

36/p.

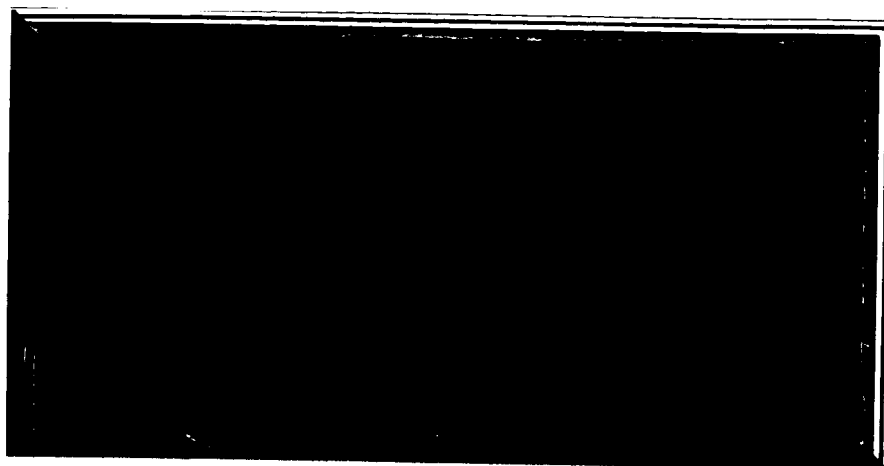
GPO PRICE \$ _____

CFSTI PRICE(S) \$ _____

Hard copy (HC) 7.00

Microfiche (MF) 2.00

ff 653 July 65



FACILITY FORM 602

N 65 - 35 277

(ACCESSION NUMBER)

(THRU)

(PAGES)

(CODE)

(NASA CR OR TMX OR AD NUMBER)

(CATEGORY)

Available
through the
General Electric
Company

GENERAL  ELECTRIC

RA-17060

DOCUMENT NO. 63SD801

15 OCTOBER 1963

VOYAGER DESIGN STUDY,

PART I,

VOLUME III :

SUBSYSTEM DESIGN

Prepared Under Contract NAS W-696

for

NATIONAL AERONAUTICS AND SPACE ADMINISTRATION

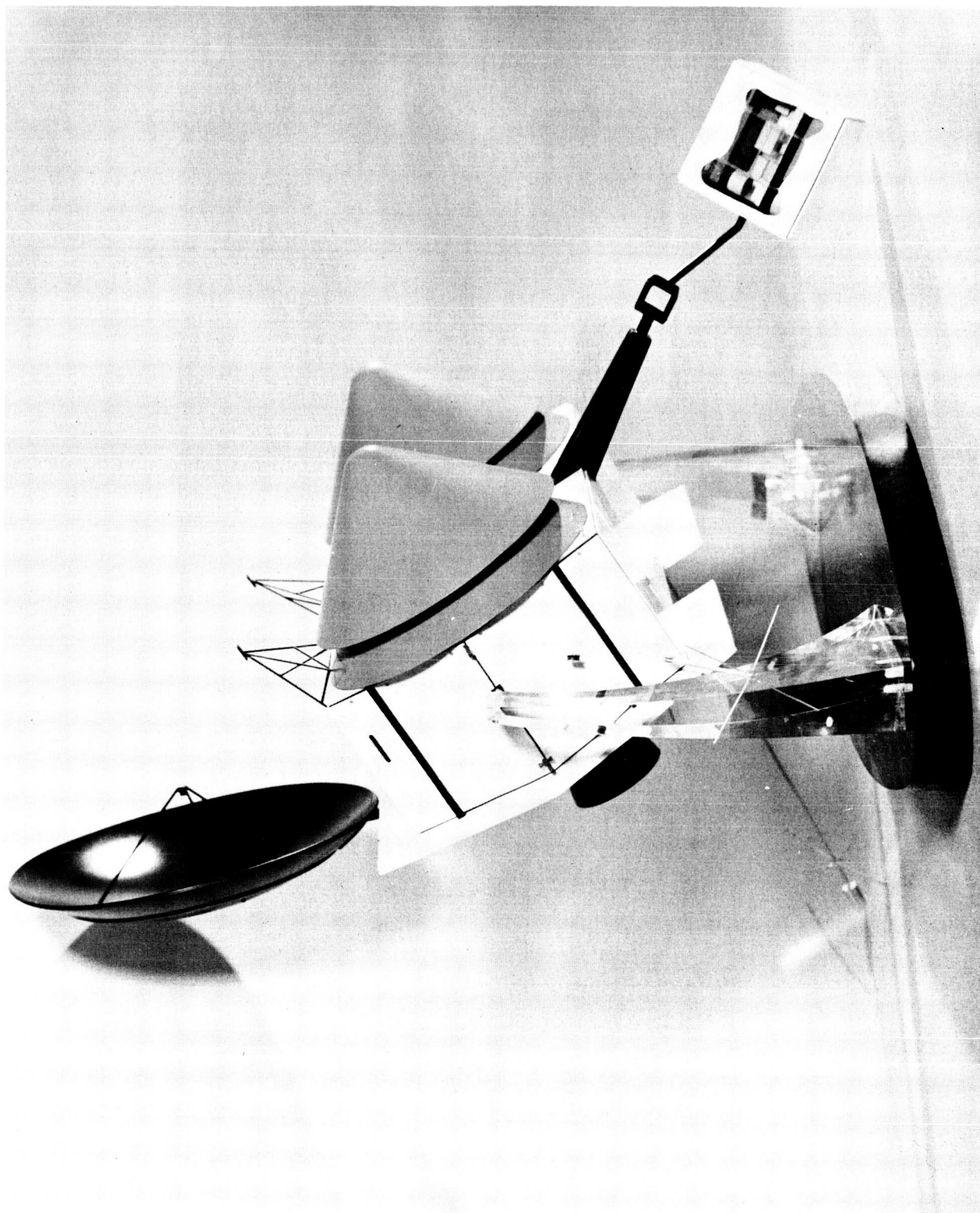
OFFICE OF SPACE SCIENCES

WASHINGTON, D.C.

~~UNCLASSIFIED TO NASA OFFICE AND~~
~~FOR OFFICIAL USE ONLY~~

GENERAL  ELECTRIC

MISSILE AND SPACE DIVISION
Valley Forge Space Technology Center
P.O. Box 8555 • Philadelphia 1, Penna.



Voyager Spacecraft Model

TABLE OF CONTENTS

Section		Page
SECTION 1.	COMMUNICATIONS SUBSYSTEM	1-1
1.1	Summary of Results	1-1
1.1.1	General	1-1
1.1.2	Description of Communications Subsystems	1-20
1.1.3	Graphical and Tabular Results	1-36
1.1.4	Tables of Size; Weight, and Power Requirements.	1-49
1.1.5	Critical Problem Areas	1-49
1.2	Command and Computer Subsystem	1-55
1.2.1	Description	1-55
1.2.2	Modes of Operation	1-58
1.2.3	Subsystem Elements	1-60
1.2.4	Implementation	1-71
1.2.5	Reliability	1-73
1.3	Data Processing and Storage Subsystem	1-75
1.3.1	Subsystem Requirements	1-75
1.3.2	Subsystem Operation	1-75
1.3.3	Data Processing Unit	1-77
1.3.4	Data Storage Unit	1-97
1.3.5	Physical Characteristics	1-103
1.4	Deep-Space Transmission Subsystem	1-105
1.4.1	Functional Requirements	1-105
1.4.2	Operational Considerations of the Deep-Space Instrumen- tation Facility (DSIF)	1-105
1.4.3	Subsystem Description	1-106
1.4.4	Component Description	1-111
1.4.5	Performance Calculations	1-111
1.4.6	Results	1-118
1.5	Relay Transmission Subsystem	1-123
1.5.1	Scope	1-123
1.5.2	The Need For A Relay Link	1-123
1.5.3	Selection of the Carrier Frequency	1-123
1.5.4	Modulation/Detection Schemes	1-126
1.5.5	Analysis	1-127
1.5.6	Subsystem Description	1-131
1.5.7	Components	1-140
1.5.8	Results	1-140
1.6	Communications Techniques	1-145
1.6.1	Analog vs Digital Television	1-145
1.6.2	Modulation and Detection	1-148
1.6.3	Error Control Coding for Voyager Communications	1-155
1.6.4	Precision Range Rate Measurement with Two-Way Doppler Tracking	1-173
1.6.5	Command Signal Structure	1-182

1.7	Component Selection	1-185
1.7.1	S-Band Power Amplifier	1-185
1.7.2	Antennas	1-189
1.7.3	Recorders	1-203
1.7.4	S-Band Transponders	1-214
1.7.5	Diplexers and RF Switches	1-217
1.7.6	High-Voltage Power Supply	1-219
1.7.7	VHF Transmitters for Relay Links	1-220
1.7.8	VHF Receivers for Relay Links	1-226
1.7.9	Command/Data Detectors	1-229
1.8	Typical Operating Sequences - Mars 1969	1-235
1.8.1	Orbiter TV Sequences	1-235
1.8.2	Television Operation	1-236
1.8.3	Orbiter-Lander Relay Link Operation - Mars 1969	1-239

TABLE OF CONTENTS

Section	Page
2.0 TELEVISION SUBSYSTEM	
2.1 Summary	2-1
2.1.1 Orbiter Television	2-1
2.1.2 Lander Television	2-1
2.1.3 Resolution Parameters	2-1
2.1.4 Cameras	2-4
2.1.5 Optics	2-4
2.1.6 Stereo	2-4
2.1.7 Artificial Illumination for Venus	
2.2 Establishment of Subsystem Requirements	2-4
2.2.1 Information Content	2-4
2.2.2 Terrain Coverage	2-5
2.2.3 Data Reduction.	2-6
2.3 Analysis	2-7
2.3.1 Optics	2-7
2.3.2 Sensors	2-12
2.3.3 Camera Electronics	2-16
2.3.4 Stereo Calculations	2-16
2.3.5 Flash Illumination on Surface of Venus	2-19
2.4 Results.	2-20
2.5 Critical Problem Areas	2-22
2.5.1 Vidicon Sterilization.	2-25
2.5.2 Image Orthicon Tube Development	2-25
2.5.3 Image Orthicon Camera Development	2-25
2.6 References	2-25
2.7 Appendices	2-27

TABLE OF CONTENTS

	Page
3. RADAR	3-1
3.1 Summary	3-1
3.1.1 Terrain Mapping	3-1
3.1.2 Radar Surface Sounder	3-2
3.1.3 Radiometer	3-2
3.1.4 Ionospheric Sounding	3-3
3.1.5 Orbiter Radar Altimeter	3-3
3.1.6 Lander Radars	3-3
3.2 Introduction	3-3
3.3 Analysis	3-4
3.3.1 Terrain Mapping Radars	3-4
3.3.2 Radar to Determine Surface Characteristics	3-43
3.3.3 Ionospheric Sounding	3-49
3.3.4 Radiometer Measurements	3-52
3.3.5 Radar Altimeters	3-55
3.4 Results and Conclusions	3-58
3.4.1 Terrain Mapping	3-58
3.4.2 Radar Surface Sounder	3-59
3.4.3 Ionospheric Sounder	3-60
3.4.4 Radiometer	3-60
3.4.5 Venus 1970 Orbiter Radar Altimeter	3-60
3.4.6 Radar Equipment for Mars-Venus Entry Vehicles	3-60
3.5 Critical Problem Areas	3-61

SECTION 4.	GUIDANCE AND CONTROL	4-1
4.1	Introduction	4-1
4.2	Summary	4-3
4.3	Approach to the Study	4-6
4.3.1	Guidance	4-6
4.3.2	Control	4-6
4.4	Guidance Analysis	4-8
4.4.1	Trajectory	4-9
4.4.2	Approach Guidance Error Analysis	4-9
4.4.3	The Terminal Problem	4-16
4.4.4	Orbit Plane Precession	4-51
4.4.5	Approach Guidance Implementation	4-51
4.5	Attitude Control	4-65
4.5.1	Summary	4-65
4.5.2	Subsystem Requirements	4-65
4.5.3	Attitude Control Subsystem	4-66
4.5.4	Subsystem Design Rationale	4-77
4.5.5	Supporting Analyses	4-87
4.6	Voyager Lander High Gain Antenna Control Subsystem	4-96
4.6.1	Introduction	4-96
4.6.2	Implementation	4-98
4.7	Alternatives	4-99
4.7.1	General	4-99
4.7.2	Canopus Vs Earth Sensing for Vehicle Attitude Reference . . .	4-99
4.7.3	Vehicle Configuration	4-99
4.7.4	On-Board Computation	4-105
4.7.5	Nonconventional Gyros	4-106
3.7.6	PHP Cable Unwinding	4-107
4.8	Bibliography	4-108
4.9	Appendices	4-109

SECTION 5. PROPULSION

5.1	Introduction	5-1
5.2	Summary	5-1
5.2.1	Orbiter Propulsion Summary	5-1
5.2.2	Lander Propulsion Summary	5-3
5.2.3	Attitude Control Propulsion Summary	5-4
5.3	Orbiter Propulsion	5-4
5.3.1	Selected System Summary - Mars 1969	5-7
5.3.2	System Type Selection	5-8
5.3.3	Use of Dual-Purpose System	5-8
5.3.4	Propellant Selection	5-8
5.3.5	System Design and Optimization	5-8
5.4	Lander Propulsion	5-58
5.5	Attitude Control Propulsion	5-58
5.5.1	Requirements	5-58
5.5.2	Cold Gas - Gaseous Stored	5-61
5.5.3	Cold Gas - Liquid Stored	5-68
5.5.4	Cold Gas - Solid Stored	5-71
5.5.5	Hot Gas	5-74
5.5.6	Cap Pistol	5-74
5.5.7	Electric Propulsion	5-75
5.5.8	Choice of System	5-75
5.5.9	Components	5-77

TABLE OF CONTENTS

SECTION 6.	POWER SUPPLY	6-1
6.1	Summary	6-1
6.1.1	Major Conclusions	6-1
6.1.2	Problem Areas	6-1
6.1.3	Orbiter Power Supply	6-3
6.1.4	Mars Lander Power Supply.....	6-5
6.1.5	Isotope Availability.....	6-9
6.1.6	Isotope Thermionic Generator Design Studies	6-10
6.2	Scope of Study	6-15
6.3	Approach	6-16
6.3.1	Selection Criteria	6-16
6.3.2	Preliminary Selection.....	6-16
6.3.3	Final Selection.....	6-19
6.4	Preliminary System Selection.....	6-20
6.4.1	Introduction	6-20
6.4.2	Tabulation of Performance Data	6-20
6.4.3	System Trade Offs	6-20
6.5	Basic Studies.....	6-34
6.5.1	Purpose	6-34
6.5.2	Concentrated Photovoltaics.....	6-34
6.5.3	Radioisotope Thermionics	6-53
6.5.4	Isotope Thermoelectric.....	6-78
6.5.5	Solar Thermionics	6-85
6.6	Final Selection - Recommended and Alternate Systems	6-104
6.6.1	Orbiters	6-104
6.6.2	Mars Lander	6-106
6.6.3	Venus Lander.....	6-106
6.6.4	Rechargeable Batteries	6-107
6.7	Performance of Recommended Power Supplies	6-108
6.7.1	Introduction.....	6-108
6.7.2	Solar Array Parameters	6-108
6.7.3	Nickel Cadmium Batteries.....	6-111
6.7.4	Silver Zinc Batteries	6-113
6.8	Mission Analysis	6-115
6.8.1	Introduction	6-115
6.8.2	Mars 1969 Orbiter	6-115
6.8.3	Mars 1971 Orbiter and 1973 Back-Up Orbiter	6-115
6.8.4	Mars 1973 Orbiter and 1975 Back-Up Orbiter	6-115
6.8.5	Mars 1975 Bus.....	6-116
6.8.6	Mars 1969 Lander	6-116
6.8.7	Mars Landers after 1969.....	6-117
6.8.8	Venus Landers	6-117

6.9	Recommendations for Future Effort	6-117
6.9.1	Earth Safety and Planet Contamination Ground Rules	6-117
6.9.2	RTG Failure Mode Analysis - Mars Lander	6-117
6.9.3	Alternative RTG Design Concepts for Mars Lander	6-118
6.9.4	Isotope Thermionic and Thermoelectric Studies	6-118
6.9.5	Isotope Availability	6-118
6.10	References	6-118

LIST OF ILLUSTRATIONS

Figure		Page
1.1.1-1	Mars 1969 and 1971 Communication Links	1-5
1.1.1-2	Mars 1973 and 1975 Communication Links	1-6
1.1.1-3	Venus 1970 Communication Links	1-7
1.1.1-4	Venus 1972 Communication Links	1-8
1.1.2-1	Mars 1969 and 1971 Orbiter Communications Subsystem . . .	1-21
1.1.2-2	Mars 1969 and 1971 Lander Communications Subsystem . . .	1-26
1.1.2-3	Mars 1973 and 1975 Orbiter Communications Subsystem . . .	1-29
1.1.2-4	Mars 1973 and 1975 Lander Communications Subsystem . . .	1-31
1.1.2-5	Venus 1970 Orbiter Communications Subsystem	1-33
1.1.2-6	Venus 1970 Lander Communications Subsystem	1-37
1.1.2-7	Venus 1972 Orbiter Communications Subsystem	1-39
1.1.2-8	Venus 1972 Lander Communications Subsystem	1-41
1.1.3-1	Data Transmission Rates (Mars 1969 and 1971)	1-42
1.1.3-2	Data Transmission Rates (Mars 1973 and 1975)	1-43
1.1.3-3	Data Transmission Rates (Venus 1970)	1-44
1.1.3-4	Data Transmission Rates (Venus 1972)	1-45
1.1.3-5	Data Rate in Orbit (Mars 1969 and 1971).	1-46
1.1.3-6	Data Rate vs Range (Venus 1970 and 1972) Missions.	1-47
1.1.3-7	Lander-to-Orbiter Data Rate During Mars Lander Descent (All Mars Missions)	1-48
1.2.1-1	Block Diagram, Command and Computer System	1-56
1.2.3-1	Power Conversion and Control Unit	1-63
1.2.3-2	Sequence Timer Unit	1-69
1.3.2-1	Data Processing and Storage Subsystem, Mars 1969 Orbiter . .	1-76
1.3.2-2	Data Processing and Storage Subsystem, Mars 1969 Lander . .	1-78
1.3.3-1	Basic Frame Format	1-80
1.3.3-2	Data Multiplexer, General Block Diagram	1-81
1.3.3-3	Pseudo Noise and Error Control Encoder, Orbiter and Lander .	1-83
1.3.3-4	Data Processor Detailed Block Diagram Orbiter Unit	1-87
1.3.3-5	Mode Selector, Orbiter and Landers	1-88
1.3.3-6	Pseudo Noise/Manchester Code Error Correction Group Gen- erator.	1-89
1.3.3-7	Analog Gate Grouping Methods	1-91
1.3.3-8	Bit and Word Generator Self Healing Logic	1-93
1.3.3-9	Data Plots Assuming One Converter Failure and Majority Logic Used	1-95
1.3.4-1	Spacecraft Video Digital Memory System	1-98
1.3.4-2	Thermoplastic Plate Format	1-100
1.3.4-3	TPR Plate Transfer Device	1-101
1.3.4-4	Phase Modulated Lateral Recording	1-102
1.3.4-5	Data Recording Technique and Sweep Waveforms	1-102
1.3.4-6	Playback Spot Position vs Time	1-104
1.3.4-7	Recording Turn-Around Detail	1-104
1.4.3-1	Orbiter Deep Space Transmission Subsystem	1-107
1.4.3-2	Mars 1969 and 1971 Lander Deep Space Transmission Sub- system	1-109
1.4.3-3	Mars 1973 and 1975 Lander Deep Space Transmission Sub- system	1-110
1.5.5-1	Free Slack Attenuation vs Orbiter Altitude	1-130
1.5.5-2	Variation in Antenna Gain With Angle From Centerline of Beam.	1-132
1.5.5-3	Transmitter Power Required Per Kilobit Per Second of Data During Mars Lander Descent.	1-133

LIST OF ILLUSTRATIONS (Cont'd)

Figure		Page
1.5.5-4	Transmitter Power Required Per Kilobit Per Second of Data During Mars Orbit	1-134
1.5.5-5	Transmitter Power Required Per Kilobit Per Second of Data . .	1-135
1.5.6-1	Mars 1969 and 1971 Orbiter Relay Transmission Subsystem . .	1-136
1.5.6-2	Mars 1969 and 1971 and Venus 1972 Lander Relay Trans- mission Subsystem	1-138
1.5.6-3	Mars 1973 and 1975 Orbiter Relay Transmission Subsystem . .	1-138
1.5.6-4	Mars 1973 and 1975 Lander Relay Transmission Subsystem . .	1-139
1.5.6-5	Venus 1970 Orbiter Relay Transmission Subsystem	1-139
1.5.6-6	Venus 1970 Lander Relay Transmission Subsystem	1-139
1.5.6-7	Venus 1972 Orbiter Relay Transmission Subsystem	1-141
1.5.8-1	Lander-to-Orbiter Data Rate During Mars Lander Descent - All Mars Missions	1-142
1.5.8-2	Data Rate in Orbit Mars 1969 and 1971	1-143
1.5.8-3	Data Rate vs Range-Venus 1970 and 1972 Missions	1-144
1.6.2-1	Signal Power Received at DSIF Ground Station vs Spacecraft Transmitter Power	1-150
1.6.2-2	Probability of Bit Error for Ideal PCM/PSK ($\pm 90^\circ$)	1-152
1.6.2-3	Signal Power Required at DSIF Ground Station vs Data Rate for Digital Modulation Systems (Zero Margin)	1-154
1.6.2-4	Total R-F Received Power Requirements as Determined by Data, Peak Phase Deviation, and Carrier (Zero Margin). . .	1-156
1.6.2-5	Typical Graphs of Data Rate vs Transmitter Power for Digital Modulation Systems	1-157
1.6.2-6	Performance at Low Data Rates Through Omni Antenna	1-158
1.6.3-1	Typical Data Link with Error Control Coding	1-160
1.6.3-2	Reduction of Power Requirements Through Error Control Coding	1-165
1.6.3-3	Encoding Subsystem	1-166
1.6.3-4	(73, 45) Encoder	1-167
1.6.3-5	Encoder Timer	1-168
1.6.3-6	Timing	1-170
1.6.3-7	Decoding Subsystem	1-171
1.6.3-8	(73, 45) Decoder	1-172
1.6.4-1	Two-Way Doppler Tracking System Simplified Functional Block Diagram	1-175
1.6.4.2	Frequency Measuring Unit Simplified Block Diagram	1-176
1.6.4.3	RMS Range Rate Error ($\Delta \dot{r}_1$) due to Coherent Oscillator In- stability	1-178
1.6.4-4	RMS Range Rate Error ($\Delta \dot{r}_2$) due to Receiver Thermal Noise .	1-180
1.6.4-5	RMS Range Rate Error ($\Delta \dot{r}_B$) due to Quantization Interval in Cycle Counting.	1-181
1.6.5-1	Command Signal Structure	1-183
1.7.2-1	Alternative Design for High-Gain Antenna (Array of 49 Helices). .	1-191
1.7.2-2	S-Band Orbiter Low Gain Antenna Array	1-194
1.7.2-3	Turnstile Antenna (S-Band Split Balun Feed)	1-195
1.7.2-4	Turnstile Antenna Over a Ground Plane (Two Different Turn- stile Heights)	1-196
1.7.2-5	Pattern of Antennas of Figure 1.7.2-2	1-197
1.7.2-6	Orbiter VHF Crossed Yogi	1-199
1.7.2-7	Arrangement of Helices in Array (Mars 1971, 1973, & 1975 Landers).	1-201
1.7.2-8	Individual Helix Element	1-201

LIST OF ILLUSTRATIONS (Cont'd)

Figure		Page
1.7.2-9	Microstrip Feed Network.	1-202
1.7.2-10	Mars Lander Low-Gain S-Band Antenna.	1-202
1.7.2-11	S-Band Turnstile Pattern.	1-204
1.7.2-12	Lander Turnstile Antenna	1-205
1.7.2-13	Lander "Transmission Line" Antenna	1-206
1.7.2-14	Installation on Lander.	1-206
1.7.3-1	Cross Section of Thermoplastic Film.	1-210
1.7.3-2	Force on Surface Charger	1-210
1.7.3-3	Deformation After Developing	1-210
1.7.3-4	Principle of Electron Beam Readout	1-212
1.7.3-5	Arrangement of Multiplier Collectors for Electron Beam Read- out.	1-212
1.7.4-1	Modified STL Receiver	1-215
1.7.4-2	Transponder-Transmitter Portion.	1-216
1.7.5-1	S-Band Diplexer.	1-218
1.7.6-1	Electrostatically Focused Klystron	1-218
1.7.6-2	Orbiter High Voltage Power Supply	1-221
1.7.6-3	Lander High Voltage Power Supply	1-222
1.7.7-1	VHF Phase Modulated Transmitter	1-223
1.7.7-2	Oscillator Schematic	1-224
1.7.7-3	Phase Modulator	1-224
1.7.8-1	VHF Pre-Amplifier and Command/Telemetry Receiver	1-227
1.7.9-1	Construction of Modulating Waveform Utilizing 7-Bit PN Sequence.	1-230
1.7.9-2	Command/Data Detector Functional Block Diagram	1-231
1.8.2-1	Television and TPR Interconnection	1-238
2.3.1-1	Focal Lengths of Lenses vs Resolution, Vidicon and Image Orthicon.	2-9
2.3.1-2	Relative Aperture vs Resolution	2-11
2.3.1-3	Maximum Exposure Time vs. Resolution	2-15
2.3.1-4	Field of View vs Resolution	2-22
2.3.2-1	Equivalent Circuit	2-36
2.3.4-1	Geometric Relationships, Camera to Objective	2-38
2.3.4-2	B/H Factor Geometry.	2-41
2.4-1	Television Subsystem Block Diagram.	2-42
C1	Solar Flux at the Average Distance of Mar's Orbit	2-46
C2	D_λ for a Sun Zenith Angle of 0°	2-53
C3	D_λ for a Sun Zenith Angle of $88^\circ 48'$	2-60
3.3.1-1	Sample Side-looking Radar Strip Map with Coordinate Grid and Point Elevation Data.	3-5
3.3.1-2	Comparison of Aerial Photograph and Side Looking Radar Image of the Same Area.	3-6
3.3.1-3	Required Reflection Coefficient vs Altitude.	3-11
3.3.1-4	Graph of Radar System Weight vs Antenna Diameter.	3-16
3.3.1-5	Equipment in Vehicle	3-20
3.3.1-6	Processing on Ground.	3-21
3.3.1-7	Shift Register Data Processor and Weighted Shift Register Chain.	3-23
3.3.1-8	Display Roster-Single Pulse Map	3-25
3.3.1-9	Geometry for Unfocused Synthetic Antenna	3-31
3.3.1-10	Azimuth Resolution as a Function of Range for Three Types of Radars	3-34
3.3.1-11	Minimum Antenna Area for Ambiguity Avoidance vs Altitude	3-35

LIST OF ILLUSTRATIONS (Cont'd)

Figure		Page
3.3.1-12	Resolution vs Average Radiated Power	3-37
3.3.1-13	Backscattering Coefficient vs Altitude	3-38
3.3.1-14	Resolution vs Altitude	3-40
3.3.2-1	Radar Sounding of the Planetary Surface at Different Aspects. .	3-45
3.3.2-2	Surface Sounder Data Handling	3-48
3.3.3-1	Ionogram	3-50

LIST OF ILLUSTRATIONS (Cont'd)

Figure		Page
4. 4. 1-1	Mars Type II Trajectory Projected Into Ecliptic Plane	4-10
4. 4. 1-2	Earth-Vehicle-Sun Angle Vs. Time From Launch 1969 Type II Mars Trajectory	4-11
4. 4. 2-1	Mars Trajectory Determination DSIF Plus Line-of-Sight Observations	4-14
4. 4. 2. 2	Venus Trajectory Determination DSIF Plus Line-of-Sight Observations	4-15
4. 4. 3-1	Lander Separation Geometry	4-17
4. 4. 3-2	Landing Site Aiming Points	4-18
4. 4. 3-3	Lander Separation and Entry	4-19
4. 4. 3-4	Entry Latitude (θ_e) Vs the Normal Velocity Increment (V_N) for Various Tangential Velocity Increments	4-28
4. 4. 3-5	Flight Path Angle (γ) Vs the Normal Velocity Increment (V_N) for Various Tangential Velocity Increments	4-29
4. 4. 3-6	Time and Down Range Travel From 10^6 Feet of Altitude to Mach 2, and Altitude at Mach 2 Vs Entry Path Angle At 10^6 Feet of Altitude	4-30
4. 4. 3-7	Time (T) From Separation to 10^6 Feet Altitude Vs the Normal Velocity Increment (V_N) For Various Tangential Velocity Increments	4-31
4. 4. 3-8	Time From Entry At 10^6 Feet of Altitude to Initiation of Chute Deployment Vs Entry Path At 10^6 Feet of Altitude	4-32
4. 4. 3-9	Mars Entry (Descent Time To Impact Vs Entry Path Angle)	4-33
4. 4. 3-10	Mars Entry (Altitude Vs Final Descent Time, After Main Chute Deployment.	4-34
4. 4. 3-11	Time From Perifocus Vs True Anomaly For Mars Hyperbolic Approved Trajectory.	4-35
4. 4. 3. 12	Lander Flight Path.	4-38
4. 4. 3-13	Apofocus Altitude Variation Due to Perifocus Errors and Retro Magnitude Errors.	4-39
4. 4. 3-14	Impulsive Velocity Increment Needed to Achieve a 1 x 19 Orbit About Mars.	4-42
4. 4. 3-15	Gravity Loss Vs Thrust-To-Final-Weight Ratio For Various Velocities at Infinity.	4-43
4. 4. 3-16	Effect of Control Mode on Gravity Loss During Injection Into A 1000 nm Circular Orbit About Mars.	4-44
4. 4. 3-17	Mars 1969 Separation.	4-47
4. 4. 3-18	Sensitivity Coefficient $\frac{\gamma T}{\gamma V}$ Relating Change In Flight Time to Change In Velocity, Vs Range From Mars.	4-49
4. 4. 3-19	Sensitivity Coefficient $\frac{\gamma T}{\gamma V}$, Relating Change In Flight Time To Change In Velocity, Vs Range From Venus	4-50
4. 4. 3-20	Propulsion Loss Vs Separation Range From Mars	4-52
4. 4. 3-21	Propulsion Loss Vs Separation Range From Venus	4-53
4. 4. 4-1	Nodal Regression Vs Inclination Angle	4-54
4. 4. 5-1	Probable Error Vs Number of Stars in the Field	4-55
4. 4. 5-2	Approach TV Picture	4-60
4. 4. 5-3	Logic Diagram	4-63
4. 5. 3-1	Voyager Guidance and Control (Attitude Control Block Diagram).	4-67
4. 5. 3-2	Voyager Guidance and Control (Earth Tracker and Antenna Drive Block Diagram)	4-68

LIST OF ILLUSTRATIONS (Cont'd)

Figure		Page
4. 4. 1-1	Mars Type II Trajectory Projected Into Ecliptic Plane	4-10
4. 4. 1-2	Earth-Vehicle-Sun Angle Vs. Time From Launch 1969 Type II Mars Trajectory	4-11
4. 4. 2-1	Mars Trajectory Determination DSIF Plus Line-of-Sight Observations	4-14
4. 4. 2. 2	Venus Trajectory Determination DSIF Plus Line-of-Sight Observations	4-15
4. 4. 3-1	Lander Separation Geometry	4-17
4. 4. 3-2	Landing Site Aiming Points	4-18
4. 4. 3-3	Lander Separation and Entry	4-19
4. 4. 3-4	Entry Latitude (θ_e) Vs the Normal Velocity Increment (V_N) for Various Tangential Velocity Increments	4-28
4. 4. 3-5	Flight Path Angle (γ) Vs the Normal Velocity Increment (V_N) for Various Tangential Velocity Increments	4-29
4. 4. 3-6	Time and Down Range Travel From 10^6 Feet of Altitude to Mach 2, and Altitude at Mach 2 Vs Entry Path Angle At 10^6 Feet of Altitude	4-30
4. 4. 3-7	Time (T) From Separation to 10^6 Feet Altitude Vs the Normal Velocity Increment (V_N) For Various Tangential Velocity Increments	4-31
4. 4. 3-8	Time From Entry At 10^6 Feet of Altitude to Initiation of Chute Deployment Vs Entry Path At 10^6 Feet of Altitude	4-32
4. 4. 3-9	Mars Entry (Descent Time To Impact Vs Entry Path Angle)	4-33
4. 4. 3-10	Mars Entry (Altitude Vs Final Descent Time, After Main Chute Deployment.	4-34
4. 4. 3-11	Time From Perifocus Vs True Anomaly For Mars Hyperbolic Approved Trajectory.	4-35
4. 4. 3. 12	Lander Flight Path.	4-38
4. 4. 3-13	Apofocus Altitude Variation Due to Perifocus Errors and Retro Magnitude Errors.	4-39
4. 4. 3-14	Impulsive Velocity Increment Needed to Achieve a 1 x 19 Orbit About Mars.	4-42
4. 4. 3-15	Gravity Loss Vs Thrust-To-Final-Weight Ratio For Various Velocities at Infinity.	4-43
4. 4. 3-16	Effect of Control Mode on Gravity Loss During Injection Into A 1000 nm Circular Orbit About Mars.	4-44
4. 4. 3-17	Mars 1969 Separation.	4-47
4. 4. 3-18	Sensitivity Coefficient $\frac{\gamma T}{\gamma V}$ Relating Change In Flight Time to Change In Velocity, Vs Range From Mars.	4-49
4. 4. 3-19	Sensitivity Coefficient $\frac{\gamma T}{\gamma V}$, Relating Change In Flight Time To Change In Velocity, Vs Range From Venus	4-50
4. 4. 3-20	Propulsion Loss Vs Separation Range From Mars	4-52
4. 4. 3-21	Propulsion Loss Vs Separation Range From Venus	4-53
4. 4. 4-1	Nodal Regression Vs Inclination Angle	4-54
4. 4. 5-1	Probable Error Vs Number of Stars in the Field	4-55
4. 4. 5-2	Approach TV Picture	4-60
4. 4. 5-3	Logic Diagram	4-63
4. 5. 3-1	Voyager Guidance and Control (Attitude Control Block Diagram).	4-67
4. 5. 3-2	Voyager Guidance and Control (Earth Tracker and Antenna Drive Block Diagram)	4-68

LIST OF ILLUSTRATIONS (Cont'd)

Figure		Page
5.3-1	Orbiter Propulsion System Schematic	5-5
5.3.5-1	Simplified Pumped System Schematic.	5-11
5.3.5-2	Effect of Thrust on Total Firing Duration	5-19
5.3.5-3	ΔV Vs. Thrust at End of Burn	5-21
5.3.5-4	Thrust Chamber Length Vs. Thrust Level	5-23
5.3.5-5	Ablative/Radiative Skirt Thrust Chamber Weight Vs. Thrust Level.	5-24
5.3.5-6	Radiative Thrust Chamber Weight Vs. Thrust Level.	5-24
5.3.5-7	Regenerative Fuel Cooling Feasibility	5-30
5.3.5-8	Radiative Chamber Wall Temperature	5-33
5.3.5-9	Expansion Coefficient Vs. Fabric Orientation for Phenolic Impregnated High Silica Glass	5-36
5.3.5-10	Thermal Conductivity of Phenolic Impregnated High Silica Glass	5-37
5.3.5-11	Specific Impulse Vs. Expansion Area Ratio.	5-40
5.3.5-12	Payload Increase Vs. Expansion Ratio - Realistic Skirt Weights.	5-41
5.3.5-13	Payload Increase Vs. Expansion Ratio - Conservative Skirt Weights	5-41
5.3.5-14	Exhaust Plumbing Angle	5-42
5.3.5-15	Payload Increase Vs. Percent Bell	5-43
5.3.5-16	Vacuum Theoretical Specific Impulse Vs. Mixture Ratio	5-44
5.3.5-17	Composition of Exhaust Gases	5-46
5.3.5-18	Exhaust Plumbing Angle Shift Vs. Mixture Ratio	5-47
5.3.5-19	Condition of Stability Between Acceleration Force and Surface Tension	5-48
5.3.5-20	Partial Bellows Tank	5-51
5.3.5-21	Orbiter Propulsion System Schematic	5-53
5.5.2-1	Cold Gas - Gaseous-Stored Schematic	5-67
6.1.3-1	Orbiter Power Supply Schematic	6-4
6.1.4-1	Radioisotope Thermoelectric Generator - Mars 1969 Lander.	6-6
6.1.5-1	Comparison of Isotope Requirements and Availability Estimates.	6-11
6.1.6-1	Radioisotope Thermionic Generator Design with Helium Volume.	6-13
6.1.6-2	Radioisotope Thermionic Generator Design Without Helium Void Volume	6-14
6.4-1	Weight of Power Supplies for Venus Orbiter, No Energy Storage Considered.	6-28
6.4-2	Weight of Power Supplies for Mars Orbiter, No Energy Storage Considered.	6-30
6.4-3	Weight of Venus Lander Power Supplies.	6-32
6.5.2-1a	Solar Cell Array and Concentrator (Conical System - 1 KW Power Level)	6-39
6.5.2-1b	Solar Cell Array and Concentrator (Conical System - 1 KW Power Level)	6-41
6.5.2-1c	Solar Cell Array and Concentrator (Conical System - 1 KW Power Level)	6-43
6.5.2-1d	Solar Cell Array and Concentrator (Conical System - 1 KW Power Level)	6-45
6.5.2-2	Solar Cell Array and Concentrator (Inverted Flat Plate System).	6-49
6.5.2-3	Solar Cell Array and Concentrator (Parabolic)	6-51
6.5.3-1	Schematic of Radioisotope Thermionic Generator.	6-53
6.5.3-2	Radioisotope Thermionic Generator	6-55
6.5.3-3	Development Schedule - Isotope Thermionic Generator for Voyager	6-61

LIST OF ILLUSTRATIONS (Cont'd)

<u>Figure</u>		<u>Page</u>
6.5.3-4	AEC Availability Estimates for C 244 and Pu 238	6-67
6.5.3-5	Thermionic Converter Design for Radioisotope Thermionic Generator	6-72
6.5.4-1	Selection Curves for Using an RTG or an RTG With Nickel Cadmium Batteries for Repetitive Cyclic Loads.	6-84
6.5.5-1	Solar Thermionic System Schematic	6-86
6.5.5-2a	Vehicle Layout for Solar Thermionic Experiment.	6-97
6.5.5-2b	Vehicle Layout for Solar Thermionic Experiment.	6-98
6.5.5-2c	Vehicle Layout for Solar Thermionic Experiment.	6-99
6.5.5-3	Development Schedule - Solar Thermionic Generator for Voyager .	6-100
6.5.5-4	Solar Thermionic Generator.	6-102
6.7-1	Solar Flare Proton Environment	6-110
6.7-2	Solar Cell Radiation Degradation Factors Due to Solar Flare Protons	6-112
6.7-3	Estimated Charging Efficiency of Nickel Cadmium Battery . . .	6-114

LIST OF ILLUSTRATIONS

Figure		Page
A-1	Configuration A High Power Efficiency On Near Ecliptic Orbits Only	4-114
A-2a	Configuration B For Near Ecliptic Orbits	4-115
A-2b	Configuration B For Near Polar Orbits	4-115
*B-1	Solar Power Efficiency Vs Orientation	4-117
B-2	Geometry	4-119
B-3	Orbit No. 1, Orbit Inclination 30°	4-120
B-4	Orbit No. 2, Orbit Inclination 70°	4-121
B-5	Orbit No. 3, Orbit Inclination 77.5°	4-122
B-6	Orbit No. 4, Orbit Inclination 68°	4-123
E-1	Mars Approach Geometry	4-131
E-2	Mars Approach Geometry, Approach Trajectory Plane	4-132
F-1	Geometry For In-Plane Landing Sites	4-134
F-2	Geometry In-Plane Perpendicular to Trajectory Plane	4-135
G-1	Coordinates For Linearized Orbiter Error Analysis	4-138
G-2	Angles Used to Define Orbit	4-139
*G-3	Effects of e (η)	4-144
H-1	Effect of the Thrust to Weight Ratio On Gravity Loss During Injection Into a 1000 nm Circular Orbit About Mars Using A Gravity Turn	4-159
H-2	Effect of the Thrust to Weight Ratio On Gravity Loss During Injection Into An Ecliptical Orbit About Mars Using a Gravity Turn	4-160
H-3	Effect of Control Mode On Gravity Loss During Injection Into A 1000 nm Circular Orbit About Mars	4-161
H-4	Sketch of Trajectories	4-162
H-5	Effect of the Velocity at Infinity On Gravity Loss During Injection Into a 1000nm Circular Orbit About Mars Using a Gravity Turn	4-164
H-6	Effect of the Velocity at Infinity On Gravity Losses During Injection Into An Elliptical Orbit About Mars Using a Gravity Turn	4-165
I-1	Thrust Vector Static Requirement Vs Propellant Ratio Error	
I-2	Effect Of Temperature Differential of Propellants On Flow Rate Ratio And On Residual Propellant (Shown For Two Different Oxidizers)	4-169
I-3	Effect of Tank Pressure Differential	4-170
I-4	Flow Rate Ratio Vs TV Requirement For Representative Amplification Factors	4-171
I-5	Auxiliary Propellant And Tank Weights For Outrigger Vernier Nozzle TVC	4-174
I-6	Condition of Stability Between Acceleration Force and Surface Tension	4-175
I-7	Comparison of Natural Frequencies of Spherical Tank And Cylindrical Tank	4-176
I-8	Fundamental Mode, Tank Diameter 39.9 Inches	4-178
I-9	Spherical Tank Fluid Frequency Parameter	4-179
I-10	Spherical Tank Fullness Vs η/a	4-180
I-11	Oscillating Mass Ratio Vs Fluid Height Ratio	4-181
I-12	Moment Factor As a Function of Frequency Ratio η/a	4-182
I-13	Force Factor Vs Frequency Ratio	4-183
I-14	Excitation Amplitude, X_0 , Which Sloshing Occurs And Below Which Oscillation Occurs	4-184
I-15	Lander Rigid Body Response to Thrust Vectoring End of Midcourse Correction Conditions	4-186

LIST OF ILLUSTRATIONS (Cont'd)

Figure		Page
I-16	Lander Rigid Body Motions I_u Response to Thrust Vectoring Near Empty Condition (End of Orbit Injections)	4-187
I-17	Voyager Assembly Geometry	4-188
I-18	Oscillating Fluid Amplitude At Wall As Function of Fluid Height Ratio And Control To Natural Frequency Ratio	4-189
J-1	Control Loop Block Diagram	4-193
J-2	Geometry of Vehicle cg Shift	4-194
J-3	Shift In cg Due to Fuel Oscillations	4-196
J-4	Shift In cg With Fuel Oscillation Effects	4-197
J-5	Shift In cg Without Fuel Oscillation Effects	4-198
L-1	Atmospheric Density Vs Altitude	4-205
L-2	G. Schillig's Model II Martian Atmosphere	4-207
L-3	Relative Photocathode Response Through Martian Atmosphere To Earth Reflected Sunlight Vs Wavelength	4-208

LIST OF TABLES

<u>Table No.</u>	<u>Title</u>	<u>Page</u>
	Mission Characteristics Affecting Communications	1-2
1.1.1-1	Summary of Communications Subsystem Requirements	1-4
1.1.1-2	Communication Mode Sequence - Mars 1969 and 1971	1-9
1.1.1-3	Communications Mode Sequence - Mars 1973 and 1975	1-11
1.1.1-4	Communication Mode Sequence - Venus 1970	1-13
1.1.1-5	Communication Mode Sequence - Venus 1972	1-14
1.1.1-6	Summary of Communication Link Parameters, Mars 1969 and	
1.1.1-7	1971	1-16
1.1.1-8	Summary of Communication Link Parameters, Mars 1973 and	
	1975	1-17
	Summary of Communication Link Parameters, Venus 1970	1-18
1.1.1-9	Summary of Communication Link Parameters, Venus 1972	1-19
1.1.1-10	Data Rates (Bits/Second).	1-35
1.1.3-1	Size, Weight, and Power Requirements for Orbiter Communica-	
1.1.4-1	tions Subsystem	1-50
1.1.4-2	Size, Weight, and Power Requirements for Lander Communica-	
	tions Subsystem	1-52
1.2.3-1	Typical Vehicle Status Inputs	1-67
1.2.4-1	Size, Weight and Power for Three Units.	1-72
1.2.4-2	Thin-Film Plated Wire Memory Characteristics	1-73
1.3.3-1	Failure Analysis for Analog Gates.	1-92
1.3.3-2	Packaging Approach Summary	1-94
1.3.3-3	Packaging Approach Summary	1-96
1.3.5-1	Size, Weight and Power Requirements for Data Processing and	
	Storage Subsystem	1-103
1.4.5-1	Deep Space Link Performance Calculations.	1-112
1.4.6-1	Carrier - Lock Range in Millicon of Nautical Miles (Telemetry	
	Links)	1-120
1.4.6-2	Carrier - Lock Range in Millions of Nautical Miles (Command	
	Links)	1-121
1.5.2-1	Factors Influencing Choice of Lander to Earth Communications	
	Link	1-124
1.5.5-1	Significant Parameters for Transmitter Power Calculation	1-128
1.6.2-1	Deep-Space Communication Link Calculations.	1-151
1.6.3-1	Random-Burst and Random Correction Capabilities	1-163
1.6.3-2	Data Bit Errors.	1-163
1.6.3-3	Error Control System Parts Count	1-173
1.7.4-1	Characteristics of Available Transponders.	1-214
1.7.7-1	Operating Characteristics of Power Transistors	1-226
1.7.8-1	Performance Characteristics of VHF Receivers	1-228
1.7.9-1	Characteristics of Command/Data Detectors (Mars 1969 and 1971).	1-233
1.8.1-1	Types of Frames	1-235
1.8.1-2	Summary of Number of TV Frames per Orbit	1-236
1.8.2-1	Individual Camera Inputs.	1-236
1.8.2-2	Camera Outputs.	1-237
2.1-1	Mars Television Mission.	2-2
2.1-2	Venus Television Mission	2-2
2.1-3	Voyager Systems Constraints	2-3
2.1-4	Television Camera Characteristics	2-3
2.3.1-1	Optical Characteristics	2-9
2.3.1-2	Television Lens Characteristics for One-Meter Resolution	2-12
2.3.2-1	Vidicon Parameters	2-15
2.3.2-2	Image Orthicon Parameters.	2-15

LIST OF TABLES (Cont'd)

<u>Table No.</u>	<u>Title</u>	<u>Page</u>
2.4-1	Lens Weights and Sizes	2-22
2.4-2	Television Subsystem Characteristics	2-23
A	Comparison - Television Vs. Photography	2-30
B	Photographic Lens Characteristics for One-Meter Ground Resolution	2-31
3.3.1-1	Mapping Conditions.	3-8
3.3.1-2	Azimuth Resolution.	3-9
3.3.1-3	Weight and Power for Equal Performance at all Altitudes	3-12
3.3.1-4	Antenna Weight vs. Diameter	3-14
3.3.1-5	Power Requirement for the SAHARA Radar, 1 NM x 1 NM Resolution	3-15
3.3.1-6	Power Requirements for the SAHARA Radar, 2 NM x 2 NM Resolution	3-15
3.3.1-7	Total Radar System and Subsystem Weights, Function of Antenna Diameter for 1 NM x 1 NM Resolution	3-17
3.3.1-8	Total Radar System and Subsystem Weights, Function of Antenna for 2 NM x 2 NM Resolution	3-17
3.3.1-9	Total Radar System Weight of Recommended System	3-26
3.3.1-10	Radar System Parameters of Recommended System.	3-27
3.3.1-11	Input-Output Parameters of Recommended System	3-28
3.3.1-12	Operating Mode Parameters of Recommended System	3-28
3.3.1-13	Summary of Weight, Volume, and Power Requirements for Coherent Pulse Doppler System	3-42
3.3.2-1	Polarization Effects	3-43
3.3.2-2	Return vs. Aspect Angle	3-44
3.3.2-3	Estimated (High Frequency) Radar Characteristics	3-47
3.3.3-1	Estimated Ionospheric Sounder Characteristics	3-52
3.3.5-1	Mars Altimeter Parameters and Performance.	3-56
3.3.5-2	Mars Altimeter Physical Characteristics	3-56
3.4.2-1	Characteristics of Radar Sounder - 10 Ft. Antenna	3-60
4.4.1-1	Various Trajectory Parameters	4-18
4.4.3-1	Lander Dispersion 10 January 1969 Launch.	4-23
4.4.3-2	Lander Dispersion 9 February 1969 Launch	4-37
4.4.3-3	Time Margins (Minutes) to Loss of Line-of-Sight for 10 January 1969 Mars Approach.	4-39
4.4.5-1	Calculated Relative Brightness.	4-62
4.4.5-2	Typical Image Orthicon Experimental Sequence	4-75
5.3.5-1	Pressurization Systems Comparison	5-9
5.3.5-2	Thrust Level Comparison, Ablative Chamber or Ablative/Radiative Skirt Chamber.	5-25
5.3.5-3	Thrust Level Comparison Radiative Chamber	5-26
5.3.5-4	System Weight Comparison - Radiative and Ablative/Radiative Systems	5-32
5.3.5-5	Chamber Type Selection	5-38
5.3.5-6	Chamber Pressure Comparison	5-39
5.3.5-7	Propellant Supply System Comparison	5-50
5.5.2-1	Gaseous Stored Cold Gas Comparison	5-63
5.5.3-1	Liquid Stored Cold Gas Comparison	5-69
5.5.8-1	Attitude Control System Comparison	5-76

LIST OF TABLES (Cont'd)

<u>Table No.</u>	<u>Title</u>	<u>Page</u>
6.1.1-1	Orbiter Power Supply Summary	6-2
6.1.1-2	Lander Power Supply Summary.	6-2
6.1.3-1	Detailed Solar Array Performance	6-7
6.1.3-2	Solar Cell Performance Factors	6-8
6.1.3-3	Solar Array Thermal Factors	6-8
6.1.4-1	Isotope Thermoelectric Generator Design	6-9
6.1.6-1	Isotope Thermionic Generator Design	6-12
6.3-1	Systems Considered for Orbiters	6-17
6.3-2	Systems Considered for Landers	6-18
6.4-1	Performance Data Used in Preliminary System Selection	6-21
6.5.2-1	Concentrating Photovoltaic Power Supplies for Mars Orbiter.	6-36
6.5.2-2	Concentrator Comparison	6-37
6.5.2-3	Comparison of Concentrated, Flat Paddle, and V-Ridge Photo- voltaics	6-38
6.5.3-1	Schedule for Development of an Orbital Isotope Thermionic Experimental Vehicle	6-57
6.5.3-2	Schedule for Development of a 300-Watt Isotope Thermionic Power Supply for Voyager	6-63
6.5.3-4	Radioisotope Requirements for Mars 1969 Mission	6-69
6.5.3-5	Isotope Thermionic Generator Parameters.	6-71
6.5.3-6	Performance of Modulus Radioisotope Thermionic Generators	6-73
6.5.4-1	Consideration of RTG Failure Modes.	6-80
6.5.5-1	Schedule for Development of an Orbital Solar Thermionic Experimental Vehicle	6-89
6.6-1	Performance Comparison of Orbiter Power Supplies	6-105

FOREWORD

Early in the Voyager study General Electric recognized that the size and complexity of the Voyager Program would inevitably require the participation of a broad segment of industry in the design, development, and manufacture of major components and subsystems. To permit the GE system study to take advantage of the capabilities of industry and to ensure that the GE conceptual design incorporated the best ideas and designs available, a series of briefings were held during the first half of 1963 for a number of companies able to contribute to the program. Agreements were negotiated with some of these companies under which General Electric provided information and technical data on the overall Voyager system, and the individual companies then developed their own ideas for the design of the component or subsystem of interest to them. All of this associated work was on a completely unfunded, nonexclusive basis.

Progress meetings were held during the course of the studies to review the subsystem design and to update the system data on which the designs were based. Each of the separate subsystem studies submitted is based on a system design which is close to the final Voyager System recommended by GE, although no attempt was made to accommodate all of the system revisions as they were made.

The Missile and Space Division of General Electric also conducted its own studies in all subsystem areas and was not dependent on the work of any other company for the successful completion of its Voyager study. However, the work done by the associated companies has proved to be of much value and in some instances is reflected in the GE final report, appropriately attributed to the proper company.

The work reported shows a very strong interest by industry in the Voyager Program and is tangible evidence of the detailed design available to substantiate the Voyager system recommendations.

The following companies have submitted reports, as shown, on their nonexclusive unfunded studies to General Electric, and five copies of each plus a reproducible has been submitted to NASA as a part of the General Electric Co. final report on its Voyager Study:

- Aerojet-General Corporation, "Voyager Orbiter Propulsion," "Voyager Propulsion Analysis (Lander Portion)"
- Barnes Engineering Company, "Approach Guidance Subsystem"
- Bell Aerosystems Company, "Voyager Orbiter Propulsion"
- Conduction Corporation, "Voyager Radar Subsystem Experiments"
- Electromechanical Research, Inc., "Digital Television Subsystem for Project Voyager"
- General Electric Company, Light Military Electronics Department, "Voyager Radargrammetry"
- General Electric Company, Light Military Electronics Department, "Voyager Guidance and Control"
- General Precision Incorporated, "Study Report of Approach Guidance System for the Voyager Spacecraft"
- Hazeltine Corporation, "Engineering Study Report on TV Camera Subsystem for Mars-Venus Voyager Missions"
- North American Aviation Inc., Autonetics Division, "Autonetics Studies of the Voyager Mission"
- North American Aviation Inc., Rocketdyne Division, "Voyager Orbiter Propulsion"

- Radio Corporation of America, "Report on: S-Band and VHF Design Considerations for Project Voyager"
- Rocket Research Corporation, "Voyager Subliming Solid Control Rocket"
- Texas Instruments Incorporated, "Proposal for Voyager Telecommunications and Data Handling Equipment"
- Thiokol Chemical Corporation, Elkton Division, "Proposal Study for Voyager Spacecraft Orbital Adjustment and Lander Insertion Motors"
- Thiokol Chemical Corporation, Reaction Motors Division, "Voyager Orbiter and Lander Propulsion"

SECTION 1. COMMUNICATIONS SUBSYSTEM

1.1 SUMMARY OF RESULTS

1.1.1 GENERAL

The recommended Communications Subsystems for the Mars 1969, 1971, 1973, and 1975 and the Venus 1970 and 1972 Voyager missions are described in the following sections.

Although differences exist between subsystems recommended for the various missions, the goal has been to utilize the same techniques and components where possible in all subsystems with changes only in subsystem parameter values and component interconnections. These changes can be made in most cases with little or no equipment re-development. Most of the components are either readily available or are in the advanced stages of development.

Only two major components are recommended that are in the early stages of development - an electrostatically focused klystron and a thermoplastic recorder. Although they are described and discussed in detail in subsequent sections, it should be noted here that the versatility of both of these components throughout the various missions makes them extremely attractive. A single development program will suffice for all the mission requirements in each case.

The high-gain klystron can be driven with a very low-power (and therefore highly reliable) transmitter. Its saturated power output can be changed across a wide range with little loss in efficiency so that a single tube can be developed for all the power levels anticipated in the Voyager missions.

Thermoplastic recorders appear to offer the ultimate in versatility in high-volume storage devices. Not only can a single recorder be read-in and read-out at bit rates covering an extremely broad range and synchronized with the spacecraft clock, but it can also provide random access as required.

Subsystem versatility is also enhanced by the exclusive utilization of digital techniques. Although the relative performance of analog and digital techniques was debatable in the case of wideband TV data (as discussed in Section 1.6.1) the incorporation of the narrow-band digital data into a hybrid system was found to be cumbersome and relatively inflexible as compared to a completely digital subsystem.

A single modulation and detection technique is utilized in all transmission links. Both data and bit synchronization signals are placed on a single square-wave subcarrier. The two-level composite signal phase-modulates the transmitted carrier between two values, ± 60 degrees being utilized in most links.

Because of the many similarities among subsystems, components, and techniques recommended for the missions, each of the subsequent sections covers all the missions, so that by indicating the similarities and differences redundancy of description can be minimized.

A. Description of Mission Characteristics

The parameters and requirements which characterize the role of each vehicle with respect to communication for each mission are shown in Table 1.1.1-1. Although two Landers are to be utilized for each Mars mission, their communication subsystems are identical except for a frequency separation.

TABLE 1.1.1-1. MISSION CHARACTERISTICS AFFECTING COMMUNICATIONS

Characteristic	Mars 1969 and 1971			Mars 1973			Mars 1975			Venus 1970			Venus 1972	
	Orbiter	Landers (2)	Landers (2)	Orbiter	Landers (2)	Bus	Landers	Orbiter	Lander	Orbiter	Lander	Orbiter	Landers (2)	
Orbital Altitude (n. mi.)	1000 x 19000	—	—	200 x 9000	—	Flyby	—	1000 x 4300	—	1000 x 7300	—	—	—	
Primary Data Source	TV and Landers	TV and Microphone	TV	Guidance TV	Mobile TV	Guidance TV and Lander	TV and Radar (Altimeter & Doppler)	Radar, TV, and Lander	TV and Radar (Altimeter & Doppler)	TV and Lander	TV and Radar (Altimeter & Doppler)	TV and Lander	TV	
Prime Data Link	Direct to Earth	Relay Via Orbiter	Direct to Earth	Direct to Earth	Direct to Earth	Direct to Earth	Direct to Earth	Direct to Earth	Relay Via Orbiter	Direct to Earth	Relay Via Orbiter	Direct to Earth	Relay Via Orbiter	
Alternate Data Link	None	Direct to Earth	Relay Via Orbiter During Descent Phase	None	Relay Via Orbiter During Descent Phase	None	Relay Via Orbiter During Descent Phase	None	None	None	None	None	None	
Prime Command Link	Direct from Earth	Relay Via Orbiter	Direct from Earth	Direct from Earth	Direct from Earth	Direct from Earth	Direct from Earth	Direct from Earth	None	Direct from Earth	None	Direct from Earth	Relay Via Orbiter	
Alternate Command Link	None	Direct from Earth	None	None	None	None	None	None	None	None	None	None	None	
Designed Lifetime after Encounter	90 days	6 months	6 months	10 days	6 months	2 days	6 months	90 days	10-30 minutes	90 days	10-30 minutes	90 days	6 hours	
Maximum Encounter Range from Earth	$\approx 100 \times 10^6$ n. mi.			$\approx 130 \times 10^6$ n. mi.		$\approx 190 \times 10^6$ n. mi.		$\approx 38 \times 10^6$ n. mi.		$\approx 75 \times 10^6$ n. mi.				
Sterilization Requirement	No	Yes	Yes	Yes	Yes	No	Yes	No	Yes	No	Yes	No	Yes	
Maximum Required Data Storage Volume (bits)	10^9	10^8	10^9	10^9	10^9	10^9	10^9	10^9	10^5	10^9	10^5	10^9	10^9	

B. Subsystem Functional Requirements

Table 1. 1. 1-2 summarizes the functional requirements of the Communications Subsystems of all vehicles.

C. Communication Links and Their Utilization

Figures 1. 1. 1-1, 1. 1. 1-2, 1. 1. 1-3 and 1. 1. 1-4 illustrate the communication links recommended for each mission. Tables 1. 1. 1-3, 1. 1. 1-4, 1. 1. 1-5 and 1. 1. 1-6 indicate the utilization of each link as a function of mission phase. Also included in the tables are descriptions of the type of data being collected and transmitted during each phase and the source of commands.

The parameters of each of the links are summarized in Tables 1. 1. 1-7 through 1. 1. 1-10.

The numbering system used to designate the various communication links is identical for all missions. Links (1) through (6) are utilized for telemetry and links (7) through (11) are utilized for command. Specifically, each link may be described as follows:

- Link (1): Prime data link from Orbiter to earth utilizing Orbiter high-gain antenna.
- Link (2): Secondary data link from Orbiter to earth utilizing Orbiter omni antenna. To be used during early transit, during maneuvers, and as back-up to link (1).
- Link (3): Data link from Lander to earth utilizing Lander high-gain antenna. To be used as secondary data link if link (5) exists or as prime data link to earth if (5) does not exist.
- Link (4): Data link from Lander to earth utilizing Lander omni antenna. To be used to assist in initial acquisition of link (3) and as a back-up to link (3).
- Link (5): Data link from Lander to Orbiter to be used after Lander is on planet surface.
- Link (6): Data link from Lander to Orbiter to be used after Lander separation from Orbiter until Lander impact.
- Link (7): Prime command link from earth to Orbiter utilizing Orbiter high-gain antenna.
- Link (8): Secondary command link from earth to Orbiter utilizing Orbiter omni antenna. To be used during early transit, during maneuvers, and as a back-up to link (7).
- Link (9): Command link from earth to Lander utilizing Lander high-gain antenna. To be used as secondary command link if link (11) exists or as prime command link if (11) does not exist.
- Link (10): Command link from earth to Lander utilizing Lander omni antenna. To be used for initial acquisition of link (3) and as a back-up to link (3).
- Link (11): Prime command link from Orbiter to Lander to be used after Lander is on the surface.

TABLE 1.1.1-2. SUMMARY OF COMMUNICATIONS SUBSYSTEM REQUIREMENTS

Requirement	Mars 1969 & 1971		Mars 1973 & 1975		Venus 1970		Venus 1972	
	Orbiter	Lander	Orbiter	Lander	Orbiter	Lander	Orbiter	Lander
a. Receive command data from Earth	X	X	X	X	X	-	X	-
b. Relay selected command data to Lander(s)	X	-	-	-	-	-	X	-
c. Receive command data from Orbiter	-	X	-	-	-	-	-	X
d. Provide command data storage	X	X	X	X	X	X	X	X
e. Issue commands to all vehicle subsystems	X	X	X	X	X	X	X	X
f. Collect data from all vehicle science and eng. sensors	X	X	X	X	X	X	X	X
g. Receive data from Lander (s)	X	-	X	-	X	-	X	-
h. Provide storage for all collected data	X	X	X	X	X	X	X	X
i. Transmit data to Earth	X	X	X	X	X	-	X	-
j. Transmit data to Orbiter	-	X	-	X	-	X	-	X
k. Provide doppler and angular tracking of vehicle from Earth at all ranges	X	-	X	-	X	-	X	-
l. Provide ranging from Earth during early transit	X	-	X	-	X	-	X	-
m. Provide computer functions as required	X	X	X	X	X	-	X	X

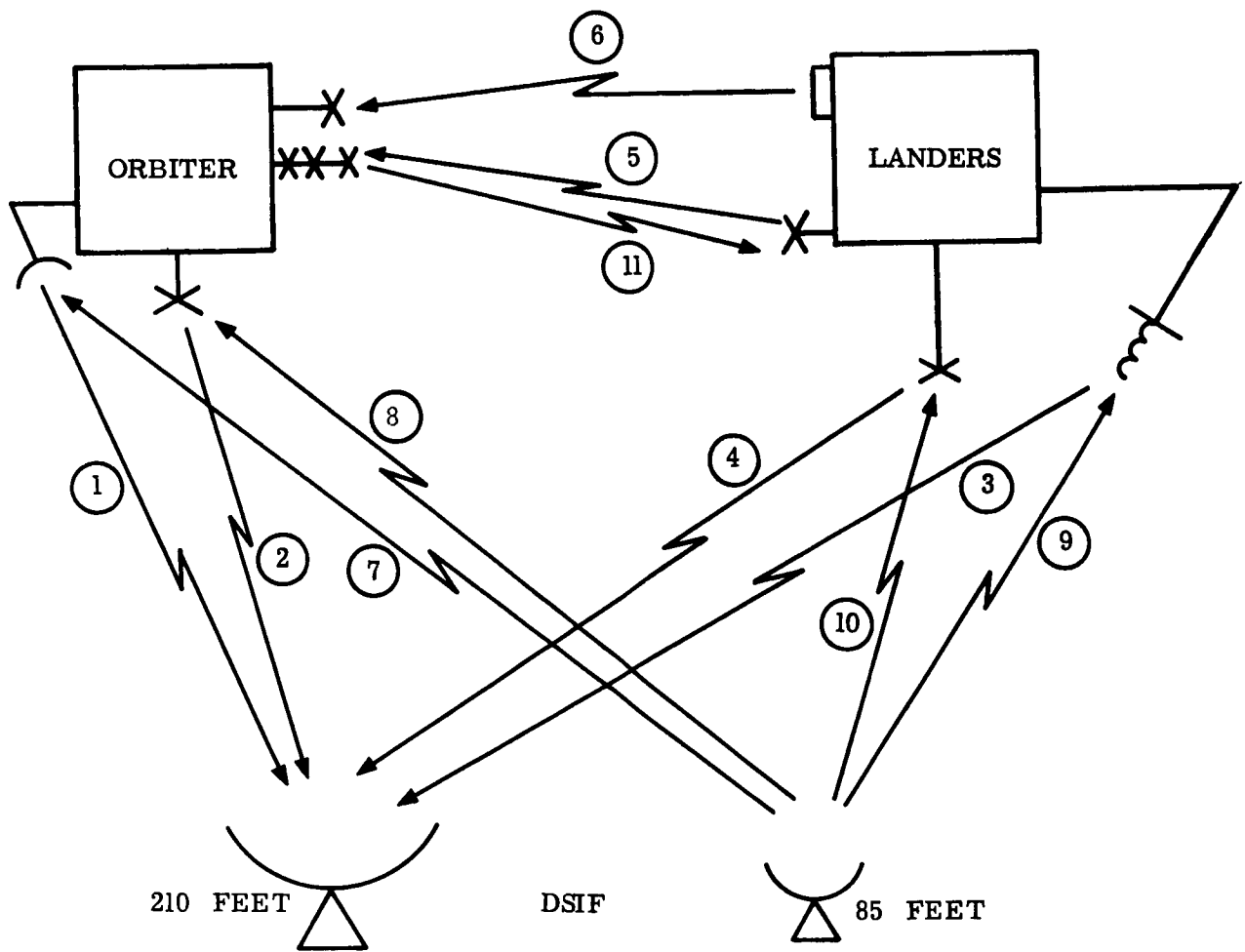


Figure 1.1.1-1 Mars 1969 and 1971 Communication Links

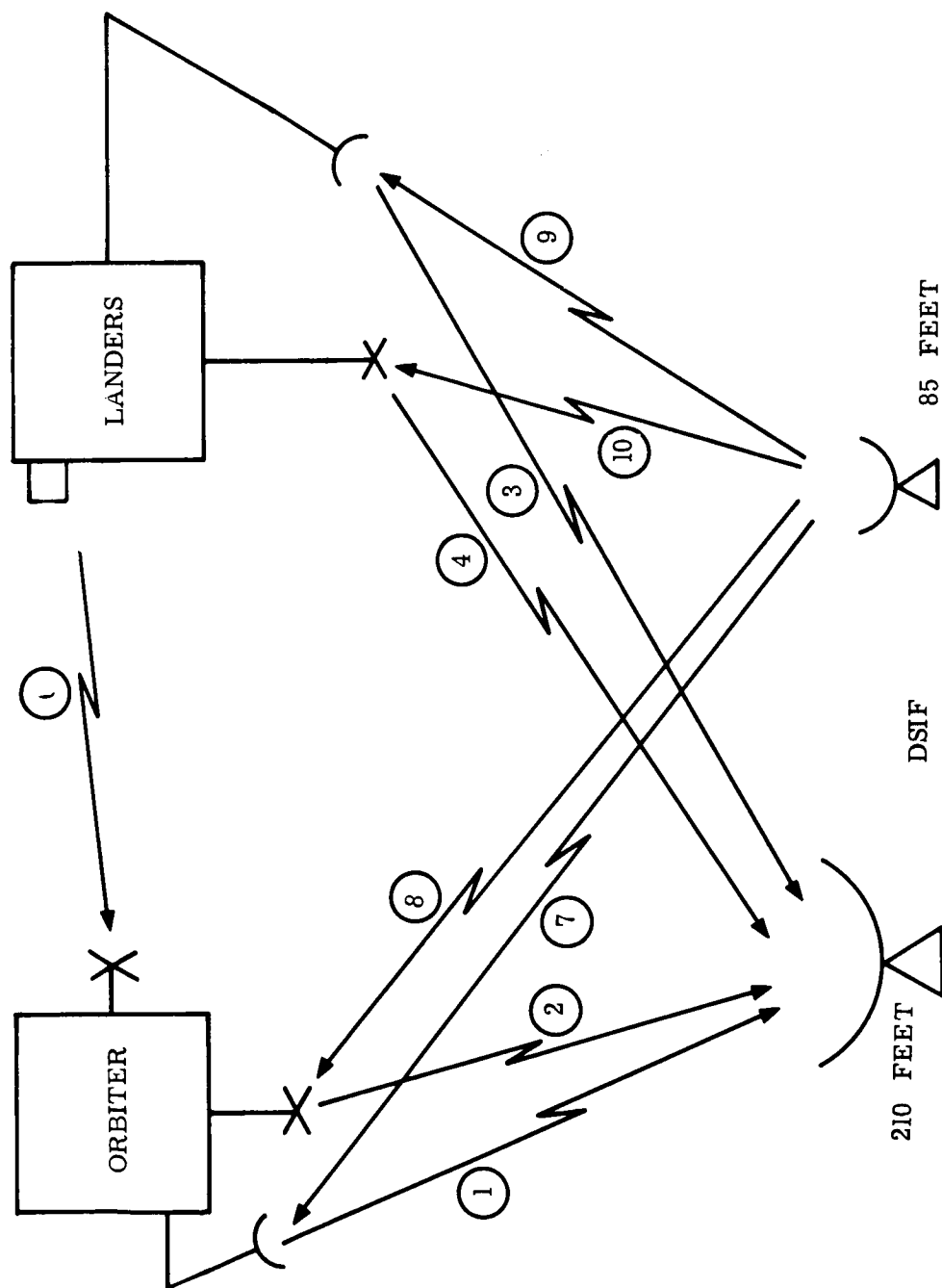


Figure 1.1.1-2 Mars 1973 and 1975 Communication Links

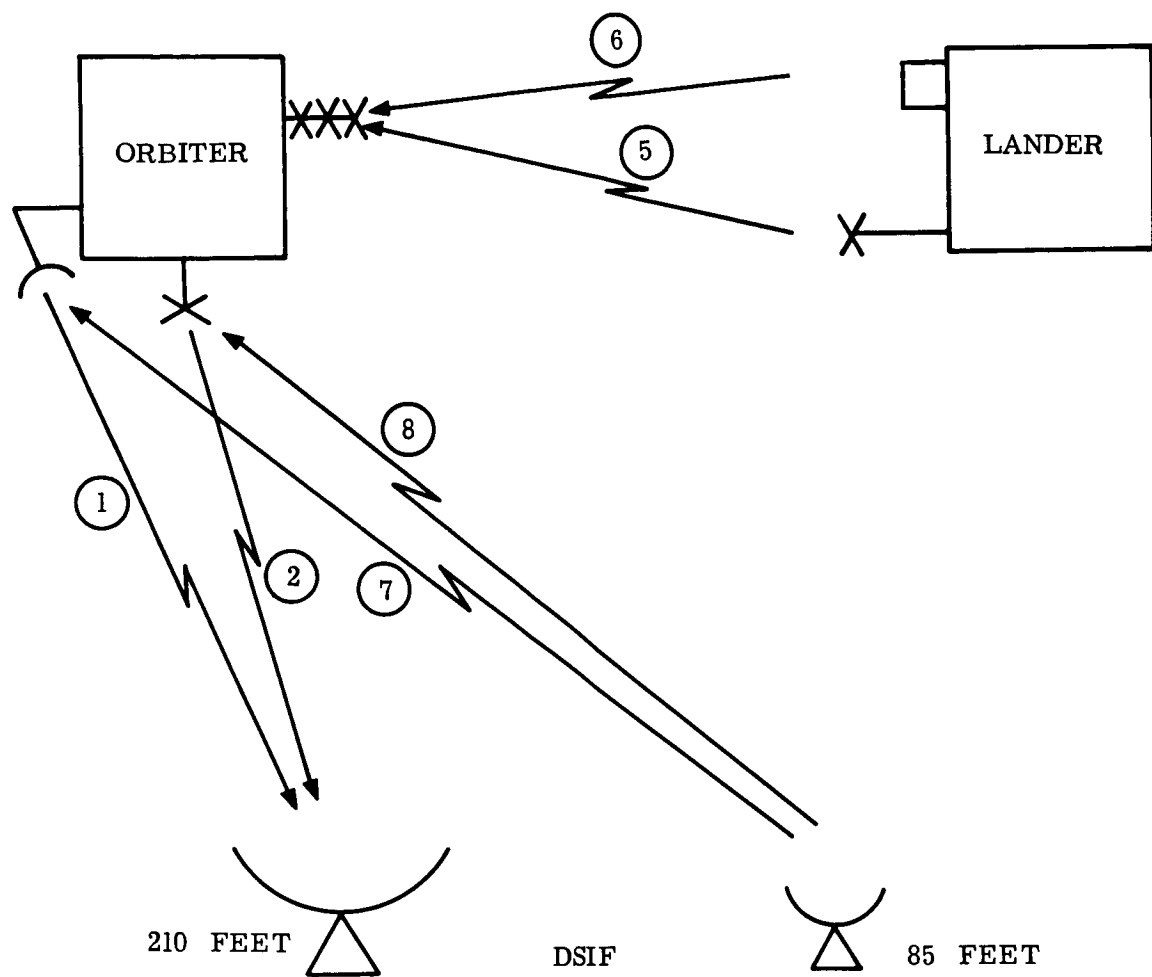


Figure 1. 1. 1-3 Venus 1970 Communication Links

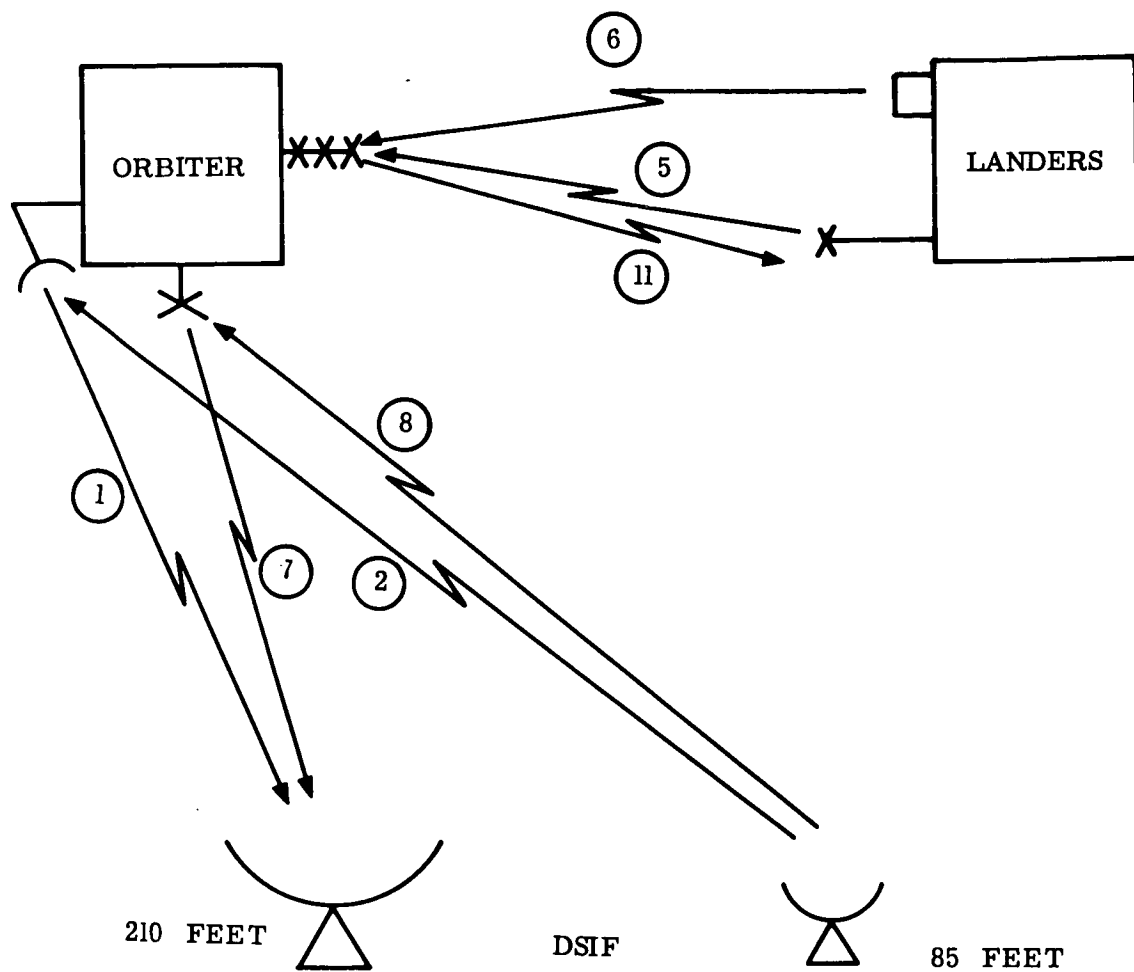


Figure 1.1.1-4 Venus 1972 Communication Links

TABLE 1.1.1-3. COMMUNICATION MODE SEQUENCE - MARS 1969 AND 1971

Phase	Time after Launch (days)	Range to Earth (NM)	Range between Orbiter and Landers (NM)	Links being Utilized	Type of Data being Collected and Transmitted		Command Source	
					Orbiter	Landers	Orbiter	Landers
1. Pre-launch	0-	0	0	Umbilical	Checkout	Checkout	Umbilical	Umbilical
2. Launch	0+	0+	0	Booster or through shroud	Selected Eng.	Selected Eng.	Orbiter Storage	Orbiter Storage
3. Parking Orbit and Entry Into Transit	0+ to one day	$< 10^6$	0	(2) (8)	Selected Eng.	Selected Eng.	Orbiter Storage or Earth	Orbiter Storage
4. Early Transit		$\approx 10^6$ to 5×10^7						
a. Normal			0	(2) (8)	Sci. and Eng.	Selected Eng.	Orbiter Storage or Earth	Orbiter Storage
b. Mid-course Corrections			0	(2) (8)	Selected Eng.	—	Orbiter Storage	—
c. Emergency			0	(2) (8)	Selected Eng.	—	Orbiter Storage or Earth	—
d. Prime Link Checkout			0	(1) (7)	Selected Eng.	—	Orbiter Storage or Earth	—
5. Late Transit	≈ 185 to 270	$\approx 5 \times 10^7$ to 10^8						
a. Normal			0	(1) (7)	Sci. and Eng.	Selected Eng.	Orbiter Storage or Earth	Orbiter Storage
b. Final Correction Measurements			0	(1) (7)	TV	—	Orbiter Storage or Earth	—
c. Final Correction			0	(2) (8)	Selected Eng.	—	Orbiter Storage	—
d. Lander Separation			0+	(2) (3)	Selected Eng.	Store Selected Eng. Transmit Stored data and Selected Eng.	Orbiter Storage	Lander Storage
e. Lander Cruise			0+ to 3500	(1) (7) (6)	Sci., Eng. and Lander		Orbiter Storage or Earth	Lander Storage

TABLE 1.1.1-3. COMMUNICATION MODE SEQUENCE - MARS 1969 AND 1971 (Cont)

Phase	Time after Launch (days)	Range to Earth (NM)	Range between Orbiter and Landers (NM)	Links being Utilized	Type of Data being Collected and Transmitted		Command Source	
					Orbiter	Landers	Orbiter	Landers
f. Lander Entry			3500 max.	① ⑦	Sci. and Eng.	Store Entry Data	Orbiter Storage or Earth	Lander Storage
g. Lander Descent			3500 max.	① ⑦ ⑥	Sci., Eng. and Lander	Collect atmospheric data, transmit entry and atmospheric	"	"
h. Lander Surface			3500 max.	① ⑦ ⑤	"	Transmit stored entry, atmospheric, landing and selected engineering	"	"
i. Emergency (before separation)			0	② ⑧	Selected Eng.	—	"	—
j. Emergency (after separation)			3500 max.	② ⑧ and ⑤ or 6	Store Lander transmit selected eng.	Selected Eng.	"	"
6. Orbit Insertion (Orbiter)	≈270	≈10 ⁸	3500 max.	② ⑧ and ⑤ or 6	Selected Eng. Store Lander Data	Descent or Surface Phase	Orbiter Storage	"
7. Orbit (Orbiter)								
a. Normal	≈270 to 360	≈10 ⁸ to 2x10 ⁸	1000 to 19000	① ⑦ ⑤ ⑩	TV, Sci., Eng. and Lander	TV, Sci., and Eng.	Orbiter Storage, Earth or Computer	Lander Storage or Orbiter
b. Emergency			1000 to 19000	② ③ ④ ⑨	Selected Eng.	"	Orbiter Storage or Earth	Lander Storage or Earth
8. Surface (Lander)								
a. Normal	≈270 to 360	≈10 ⁸ to 2x10 ⁸	1000 to 19000	① ⑦ ⑤ ⑩	TV, Sci., Eng., and Lander	TV, Sci., and Eng.	Orbiter Storage, Earth or Computer	Lander Storage or Orbiter
b. Lander-Earth Link Checkout	≈270+	10 ⁸ +	1000 to 19000	① ⑦ ③ ④ ⑨ ⑩	TV, Sci., and Eng.	Science and Eng.	"	Lander Storage Orbiter or Earth
c. Post Orbiter Life Time	≈360 to 450	2x10 ⁸ to 2.16x10 ⁸	—	③ ⑨	—	TV, Sci., and Eng.	—	Lander Storage or Earth
d. Emergency			1000 to 19000	④ ⑩	—	Selected Eng.	—	"

TABLE 1.1.1-4. COMMUNICATIONS MODE SEQUENCE - MARS 1973 AND 1975

Phase	Time after Launch (Days)	Range to Earth (NM)	Range between Orbiter and Landers (NM)	Links being Utilized	Type of Data being Collected and Transmitted		Command Source	
					Orbiter	Landers	Orbiter	Landers
1. Pre-launch	0-	0	0	Umbilical	Checkout	Checkout	Umbilical	Umbilical
2. Launch	0+	0+	0	Booster or through shroud	Selected Eng.	Selected Eng.	Orbiter Storage	Orbiter Storage
3. Parking orbit and Entry into Transit			0	(2) (3)	Selected Eng.	Selected Eng.	Orbiter Storage or Earth	Orbiter Storage
4. Early Transit								
a. Normal			0	(2) (3)	Sci. and Eng.	Selected Eng.	Orbiter Storage or Earth	Orbiter Storage
b. Midcourse corrections			0	(2) (8)	Selected Eng.		Orbiter Storage	
c. Emergency			0	(2) (3)	Selected Eng.		Orbiter Storage or Earth	
d. Prime Link Checkout			0	(1) (7)	Selected Eng.		Orbiter Storage or Earth	
5. Late Transit			0	(1) (7)	Sci. and Eng.	Selected Eng.	Orbiter Storage or Earth	Orbiter Storage
a. Normal			0	(1) (7)	TV		Orbiter Storage or Earth	
b. Final Correction Measurements	~ 205	0.96×10^8 to 1.32×10^8	0	(2) (8)	Selected Eng.		Orbiter Storage	
c. Final Correction			0+	(2) (8)	Selected Eng.	Store Selected Eng.	Orbiter Storage	Lander Storage
d. Lander separation			0+ to 3500	(1) (7) (6)	Sci., Eng. and Lander	Transmit stored data and Selected Eng.	Orbiter Storage or Earth	Lander Storage
e. Lander Cruise					Sci. and Eng.	Store Entry Data	Orbiter Storage or Earth	Lander Storage
f. Lander Entry			~ 3500	(1) (7)			Orbiter Storage or Earth	Lander Storage
g. Lander Descent				(1) (7) (6)	Sci., Eng. and Lander	Collect Atmospheric Data, Transmit Entry and Atmospheric	Orbiter Storage or Earth	Lander Storage
h. Lander surface				(1) (7) (4) (10)	Sci. and Eng.	Transmit stored Entry, Atmospheric, Landing, and Selected Eng.	Orbiter Storage or Earth	Lander Storage or Earth
i. Emergency (before separation)				(2) (8)	Selected Eng.		Orbiter Storage or Earth	
j. Emergency (after separation)				(2) (3) and (6)	Selec. Eng. transmitted; Store Lander Data	Selected Eng.	Orbiter Storage or Earth	Lander Storage

TABLE 1.1.1-4. COMMUNICATIONS MODE SEQUENCE - MARS 1973 AND 1975 (Continued)

Phase	Time after Launch (Days)	Range to Earth (NM)	Range between Orbiter and Landers (NM)	Links being Utilized	Type of Data being Collected and Transmitted		Command Source	
					Orbiter	Landers	Orbiter	Landers
6. Orbit Insertion (Orbiter-1973)	205-220	0.96 to 10^8 to 1.32×10^8		② ⑧ and ⑥	Selected Eng.	Descent or surface phase	Orbiter Storage	Lander Storage
7. Orbit (Orbiter-1973)				① ⑦	Sci. and Eng.		Orbiter Storage, Earth or Computer	
a. Normal				② ③	Selected Eng.		Orbiter Storage or Earth	
b. Emergency				① ⑦	Sci. and Eng.		Storage or Earth	
8. Encounter and Post-Encounter (BUS - 1975)						Selected Eng.		Lander Storage or Earth
a. Antenna Pointing Procedure				③ ⑨ ④ ⑩		Previously stored data plus TV, Sci., and Eng.		Lander Storage or Earth
b. Normal				③ ⑨		Selected Eng.		Lander Storage or Earth
c. Emergency (Loss of HI-Gain)				④ ⑩				Lander Storage or Earth

TABLE 1.1.1-5. COMMUNICATION MODE SEQUENCE - VENUS 1970

Phase	Time after Launch (Days)	Range to Earth (NM)	Range between Orbiter and Lander (NM)	Links being Utilized	Type of Data being collected and transmitted		Command Source	
					Orbiter	Lander	Orbiter	Lander
1. Pre-launch	0-	0	0	Umbilicals	Checkout	Checkout	Umbilical	Umbilical
2. Launch	0+	0+	0	Booster or through shroud	Selected Eng.	Selected Eng.	Orbiter Storage	Orbiter Storage
3. Parking Orbit and Entry into Transit			0	(2) (3)	Selected Eng.	Selected Eng.	Orbiter Storage or Earth	Orbiter Storage
4. Early Transit			0	(2) (8)	Sci. and Eng.	Selected Eng.	Orbiter Storage or Earth	Orbiter Storage
a. Normal			0	(2) (8)	Selected Eng.	_____	Orbiter Storage	_____
b. Midcourse corrections			0	(1) (7)	Selected Eng.	_____	Orbiter Storage or Earth	_____
c. Prime link checkout			0	(2) (3)	Selected Eng.	_____	Orbiter Storage or Earth	_____
d. Emergency			0	(1) (7)	Sci. and Eng.	Selected Eng.	Orbiter Storage or Earth	Orbiter Storage
5. Late Transit			0	(1) (7)	TV	_____	Orbiter Storage or Earth	_____
a. Normal			0	(2) (8)	Selected Eng.	_____	Orbiter Storage	_____
b. Final correction Measurement			0	(2) (3)	Selected Eng.	Store Selected Eng.	Orbiter Storage	Lander Storage
c. Final correction			0+	(1) (7) (6)	Sci., Eng., and Lander	Transmit stored data and Selected Eng.	Orbiter Storage or Earth	Lander Storage
d. Lander separation			0+ to 11,000	(1) (7) (6)	Sci. and Eng.	Selected Eng. stored	Orbiter Storage or Earth	Lander Storage
e. Lander cruise			≈ 11,000	(1) (7) (6)	Sci., Eng., and Lander	Stored data plus atmospheric and Selected Eng.	Orbiter Storage or Earth	Lander Storage
f. Lander Entry				(1) (7) (5)	Selected Eng.	TV, Sci., and Eng.	Orbiter Storage or Earth	Lander Storage
g. Lander Descent				(2) (8)	Selected Eng. transmitted; Lander data stored	Selected Eng.	Orbiter Storage or Earth	Lander Storage
h. Lander surface				(2) (8) (5)	Selected Eng.	Descent or surface phase	Orbiter Storage	Lander Storage
i. Emergency (before separation)				(1) (7)	Lander Data, Radar, TV, Sci., and Eng.	_____	Orbiter Storage or Earth	_____
j. Emergency (after separation)				(2) (3)	Selected Eng.	_____	Orbiter Storage or Earth	_____
6. Orbit Insertion	121-98	.32 x 10 ⁸ to .38 x 10 ⁸						
7. Orbit (Lander Dead)								
a. Normal				(1) (7)			Orbiter Storage or Earth	_____
b. Emergency				(2) (3)			Orbiter Storage or Earth	_____

TABLE 1.1.1-6. COMMUNICATION MODE SEQUENCE - VENUS 1972

Phase	Time after Launch (Days)	Range to Earth (NM)	Range between Orbiter and Lander (NM)	Links being Utilized	Type of Data being collected and Transmitted		Command Source	
					Orbiter	Lander	Orbiter	Lander
1. Prelaunch	0-	0	0	Umbilicals	Checkout	Checkout	Umbilical	Umbilical
2. Launch	0+	0+	0	Booster or through shroud	Selected Eng.	Selected Eng.	Orbiter Storage	Orbiter Storage
3. Parking Orbit and Entry into Transit			0	(2) (8)	Selected Eng.	Selected Eng.	Orbiter Storage or Earth	Orbiter Storage
4. Early Transit								
a. Normal			0	(2) (8)	Sci. and Eng.	Selected Eng.	Orbiter Storage or Earth	Orbiter Storage
b. Midcourse corrections			0	(2) (8)	Selected Eng.	_____	Orbiter Storage	_____
c. Prime Link Checkout			0	(1) (7)	Selected Eng.	_____	Orbiter Storage or Earth	_____
d. Emergency			0	(2) (8)	Selected Eng.	_____	Orbiter Storage or Earth	_____
5. Late Transit								
a. Normal			0	(1) (7)	Sci. and Eng.	Selected Eng.	Orbiter Storage or Earth	Orbiter Storage
b. Final Correction Measurement			0	(1) (7)	TV	_____	Orbiter Storage or Earth	_____
c. Final Correction			0	(2) (8)	Selected Eng.	_____	Orbiter Storage	_____
d. Lander Separation			0+	(2) (8)	Selected Eng.	Store Selected Eng.	Orbiter Storage	Lander Storage
e. Lander Cruise			0+ to 11,000	(1) (7) (6)	Sci., Eng. and Lander	Selected Eng.	Orbiter Storage or Earth	Lander Storage
f. Lander Entry			≈ 11,000	(1) (7)	Sci. and Eng.	Store Selected Eng.	Orbiter Storage or Earth	Lander Storage
g. Lander Descent			≈ 11,000	(1) (7) (6)	Sci., Eng. and Lander	Stored data plus atmospheric and selected Eng.	Orbiter Storage or Earth	Lander Storage
h. Lander Surface			≈ 11,000	(1) (7) (5) (11)	Sci., Eng., and Lander	Stored data plus TV Sci. and Eng.	Orbiter Storage or Earth	Lander Storage or Orbiter
i. Emergency (before separation)				(2) (8)	Selected Eng.	_____	Orbiter Storage or Earth	_____
j. Emergency (after separation)				(2) (8) and (5) or (6)	Store lander, transmit Selected Eng.	Selected Eng.	Orbiter Storage or Earth	Lander Storage

TABLE 1.1.1-6. COMMUNICATION MODE SEQUENCE - VENUS 1972 (Continued)

Phase	Time after Launch (Days)	Range to Earth (NM)	Range between Orbiter and Lander (NM)	Links being Utilized	Type of Data being Collected and Transmitted		Command Source	
					Orbiter	Lander	Orbiter	Lander
6. Orbit Insertion	190-163	0.69×10^8 to 0.76×10^8		(2) (8)	Store Lander; transmit Selected Eng.	Descent or surface phase	Orbiter Storage	Lander Storage
7. Initial Orbits (Lander alive)				(1) (7) (5) (11)	TV, Sci., Eng. Lander data and commands	Stored Data plus TV, Sci., and Eng.	Orbiter Storage, Earth or Computer	Lander Storage or Orbiter
b. Emergency				(2) (8) (5) (11)	Transmit Selected Eng. and Lander commands, Store Lander Data	Stored Data plus TV, Sci., and Eng.	Orbiter Storage or Earth	Lander Storage or Orbiter
8. Orbit (Lander Dead)				(1) (7)	TV Sci. and Eng. transmit stored lander until all data is received accurately		Orbiter Storage Earth or Computer	
a. Normal								
b. Emergency				(2) (8)	Selected Eng.		Orbiter Storage or Earth	

TABLE 1.1.1-7. SUMMARY OF COMMUNICATION LINK PARAMETERS, MARS 1969 AND 1971

Link	1	2	3	4	5	6	7	8	9	10	11
Purpose	O-E TLM	O-E TLM	L-E TLM	L-E TLM	L-O TLM	L-O TLM	E-O Command	E-O Command	E-L Command	E-L Command	O-L Command
Frequency (mc)	2295	2295	2295	2295	94 96	94 96	2115	2115	2115	2115	105
Power Transmitted (watts)	50	50	70	70	25	25	10,000	10,000 (100,000 backup)	10,000	10,000 (100,000 backup)	5
Transmitting Antenna	10-ft. Dish	Turnstile	(21-db Helix)** (26.7-db Helix Array)***		Turnstile	Transmission line	85-ft. Dish	85-ft. Dish	85-ft. Dish	85-ft. Dish	10-db Yagi
Receiving Antenna	210-ft. Dish	210-ft. Dish	210-ft. Dish	210-ft. Dish	10-db Yagi	Turnstile	10-ft. Dish	Turnstile	(20.3-db Helix)** (26-db Helix Array)***	Turnstile	Turnstile
Receiver Noise Figure	--	--	--	--	4-db	4-db	10-db	5-db	10-db	10-db	4-db
Receiving System Noise Temp. (°K)	35	35	35	35	--	--	--	--	--	--	--
Probability of Bit Error	1.4×10^{-3}	1.4×10^{-3}	1.4×10^{-3}	1.4×10^{-3}	10^{-3}	10^{-3}	10^{-5}	10^{-5}	10^{-5}	10^{-5}	10^{-5}
Transmitting Ant. Pointing Error (Degrees)	1.0	--	3.0	--	--	--	Neg.	Neg.	Neg.	Neg.	Function of Orbital Altitude
Receiving Ant. Pointing Error (Degrees)	Neg.	Neg.	Neg.	Neg.	Function of Orbital Altitude	--	1.0	--	3.0	--	--

*O - Orbiter
L - Lander
E - Earth

**Mars 1969 only

***Mars 1971 only

TABLE 1.1.1-8. SUMMARY OF COMMUNICATION LINK PARAMETERS, MARS 1973 AND 1975

Link	1	2	3	4	5	6	7	8	9	10	11
Purpose	O-E TLM	O-E TLM	L-E TLM	L-E TLM	None	L-O TLM	E-O Command	E-O Command	E-L Command	E-L Command	None
Frequency (mc)	2295	2295	2295	2295	--	94 96	2115	2115	2115	2115	--
Power Transmitted (watts)	35	35	70	70	--	25	10,000	10,000 (100,000 backup)	10,000	10,000 (100,000 backup)	--
Transmitting Antenna	10-ft. Dish	Turnstile	Helix Array (26.75 db)	Turnstile	--	Transmission line	85-ft. Dish	85-ft. Dish	Helix Array (26 db)	85-ft. Dish	--
Receiving Antenna	210-ft. Dish	210-ft. Dish	210-ft. Dish	210-ft. Dish	--	Turnstile	10-ft. Dish	Turnstile	Turnstile	Turnstile	--
Receiver Noise Figure	--	--	--	--	--	4-db	10-db	10-db 5-db(1975)	10-db	10-db	--
Receiving System Noise Temp. (⁰ K)	35	35	35	35	--	--	--	--	--	--	--
Probability of Bit Error	1.4×10^{-3}	1.4×10^{-3}	1.4×10^{-3}	1.4×10^{-3}	--	10^{-3}	10^{-5}	10^{-5}	10^{-5}	10^{-5}	--
Transmitting Ant. Pointing Error (Degrees)	1.0	--	3.0	--	--	--	Neg.	Neg.	Neg.	Neg.	--
Receiving Ant. Pointing Error (Degrees)	Neg.	Neg.	Neg.	Neg.	--	--	1.0	--	3.0	--	--

TABLE 1.1.1-9. SUMMARY OF COMMUNICATION LINK PARAMETERS, VENUS 1970

Link	1	2	3	4	5	6	7	8	9	10	11
Purpose	O-E TLM	O-E TLM	None	None	L-O TLM	L-O TLM	E-O Command	E-O Command	None	None	None
Transmission Frequency (mc)	2295	2295	--	--	95	95	2115	2115	--	--	--
Power Transmitted (watts)	50	50	--	--	25	25	10,000	10,000 (100,000 back-up)	--	--	--
Transmitting Antenna	10-ft. Dish	Turnstile	--	--	Whip	Transmission line	85-ft. Dish	85-ft. Dish	--	--	--
Receiving Antenna	210-ft. Dish	210-ft. Dish	--	--	10-db Yagi	10-db Yagi	10-ft. Dish	Turnstile	--	--	--
Receiver Noise Figure	--	--	--	--	4-db	4-db	10-db	5-db	--	--	--
Receiving System Noise Temperature ($^{\circ}\text{K}$)	35	35	--	--	--	--	--	--	--	--	--
Probability of Bit Error	1.4×10^{-3}	1.4×10^{-3}	--	--	10^{-3}	10^{-3}	10^{-5}	10^{-5}	--	--	--
Transmitting Antenna Pointing Error (Degrees)	1.0	--	--	--	--	--	Neg.	Neg.	--	--	--
Receiving Antenna Pointing Error (Degrees)	Neg.	Neg.	--	--	Neg.	--	1.0	--	--	--	--

TABLE 1.1.1-10. SUMMARY OF COMMUNICATION LINK PARAMETERS, VENUS 1972

TABLE 1.1.1-10. VENUS 1972

Link	1	2	3	4	5	6	7	8	9	10	11
Purpose	O-E TLM	O-E TLM	None	None	L-O TLM	L-O TLM	E-O Command	E-O Command	None	None	O-L Command
Transmission Frequency (mc)	2295	2295	--	--	95	95	2115	2115	--	--	105
Power Transmitted (watts)	35	35	--	--	25	25	10,000	10,000 (100,000 back-up)	--	--	5
Transmitting Antenna	10-ft. Dish	Turnstile	--	--	Turnstile	Transmission line	85-ft. Dish	85-ft. Dish	--	--	10-db Yagi
Receiving Antenna	210-ft. Dish	210-ft. Dish	--	--	10-db Yagi	10-db Yagi	10-ft. Dish	Turnstile	--	--	Turnstile
Receiver Noise Figure	--	--	--	--	4-db	4-db	10-db	5-db	--	--	4-db
Receiving System Noise Temperature ($^{\circ}\text{K}$)	35	35	--	--	--	--	--	--	--	--	--
Probability of Bit Error	1.4×10^{-3}	1.4×10^{-3}	--	--	10^{-3}	10^{-3}	10^{-5}	10^{-5}	--	--	10^{-5}
Transmitting Antenna Pointing Error (Degrees)	1.0	--	--	--	--	--	Neg.	Neg.	--	--	Neg.
Receiving Antenna Pointing Error (Degrees)	Neg.	Neg.	--	--	Neg.	--	1.0	--	--	--	--

1. 1. 2 DESCRIPTION OF COMMUNICATIONS SUBSYSTEMS

A. General

The communications subsystem of each vehicle comprises the following subsystems:

1. Deep space transmission subsystem
2. Relay transmission subsystem
3. Command and computer subsystem
4. Data processing and storage subsystem

Their functions and general implementations are summarized for each mission in the subsequent sections. The early Mars missions are described in the most detail and only the differences are noted for the other missions.

B. Mars 1969 and 1971

(1) Orbiter

Figure 1. 1. 2-1 shows the functional block diagram of the Orbiter Communications Subsystem for the Mars 1969 and 1971 missions. The Deep Space Transmission Subsystem provides for transmission of all data from the Orbiter to Earth, reception of commands from Earth and cooperates with the DSIF in the tracking (doppler, angle, and turn-around ranging) of the Spacecraft from Earth. Independent equipments are utilized in the functions associated with the high-gain and low-gain antennas, each utilizing a separate 50-watt klystron for transmission of data to Earth. The high-gain antenna used in the normal mode after early transit is a ten-foot parabolic dish having a beamwidth of three degrees and capable of being pointed with an accuracy of \pm one degree. The low-gain antenna gives nearly omnidirectional coverage except in the meridial plane between the two radiating elements and is used during early transit and as a back-up for the normal mode.

When in the normal mode, the Deep Space Transmission Subsystem is capable of transmitting 16 kilobits per second at encounter range. The digital data is combined with a pseudo-noise (PN) sequence on a square-wave subcarrier prior to transmission. This composite signal is used at the receiver to derive bit sync. In addition it moves the sidebands of the transmitted signal away from the RF carrier so that an uncluttered carrier will be available for tracking purposes.

In the normal command mode, commands are transmitted from the Earth using the 85-foot DSIF antenna and ten-kw transmitter, and reception is through the high-gain antenna after early transit. As a back-up mode, reception is through the omni, and the 100-kw transmitters must be used at the longer ranges.

The Orbiter is visible full-time from the earth for the first 30 days after orbit insertion. Also, it is within line of sight of the sun during that period. Continuous transmission to and from the vehicle is therefore allowable.

The command word unit accepts digital data and associated sync pulses from the command detector when a lock signal is received; otherwise, it will not accept or act on any data. The command word unit interprets the word-start symbols, determines its destination, verifies the validity of the received data and, if accepted, delivers real-time data to the Command Execution and Computation Unit and stored data to the Memory Unit. All commands to the Lander are stored until another command, either real-time or stored, directs a read-out to the Lander through the Relay Transmission Subsystem.

S

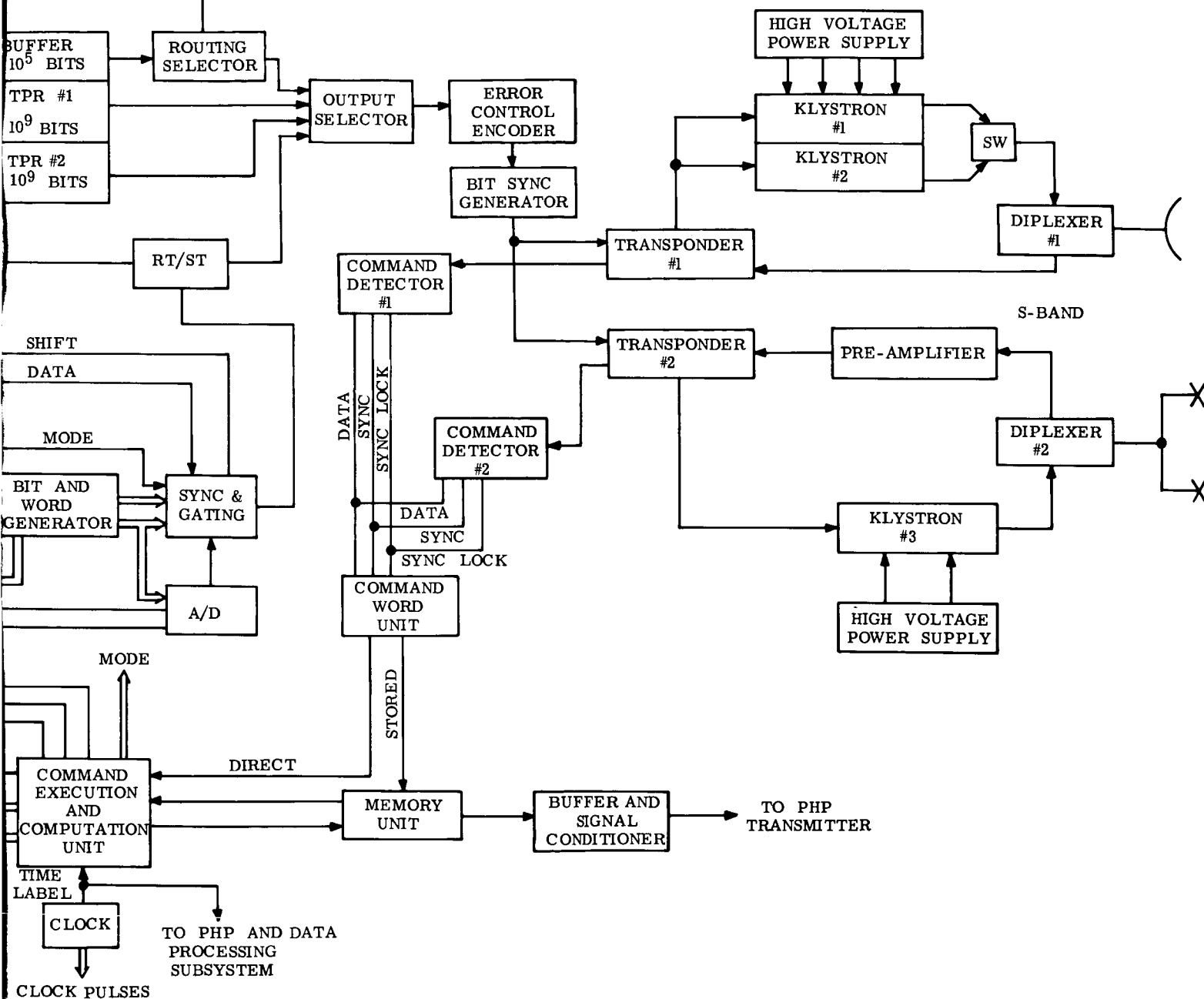
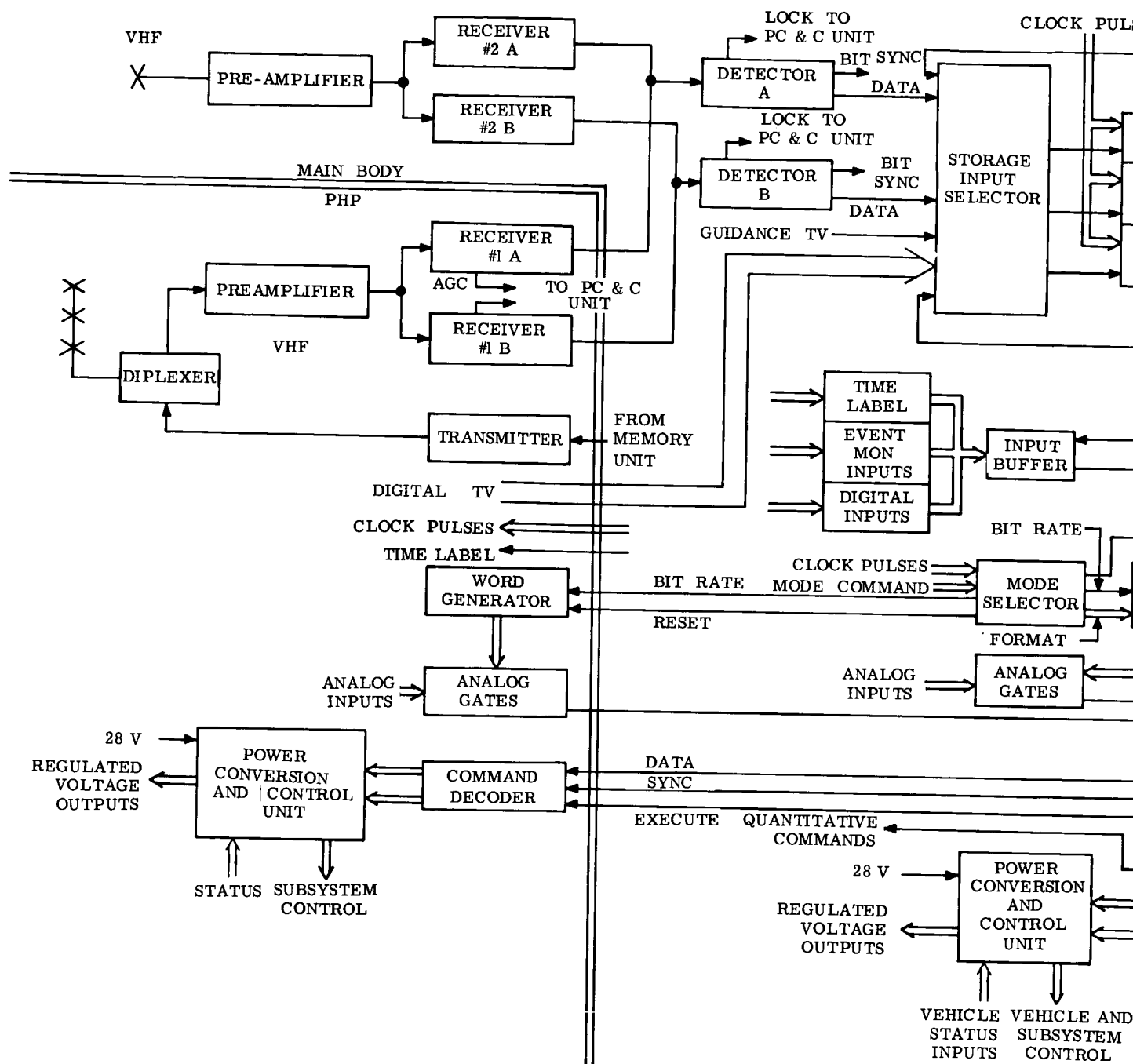


Figure 1.1.2-1 Mars 1969 and 1971 Orbiter Communications Subsystem



The Command Execution and Computation Unit executes all real-time commands upon reception. It also selects the command in the Memory Unit to be executed next and holds it in a register until its time label coincides with that of the spacecraft clock. It then executes the command and selects the next command from the memory to be executed and holds it in the register until executed. This process is repeated until all commands in the memory have been executed. Such a technique minimizes the number of times the memory must be interrogated and therefore minimizes the probability of producing an error in the process. A parity check is also made before a stored command is executed, thereby further reducing the probability of initiating an incorrect command. Both quantitative and discrete (on-off) commands are initiated by the Command Execution and Computation Unit. This unit in conjunction with the Memory Unit forms a special-purpose computer which can be used to compute such things as mapping time sequences upon receipt of the appropriate coefficients from earth.

The clock is the central time reference for the space craft. It provides a time label and timing pulses for all subsystems as required. The time label is used to determine the time at which a command is to be executed and also is inserted into each frame of data being taken by the Data Processing Unit.

To minimize the number of lines to the Planet Horizontal Package (PHP) a separate Decoder and Power Conversion and Control Unit are utilized on the PHP. Only the data and control lines are therefore required.

The Data Processing and Storage Subsystem has four different functions:

1. Digitize and multiplex data
2. Store data
3. Encode data for error control
4. Generate bit sync signal

The first function applies only to the narrow-band data sensors as used in most cases for both science and engineering data. Wide-band data such as TV is encoded by an A/D encoder within the TV subsystem and separate from that used for the narrow-band data. Multiplexing of TV data with narrow-band data is directed by the Command Subsystem. The data format and rate are also determined by the Command Subsystem. The format determines which sensors are sampled in a particular frame. For instance, during maneuvers only selected diagnostic sensors will be sampled, while during orbit most of the data collected will be scientific. The data collection rate will be commanded from earth, based on the anticipated rate of change of sensor outputs and will be constrained by the rate at which data can be sent to earth over an available time period. The narrow-band data can be either stored or transmitted directly. The storage devices utilized are a 100-kilobit plated-wire storage and two 10^9 -bit thermoplastic plate recorders. Because of their ability to record over an extremely wide range of data rates, the TPR's could probably be utilized for all recording and the plated-wire storage eliminated; however, there are periods of time such as during maneuvers in which it is desirable to record low-rate data with a minimum of power expenditure. In this case the plated-wire storage can be utilized with a power requirement of milliwatts, as opposed to the TPR's which would require about 25 watts. The TPR's would then be activated only for short periods of time if required to accept data from the wire storage when the latter is filled.

One of the primary features of the TPR's is that data can be clocked in and out. This means that during read-in a constant number of bits are stored on each line of a TPR plate regardless of the read-in rate. If magnetic tape recorders were used, either the tape speed would have to be changed for each new rate, or a tape

speed higher than that actually required would be necessary. The ability to read in at various speeds in a tape recorder can result in considerable waste of storage volume. The disadvantage of start-stop time is also eliminated in the TPR's. This is especially important during the in-orbit mapping procedure, since the frame rate is not constant.

The ability to clock-out the data also results in ease of implementation by automatically satisfying the requirements imposed by the error control encoding and bit sync techniques. The Error Control Encoder requires that a burst of 45 bits be read into the encoder at the transmitted bit rate and that no data be read-in during the subsequent 28 bit periods. The TPR output can be presented in this fashion without the use of buffers, whereas a magnetic tape recorder output must first be fed into buffers at 45/73 times the transmitted bit rate and the buffers clocked out in bursts as described previously. This would present a problem in that the data rate from the tape must be extremely close to that required so that the buffers do not overflow or become empty. Running the tape at a higher speed into a high-volume buffer and stopping it when the buffer filled would alleviate this problem; however, this again would result in added complexity and reduced reliability.

If the Error Control Encoder were not in the system, or, if it were by-passed during portions of the mission, the bit sync requirements still make clocked data desirable. The more precisely the PN sequence is combined in phase with the data and the more stable the bit rate, the better the detection capability at the receiver. Therefore, for tape recorders either the inferior detection capability must be accepted or a buffer must still be utilized to allow clocking out the data.

The TPR's also accept data directly from the TV Subsystem and the Lander Data Detector. The TV sampling and digital encoding processes as well as the TPR read-in are controlled by synchronous clock pulses from the Command Subsystem. Recording of data from the Lander Data Detectors is clocked by the bit sync pulses from the detectors.

The Error Control Encoder, a unit of the Data Processing and Storage Subsystem, accepts bursts of 45 bits as described previously and computes and appends 28 check bits in a cyclical register. Its output to the bit sync generator is then a serial string of 73 bits. Approximately 1.5 db reduction of required transmitter power is accomplished by the error control encoding.

The Bit Sync Generator combines a 511-bit PN sequence on a square-wave subcarrier with the 73 data bits. This allows seven PN bits per data bit. At the receiver, the subcarrier and PN sequence are cross-correlated with identical locally generated waveforms. When the two PN sequences are in phase or correlated, the PN generator in the receiver provides outputs indicating the beginning of each data bit period and the beginning of each group of 73 bits. The former output allows accurate detection of each bit in an integrate-and-dump circuit, while the latter resets the error control decoder each time a group of 73 bits is decoded.

The composite signal from the Bit Sync Generator is a two-level waveform. This signal is used to phase-modulate the carrier generated in the transmitter portion of the transponder. The carrier is shifted, therefore, between two values of phase (± 60 degrees utilized in this case) resulting in a spectrum with a discrete carrier frequency and sidebands containing the data and synchronization information. The sidebands are sufficiently removed in frequency from the carrier so that the spectrum is relatively uncluttered near the carrier as required for tracking.

The Relay Transmission Subsystem on the Orbiter is divided between the Main Body and the PHP. The detectors in the Main Body are used to detect all received data, since only one of the sets of receivers will be utilized at one time. The receivers in the Main Body are fed by a turnstile antenna. They are used only during the cruise and descent phases of the Landers. The receivers in the PHP cannot be used at that time, since the PHP is

stowed until after retro firing for orbit insertion, which is not accomplished until the Lander has completed or nearly completed its descent phase. The turnstile antenna is located on the Main Body so as to give complete coverage of the planet when the Orbiter is in the retrofire attitude.

After orbit insertion the PHP is deployed, and a 10-db yagi on the PHP is extended toward the planet. Reception thereafter is through this antenna and the receivers on the PHP, although the omni can serve as back-up.

The modulation technique utilized in all relay links is PCM/PSK (± 60 degrees). Synchronous reception and matched-filter data detection are also used. Bit sync is similar to that described for the deep-space links; however, faster lock is attained by reducing the length of the PN sequence (used for bit sync) to three bits in the Lander-Orbiter telemetry links and 31 bits in the Orbiter-Lander command link. The PN sequence is repeated each data bit rather than for a group of 73 bits as described for the deep-space links. The latter is not a requirement in the relay links since error control encoding is not used.

Each Lander has its own associated receiver in the PHP and a receiver and detector in the Main Body of the Orbiter. The Landers transmit on separate frequencies, since there are periods when they must operate simultaneously. Transmission to the Landers is on a single frequency, and all commands are received by both vehicles if they are within line of sight of the Orbiter. Each command contains an address that indicates which Lander is to accept the command. The five-watt command transmitter in the PHP is modulated by commands sent from the Command and Computer Subsystem. The Command and Computer Subsystem also initiates and controls the lock procedure which ensures both carrier and bit-sync lock in the relay links. Carrier-lock signals from the PHP receivers and sync-lock signals from the data detectors are sent to the Command and Computer Subsystem as a part of this procedure.

(2) Lander

The functional block diagram of the Lander Communications Subsystem for the Mars 1969 and 1971 missions is shown in Figure 1.1.2-2. It comprises the same four subsystems (Deep Space Transmission, Command and Computer, Data Processing and Storage, and Relay Transmission). However, each subsystem differs to a certain extent from its counterpart in the Orbiter.

The Deep Space Transmission Subsystem has been relegated to a secondary role in the Lander and is a reduced version of that in the Orbiter. Only one 70-watt klystron, one transponder and one command detector have been used. Transmission and reception can be switched between a low-gain turnstile antenna and a high-gain antenna. The high-gain antenna is a 21-db helix for the 1969 mission and a 26.7-db helix array for the 1971 mission. Each of these antennas is to be pointed to earth with an accuracy of \pm three degrees.

The prime data links to and from the Landers are provided by the Relay Transmission Subsystem. Link (6) as described previously is used during the Lander cruise and descent phases. A separate power amplifier and antenna are used in the Lander for this link. The "transmission line" antenna will survive entry but can be damaged upon landing. Therefore, a turnstile antenna is erected after the Lander is on the surface and the aft cover has been removed. Individual power amplifiers are utilized to eliminate RF switching.

The Lander Command and Computer Subsystem function is reduced from that in the Orbiter in that the commands to the PHP and those relayed through the Orbiter to the Lander are not required in this case. The Memory Unit capacity and the number of command words are also reduced.

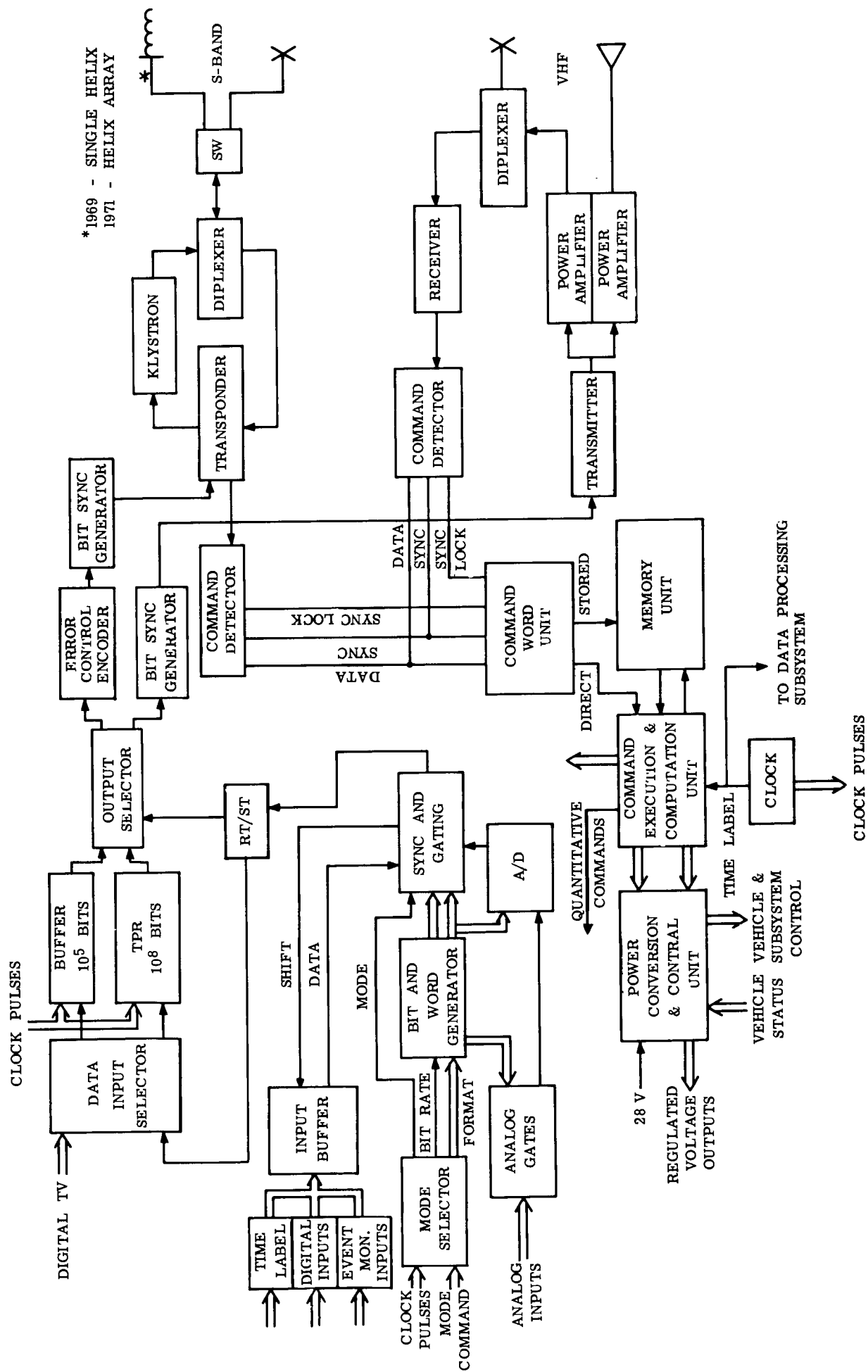


Figure 1.1.2-2 Mars 1969 and 1971 Lander Communications Subsystem

The number of inputs to the Data Processing and Storage Subsystem is also reduced, and, since transmission can occur for only one-half hour every six hours because of energy storage limitation, the data storage volume is reduced. A plated-wire storage and a thermoplastic recorder provide capacities of 10^5 and 10^8 bits, respectively. The small plated-wire storage is used primarily for narrow-band data and data accumulated during entry and descent. Actuation of the TPR is not required until after the Lander has reached the planet surface.

Only the direct links to earth utilize error control encoding. When data is being transmitted via the Relay Transmission Subsystem to the Orbiter, the encoder is bypassed.

C. Mars 1973 and 1975

(1) Orbiter

Figure 1.1.2-3 shows the block diagram of the Orbiter Communication Subsystem for the 1973 and 1975 missions. It is identical to that described for the 1969 and 1971 missions with the elimination of some components and the reduction of radiated power. In particular, the PHP and its associated electronics have been removed, only one TPR is used, and the S-band pre-amplifier has been eliminated for the 1973 mission, because no pre-amplifier has been found capable of meeting the heat sterilization requirements. Each klystron here radiates only 35 watts, instead of 50.

The relay receivers are used only during the Lander cruise and descent phases to monitor the Lander before it reaches the surface. After landing, the Lander Deep Space Transmission Subsystem provides all communications. There is no command transmission from the Orbiter to the Lander at any time.

(2) Lander

The block diagram of the Lander Communications Subsystem for the Mars 1973 and 1975 missions is shown in Figure 1.1.2-4. Because the Deep Space Transmission Subsystem provides the prime link to and from earth, it is constructed in two independent sections to increase its reliability - one section is associated with the high-gain antenna and the other with the low-gain antenna. A back-up klystron, which can be switched into the high-gain section, is provided. The high-gain antenna is a helix array giving a gain of approximately 26.7 db. This antenna is to be pointed at the earth with an accuracy of \pm three degrees.

The Relay Transmission Subsystem comprises only a VHF transmitter, power amplifier, and a "transmission line" antenna. Upon Lander impact, the latter is discarded, and the relay link can no longer be utilized.

D. Venus 1970

(1) Orbiter

The block diagram of the Orbiter Communications Subsystem for the Venus 1970 mission is shown in Figure 1.1.2-5. The Deep Space Transmission and Data Processing and Storage Subsystems are identical to those described for the Mars 1969 and 1971 missions. The Command Subsystem differs only in that no commands are relayed to the Lander.

In the Relay Transmission Subsystem, a 10-db planet-tracking yagi antenna is used to receive data from the single Lander both before and after impact. Communication time after Lander impact is expected to be in the order of 10 to 30 minutes. The Lander will be dead on the second orbit; therefore, the yagi pointing need be programmed only for the first pass.

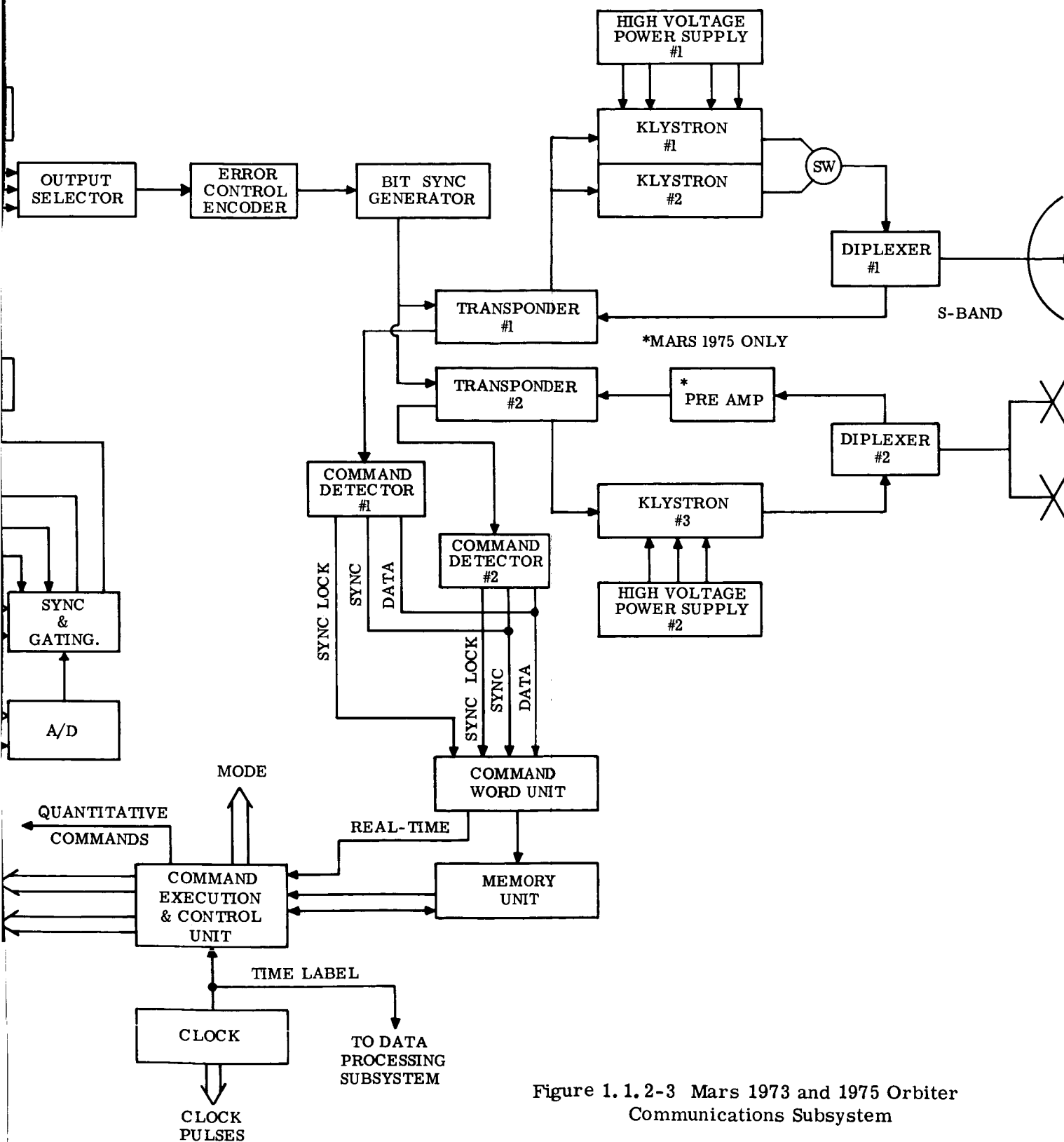
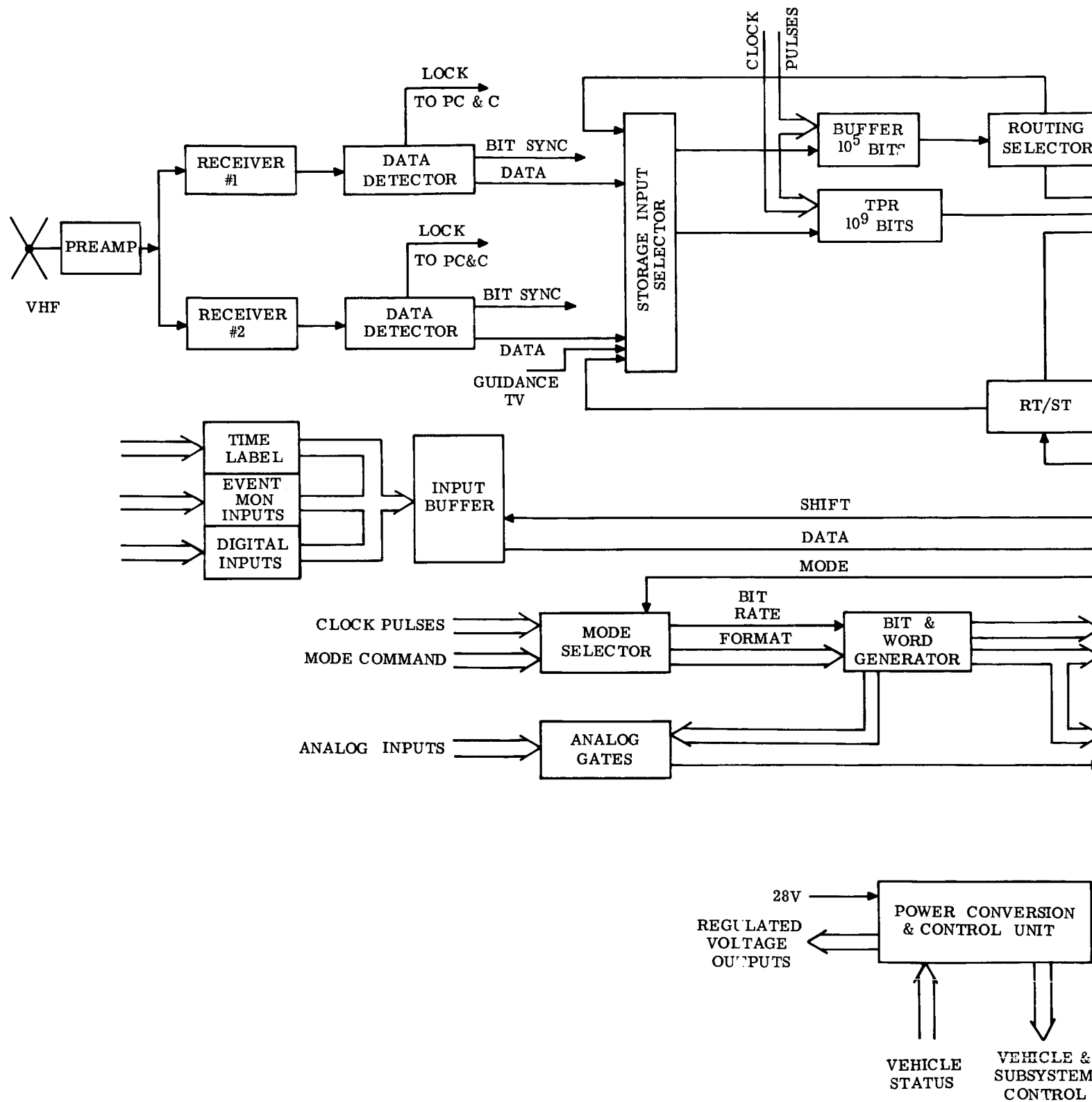


Figure 1.1.2-3 Mars 1973 and 1975 Orbiter Communications Subsystem



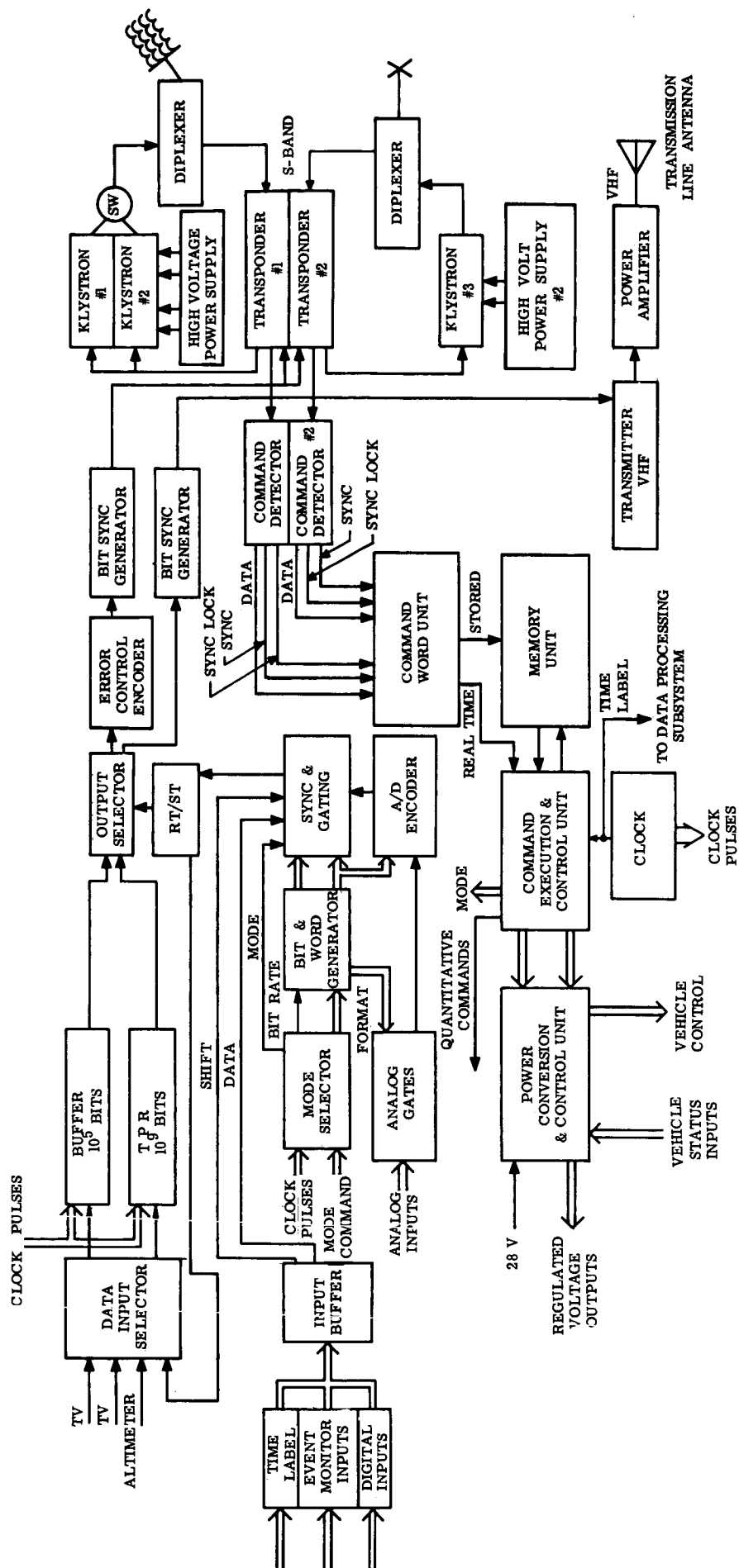


Figure 1.1.2-4 Mars 1973 and 1975 Lander Communications Subsystem

INSTRUMENT PACKAGE ON
SUB-REFLECTOR OF
RADAR ANTENNA

TV

WORD
GENERATOR

ANALOG
INPUTS

ANALOG
GATES

COMMAND
DECODER

REGULATED
VOLTAGE OUTPUTS

28V

SUBSYSTEM
CONTROL

POWER
CONVERSION
& CONTROL

V H F

PREAMP

RECEIVER

DATA
DETECTOR

LOCK
TO PC & C UNIT

BIT SYNC

DATA

RADAR

DATA

STORAGE INPUT
SELECTOR

BUFFER
10⁵ BITS

T P R
10⁹ BITS

T P R
10⁹ BITS

TIME
LABEL
EVENT
MONITOR
INPUTS
DIGITAL
INPUTS

INPUT BUFFER

DATA

SHIFT

MODE

CLOCK
PULSES
MODE
COMMAND

MODE
SELECTOR

BIT RATE
FORMAT

BIT & WORD
GENERATION

RESET

ANALOG
INPUTS

ANALOG
GATES

QUANTATIVE COMMANDS

EXECUTE

28 V

REGULATED
VOLTAGE
OUTPUTS

POWER
CONVERSION
& CONTROL UNIT

VEHICLE
STATUS
INPUTS

SUBSYSTEM
& VEHICLE
CONTROL

MAIN BODY

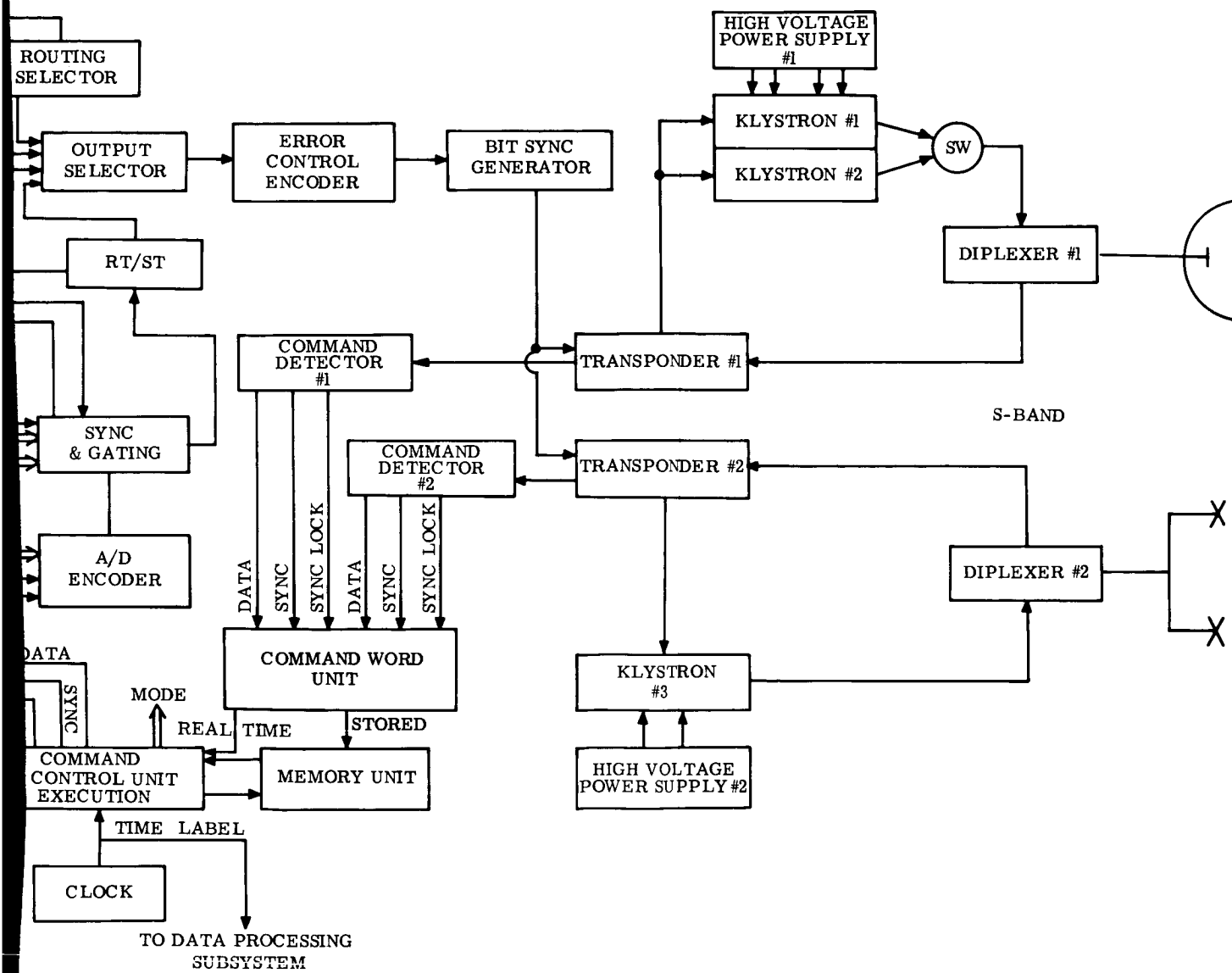


Figure 1.1.2-5 Venus 1970 Orbiter Communications Subsystem

TABLE 1.1.3-1. DATA RATES (BITS/SECOND)

Link Purpose* Mission	1		2		3		4		5		6		7		8		9		10		11	
	O-E	TLM	O-E	TLM	L-E	TLM	L-E	TLM	L-O	TLM	L-O	TLM	E-O	Command	E-O	Command	E-L	Command	E-L	Command	O-L	Command
Mars 1969 1971	16,000	1,000	1,000	1,000	1,000	4	16,000															
	8,000	125	500				8,000															
	4,000	4	250				4,000		500				10		0.5		0.5		0.5		10	
	2,000		125				2,000															
Mars 1973 1975	8,000	1,000	4,000																			
	4,000	125	2,000	4					500				10		0.5		2.0		0.5		--	
	2,000	4	1,000																			
	1,000		500																			
Venus 1970	64,000	1,000																				
	32,000	125	4				8,000		500 (Pre-entry)				10		0.5		---		---		--	
	16,000								8,000 (Post-entry)													
	8,000																					
Venus 1972	16,000	1,000	-----				16,000															
	8,000	125							500 (Pre-entry)				10		0.5		---		---		10	
	4,000	4							8,000 (Post-entry)													
	2,000																					

*O - Orbiter
L - Lander
E - Earth

(2) Lander

The block diagram of the Lander Communications Subsystem for the Venus 1970 mission is shown in Figure 1.1.2-6. This subsystem has no Deep Space Transmission Subsystem and therefore depends solely on the relay links to retrieve cruise, descent, and surface data. A "transmission line" antenna is used during the first two phases but is disconnected upon impact, and a whip antenna is used for the surface phase.

Only a 10^5 -bit plated-wire storage is used in the Lander. This will allow storage of entry data. Because TV pictures must be taken and transmitted in a short period of time, the TV camera itself will be used for short-term storage, and the picture will be transmitted directly as it is scanned from the target element of the camera tube.

Because there is no radio command capability to the Lander here, the Command Subsystem takes the form of a Sequence Timer. It is pre-programmed either on the earth or through the Orbiter Command Subsystem prior to separation. It also accepts signals such as that from a "g"-switch which initiates programs during and after entry.

E. Venus 1972

(1) Orbiter

The block diagram of the Orbiter Communication Subsystem for the Venus 1972 mission is shown in Figure 1.1.2-7. It is identical to that described for the Venus 1970 mission, except that the klystrons radiate only 35 watts instead of 50 and it provides for command transmission to the single Lander. The 10-db yagi is body-mounted and is programmed to point in the direction of the Lander both on the first pass and after completion of the first orbit. The program can be updated in the latter case after the parameters of the attained orbit has been determined by the tracking station. The Lander will be designed for only a one-orbit lifetime, and the relay link will be de-activated after that time.

Commands will be sent to the Lander only when the Lander comes within line-of-sight at the completion of the first orbit. This allows time for transmission to earth and evaluation of the pictures taken on the first pass. The commands will, therefore, be based on information obtained from the first pictures.

(2) Lander

The Venus 1972 Lander Communication Subsystem is most nearly like that described for the Mars 1969 and 1971 Landers. Its block diagram is shown in Figure 1.1.2-3. The two subsystems differ in that the Venus 1972 Lander does not have a Deep Space Transmission Subsystem. The other subsystems are identical.

1.1.3 GRAPHICAL AND TABULAR RESULTS

A. Performance of Data Transmission Links

The data rate capability of each of the deep space communication links for each mission is shown in Figures 1.1.3-1 through 1.1.3-4 as a function of transmission range. All parameter values and assumptions utilized in the derivation of the rates are given in Section 1.4.5.

Figure 1.1.3-5 shows the capability of the relay links from Lander to Orbiter (link 5) and Orbiter to Lander (link 11) for the Mars 1969 and 1971 missions as a function of Orbiter altitude. In each case the Lander is assumed to be on the planet's horizon and the Orbiter antenna is pointed at the center of the planet. The antenna gain in the direction

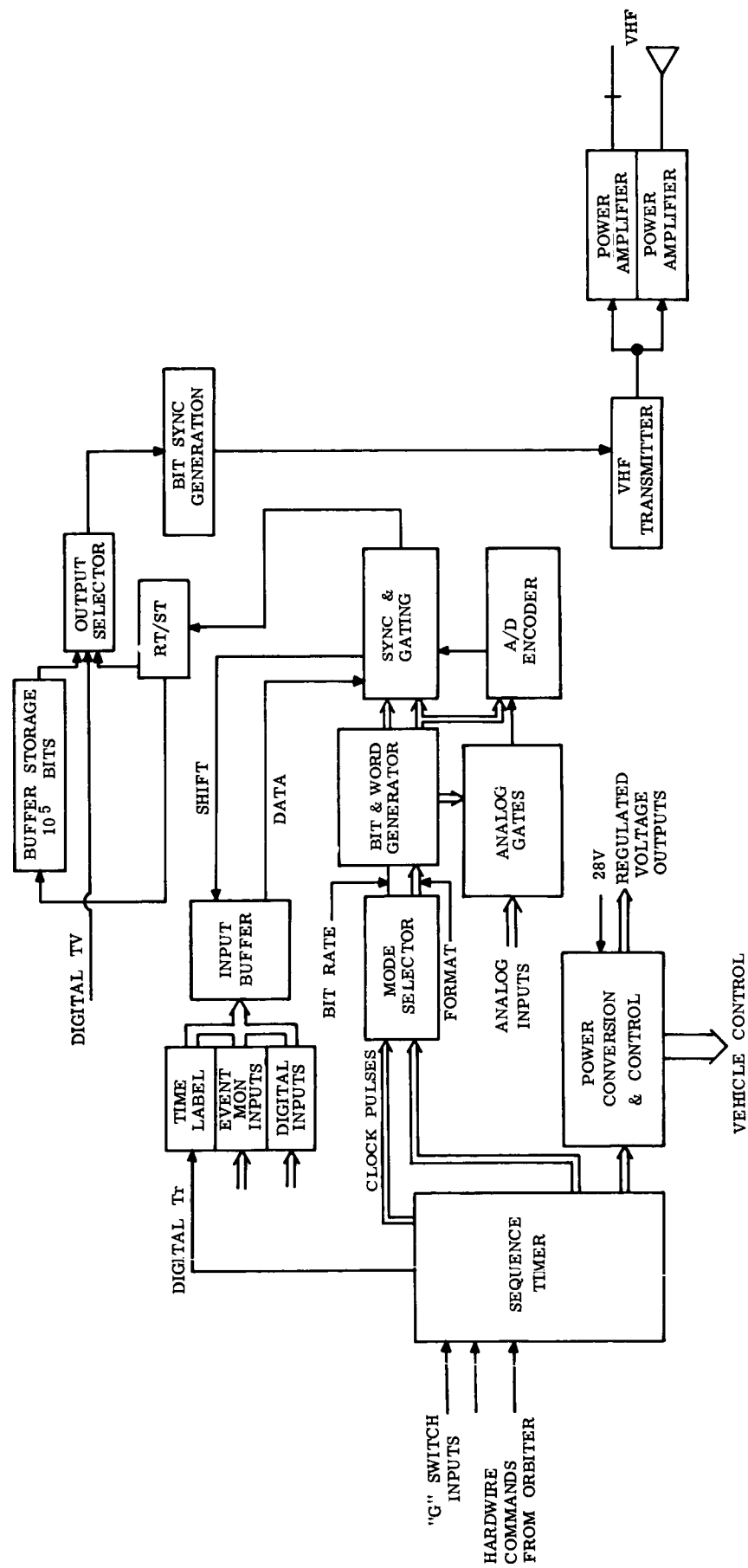
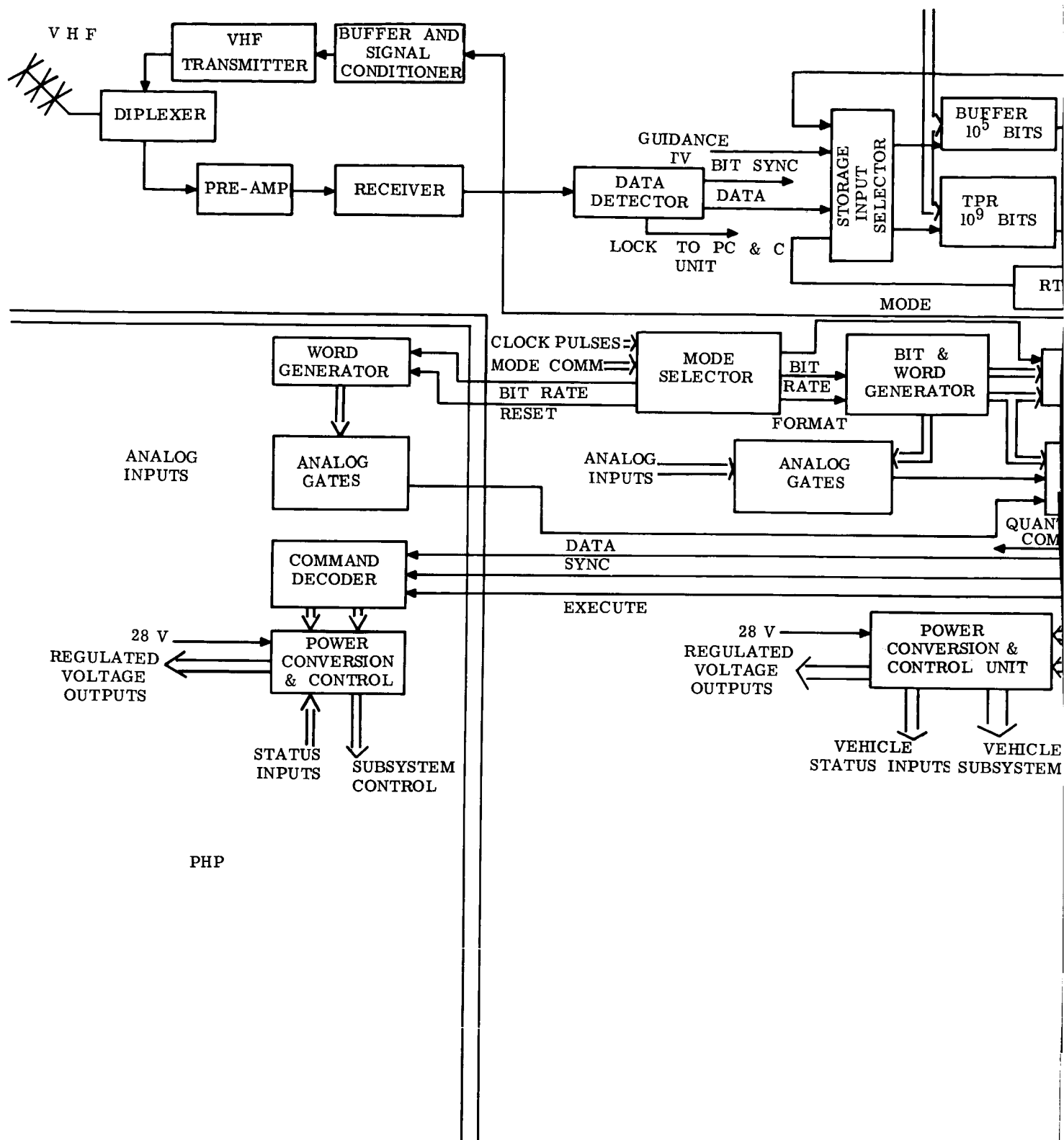


Figure 1. 1. 2-6 Venus 1970 Lander Communications Subsystem



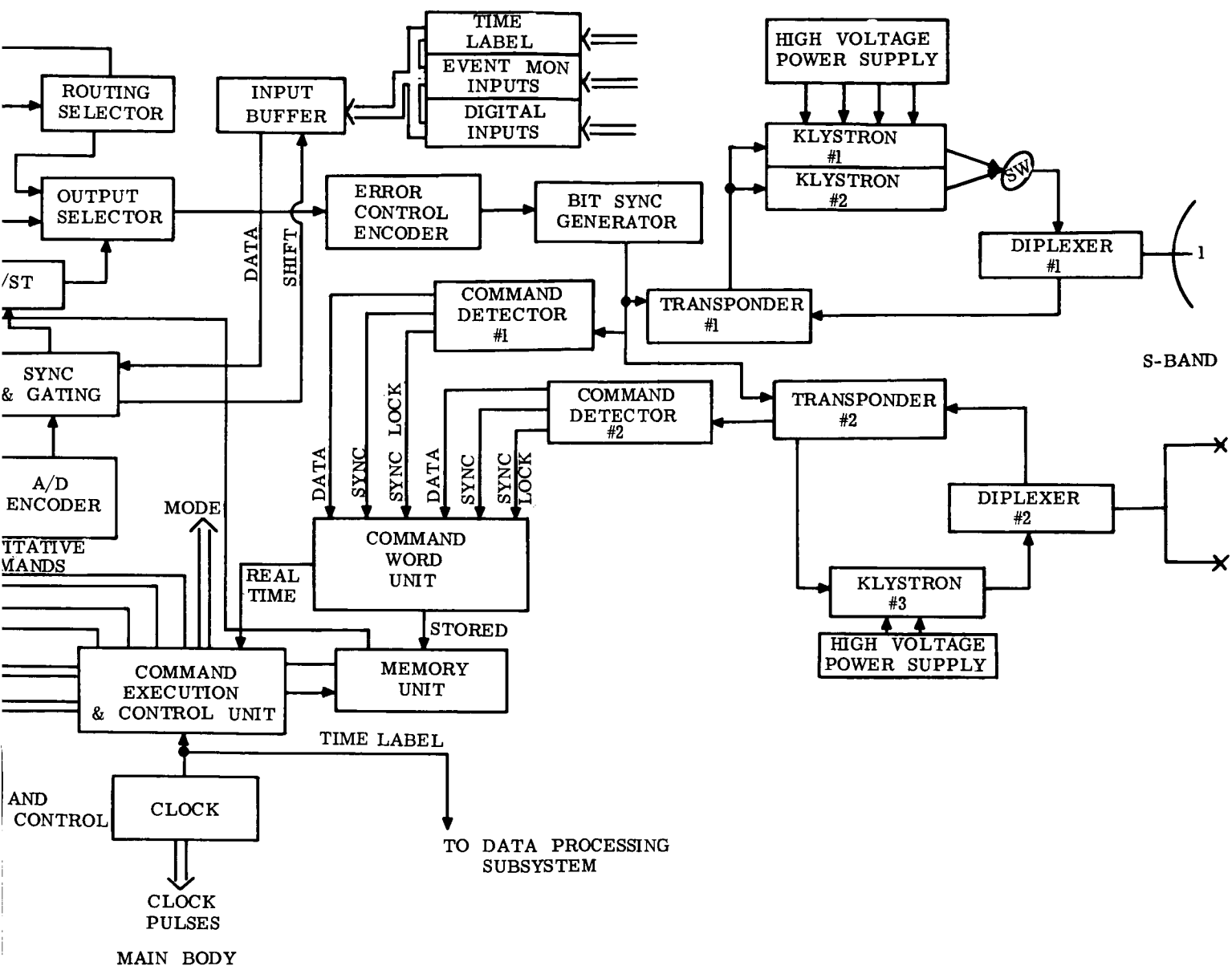


Figure 1.1.2-7 Venus 1972 Orbiter Communications Subsystem

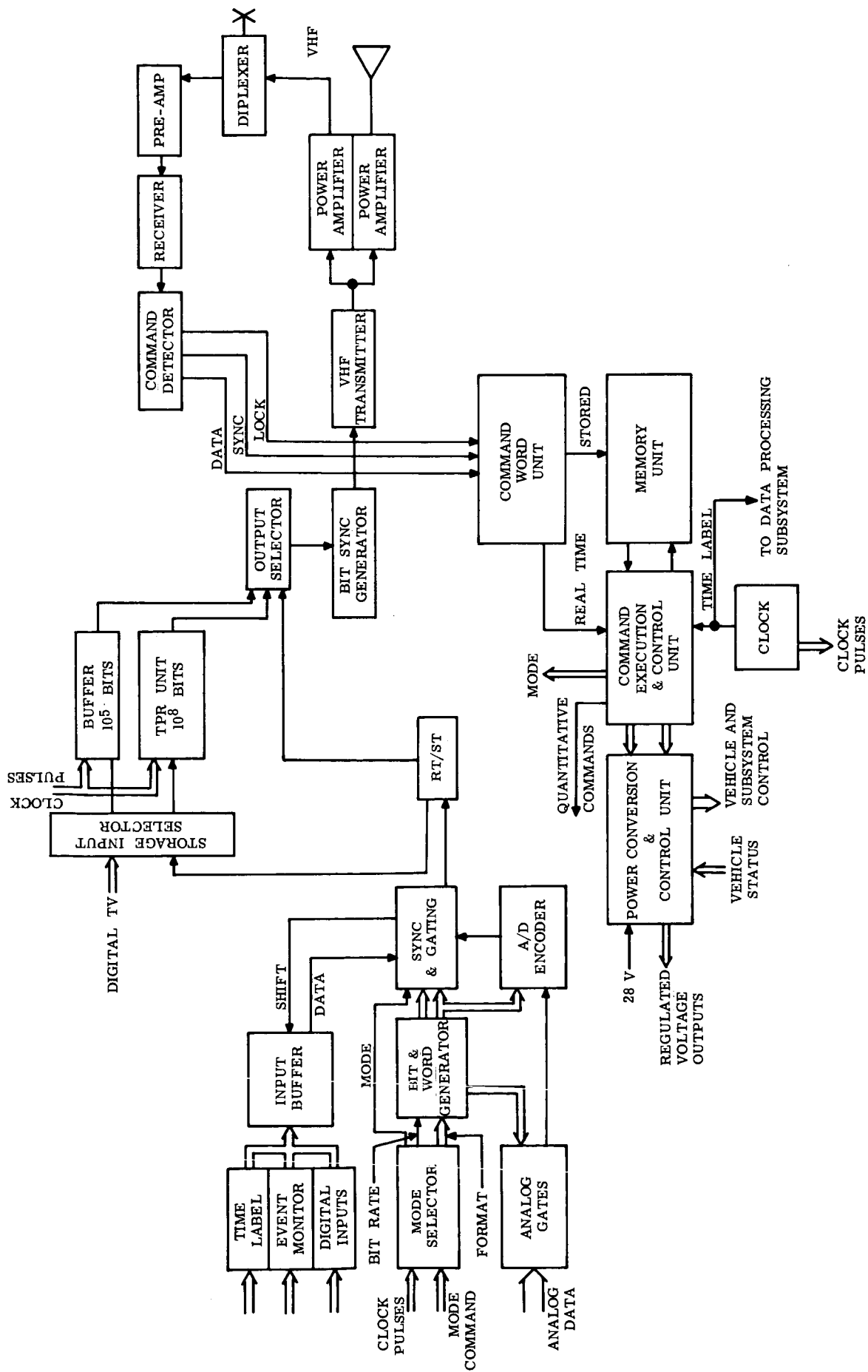


Figure 1.1.2-8 Venus 1972 Lander Communications Subsystem

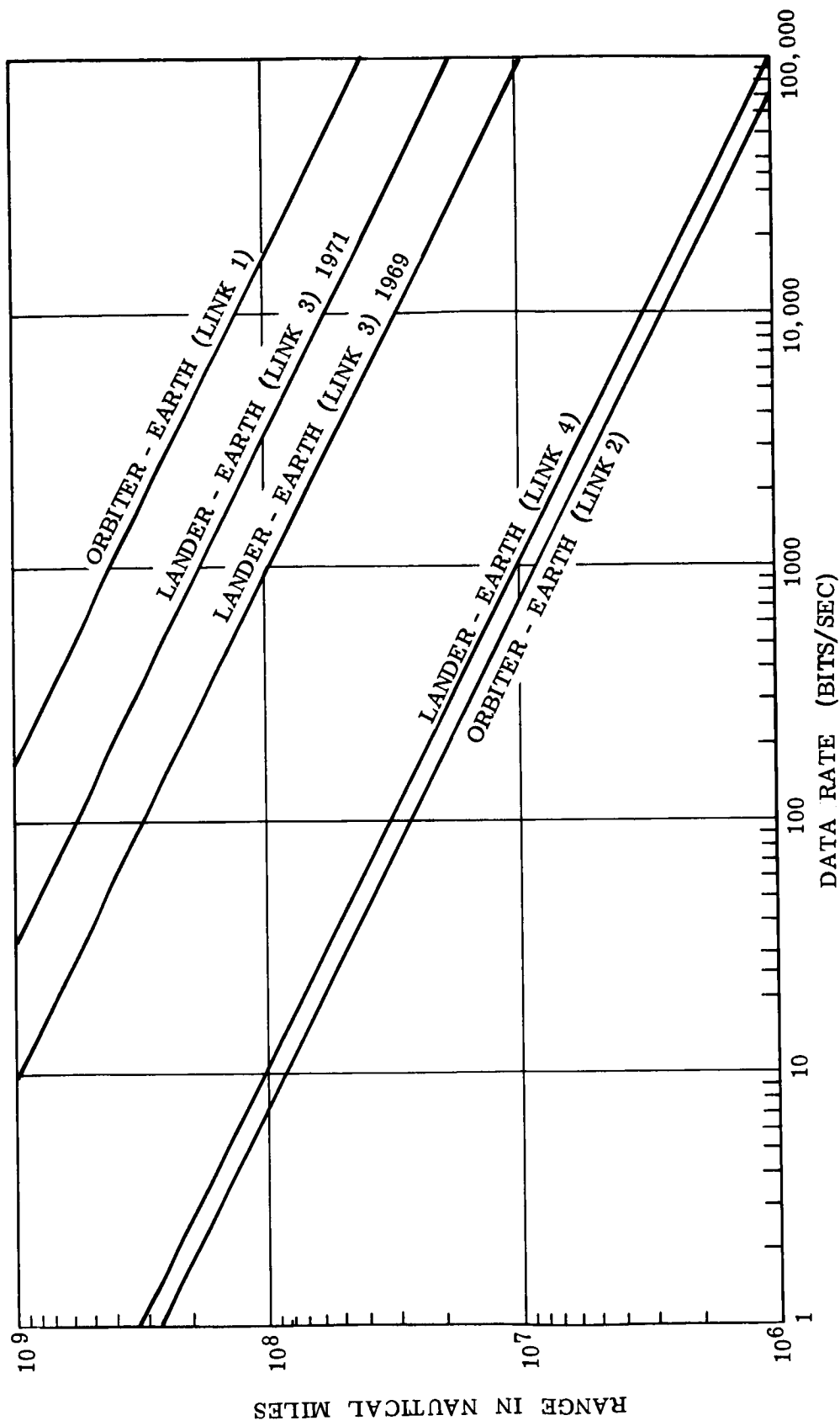


Figure 1.1.3-1 Data Transmission Rates (Mars 1969 and 1971)

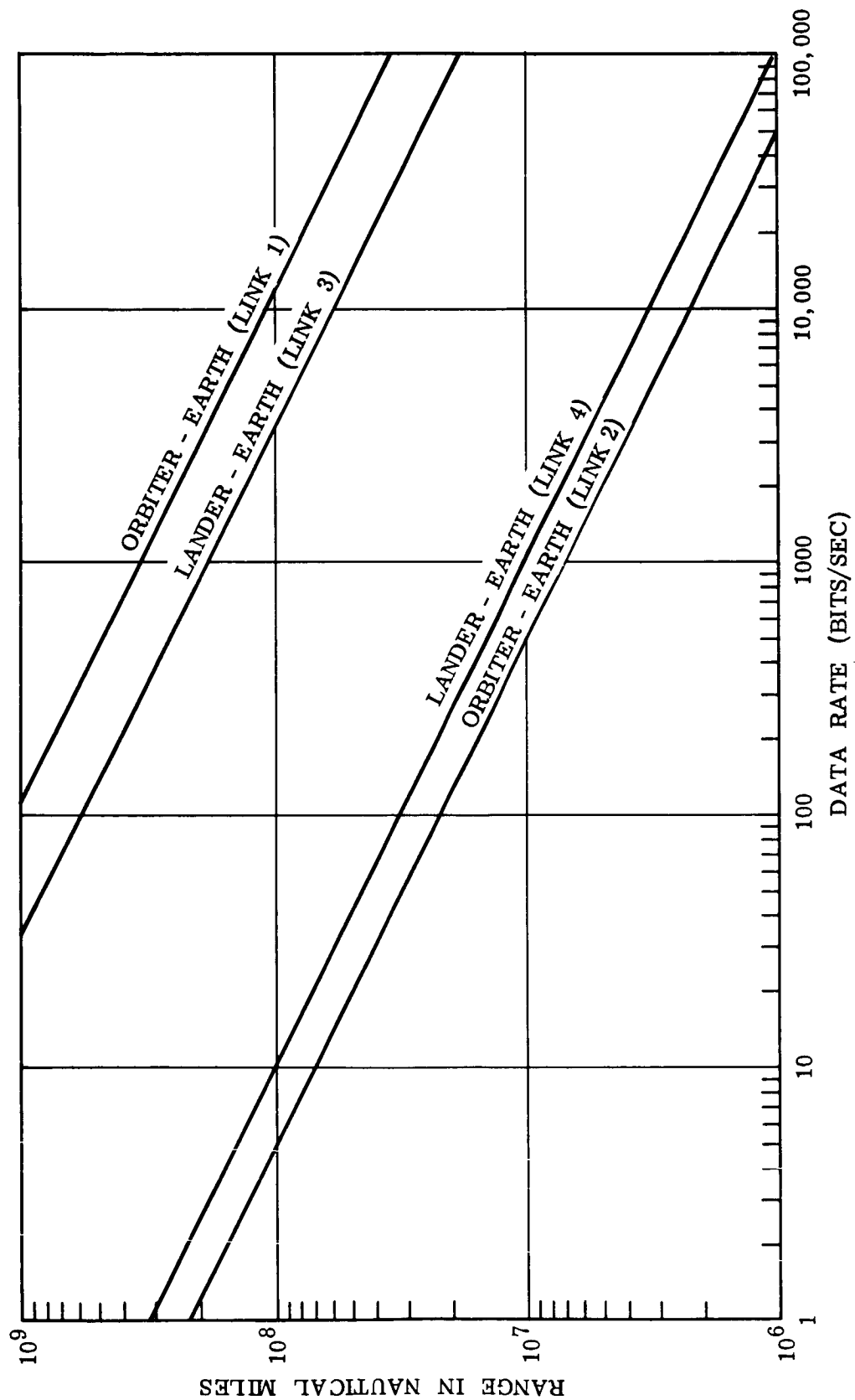


Figure 1.1.3-2 Data Transmission Rates (Mars 1973 and 1975)

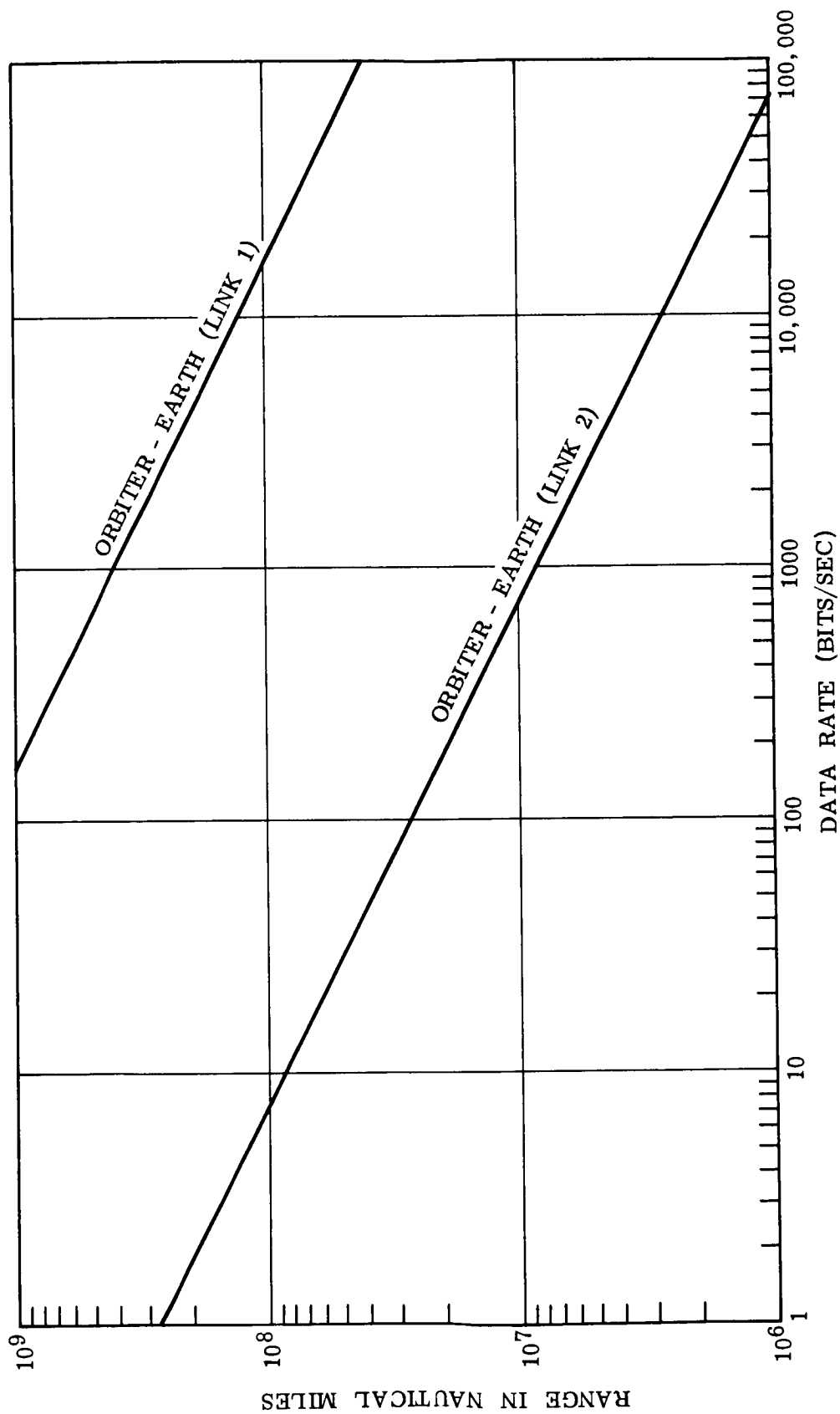


Figure 1.1.3-3 Data Transmission Rates (Venus 1970)

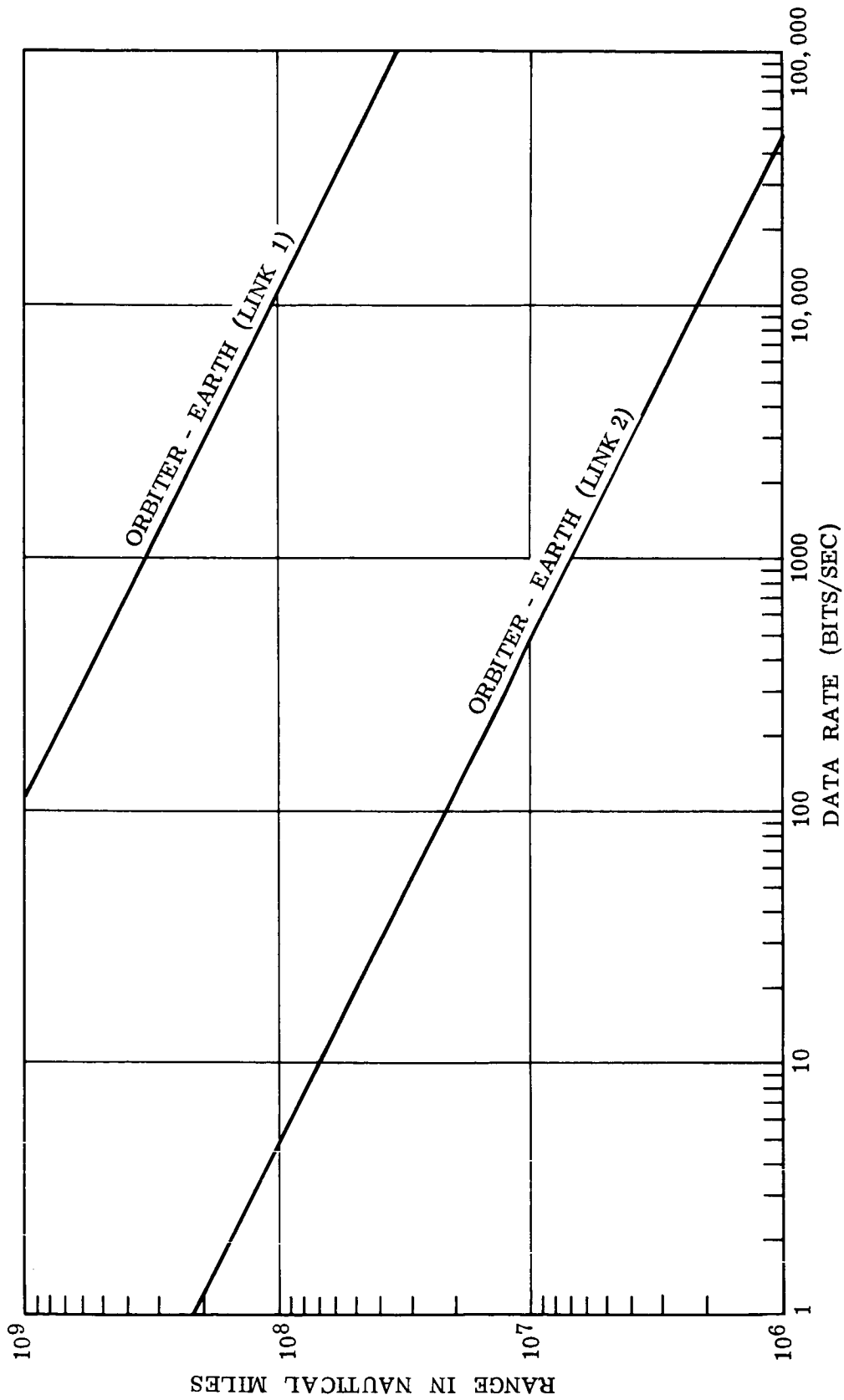


Figure 1.1.3-4 Data Transmission Rates (Venus 1972)

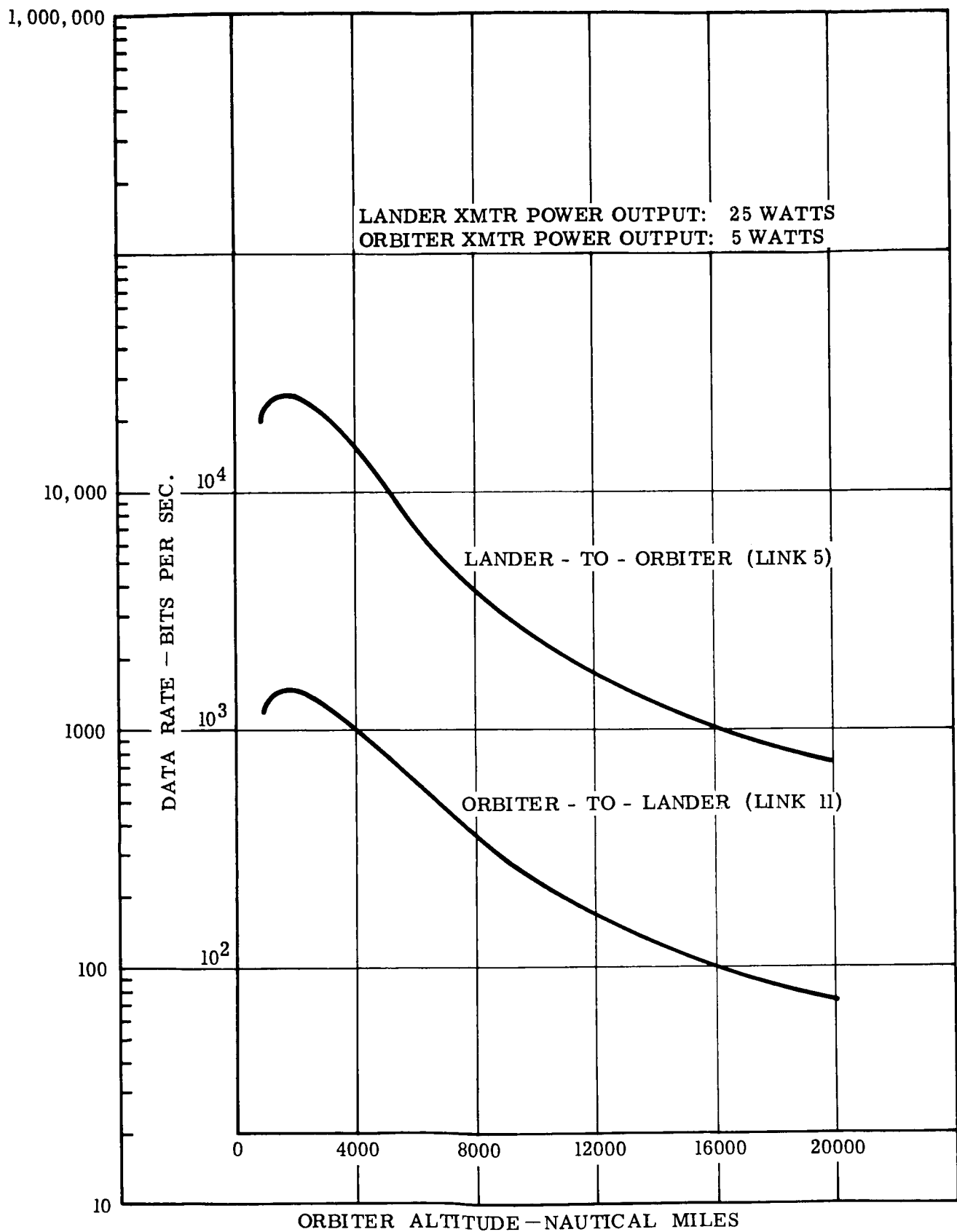


Figure 1.1.3-5 Data Rate In Orbit (Mars 1969 and 1971)

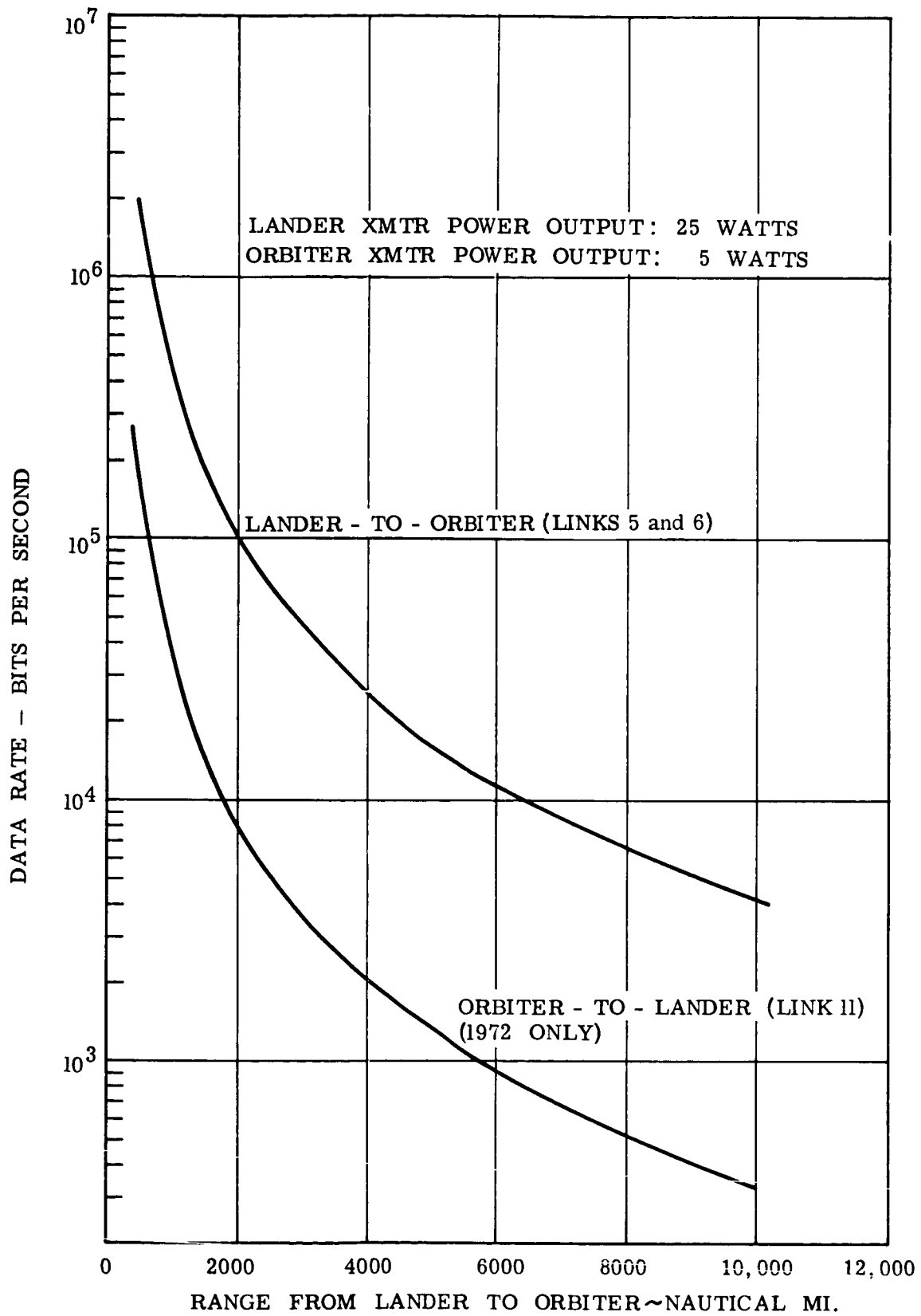


Figure 1. 1. 3-6 Data Rate vs Range (Venus 1970 and 1972) Missions

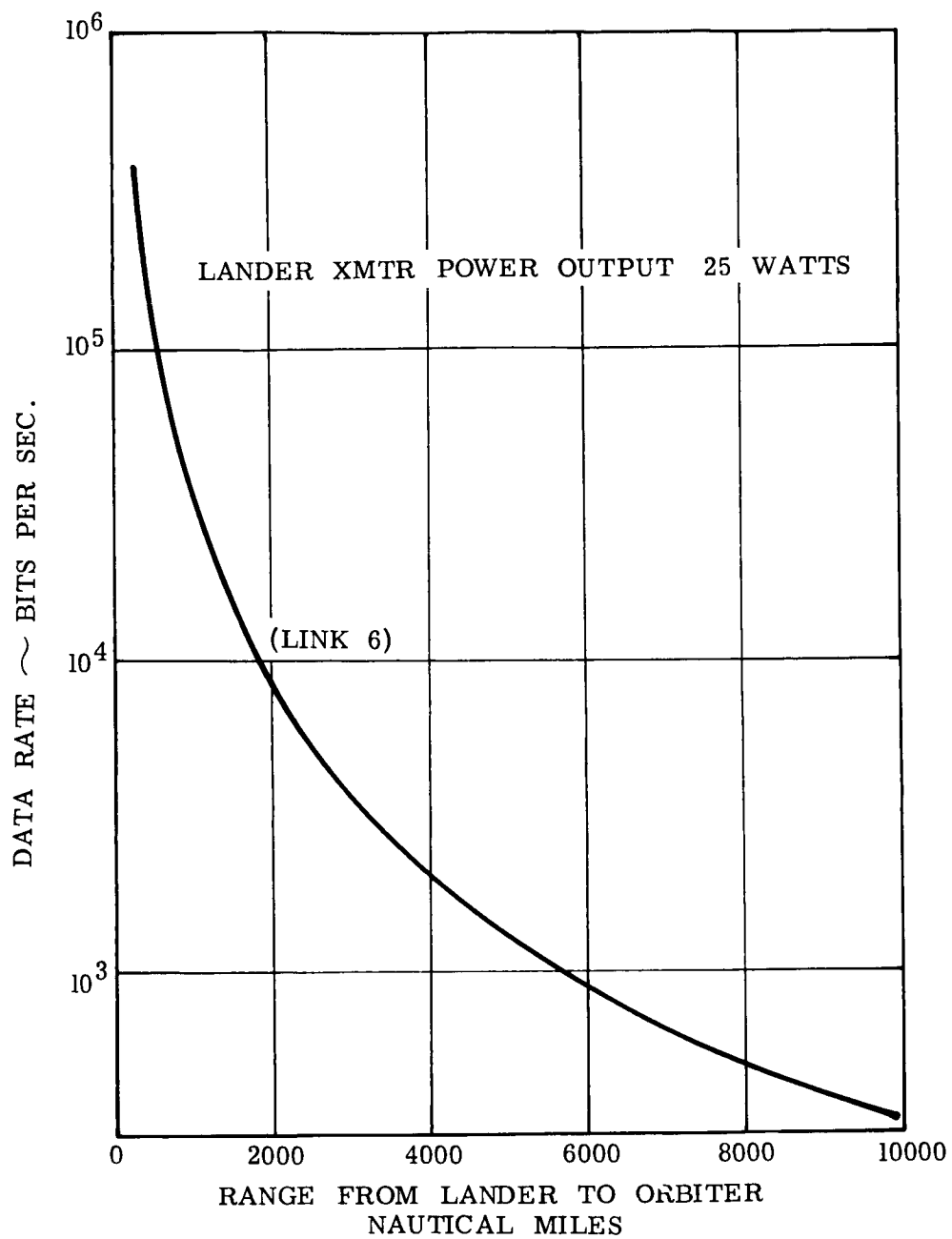


Figure 1. 1. 3-7 Lander-to-Orbiter Data Rate During Mars Lander Descent (All Mars Missions)

of the Lander is therefore varied with Orbital altitude to account for the angle between the Lander and antenna boresight.

Figure 1.1.3-6 indicates the data rate capability of the Lander-to-Orbiter links (links 5 and 6) and Orbiter-to-Lander link (link 11) as functions of range for the Venus 1970 and 1972 missions. In this case the 10-db antenna is programmed to be pointed at the Lander so that the pointing error is negligible.

The Lander-to-Orbiter data rate is given as a function of range in Figure 1.1.3-7 for the Lander cruise and descent phases of all Mars missions. A low-gain turnstile antenna is utilized on the Orbiter during these phases.

B. Selected Data Rates

Based on the data-rate capabilities shown in the previous section one or more nominal discrete data rates were selected for each link. The selection of multiple data rates for a single telemetry link indicates the ability to change the rate on command from earth or by stored command. Changes can be made to approach the maximum allowable data rate as the transmission range and system parameter values vary. All selected values including those for command links are listed in Table 1.1.3-1.

1.1.4 TABLES OF SIZE; WEIGHT, AND POWER REQUIREMENTS

Table 1.1.4-1 shows size, weight and power requirements for the Orbiter Communications Subsystems. Table 1.1.4-2 shows similar data for the Lander.

1.1.5 CRITICAL PROBLEM AREAS

A. Electrostatically Focused Klystron (ESFK)

The electrostatically focused klystron has been selected for the S-band power amplifier because of its favorable characteristics in the categories of weight, gain, efficiency, and predicted lifetime. To date only prototype units have been built and tested. A program for further development, qualification, and life-testing will be necessary. It is estimated that this will require about two years plus life-test.

B. Thermoplastic Recorder (TPR)

Thermoplastic recorders have been selected for both the Lander and the Orbiter because of their high data storage density, ease of operation and lack of rotating parts. It is also expected that these will prove to be more amenable to heat sterilization than magnetic tape.

A breadboard model of a thermoplastic recorder is presently being developed at the GE Advanced Technologies Laboratory under contract to JPL. Rather extensive development and testing will be required to qualify this for spacecraft use, but the time schedule will allow this. About three years plus life-test should suffice.

C. Sterilization of Magnetic Tape

In the event that unforeseen difficulties arise in the development of the thermoplastic recorder, it is recommended that a magnetic tape recorder development program be started. Heat sterilization of magnetic tape will cause material problems, thus requiring the development of perhaps a metal-backed tape. Several companies claim to be studying this problem already, and such programs should be continued. About a two-year development program will be required.

TABLE 1.1.4-1. SIZE, WEIGHT, AND POWER REQUIREMENTS FOR ORBITER COMMUNICATIONS SUBSYSTEM

	Mars '69 and '71				Mars '73 and '75				Venus '70				Venus '72			
	Quan	Size	Weight (lbs)	Power (watts)	Quan	Size	Weight (lbs)	Power (watts)	Quan	Size	Weight (lbs)	Power (watts)	Quan	Size	Weight (lbs)	Power (watts)
Deep Space Transmission Subsystem																
1. S-Band Diplexer	2	6 x 3.25 x 2 in.	1	0	2	Same	—	—	2	Same	—	—	2	Same	—	—
2. Parabolic Antenna	1	10 ft. Dia.	32	0	1	Same	—	—	1	Same	—	—	1	Same	—	—
3. Omnidirectional S-Band Antenna	2	2.3 x 2.7 x 1.3 in.	2	0	2	Same	—	—	2	Same	—	—	2	Same	—	—
4. Transponder	2	184 cu in.	5.4	2	2	Same	—	—	2	Same	—	—	2	Same	—	—
5. Klystron	3	3 in. dia x 4 in.	1.5	6	3	Same	—	—	3	Same	—	—	3	Same	—	—
6. High Voltage Power Supply	2	4 x 4 x 6 in.	5	232	2	4 x 4 x 6 in.	5	140	2	4 x 4 x 6 in.	5	232	2	4 x 4 x 6 in.	5	140
7. Command Demodulator	2	4 x 4 x 5 in.	3	1.75	2	Same	—	—	2	Same	—	—	2	Same	—	—
8. RF Switch	1	2 x 2 x 2 in.	1	0	1	Same	—	—	1	Same	—	—	1	Same	—	—
Relay Transmission Subsystem																
9. VHF Antenna (Yagi)	1	13 ft x 2.1 ft x 2.1 ft	16	0	None	--	--	--	None	--	--	--	1	Same	—	—
10. VHF Antenna (Turnstile)	1	4.2 ft x 4.2 ft x 2.5 ft	5	0	1	Same	—	—	1	4 ft x 4 ft Dia	5	0	1	Same	—	—
11. VHF Diplexer	1	2 x 2 x 2 in.	1	0	None	--	--	--	None	--	--	--	1	Same	—	—
12. VHF Transmitter	1	1.3 x 3 x 3 in.	0.6	15	None	--	--	--	None	--	--	--	1	Same	—	—
13. VHF Receiver	4	7 x 4 x 2 in.	2	1.5	2	Same	—	—	1	Same	—	—	2	Same	—	—
14. Data Demodulator	2	6 x 5 x 3 in.	3.5	1.75	2	Same	—	—	1	Same	—	—	1	Same	—	—
Data Processing and Storage Subsystem																
15. Data Processing Unit	1	3 x 6 x 10 in.	12.25	2.5	1	Same	—	—	1	Same	—	—	1	Same	—	—
16. Multicoder	1	7 x 2 x 10 in.	10	1	None	--	--	--	1	Same	—	—	1	Same	—	—
17. Buffer Unit	1	3.5 x 2 x 10 in.	3.5	0.5	None	--	--	--	None	--	--	--	None	--	--	--
18. Thermoplastic Recording Unit	2	12 x 10 x 10 in.	25	25	1	Same	—	—	2	Same	—	—	1	Same	—	—

TABLE 1.1.4-1. SIZE, WEIGHT, AND POWER REQUIREMENTS FOR ORBITER COMMUNICATIONS SUBSYSTEM (Continued)

	Mars '69 and '71				Mars '73 and '75				Venus '70				Venus '72			
	Quan	Size	Weight (lbs)	Power (watts)	Quan	Size	Weight (lbs)	Power (watts)	Quan	Size	Weight (lbs)	Power (watts)	Quan	Size	Weight (lbs)	Power (watts)
Command and Computer Subsystem																
19. Command Decoder	1	2 x 2.5 x 10 in.	4	0.3	None	--	--	--	1	Same	Same	Same	1	Same	Same	Same
20. Command and Computer Equipment	1	3.5 x 10 x 10 in.	20	6.4	1	Same	Same	Same	1	Same	Same	Same	1	Same	Same	Same
21. Power Control and Conversion	1	3 x 10 x 10 in.	12	5	1	Same	Same	Same	1	Same	Same	Same	1	Same	Same	Same
22. PHP — Power Control and Conversion	1	2 x 2.5 x 11 in.	2	10	None	--	--	--	1	Same	Same	Same	1	Same	Same	Same

TABLE 1.1.4-2. SIZE, WEIGHT, AND POWER REQUIREMENTS FOR LANDER COMMUNICATIONS SUBSYSTEM

	Mars '69 and '71				Mars '73 and '75				Venus '70				Venus '72			
	Quan Per Lander	Size (in.)	Weight (lbs)	Power (watts)	Quan	Size (in.)	Weight (lbs)	Power (watts)	Quan	Size (in.)	Weight (lbs)	Power (watts)	Quan	Size (in.)	Weight (lbs)	Power (watts)
Relay Transmission Subsystem																
1. VHF Antenna System	1*	--	10	0	1	**	8	--	1 ¹ / ₂	--	10	0	1*	--	10	0
2. VHF Diplexer	1	2 x 2 x 2	1	0	None	--	--	--	None	--	--	--	1	Same	--	--
3. VHF Transmitter	1	3.5 x 3 x 3	1.3	115	1	2.5 x 3 x 3	0.95	115	1	3.5 x 3 x 3	1.3	115	1	3.5 x 3 x 3	1.3	115
4. VHF Receiver	1	7 x 4 x 2	2	2	None	--	--	--	None	--	--	--	1	Same	--	--
5. Command Demodulator	1	4 x 5 x 4	3	1.75	None	--	--	--	None	--	--	--	1	Same	--	--
Deep Space Transmission Subsystem																
6. S-Band Antenna	$\begin{Bmatrix} 1 \\ 1 \end{Bmatrix}$	$\begin{Bmatrix} 28 \times 3.3 \text{ Dia } 1969 \\ 33 \times 33 \times 9 \text{ } 1971 \end{Bmatrix}$	$\begin{Bmatrix} 4 \\ 10 \end{Bmatrix}$	$\begin{Bmatrix} 0 \\ 0 \end{Bmatrix}$	1	33 x 33 x 9	10	10	None	--	--	--	None	--	--	--
7. S-Band Omnidirectional Antenna	1	2.3 x 2.7 x 1.3	2	0	1	Same	--	--	None	--	--	--	None	--	--	--
8. S-Band Diplexer	1	6 x 3.25 x 2	1	0	2	Same	--	--	None	--	--	--	None	--	--	--
9. Transponder	1	184 cu in.	5.4	2	2	Same	--	--	None	--	--	--	None	--	--	--
10. Klystron	1	3 Dia x 4	1.5	6	3	Same	--	--	None	--	--	--	None	--	--	--
11. High Voltage Power Supply	1	4 x 4 x 6	5	280	2	Same	--	--	None	--	--	--	None	--	--	--
12. Command Demodulator	1	4 x 5 x 4	3	1.75	2	4 x 5 x 4	3	1.75	None	--	--	--	None	--	--	--
13. S-Band Switch	None	--	--	--	1	2 x 2 x 2	1	0	None	--	--	--	None	--	--	--
Command and Computer Subsystem																
14. Command and Computer Equipment	1	4 x 5 x 10	14	1.8	1	4 x 5 x 10	14	1.8	None	--	--	--	1	4 x 5 x 10	14	1.8
15. Sequence Timer	None	--	--	--	None	--	--	--	1	3 x 4 x 6	4	2.5	None	--	--	--
16. Power Control and Conversion Unit	1	3.5 x 5 x 11	7	10	1	Same	--	--	1	Same	--	--	1	Same	--	--

TABLE 1.1.4-2. SIZE, WEIGHT, AND POWER REQUIREMENTS FOR LANDER COMMUNICATIONS SUBSYSTEM (Continued)

	Mars '69 and '71				Mars '73 and '75				Venus '70				Venus '72			
	Quan Per Lander	Size (in.)	Weight (lbs)	Power (watts)	Quan	Size (in.)	Weight (lbs)	Power (watts)	Quan	Size (in.)	Weight (lbs)	Power (watts)	Quan	Size (in.)	Weight (lbs)	Power (watts)
Data Processing and Storage Subsystem																
17. Data Processing Unit	1	5 x 5 x 10	16	3.5	1	5 x 5 x 10	16	3.5	1	5 x 5 x 8	11	3.5	1	5 x 5 x 10	16	3.5
18. Buffer Storage Unit	1	3.5 x 2 x 10	3.5	0.5	1	Same	Same	Same	1	Same			1	Same		
19. Thermoplastic Recorder Unit	1	8 x 10 x 10	25	25	1	8 x 10 x 10	25	25	None	--	--	--	1	8 x 10 x 10	25	25
**"Transmission Line" and turnstile antenna																
***"Transmissior Line" antenna only																
-/- "Transmission Line" and whip antenna																

1.2 COMMAND AND COMPUTER SUBSYSTEM

This section covers the functional requirements for the Voyager Command and Computer Subsystem including the functions of command word reconstitution, command storage, subsystem time pulse generation, command selection and execution, and computation required by the vehicle for the operation of control functions, selection and operation of on-board equipment and control of acquisition of scientific and engineering data. The Power Conversion and Control Unit is also included in this subsystem.

1.2.1 DESCRIPTION

The functional requirement and operation of the Orbiter and Lander Command Subsystems are the same. Only the memory size needs to be changed in the Lander since fewer commands need to be stored. Therefore, there is no loss in completeness by limiting the following description to the Orbiter subsystem.

A. Functional

The Voyager Command and Computer Subsystem will be designed to perform the following functions:

- (1) Receive and verify command words, prepare the word format for use by the subsystem and determine if the command is to be stored or operated upon directly.
- (2) Store command words for later use by the vehicle and, in the case of the Orbiter Command and Computer Subsystem, to hold command words to be relayed to the Landers.
- (3) Generate and supply to the subsystems, timing pulses of required repetition rates and provide a present time clock for the timing and execution of stored commands.
- (4) Search the memory and retain the time tag and command for the next event to be executed.
- (5) Provide magnitude information to designated elements in the control system and provide decoded output with sufficient drive capability to operate command relays.
- (6) Compute a time increment, for certain data channels when selected, and add to the command's time tag before returning both to memory.

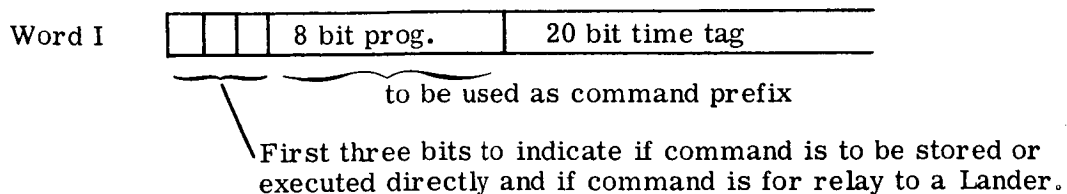
B. Block Diagram

The elements and their interconnections are shown in Figure 1.2.1-1.

C. Command Word Format

The command word formats with which this system will be required to operate are as follows:

Type I Command Input; Requires two words



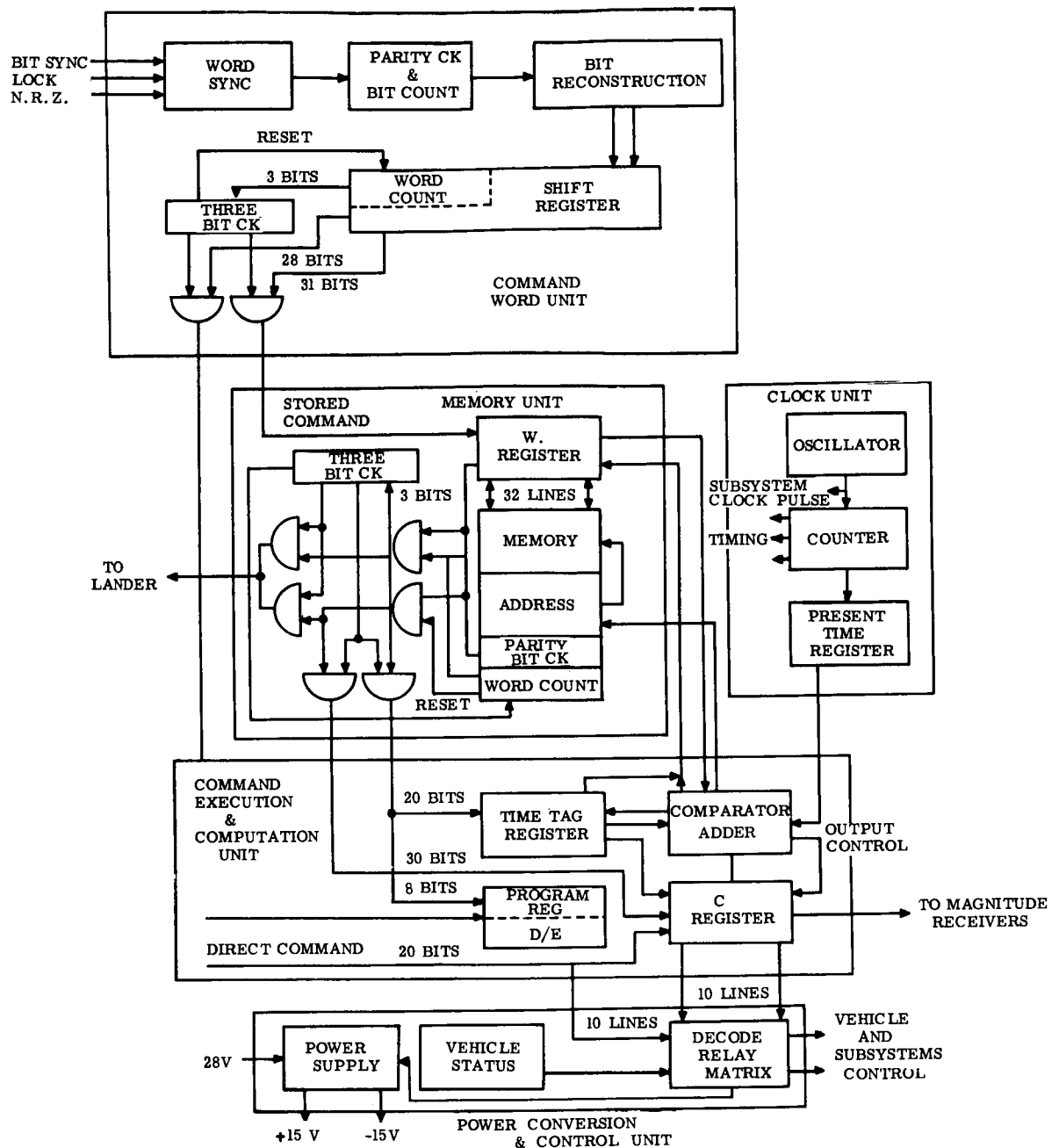
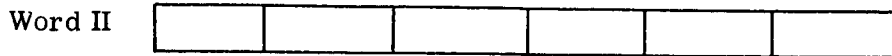
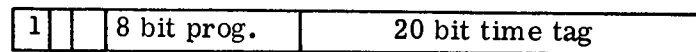


Figure 1.2.1-1. Block Diagram, Command and Computer Subsystem



Six 5-bit command suffix, or up to 30-bit magnitude word.

Type II Command Correction; Requires one word.



The code word indicates to the program encoder/decoder that the command stored with the same time tag is to be erased.

Type III Clear Commands stored; Requires 1 word



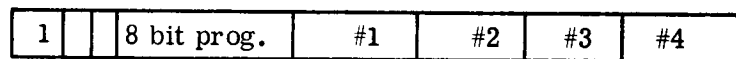
The code word indicates that all commands with time tags greater than the time given are to be erased.

Type IV Computer Constant; Requires 1 word



Provides, through the program decoder/encoder, the address for storing the magnitude word.

Type V Immediate Commands; Requires 1 word



Four, 5-bit command suffix words

Command prefix word

Indicated immediate action and along with the other two bits, indicates if it is for the Orbiter or for the Landers.

The first three bits, as indicated, are used to indicate the recipient of the following command. For the condition of one Orbiter and two Landers, the code assignment may be as follows:

000	Orbiter stored command
001	Lander #1 stored command
010	Lander #2 stored command
101	Lander #1 immediate command
110	Lander #2 immediate command
111	Orbiter immediate command

The next eight-bit program portion of the command word is used in conjunction with the Program Register Decoder/Encoder Unit. The eight-bit code may be partitioned into three groups as follows:

Group I:	From	00000000	32 code words to represent first half of the command word.
	To	00011111	
Group II:	From	00100000	96 to be reserved for use by the Command Subsystem; this is to include the computer operations.
	To	01111111	

Group III:	From	10000000	128 code words to be used to select
	To	11111111	data blocks for acquisition.

The following twenty-bit time tag, at a four-second time increment, will allow for a 48-day unambiguous command period. Second-half, or suffix, command words are decoded, five bits at a time, and used in conjunction with the outputs generated by the eight-bit program word.

1.2.2 MODES OF OPERATION

A. Command Acquisition

When a sub-carrier lock signal is received by the Command and Computer Subsystem, a search is initiated for a combination of incoming data in the form of 111000. This is the signal that the following data is to be interpreted as a command word. The Command and Computer Subsystem receives information from the Command Demodulator in a Manchester format at a command rate of ten bits per second. A command bit of data requires two Manchester bits of data, where certain combinations of bits in the Manchester code are recognized as errors. The system processes the Manchester data by bit counting, parity checking, and command-bit verification. It then converts the Manchester binary data to the conventional format and transfers the data to a shift register. Reject and accept signals are generated in the command acquisition phase.

With the command word in the shift register, the first three bits are checked and the appropriate output gate opened. If it is to be stored, the contents of the shift register are transferred to the "W" register in the Memory Unit. If the Command is to be operated on immediately, the eight-bit program word is sent to the Program Register Decoder/Encoder element and the twenty-bit suffix portion to the "C" register.

B. Command Storage

All command and control information is stored in the Memory Unit. Inputs are in serial form into the "W" registers and may be received from the following elements:

1. Shift register in the command word unit
2. Time tag register
3. Comparator/Adder
4. TPR Memory System

The information is transferred into the memory storage cells and received back through the "W" register.

Since command words are stored in pairs, a first-second word control is exercised over the decoding of the output of the "W" register. On the first word the first three bits are checked for the destination of the command. If, in the case of the Orbiter, it is an Orbiter command, then the next eight bits are sent to the Program Register and the following twenty to the time tag register. The second word is sent to the "C" Register. If the command is intended for a Lander and transmission to the Lander is available as indicated by the Vehicle Status Elements, then the two words are shifted out for relay via the communication link.

Computer words are stored in a separate part of the memory and are selected by direct addressing. Command words are selected through a sequential search. The output of the "W" Register is checked for parity. This check insures that the information has been properly stored and retrieved from the memory. Only command words to be sent out of the Command Storage Unit will contain a parity check bit.

C. Subsystem Time Pulse Generation (Clock Unit)

The clock unit, as indicated in the block diagram, is composed of three elements - the Oscillator, the Counter, and the Present Time Register.

(1) Oscillator

The Oscillator will be crystal-controlled with a long-term stability of 50 parts per million. The frequency selected is 524.29 kc, since this frequency is needed in other subsystems, such as digital TV. It also provides the standard binary number system.

(2) Counter

The functional requirement for multiplication by powers of two is performed by the Counter. With an input pulse period of 1.91 microseconds, all binary values up to one pulse in four seconds are available. The 0.125 second pulse period will be used in timing data acquisition in the Data Processing and Storage Subsystem. The shorter pulse periods will be used in timing the duration of commands used in the guidance subsystem and in the communication equipment.

(3) Present Time Register

The four-second pulse period output of the Counter is accumulated in the Present Time Register. This provides a continuous indication of elapsed time for the comparison of command time tags and for their execution. After 48.5 days the register will restart from zero. If stored commands span the time period when the register reverts to zero time, then the command search program must take this into account.

D. Command Selection and Execution

After a command has been executed, the subsystem will start a routine search of the Memory Element. The objective will be to locate the next command by finding the lowest time tag that is greater than the time given by the Present Time Register. The double constraint, of (1) lowest of all stored values and (2) greater than the value of the present time, allows command time tags to span the period when the clock restarts from zero.

Only Type I command inputs, containing two words, are kept in storage. The command search starts by extracting the first command encountered in the memory and storing both of its words in the appropriate registers: Three bits to the Three-Bit Check Register; eight bits to the Program Register; twenty bits to the Time Tag Register; thirty bits to the "C" register. The next command encountered is held in the "W" Register and its time tag compared with the one stored in the Time Tag Register. If it meets the conditions with respect to the Time Tag Register and the Present Time Register, then both its words are transferred out of the "W" Register, replacing the previous command which is then returned to the memory. If it does not meet the required conditions, it is transferred back to the memory, and the next command is similarly checked. Following this procedure, all of the stored commands are tested. After this search is concluded, the command to be executed next will be in the "C" Register, its program part in the Program Register, and the time of execution in the Time Tag Register.

With the search over, the comparator element determines when time for execution occurs. During this period, between search and execution, the only parts of the subsystem that are active are the Registers, the Comparator and Clock Unit. During this phase of the operation, the power expended is at a minimum, and increases only as a function of the command activity of the subsystem. At the time of execution, the program word in the Program Register Decoder/Encoder selects one out of 10 output lines. The second word in the "C" Register is decoded, five bits at a time, to select one out of another set of 10 lines. It is the combination of selected lines that, through the Decoder Relay Matrix, selects one out of 1024 output lines. After each selection, the word in the "C" Register is shifted, five bits at a time, so that each of the six parts may be decoded.

The vehicle status element is to be used to modify the operation of the Decoder Relay Matrix in accordance with the condition of the vehicle audit sensors. This allows for

interlocking of commands with system performance. It will also allow recalling subsystem commands as may be required by the vehicle.

E. Computation

Data acquisition, as a function of time, forms the basis for an on-board computational requirement. The routine operations during the transit phase will be accomplished by selecting from among preset modes. Once in orbit about the target planet, however, it may be found necessary to change the mode and rate at which data is acquired so as to adapt to the conditions actually observed.

The computer capability is inherently available with the elements required to perform the command function. This includes all elements with the exception of the following:

1. Vehicle Status
2. Decode Relay Matrix
3. All elements in the Command Word Unit

The essential changes are the addition of ADD logic to the Comparator element and the addition of related transfer and control lines. The limited forms of computation required allow the functional organization to be most efficient for the intended programs. Specialized instructions and programs will be written to take maximum advantage of the design.

The computational requirements are as follows:

1. Given selected sensor channels and assigned time increments, update the time tag of each selected channel by the assigned increment after the data has been obtained.
2. For orbital-sensitive channels, such as television pictures, radar mapping and infrared, the time increment for each succeeding operation will be computed by evaluating a polynomial with constants, related to the orbit obtained, to be supplied from earth. The time increment will be added to the time tag before it is returned to the memory.

The inclusion of the computer function in no way obstructs the Command Execution and Computation Unit to operate in either the stored pre-programmed mode or the direct command mode. It does, however, provide a degree of flexibility and adaptability that could only be achieved by expanding the storage capacity of the system and increasing the command load on the communication link.

1.2.3 SUBSYSTEM ELEMENTS

A. Command Word Unit

(1) Word Synchronization Element

The Command Demodulator extracts the Manchester bits and synchronization data from the received command signal. The Command and Computer Subsystem receives the data in the form of a sub-carrier lock indicator signal, bit sync and the Manchester representation of the command word. The function of the word sync is to determine the start of each word and forward the binary data and sync pulses to a Parity Check and Bit Count Element. The Word Sync Element is inhibited by the sub-carrier lock indicator until the receiver is locked to the received signal for more than ten seconds. The bit sync signal will always be present, but it will only be synchronous with the ground station when the sub-carrier is locked. The word sync will search the Manchester bits for a 111000 combination. Upon recognizing this format, the word sync unit will cause the appropriate registers

and counters to be reset to initial conditions. When commands are not being sent, all decoded Manchester bits will be zeros.

(2) Parity Check and Bit Count Element

The Parity Check and Bit Count Element verifies that an odd number of bits have changed or that a bit was lost. One-bit parity is used. A single flip-flop that is initialized before checking parity is sampled again after the command is received. A bit counter determines if the proper number of bits have been received, and also sends an end-of-word signal to other units.

(3) Bit Reconstruct Element

The function of the Bit Reconstruct Element is to change the Manchester bit information to a standard command format. It also provides a control pulse to a shift register where the data is stored. Upon receiving a "00" or a "11" combination which is not a valid command bit, all counters and registers are reset to initial conditions. The Bit Reconstruct Element provides an accept or reject output signal after receiving a valid command word having the proper bit count, parity, and binary format. The accept and reject signals are sampled by the Data Processing Subsystem so that a complete record of the command information is transmitted to the ground station.

(4) Shift Register Element

The Shift Register Element will accept the command word and shift pulse control from the Bit Reconstruct Element. Once in the shift register, the command word may be operated upon in accordance with the assigned format. For example, if it is the first word of a command (the first word being indicated by a word count flip-flop in the element) then the states of the first three bits are transmitted to the three-bit check element.

The output of the Shift Register Element is under the control of the Three-Bit Check Element. Depending on the code of the first three bits, the command will be shifted out as follows:

1. For a stored command, to the "W" Register in the Memory Unit. The second word will also take the same route.
2. For a direct command, bits four through eleven to the Program Register and bits twelve through thirty-one to the "C" Register, both in the Command Execution and Computer Unit. Since direct commands are one-word messages, the word count flip-flop will be reset after the transmission is completed. Transfer of information out of the Shift Register Element will be at the clock-pulse rate, 8.2 kilocycles.

(5) Three-Bit Check Element

In the event of a 111 input to the Three-Bit Check Element from the Shift Register Element, the decoded output will open the gate necessary for the routing of a direct command. After such a direct command has been shifted out, the Three-Bit Count Element will send a reset pulse to the word-count flip-flop.

Under all other codes, the contents of the Shift Register Element are transferred to the "W" Register in the Memory Unit.

B. Memory Unit

(1) "W" Register Element

This Element will receive data in serial form from the Command Word Unit and from the Command Execution and Computation Unit. It will provide serial data output to the Command Execution and Computation Unit and to the Lander Communication Link. Internal transfer of data to and from the Memory Element will be in parallel form.

Through its connection with the Command Execution and Computation Unit, the "W" Register will be used as a part of the computer mechanization as well as to provide access to stored data. During the command search phase, the contents of the Memory Element as sequentially held by the "W" Register are compared with the Time Tag Register and with the Present Time Register.

Transfer of information into and out of the "W" Register will be at the clock-pulse rate of 8.2 kilocycles.

(2) Memory Element

The Memory Element will store command words, computer words and interim results from the computer. Data access to the memory is in parallel through the "W" Register. A word-organized magnetic storage implementation will be used.

If a non-destruct read-out technique is available, (as is presently under development for NASA by UNIVAC), the time for the memory search function will be reduced. With a non-destruct readout, only the selected Time Tag need be retained while the search looks for the lowest time value. When the search is completed, the memory will be re-cycled to the location of the lowest value, the complete command words read out to the appropriate registers, and the contents of the selected memory address erased.

If it is necessary to use a read-write destruct memory, the number of shift and write operations will be increased. In either case, the memory is cycled once to locate the next command and then waits for the selected event to occur. During this period, the power expenditure will be that necessary to bias off all drive and sense circuits.

The determination of the time required for a command search is as follows:

(a) For a non-destruct read memory. Given a memory of "N" word capacity, $N/2$ words will be read and compared with the contents of the two time registers. To read a word takes one clock period; to make a comparison requires a clock period for each bit of the time tag. If it is assumed that half the tags encountered are less than the one held in the Time Tag Register, then this will require $N/4$ shifts. At this point the search is done, but now the memory must be recalled to the address of the last time tag transferred into the Time Tag Register. At this time, the eight bits of the program and the thirty bits of the second word are read out and shifted to the appropriate registers. The average total time is then $(N/2 + 2 N/2B + N/4 B + 1 + 8 + 30) t$ where B is the number of bits in the time tag and t is the clock period. For the values $N = 512$, $B = 20$ and $t = 122.07$ microseconds, the average time will be 1.6 seconds. If the 200 addresses reserved for Lander storage are excluded from the search, the average time will be 1.01 seconds.

(b) For a read-write destruct memory. Given the same size memory, the sequence of operations will be the same with the exception that each memory read cycle must be followed by a write period. For a complete search, the average time will be 1.64 seconds and for a search excluding Lander addresses the time will be 1.04 seconds.

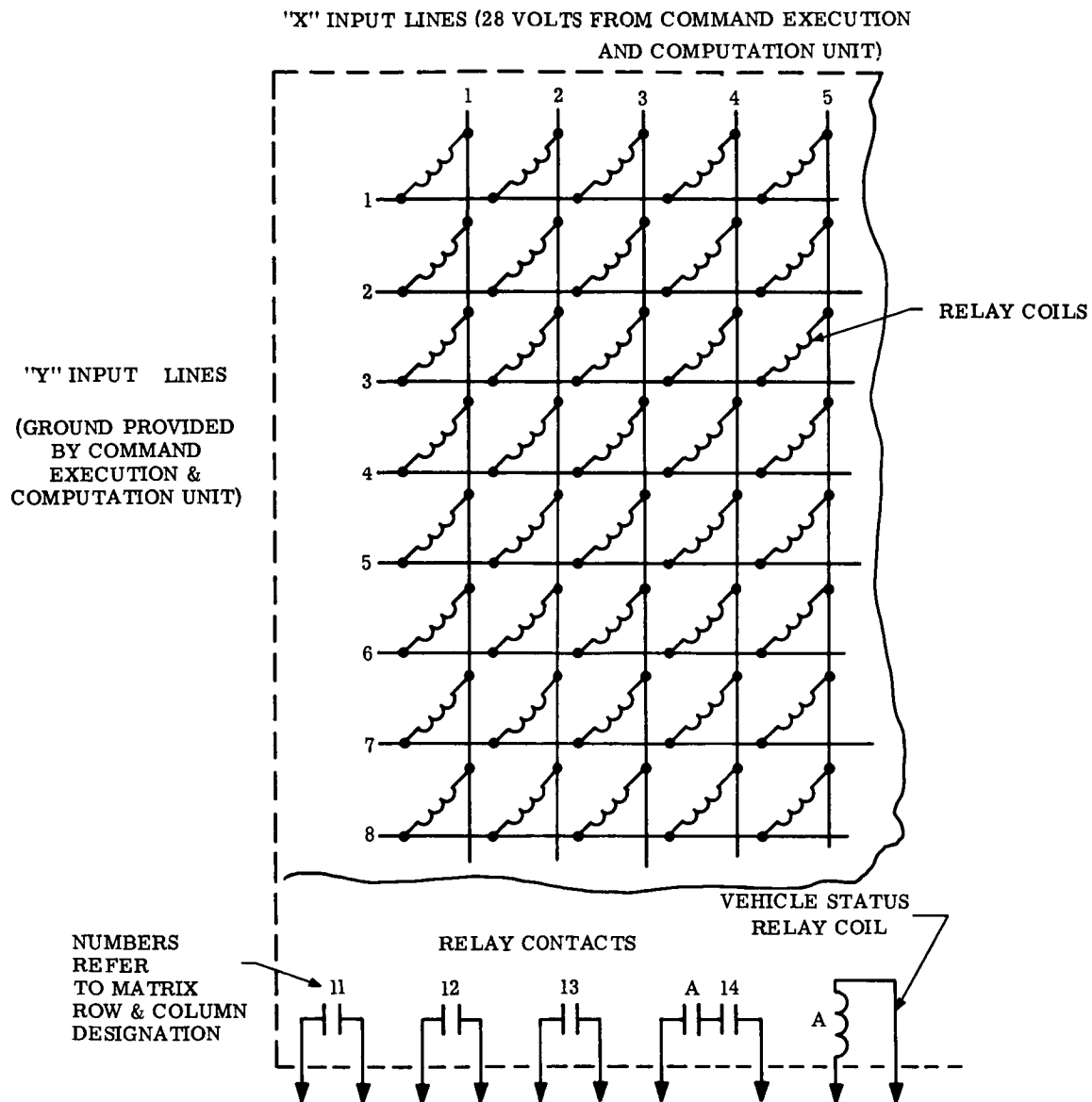


Figure 1.2.3-1. Relay Matrix for Power Conversion and Control Unit

(3) Address Element

During memory search, the addresses are selected in serial order. Then a time tag is located that is to be transferred to the Time Tag Register and the address of the location is stored in the Address Element. The search is then continued, with the Address Element taking on the value of any new location found to be a better fit to the selection criteria. After the search, the Address Element is used to relocate the desired command words.

(4) Parity Bit Check Element

All words read out of the Memory Element through the "W" Register will be checked by the Parity Bit Check Element. A loss of parity will indicate a fault in the system and this will be reported to earth by way of the telemetry. The internal action to be taken will depend on the type of redundancy to be used.

(5) Word Count Element

Since command words are stored in pairs, the Word Count Element will be used to indicate first or second word to the output control gates. During memory search, this Element will be used to gate the selection of only the time-tag word for read-out.

(6) Three-Bit Check Element

The function of this Element in the Memory Unit is to separate Lander and Orbiter commands. Lander command codes are used to set a flip-flop and open the gates to the Lander Communication Link. After the second word, the flip-flop is reset by a pulse from the Word Count Element. It is this decoding action taken on the first three bits that can be used to block Lander commands from the Command Search Sequence.

C. Clock Unit

(1) Oscillator Element

The highest frequency available to the subsystem will be generated by a crystal-controlled oscillator. The frequency of operation will be 524.29 kc, and the stability will be $\pm 0.005\%$ over all environmental conditions. Division of this frequency by 64 will produce the required subsystem clock frequency of 8.2 kc.

Output of the oscillator will be used to drive the Counter Element and through buffer amplifiers supply clock pulses to the subsystem.

(2) Counter Element

The Counter Element will be a series of flip-flops which will divide the input frequency down to one output pulse every four seconds. This will require fifteen stages. The output will be sent to the Present Time Register Element. Of all the other frequencies available, only a few will be required for the subsystem. The pulses will be amplified before being sent out of the Clock Unit.

(3) Present Time Register Element

The Present Time Register Element accumulates the Counter output and presents to the Comparator/Adder a continuous indication of the elapsed time. For a twenty-bit register and a four-second time increment, the maximum time period that can be indicated will be 48.5 days. At that time, the register will revert to zero and start over.

D. Command Execution and Computation Unit

(1) Time Tag Register Element

This register, twenty bits in length, will be capable of receiving data in serial form from the memory unit and from the Comparator/Adder Element. Outputs, also in serial form, may go to the Memory Unit, to the Comparator/Adder Element, and to the "C" Register Element. Shift pulse rate will be at the 8.2 kc clock frequency.

(2) Program Register - Decoder/Encoder Element

The eight-bit program word is held in the Register and decoded to determine the type of control required. The decoded command will be distributed to the elements to be controlled. In the case of decoded commands related to the computer function, an encoded output may be required. The encoded output may be used to select addresses in the Memory Unit and to set new program words into the Program Register.

Under the condition that an immediate command is to be executed when there is a program word in the Register, an eight-bit temporary storage will be required.

(3) "C" Register Element

The "C" Register Element will be thirty bits in length and will receive data in serial form. Inputs will be obtained from (a) the Command Word Unit (on immediate command); (b) the Memory Unit (on stored command); (c) the Time Tag Register when performing computation; and (d) the "C" Register output so as to be able to do shift and restore operations. Outputs are sent in serial form (a) to the Comparator/Adder; (b) the magnitude receivers in the vehicle control subsystem; and (c) in parallel, five bits at a time, to the Decode Relay Matrix Element. Shift pulse rate will be at the 8.2 kc clock frequency.

Magnitude receivers in the control subsystem can have two functions. In the first case they serve to hold a reference number such as an angular position. In the second case they serve to measure a time duration. This is done by counting down the number held. For this function, any binary rate up to 524.29 kc can be used. In this way the time duration of the command may be accomplished within a wide selection of time resolutions.

(4) Comparator/Adder Element

Under the condition of command search, inputs are taken from the "W" Register, Time Tag Register, and the Present Time Register. Inputs are taken in serial form, most significant bit first. With the first located time tag in the Time Tag Register, the succeeding time tags in the "W" Register are checked by the logic in the Comparator/Adder Element to determine if it is less than the contents of the Time Tag Register and equal to or greater than the contents of the Present Time Register. The output generated by this check will determine if the address of the word in the "W" Register should be retained in the Address Element and its contents be transferred to the Time Tag Register.

For the condition of command execution, the contents of the Time Tag Register and the Present Time Register are compared and, at the time of coincidence, produce an output pulse. This pulse will allow the output of the "C" Register Element and Decode Relay Matrix Element to go to the vehicle and other subsystems.

For the computational requirements, the Comparator/Adder Element will, under the control of the Program Register Decoder/Encoder, do the following:

1. Add the contents of the "W" Register to the contents of Time Tag Registers.

2. Subtract the contents of the "W" Register from the contents of Time Tag Register.
3. Multiply the contents of the "W" Register by the contents of the "C" Register. This is done by successively adding the contents of "W" Register and Time Tag Register, shifting the contents of the Time Tag Register one bit after each cycle. The add and shift are done under the control of the "C" Register.

E. Power Conversion and Control Unit

The Power Conversion and Control Unit in the Orbiter main body and on the PHP will switch voltages to the various units controlled by the Command and Computer Subsystem and also provide regulated voltages to the transponder Command/Data Demodulator and the VHF transmitter.

The inputs to this Unit will be from the Decoder/Encoder Element and the "C" Register of the Command Execution and Computation Unit, 28 volts d. c. from the vehicle power supply and approximately nine vehicle status inputs. The output functions are the opening and closing of relay contacts, regulated voltages for the above-mentioned units and various changes of state in the Communications Subsystem in response to the vehicle status inputs. The vehicle status inputs which cause several operations to take place automatically can be overruled by the Command Subsystem. Thus, with this unit and the Command and Computation Subsystem, a very flexible and adaptable system is realized, which can perform almost without direction from the earth or be controlled directly from earth.

Ten lines, received from each element, are decoded to select one of thirty-two input lines. The total number of line intersections for the Orbiter form a 32 x 32 matrix of 1024 intersections. In the Lander only 512 are needed.

The relay control for the Orbiter Main Body will be implemented as shown in Figure 1.2.3-1. An "X" input (28 v.) and a "Y" input (ground) are required to energize the coil at the intersection of the respective input lines. All relays will be of the magnetic latching type, and the voltage must be present for 30 milliseconds to change the state of a relay. If more than one function is required at a time, more than one coil can be placed at the proper intersection in the matrix. Other basic logic operations can be performed in this unit such as interlock functions and automatic commands in response to vehicle status. It is envisioned that various relay logic modes will be changed from flight to flight and therefore the design allows changing the interconnection circuits quite easily.

The power supply in the unit in the Main Body of the Orbiter will have the following outputs:

+ 15 v.	60 ma.	} 1% Regulation
- 15 v.	360 ma.	

The power supply in the PHP unit will have the following output:

+ 50 v.	300 ma.	1% Regulation
---------	---------	---------------

The design of the power supply will be based on a pulse-width modulated (PWM) constant-frequency primary voltage. A reference voltage on the secondary of the transformer will be used to attain the desired regulation by varying the width of the pulses in the PWM waveform. The unit will have an input line filter to isolate it from noise and switching transients. The unit will be designed for an input voltage variation of $\pm 10\%$. Each output will be separately rectified, filtered and further regulated to provide the required regulation and minimum ripple voltage.

F. Vehicle Status Element

The Vehicle Status Element gives the Command and Computer Subsystem the capability to adjust to requirements or signals received from other subsystems. It has two functions: (1) an input can cause a latching relay to go to a specific condition, regardless of any normal command generated by the Command and Computer Subsystem; (2) it can prevent an electrical system from operating until a specific signal or group of signals is received by the Vehicle Status Element. A command word will be available which will disconnect the Vehicle Status Element.

Typical inputs to the Vehicle Status Unit are given in Table 1.2.3-1. Additional requirements can also be accommodated since the inputs cause a relay or set of relay contacts to close, open, or be inhibited, and this is accomplished by making the proper connections into the relay matrix.

TABLE 1.2.3-1. TYPICAL VEHICLE STATUS INPUTS

<u>INPUTS</u>	<u>RESULTANT ACTION</u>
1. Sun gate or Canopus gate off.	Telemetry turned on, G&C information mode.
2. VHF Data Demodulator PN sync.	Command subsystem transmits Lander commands.
3. Lander Separation signal.	Command transmissions via hardwire to Lander inhibited.
4. High-gain antenna stowed.	S-Band transmission subsystem inhibited through 10-ft dish.
5. Command Demodulator Synchronization #1 or #2.	Transmit telemetry data.
6. Light Level, Nadir Vidicon.	Inhibits camera sequence until sufficient light is present.

G. Sequence Timer for Venus 1970 Lander

The following covers the functional requirement for the Voyager Lander Sequence Timer including the functions of vehicle event timing, mode selection, and timing for the Data Processing and Storage Subsystem. This will replace the Command and Computer Subsystem on the Venus 1970 Lander, since its short lifetime precludes the transmission of commands to it.

The operational life of the Lander is divided into the four modes as follows:

- | | |
|-----------|---|
| Mode I: | Transit phase from initiation of separation from Orbiter until the start of entry into the planet's atmosphere. |
| Mode II: | Black-out phase from entry until deceleration is below 0.1 g. |
| Mode III: | Descent phase from the end of blackout until impact. |
| Mode IV: | Terminal phase from impact until the end of life of the vehicle. |

The Sequence Timer Subsystem will be designed to perform the following functions:

- (1) To receive from the Orbiter Command and Computer Subsystem a start pulse to initiate the launch and data acquisition sequences. To receive from a 0.1 g accelerometer a signal to indicate the start of the entry phase. To receive from an impact sensor a signal to indicate that the vehicle has landed.
- (2) To generate timing signals for this unit and for the Data Processing and Storage Subsystem.
- (3) To generate timing pulses required for vehicle launch and transit operation.
- (4) To generate Mode I timing signals and to switch in sequence, as a function of sensor inputs, to Mode II, Mode III and Mode IV.

The elements and their interconnection are shown in Figure 1.2.3-2.

(a) Modes of Operation

1) Mode I

Basic timing for this subsystem and for the Data Processing and Storage Subsystem is generated by an oscillator at 24 kilocycles per second. For use by the Sequence Timer, this is counted down by a factor of 2^{15} to produce a pulse output of 0.73 seconds duration. At the start flip-flop A, upon an input command, will gate the pulses into the counter element.

The Mode I output is a series of pulses of 175 seconds duration at a pulse interval period of 0.778 hours. The pulse duration is controlled by the seven-bit portion, the pulse interval period is controlled by the five-bit portion.

During the first Mode I pulse period, the In-flight Disconnect, Separation Bolt Firing, Lander Spin-up, and ΔV Rocket Firing events are sequenced. These events occur at the eighth, ninth, tenth, and ninety-eighth time increment from start.

During the fourth Mode I pulse period and at the ninety-eighth time increment, the aft fairing separation signal is generated.

At the eighth pulse period, the gates that control the events as a function of time increments are turned off by flip-flop B, and the "g" sensor gates are enabled. The pulse period selection is done by the last three bits of the counter element. Mode I output is available until the 0.1 g. accelerometer produces an input.

2) Mode II

At the time of a 0.1 g accelerometer input, and with its gate enabled, the C flip-flop is set to switch the output from the Mode I gate to the Mode II gate. This output is continuous and will last as long as there is an accelerometer input.

3) Mode III

At the end of the 0.1 g accelerometer input the Mode II gate will be closed. The condition of the sensor flip-flop C in the one state and the input at zero will, through the inverter, cause the Mode III gate to open and produce a continuous output.



4) Mode IV

On impact, an impact sensor input will set flip-flop D to the "one" state. The flip-flop "one" is the Mode IV output. The "zero" side will close the Mode II and III gate and hence block their output.

(b) Unit Elements

1) Oscillator Element

The Oscillator Element will generate and provide as an output a 24 kilocycle per second square wave for use by the Count Down Element and by the Data Processing and Storage Subsystem.

2) Count Down Element

The input from the Oscillator Element will be used to drive a series chain of fifteen flip-flops. The output, a square wave of 1.37 seconds duration from the last flip-flop, represents the basic time increment used in this unit. Output of the Count Down Element is gated by the start flip-flop A.

3) Counter Element

Input is from the Count Down Element after the start command has been received. The counter (made up of fifteen flip-flops) provides through suitable decoding networks on the first seven flip-flops, an output of 0.68 seconds duration when the eighth, ninth, tenth and ninety-eighth input time increments are counted. These outputs, through the Event Control Elements, are used to time Lander functions.

The next five flip-flops are decoded to provide a pulse of 175 seconds duration with a repetition period of 0.778 hours. This output is required by the Data Processing and Storage Subsystem during Mode I operation.

The last three flip-flops are used to provide three timing control signals. The first output is at the time of the first pulse sent to the DPSS. The second output is available during the fourth DPSS pulse. The third output is at the eighth DPSS pulse. All three outputs are sent to the Event Control Element.

4) Event Control Element

Inputs to the Event Control Element are from the Counter Element (8 inputs), from the 0.1 g accelerometer and from the impact sensor. Mode output signals are a logical function of the inputs. The conditions for each mode output are as follows:

<u>Mode</u>	<u>Condition</u>
I	Start and no 0.1 g signal
II	Start, 0.1 g signal, and no impact signal
III	Start, 0.1 g signal occurred, and no impact signal
IV	Start, and impact signal

Vehicle event outputs have sufficient power capability to operate relays. In-flight Disconnect, Separation Bolt Firing, Lander Spin-up, and ΔV Rocket Firing signals are available only during the first DPSS pulse period. The aft fairing separation signal is available only during the fourth DPSS pulse period.

H. Power Supply

The Command and Computer Subsystem consists of basically digital logic circuits such as one-shots, flip-flops and NAND gates. These circuits are susceptible to noisy power supply voltages and ground. To insure that the Command and Computer Subsystem is not sensitive to system voltage variations, a self-contained power supply having a large immunity to variations on the power source is included. Low-impedance distribution lines and capacitive filtering are provided on the voltage and ground lines to further reduce the electrical noise problem. The built-in power supply also reduces the probability of transients from the Command and Computer Subsystem interfering with other equipment.

1.2.4 IMPLEMENTATION

The Command and Computer Subsystem study effort did not permit a detailed logic and circuit design, thus the reliability, size, weight, and power figures are estimates of an implementation that would satisfy the system requirements. The following sections discuss the implementation of the Command and Computer Subsystem by using thin-film circuits with discrete components.

A. Equipment Location

Since the Orbiter has a Main Body - PHP joint, separate equipment is required in the PHP. Approximately thirty wires are required across the joint, and this number will increase if a significant number of vehicle status signals are to be included.

The equipment on the Orbiter and Lander use basically the same parts and logic. The difference is in the number of outputs and in the storage requirements. The block diagram shown in Figure 1.2.1-1 applies to both systems.

B. Majority Logic and Redundancy

Majority Logic and Redundancy are built into the Command and Computer Subsystem wherever a component failure would constitute a mission failure. The Command Word Unit processes the incoming commands and verifies that the command is correct. Majority logic is used to insure that the subsystem reliability is much greater than the reliability of the command data.

The Memory Unit consists of three 16,000-bit redundant units which can be used independently. Parity is checked on each command read from the memory. The clock unit incorporates majority logic techniques similar to those used in the Data Processing Subsystem. The Command Execution and Computation Unit uses majority logic except where alternate or redundant data paths are provided. The Decode Relay Matrix and Vehicle Status Units are redundant in only the critical relays. A back-up mode is provided such that the Vehicle Status Unit can be disconnected.

C. Size, Weight and Power

The size, weight, and power of the Command and Computer Subsystem are based on the use of thin-film circuits containing discrete active devices. A standard flip-flop containing two transistors requires approximately 0.22 cubic inches, 0.96 ounces and two milliwatts. The size and weight estimates include all connectors, harness, container, etc. The memory size, weight, and power are based on the published literature and an informal discussion with UNIVAC. See the following section on Producibility.

The Orbiter Command and Computer Subsystem contains 1000 circuits not including the UNIVAC memory, requires a total of 350 cubic inches, weighs 20 pounds and requires 2.5 watts.

Table 1.2.4-1. Size, Weight and Power of Three Units.

<u>EQUIPMENT</u>	<u>LOCATION</u>	<u>SIZE</u>	<u>WEIGHT</u>	<u>POWER</u>
1. Electronics	Orbiter - Main	350 in. ³	20 lb	2.5 watts
2. Power Conversion and Control Unit	Orbiter - Main	300 in. ³	12 lb	5.0 watts*
3. Electronics	Orbiter - PHP	50 in. ³	4 lb	0.3 watts
4. Power Conversion and Control Unit	Orbiter - PHP	55 in. ³	2 lb	10 watts*
TOTAL ORBITER		755 in. ³	38 lb	2.8 watts
5. Electronics	Lander	200 in. ³	14 lb	1.8 watts
6. Power Conversion and Control Unit	Lander	175 in. ³	7 lb	10.0 watts*
TOTAL LANDER		375 in. ³	21 lb	1.8 watts

* This power is dissipated in the Power Supply in the PC&C Unit and is not charged to the Command and Computer Subsystem Power.

The weight and size of the relays are not included since they are included in the Power Conversion and Control Unit. The PHP section of the Orbiter Command and Computer Subsystem requires 120 circuits, 50 cubic inches, 4 pounds and 0.3 watts. Each Lander requires 800 circuits, 200 cubic inches, 14 pounds and 1.8 watts.

Since the Command and Computer Subsystem must control currents as high as two amps, it is desirable to implement the Decode Relay Matrix and Vehicle Status Units in the Power Conversion and Control Unit with high reliability latching relays. The size, weight and power requirements of the three units are given in Table 1.2.4-1.

D. Producibility

The logic circuits and the packaging techniques which are recommended for the implementation of the Command and Computer Subsystem are discussed in detail in the description of the Data Processing and Storage Subsystem (see section 1.3.3-G).

The Memory Unit of the system requires 16,000-bit non-destructive read-out memories that operate at a low data rate. Although many types of memories would be acceptable in this application, a core memory offers many advantages. The primary advantage to Voyager is that it can store data without power, thus keeping the system power requirements to a minimum. Also, the reliability of a core memory is superior to a tape recorder.

Many vendors can satisfy the memory requirements, but at the present the UNIVAC Division of the Sperry Rand Corporation has a memory system with very low power requirements, small size, low weight, and a non-destructive read-out capability. The published data provided by UNIVAC in Blue Bell, Pennsylvania is summarized in Table 1.2.4-2. It discusses a 100,000 bit magnetic thin-film plated wire spacecraft memory presently being developed for the National Aeronautics and Space Administration. The approximate cost per bit will be twenty cents after the initial prototype for NASA is completed in March 1964.

TABLE 1.2.4-2

THIN-FILM PLATED-WIRE MEMORY CHARACTERISTICS

Capacity	10^5 Bit (nondestructive)
Power Consumption	133 milliwatts
Weight	3.5 pounds
Volume	70 cubic inches
Temperature Range	-25°C to $+100^{\circ}\text{C}$ (operating)
Output Signal	+15 millivolts "1" -15 millivolts "0"

1.2.5 RELIABILITY

The selection of thin-film technology and the forms of redundancy used are based on a best estimate of the components required for the implementation of this subsystem. Since reliability is a sensitive function of the components used, it may be necessary to review this decision when a more detailed logic design is available. For any one implementation, the predicted values of size, weight, power and reliability will be different and for a comparison to be valid, the logic must be sufficiently detailed to indicate all required components. The techniques or implementation that are available are as follows:

- (1) Standard components
- (2) Thin-film circuits
- (3) Functional electronic blocks (microelectronics)
- (4) Magnetic core circuits

Each of the above will have specific advantages depending on the application and the design objectives. A design study with each as the predominant component will indicate which is best suited for the subsystem or for its elements. It will be at this point that the level of redundancy required to meet the subsystem specification can be determined. One form that this may take is at the component level. Redundancy at the element or unit level can be effected by the subsystem organization. For example, since direct command can be performed by using only a portion of the elements involved, switching of some redundant parts may be accomplished through the Decoder Relay Matrix Element. Other elements may require triplication because of the essential functions they perform.

Reliability, as one of the design objectives, must take into account the effects of the anticipated in-flight radiation on the components used. Even within one class of components, functional electronic blocks for example, this effect can be widely different for units made by different manufacturers. The selection of a suitable set will require a detailed search of the pertinent information available or a separate evaluation test program.

1.2.6 CRITICAL COMPONENTS

The components which are recommended for the Command and Computer Subsystem have been selected to tolerate the environmental, sterilization, and reliability requirements. Although the Voyager system offers some complex development problems, they should not be considered critical in a twenty-four month development program. The UNIVAC memory system is presently ahead of schedule, and should be a practical memory for the system.

1.3 DATA PROCESSING AND STORAGE SUBSYSTEM

1.3.1 SUBSYSTEM REQUIREMENTS

The Data Processing and Storage Subsystems on the Voyager Landers and Orbiters are the gathering points for all data including diagnostic, scientific, and television information which is to be prepared for transmission to earth. As such, extreme flexibility and reliability are imperative to mission success: the derivation of both characteristics will be discussed specifically in later portions of this section.

In general, the Voyager Data Processing and Storage Subsystem is required to perform the following functions: It must sample selected groups of scientific and diagnostic data inputs from other subsystems, digitize those inputs which are analog voltages, organize the data into identified frames and route the resultant information into the storage unit, to the transmitter, or both, at the desired data rate. It must be capable of storing large quantities (10^9 bits) of digital television data at variable bit rates up to 300 kilobits/sec in addition to the vehicle data. On command it must read out both TV and a relatively small quantity of vehicle data, pseudo noise and Manchester coded for transmission, to the transmitting equipment at the desired bit rate. It must be capable of generating error control code groups for all links transmitting directly to earth.

The Data Processing and Storage Subsystem must be capable of meeting the environments of launch, transit, entry and impact and will, accordingly, be designed to operate through the following specific environments:

1. High Temperature	71°C
2. Low Temperature	-10°C
3. Shock	125 g's
4. Vibration	0.2 g ² /cps
5. Acceleration	300 g's
6. Integrated Neutron Radiation	10^{14} - 10^{15} nvt
7. Integrated Gamma Radiation	10^5 rads (10^4 rads/hr max)

The equipment will be designed to operate for the mission duration in a vacuum environment without physical or operational degradation.

1.3.2 SUBSYSTEM OPERATION

It will be found in reading the following sections that the Voyager Data Processing and Storage Subsystem is very adaptable, and its operation can vary greatly from mission to mission without affecting the size or type of either the Storage Unit or the Data Processing Unit. Accordingly, the discussion of subsystem operation will be quite general, using storage capacity figures for the Mars 1969 mission.

A. Orbiter Subsystem Operation

The Orbiter Subsystem block diagram is shown in Figure 1.3.2-1. The subsystem consists of the Data Processing Unit, two thermoplastic recorders (TPR), and a 100-kilobit buffer. Each of the TPR's has a storage capacity of 10^9 bits of data. The use of two recorders improves reliability through component redundancy and provides the capability of storing data from two sources simultaneously, e.g., data received simultaneously from both Landers between time of separation and impact. The 100-kilobit buffer (discussed in Section 1.2) is small, lightweight and has an extremely low operating power requirement (0.25 watts). It is utilized for two purposes: First, it provides temporary storage for data sampled at low rates thereby eliminating the need for the comparatively high-powered (25-watt) TPR's to record this data. Second, it provides speed differential

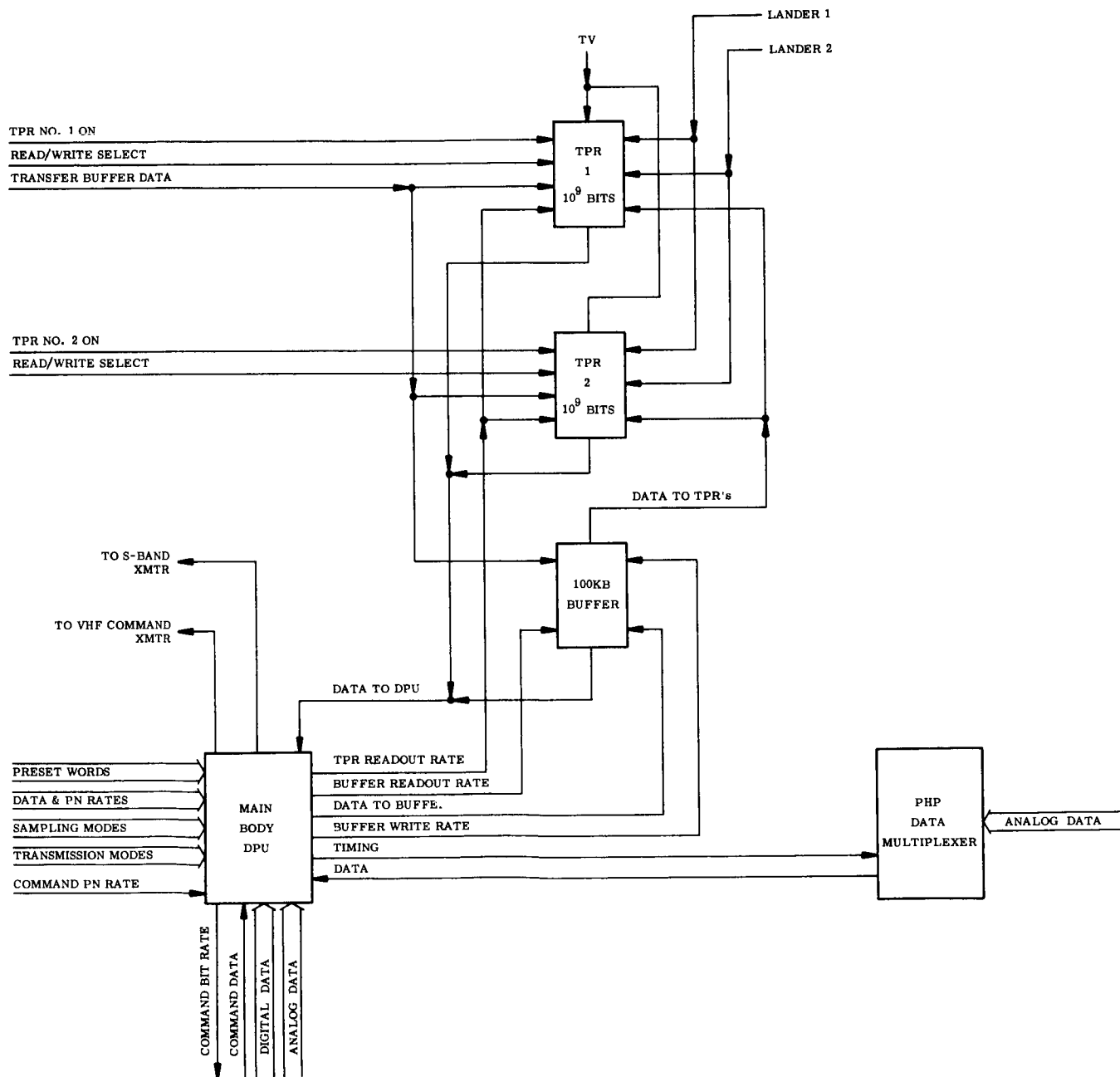


Figure 1.3.2-1. Data Processing and Storage Subsystem, Mars 1969 Orbiter

buffering between the Data Processing Unit (DPU) and the Error Control Generator. It is shown in Figure 1.3.2-2 that the Data Processing and Storage Subsystem is operated through the Command & Computer Subsystem. Sequencing of input data sources, selection of sampling rates, data formats, and data routing are requested by the Command Subsystem and fulfilled by the DPU. Likewise, selection of data sources for transmission, control of data encoding, and selection of transmission rates is performed by the DPU upon request from the Command & Computer Subsystem. In addition, command data to the Landers is pseudo-noise (PN) and Manchester coded in the DPU and routed to the command transmitters at the proper data rate.

B. Lander Subsystem Operation

The Lander Subsystem block diagram is shown in Figure 1.3.2-2. As in the Orbiter, the subsystem obtains all its operational inputs from the Command Subsystem. Its functions, with respect to sampling and transmission control are also similar to Orbiter operation. The Lander, however, requires only a 10^7 bit maximum storage capacity for collection of data after impact.

The 100 kilobit recorder will be of the type used in the Orbiter. In addition to the desirable physical characteristics mentioned, it also provides non-destructive readout so that data may be re-transmitted after impact if desired, and non-volatile storage which prevents loss of data in event of power interruption upon impact. The Lander DPU will provide PN and Manchester coding for data transmitted in the direct link with capability of addition of error control coding upon command.

Detailed descriptions of the Data Processing and Storage Units follow.

1.3.3 DATA PROCESSING UNIT

A. Functional Capabilities

Specifically, the data processing unit will perform the following functions:

1. It will accept:
 - a. High-level analog inputs, 0-5vdc
 - b. Low-level analog inputs 0-50 mv dc
 - c. Digital data
 - d. Event occurrence pulses.

The analog voltages will be converted in the data multiplexer to a six-bit digital equivalent, thereby providing a measurement resolution of 1.6%.

2. It will assemble the data into frames containing 1024 words, uniquely locating the data from each of the input lines within the frame.
3. It will generate any one of many programmed sampling modes upon receipt of a mode-select pulse and preset word from the Command and Computer Subsystem. A mode is defined as a particular combination of frame format and bit rate. The basic frame consists of 1024 words, each from a different input line. The format may be changed by sampling sub-groups of the total 1024 more often than once per frame, e.g., 512 inputs sampled twice per frame, 32 inputs sampled 32 times per frame, etc. The ability to create a variety of modes during a mission permits most efficient use of the Data Processor through format control, and flexibility of sampling rate through

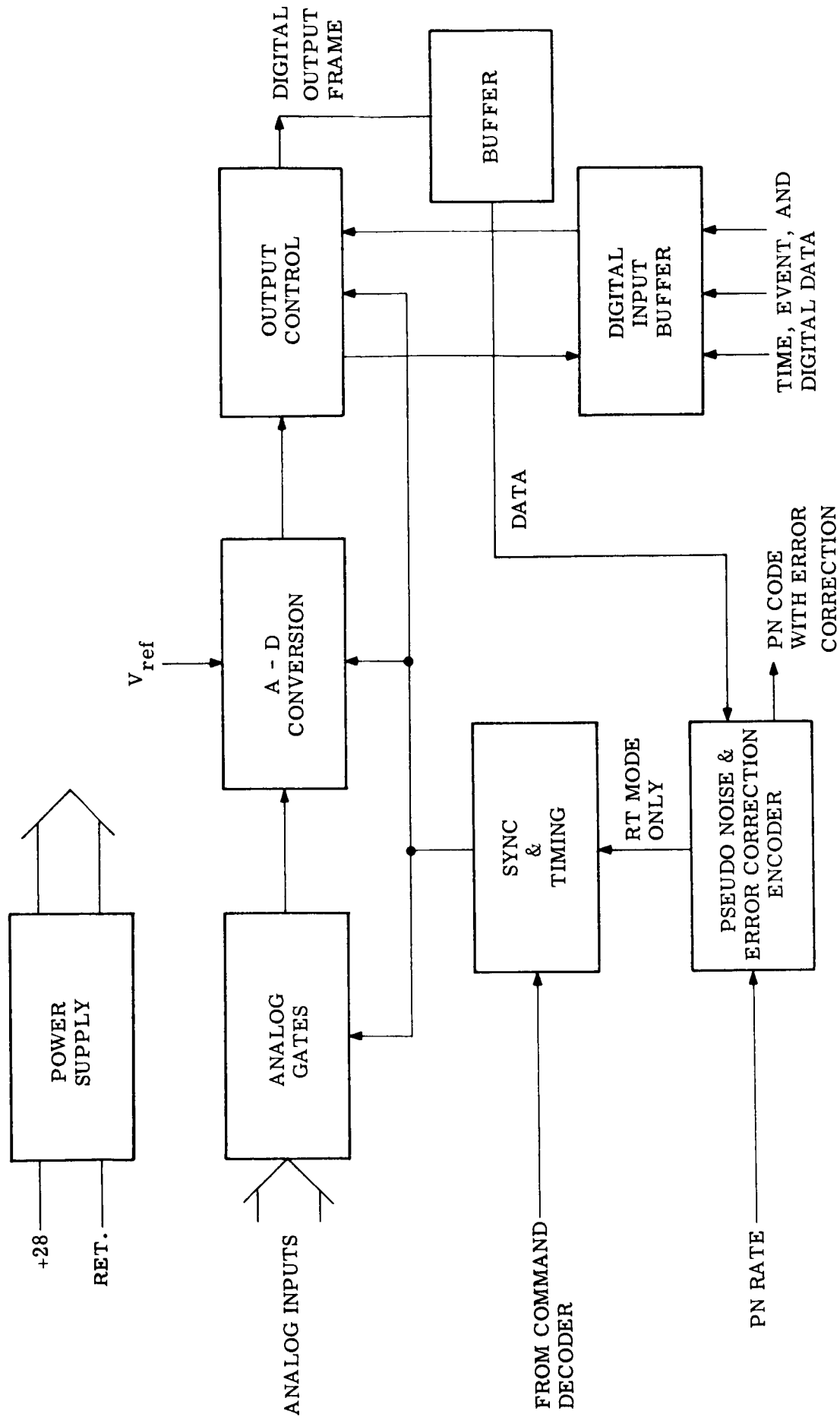


Figure 1.3.2-2. Data Processing and Storage Subsystem, Mars 1969 Lander

bit rate control. This capability permits utilization of the same Data Processor on all Voyager missions.

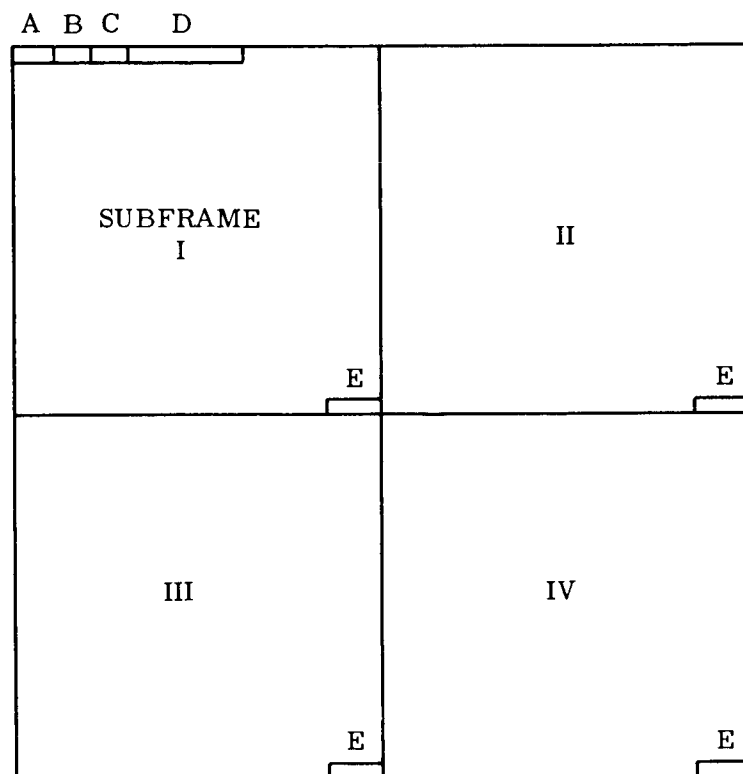
4. It will provide either recycling sampling operation or one-cycle-per-command pulse operation, depending on the mode selected as shown in Figure 1.3.3-5.
5. It will insert proper identification and synchronization data into each frame of 1024 words (Figure 1.3.3-1). These include:
 - a. Barker code for frame synchronization of ground equipment (Other suitable codes are available; the Barker code is herein used as an example).
 - b. Time label having a four-second resolution
 - c. Mode identification for locating specific data in a given frame
 - d. Data origin point identification, i. e., Lander No. 1, Lander No. 2, or Orbiter
 - e. Four sub-frame identification words spaced 256 words apart for ease of data location.
6. It will route the output data train to the Data Storage Unit, the transmitter, or both, depending on the mode.
7. It will provide digital output buffering for simultaneous storage and real-time transmission at different bit rates.
8. It will generate any one of several transmission modes upon receipt of a transmission mode select pulse from the Command and Computer Subsystem. A transmission mode is defined as a particular combination of data source (TPR, DPU, Buffer), data rate, and encoding scheme.
9. It will provide a Manchester-coded 511-bit PN code for encoding all data for transmission to Earth.
10. It will provide 28 bits of error control code for each 45 data bits if requested by mode select pulse. Then it will be PN and Manchester coded for transmission.
11. It will apply a Manchester-coded 31-bit PN code to command data being transmitted to the Landers from the Orbiter. It will apply a Manchester coded three-bit PN code to data being transmitted from the Landers to the Orbiter.

B. General Description and Method of Operation

The following description and discussion of operation deals with the basic Data Processor exclusive of mode generation. Adaptability through mode construction will be discussed as an extension of this description in Section 1.3.3D. A general block diagram is shown in Figure 1.3.3-2.

The basic Data Processing Unit consists of the following seven sections:

1. Analog gates
2. Sync and timing logic
3. Analog/digital converter
4. Digital input buffer



A = MODE IDENTIFICATION - 1 WORD
 B = DATA ORIGIN IDENTIFICATION - 1 WORD
 C = TIME LABEL - 4 WORDS
 D = BARKER CODE - 3 WORDS
 E = SUBFRAME IDENTIFICATION - 4 WORDS
 TOTAL REMAINING DATA WORDS - 1011

Figure 1.3.3-1. Basic Frame Format

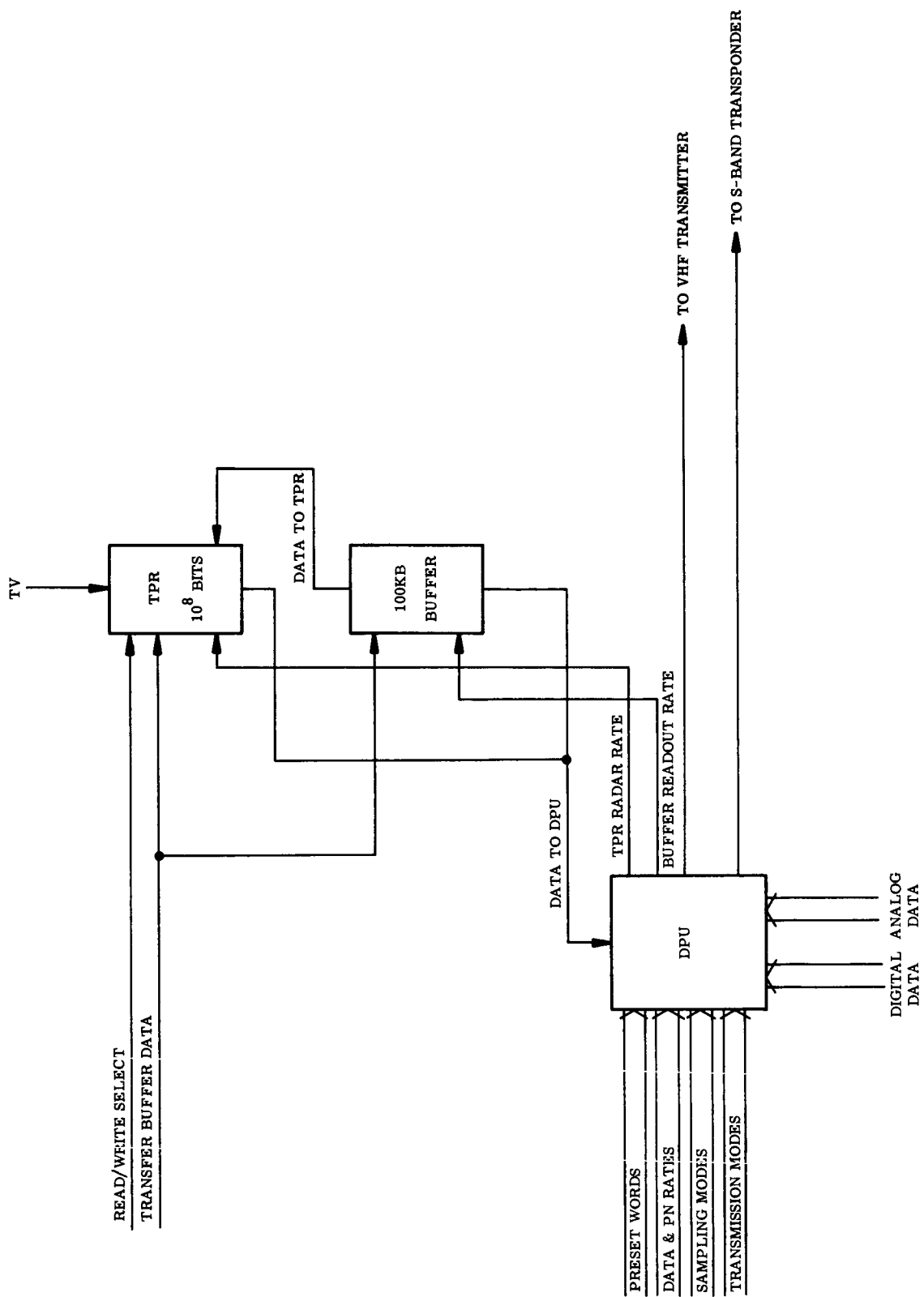


Figure 1.3.3-2. Data Multiplexer, General Block Diagram

5. Output control
6. Pseudo noise and error control encoder
7. Low-voltage power supply

Analog information from diagnostic and scientific sensors is routed through the solid state analog gates. The analog gates are sequentially sampled by "word gate" pulses generated in the timing logic. Upon selection of a particular analog information line or channel, the selected analog voltage is transferred to the A/D encoder for digitizing. The A/D conversion technique utilized is that of successive digital approximations of the analog information. The analog voltage to be digitized is repetitively compared with an accurate reference voltage from the low-voltage power supply. The initial comparison is usually made at the midpoint of the sensitivity range of the unit. For example, the first comparison in a 0-5 volt full-scale system would utilize an initial 2.5 volt reference. Should the initial comparison show the input analog voltage to be greater than the reference voltage, the digital value "1" is given to the most significant bit of the digital word and the reference voltage (V_R) is switched from its initial value to $(V_R + V_R/2)$.

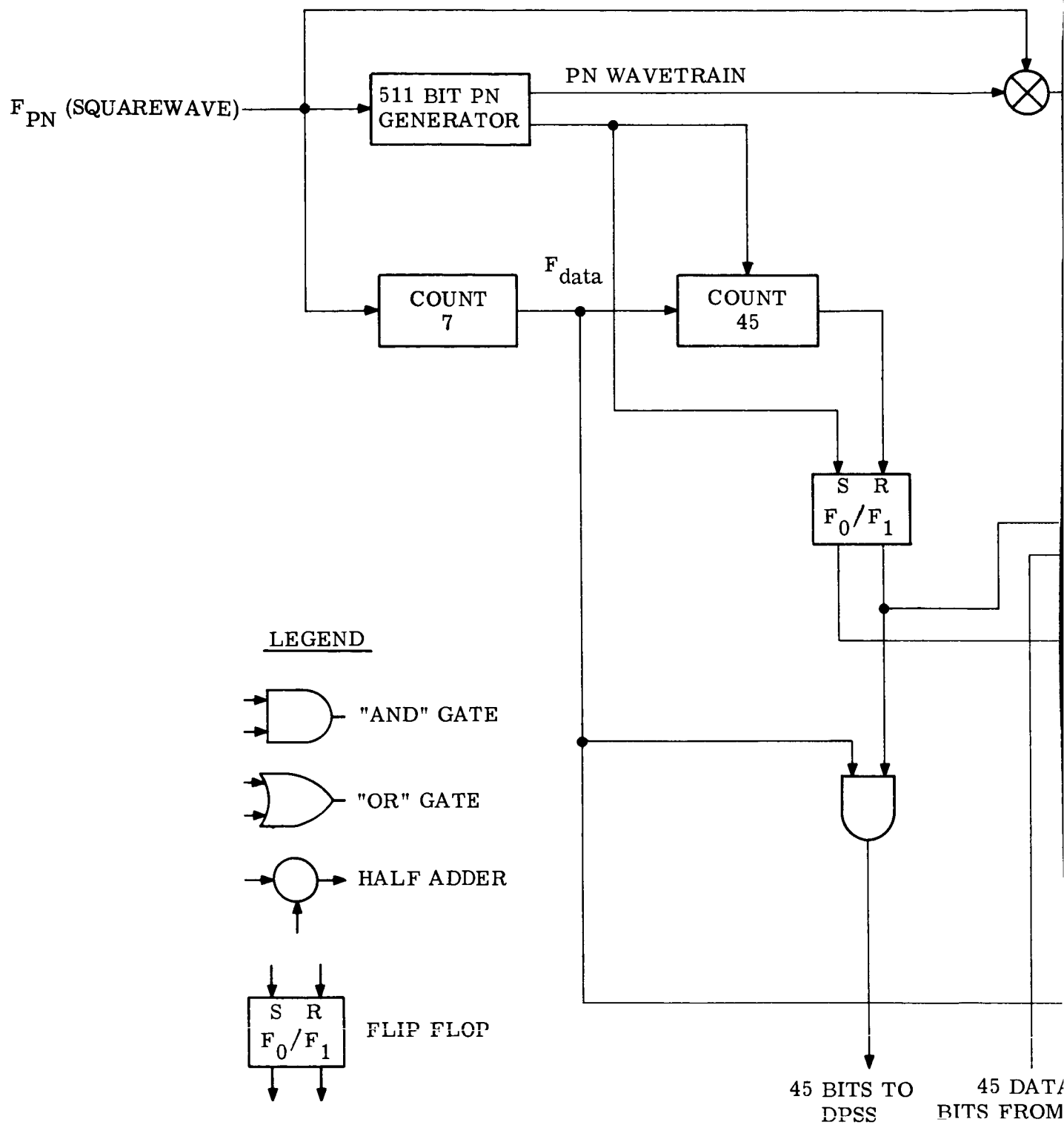
Similarly, if the value of the input analog voltage is smaller than the initial value of the reference voltage, the digital value "0" is assigned to the most significant bit of the digital word and the reference voltage is switched from its initial value (V_R) to $(V_R - V_R/2)$. At the completion of each successive comparison, one-half of the previous addition or subtraction is either added to (input less than reference voltage) or subtracted from (input greater than reference voltage) the reference voltage. Incremental reference voltages ($V_R, V_R/2^1, V_R/2^2, V_R/2^3, V_R/2^4, \dots, V_R/2^{m-1}$) for the comparator are provided by a conventional ladder network.

The digitized information from the A/D converter is transferred serially (most significant bit first) to the output control logic. The purpose of the output control logic is to insert the Barker code, subframe identification, mode and data origin identification into the data frame at the proper word locations. The output control logic also sends timing pulses to the digital input buffer to sample time label, event monitor data and digital information at the proper word locations in the frame.

The sync and timing logic consists of a bit generator which provides six time-spaced cyclical bit pulses and a word generator which provides 1024 time-spaced cyclical word pulses. Specifically, it provides a selection and sampling "word" pulse for each of the analog input gates; bit and word sampling pulses to the conversion unit; bit, word, frame and subframe timing pulses to the output control logic.

The digital input buffer consists of a shift register and three separate input gating sections. The input gating sections provide event occurrence data, time label and digital data as parallel data, using as inputs to the shift register a single group of time-shared parallel lines. Data stored in the shift register is shifted serially into the output control logic at the data multiplexer bit rate timed so that it occupies the proper word locations in the data frame.

The PN and Error Control Generator shown in Figure 1.3.3-3 performs the following functions: First, it generates a 511-bit PN code in a nine-stage shift code counter at data rate F_{PN} and converts this to a Manchester coded pulse train in a half-adder. Second, it divides the F_{PN} rate by seven in a three-stage counter to generate the actual data rate ($F_{data} = F_{PN}/7$), which will synchronize the data source with the PN generator. It generates groups of 45 data pulses, at rate F_{data} , which are sent to the data source and then receives 45 data bits from the source. These bits are combined in a half-adder with the Manchester coded PN chain and transmitted. Simultaneously, they are shifted into a 28-stage shift register which generates 28 error control bits which are shifted into the half adder, PN coded and transmitted after the last of the 45 data bits has passed.



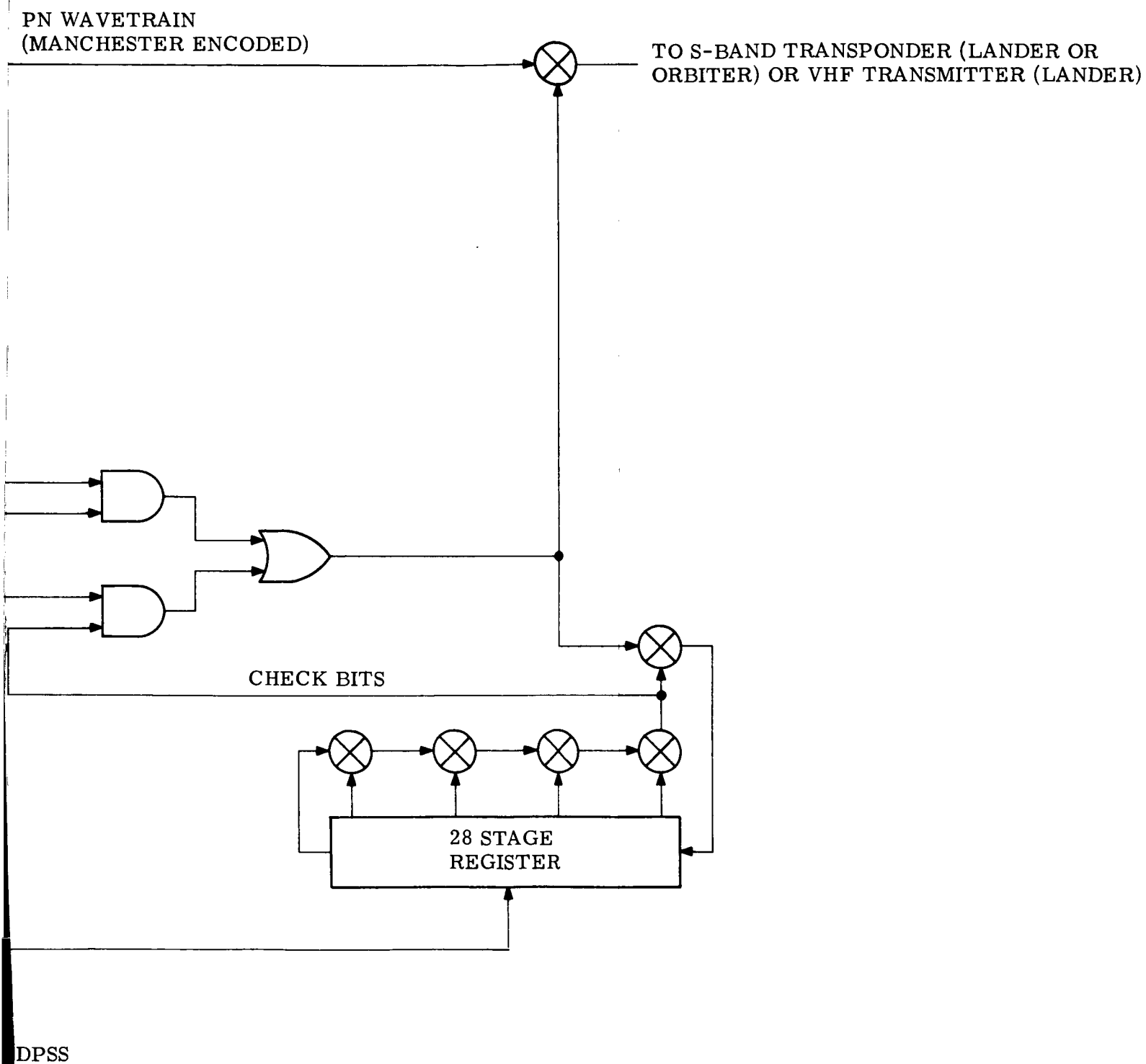


Figure 1.3.3-3. Pseudo Noise and Error Control Encoder, Orbiter and Lander

It should be noted that a total group of 45 data bits plus 28 error correction bits has been transmitted. Each bit contains seven PN bits, making a total of 511 PN bits per group. Therefore, the PN generator has a unique cycle for each group of data plus error correction bits.

A self-contained regulated power supply is included as an integral part of the equipment. It provides all necessary regulated supply voltages and a highly accurate and regulated reference voltage for use in the conversion section. Utilization of a separate power supply for the Data Processing Unit is recommended because of the buffering it provides against system line noises, spikes and oscillations which could normally cause mis-counting of counters, false one-shot firing, etc. A secondary benefit is accrued in that it also effectively isolates other subsystems from any timing noise which is generated in the Data Processor.

C. Equipment Location

In examining the Voyager System with respect to the location of sensors which are to be sampled, it is seen that there are large quantities of sensors in both the main body and the PHP. Since the number of wires which must be carried across the main body-PHP joint should be kept to a minimum, it is necessary either to install a separate Data Processor on each section or to relocate a section of analog gates and a word generator from the main body to the PHP. The latter course appears much more practical than the former. The analog gates are evenly divided between the main body and the PHP, and an identical word generator is employed in each section. Word rate pulses from the bit generator on the main body are fed in parallel to counters in both word generators. Each generator has a 1024 gate-selection capability but supplies only 512 analog gates in each section, giving a total of 1024 inputs (disregarding identification and coding words) time-multiplexed between the main body and the PHP. It is seen that there is one extra counter stage in each section; this is the least complex choice of several for implementing the multiplexer division. The word counters will be reset to zero each time power is reapplied or upon command to insure that both counters are operating in phase. The capability of varying the sampling format in the PHP section has not been justified by examination of the operating schedule of equipment located there and has been disregarded in favor of maintaining a minimum of interconnecting wires. The interface wiring between the main body section and the PHP section, therefore, consists of:

1. + 6V
2. - 6V
3. Reset line
4. Word rate line (three redundant)
5. Analog data line.

The voltage lines, reset line and analog data line should be redundant for reliability; the word rate lines are necessarily redundant due to utilization of redundant word counters in both sections. This will be discussed in Section 1.3.3G on reliability.

The Lander Data Processers are single, self-contained units requiring no mechanical separation.

D. Adaptability

An examination of lists of the diagnostic and scientific monitors to be sampled on a typical Voyager mission reveals a wide range of sampling rates from 100 samples/sec to 1 sample/hr and even 1 sample/day; it lists groups of monitors which must be sampled at specific mission phases and omitted during others; it lists monitors which appear in several otherwise different groups of monitors and do not appear in others. Various requirements for real time and stored time operation transmission and encoding are

evident. In order to be an efficient functional part of the Voyager Communications Subsystem, the Data Processor must be capable of meeting all the requirements of sampling rate, frame format and data routing for a particular mission without either impairing mission flexibility or becoming so complex that it becomes unreliable.

The discussion heretofore has presented a detailed description of the basic Data Processor. The following discussion describes the extensions to the basic concept which result in the universal Voyager Data Processor. The description of the operation is designed to show the capability rather than to implement it with respect to all missions.

(1) Description of Mode Selector

DPU adaptability is provided by the mode selector. This is shown in Figures 1.3.3-4 and 1.3.3-5. Figure 1.3.3-6 shows its connection to the basic PN and error correction generator. Inputs to the mode selector from the Command and Computer Subsystem consist of a multiplicity of PN and data rate lines from the clock, sampling and transmission mode-select commands and word counter preset words. Its output is comprised of a format-select signal, data bit rate and cycling-select signal for sampling control, a source-select signal, PN bit rate, and error control signal. Sampling and transmission modes may be selected independently without interaction except in the case of real-time transmission (Mode 1 in Figure 1.3.3-5) at which time the transmission mode is determined by the sampling mode.

The mode selector contains groups of flip-flops for each function, i.e., format control, bit-rate, data source, etc. Sampling and transmission mode programming are accomplished by connecting each mode-select input line to one flip-flop in each group that it is required to control. Connections are made through diodes for isolation between lines. The number of permutations possible in the diode matrix is limited solely by the numbers of bit rates and formats desired. Any number of programs can be wired in for a specific mission. A mode-reset pulse will set all flip-flops to the disable state just prior to a change in mode to eliminate the possibility of having any more than one flip-flop in a given group enabled at a given time.

The modification necessary to change the mode programming from mission to mission consists of inserting the proper diode interconnection matrix into the selector. This will be a plug-in unit in the form of a printed circuit board containing a unique diode interconnection matrix for each mission.

The ability to change the data frame format upon command is provided by modifying the counting sequence of the word generator and, therefore, the number and location in the frame of analog input samples. The format signal from the mode selector inhibits the specific counter stage or stages required to formulate a desired sampling sequence of the analog input gate. The counter preset words are inserted in the disabled counter stages, thereby locating the exact group which is to be sampled. For example, assume the last seven stages of the ten-stage counter are disabled. The DPU will then sample a group of eight inputs by counting in only the first three stages. By inserting various seven-bit words in the disabled stages, any group of eight sensors may be selected for sampling.

It is imperative, due to ground synchronization techniques, that the Barker code be inserted every 1024 words regardless of the sampling mode. It is, therefore, necessary to add an auxiliary counter at the end of the ten-stage word counter. A number of stages in this counter will be enabled equal to the number disabled in the word counter, thus providing a full 1024 count for gating in the identification words, time label and Barker code each 1024 words independent of the frame format.

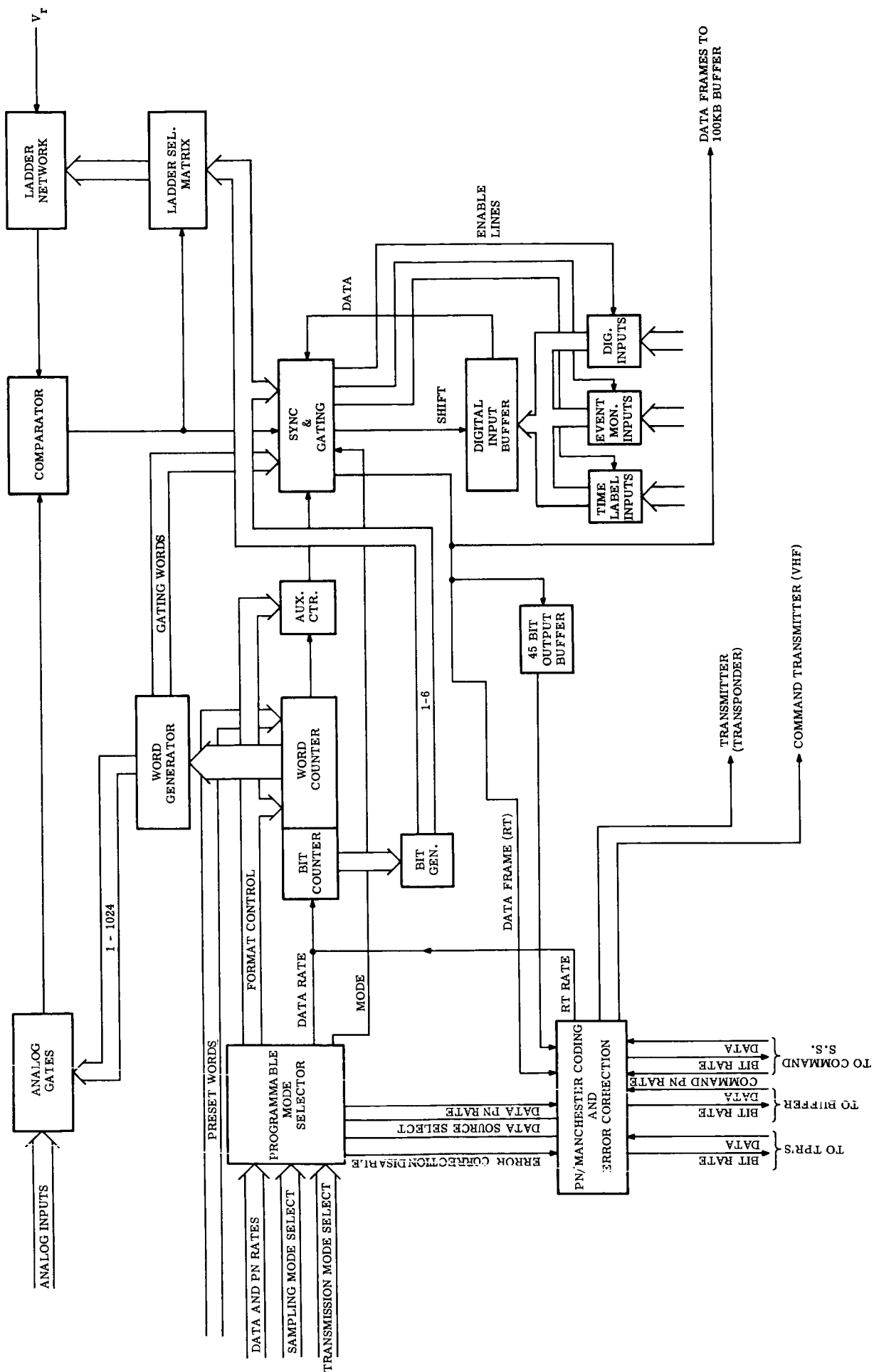


Figure 1.3.3-4. Data Processor Detailed Block Diagram, Orbiter Unit

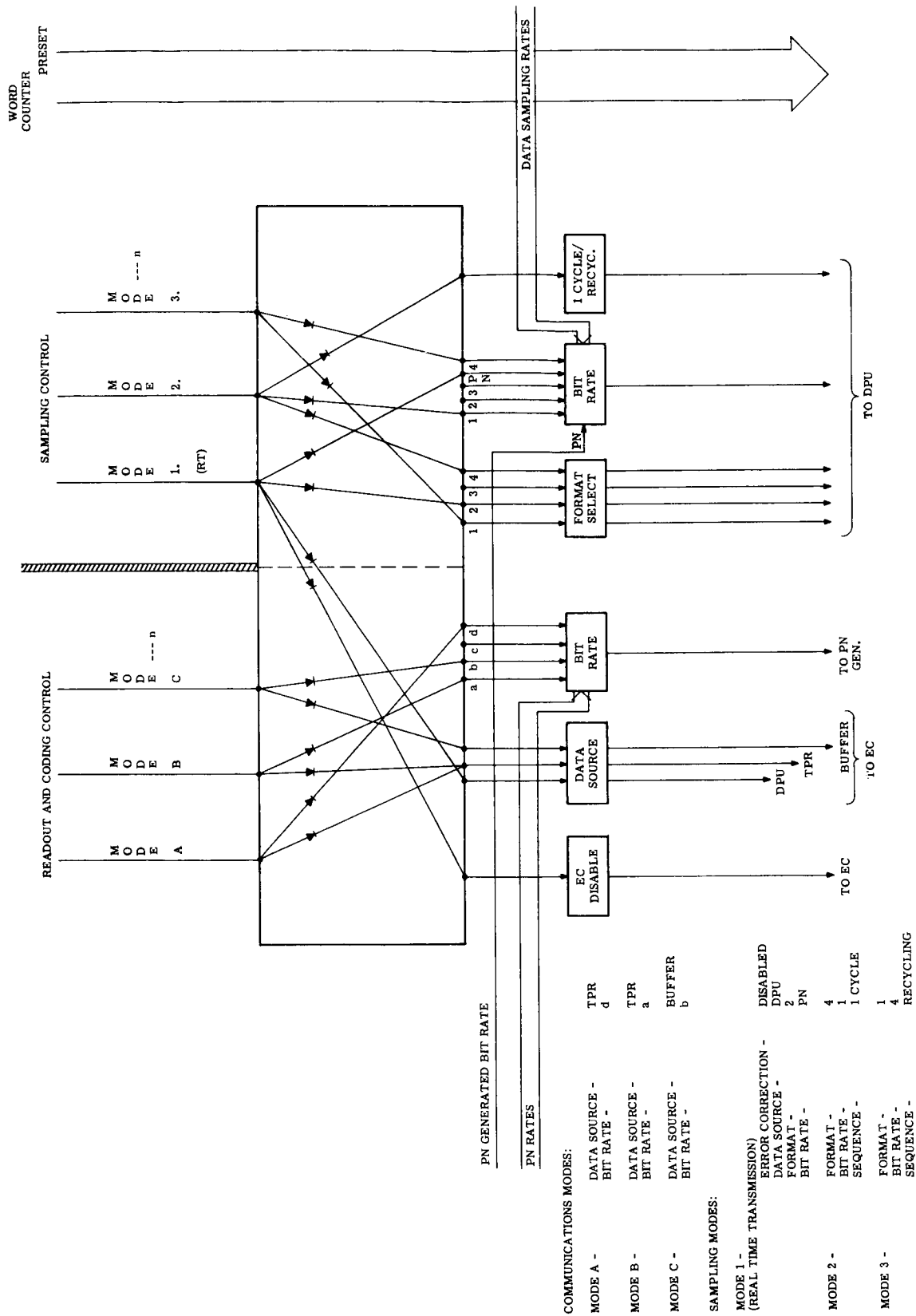


Figure 1.3.3-5. Mode Selector, Orbiter and Landers

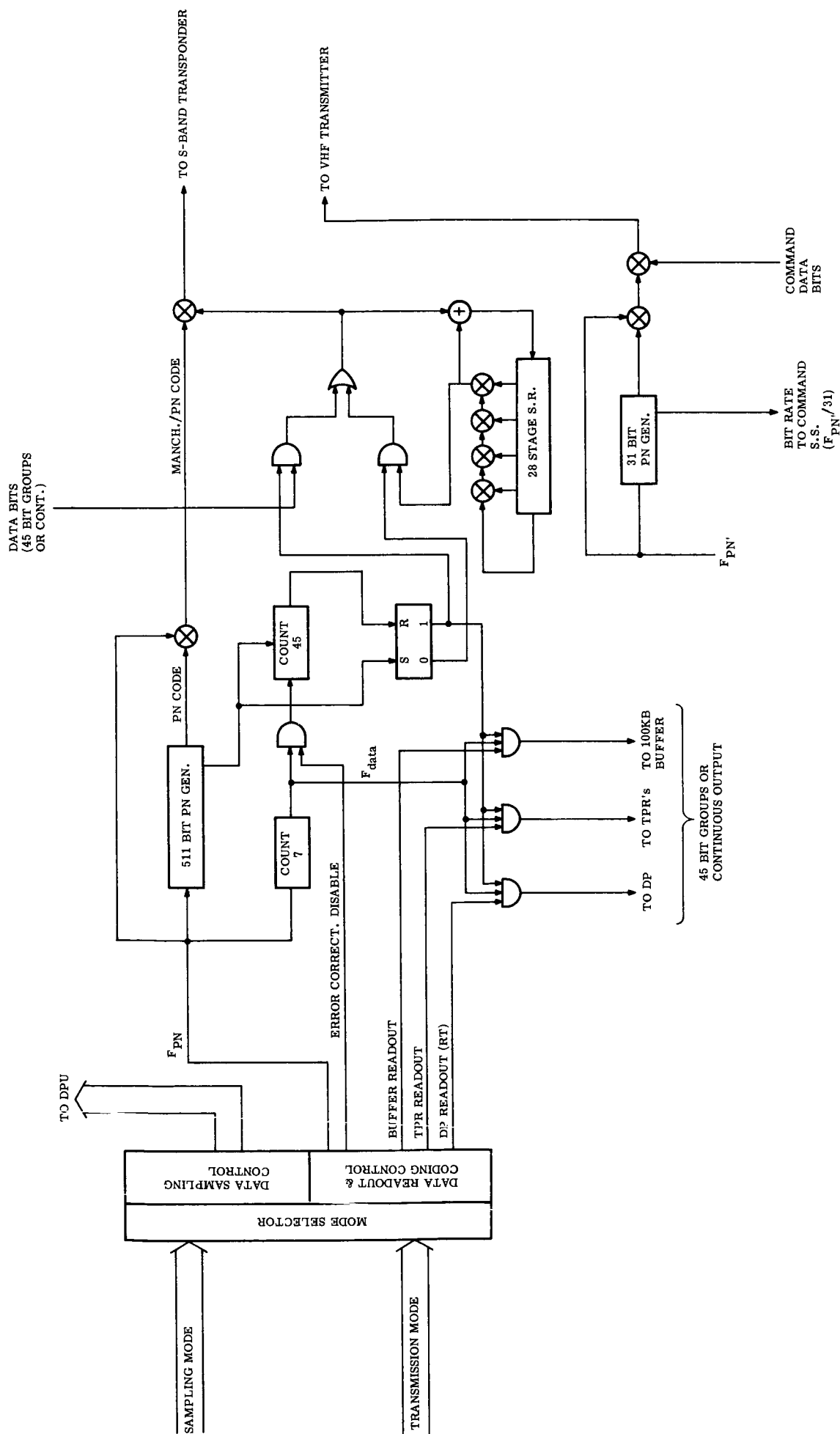


Figure 1.3.3-6. Pseudo Noise/Manchester Code Error Correction Group Generator

Additions to the basic PN and Error Control Code Generator consist of gates to select the data source and apply bit rates to the source selected and a gate to disable the Error Control Encoder. In the event that this is activated, the output rate to the selected source will be a continuous rate as opposed to the 45-bit group used with error correction.

(2) Real Time/Stored Time Operation

In real-time operation, the Data Processing Unit bit rate and the transmission data bit rate are the same. The rates are obtained from the pseudo noise generator and to each group of 45 data bits, 28 bits of error control coding are added. In the storage mode, the Data Processing Unit operates at the bit rate selected by the mode command and is completely independent of the transmission rate.

Parallel real-time and storage modes at the same bit rates are accomplished as in the real-time mode discussed above, except that in this case the 100-kilobit buffer line is also enabled.

During periods when it is desired to sample, store data at a high rate, and transmit selected words at a low rate simultaneously, a low-capacity speed-differential buffer will be utilized. As the frame is generated, the data will be sent to the main storage device, while the selected words will also be placed in the output buffer. The buffer will subsequently be read out at the data rate of the Communications Subsystem.

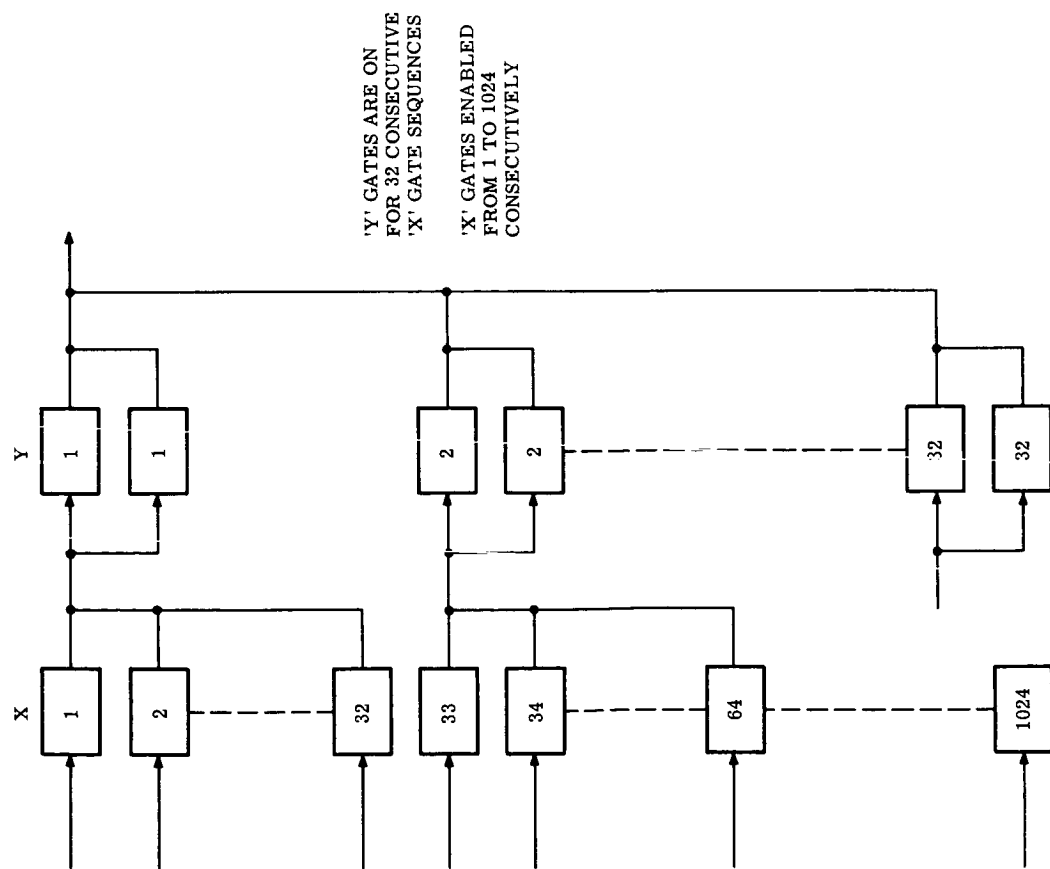
E. Reliability Through Logic Technique

Since the Data Processing Unit is the sampling and coordinating center for all scientific and engineering data (exclusive of television) for the Voyager mission, it is essential that extreme reliability be designed into the unit at the circuits, logic, and packaging levels. Reliability through circuit design and packaging will be described in a later section on producibility; reliability through logic techniques will be discussed here.

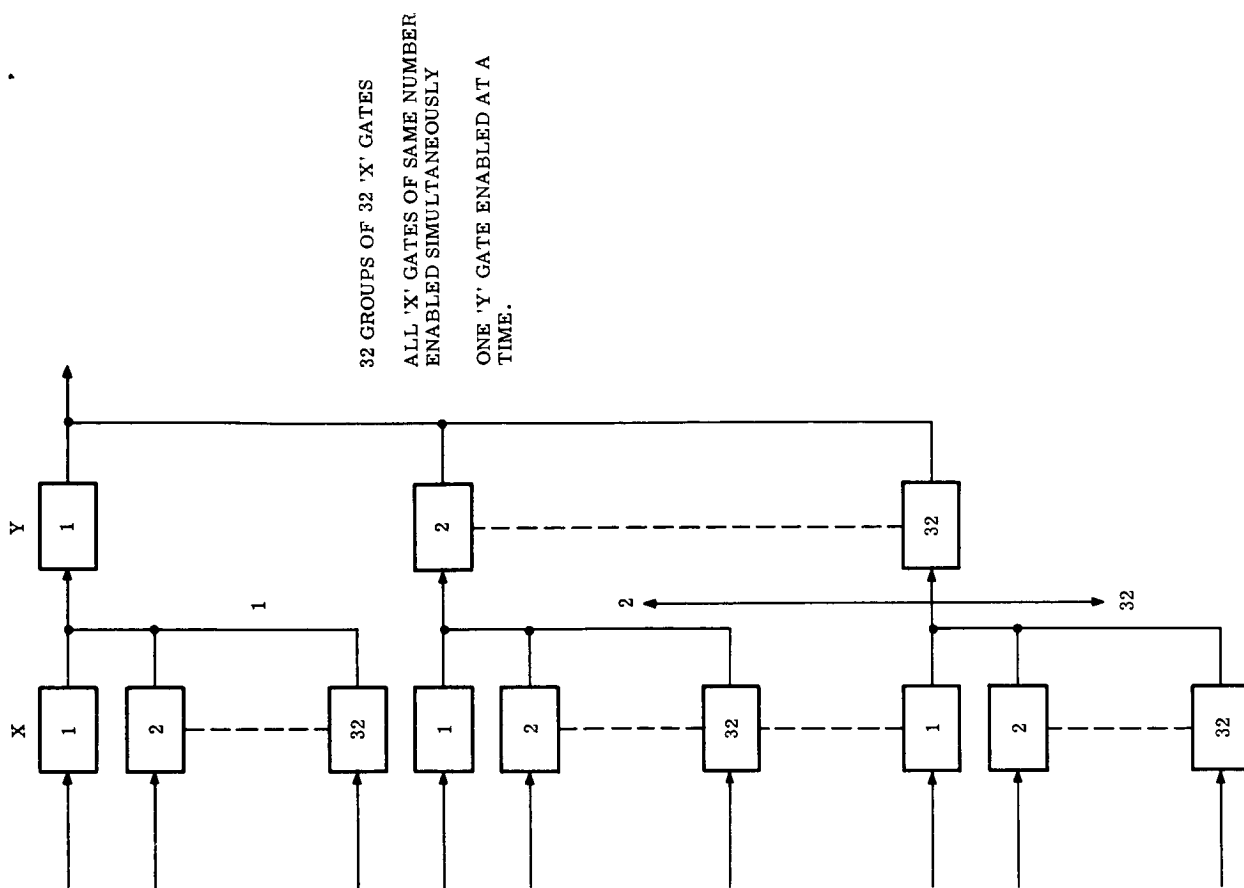
It has been the intent of the design to apply redundancy and self-healing techniques to all functions which are "in-line" with overall data flow and control, i. e., any point at which a failure would cause complete loss of data. This includes analog gates, bit and word counter, A/D converter and a small number of gates in the output control section.

(1) Analog Gates

Reliability in the input gate section is basically inherent in the gates themselves. They do not pass current in excess of the few microamperes of drive needed for transfer of the input voltage across the transistor junctions. This reliability is enhanced by judicious grouping of the gates, as shown in Figure 1.3.3-7A. There are 32 groups of 32 "X" input gates and 32 pairs of redundant "Y" gates, each pair receiving inputs from a group of "X" gates. Assuming the basic 1024 word frame, the "X" gates are sampled sequentially for one word-time each; the "Y" gate pairs are sampled sequentially for 32 consecutive word-times. The "Y" gate pairs are then opened for the time necessary to sample all of the "X" gates which provide inputs to it. Failure analysis with this grouping is compared with the more conventional method shown in Figure 1.3.3-7B in Table 1.3.3-1.



A.
VOYAGER METHOD



B.
CONVENTIONAL METHOD

Figure 1.3.3-7. Analog Gate Grouping Methods

TABLE 1.3.3-1. FAILURE ANALYSIS FOR ANALOG GATES

<u>FAILURE MODE</u>	<u>LOSS BY VOYAGER METHOD</u>	<u>LOSS BY CONVENTIONAL METHOD</u>
1. Short in any "X" gate	32 inputs	32 inputs
2. Open in any "X" gate	1 input	1 input
3. Short in any "Y" gate	No effect	1024 inputs
4. Open in any "Y" gate	No effect	32 inputs

Using the approach of Figure 1.3.3-7A, the maximum effect in case of the worst failure mode is loss of 32 out of 1024 inputs in the basic frame. The approach of Figure 1.3.3-7B permits loss of all data in the worst case single failure.

In cases where the format is other than the basic frame, the effect of the worst case failure is minimized by locating the inputs to be sensed in different groups of the 32 "X" gate group. For example, assume the format requires 32 sensors sampled 32 times per frame; the sensor inputs would be located one in each group of "X" gates rather than all 32 inputs in the same "X" group. In the former case, a shorted "X" gate causes the loss of only one out of 32 inputs, while in the latter case all 32 inputs would be lost.

(2) Bit and Word Generator

Reliability in the bit and word generator is attained by using majority comparison of redundant counters to provide a self-healing capability. This is shown in Figure 1.3.3-8. Specifically, three redundant bit and word counters are operated in parallel, and their last stage outputs are checked for agreement.

One of the counters is "enabled" to provide inputs to the bit and word generating matrices; the outputs of a second stand-by counter are connected to the same inputs but are in a "disabled" condition. The third counter provides only a last stage output for majority comparison with the other two.

In the event that one counter falls out of agreement with the other two, the error detection section will determine which counter is in disagreement and perform one of two possible actions. First, if the failure is in the "disabled" counter or the comparison counter, no action is taken other than to disable itself from making any further comparisons based on the remaining two valid counters. Second, if the failure is sensed in the "enabled" counter, it will disable its outputs, enable the outputs of the standby section and disable itself from making further comparison. Calculations have shown that an 8:1 improvement in failure rate of the bit and word counter is achieved by using this technique instead of the basic non-redundant method.

(3) Analog-to-Digital Converter

High reliability in the conversion circuitry will be assured through the use of majority logic. The comparator, ladder network, and ladder selection matrix will be triplicated to form three parallel A/D converters, whose outputs will be compared in a majority output gate. Since the comparator is an analog device, it is subject to finite inaccuracies which may be minimized but not eliminated. These appear as "indecision bands" at those discrete analog threshold voltages which cause a change from one digital number to the next higher or lower, e.g., 2.500 volts may be represented by 100000 or 011111 over a range of variation in the analog voltage determined by the comparator accuracy. Use of majority logic with this device can produce a wrong word, assuming one converter failed, since the two operating sections can differ at 1.6% intervals over the input range from 0 to 100% of full scale.

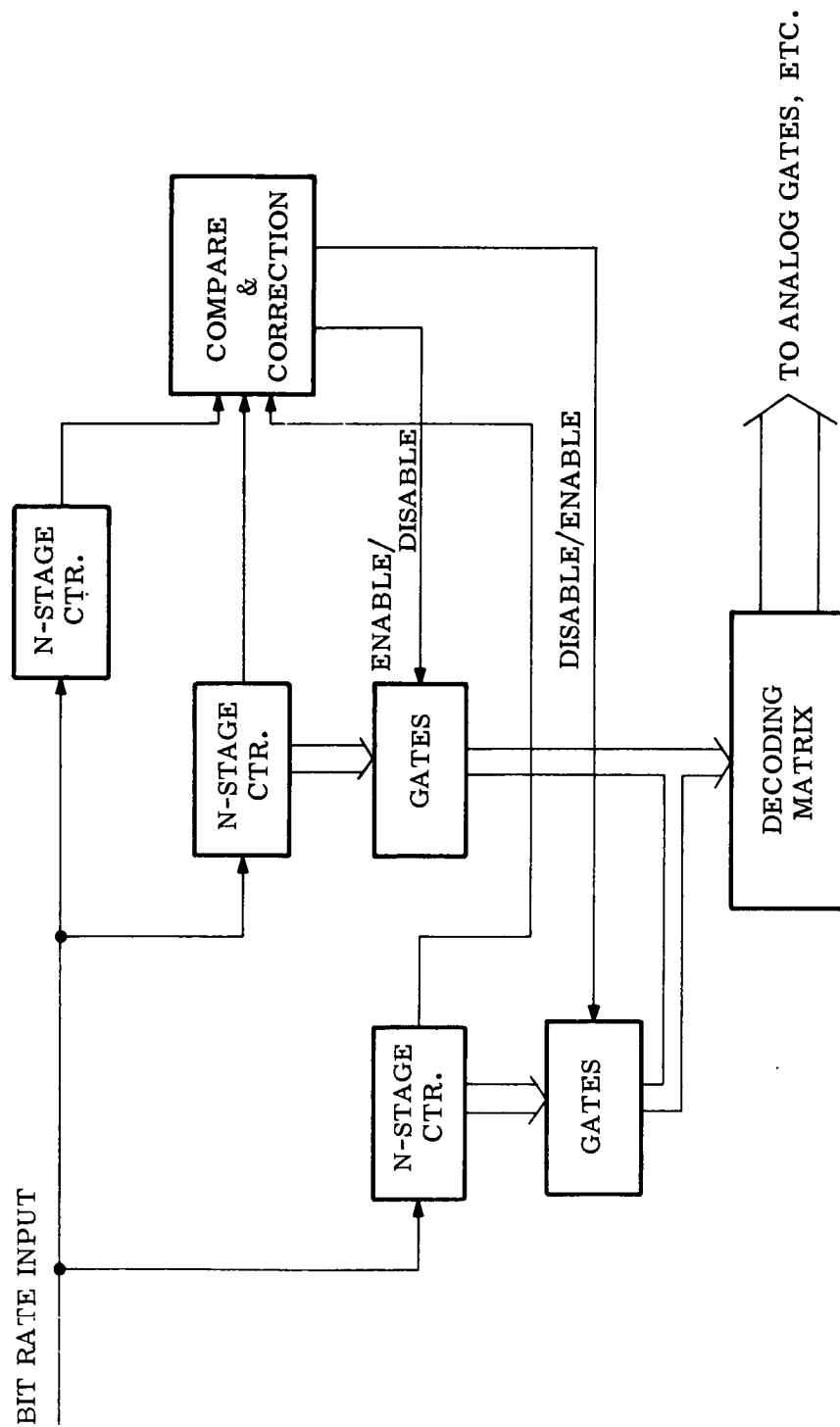


Figure 1.3.3-8. Bit and Word Generator Self Healing Logic

At first this appears to invalidate the use of majority logic in this section of the Data Processor. The following facts, however, prove its merit:

1. The comparator inaccuracy may be made as small as $\pm 0.05\%$ of full-scale input voltage (i. e., ± 2.5 mv for 5.00 v full-scale).

This permits a maximum of 0.1% "indecision band" for each 1.6% analog voltage change, or a 6.3% possibility of wrong word occurrence.

2. A converter failure will become evident in the received data as discontinuities at the 1.6% increments, and once evident, can be eliminated by plotting data and eliminating erroneous data which occurs in the indecision band. (Figure 1.3.3-9.)

Majority logic in this section then will permit a quantitative loss of 6.3% of data taken with little or no loss after evaluation of the plotted data.

F. Similarity to Flight-Proven Equipment

The flight performance of equipment designed and produced at GE-MSD utilizing the circuits and logic techniques which will be applied to the Voyager Data Processor has been impressive over the last few years. While exact implementations of the Voyager unit have not been flown, a high-accuracy data multiplexer for the Mark 6 program has been designed and flown. Extremely complex command decoders and programmers have been flown on several classified programs, and various routine and sub-routine timers have been utilized on Bios, Mark 6 and classified programs. The reliable performance attained during flight use has proven the validity of the logic techniques and adequacy of the circuit design under the stresses of the launch, orbit, re-entry and impact environments.

G. Producibility and Packaging

A study was conducted to determine the optimum packaging method to be utilized in both the Command Subsystem and the Data Processor.

This packaging study has determined that a microelectronic approach is the most feasible method of design and production for highest reliability of the subsystem. This task has compared designs of conventional electronic parts with two types of microelectronic parts: thin-film microelectronics and integrated-circuit microelectronics. The following criteria were compared: size, weight, power, reliability, producibility, and performance. The results of this task have determined that the thin-film microelectronic method of packaging will be used in the Data Processor. This method best meets the design goal and criteria of the subsystem.

The following tables summarize the factors for determining the approach to be used.

TABLE 1.3.3-2 PACKAGING APPROACH SUMMARY

	THIN FILM MICROELEC - TRONICS	INTEGRATED ELECTRONIC MICROCIRCUITS	CONVENTIONAL ELEC. PARTS
SIZE	1/4 : 1	1/5 : 1	1 : 1
WEIGHT	1/9 : 1	1/10 : 1	1 : 1
POWER	1 : 1	2 : 1	1 : 1
ELECTRONIC PIECE PARTS	1/3 : 1	1/5 : 1	1 : 1
INTERCONNECTORS	1/4 : 1	1/8 : 1	1 : 1

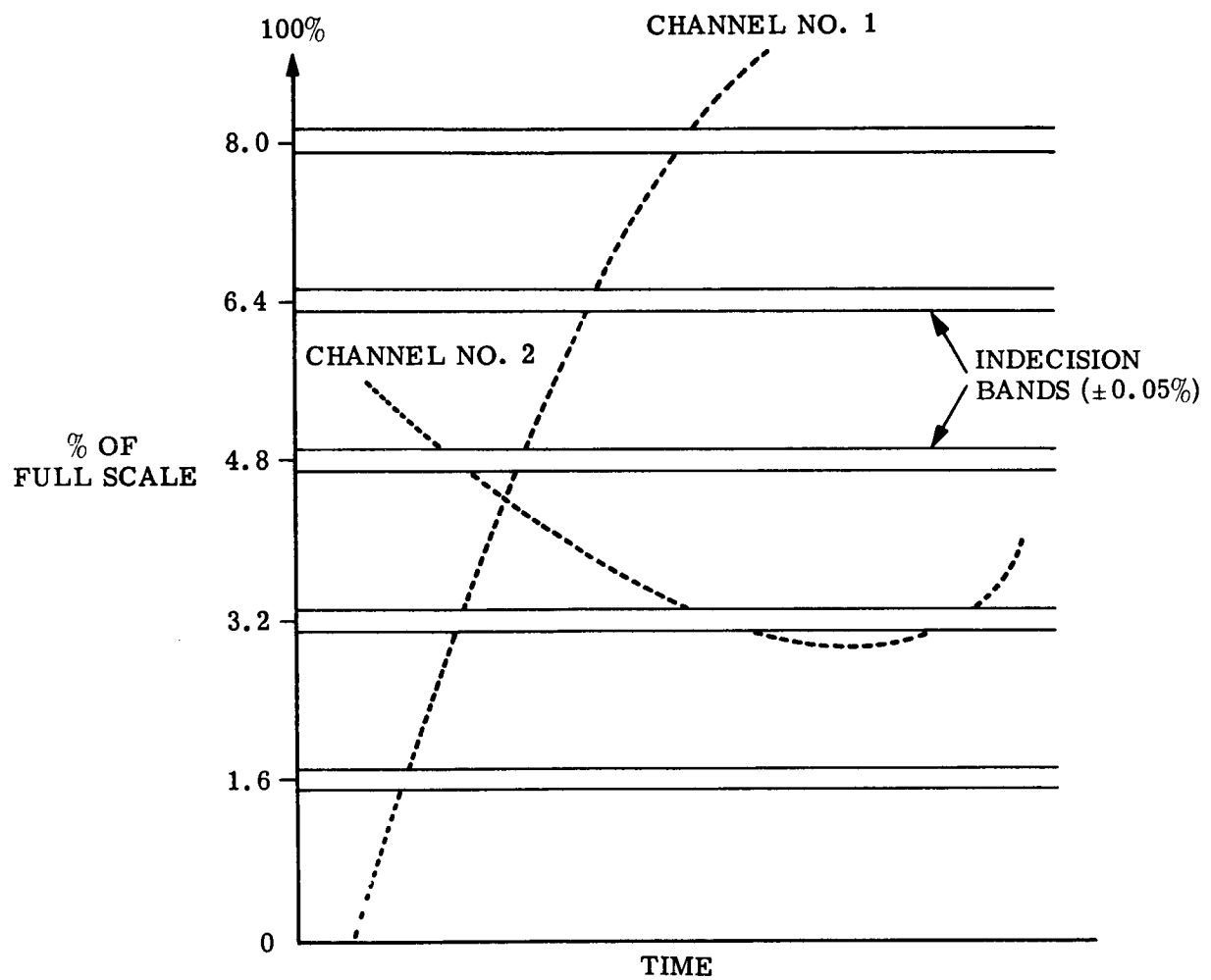


Figure 1.3.3-9. Data Plots Assuming One Converter Failure and Majority Logic Used

TABLE 1.3.3-3 PACKAGING APPROACH SUMMARY

	<u>THIN FILM MICROELEC- TRONICS</u>	<u>INTEGRATED MICROELEC- TRONICS</u>	<u>CONVENTIONAL (CORDWOOD) ELEC. PARTS</u>
Readily Changed or Modified	good	fair	best
Most easily produced	best	fair	good
Most readily available Multi-sources	good	poor	best
Radiation Resistant	good	poor	good
Lowest power custom circuits	best	poor	good
Size, Weight	good	best	poor
Inter-connection	good	best	poor
Volumetric change due to additions	good	best	poor
Order of Solution for applica- tion to the Voyager Mission	1	2	3

(1) Circuit Packaging Concepts

The packaging of the Command and Data Processing Subsystem will be accomplished using circuits developed on thin-film substrates. The repeated number of functional circuits (flip-flops, gates, drivers, etc.) used within the subsystems allows most efficient use of printed circuit boards and microelectronics. The combination of printed circuit boards and thin-film circuits has been selected for the following reasons: 1) size, 2) weight, 3) volume, 4) repeatability, 5) producibility, and 6) reliability. The board assembly size will be about 3 x 3.24 x 0.2 inches or 1.9 cubic inches. Approximately 216 circuit parts will occupy this volume. The interface wiring of the modules and the heat sink are included in this volume. The comparable volume for the same circuits using high reliability parts of equivalent power rating will be about 8.0 cubic inches. The weight of this board will be approximately 0.078 pounds. Comparable weight of the same circuitry using high reliability parts within encapsulated cordwood modules will be 0.65 pounds; the apparent weight saving of 9:1, and volume saving of 4:1, can be used generally for comparison purposes throughout the subsystems.

The thin-film module is comprised of a stable glass base called the substrate, upon which film-type resistors and capacitors are vapor deposited. The thin-film components are interconnected by deposited film conductor patterns. A heavy glaze of protective glass is fired over the thin-film parts to provide a barrier coating against environmental and assembly damage. The passive components of diodes and transistors are soldered to the film-masked conductor pattern areas. These pad areas also provide test points for checkout and inspection.

A module heat sink is designed onto the printed circuit board foil. The copper cladding is not removed from beneath the modules. Thus the module, when bonded and wired to the board, has a heat sink and a natural noise shield of copper within 0.020 inches of the resistors or heat producing parts of the substrate. This distance compares to 0.70 inches to the center of parts mounted with cordwood modules. The foil then conducts the heat to the frame or structure heat sink. It has been determined that a structural heat sink will not be required. A blanket of super-insulation material will be used to provide a uniform temperature within the subsystem. Insulation washers between the unit, mounting, and the structure may be desirable to retain the heat within the units.

(2) Harness and Frame

The harness is the largest single item of the equipment. It will contribute to at least 1/3 of the overall weight, occupy 20 percent of the volume, will absorb 25% of all heat generated within the package, and will be the least reliable part of the entire subsystem, primarily because connectors must be used to interconnect the subsystem to the vehicle. The harness will be designed to allow the most reliable method of test and alteration or modification. It will also be designed to reduce or suppress noise for maximum performance of the system.

After final test and acceptance of the subsystem, the harness will be foam-potted in place.

The design of the harness will incorporate means to overcome the inherent problems of accessibility and bulk. Complete access to the harness will allow inspection to review all joints, connections and workmanship. The design will allow easy access to all connectors for modification or test. The harness raceway will have metal covers to protect the harness from noise and mechanical damage. The design will provide for pre-wiring the cable harness on jigs prior to assembly into the frame. This will allow inspection and workmanship of the highest quality to be performed in an unobstructed area.

1.3.4 DATA STORAGE UNIT

A. Data Storage Requirements

The purpose of the Data Storage Unit is to store orbital television, scientific, and engineering data accumulated at a high bit rate and to play back at any one of a number of reduced bit rates, compatible with the transmitter capabilities; to record and play back data transmitted from the Lander; and to reproduce pre-recorded stored programs on command. Data originating in the Orbiter is to be recorded at rates up to 3×10^5 bits per second and read out at much lower rates (16,000 bits per second or less). The Lander data rate is on the order of 10,000 bits per second. The total data storage requirement is 10^9 bits. The stored program data requirement is 10^6 bits. It is not required to record and play back simultaneously. The Orbiter TV data format is four bits per word, NRZ; the Lander data format and the Orbiter scientific and engineering data format is six bits per word, NRZ.

Reliability considerations make redundancy of recording devices desirable. If possible, there should be complete redundancy, i.e., two recorders, each capable of storing 10^9 bits. If this is not feasible, the 10^9 storage capability should be divided among two or more separate recorders. The error rate should be no more than one bit in 10^4 bits.

In addition to these explicit requirements, the recording devices must have the inherent flexibility to accept changes in requirements, such as increased storage capacity and changes in recording and read out rates. While there is no requirement for the orbital storage device to withstand sterilization in the early phases of the program, it seems probable that there will be such a requirement in the later phases. Consequently, this should be considered.

To meet these requirements, many different types of storage devices were considered. After careful evaluation, it was decided that a thermoplastic recorder (TPR) was the only type of device capable of the high storage capacity and flexibility of read-in and play-back rates. This decision is discussed in greater detail in Section 1.7.3.

B. Description of Proposed TPR

Figure 1.3.4-1 shows a block diagram of the proposed thermoplastic recorder. Data will be stored in 1 in. x 1 in. thermoplastic plates by an electron beam modulated in

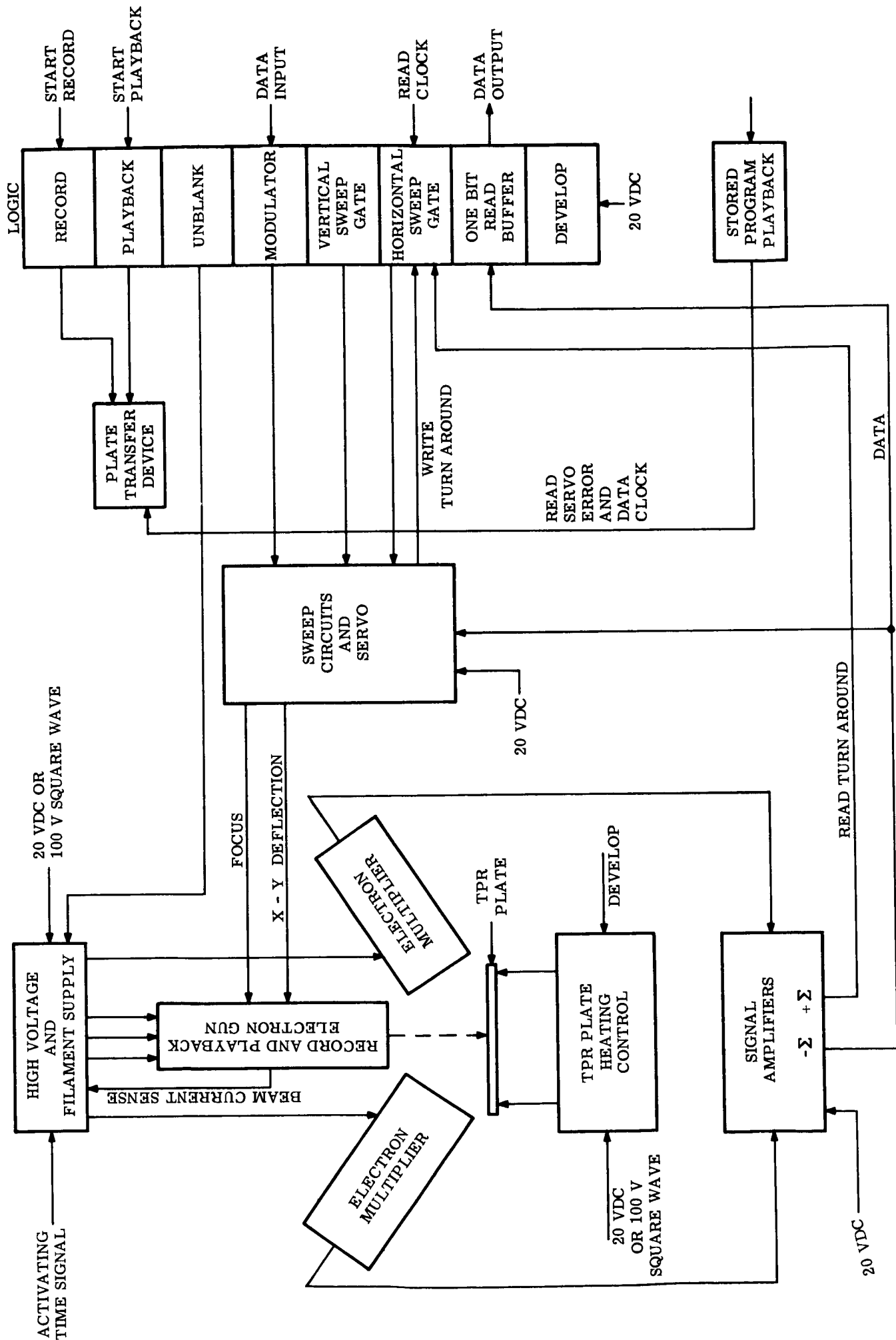


Figure 1.3.4-1. Spacecraft Video Digital Memory System

accordance with the data being stored. The digital data will be written using lateral beam deflection. With this technique, a one causes an upward deflection from an imaginary center line and a zero causes a downward deflection. The lateral motion of the groove beneath the read-out electron beam modulates the secondary electrons' direction back and forth between the collectors. This provides a push-pull data signal.

Each 1 in. x 1 in. plate will store 10^7 bits. A possible format is shown in Figure 1.3.4-2. The left-hand portion of the top line will be used to find the start of data during play back. Each line will be approximately 3150 bits in length and approximately 3150 lines will be recorded on the plate. Bits are serially recorded along the line. Since bits are synchronously supplied with no gaps during recording, it is not necessary to make the thermoplastic lines an integral multiple of picture lines. To store the required 10^9 bits, 100 plates will be required. An additional plate will contain the stored programs. A plate transfer device will be used to shift plates into position. A possible configuration is shown in Figure 1.3.4-3. The operating procedure would be as follows:

Initially the first plate will be in position and the caging frame, shown in the diagram, will be in place. This will prevent movement of the plates during the period of lift-off acceleration and vibration. The frame will uncage prior to start of recording. When recording has been completed on plate No. 1, the plate will be developed, the second plate will be shifted into position, and recording will be resumed. When the signal for play back is received, the plate transfer device will cycle back to plate No. 1, and proceed to read out. At the conclusion of read out of plate No. 1, the plate will be erased, and the next plate will be shifted into position.

The stored program plate functions separately from the normal read-in and playback sequence. Since there are only 10^6 bits stored on this plate, each program can be stored in a separate section of the plate with a gap between programs. When the command to play out a stored program is received, the plate transfer device will cycle the stored program plate into playback position. The next part of the command signal determines the particular program to be read. The left-hand portion of the top line of the selected program will be used to find the start of data for playback. At the conclusion of program readout, the recorder will cease to function until the next command is received.

Data can be recorded as phase-modulated lateral displacement of the groove. Figure 1.3.4.-4 shows the groove shape for an arbitrary sequence of bits. Data recorded with this technique using a two-phase clock provides a self-clocking feature during read-out. The clocking signals will be used to control incrementing of the electron beam motion during readout.

To prevent the loss of data during recording and to provide for continuous synchronous playback, alternate grooves of data will be recorded in opposite directions as shown in Figure 1.3.4-5. The horizontal and vertical waveforms are also shown. The turn-around sequence can be started by sensing a threshold on the horizontal waveform voltage. The vertical sweep is incremented and the direction of the horizontal sweep reversed. A one-microsecond reversal of the horizontal sweep will require only 100 milliwatts average power input to the horizontal sweep circuit during recording. Each turn-around is executed subsequent to the recording of a bit, but prior to recording of a clock pulse. This action is initiated once the turn-around signal has been received from the horizontal-sweep threshold sensing circuit. The end-of-plate sequence can be started by sensing a threshold on the vertical voltage waveform.

If information is recorded in self-clocking form as shown in Figure 1.3.4-4, it is proposed to read it with a scanning electron beam which precisely follows the groove. The vertical deflection signals will then duplicate the recorded waveform shown in the figure. In order to playback synchronously with the internal playback clock, the reading beam will scan at slightly higher than average velocity and cease scanning on each encounter with a recorder clock mark. It will then wait for the playback clock pulse before resuming

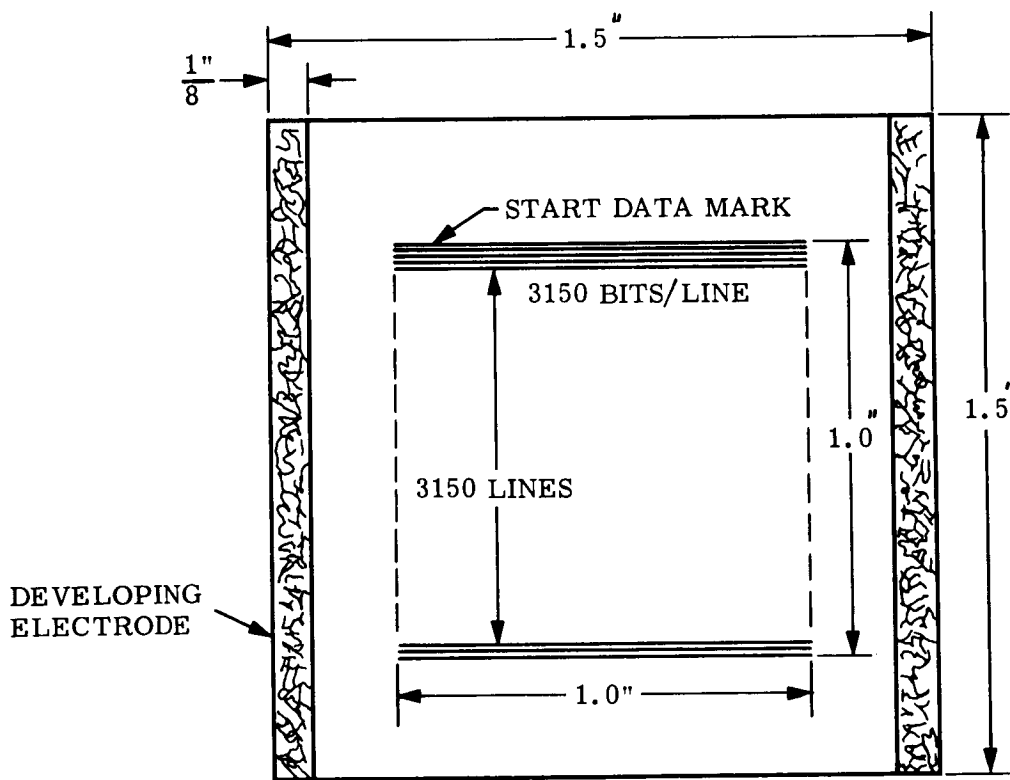


Figure 1.3.4-2. Thermoplastic Plate Format

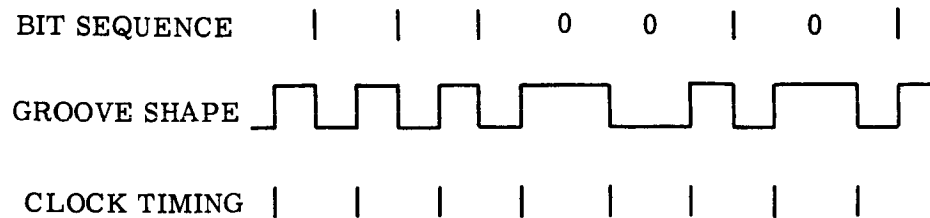


Figure 1.3.4-4. Phase Modulated Lateral Recording

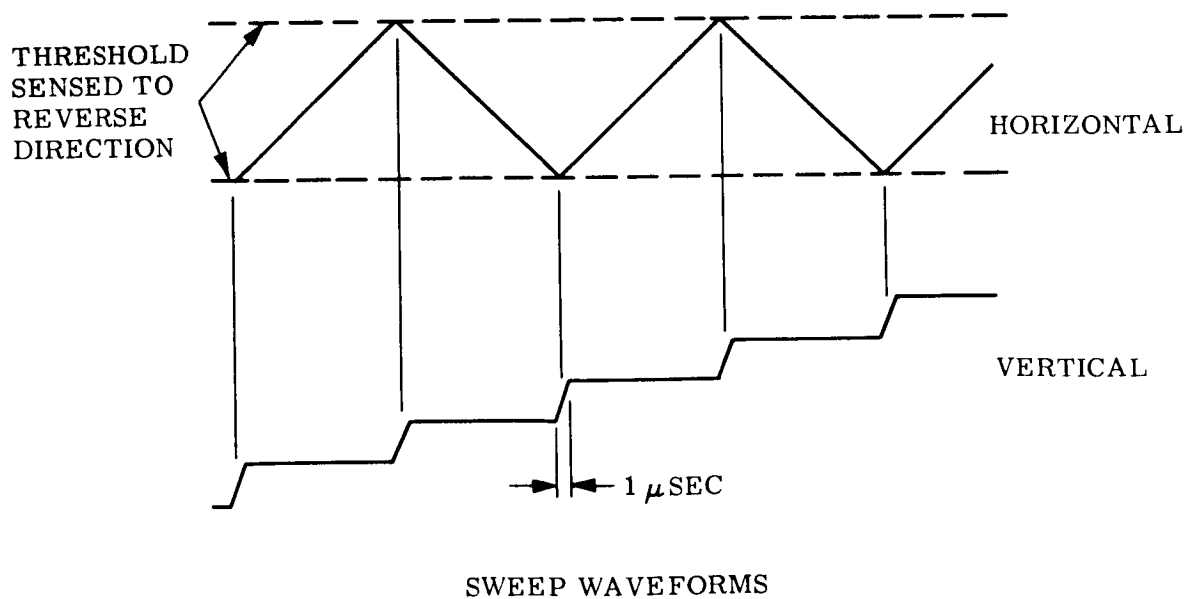
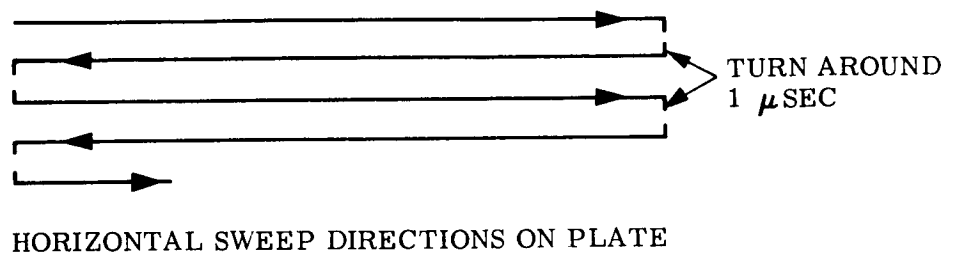


Figure 1.3.4-5. Data Recording Technique and Sweep Waveforms

its sweep. The horizontal sweep position vs time will be that shown in Figure 1.3.4-6. If the information bit is stored in a one-bit buffer at the instant of read out, it may be clocked out of the buffer in exact synchronism by the playback clock. The buffer will then be ready to receive the next bit read from memory. It is here assumed that the timing of data directly from the memory is not sufficiently accurate for transmission in the communications channel. If this is not the case, the buffer can be eliminated. The method of read out near the point of sweep turn-around is important. As described earlier, the last thing recorded on a groove is a bit and this action is followed by a writing beam transfer to the position of the next lower groove in about one microsecond or less. This means that the ends of two adjacent recorded grooves will appear as shown in Figure 1.3.4-7.

The readout electron beam will be following these grooves in the directions indicated at a different velocity than when it was recorded. The jump between successive grooves, however, will be at the same rate, so that a very negligible longitudinal motion will occur during transit. The deflection circuits will be triggered by sensing the end of the recorded groove on one line, transferring at that point to the next line, and starting scan in the opposite direction on that line. The first clock mark will again stop horizontal scan until the communications clock restarts the sweep, as previously described. Since the first mark on a groove will always be a clock, it will furnish an opportunity for re-establishing the clock in case an error in recording or reading the previous groove has caused loss of synchronism of data and clock. The end of a recorded groove is sensed while reading by observing the sum signal from the two collector electron multipliers. This signal suddenly drops in amplitude when the groove disappears. Since the jump between grooves is very short, little precision is necessary to assure that the reading beam will be well registered with the next groove when the scan is resumed.

1.3.5 PHYSICAL CHARACTERISTICS

Table 1.3.5-1 shows the size, weight, and power requirements of both the Data Processor and Thermoplastic Recorders for the Mars 1969 mission.

TABLE 1.3.5-1. SIZE, WEIGHT, & POWER REQUIREMENTS FOR DATA PROCESSING & STORAGE SUBSYSTEM

EQUIPMENT	LOCATION	SIZE (IN. ³)	WEIGHT (LBS)	POWER (W)
1. Data Processor	Lander	251	16	3.5
2. TPR	Lander	800	22	25
3. 100-kilobit Storage	Lander	80	3.5	0.25
TOTAL LANDER FIGURES		<u>1131</u>	<u>41.5</u>	<u>28.75</u>
4. Data Processor	Orbiter Main	183	12.3	2.5
5. Data Processor	Orbiter PHP	138	8.3	1.0
6. TPR (2 Units)	Orbiter Main	2400	50	50
7. 100-kilobit Storage	Orbiter Main	80	3.5	0.25
TOTAL ORBITER FIGURES		<u>2801</u>	<u>74.1</u>	<u>53.75</u>

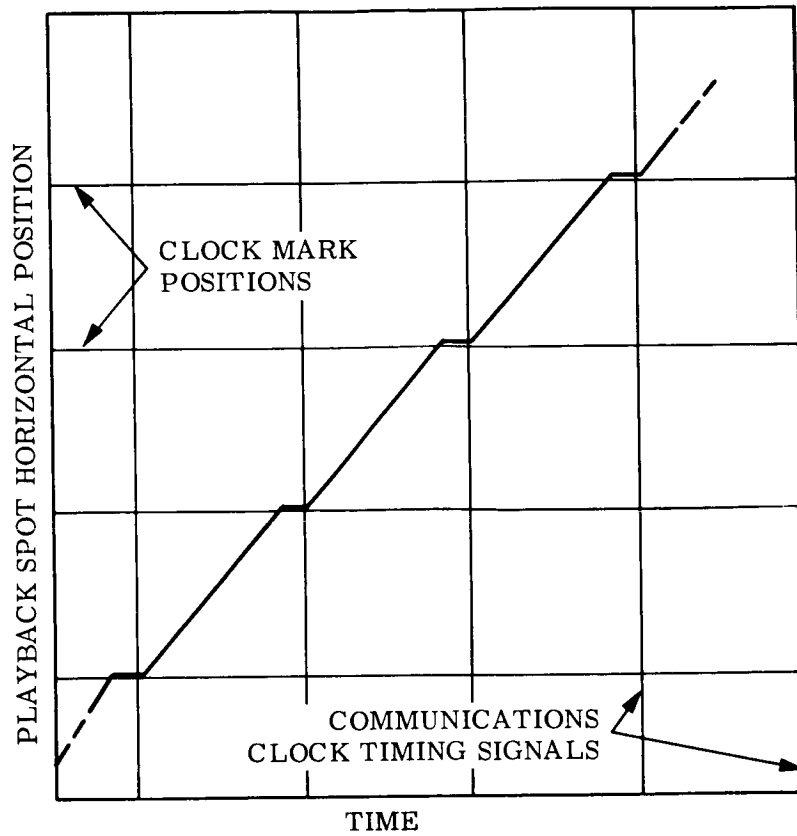


Figure 1.3.4-6. Playback Spot Position vs Time

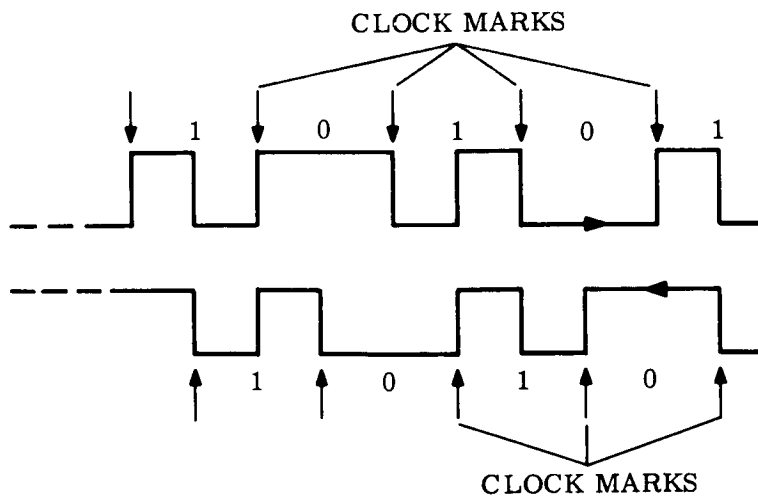


Figure 1.3.4-7. Recording Turn-Around Detail

1.4 DEEP SPACE TRANSMISSION SUBSYSTEM

1.4.1 FUNCTIONAL REQUIREMENTS

The Deep Space Transmission Subsystems of all Orbiters are required to:

1. Accept a serial digital waveform containing both data and bit synchronization information from the Data Processing and Storage Subsystem
2. Phase-modulate an RF carrier with the composite signal and transmit it to Earth
3. Receive command data on a phase-modulated RF carrier from Earth
4. Demodulate the command signals
5. Provide the demodulated data along with bit-synchronization pulses and a bit-synchronization lock signal to the Command and Computer Subsystem
6. Accept mode change commands from the Command and Computer Subsystem
7. Coherently translate the frequency and phase of the received RF carrier by a ratio of 240/221 to obtain the transmitted frequency
8. Provide an auxiliary stable frequency source which controls the transmitted frequency when no signals are being received from earth
9. Receive and transmit a ranging code

All of the above functions except the last three are also required of all Mars Lander Deep Space Transmission Subsystems; however, since the same Transponder is recommended for both Orbiters and Landers, functions (7) and (8) will be included. The ranging function (9) will be omitted in the Landers.

1.4.2 OPERATIONAL CONSIDERATIONS OF THE DEEP SPACE INSTRUMENTATION FACILITY (DSIF)

The DSIF will receive telemetry data from the vehicles, transmit commands to the vehicles, and determine the angle and radial velocity of the vehicles with respect to the Earth. In addition it will determine the range of the spacecraft from the Earth during the early portion of the transit period.

Reception and transmission at the DSIF sites will be via 85-foot and 210-foot dishes. At the time that the first recommended Voyager mission takes place (1969), at least two 85 foot antennas and one 210-foot antenna are expected to be operational at each of three DSIF ground stations, which are separated by approximately 120 degrees in longitude. The 210 foot antennas are to be used only for reception. The 85 foot antennas can be used for both transmission and reception; however, the latter function will probably only be performed during early transit and for tracking. Both 10-kilowatt and 100-kilowatt transmitters will be available; however, the higher power is expected to be used only as a back-up and may be available at only the Goldstone site.

1.4.3 SUBSYSTEM DESCRIPTION

A. Mars 1969 and 1971

(1) Orbiter

A block diagram of the Mars 1969 and 1971 Orbiter Deep Space Transmission Subsystem is shown in Figure 1.4.3-1. To achieve high reliability the subsystem is divided into two independent parts — one part associated with the high-gain antenna and the other associated with the omni or low-gain antenna. Transmission links 1 and 7 as defined in Section 1.1 are provided by the first part and links 2 and 8 by the second. Although the Power Amplifiers and Transmitters are identical in both parts, no switching is provided between the parts to give added redundancy. This capability could easily be added if a detailed reliability analysis shows it to be advantageous.

The waveform provided to the Transponders by the Data Processing and Storage Subsystem is a two-level digital signal which contains both the data and bit synchronization information. This signal phase-modulates the 2295 megacycle carrier between two levels — ± 60 degrees. The power in the resulting spectrum is divided such that 25 percent is in the discrete carrier and 75 percent in the sidebands. Up to fifty milliwatts of RF power are provided by the transmitter portion of the Transponder to drive the klystron power amplifiers. Two identical klystrons are utilized for redundancy. The RF switch allows signal transmission to the antenna from the klystron to which DC power is applied while isolating the other klystron from the high-level signal. Fifty watts of RF power are provided by either klystron. Isolation of the receiver portion of the Transponder from the transmitted signal is provided by a diplexer. The antenna is a ten-foot diameter horn-fed parabola resulting in a three-degree beamwidth.

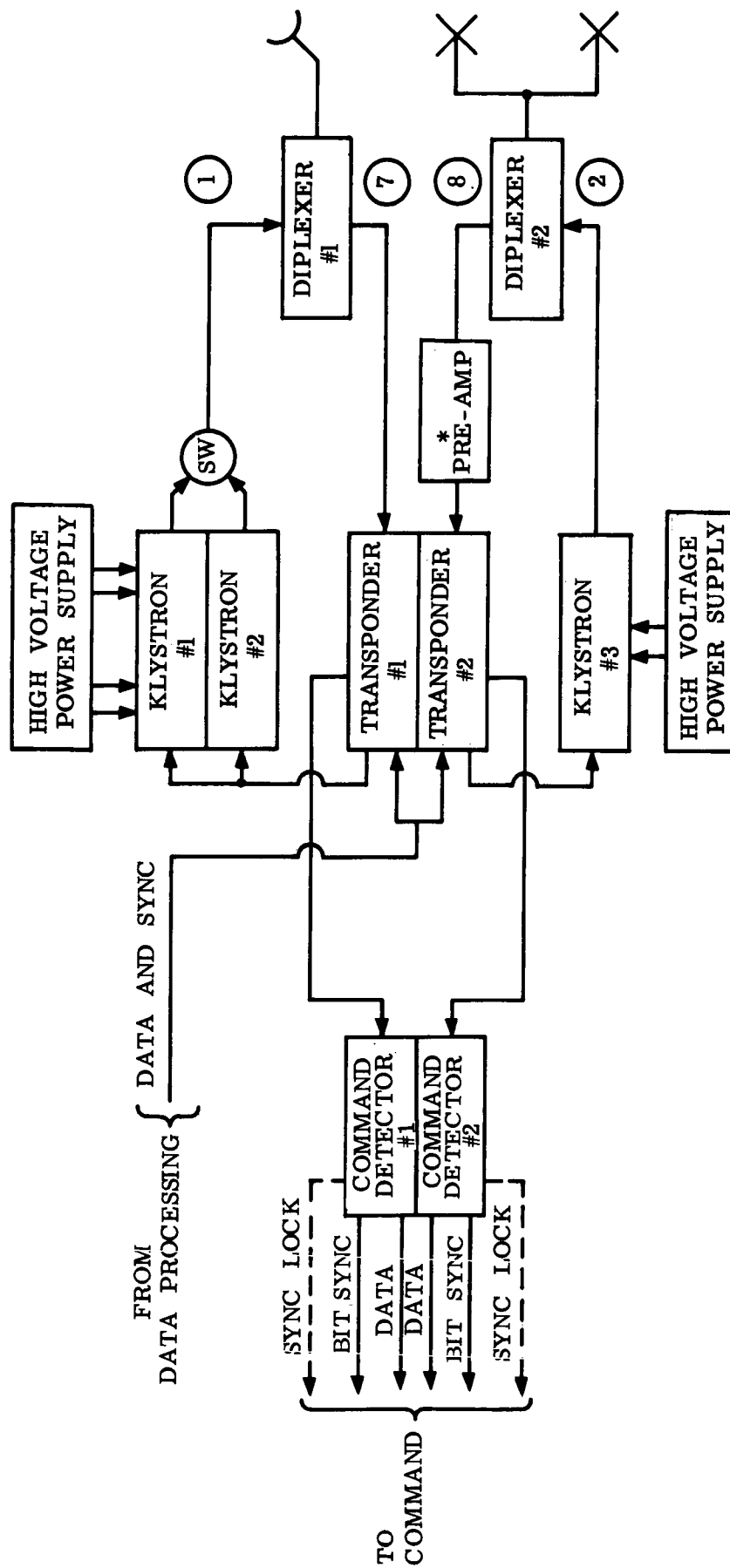
The signal received from the earth is a 2115-megacycle carrier which has been phase-modulated by a two-level waveform similar to that described previously. A triple-conversion synchronous receiver is utilized to detect the baseband waveform. The receiver has a nominal ten-db noise figure and a 20-cps carrier automatic phase-lock-loop bandwidth.

In addition to the demodulated waveform output, the receiver also provides a signal to the transmitter which is derived from the voltage controlled oscillator (VCO) and is both phase and frequency coherent with the received signal. After further frequency multiplication in the transmitter, the final transmitted carrier frequency is exactly 240/221 times the received signal and is utilized at the DSIF for the doppler tracking functions. When no signal is received by the Transponder, an AGC signal switches the transmitter frequency source from that just described to one derived from an auxiliary oscillator.

A turn-around ranging unit on the Transponder provides ranging out to lunar distances. The ranging signal is received by the Transponder, phase-detected, and re-transmitted on the coherent carrier.

The Command Detector accepts the demodulated command waveform from the receiver and separates the data from the bit sync information. The state of each bit ("1" or "0") is detected at the output of a matched filter, and the resulting two-level data waveform is sent to the Command and Computer Subsystem so that commands can be rejected if they are not being detected properly.

Other than utilizing a low-gain antenna, the second part of the subsystem differs from the first part in that a tunnel-diode pre-amplifier precedes the receiver to reduce the overall noise figure to approximately five db, no redundant klystron is utilized, the carrier phase-lock-loop bandwidth of the receiver is reduced from 20 cps to 10 cps, and the Command Detector operates at one half bit per second rather than ten bits per second. The latter two changes require only minor modifications to the Receiver and the Command Detector.



* ALL ORBITERS EXCEPT MARS 1973

Figure 1.4.3-1. Orbiter Deep Space Transmission Subsystem

The low-gain antennas selected for all Orbiters consist of two turnstiles located on opposite sides of the spacecraft. An equal division of power is utilized; however, since only one of the turnstiles will be within line-of-sight of the earth during transit under normal conditions, a higher portion of the power could be diverted through that turnstile, if desired, by adding a power divider. Undesirable partial interference nulls in the meridial plane between the two turnstiles will occur. Techniques to eliminate this problem are discussed in Section 1.7.2; however, the best technique cannot be determined until a more detailed study is made of the possible maneuver and emergency orientations and a transmission philosophy selected for these periods.

(2) Landers

The Mars 1969 and 1971 Lander Deep Space Transmission Subsystem block diagram is shown in Figure 1.4.3-2. This subsystem is a back-up to the Relay Transmission Subsystem and contains no component redundancy. The single RF input-output line is switched between the high-gain and low-gain antennas to provide links 3, 4, 9, and 10 as defined in Section 1.1. The Transponder and Command Detector are identical to those associated with the low-gain antenna in the Orbiter. Although the klystron design is identical to that of the orbiter klystrons, 70 watts are radiated instead of 50 watts. An RF switch similar to that used in the Orbiter provides antenna switching. The high-gain antenna of the 1969 Lander is a helix with 21 db gain and a beamwidth of approximately 14.5 degrees. A 26.7 db helix array with a beamwidth of approximately 7.5 degrees is used in the 1971 Lander. The low-gain antenna utilizes radiating crossed dipoles backed by a parasitic crossed-reflector to achieve a hemispherical pattern.

B. Mars 1973 and 1975

(1) Orbiter

The block diagram for the Mars 1973 and 1975 Orbiter Deep Space Transmission Subsystem is identical to that for Mars 1969 and 1971 as shown in Figure 1.4.3-1; however, the klystron is operated at a power level of 35 watts instead of 50 watts and the preamplifier is eliminated for 1973 because of the sterilization requirement.

(2) Landers

Both the 1973 and 1975 Orbiters are short-lived; therefore, the Lander Deep Space Transmission Subsystem provides the prime communication links with earth. To increase reliability, the subsystem is divided into two independent parts as described for the Mars 1969 and 1971 Orbiters. Its block diagram is shown in Figure 1.4.3-3. The klystrons radiate 70 watts. Both antennas are identical to those used on the 1971 Lander. The Command Detectors are identical to those of the 1969 and 1971 Orbiters except that the bit rate of the detector associated with the high-gain antenna operates at a command rate of 2 bits per second.

C. Venus 1970

There is no Deep Space Transmission Subsystem in the Venus 1970 Lander. The Orbiter subsystem is identical in every respect to that of the Mars 1969 and 1971 Orbiters. Its block diagram is shown in Figure 1.4.3-1.

D. Venus 1972

The Orbiter Deep Space Transmission Subsystem for the Venus 1972 is identical to that described for the Mars 1975 mission. Figure 1.4.3-1 shows the block diagram of the subsystem. There are no direct communication links between the Lander and Earth.

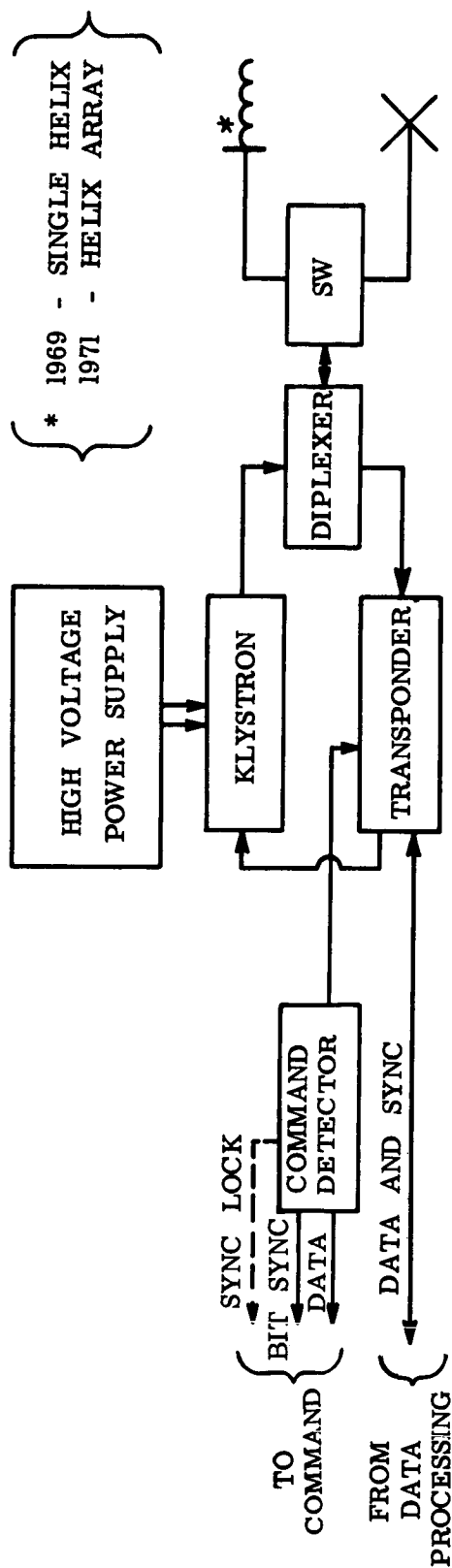


Figure 1.4.3-2. Mars 1969 and 1971 Lander Deep Space Transmission Subsystem

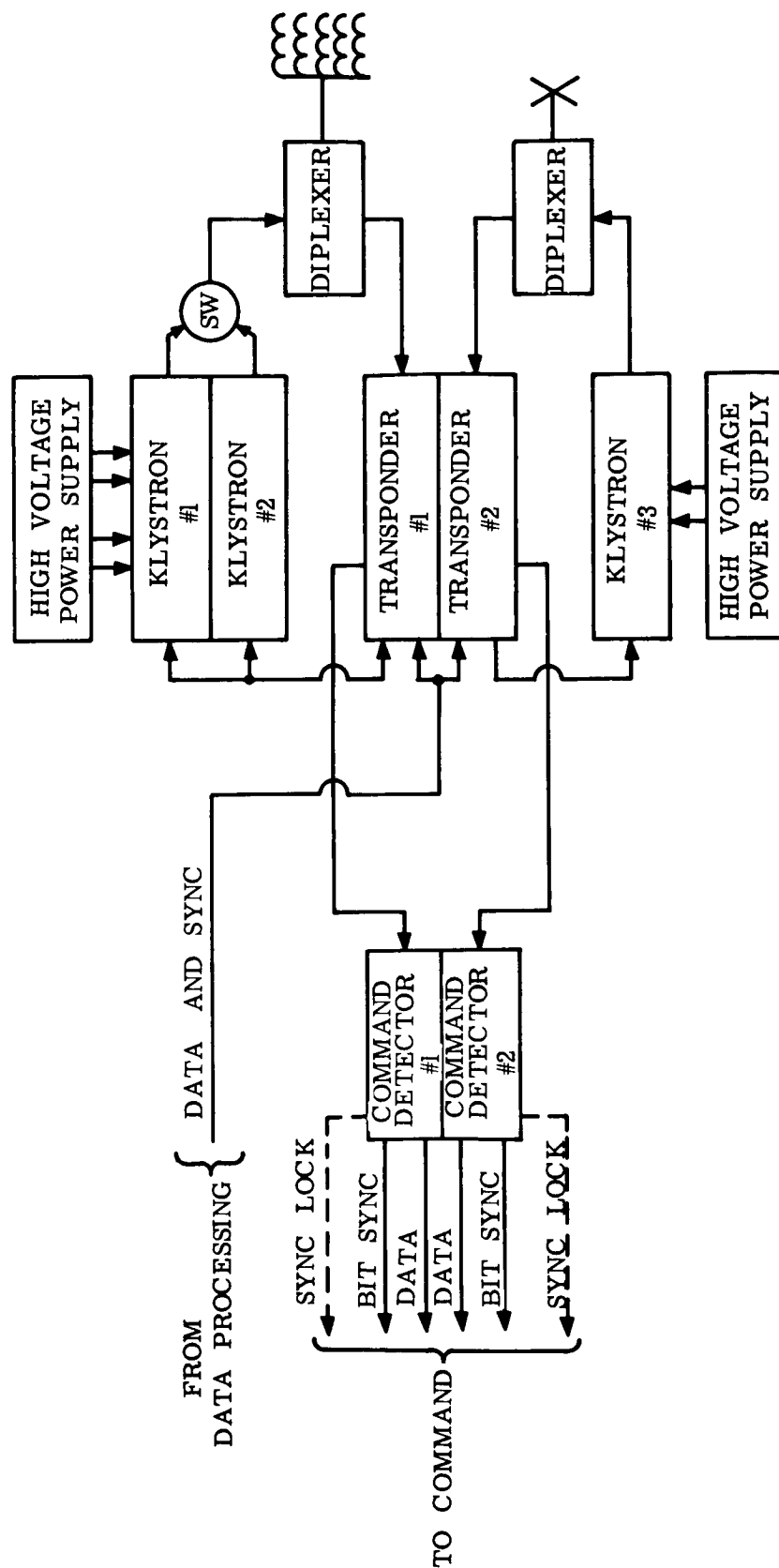


Figure 1.4.3-3. Mars 1973 and 1975 Lander Deep Space Transmission Subsystem

1.4.4 COMPONENT DESCRIPTION

All components are described in Section 1.7. In addition to the description of recommended components, alternate configurations and selection considerations are given there.

1.4.5 PERFORMANCE CALCULATIONS

The parameters and resulting performance equations for the eight links are listed in Table 1.4.5-1. Parameter values that are identical for all missions are stated numerically in db. Where values are not identical, the parameters are only listed in the table and retained in the equations as variables. A transmission range of one AU (81×10^6 nautical miles) is used in each case; however, the results are extended to indicate performance as a function of range in Section 1.4.6. All values utilized to evaluate the performance of each link are discussed below.

A. Telemetry Links — Links (1), (2), (3), and (4)

1. Transmitter Power

Mars 1969 and 1971 (Orbiters):	50 watts
Mars 1969 and 1971 (Landers):	70 watts
Mars 1973 and 1975 (Orbiters):	35 watts
Venus 1970 (Orbiter):	50 watts
Venus 1972 (Orbiter):	35 watts

2. Transmitting Circuit Loss

All vehicles: 2 db estimated

3. Transmitting Antenna Gain

a. High-gain Antennas

All Orbiters:	34.7 db (10 ft dish)
Mars 1969 (Landers):	21.0 db (Helix)
Mars 1971, 1973, and 1975 (Landers):	26.7 db (Helix Array)

b. Low-gain Antennas

The product of the gain, pointing loss, and polarization loss of all omni or low-gain antennas has been taken to be unity in the margin calculations. The actual values in each case will depend on the interacting effects of the radiating elements and the vehicle in addition to the orientation of the vehicle with respect to the earth. For the Landers the interaction and possible obstruction due to the planet surface is also a factor. More refined values can be presented when the above aspects are clearly defined for each vehicle as a function of mission phase; however, preliminary results indicate that the product of the refined values will not vary significantly from unity as assumed, except during some emergency and Orbiter maneuver modes.

TABLE 1.4.5-1. DEEP SPACE LINK PERFORMANCE CALCULATIONS (db)

Link Parameter	(1)	(2)	(3)	(4)	(7)	(8)	(9)	(10)
1. Transmitter Power	P_t	P_t	18.5	18.5	40.0	40.0 (50.0)	40.0	40.0 (50.0)
2. Transmitting Ckt. Loss	-2.0	-2.0	-2.0	-2.0	-0.5	-0.5	-0.5	-0.5
3. Transmitting Antenna Gain	34.7	0.0	G_t	0.0	51.0	51.0	51.0	51.0
4. Transmitting Antenna Pointing Loss	-1.2	0.0	L_{pt}	0.0	-	-	-	-
5. Space Loss	-263.2	-263.2	-263.2	-263.2	-262.5	-262.5	-262.5	-262.5
6. Polarization Loss	-	0.0	-	0.0	-	0.0	-	0.0
7. Receiving Antenna Gain	61.0	61.0	61.0	61.0	34.0	0.0	G_r	0.0
8. Receiving Antenna Pointing Loss	-	-	-	-	-1.1	0.0	L_{pt}	0.0
9. Receiving Ckt. Loss	-0.2	-0.2	-0.2	-0.2	-2.0	-2.0	-2.0	-2.0
10. Net Ckt. Loss	-170.9	-204.4	$G_t + L_{pt} - 204.4$	-204.4	-181.9	-214.0	$G_r + L_{pt} - 214.0$	-214.0
11. Total Received Power	$P_t - 120.9$	$P_t - 204.4$	$G_t + L_{pt} - 185.9$	-185.9	-141.9	-174.0 (-164.0)	$G_r + L_{pt} - 174.0$	-174.0 (-164.0)
12. Receiver Noise Spectral Density	-213.2	-213.2	-213.2	-213.2	-194.0	N_o	-194.0	-194.0
13. Carrier Modulation Loss	-6.0	-6.0	-6.0	-6.0	-4.4	-4.4	-4.4	-4.4

TABLE 1.4.5-1. DEEP SPACE LINK PERFORMANCE CALCULATIONS (Continued)

Link Parameter	(1)	(2)	(3)	(4)	(7)	(8)	(9)	(10)
14. Received Carrier Power	$P_t - 176.9$	$P_t - 210.4$	$G_t + L_{pt} - 191.9$	-191.9	-145.5	-178.4 (-168.4)	$G_r + L_{pt} - 178.4$	-178.4 (-168.4)
15. Carrier APC Loop Noise Bandwidth ($2B_{LO}$)	4.8	4.8	4.8	4.8	13.0	10.0	$2B_{LO}$	10.0
16. Threshold SNR in $2B_{LO}$	6.0	6.0	6.0	6.0	6.0	6.0	6.0	6.0
17. Threshold Carrier Power	-202.4	-202.4	-202.4	-202.4	-175.0	$N_o + 16.0$	$2B_{LO} - 188.0$	-178.0
18. Carrier Performance Margin	$P_t + 25.5$	$P_t - 8.0$	$G_t + L_{pt} + 10.5$	10.5	29.5	$-N_o - 194.4$ ($-N_o - 184.4$)	$G_r + L_{pt} - 2B_{LO} + 9.6$	-0.4 (9.6)
19. Data Modulation Loss	-1.3	-1.3	-1.3	-1.3	-1.9	-1.9	-1.9	-1.9
20. Received Data Sub-carrier Power	$P_t - 172.2$	$P_t - 205.7$	$G_t + L_{pt} - 187.2$	-187.2	-143.0	-175.9 (-165.9)	$G_r + L_{pt} - 175.9$	-175.9 (-165.9)
21. Bit Rate ($1/T$)	$P_t + 27.0$	$P_t - 6.5$	$G_t + L_{pt} + 12.0$	12.0	13.0*	0.0*	R_s^*	0.0*
22. Required ST/(N/B)	6.0	6.0	6.0	6.0	18.5	18.5	18.5	18.5
23. Threshold Subcarrier Power per Bit/Sec	-205.2	-205.2	-205.2	-205.2	-175.5	$N_o + 18.5$	-175.5	-175.5
24. Data Performance Margin	8.0	8.0	8.0	8.0	19.5	$-N_o - 194.4$ ($-N_o - 184.4$)	$G_r + L_{pt} - R_s - 0.4$	-0.4 (9.6)

* Symbol Rate -- Two symbols per command bit

4. Transmitting Antenna Pointing Loss

a. High-Gain Antennas

All Orbiters: 1.2 db (Pointing Error =
± 1 degree)

Mars 1969 (Landers): 0.5 db (Pointing Error =
± 3 degrees)

Mars 1971, 1973 and
1975 (Landers): 1.7 db (Pointing Error =
± 3 degrees)

b. Low-Gain Antennas

See item 3 (Transmitter Antenna Gain)

5. Space Loss

Space loss has been calculated for a transmitting frequency of 2295 megacycles and a transmission range of 1.0 AU (263.2 db).

6. Polarization Loss

High-Gain Antennas: Negligible

Low-Gain Antennas: See item 3 (Transmitting Antenna Gain)

7. Receiving Antenna Gain

The proposed DSIF 210-ft. dishes with 61-db gain have been assumed in the table for reception at Earth; however, maximum tracking ranges utilizing both the 210- and 85-foot dishes are shown in Section 1.4.6.

8. Receiving Antenna Pointing Loss

Negligible

9. Receiving Circuit Loss

0.2 db (estimated)

10. Net Circuit Loss

Sum of the parameter values given in items 2 through 9.

11. Total Received Power

Sum of the parameter values given in items 1 through 9.

12. Receiver Noise Spectral Density

All links: -213.2 db (System Noise Temperature = 35°K)

13. Carrier Modulation Loss

All links: 6.0 db (PCM/PSK ± 60°)

14. Received Carrier Power

Sum of items 11 and 13.

15. Carrier APC Loop Noise Bandwidth ($2 B_{LO}$)

All links: 3 cps minimum

16. Threshold SNR in $2 B_{LO}$

All links: 6 db

17. Threshold Carrier Power

Sum of items 12, 15, and 16.

18. Performance Margin

Item 14 minus 17 (for a primary link this value should not be less than approximately 8 db, which is the estimated sum of the negative tolerances of the parameter values).

19. Data Modulation Loss

All links: 1.3 db (PCM/PSK $\pm 60^\circ$)

20. Received Data Subcarrier Power

Sum of items 11 and 19.

21. Bit Rate ($1/T$)

Links (1) through (4): item 20 minus the sum of items 12 and 23.

22. Required ST/ (N/B)

All links: 6.0 db (for bit error probability of 1.4×10^{-3}).

This value includes the effect of error control coding (1.5 db) and detection losses (1.0 db). Note that T is the reciprocal of the data bit rate and not that of the transmitted digit rate. Because of the addition of 28 coding bits to each group of 45 data bits the transmitted digit rate is 73/45 times the data bit rate.

23. Threshold Subcarrier Power Per Bit/Sec

Sum of items 12 and 22.

24. Performance Margin

All links: 8.0 db. This value is approximately equal to the sum of the anticipated negative tolerances associated with the subsystem parameters for the prime modes. In the backup modes utilizing the low-gain antennas the negative tolerances might be greater than eight db because of the variations of antenna pointing and polarization losses. However, an eight db margin should be adequate for most situations in which the backup modes would be utilized.

B. Command Links — Links (7), (8), (9), and (10)

1. Transmitter Power

Normal Mode: 10,000 watts

Backup Mode: 100,000 watts

2. Transmitting Circuit Loss

All links: 0.5 db (estimated)

3. Transmitting Antenna Gain

The DSIF 85 ft. dishes with 51.0 db gain are assumed for all transmission from the Earth.

4. Transmitting Antenna Pointing Loss

Negligible

5. Space Loss

Space loss has been calculated for a transmitting frequency of 2115 megacycles and a transmission range 1.0 AU (262.5 db).

6. Polarization Loss

a. High-gain Antenna: Negligible

b. Low-gain Antennas: See Telemetry Links - Item 3 (Transmitting Antenna Gain)

7. Receiving Antenna Gain

a. High-gain Antennas

All Orbiters: 34.0 db (10 ft dish)

Mars 1969 (Landers): 20.3 db (Helix)

Mars 1971, 1973, and
1975 (Landers): 26.0 db (Helix Array)

b. Low-gain Antennas

See Telemetry Links — Item 3 (Transmitting Antenna Gain)

8. Receiving Antenna Pointing Loss

a. High-gain Antennas

All Orbiters: 1.1 db (pointing error = ± 1 degree)

Mars 1969 (Landers): 0.4 db (pointing error = ± 3 degrees)

Mars 1971, 1973 and
1975 (Landers): 1.5 db (pointing error = ± 3 degrees)

b. Low-gain Antennas

See Telemetry Links — Item 3 (Transmitting Antenna Gain)

9. Receiving Circuit Loss

All vehicles: 2.0 db (estimated)

10. Net Circuit Loss

Sum of Items 2 through 9.

11. Total Received Power

Sum of Items 1 through 9.

12. Receiver Noise Spectral Density

Links (7), (9), and (10): -194 dbw

Link (8): -194 dbw Mars 1973
-199 dbw All Others

13. Carrier Modulation Loss

All links: 4.4 db (PCM/PSK ± 53 degrees)

This phase deviation results in equal margin in the carrier and data channels for a one symbol per second command rate. (See Section 1.6.5.) In the links operating at the higher rates the margin is unbalanced but more than adequate in both channels.

14. Received Carrier Power

Sum of Items 11 and 13.

15. Carrier APC Loop Noise Bandwidth ($2 B_{LO}$)

Prime Mode:

All Orbiters: 20 cps

Mars 1969 and 1971 (Landers): 10 cps

Mars 1973 and 1975 (Landers): 20 cps

Backup Mode:

All Orbiters and Landers: 10 cps

16. Threshold SNR in $2 B_{LO}$

All links: 6 db

17. Threshold Carrier Power

Sum of Items 11 and 13

18. Performance Margin

Items 14 minus 17 (This value should not be less than approximately 8 db for a prime link.)

19. Data Modulation Loss

All links: 1.9 db (PCM/PSK ± 53 degrees)

20. Received Data Subcarrier Power

Sum of Items 11 and 19

21. Symbol Rate (Note: 2 symbols per command bit)

Prime Mode:

All Orbiters and Mars 1963 Lander: 20 symbols/sec

Mars 1969 and 1971 (Landers): 1 symbol/sec

Mars 1973 and 1975 (Landers): 4 symbols/sec

Backup Mode:

All Orbiters and Landers: 1 symbol/sec

22. Required $ST/(N/B)$ (S = Signal Power; $1/T$ = Symbol Rate; N/B = Noise Power Spectral Density)

All links: 18.5 db (probability of symbol error = 10^{-5})

This is the value presently quoted by Motorola for their double-channel detector operating at a rate of one bit per second and for a bit-error probability of 10^{-5} . It is understood that a single-channel detector (as recommended in this report) presently being developed for JPL offers a slight improvement in detection capability. The above value is therefore expected to be conservative.

23. Threshold Subcarrier Power per Bit/Sec

Sum of Items 12 and 22

24. Performance Margin

Item 20 minus the sum of Items 21 and 23

1.4.6 RESULTS

The results of interest determined in the calculations of the previous section are:

1. Data rates of telemetering links
2. Carrier channel performance margins for telemetry links
3. Data channel performance margins for command links
4. Carrier channel performance margins for command links.

The telemetry data rates are given for each link as a function of range in Figures 1.1.3-1 through 1.1.3-4 in Section 1.1. The maximum range at which each of these links can operate is determined by the threshold constraints in the data and carrier channels. Since the data rate can be selected for a link such that threshold is not reached in the data channel before it is reached in the carrier channel and since the carrier channel threshold determines the tracking range, only the range at which carrier channel threshold occurs is considered here. This range is shown for each link in Table 1.4.6-1 under four conditions. These conditions are:

1. Reception with a 210 foot dish with a 8 db margin in the link
2. Reception with a 210 foot dish with no margin in the link (values in parentheses)
3. Reception with an 85 foot dish with an 8 db margin
4. Reception with an 85 foot dish with no margin (values in parentheses).

The first condition gives the worst case design range for each link while the range determined under the second condition indicates the maximum range which is possible if the parameters are at their nominal values. The latter is listed for all links but should be used only to indicate possible performance for an emergency or backup link. The third and fourth conditions are utilized to indicate the tracking range utilizing an 85 foot dish. A gain of 51.8 db was used for the 85 foot dish to determine each range.

Similarly, the range at which carrier threshold occurs is shown in Table 1.4.6-2 for each of the command links. The four conditions used in this case were:

1. Transmission of 10 kilowatts with 8 db margin in link
2. Transmission of 10 kilowatts with no margin in link (value in parentheses)
3. Transmission of 100 kilowatts with 8 db margin in link
4. Transmission of 100 kilowatts with no margin in link (vales in parentheses)

The first condition indicates the design range while the second condition indicates the maximum possible range if all parameter values are nominal. The latter indicates possible performances in an emergency mode if the 100-kw transmitter is not available. Conditions three and four indicate the design range and maximum range, respectively, for backup modes when the 100-kw transmitter is used.

The range at which threshold is reached in the data channel of each command link is not shown; however, the data rate has been selected in each link such that either the carrier and data channel thresholds are reached simultaneously (rate = 0.5 bits/sec) or the data channel threshold cannot be reached at the maximum earth-planet range under design conditions (8 db margin and 10 kilowatts transmitted).

It should also be noted that the carrier tracking range of each telemetry link can be doubled by removing the modulation (carrier modulation loss = 6 db). The carrier tracking range of each command can be extended by a factor of 1.3 (carrier modulation loss = 4.4 db) by the same method.

TABLE 1.4.6-1. CARRIER-LOCK RANGE IN MILLIONS OF NAUTICAL MILES (TELEMETRY LINKS)

Telemetry Link	Mars 1969 and 1971		Mars 1973 and 1975		Venus 1970		Venus 1972	
	210 ft	85 ft	210 ft	85 ft	210 ft	85 ft	210 ft	85 ft
(1)	4400* (11000)**	1480 (3700)	3560 (8900)	1240 (3100)	4400 (11000)	1480 (3700)	3560 (8900)	1240 (3100)
(2)	91 (227)	37.6 (94)	76 (190)	26 (65)	91 (227)	37.6 (94)	76 (190)	26 (65)
(3)	1969 { 1020 { (2560) 1970 { 1920 { (4800)	{ 356 { (890) { 670 { (1670)	1920 (4800)	670 (1670)	—	—	—	—
(4)	108 (270)	37.6 (94)	108 (270)	37.6 (94)	—	—	—	—

* Includes 8-db margin

** Values shown in parentheses are for zero margin

TABLE 1. 4. 6-2. CARRIER-LOCK RANGE IN MILLIONS OF NAUTICAL MILES (COMMAND LINKS)

Command Link	Mars 1969 and 1971		Mars 1973 and 1975		Venus 1970		Venus 1972	
	10 kw	100 kw	10 kw	100 kw	10 kw	100 kw	10 kw	100 kw
(7)	950* (2400)**	3000 (7600)	950 (2400)	3000 (7600)	950 (2400)	3000 (7600)	950 (2400)	3000 (7600)
(8)	55 (135)	175 (435)	32 } 1973 (78)	100 } 1973 (250)	55 (135)	175 (435)	55 (135)	175 (435)
(9)	300 } 1969 (770)	950 } 1969 (2400)	370 (920)	1150 (2900)	—	—	—	—
(10)	32 (78)	100 (250)	32 (78)	100 (250)	—	—	—	—

* Includes 8-db margin

** Values shown in parentheses are for zero margin.

1.5 RELAY TRANSMISSION SUBSYSTEM

1.5.1 SCOPE

The Voyager system requires two way communication links between the Landers and the Earth. The bulk of the data originating in the Lander which must ultimately be transmitted to Earth is from the Lander television camera. A lesser amount of the data (perhaps 10 percent of the total) will be scientific and diagnostic telemetry. The data which must be sent from Earth to the Landers consists of the commands required to select operational modes of the Lander, to enable or disable various Lander equipments, and in general to exercise control of the Lander beyond a programmed nominal sequence of events. The required command data rate will be as much as two to three orders of magnitude lower than the data rate from the Lander.

This section of the report concerns itself with the accomplishment of the above communications by use of a relay link through the Orbiter. The considerations which affect the choice between an Orbiter-to-Lander relay link and a direct Lander-to-Earth link are discussed. A discussion of the trade-offs involved in the selection of the relay link parameters such as carrier frequency and modulation/detection schemes is presented. A description of the proposed system follows, including block diagrams, size, weight, and power estimates. The performance of this system is then evaluated with respect to the planned orbits and Lander descent trajectories for the Mars and Venus missions.

1.5.2 THE NEED FOR A RELAY LINK

The choice between a direct Lander-to-Earth link and a relay link through the Orbiter for accomplishing communications between the Lander and Earth is influenced by many factors. The primary factor favoring a direct link is that it enables the Lander and Orbiter modules to be operationally independent after separation. Thus receipt of the Lander data is independent of successful injection of the Orbiter, of operation of the Orbiter equipment, of line-of-sight time between Lander and Orbiter, and of Orbiter lifetime. This consideration becomes the deciding factor in those missions which have short Orbiter lifetimes due to orbit decay or in a fly-by mission.

On the other hand there are many practical, environmental, and operational problems associated with a direct high-capacity microwave link (compatible with the DSIF network) from Lander to Earth. These factors, which are summarized in Table 1.5.2-1 clearly indicate the desirability of relaying communications through the Orbiter for certain missions. The Venus missions, for example, will employ a relay link because the short Lander lifetimes combined with the adverse environmental conditions are incompatible with the erection, acquisition, and steering of a high-gain Lander antenna.

For the MARS 1969 and 1971 missions the longer Lander lifetimes make the use of a direct link feasible, but a relay link is preferable because of the uncertain effects of terrain and environmental conditions on Lander righting capability and antenna erection and steering.

The short Orbiter lifetime of the MARS 1973 and 1975 missions becomes the deciding factor and indicates the choice of a direct link here. The uncertainties of terrain and environmental conditions will have been evaluated by the earlier missions. During the Lander descent phase, however, communications from the Lander to the Earth will be relayed through the Orbiter.

1.5.3 SELECTION OF THE CARRIER FREQUENCY

The optimum transmission frequency for the relay link appears to lie in the VHF band. The primary factors affecting the choice of carrier frequency are discussed in the following paragraphs.

**TABLE 1.5.2-1. FACTORS INFLUENCING CHOICE OF
LANDER-TO-EARTH COMMUNICATIONS LINK**

<u>Consideration</u>	<u>Venus</u>	<u>Mars</u>
(1) The electrical power available on the surface will be limited (due to limited weight of the Lander and the impracticability of installing solar-cell paddles on the Lander).	Lander: about 100 watt-hrs (batteries) Orbiter: 600 watts	70-90 watts (RTG unit) 600 watts
(2) Surface environmental conditions, such as winds, temperatures, and pressures make the erection and steering of a large antenna difficult. The dust storms also interfere with optical earth tracking sensors.	Wind: up to 200 mph Pressure: 6 to 54 atmos Temp: 800°F Other:	up to 140 mph 0.015 to 0.15 atmos -320 to +120°F Occasional dust storms of several weeks duration
(3) The planetary encounter geometry might cause the Lander to lose sight of the earth even before landing.	Important, due to short lifetime of Lander	Not applicable
(4) Effect of terrain uncertainty on righting ability of Landers.	Important	Important
(5) Design lifetimes of the Orbiters and Landers.	Orbiter: 3 months Lander: 10 min. to 6 hrs.	3 mos. (1969 and 1971) 10 days (1973) fly-by (1975) 6 months
(6) State-of-the-art in equipment suitable for the environments.	Lander requires rugged high temperature components	Lander requires rugged components
(7) The Orbiter is collecting a large amount of its own data which must somehow be transmitted to Earth anyway.	Cloud photos and radar surface mapping data	Television surface mapping data

A. Antenna Considerations

Since it is not considered technically advisable to require the Lander to track the Orbiter with a narrow-beam antenna, a hemispherical (horizon-to-horizon) antenna pattern is planned for the Lander. Circular polarization is planned, with a centerline gain of 2 db oriented along the Lander local vertical, as determined by the Lander's orientation system. More directivity is available in the Orbiter antenna, since it can be mounted on the Orbiter's planet-pointing package. The beamwidth of the Orbiter antenna may therefore be made equal to the angle subtended by the planet plus a small tolerance. Thus the antennas are gain-limited on both ends of the link, due to the required pattern geometry, and the gains are independent of frequency. The size and weight of the antennas increase as the frequency is decreased but this should not be a major factor if lightweight flexible elements are used.

B. Transmitter Efficiency

The prime power requirements of conventional tube power amplifiers tend to increase with frequency, although not appreciably within the VHF band. However, the available RF output power of solid-state transmitters drops off rapidly at frequencies above 100 mc, at which about 25 watts can be obtained. Therefore, it appears desirable from the transmitter viewpoint to operate at or below 100 mc in order to take advantage of the reduced size, weight, and power requirements of a solid-state transmitter. This will also eliminate transmitter warm-up time, be more rugged, and offer greater reliability than a tube-type transmitter.

C. Bandwidth

The frequency uncertainty due to oscillator instability and doppler shift is directly proportional to the carrier frequency. It is desirable to minimize the amount of frequency uncertainty in order to minimize the pre-detection bandwidth (hence, transmitter power) of a conventional receiver, or to minimize the acquisition time of a frequency-tracking receiver. Therefore, low carrier frequencies appear attractive here.

D. Free-Space Attenuation

Free-space attenuation is the dominant factor which degrades the communication capacity as frequency increases. This is, of course, merely a factor used in the range equation for mathematical convenience. The physical cause is a reduction of the effective area of the constant-gain receiving antenna with increasing frequency. Since the free-space attenuation is proportional to the square of the frequency, a low carrier frequency is desirable.

E. System Noise Temperature

The noise temperature of the receiving system is derived from the receiver noise and RF losses inside the Orbiter and the effective noise temperature which the antenna "sees" external to the Orbiter. Inside the Orbiter the noise will be due primarily to the receiver itself, for which a noise figure of 4 db at 100 mc, increasing gradually to 5 db at 500 mc, has been assumed. Galactic noise (min.) temperature is about 1000°K at 100 mc and decreases to about 100°K at 500 mc. This would be an important factor to consider when using an isotropic antenna, but for a directional antenna on the Orbiter the antenna noise will be determined by the surface temperature of the planet. The noise temperature of Venus has been taken to be 700°K and the maximum noise temperature of Mars to be 320°K, independent of frequency. Therefore, noise considerations indicate the desirability of a relatively low frequency.

F. Ionospheric Effects

To avoid ionospheric reflection and attenuation it is essential to keep well above the critical frequency of the ionosphere, given by:

$$f_{\text{crit.}} \approx 9 \sqrt{N_e} \quad (1)$$

where N_e is the electron density per cubic meter. The electron density in the Venusian atmosphere has been estimated to be 10^{12} electrons per cubic meter, which corresponds to a critical frequency of 9 mc. The critical frequency for the Martian atmosphere is estimated to be even less than this.

G. Selected Frequency

Most of the factors discussed tend to indicate the choice of a low VHF frequency, with the limit being established by the dimensions of the antenna elements. For the Lander con-

figurations presently being planned, it appears that a reasonable compromise will be a frequency in the neighborhood of 100 mc.

1.5.4 MODULATION/DETECTION SCHEMES

A. Detection

In order to minimize the required transmitter power and maximize the data rate, some form of coherent detection should be used. Otherwise the frequency uncertainty due to oscillator instability between the Lander and Orbiter and the doppler shift will require a significant widening of the pre-detection noise bandwidth which will unduly degrade the information capacity of the link. This is seen by considering some typical values. For an oscillator instability of 10^{-5} at a carrier frequency of 100 mc, the frequency uncertainty is ± 100 cps. The doppler shift will of course vary with the orbit, but typical values for the orbits which have been investigated range from ± 500 cps to ± 1000 cps. Thus the maximum total frequency uncertainty varies from 3 to 4 kc, which is of the same order of magnitude as the information bandwidth.

B. Video Data

Since all of the data will be in digital form (see Section 1.8.1 for discussion of digital TV vs analog TV) the first step employed in the modulation scheme will be pulse-code modulation (PCM). Assuming the analog-to-digital converter quantizes the signals to within \pm one-half a quantum level, the accuracy of the quantization may be expressed as:

$$E = \pm (1/2)^{n+1} \quad (2)$$

where E is the quantization error and n is the number of bits per sample.

For $|E| \leq 0.01$, n must be ≥ 6 . Therefore, six-bit encoding will be employed in order to achieve a quantization accuracy of $\pm 1\%$ of full scale. To be consistent with the S-band link from the Orbiter to Earth, a bit error probability of 10^{-3} will be assumed for the Lander-to-Orbiter link (see Television Subsystem, Section 2, for choice of bit error probability). For the command link from Orbiter to Lander a lower bit error probability of 10^{-5} is assumed. Because of the low command data rate, however, the power required in the Orbiter-to-Lander link is not a limiting item. Therefore, the following comparison of modulation techniques will be made with respect to the Lander-to-Orbiter link.

C. Comparison of RF Modulation Schemes

A more complete analysis of modulation techniques is given in Section 1.6.2. Results pertinent to the relay link are summarized here.

(1) PCM/PSK ($\pm 90^\circ$)

This technique involves phase-reversal keying of the RF carrier, resulting in a double-sideband, suppressed-carrier spectrum. A synchronous receiver is required with a re-set integrator (matched filter) in the output. For a 10^{-3} bit error probability, the theoretically required S/N ratio is 6.8 db in an equivalent noise bandwidth equal to the bit rate. An allowance of about 4 db will be assumed for detection losses in the Orbiter yielding a required S/N ratio of 10.8 db.

(2) PCM/PSK ($\pm 60^\circ$)

If the phase of the carrier is not completely reversed between a mark and a space, the RF carrier will not be completely suppressed, thus providing some carrier power for tracking. If θ is the phase shift, the output signal power is proportional to $\sin^2 \theta$, and the carrier power is proportional to $\cos^2 \theta$. Thus for $\theta = 60^\circ$, 75% of the power is in the

sidebands, and 25% of the power is in the carrier. Therefore, the data channel is 1.25 db inferior to PCM/PSK ($\pm 90^\circ$) so that for the same bit error probability the required S/N ratio is approximately 12 db in an equivalent noise bandwidth equal to the bit rate.

(3) PCM/PSK/PM

This technique consists of phase-modulating the main carrier with a subcarrier which has been modulated PCM/PSK ($\pm 90^\circ$). For high data rates a phase-modulation index of about 1.4 would be used, yielding a sub-carrier suppression factor of $2J_1^2(1.4) = -2.32$ db. Therefore, PCM/PSK/PM is 2.32 db inferior to PCM/PSK ($\pm 90^\circ$) and about 1 db inferior to PCM/PSK ($\pm 60^\circ$).

(4) PCM/FSK/PM

In this technique the PCM data frequency-modulates a subcarrier which in turn phase-modulates the carrier. Frequency-shift keying exploits the zero value of the correlation coefficient of two orthogonal waveforms. However, phase-shift keying ($\pm 90^\circ$) results in a correlation coefficient of -1, which is a 3 db improvement. An additional 1 db is usually lost in the FSK detection process. Thus PCM/FSK/PM is approximately 4 db inferior to PCM/PSK/PM and therefore, about 5 db inferior to PCM/PSK ($\pm 60^\circ$).

D. Recommended Method

In view of the above considerations, the selected modulation/detection scheme is PCM/PSK ($\pm 60^\circ$) with a phase-lock receiver. Of the techniques considered above, this is second only to PCM/PSK ($\pm 90^\circ$) in transmission efficiency, but allocates 25 percent of the transmitter power to the carrier for tracking, whereas the carrier is completely suppressed in PCM/PSK ($\pm 90^\circ$).

1.5.5 ANALYSIS

A. Assumptions

Calculation of the required transmitter output power as a function of data rate has been carried out for the Orbiter-to-Lander relay link using the values shown in Table 1.5.5-1. Note that it has been assumed that the Orbiter is on the Lander horizon, so that a Lander antenna pointing loss of three db is used, and a polarization loss of three db results since the antenna is to be circularly polarized. No value of Orbiter antenna pointing loss is quoted in Table 1.5.5-1, since this will be treated as a variable part of G, the Orbiter antenna gain, due to wide variations in geometry through the approach trajectory and elliptical orbits.

Using the values given in the table, the power balance equation may be written as:

$$10 \log P/B = 16 + S/N + N_O + A - G \quad \text{db} \left(\frac{\text{watts}}{\text{cps}} \right) \quad (3)$$

where

P is the transmitter output power (watts)

B is the equivalent noise bandwidth (cps)

S/N is ratio of average signal power to average noise power (db)

N_O is the noise spectral density (db)

A is the free space attenuation (db)

TABLE 1.5.5-1
SIGNIFICANT PARAMETERS FOR TRANSMITTER POWER CALCULATION

Parameter		Value (db)	Tolerance (db)
1.	Transmitter Output Power	$10 \log P$	± 1.0
2.	Transmitter Circuit Loss	3.0	± 1.0
3.	Lander Antenna Gain	2.0	± 0.5
4.	Lander Antenna Pointing Loss	3.0	± 0.3
5.	Free-space Attenuation	A	--
6.	Polarization Mismatch Loss	3.0	± 0.2
7.	Orbiter Antenna Gain	G	± 0.5
8.	Receiving Circuit Loss	1.0	± 0.5 ± 1.0
9.	Noise Spectral Density	N_o	± 2.0
10.	Required S/N Ratio	S/N	± 1.0 ± 2.0
11.	Equivalent Noise Bandwidth in db (cps)	$10 \log B$	± 0.5
12.	Performance Margin (sum of negative tolerances)	9.0	--

The required S/N ratio in the Lander-to-Orbiter link is about 12 db for a bit error probability of 10^{-3} . For the Orbiter-to-Lander link, a bit error probability of 10^{-5} is desired so that an additional three db will be required, for a total S/N ratio of 15 db.

In arriving at the system noise temperature a receiver noise figure of four db is assumed, corresponding to a noise temperature of 435°K. In the Orbiter-to-Lander link, the Lander antenna will see the galactic noise level which is about 1000°K at a carrier frequency of 100 mc. Thus the total system noise temperature for Orbiter-to-Lander communications is 1435°K which yields a noise spectral density of $N_0 = -197.0$ db. For the Lander-to-Orbiter link the Orbiter antenna may see a combination of the galactic noise level and the planet surface temperature depending on the Orbiter antenna beamwidth, the orbit altitude and antenna pointing. Since the Orbiter antenna beamwidth may vary from mission to mission, and altitude and antenna pointing will vary throughout the mission, the noise spectral density for this link will be handled as a variable. The planet surface temperatures are about 700°K for Venus and 320°K (maximum) for Mars. The corresponding noise spectral densities (including the four db receiver noise figure) are -198.0 db for Venus and -199.8 db for Mars.

The free-space attenuation, A, is given by

$$A = 37.7 + 20 \log r + 20 \log f_c \text{ (db)} \quad (4)$$

where

r is the slant range in nautical miles

and

f_c is the carrier frequency in mc

For $f_c = 100$ mc this becomes

$$A = 77.7 + 20 \log r \text{ (db)} \quad (5)$$

For the in-orbit phase of the mission we may express the maximum slant range in terms of orbit altitude (assuming the orbiter is on the lander horizon) as

$$R = \sqrt{h^2 + 2 r_0 h} \quad (6)$$

where

h is orbit altitude

and

r_0 is the planet radius

Figure 1.5.5-1 shows the attenuation as a function of orbit altitude, based on equations (5) and (6).

The Orbiter antenna which will be used depends on the particular mission and in some cases varies from one part of the mission to another. The value of Orbiter antenna gain used in the calculations has been varied accordingly. In addition, for those portions of the mission where the geometry and the antenna pointing give rise to a definite limit on the angular position on the antenna pattern at which the Orbiter sees the Lander, the corresponding value of antenna gain has been used. For this purpose it has been assumed that the gain varies as $(\sin k\theta/k\theta)^2$ where θ is the angle from the center-line of the antenna

ASSUMES ORBITER ON HORIZON
RELATIVE TO LANDER

CARRIER FREQUENCY = 100 MC

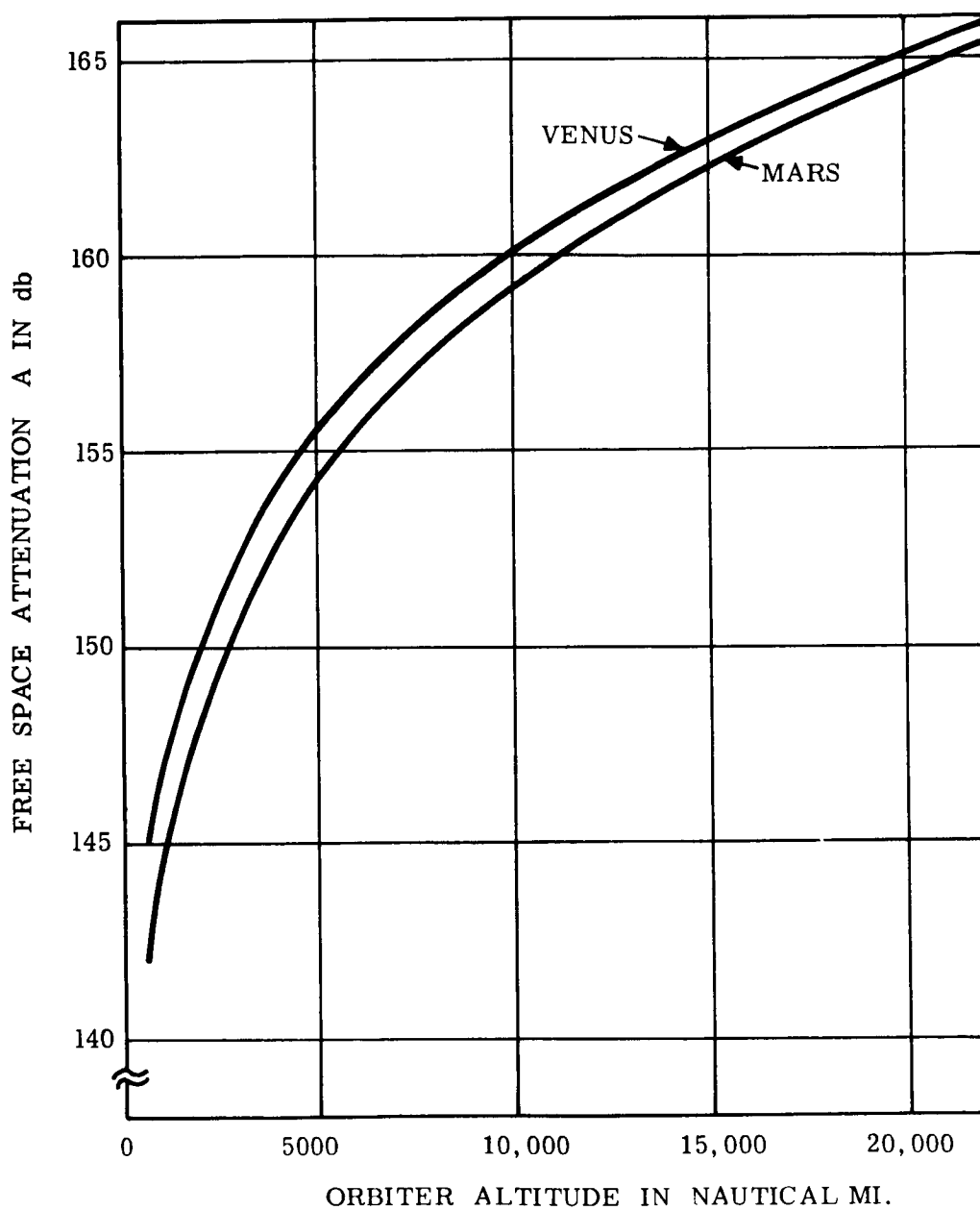


Figure 1.5.5-1. Free Space Attenuation vs Orbiter Altitude

beam, and the value of k is determined by the 3-db beamwidth. Based on this assumption, Figure 1.5.5-2 shows the variation in gain with the ratio of the angle θ to the 3-db beamwidth.

Making use of the equations and assumptions given above, calculations of transmitter output power requirements have been carried out as a function of data rate for the missions being considered.

B. Mars 1969 and 1971 Missions

The parameters of the relay link will be the same for these two missions so that one set of results applies. For the purpose of these calculations the mission is considered in two parts. The first part is Lander descent which covers the period from Orbiter/Lander separation to Lander impact. During this phase the Orbiter antenna in use will be an omnidirectional antenna. Therefore a value of 0 db antenna gain and a noise spectral density of -197 dbw, corresponding to the galactic noise level, are used in the calculations. The resulting transmitter power required per kilobit per second of data is shown in Figure 1.5.5-3 for the Lander-to-Orbiter link. The command link from Orbiter-to-Lander is not used during this phase of the mission.

During the second phase, after orbit injection, the Orbiter will employ a directional yagi antenna mounted to the planet-horizontal-package (PHP), which is aligned along the local vertical from the Orbiter to the planet. The proposed antenna has a centerline gain of 10 db and a corresponding 3 db beamwidth of approximately 52 degrees. The actual value of Orbiter antenna gain has been varied with Orbiter altitude to reflect the variation in operating point on the antenna pattern, assuming the Orbiter is on the horizon relative to the Lander. Results are shown for both the Orbiter-to-Lander and the Lander-to-Orbiter links in Figure 1.5.5-4. The difference in transmitter power required in the two links is due to a difference in required S/N ratio (due to different bit error probability) and the difference in receiving system noise temperature.

C. Mars 1973 and 1975 Missions

These missions will employ a Lander-to-Orbiter link during the Lander descent phase. Since the characteristics of this link will be the same as in the earlier Mars missions, the results of Figure 1.5.5-3 apply.

D. Venus 1970 and Venus 1972 Missions

For the Venus missions it is planned to use an Orbiter antenna having a centerline gain of 10 db. A programmed rotation of this antenna is planned which will keep the Lander in the close vicinity of the centerline of the antenna beam so that maximum gain is achieved. The ratio of transmitter output power to data rate is shown as a function of range in Figure 1.5.5-5. Since no command link is planned for the Venus 1970 mission, the Orbiter-to-Lander curve of Figure 1.5.5-5 applies only to the Venus 1972 mission.

1.5.6 SUBSYSTEM DESCRIPTION

A. Mars 1969 and 1971

(1) Orbiter

A block diagram of the Orbiter Relay Transmission Subsystem for the Mars 1969 and 1971 missions is shown in Figure 1.5.6-1. Two sets of receivers are utilized: one set in the Main Body and the other in the PHP. Each receiver in a set receives from one of the Landers; therefore, simultaneous reception from both Landers is possible. Each set is used at different times — the set in the Main Body during Lander cruise and descent and the set in the PHP after the Lander is on the surface and the PHP is deployed.

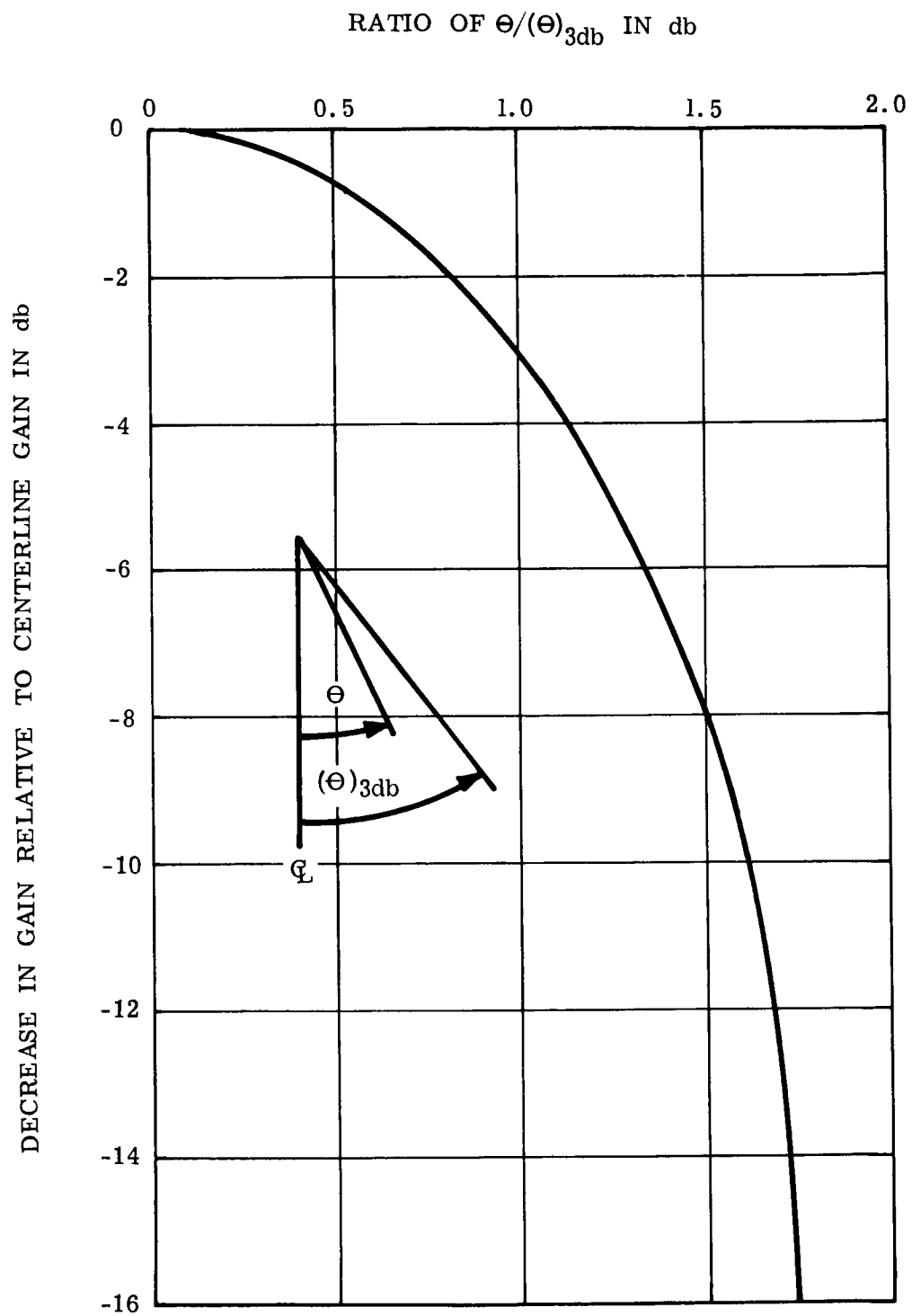


Figure 1.5.5-2. Variation in Antenna Gain With Angle From Centerline of Beam

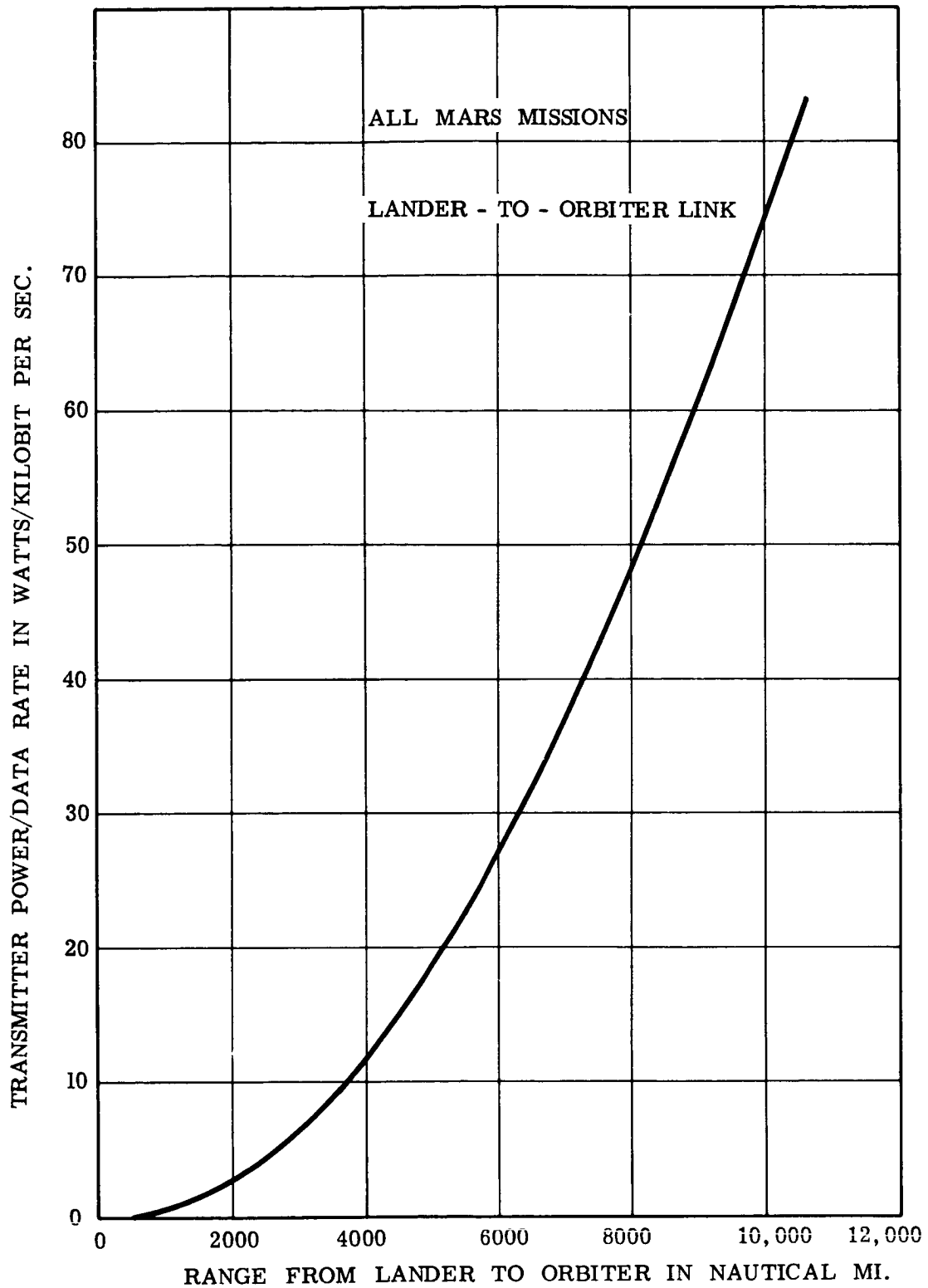


Figure 1.5.5-3. Transmitter Power Required Per Kilobit Per Second of Data During Mars Lander Descent

MARS 1969 AND 1971

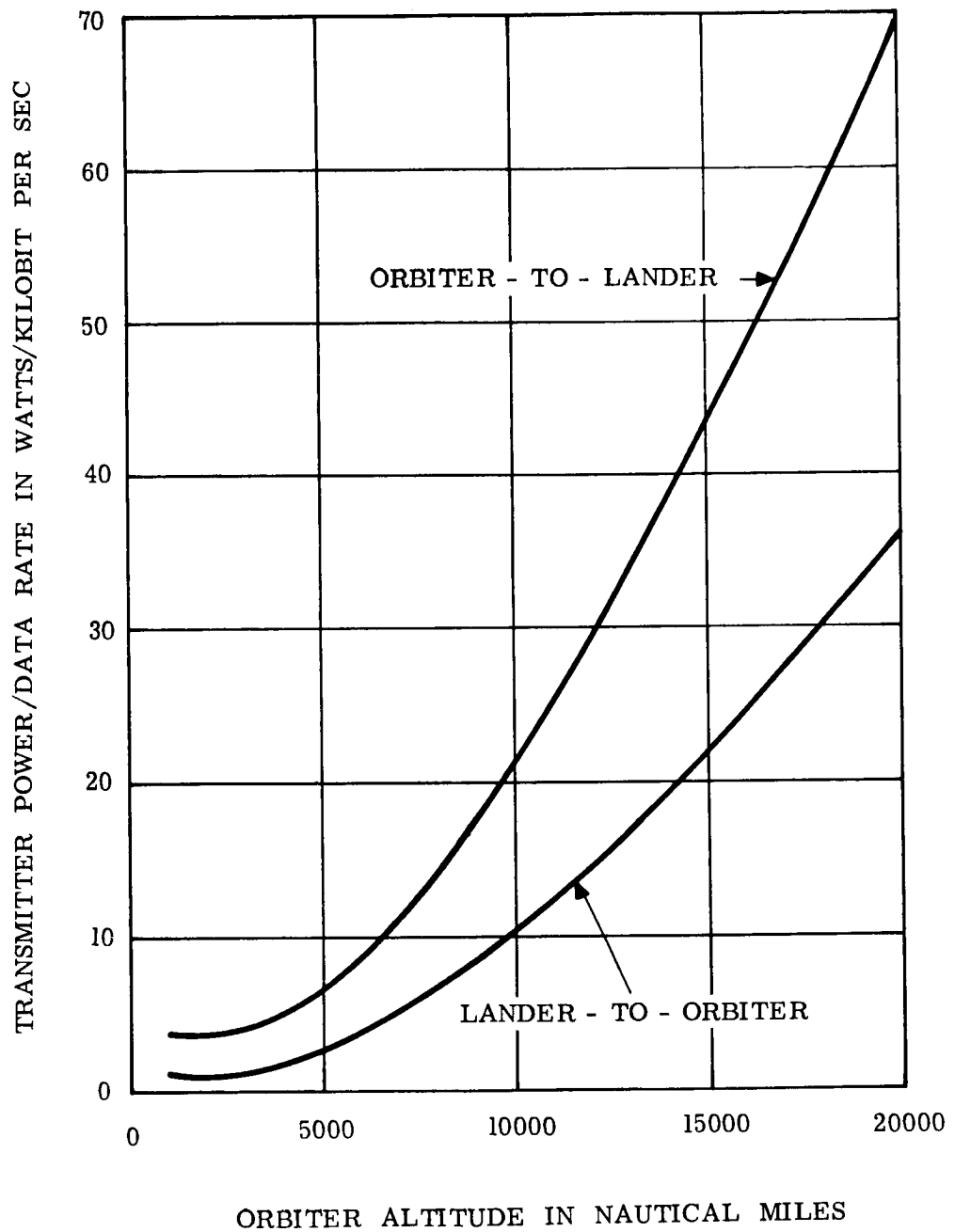


Figure 1.5.5-4. Transmitter Power Required Per Kilobit Per Second of Data During Mars Orbit

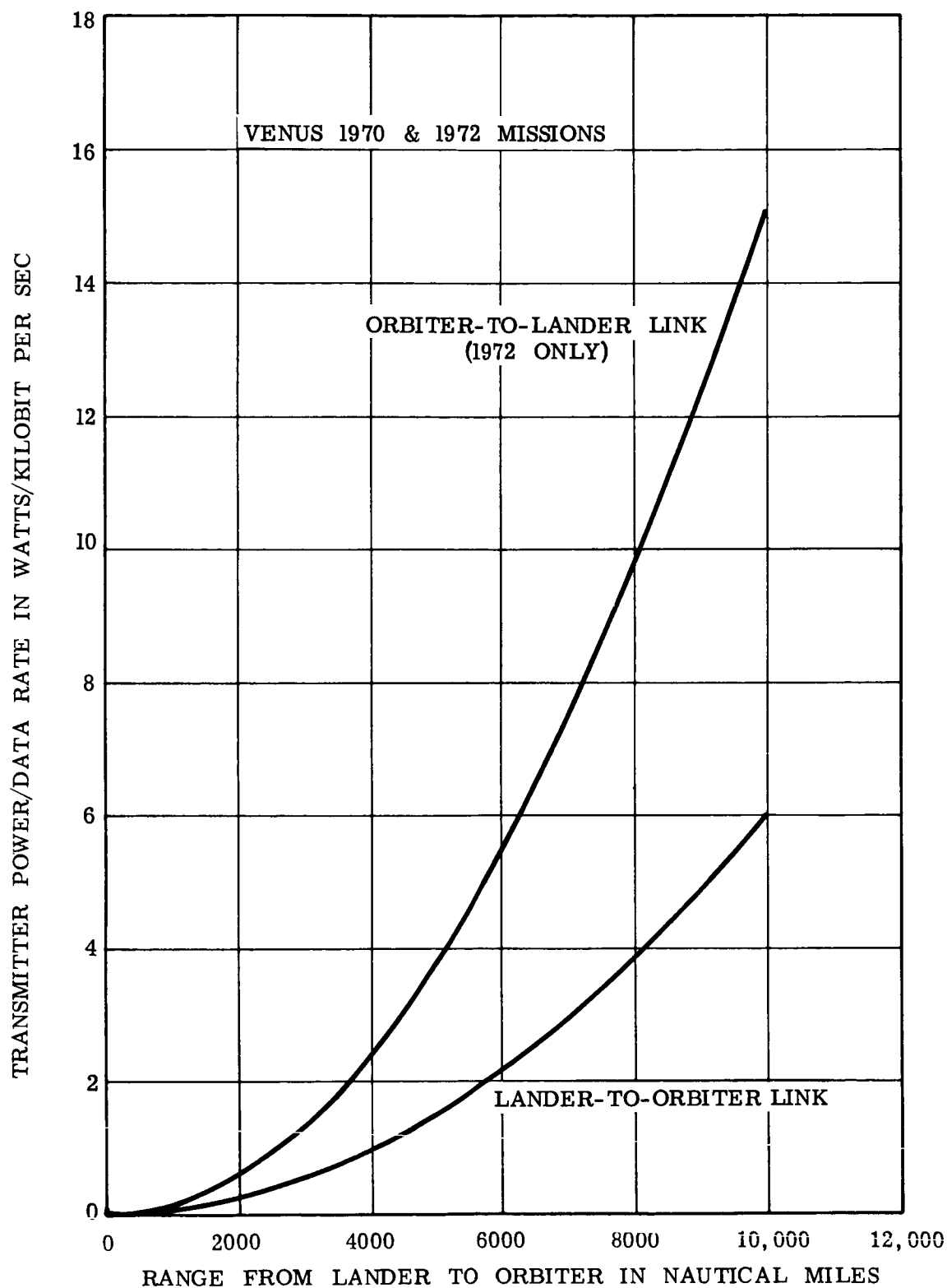


Figure 1.5.5-5. Transmitter Power Required Per Kilobit Per Second of Data

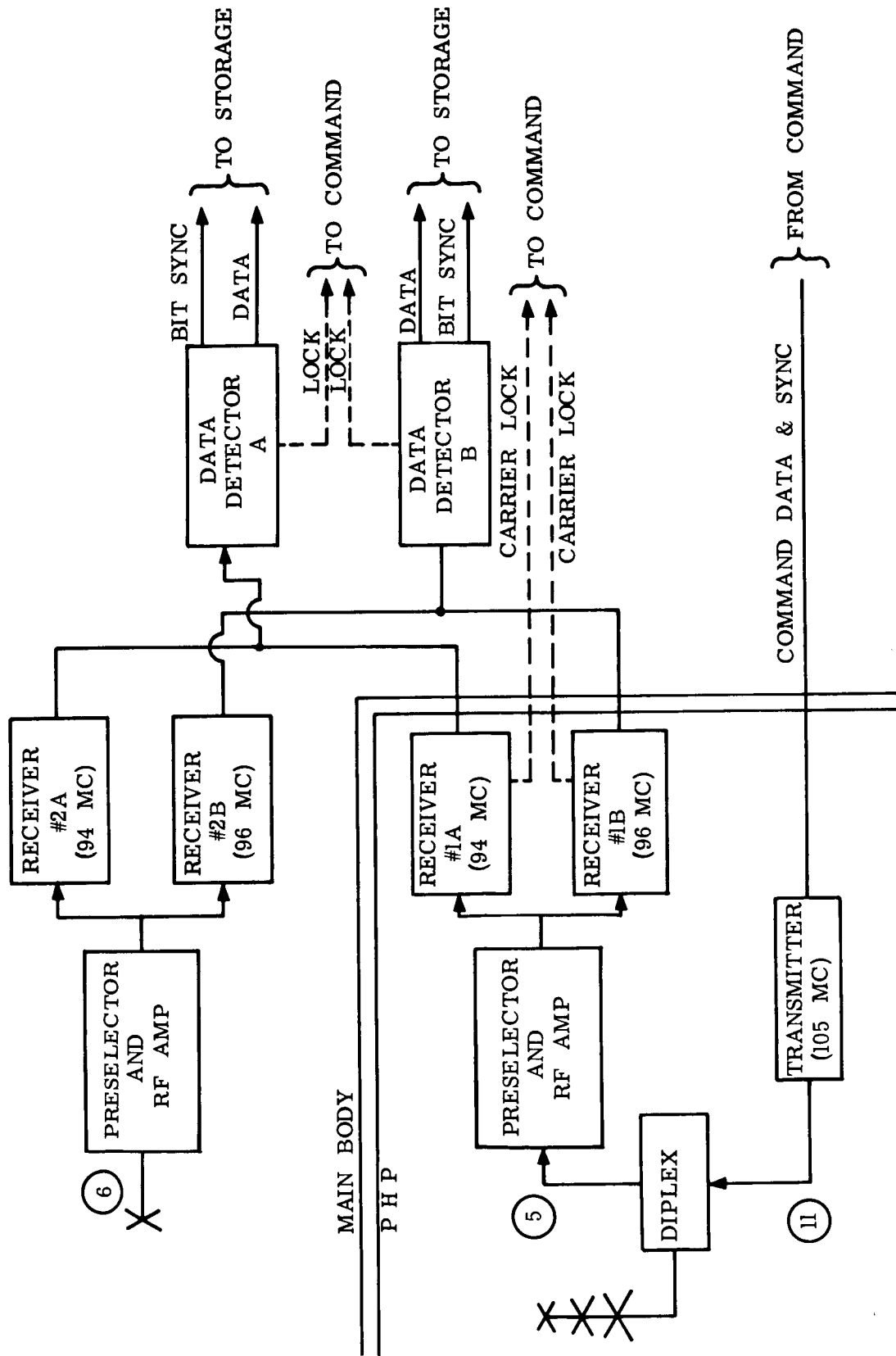


Figure 1.5.6-1. Mars 1969 and 1971 Orbiter Relay Transmission Subsystem

Transmission to the Landers is not required until after the lander is on the surface; therefore, only one transmitter, located in the PHP, is provided. The utilization of two sets of receivers instead of one eliminates the requirement for transmitting RF from the PHP to the Main Body.

The signal received at the Orbiter is a carrier at either 94 or 96 mc phase-modulated by a composite signal containing both data and bit sync. It is amplified prior to down-conversion in order to attain a reasonably low noise figure. The output of the synchronous receivers is the composite modulating waveform. Bit sync and data are separated in the detector and the data is stored in the TPR's using the sync pulses to clock it in. Each detector can receive at any one of five bit rates: 16,000, 8,000, 4,000, 2,000, and 500 bits per second. The operating rate is selected by command. The detector also provides a lock signal to the Command and Computer Subsystem which routes the data to storage and also controls the Orbiter-Lander lock sequence. Carrier-lock signals provided by the receivers on the PHP also go to the Command and Computer Subsystem as a part of the Orbiter-Lander lock sequence

The Command and Computer Subsystem also controls the data being transmitted to the Landers. When received at the transmitter, the waveform contains command data, bit sync, word-start, and parity information. The two-level waveform bi-phase modulates a 105-mc carrier which is amplified to five watts before transmission. Transmission is at a rate of 10 command bits per second.

The two antennas being utilized are a turnstile on the Main Body and a 10-db yagi on the PHP.

(2) Lander

The Lander Relay Transmission Subsystem block diagram is shown in Figure 1.5.6-2. Transmission to the Orbiter is via a single phase-modulated transmitter feeding two 25-watt solid-state power amplifiers. One of the power amplifiers feeds a "transmission line" antenna and operates during cruise and descent. The other amplifier is actuated after the Lander reaches the surface, releases the aft cover and extends the turnstile antenna. This antenna is also used for reception from the Orbiter. The receiver and detector are the same type used in the Orbiter; however, the receiver operates at 105 mc and the command detector operates at a rate of 10 command bits per second (20 symbols per second).

B. Mars 1973 and 1975

(1) Orbiter

The Orbiter Relay Transmission Subsystem as shown in Figure 1.5.6-3 is identical to that part of the Mars 1969 and 1971 subsystem located in the main body; however, the data detectors operate only at a rate of 500 bits per second.

(2) Lander

The Lander Subsystem (Figure 1.5.6-4) is a 95 mc transmitter with a 25 watt power amplifier feeding a "transmission line" antenna. The antenna is removed with the aft cover after landing, terminating all transmission to the Orbiter.

C. Venus 1970

Figure 1.5.6-5 shows a block diagram of the Orbiter subsystem. The receiving antenna is a 10 db planet-tracking yagi mounted on the main body. The receiver and detector are

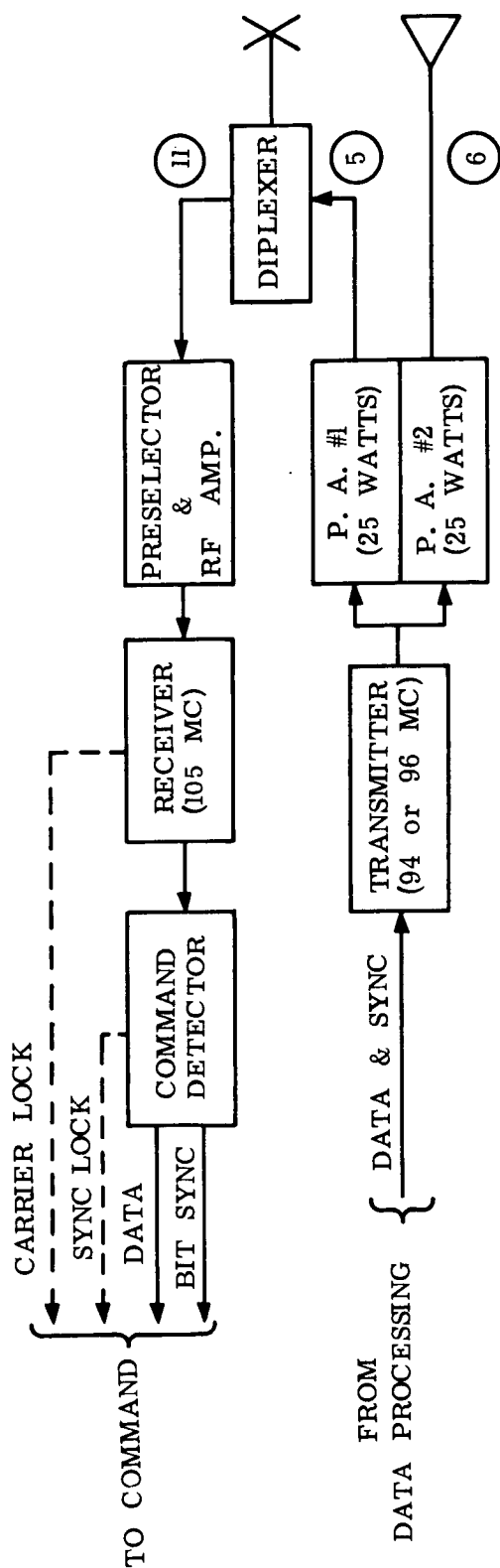


Figure 1.5.6-2. Mars 1969 and 1971 and Venus 1972 Lander Relay Transmission Subsystem

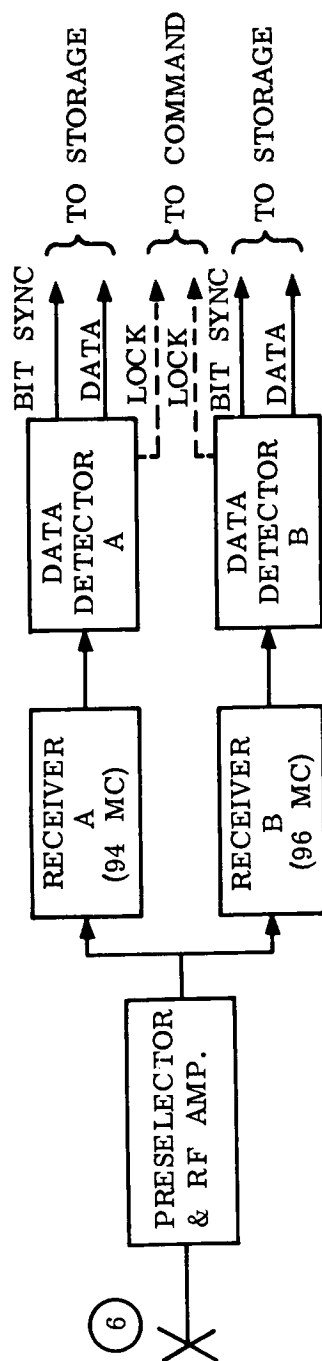


Figure 1.5.6-3. Mars 1973 and 1975 Orbiter Relay Transmission Subsystem

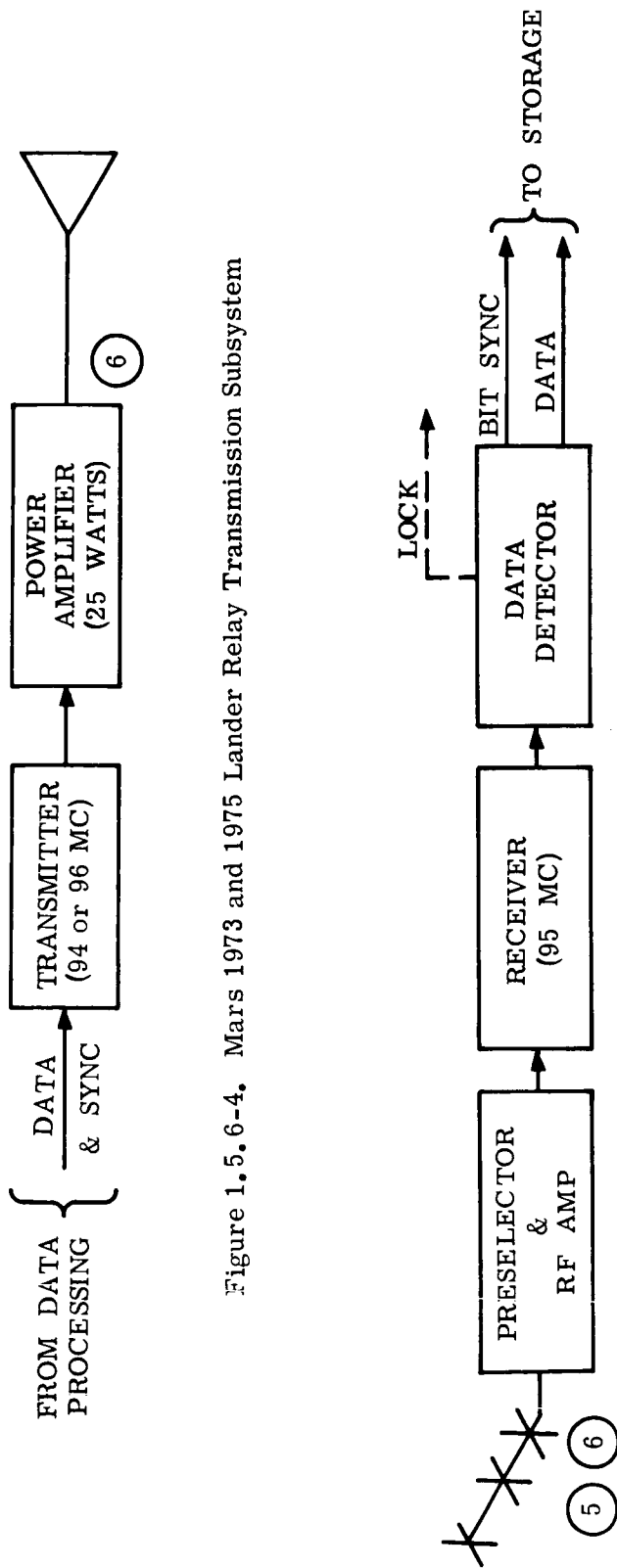


Figure 1.5.6-4. Mars 1973 and 1975 Lander Relay Transmission Subsystem

Figure 1.5.6-5. Venus 1970 Orbiter Relay Transmission Subsystem

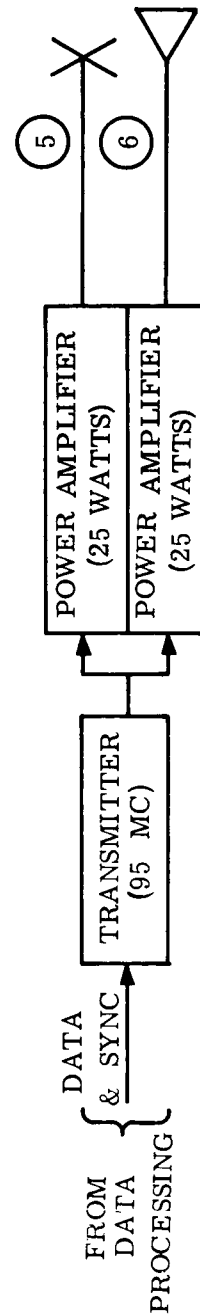


Figure 1.5.6-6. Venus 1970 Lander Relay Transmission Subsystem

the same as described previously for the Mars 1969 and 1971 missions; however, the detector operates only at rates of 8000 and 500 bits per second.

The Lander subsystem (Figure 1.5.6-6) is the same as that for Mars 1969 and 1971 missions without a receiving capability.

D. Venus 1972

The Venus 1972 Orbiter Relay Transmission Subsystem provides for both reception of data from a single Lander and transmission of commands to the Lander. The block diagram is shown in Figure 1.5.6-7. Command transmission is at a rate of 10 bits per second and data reception is at any one of three selected rates: 16,000, 8,000, and 500 bits per second. The antenna is a 10 db planet-tracking yagi mounted on the main body.

The Lander Relay Transmission Subsystem is identical to that of the Mars 1969 and 1971. It is shown in Figure 1.5.6-2.

1.5.7 COMPONENTS

The basic components utilized in the Relay Transmission Subsystems are transmitters, power amplifiers, receivers, detectors, antennas and diplexers. These are described in Section 1.7.

1.5.8 RESULTS

As discussed above, the Lander transmitter will have an output power of 25 watts and the Orbiter transmitter will have an output power of 5 watts. The data rate capability of these transmitters can be obtained from the curves of Section 1.5.5 which show the transmitter power required per kilobit per second of data. Based on these curves the data rates which can be achieved using the selected transmitters are shown for the various missions in Figures 1.5.8-1 through 1.5.8-3.

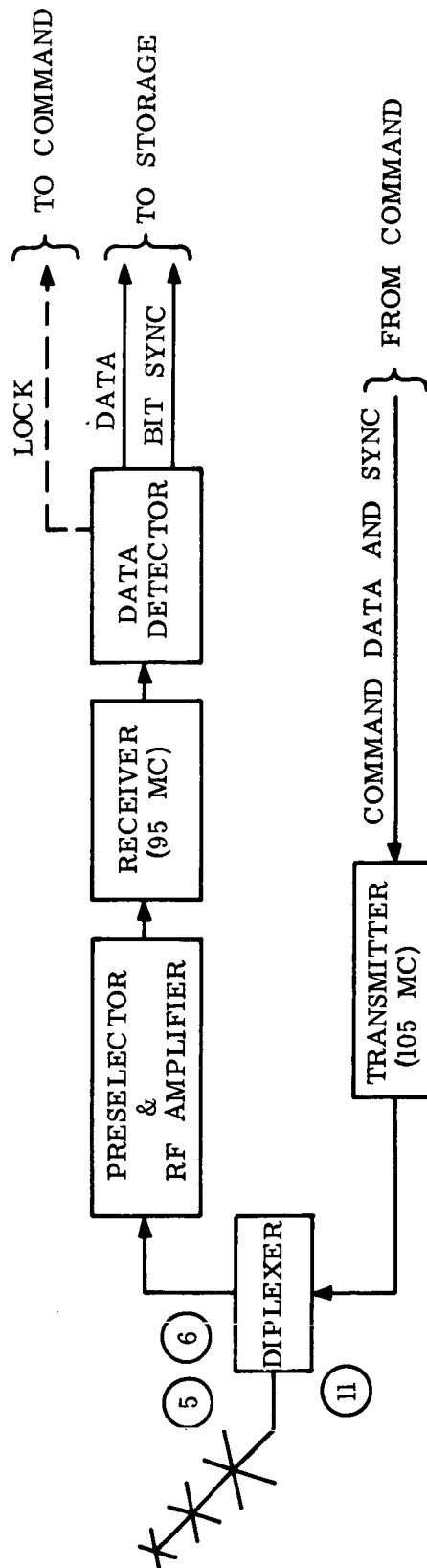


Figure 1.5.6-7. Venus 1972 Orbiter Relay Transmission Subsystem

LANDER XMTR POWER OUTPUT~25 WATTS

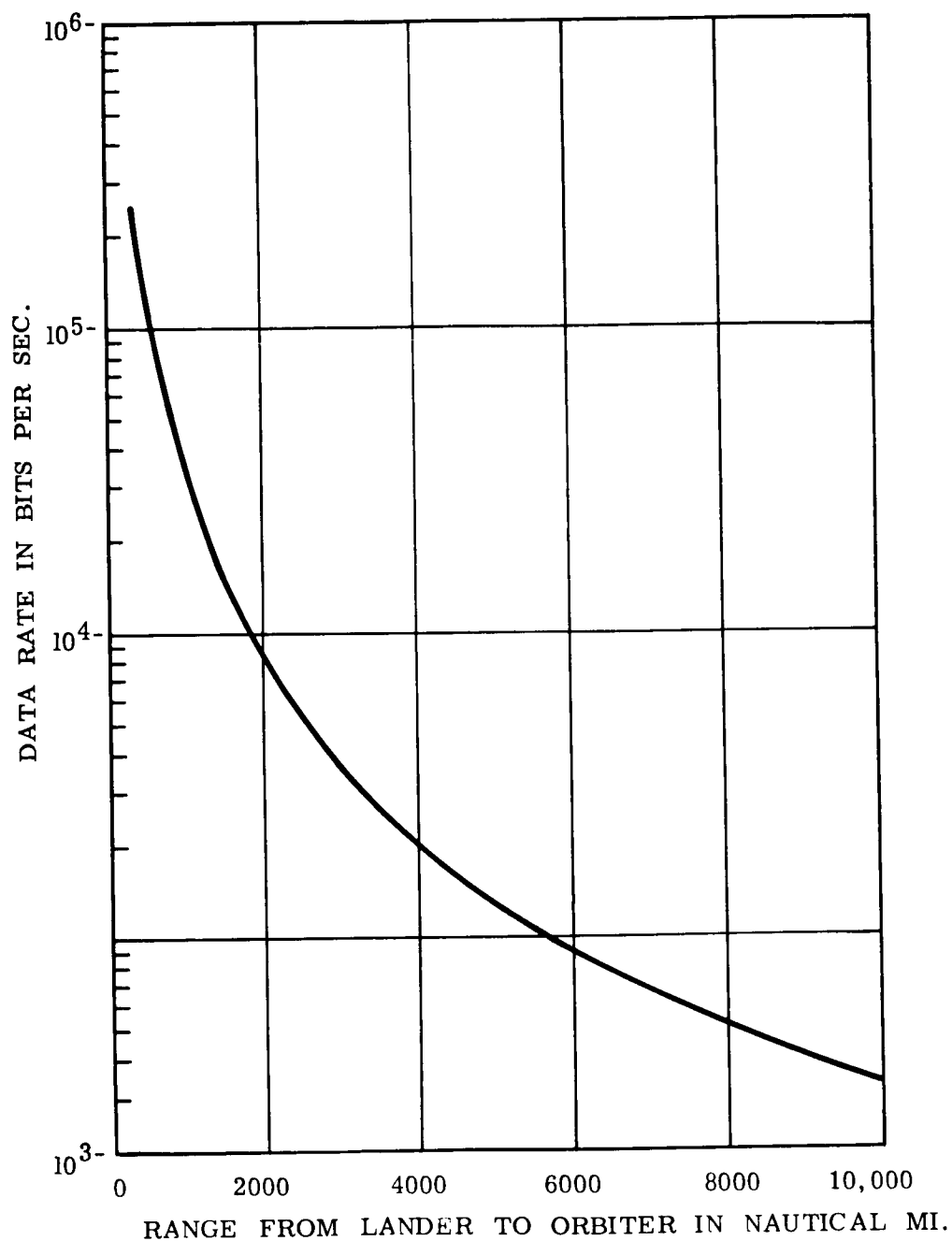


Figure 1.5.8-1. Lander-to-Orbiter Data Rate During Mars Lander Descent - All Mars Missions

LANDER XMTR POWER OUTPUT~ 25 WATTS
ORBITER XMTR POWER OUTPUT~ 5 WATTS

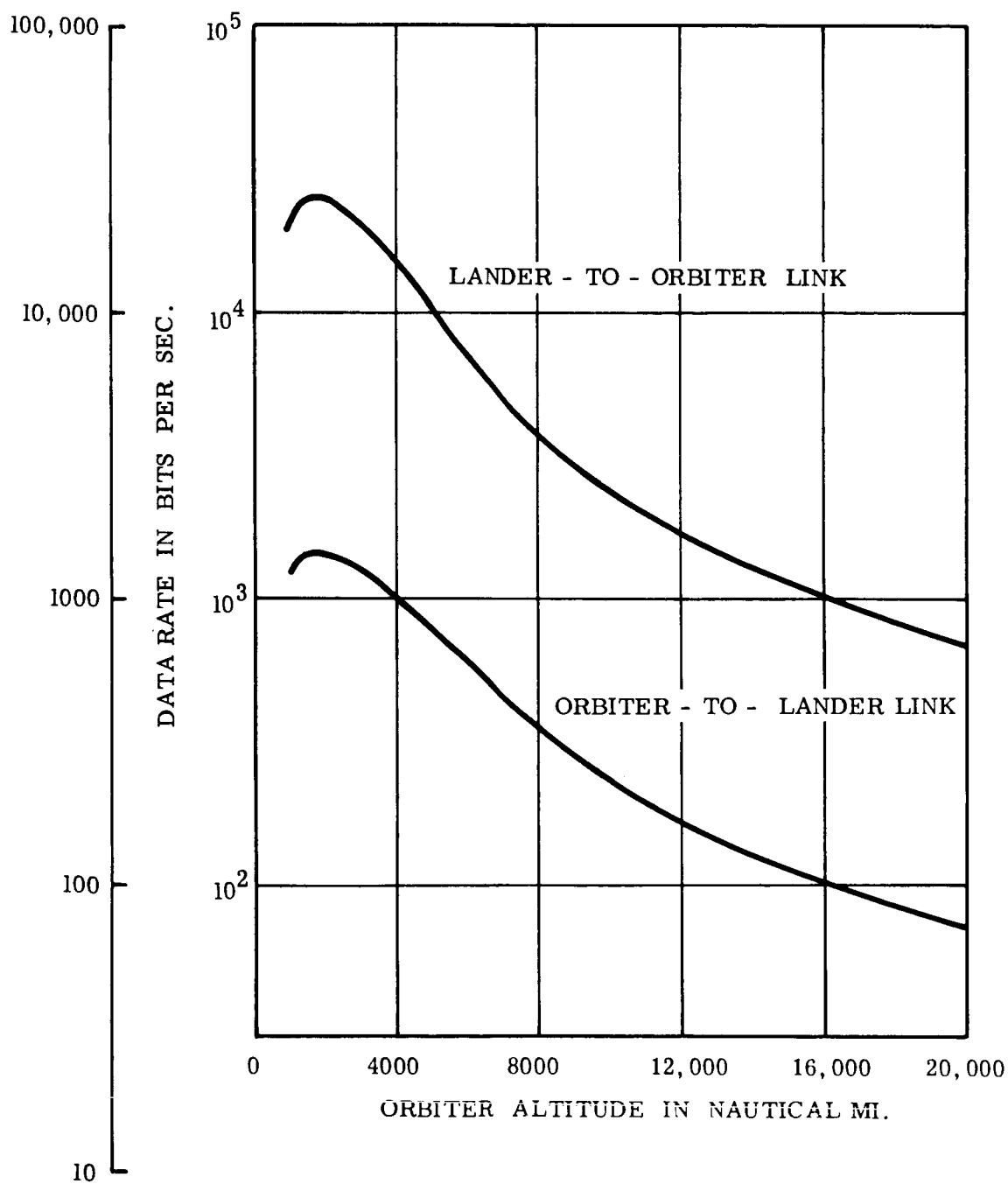


Figure 1.5.8-2. Data Rate in Orbit-Mars 1969 and 1971

LANDER XMTR POWER OUTPUT: 25 WATTS
ORBITER XMTR POWER OUTPUT: 5 WATTS

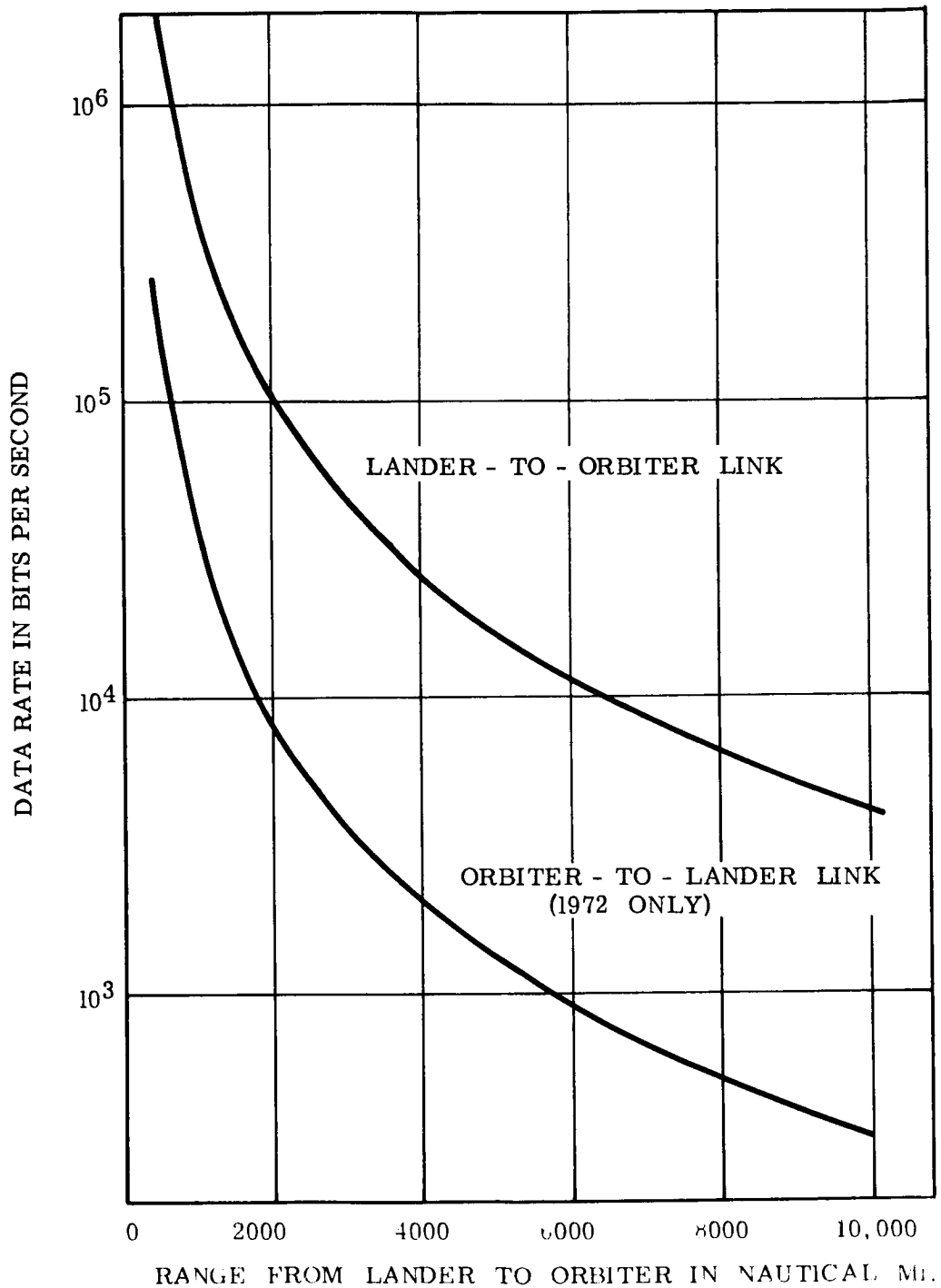


Figure 1.5.8-3. Data Rate vs Range-Venus 1970 and 1972 Missions

1.6 COMMUNICATIONS TECHNIQUES

1.6.1 ANALOG VS. DIGITAL TELEVISION

A. Summary

One of the tasks performed in the Voyager study was a comparison of analog television with digital television for the Voyager mission. Although a strong case can be made for either technique, a digital TV subsystem has been selected. Since the main factors affecting the choice include such details as orbital parameters, recorder availability, and year of launch, the decision will have to be reviewed if these change significantly from the values presented in this report.

Early in the study the system mapping concept was centered about a circular orbit with up to 250 kc of continuous data transmission required. It was also considered desirable to employ the same equipment for the Mars 1969 mission as would be used for Venus 1967. Therefore, existing flight-proven analog TV techniques using FM with feedback appeared to be the best choice. Digital TV was investigated but not favored.

However, during the course of the study, the trend toward highly elliptical orbits, with relatively short periods of mapping (near periapsis), large recording requirements, and long available playback times at lower data rates evolved, together with a growing indication that Mars 1969 will probably be the earliest flight. These factors now indicate that it would be desirable to select a digital TV system, with its inherent advantages in data-handling versatility and adaptability, for the Voyager program.

The major factors considered during the course of the study are described in the following paragraphs.

B. Factors Which Appear to Favor Analog (FM) Television

(1) Transmission Efficiency

Theoretical analysis has shown that for the assumed 32-db average output S/N ratio requirement, FMFB requires about 3 db less transmitter power than PCM/PSK. This assumes no processing has been done on the data and that all amplitude levels are equally likely with no correlation between elements. It should be noted that for somewhat higher output S/N ratios PCM/PSK would become more efficient than FMFB.

(2) Output S/N Ratio Limitation

The output S/N ratio of a digital TV system is limited by the quantization noise introduced in the encoding process, irrespective of how great the received RF S/N ratio might be. However, the output S/N ratio from an FM television system increases directly as the received RF S/N ratio increases. Thus one could conceivably achieve S/N performance in excess of the specification value from an FM system, if all system tolerances are not at their worst extreme. Graceful degradation of picture quality at longer transmission distances is also possible with FM, but not with PCM.

(3) No Contouring Effect

The video contouring effect caused by gradually crossing a PCM quantization level has been the subject of several IRE papers in the last several years. Although this will distort an aerial mapping picture somewhat, it is not apparent that it is entirely undesirable for our purposes, since it will serve to enhance outlines. If this does turn out to be desirable, quantization and contouring can always be done on Earth after reception of the picture.

(4) More Background Available on Analog TV

Analog TV systems have been flown or are being built for such programs as Tiros, Nimbus, Ranger, Surveyor, and Apollo. Almost all terrestrial TV systems are analog. Therefore, if work were to begin today on a television system for Voyager, this background should be a strong factor in deciding between analog and digital.

However, the Voyager program has sufficient lead time to make this consideration almost irrelevant. Current programs such as OAO and Mariner C should demonstrate the capabilities of digital TV.

(5) Smaller Recorder Requirement

For the same data storage requirement, an analog magnetic tape recorder will be somewhat smaller than a digital magnetic tape recorder. However, the time scale of the Voyager program again permits us to recommend a thermoplastic recorder (TPR) with reasonable confidence. The digital storage capacity available with TPR will obviate this problem.

(6) Analog Circuitry Less Complex

Since a digital television system must in general contain almost all the analog circuitry in addition to the analog-to-digital encoding equipment, there will certainly be some increase in the circuitry involved in the latter, although it will be small. However, as will be pointed out later, the digital circuitry is not so critical as the analog circuitry.

(7) Weight of an Analog TV System

If conventional packaging is assumed, the fact that more circuitry is required for a digital television system than for an analog system implies that a digital system should be heavier. It is expected, however, that the increasing use of micro-electronics, integrated components, and packaging techniques will probably make any differential almost insignificant.

C. Factors Which Appear to Favor Digital (PCM) Television

(1) Ease of Multiplexing

The Voyager missions will require the transmission of a small amount of narrow-band scientific and engineering data (perhaps 10% of the total data) along with the television data. Amplifier linearity specifications and diplexer insertion loss problems indicate that this can better be done by time-sharing than by frequency-division multiplex. Although this can be done with analog TV, a digital TV system adapts to it more naturally, especially if the frame periods are short.

(2) Ease of Changing Data Rate

Since each Voyager mission extends over a period of several months, during which period the transmission distance will increase significantly and the equipment performance might degrade somewhat, and also because we have only limited a priori knowledge of what we will find on the planets, it will be highly desirable to be able to change recorder readout speed in discrete steps upon command. For an analog system the high output S/N ratio specification would require that an FM recording technique be used. Therefore, to change readout speeds it would be necessary to switch to a separate FM discriminator. With digitally recorded data this is not necessary. One merely switches to a new readout speed.

(3) Uncluttered Carrier for Tracking

In order to provide an uncluttered carrier for tracking purposes with an FM system, it would be necessary to frequency-modulate a subcarrier with the television data and then phase-modulate the carrier with the subcarrier signal. The detection process limits the phase-modulation index to about 1.4 radians, so the carrier power component reduces the signal power available from the transmitter by a factor of $2J_1^2(1.4)$, which is -2.32 db.

The PCM/PSK technique, on the other hand, can be encoded with a pseudo-noise or Manchester code before performing the rf modulation. This will move the peak of the signal spectral density away from the carrier and provide a relatively clear region near the carrier for tracking purposes. Limitation of the peak phase deviation to angles less than 90° will result in leaving a discrete carrier frequency component.

(4) Allows Pulse Reshaping

The use of recorders and relay modes in the Voyager system results in the overall communications link having many of the features of a multiple-station relay system. In such a system the noise is additive in each link, so the S/N ratio degrades quite rapidly in analog systems. However, in a PCM system, only the digit error rates add in each link, since the pulses can be cleaned up at each intermediate station, and the effect is much less severe.

(5) Camera S/N Ratio

EMR has stated that digital TV cameras provide a higher S/N ratio than analog cameras for a slow-scan (greater than 1/2 second per frame) system. This is because the charge replacement is less with a sampled scan.

(6) Television Terminal Guidance

The terminal guidance television pictures will consist of a number of stars plus a part of the target planet. Most of the frame will be black. Such a scene could be quite efficiently transmitted by using the random-scan technique which EMR is using for the OAO Telescope experiment. In such a technique, the camera scanning beam moves rapidly until it detects a light source - then reads out the magnitude and X-Y coordinates of the source to a high accuracy. This can be handled easily by a digital TV system.

(7) Bandwidth Compression and Error-Correction Coding

Digital television lends itself well to such signal-processing techniques as bandwidth compression (through redundancy elimination) and error-correction coding. Each of these techniques reduces the transmitter power requirement, but increases the circuit complexity considerably. Therefore, they are not in popular use today, but may be well-established in the next few years.

(8) Common Memory

The scientific and engineering data are digital (since they consist of many channels of narrow-band data, which can be more efficiently handled through time-division multiplex than through frequency-division). If a digital television recorder is used, it would be convenient to use the same recorder for the narrow-band data. Otherwise a separate recorder might be required.

(9) Reliability

In general, a stage of digital circuitry is more tolerant to perturbations than a stage of analog circuitry. This is because the digital circuit has only two stages between which

it must distinguish. Therefore, it should be more reliable than an analog stage. This is partially offset, however, by the fact that a digital television system has more stages than an analog television system.

(10) Subsequent Computer Analysis

The digital data format lends itself well to subsequent computer analysis, such as statistical calculations and cleaning up the picture element-by-element. This can, of course, be done with analog signals, too, by digitizing on the ground. However, the digital TV signal does have the slight advantage of already being in this format.

(11) Asynchronous Operation

A digital TV system can be operated (as proposed by EMR) with the Huffman encoder an integral part of the scanning system. The scanning rate is then adjusted to provide a fairly constant bit rate out of the encoder. This results in the most efficient use of the frame transmission time.

(12) Security Coding

Analog signals can be encoded (e.g., by scrambling), but the most efficient cryptographic techniques require digital signals. Although secure communications systems have not been required on NASA missions to date, the advantage of digital TV for this purpose should be kept in mind if it becomes a possible requirement in the future.

(13) Synchronization and Identification Time

The fraction of the frame time required for synchronization and identification will be less for a digital TV system than for an analog TV system, assuming that both systems use digital words for these purposes. This is because an identification or sync bit requires the time duration of an element scanning time in the analog system, while it takes only the time of a bit in a digital system. Hence, synchronization and identification might require as much as 15-20% of the frame time for an analog frame, but only about 3-4% for a digital frame.

1.6.2 MODULATION AND DETECTION

A. Introduction

This section shows calculations for the data rate capabilities of a digital communication link from the Voyager spacecraft to Earth. Results are shown for the transmission to Earth of both wideband data through a 10-foot dish and narrow-band data through an omnidirectional antenna, using a 50-watt transmitter. Modifications can be made conveniently for other antenna gains and transmitter power levels.

B. Link Parameters

The parameter values for the Deep Space Transmission Subsystem are given in Section 1.4 and summarized below:

Modulation Technique:	PCM/PSK with PN coding and ±60 peak phase deviation
Bit Error Probability:	1.4×10^{-3}
Demodulation Loss:	1.0 db

Improvement due to Error Control Coding:	1.5 db
C/N Ratio Required for Telemetry:	6.0 db
Minimum Carrier Phase-Lock Loop Bandwidth ($2 B_{LO}$):	3 cps
Receiving System Noise Temperature:	35° K
Corresponding Noise Spectral Density:	-213.2 db (w/cps)
Operating Margin:	8 db
Calculations Made at Range of one AU:	81×10^6 nm
Range at Mars Encounter:	103×10^6 nm

C. Total Received Power

The calculation of the total power received on Earth is shown in Table 1.6.2-1 and plotted in Figure 1.6.2-1 as a function of range from the spacecraft to Earth.

D. Total Receiver Power Required

The required receiver power will depend in general on the data rate and the modulation technique employed. The required receiver power level is derived in this section for several promising digital modulation techniques.

(1) Theoretically Ideal System

For the theoretically ideal system the data rate is equal to the channel capacity given by Shannon's theorem:

$$C = B \log_2 (1 + S/N) \text{ bits/sec.} \quad (1)$$

where B is the RF bandwidth occupied. For wide bandwidths and low received S/N ratios, this reduces to

$$\begin{aligned} C &= B \frac{S}{N} \log_2 e \\ &= \frac{S}{N/B} \log_2 e \\ &= 1.44 S/(N/B) \text{ bits/sec} \end{aligned} \quad (2)$$

which yields:

$$\begin{aligned} \frac{S}{C} &= ST = 0.695 \frac{N/B \text{ watts}}{\text{bit/sec.}} \\ &= 0.695 N/B \text{ joules/bit} \end{aligned} \quad (3)$$

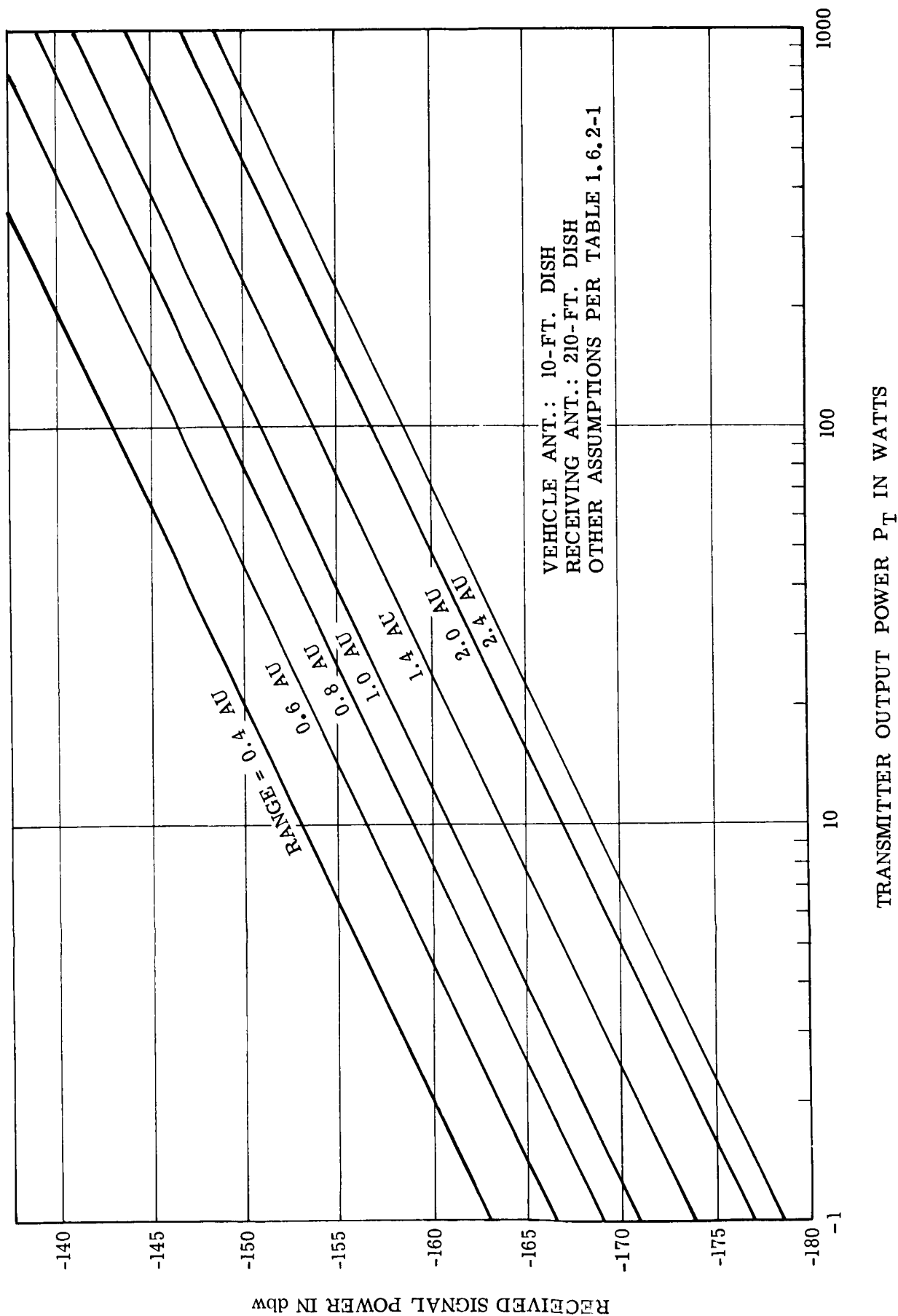


Figure 1.6.2-1. Signal Power Received at DSIF Ground Station Vs. Spacecraft Transmitter Power

This is the absolute minimum received energy required per bit of data. However, it would require an infinite encoding time delay, and no suitable code has yet been discovered.

TABLE 1.6.2-1. DEEP-SPACE COMMUNICATION LINK CALCULATIONS

Link: Spacecraft-to-Earth		
Mode:	Transmitter Frequency:	2295 mc
	Transmitter Power:	50 watts
	Modulation:	PCM/PSK
	Vehicle Antennas:	Omni/10-ft. dish
	Ground Antenna:	210-ft. dish
	Ground Receiver:	Maser
ITEM	PARAMETER	VALUE
1.	Total Transmitter Power	$10 \log P_T$ dbw
2.	Transmitting Circuit Loss	- 2.0 db
3.	Transmitting Antenna Gain (omni) (10-ft dish)	+ 0.0 db + 34.7 db
4.	Transmitting Antenna Pointing Loss (10-ft dish)	- 1.2 db
5.	Space Loss (2295 mc, one AU)	-263.2 db
6.	Polarization Loss	- 0.0 db
7.	Receiving Antenna Gain (210-ft dish)	+ 61.0 db
8.	Receiving Antenna Pointing Loss	- 0.0 db
9.	Receiving Circuit Loss	- 0.2 db
10.	Net Circuit Loss (omni) (10-ft dish)	-205.6 db -170.9 db
11.	TOTAL RECEIVED POWER	$10 \log P_T - \begin{cases} 205.6 \text{ dbw (omni)} \\ 170.9 \text{ dbw (10-ft dish)} \end{cases}$

(2) PCM/PSK ($\pm 90^\circ$)

The optimum modulation technique for transmitting uncoded binary information in the presence of additive white gaussian noise is phase-reversal keying of the rf carrier, resulting in a DSB(SC) spectrum. A synchronous receiver is required with a reset integrator (matched filter) in the output. For a 1.4×10^{-3} bit error probability, Figure 1.6.2-2 shows that a value of $ST/(N B) = 6.5$ db is theoretically required. Comparison with Equation (3) shows that this is 8.1 db inferior to Shannon's ideal.

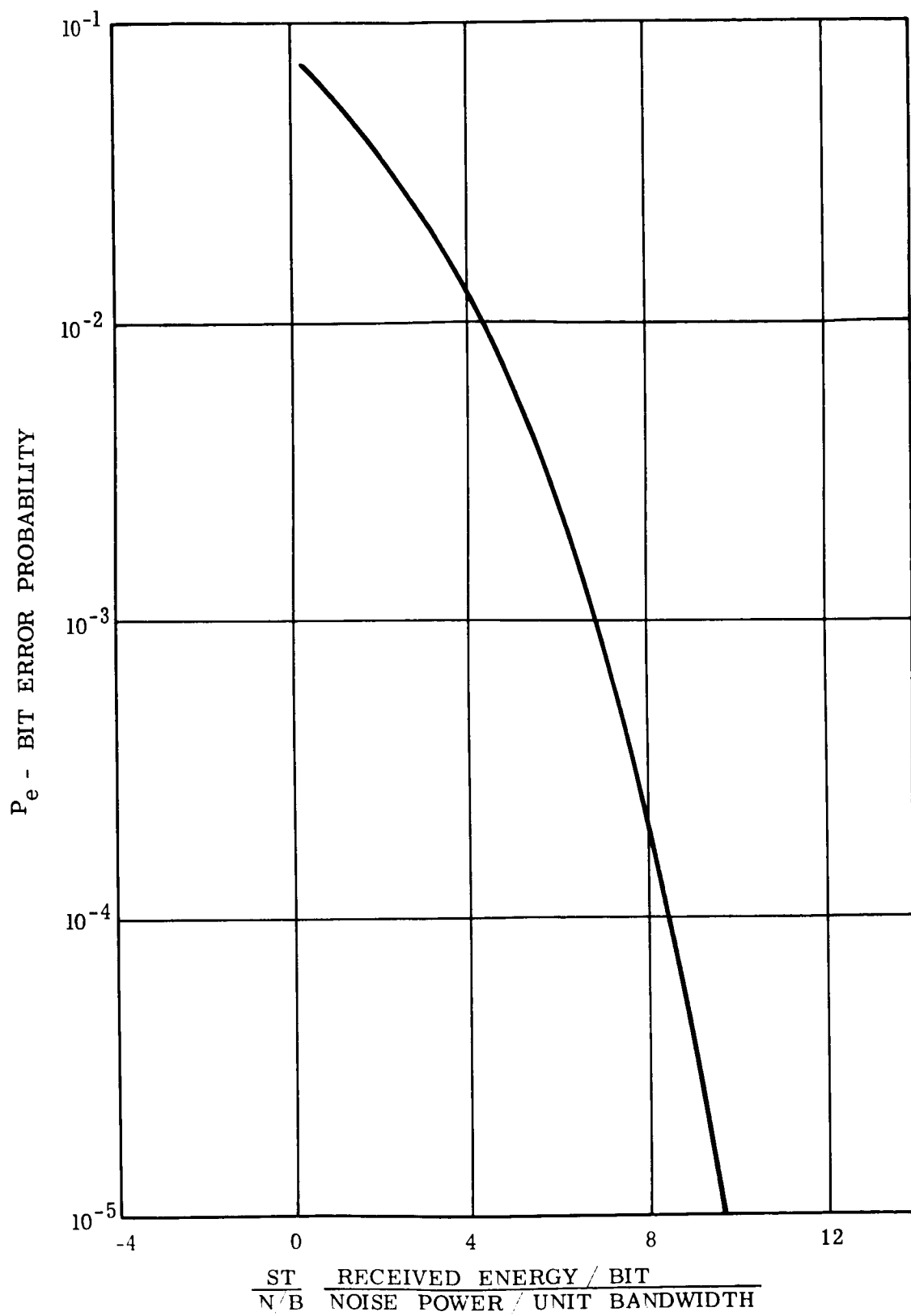


Figure 1.6.2-2. Probability of Bit Error for Ideal PCM/PSK ($\pm 90^\circ$)

It is felt that during the Voyager era it will be possible to come within one db of the theoretical PSK detection efficiency at a DSIF ground station. Error control coding, as described in Paragraph 1.6.3, can be used to reduce the required signal strength by about 1.5 db. Therefore, the required value of $ST/(N/B)$ for this link has been taken to be

$$ST/(N/B) = 6.0 \text{ db} \quad (4)$$

which is about 7.6 db inferior to Shannon's ideal.

(3) PCM/PSK ($\pm 60^\circ$)

If the phase of the carrier is not completely reversed between a mark and a space, the RF carrier will not be completely suppressed, thus leaving some carrier power for tracking. Conventional NRZ transmission will produce significant sidebands near the carrier frequency, however, thus interfering with carrier tracking; but an uncluttered band in the vicinity of the carrier can be provided by simple modulo-two addition of the NRZ data with a squarewave or pseudo noise carrier of the correct phase and frequency.

For a peak phase deviation ϕ , the output signal power will be proportional to $\sin^2 \phi$, and the carrier power will be proportional to $\cos^2 \phi$. For example, for $\phi = 60^\circ$, 75% of the power is in the sidebands, and 25% is in the carrier. In this case the data channel would be 1.25 db inferior to PCM/PSK with $\pm 90^\circ$ keying.

(4) PCM/PSK/PM

PCM/PSK/PM, such as was used on Mariner II, denotes a PCM/PSK ($\pm 90^\circ$) signal on a subcarrier which phase-modulates the main carrier. For high data rates the phase modulation index should be about 1.4 radians. This yields a subcarrier suppression factor of $2J_1^2(1.4) = -2.32$ db. Therefore, PCM/PSK/PM is about 2.32 db inferior to PCM/PSK at high data rates.

(5) PCM/FSK/PM

PCM/FSK/PM exploits the zero value of the correlation coefficient of two orthogonal waveforms. But $\pm 90^\circ$ PSK results in a correlation coefficient of -1, which is even three db better than FSK. Also, an additional one db is usually lost in the FSK detection process. Therefore, PCM/FSK/PM is approximately four db inferior to PCM/PSK/PM at these error rates.*

(6) Comparison of Techniques

Multiplication of Equation (3) by the data rate yields the ideal required signal power as a function of N/B , the noise spectral density. Assuming this to be -213.2 db (w/cps) the relationship has been plotted in Figure 1.6.2-3.

The required power for the other modulation techniques has been plotted relative to the ideal Shannon relationship.

E. Minimum Carrier Power Requirements

For high data rates and high received signal levels, such as will be provided by the high-gain spacecraft antenna, supplying the minimum carrier power required by the phase-lock loop is not a problem. However, the weak signals provided by the spacecraft

* Glenn, A. B., "Comparison of PSK vs. FSK and PSK-AM vs. FSK-AM Binary Coded Transmission Systems", IRE Transactions on Communications Systems, June, 1960, p. 92.

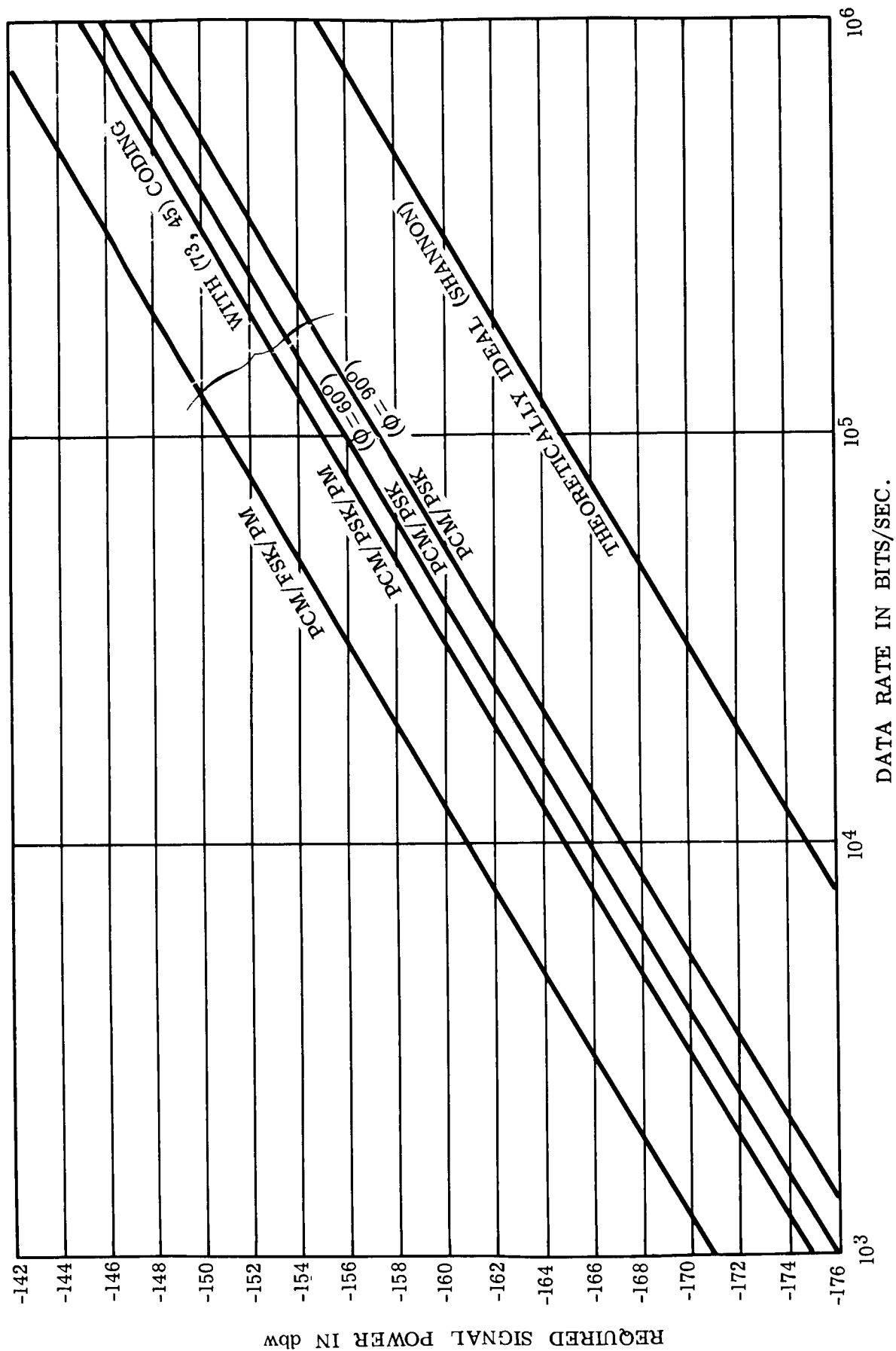


Figure 1.6.2-3. Signal Power Required at DSIF Ground Station Vs. Data Rate for Digital Modulation Systems (Zero Margin)

omnidirectional antennas in a back-up mode require an analysis of the carrier threshold level.

Using the link parameter values of Paragraph B, the minimum carrier power required is:

$$\begin{aligned} P_c &= (C/N) (N/B) (2B_{LO}) \\ &= 6 - 213.2 + 4.8 \text{ dbw} \\ &= -202.4 \text{ dbw} \end{aligned} \tag{5}$$

This has been plotted as a horizontal asymptote in Figure 1.6.2-4.

Equation (4) shows that the required value of $ST/(N/B)$ in the sidebands is 6.0 db.

With $\pm 90^\circ$ phase-shift keying, all the RF power can be used for data. For $\phi < 90^\circ$ the total RF power required will be proportional to $1/\sin^2 \phi$, provided that this exceeds the carrier power requirement given by equation (5). Addition of the power required by the carrier yields the curved line in Figure 1.6.2-4, showing the power required for equal thresholds in the data and carrier channels. The intersections of this curve with the members of the family of $\phi < 90^\circ$ curves indicate the optimum phase deviation as a function of received power level.

F. Results

Figure 1.6.2-5 has been plotted for wideband transmission through the high-gain antenna by combining Figures 1.6.2-1 and 1.6.2-3 and including eight db margin.

The curve of Figure 1.6.2-4 has been re-plotted in Figure 1.6.2-6 to show the narrow-band performance through an omni antenna. This shows that at 1969 Mars encounter (103×10^6 nm) a 50-watt transmitter with $\pm 50^\circ$ peak phase deviation will provide about four bits/sec, with eight db margin. It also indicates the possibility of operating out to 1.5 times that distance at a data rate of 0.4 bits/sec, if the peak phase deviation is gradually reduced (on command) to 20 degrees.

1.6.3 ERROR CONTROL CODING FOR VOYAGER COMMUNICATIONS

A. Codes for Deep-Space Telemetry

(1) Information Theory and Coding

For binary transmission, the upper bound for the capacity of a communication channel perturbed by additive random noise has been defined by Shannon to be

$$C = B \log_2 \left(1 + \frac{S}{N} \right) \tag{1}$$

where B = receiver bandwidth

S = received signal power

N = received noise power

Assuming that the noise energy density N_0 is constant over the bandwidth of interest, $N = N_0 B$, the received noise power N is directly proportional to the receiver bandwidth B and the channel capacity C is a monotonically increasing function to the limit $(S/N_0) \log_2 e$ as $B \rightarrow \infty$

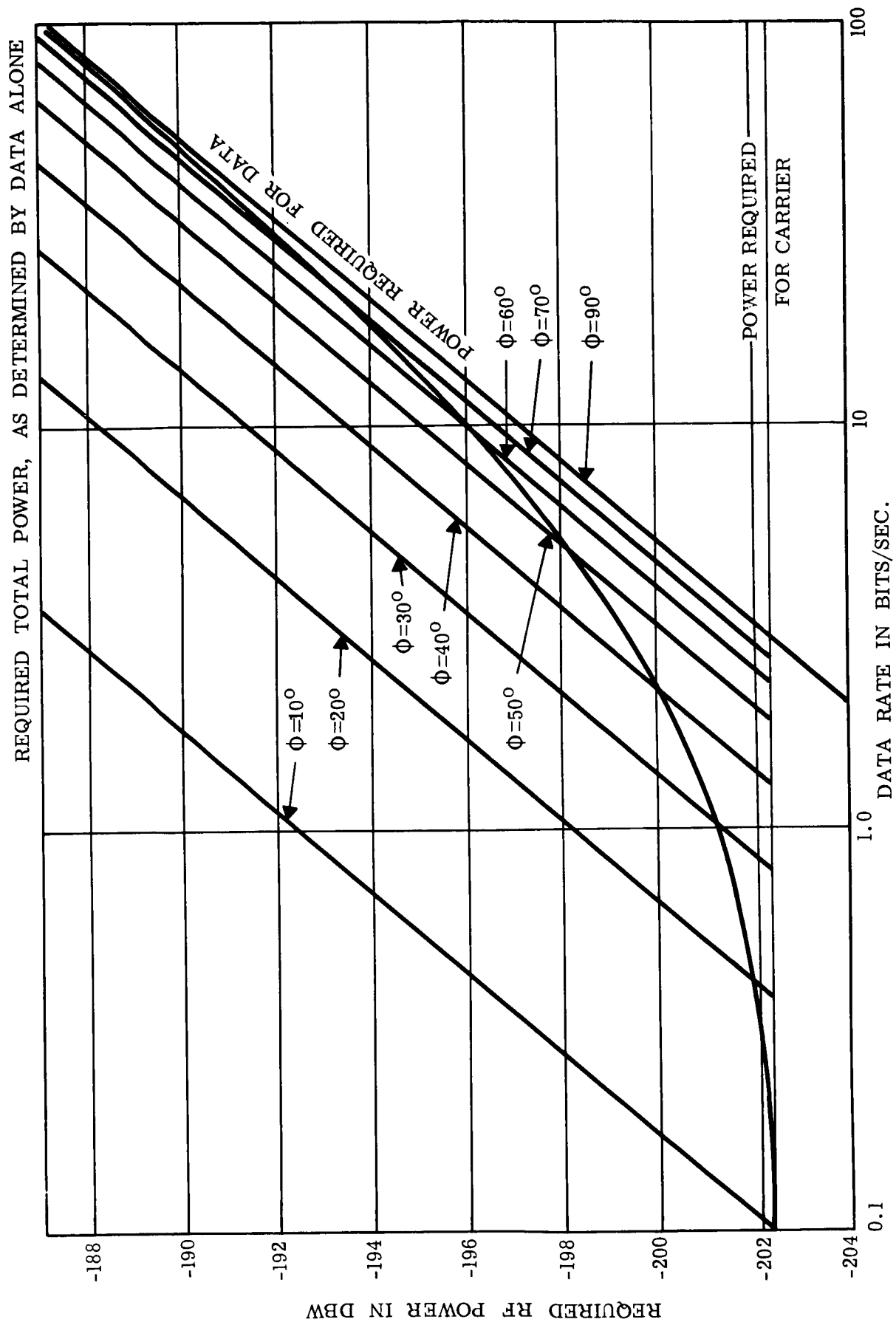


Figure 1.6.2-4. Total R-F Received Power Requirements as Determined by Data, Peak Phase Deviation, and Carrier (Zero Margin)

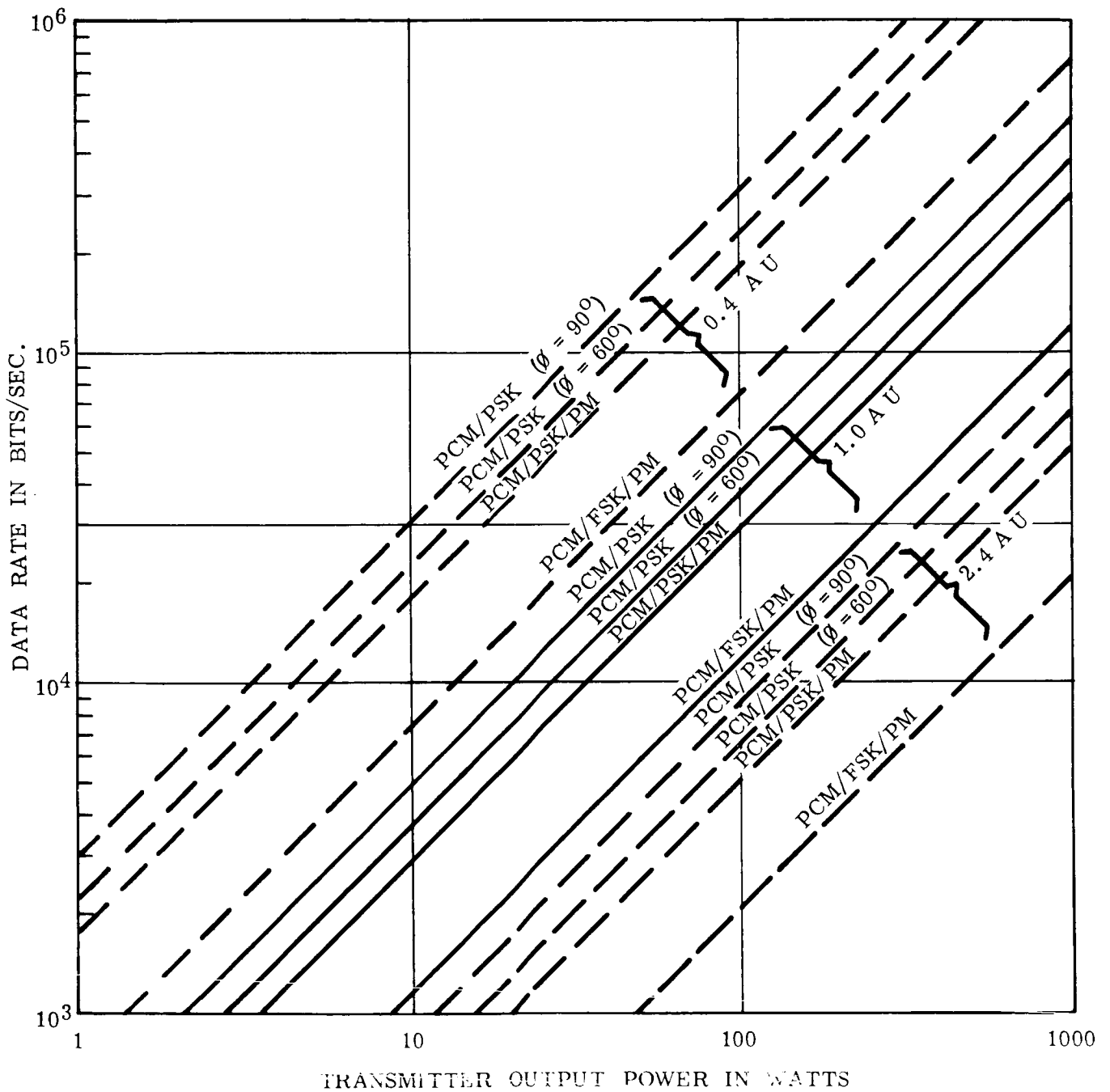


Figure 1. 6. 2-5. Typical Graphs of Data Rate Vs. Transmitter Power for Digital Modulation Systems

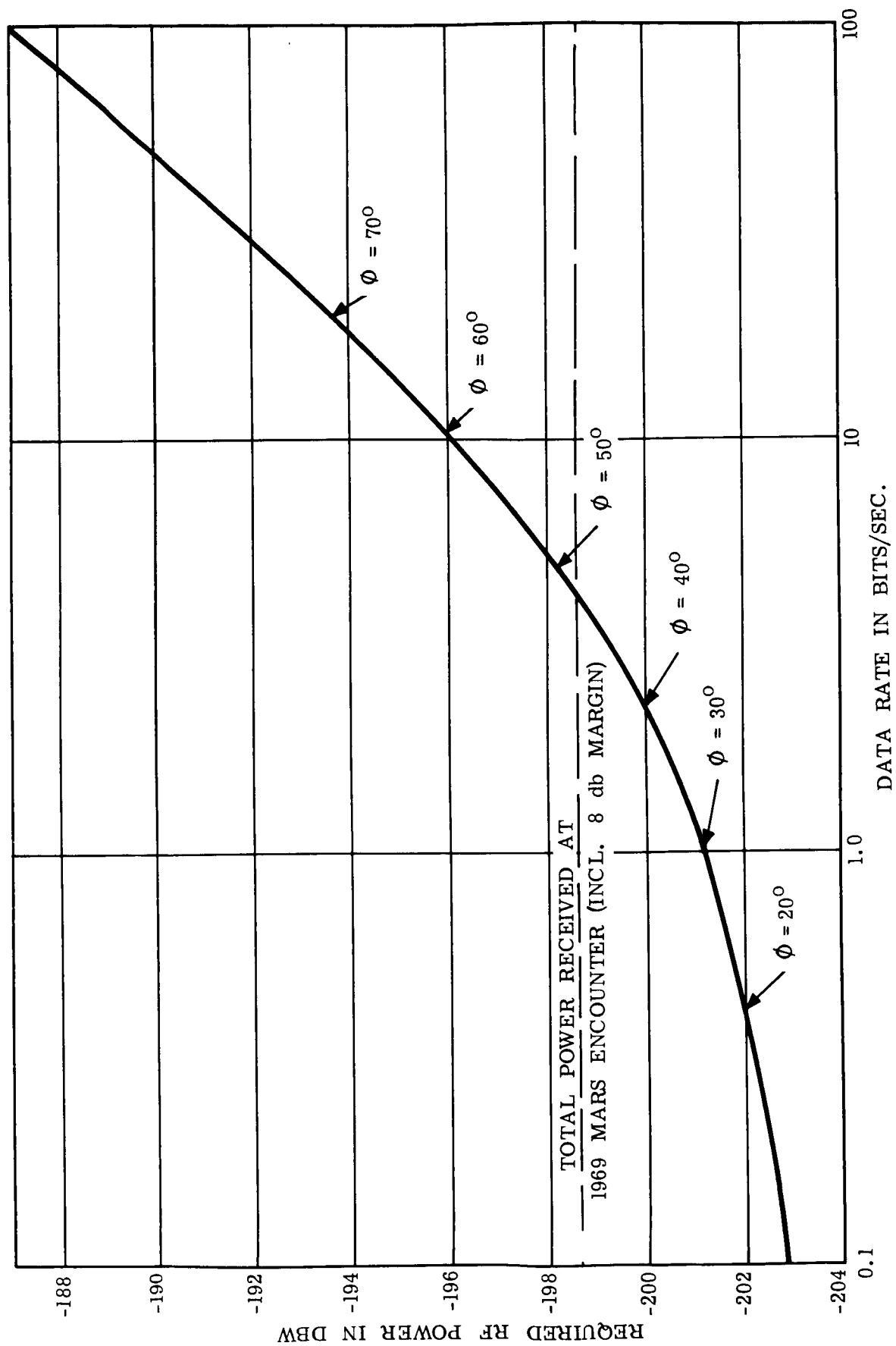


Figure 1.6.2-6. Performance at Low Data Rates Through Omni Antenna

This relationship implies that for a fixed received power level S , it should be possible to increase the channel capacity by increasing the bandwidth B . It is important to note, however, that unless this increase in bandwidth is obtained in the correct manner, system performance will not be improved, and may even be degraded.

A clarification of the terms "information bit rate", "data bit rate", and transmitted "digit rate" will be helpful at this point. Information has a precise definition in communication theory; it is synonymous with intelligence, but not necessarily synonymous with data. The maximum amount of information which can be obtained from a signal source is a function of the accuracy and bandwidth of the sensor. The rate at which samples should be taken to obtain the information from the source is specified by the sampling theorem, and the number of data bits required for each sample is determined by the accuracy of the sensor. The resultant minimum transmission rate is the information bit rate. The data bit rate is the actual number of digits used to convey the information, and may exceed the information bit rate. The transmitted digit rate is the same as the data rate unless error control coding is used, in which case the digit rate exceeds the data rate.

The use of excess bandwidth for transmission of a signal is known as redundancy. It can be classified as desirable or undesirable according to whether it improves the information transmission efficiency or not. Examples of undesirable redundancy are:

1. Data samples in excess of the sampling theorem criterion or practical filtering requirements.
2. Data bits per sample in excess of that dictated by sensor accuracy.
3. Repetition of sampled data.

All desirable redundancy may be considered a form of error-control coding.

The role of error-control coding in a digital data link is illustrated in Figure 1.6.3-1. The encoding function is a binary-to-binary conversion which adds r digits of useful redundancy to the m data bits to form an $n = m + r$ digit code word. The electrical signal, representing a sequence of binary "1"s and "0"s from the encoder, is transmitted via a communication channel in which noise may be added to the signal. Upon arrival at its destination, the signal (code word plus noise) enters a receiver that is kept in synchronism with the transmitter. The signal is demodulated by the receiver and then quantized, after which the error-control decoder operates on the quantized binary digits to extract the information contained in the original message.

This method of processing a received code word is referred to as digital decoding, where decisions are made on a digit-by-digit basis (quantizing), and the error correction is performed by logical circuits.

An alternate method of processing the received code word is by correlation, where decisions are made on a word basis, and the "error correction" is implicit in the maximum likelihood mechanism which decides which word was sent. It is well known that correlation detection is optimum in a Gaussian environment, but the receiving equipment becomes unduly complex for all but relatively weak codes.

(2) Code Options

Error control codes range from the least redundant Wagner codes, where one redundant digit is added to a block of data bits, to the most redundant orthogonal codes, where $2^m - m$ redundant digits are added to a block of m data bits.

For a given block of m data bits, the greatest increase in channel capacity in a Gaussian noise environment is obtained by using a highly redundant code, such as a maximal length

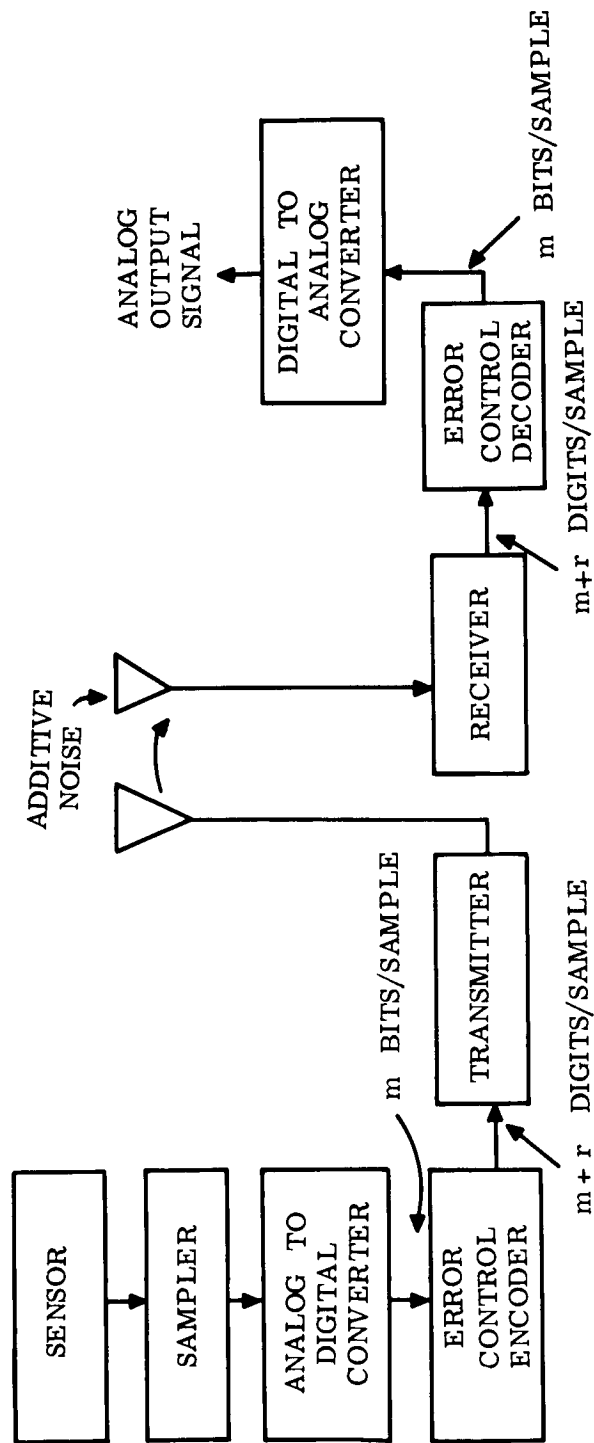


Figure 1.6.3-1. Typical Data Link with Error Control Coding

sequence, orthogonal, or bi-orthogonal code, together with correlation processing at the receiver. There are several practical drawbacks, however.

First, the ratio of total bandwidth to information bandwidth becomes extremely large. For example, the maximal length sequence code with 20 data bits per code word has a code word length of $2^{20} - 1$ digits. This means that roughly one megacycle of bandwidth would be required to transmit 20 bps. Although theoretically this is feasible, practical considerations such as receiver thresholds and synchronization requirements ordinarily rule out such a large bandwidth increase.

Second, correlation processing requires that an incoming code word be compared to all possible code words which could have been transmitted. For a maximal length sequence code with 20 data bits per code word, this would require 2^{20} comparisons for every received code word. Even at very low data rates, this would be impractical. Also correlation processing does not adapt easily to data rates which vary over a wide range, although devices have been developed which are capable of variable data rate operation over a limited range.

To keep the bandwidth increase small and at the same time obtain a significant increase in data transmission rate requires the use of a medium redundancy code with a relatively large number of data bits per code word. The large number of data bits per code word usually rules out the use of correlation processing at the receiver. Digital decoding techniques are available, however, which increase in complexity only linearly with code length, so that very powerful, low-redundancy codes can be implemented with relative ease.

The usual choice, then, is between a high-redundancy code with very few data bits per code word and correlation processing at the receiver, and a low-redundancy code with a large number of data bits per code word and digital decoding at the receiver. The net performance increase is about the same in either case for comparable receiver data processor complexity. The encoding equipment is the same for either system when shift-register codes are used, which is almost always the case.

B. Choice of Code

(1) Selection Criteria

The system performance increase afforded by coding is realized only when a code is selected which is appropriate for the channel and compatible with other subsystems. Some of the selection criteria are discussed in the following paragraphs.

In many applications, it is difficult to choose from among the various coding schemes such as error correction alone, error detection with retransmission, and combinations of error detection and correction. However, for deep-space telemetry, a detection and retransmission scheme is impractical because of the large propagation time involved, so that error correction alone is recommended.

The choice of code depends in part upon the channel noise statistics. For an S-band telemetry system, the noise is expected to be Gaussian, so that a random error-correcting code is appropriate.

Because of receiver thresholds and synchronization requirements, the bandwidth increase should generally not exceed 100%. A smaller increase would, of course, be preferable.

If possible, a code length should be chosen which divides the period of the pseudo-random stream used for synchronization. This enables word synchronization to be established automatically. The quotient (number of PN digits per coded data bit) should be large enough to insure sufficient resolution for synchronization.

Normally, the relationships of the number of data bits per code word to the total number of digits per code word and to the number of data bits per sample would be of importance from a timing standpoint. In the present application, however, the source will provide data bits individually on command so that no rate changes will be involved and so that the number of data bits per code word need not be divisible by the number of data bits per sample.

The complexity of the encoding equipment in the spacecraft should be held to a minimum, of course. This implies the use of a shift-register code of short or intermediate length.

(2) Selected Code

Application of the above selection criteria to available error-control codes has resulted in recommendation of the (73, 45) Bose-Chaudhuri code for use in the Voyager Communications Subsystem. This code has a block length of 73 digits, 45 of which are data bits. The general characteristics and specific performance data for this code in conjunction with the appropriate decoder are summarized in the next two subsections.

(a) General Characteristics

The (73, 45) code is a four-error correcting/five-error detecting shift-register code which can be decoded with remarkable simplicity. The code length 73 divides the PN sequence length of 511 digits, resulting in seven PN digits per coded data bit, which is quite sufficient for synchronization purposes.

Another characteristic of this code is its capability of correcting a relatively large number of error patterns of weight greater than four, in addition to the correction of all error patterns of weight four and less. This higher order error-correction capability may take either of two alternative forms, corresponding to error-correction options called "random-burst" and "random". Lower bounds on the correction capability for these two options are indicated in Table 1.6.3-1.

Based on a consideration of the expected noise in the Voyager communication channels, it appears that the random error correction option is the more appropriate.

Consider now some of the additional characteristics of the selected code for the random error correcting option. Given that an uncorrectable error occurs, it is important to have a characterization of its effect on the 45 decoded data bits. Although a complete specification of the output error statistics for the (73, 45) code together with its recommended decoder would require a prohibitive amount of computation, partial results of this type are fortunately available.* These results are for the case of low-level random interference, such as Gaussian noise at high S/N. In this environment, almost all of the uncorrected errors are of weight $e+1=5^{**}$, and it has already been noted that only $100-50.11 = 49.89$ percent of the five-digit errors cause decoded data bit errors. Table 1.6.3-2 also indicates this percentage, as a part of the complete probability density distribution of decoded data bit errors caused by five-digit errors in the 73-digit code block.

* M. Mitchell, "Performance of Error Correcting Codes, "I. E. E. Trans. on Communication Systems, Vol. CS-10, No. 1, March 1962, p. 77.

** The symbol e designates the maximum number of errors per word which can be corrected with complete certainty.

TABLE 1.6.3-1. RANDOM-BURST AND RANDOM CORRECTION CAPABILITIES

Correction Option	Lower Bound on Correction Capability
Random-burst	All random error patterns of weight 4 or less, plus all burst error patterns of width 11 or less.
Random	All random error patterns of weight 4 or less, plus 50.11 percent of the random error patterns of weight 5.

TABLE 1.6.3-2. DATA BIT ERRORS

Number of Decoded Data Bit Errors	Probability of E Decoded Data Bit Errors
E	P(E)
0	0.5011
1	0.1920
2	0.1105
3	0.0979
4	0.0762
5	0.0223
P(E) = 0 for E > 5	
$\sum_{E=0}^5 P(E) = \binom{73}{5}$	

It is interesting to observe from Table 1.6.3-2 that a five-digit error in the 73-digit code block causes at most five errors in the 45-bit decoded data block. Also note that about 70% of the time fewer than two decoded data bit errors result.

The data in Table 1.6.3-2 can, of course, also be used to calculate the conditional probability $P_b(5)$ of decoded data bit error given that a five-digit error occurs. This calculation is:

$$P_b(5) = \frac{1}{45} \sum_{E=0}^5 E P(E) = 0.0250 \quad (2)$$

which says that the corresponding expected number of incorrectly decoded data bits is $(0.025)(45) = 1.125$ per block of 45.

There is an alternative approach to calculating the conditional probability $P_b(5)$, based on the cyclic property of this code. The reasoning is as follows. First, if a pattern of $e+1(=5)$ errors is decoded incorrectly, a maximum likelihood (optimum) decoder (and all

"good" decoders also) will output a block of $m(=45)$ data bits corresponding to a "nearest neighbor" of the transmitted code word. Since all nearest neighbor code words differ in $d(=10)$ places from the code word that was transmitted, this means that the conditional probability $P_b(5)$ of decoded data bit error can (assuming all 5-digit errors to be uncorrectable) be approximated by $P_b(5) \approx 10/73 \approx 0.137$. This is more than 5 times greater than the exact calculation of the preceding paragraph, and shows that the $P_b(e+1) \approx d/n$ approximation is definitely conservative in the case of (73, 45) code with the recommended random error correcting decoder. (If this approximation is modified by taking into account the known fact that about 1/2 of the five-digit errors are actually correctable, the resulting approximation would still be conservative by a factor greater than 2.)

(b) Specific Performance Data

Figure 1.6.3-2 is a curve specifying the expected telemetry receiver input-output characteristic both with and without coding. It is given in terms of receiver output data bit error probability P_{ud} as a function of E/N_0 (ratio of received signal energy E per data bit to Gaussian noise power density N_0).

The curve labeled "coded: (73, 45)" was obtained as follows. First, the receiver output digit error probability P_{cd} with coding was obtained from Figure 1.6.3-1 by using the degradation factor 45/73 in db. Second, the (73, 45) decoder output word error probability $P_c(W)$ was computed, under the (conservative) simplifying assumption that no errors of weight greater than four were correctable, using an approximation to the formula:

$$P_c(W) = \sum_{i=5}^{73} \binom{73}{i} (P_{cd})^i (1-P_{cd})^{73-i} \quad (3)$$

where $\binom{73}{i} = \frac{(73)!}{(i)! (73-i)!}$

Third, the decoder output data bit error probability P_{cb} was approximated by

$$P_{cb} \approx \frac{10}{73} P_c(W). \quad (4)$$

C. Error Control System Description

The error control system consists of the encoding subsystem, located on the spacecraft, and the decoding subsystem, located at the earth receiving site.

(1) Encoding Subsystem Description

The encoding subsystem consists of an encoder for the (73, 45) code, and an encoder timer, as shown in Figure 1.6.3-3.

The (73, 45) encoder performs the function of transforming a sequence of 45 data bits into a 73-digit code word. The encoder consists of the 28-stage shift register and associated logic shown in Figure 1.6.3-5.

The encoder is sequenced through two modes during encoding of a (73, 45) code word. In the first mode, the sequence of 45 data bits is transmitted, and at the same time is also read into the encoder logic to establish the proper "initial condition". In the second mode the encoder sequentially computes the 28 redundant code digits (called "check digits") from the initial condition, and simultaneously reads them out to the transmitter.

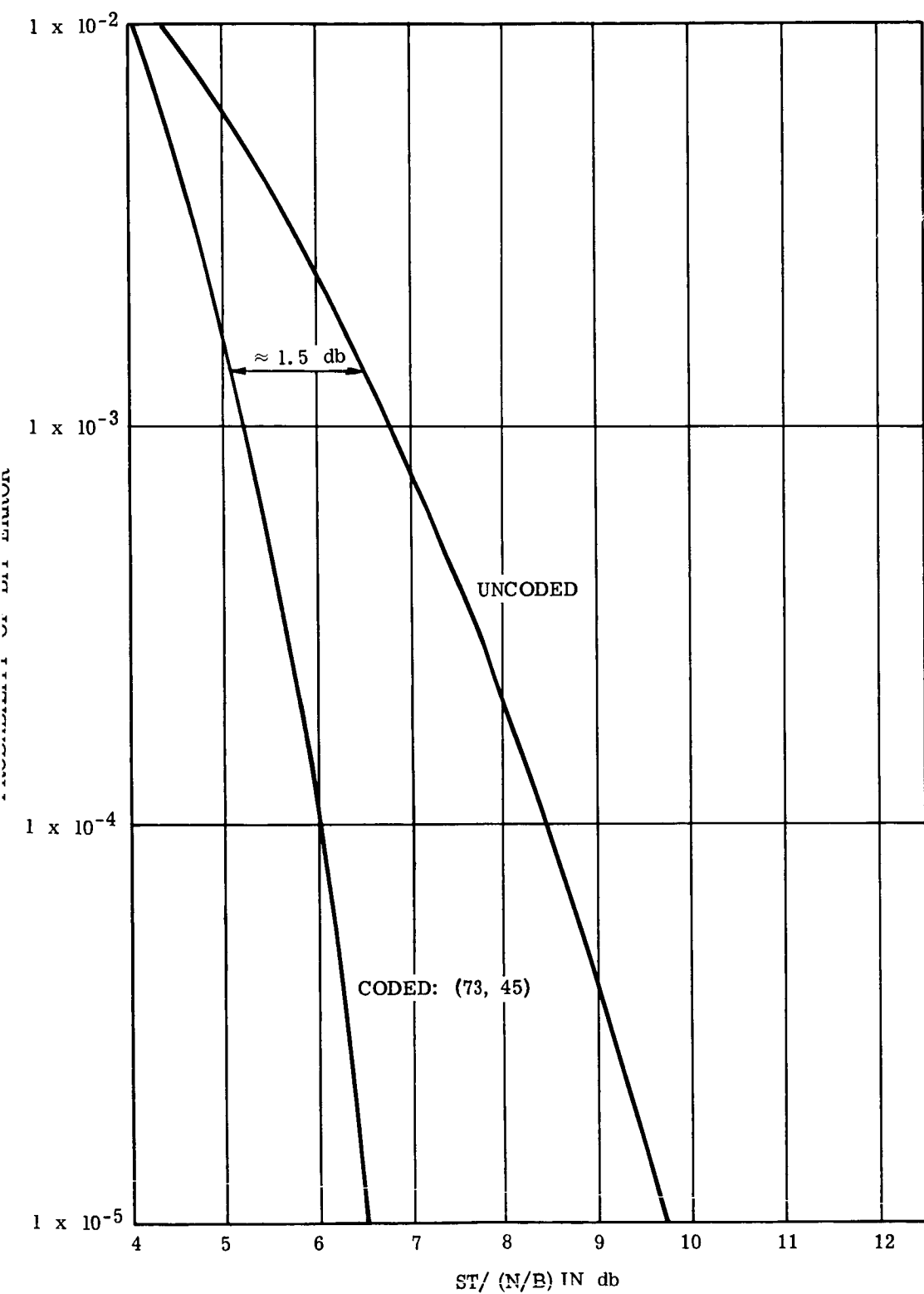
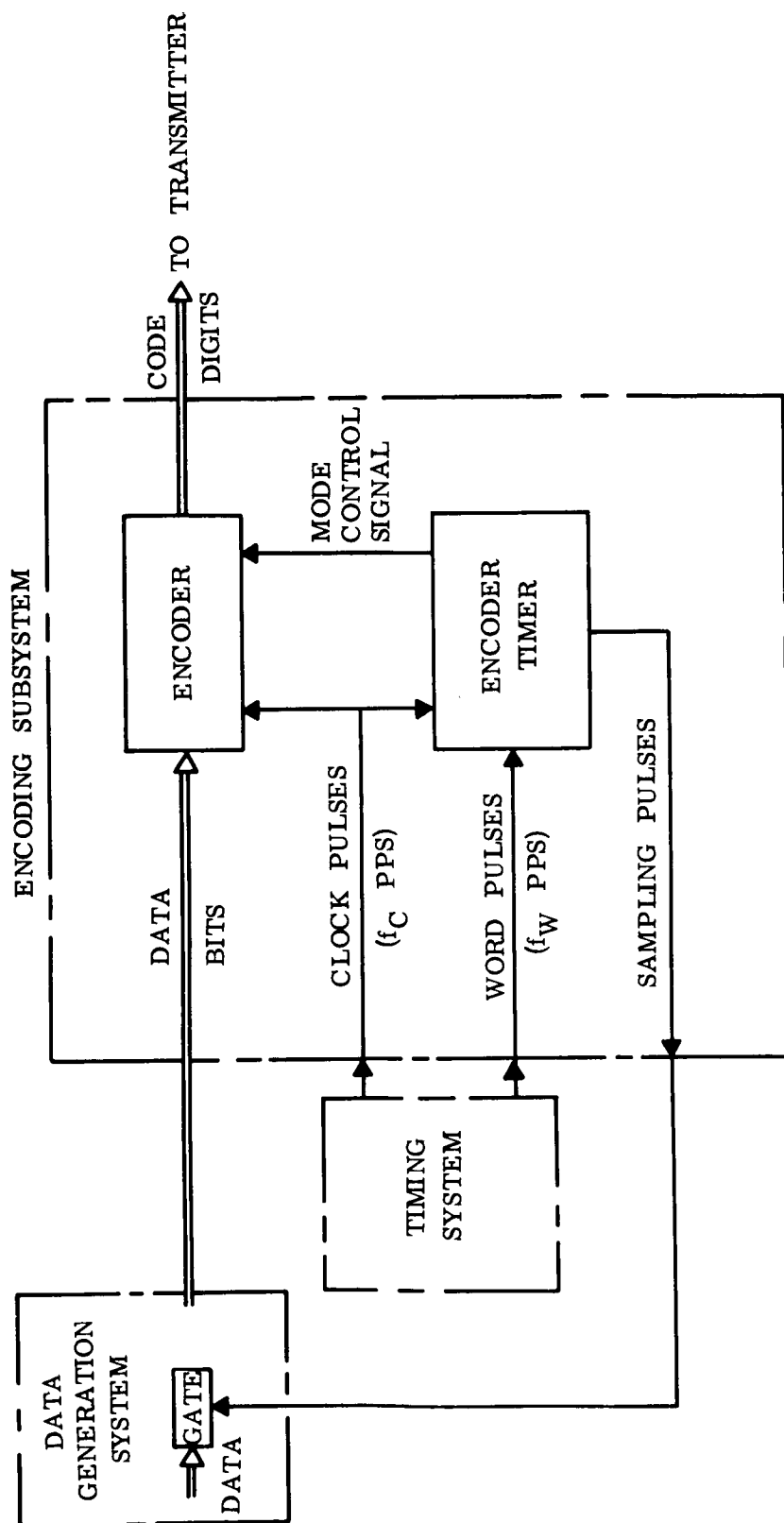


Figure 1. 6. 3-2. Reduction of Power Requirements Through Error Control Coding



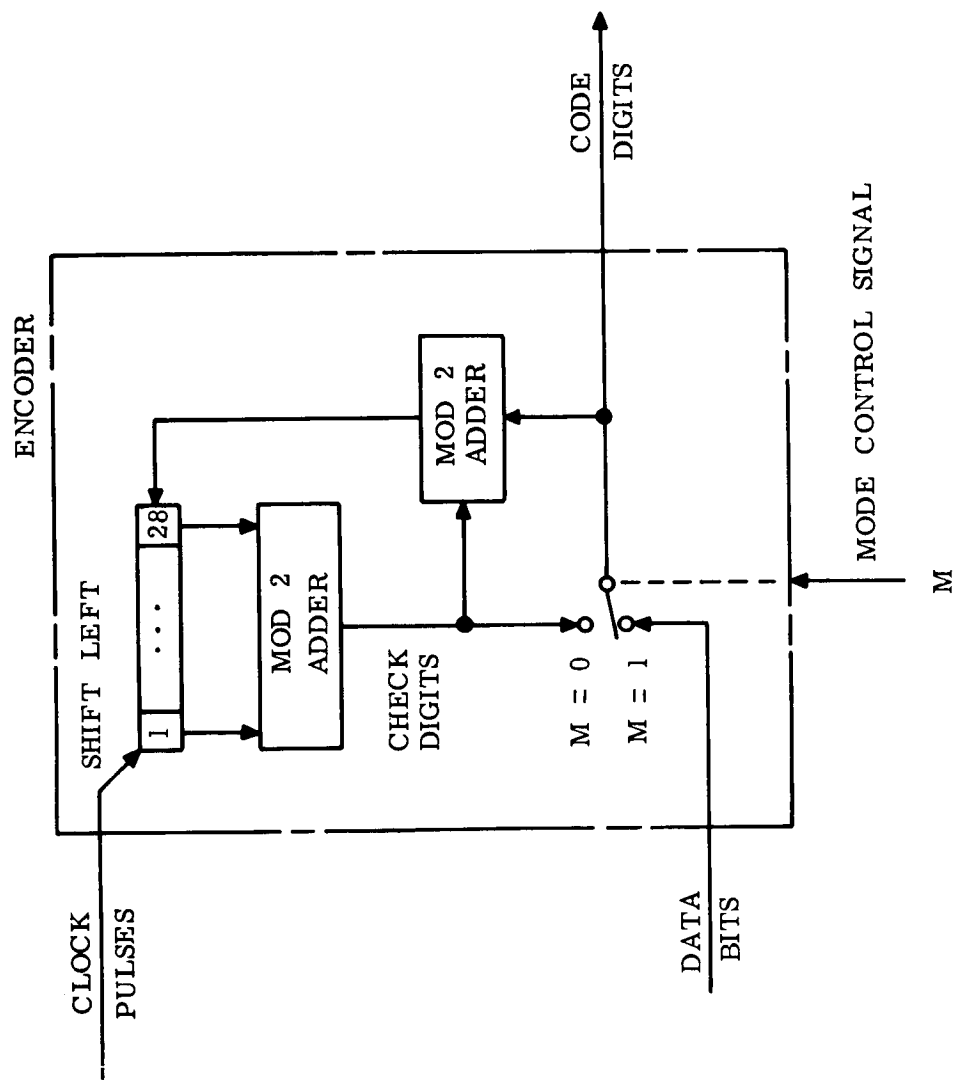


Figure 1. 6. 3-4. (73, 45) Encoder

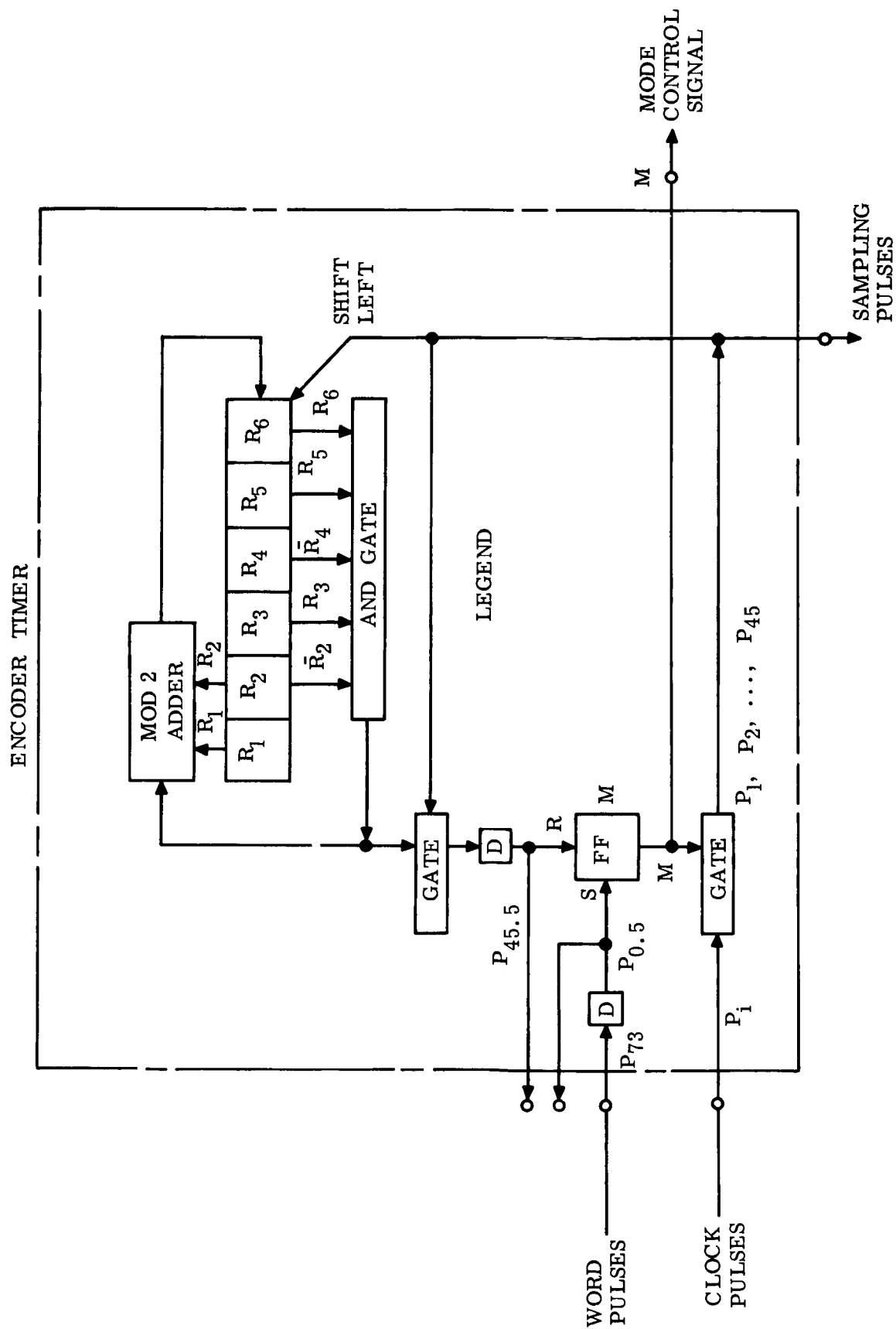


Figure 1.6.3-5. Encoder Timer

The encoder timer consists of a novel preset (45-digit) counter and the associated logic shown in Figure 1.6.3-6. It performs two functions which may be described as follows:

The encoder timer first of all performs the function of deriving a burst of 45 consecutive "data sampling pulses" from the word sync pulse train (at f_w PPS) and the clock pulse train (at $f_c = 73 f_w$ PPS) as indicated in Figure 1.6.3-6. This burst of sampling pulses consists of clock pulses 1 through 45 from each block of 73. The sampling pulse burst is fed back to the sampling gate located in the data generation system, as indicated in Figure 1.6.3-3.

A second function of the encoder timer is to sequence the encoder through its (repetitive) cycle of first transmitting a block of 45 information bits, and then transmitting the corresponding block of 28 redundant code digits of the 73 digit code word. The output of flip-flop M of the encoder timer (Figure 1.6.3-5) controls the operating mode (information or redundant half-cycle) of the encoder as indicated.

(2) Decoding Subsystem Description

The decoding subsystem consists of a 45-stage buffer, a (73,45) decoder, a decoder timer, and the interconnecting gates shown in Figure 1.6.3-7.

The (73,45) decoder performs the function of transforming a received 73-digit code word, with any of its correctable errors, into a sequence of 45 data bits identical to that read into the encoder. The decoder consists of a 73-stage shift register, a block of mod 2 adders, and a majority decision element, as shown in Figure 1.6.3-8.

The 45-stage buffer is merely a 45-stage shift register with serial input and parallel output. The buffer is used to accumulate received digits while the 45 data bits of the previously received 73 digit word are being decoded.

The decoding subsystem sequences through four modes during each complete 73-digit cycles of its operation. Assuming that a sequence of (73,45) code words $A_1, A_2, \dots, A_j, \dots$ is transmitted, and that each A_j is received as B_j , the operation of the decoding subsystem can be summarized as follows:

MODE 1 (Clock times $t=1, 2, \dots, 45$)

- A. Decode B_j into 45 decoded data bits
- B. Read first 45 digits of B_{j-1} into the 45-stage buffer.

MODE 2 (Clock time $t=45.5$)

Transfer (in parallel) first 45 digits of B_{j-1} from 45-stage buffer into first 45 stages of 73-stage decoding register, and switch the input of the 73-stage decoding register from the output of the majority element to the decoding subsystem input terminal.

MODE 3 (Clock times $t=46, 47, \dots, 73$)

Read digits 46-73 of B_{j-1} into 73-stage decoding buffer.

MODE 4 (Clock time $t=0.5$)

Switch input of 73-stage decoding register from input terminal to output of majority element, and switch decoding subsystem input terminal to input of 45-stage buffer.

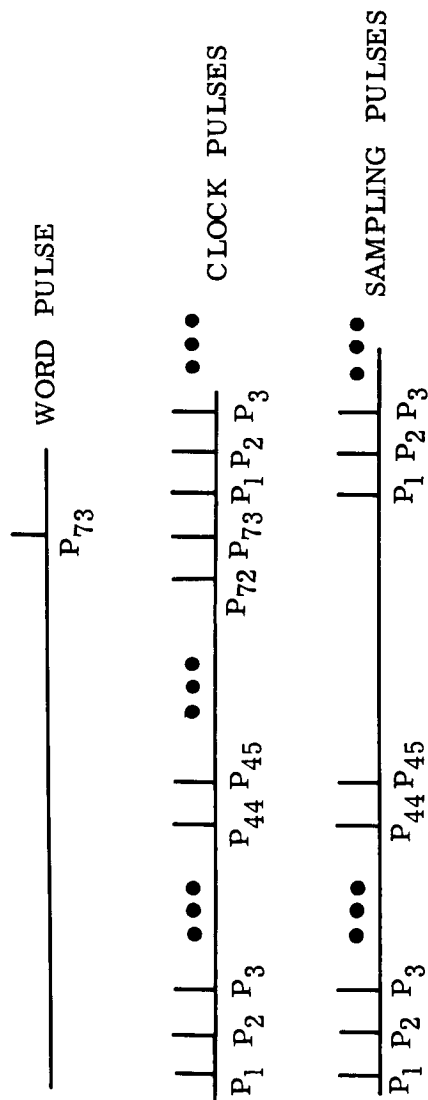


Figure 1. 6. 3-6. Timing

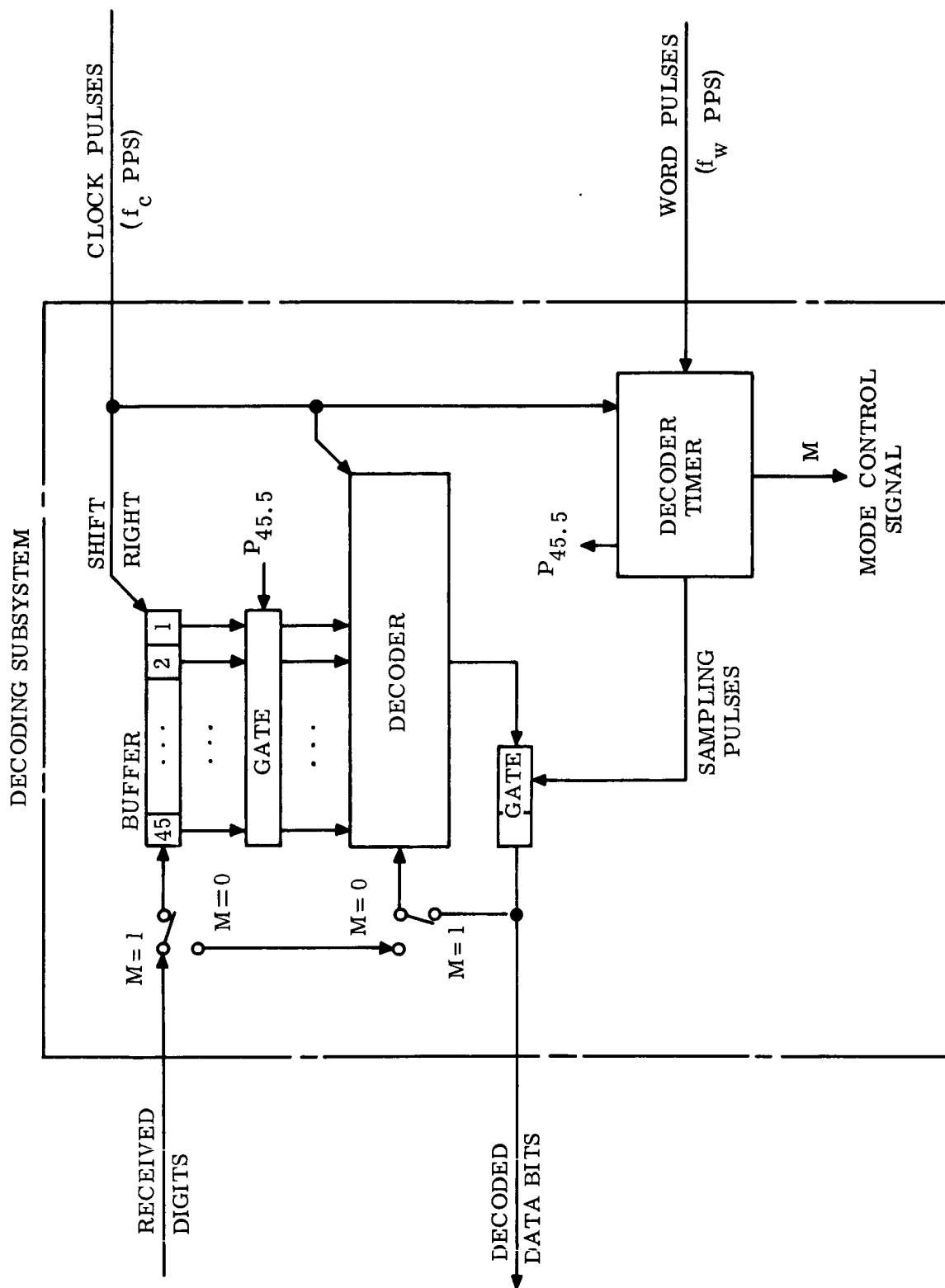


Figure 1.6.3-7. Decoding Subsystems

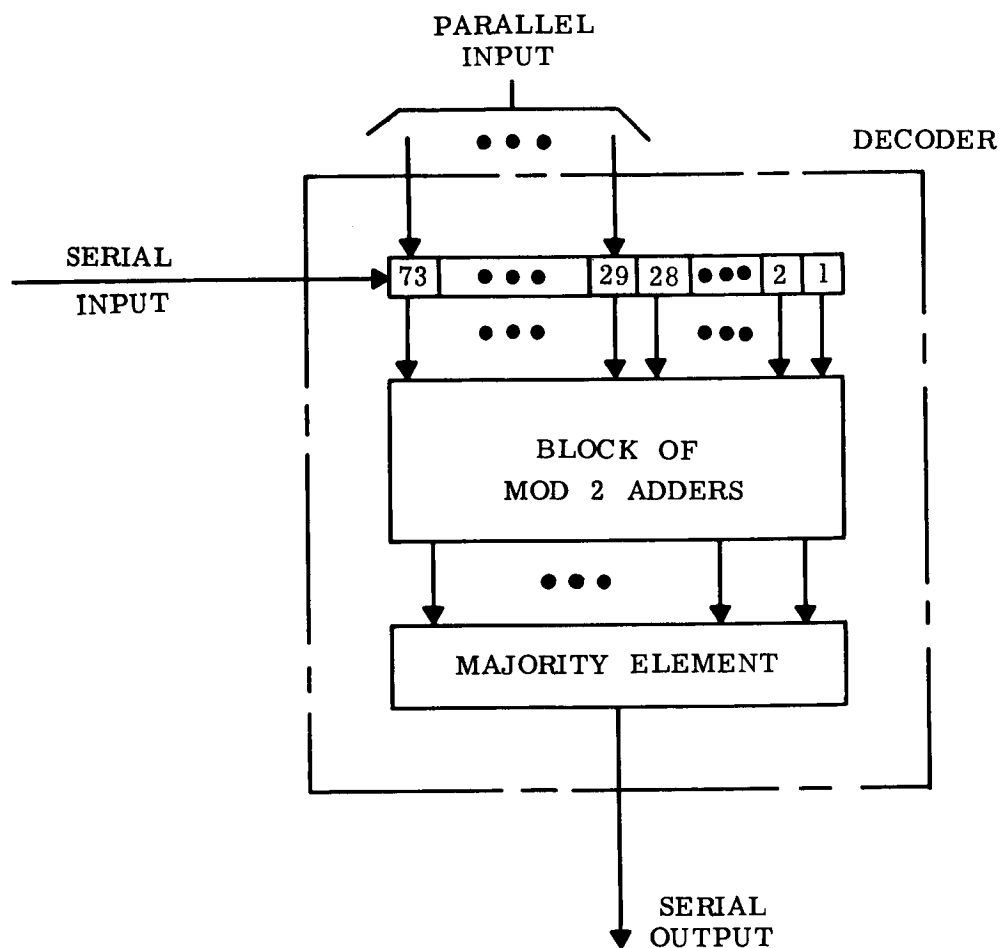


Figure 1. 6. 3-8. (73, 45) Decoder

The decoder timer is identical to that for the encoder just discussed. However, its outputs are used somewhat differently. One difference is that the 45-bit sampling burst is used for output rather than input gating, and the output of flip-flop M controls the decoder mode switches (instead of the encoder mode switch). A second difference is the use of the special pulse P45.5 generated in mode 4, as indicated.

(3) Parts Count for Error Control System

The parts count, for the encoding and decoding subsystem, are summarized in Table 1.6.3-3. The indicated number of mod 2 adders can be converted to a corresponding number of transistors by multiplying by 2 if a high-speed mod 2 adder design is assumed. At the relatively low bit rates expected, however a mod 2 adder design using only one transistor should be adequate.

TABLE 1.6.3-3. ERROR CONTROL SYSTEM PARTS COUNTS

	FLIP FLOPS	MOD 2 ADDERS	NANDS
ENCODER	28	9	3
ENCODER TIMER	7	2	6
ENCODING SUBSYSTEM	35	11	9
DECODER	73	63	30
DECODER TIMER	7	2	6
BUFFER	45	0	0
GATES	0	0	50
DECODING SUBSYSTEM	125	65	86

1.6.4 PRECISION RANGE RATE MEASUREMENT WITH TWO-WAY DOPPLER TRACKING

A. Introduction

One of the experiments being planned for the Voyager mission is a high-precision determination of the spacecraft's orbit about Mars or Venus in order to provide information on the planetary mass, potential field, and internal structure. It is therefore desired to measure the radial range rate as precisely as possible, and a goal of ± 0.01 ft/sec rms instrumentation error has been specified. Note that it is the precision with which the tracking system equipment can make this measurement that is being discussed here and not the absolute accuracy of the measurement. The absolute accuracy of the range rate determination will be limited by the uncertainty in the speed of light, which is not considered here.

An investigation of the two-way doppler tracking capability provided by the DSIF in conjunction with the spacecraft transponder and an analysis of the contributing error sources has indicated the feasibility of determining range rate with the desired precision. A discussion of the tracking system and the instrumentation errors in range rate measurement is presented below.

B. System Description

A simplified functional block diagram of the two-way doppler tracking system is shown in Figure 1.6.4-1. A stable 2113.312 mc carrier is transmitted to the spacecraft. The spacecraft transponder receives the signal which is then filtered, has its frequency multiplied by the exact ratio of 240/221, and is subsequently re-transmitted to the ground. The exact relationship between received and transmitted signals is achieved by use of a phase-lock loop in the transponder which insures phase coherence of the transponder local oscillator.

At the ground station the return carrier is mixed with the transmitter signal (multiplied by 240/221), to produce a beat frequency which is equal to the doppler frequency plus a bias which is added to prevent the doppler signal from going to zero when the range rate goes to zero. From Figure 1.6.4-1 the doppler frequency, f_D , is seen to be

$$f_D = \frac{240}{221} f_T \left(2 \frac{\dot{r}}{c} \right) \quad (1)$$

where f_T is the transmitter frequency, \dot{r} is the radial range rate, and c is the speed of light. The sum of the doppler frequency and the bias frequency, $f_D + f_B$, is then sent to a frequency measurement unit.

The frequency may be determined either by counting the number of cycles appearing in a fixed interval of time or by measuring the time interval required for a fixed number of cycles. A simplified functional block diagram of a system employing the latter technique is shown in Figure 1.6.4-2. Upon receipt of a command pulse, a gate opens which admits the unknown frequency, $f_D + f_B$, to a cycle counter which detects zero crossings of the signal. At a count of one cycle, a pulse from the cycle counter gates pulses at a frequency f_P into the pulse counter. At a count of $n + 1$ cycles a pulse from the cycle counter gates off the pulse counter. This pulse also closes the input to the cycle counter and resets the counters. The measured frequency is thus given by

$$f_D + f_B = nf_P/k \quad (2)$$

where n is the number of cycles of the unknown frequency

k is the number of pulses counted

and f_P is the pulse frequency

C. Error Sources

The three basic contributors to the instrumentation error in range rate determination which will be considered here are:

1. Coherent oscillator instability
2. Receiver thermal noise
3. Quantization error of frequency measurement unit

Uncertainty in the velocity of light is not considered as part of this study, since it is a fundamental limitation which is independent of the tracking system equipment.

(1) Coherent Oscillator Instability

Coherent oscillator instability is a limitation in all systems which require a stable time reference. All oscillators drift randomly in phase. It is the coherent oscillator drift

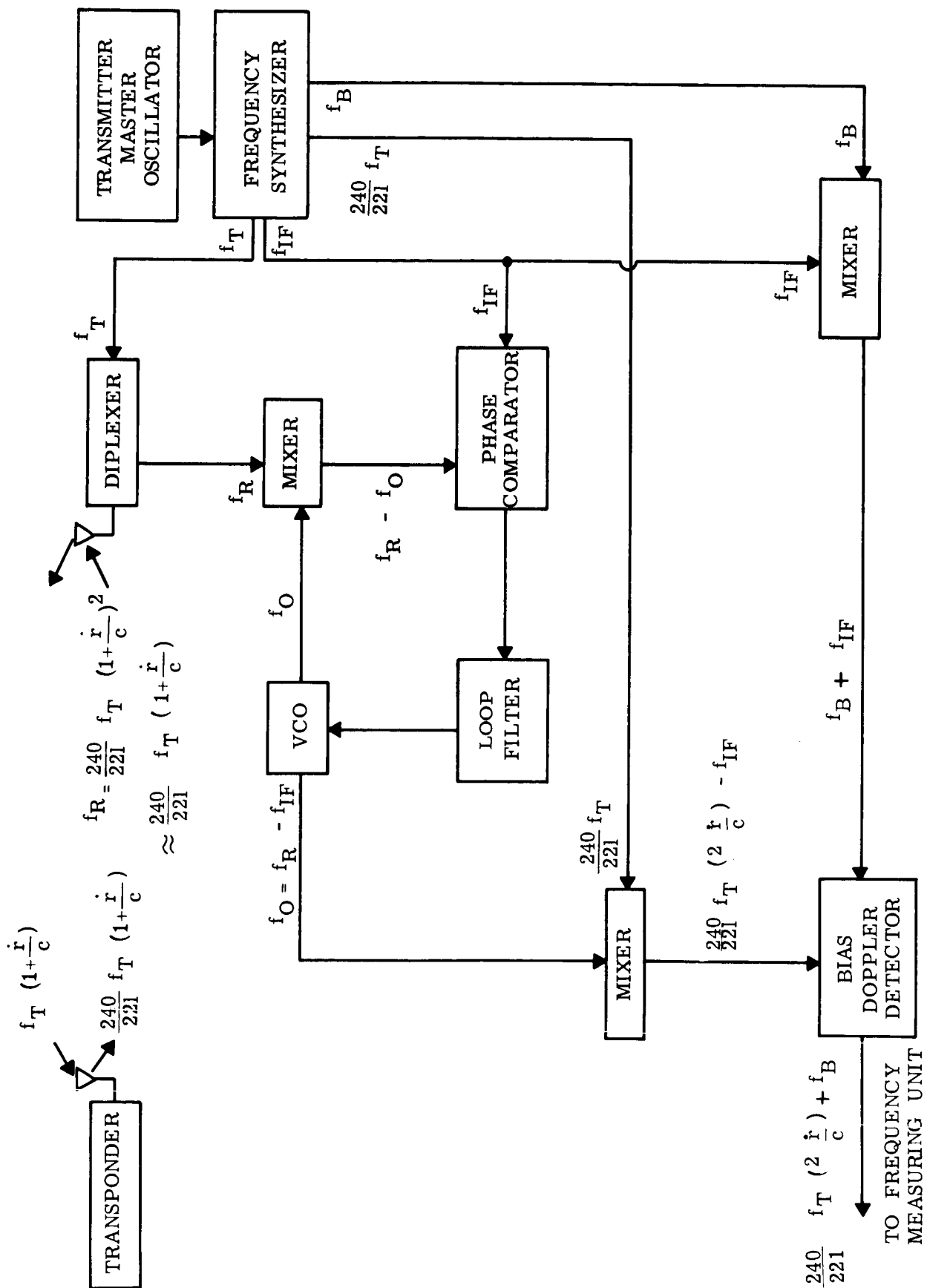


Figure 1. 6. 4-1. Two-Way Doppler Tracking System Simplified Functional Block Diagram

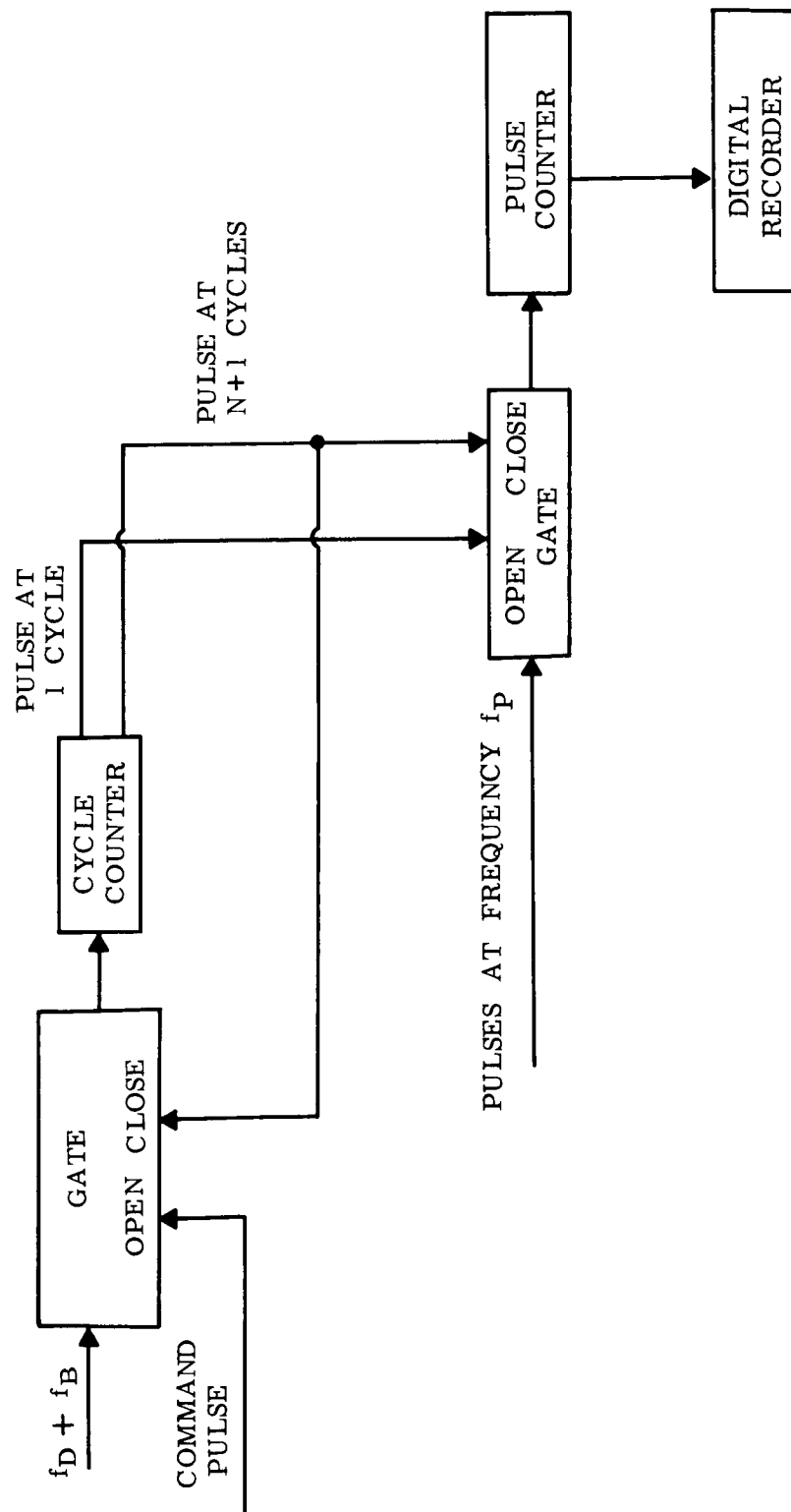


Figure 1.6.4-2. Frequency Measuring Unit Simplified Block Diagram

during the transit time, τ , between the transmitter, spacecraft, and ground receiver which causes an error in range rate determination. This drift can be quantitatively defined by a parameter known as coherence time, which is the time it takes an oscillator to drift one radian rms. Develet¹ has derived an expression for the rms error in range rate caused by coherent oscillator instability:

$$\Delta \dot{r}_1 = \frac{c}{2\pi f_T \sqrt{2 T T_c}}, \quad \frac{\tau}{T} \geq 1 \quad (3)$$

where

$\Delta \dot{r}_1$ = range rate error (rms) due to coherent oscillator instability, ft/sec

c = velocity of light, 9.84×10^8 ft/sec

f_T = transmitted frequency, cps

T = cycle-counting interval (smoothing time), sec

T_c = coherence time at transmitted frequency, sec

τ = round-trip propagation time, sec

Since we are concerned here with distances on the order of one astronomical unit, at which the round-trip propagation time is about 16 minutes, the condition $\tau/T > 1$ holds. Using $f_T = 2113$ mc, the curves of Figure 1.6.4-3 have been constructed from Equation (3) showing range rate error vs. smoothing time for various values of coherence time, T_c .

2. Deep Space Instrumentation Facility, Space Programs Summary No. 37-16, Volume III, p. 40, Jet Propulsion Laboratory, Pasadena, 31 July 1962.

The coherence time at the transmitter frequency may be related to the value of oscillator instability by the expression:

$$T_c = \frac{1}{(2\pi f_T)^2 s^2 \rho} \quad (4)$$

where s = oscillator instability

and ρ = time interval over which the value of s is determined.

The transmitter master oscillator at the DSIF is slaved to a rubidium frequency standard providing a short-term stability of at least one part in 10^{11} over a ten minute interval.² Using these values and a transmitter frequency of $f_T = 2113$ mc, equation (4) yields a coherence time of approximately 0.1 seconds. From Figure 1.6.4-3 it may be seen that a cycle-counting interval of approximately 270 seconds is required to restrict the range rate error to ± 0.01 ft/sec with this 0.1 second coherence time.

(2) Receiver Thermal Noise

For a second-order phase-lock receiver of high open-loop gain, the effect of additive receiver noise on range rate error in a two-way coherent doppler tracking system has been derived by Develet¹:

$$\Delta \dot{r}_2 = \frac{c}{4\pi f_T T \sqrt{S/N}} \quad (5)$$

1. Develet, J. A., "Fundamental Accuracy Limitations in a Two-way Coherent Doppler Measurement System", IRE Transactions on Space Electronics and Telemetry, Volume SET-7, No. 3, pp. 80-85, September 1961.

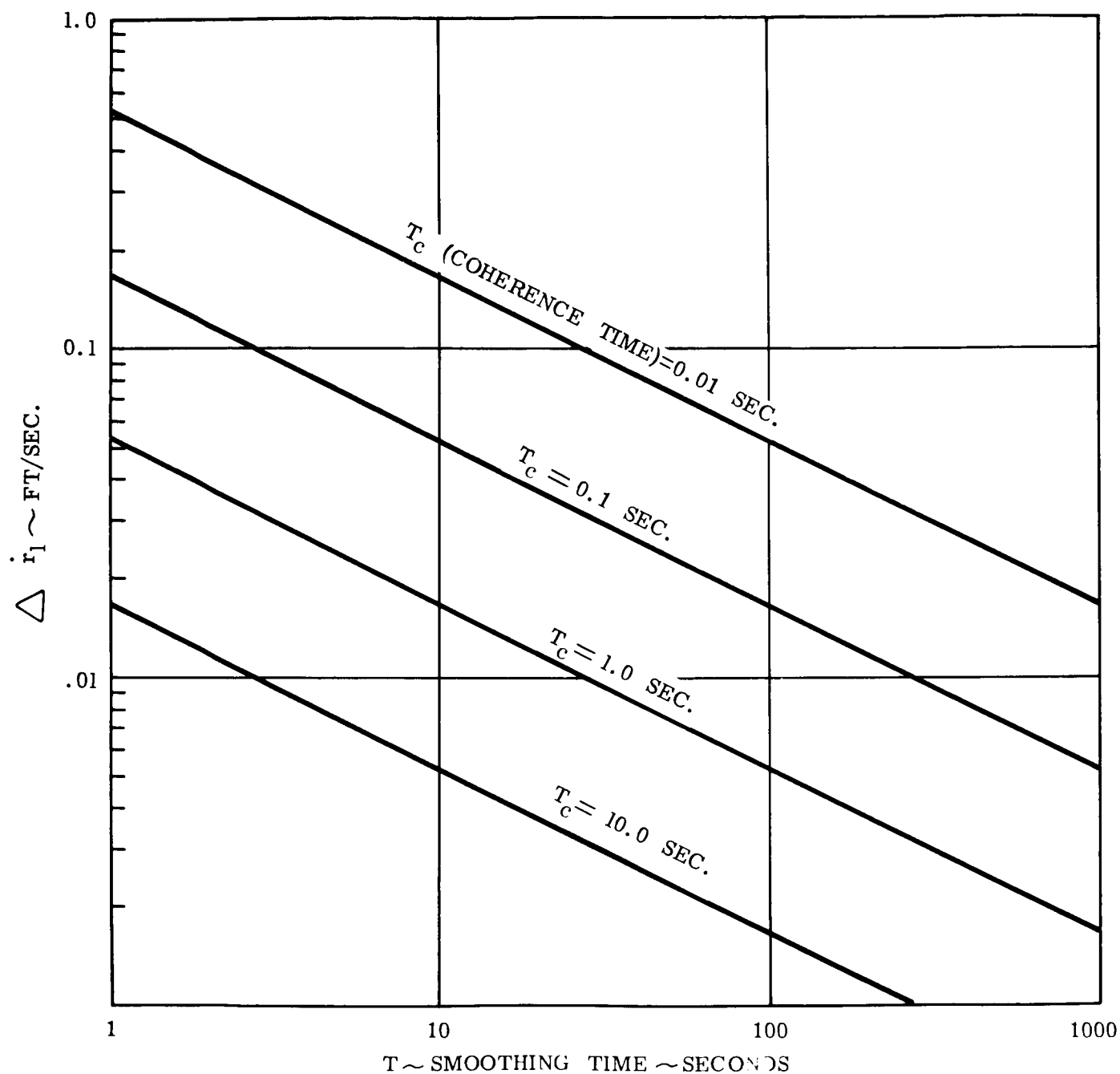


Figure 1.6.4-3. RMS Range Rate Error ($\Delta \dot{r}_1$) Due to Coherent Oscillator Instability

where S/N is the signal-to-noise power ratio in the phase-lock loop two-sided noise bandwidth and the other symbols are as previously defined. Figure 1.6.4-4 is a plot of Equation (5) showing the rms error in range rate vs. smoothing time for various values of S/N in db. A value of $f_T = 2113$ mc has been used. As indicated by this figure, even at the threshold value of $S/N = 6$ db, which is a worst case, only a two-second smoothing time is required to limit the range rate error to ± 0.01 ft./sec. At the more realistic values of S/N equal to 10 to 20 db, a smoothing time of one second or less will suffice.

(3) Cycle-Counting Quantization Error

With the frequency measurement unit described in Paragraph 1.6.4-B, the measured frequency is expressed by Equation (2):

$$f_D + f_B = n f_P / K \quad (2)$$

Due to the quantization interval of the reference pulses which are being counted, there will be an error in the pulse count, k . Assuming that the time at which the counting interval starts and the time at which the counting interval ends both have a uniform probability distribution over the pulse interval, there is an rms error of $1/\sqrt{12}$ associated with each. Since these are uncorrelated, the total quantization error is the root-sum-square of the two errors, i. e., Δk (rms) = $1/\sqrt{6}$.

The resulting rms error in range rate may be obtained from

$$\begin{aligned} \Delta \dot{r}_3 &= \left(\frac{\partial \dot{r}}{\partial f_D} \right) \left(\frac{\partial f_D}{\partial k} \right) \Delta k \\ &= \frac{c (f_D + f_B)^2}{2 f_T n f_P} \frac{1}{\sqrt{6}} \end{aligned} \quad (6)$$

Note that the ratio of the number of cycles counted, n , to the frequency being measured, $f_D + f_B$, is just the smoothing time (cycle-counting time), T , i. e.,

$$T = \frac{n}{f_D + f_B} \quad (7)$$

Equation (6) may therefore be rewritten:

$$\Delta \dot{r}_3 = \frac{c (f_D + f_B)}{2 \sqrt{6} f_T f_P T} \quad (8)$$

Using 2113 mc for the transmitted frequency (f_T) and assuming a value of 10 mc for the pulse frequency (f_P), Figure 1.6.4-5 has been plotted from Equation (8). The figure shows the range rate error vs. smoothing time for various values of $f_D + f_B$, the sum of the doppler frequency and the bias. The figure indicates that rms errors in range rate of ± 0.01 ft./sec are easily achievable with relatively short smoothing times.

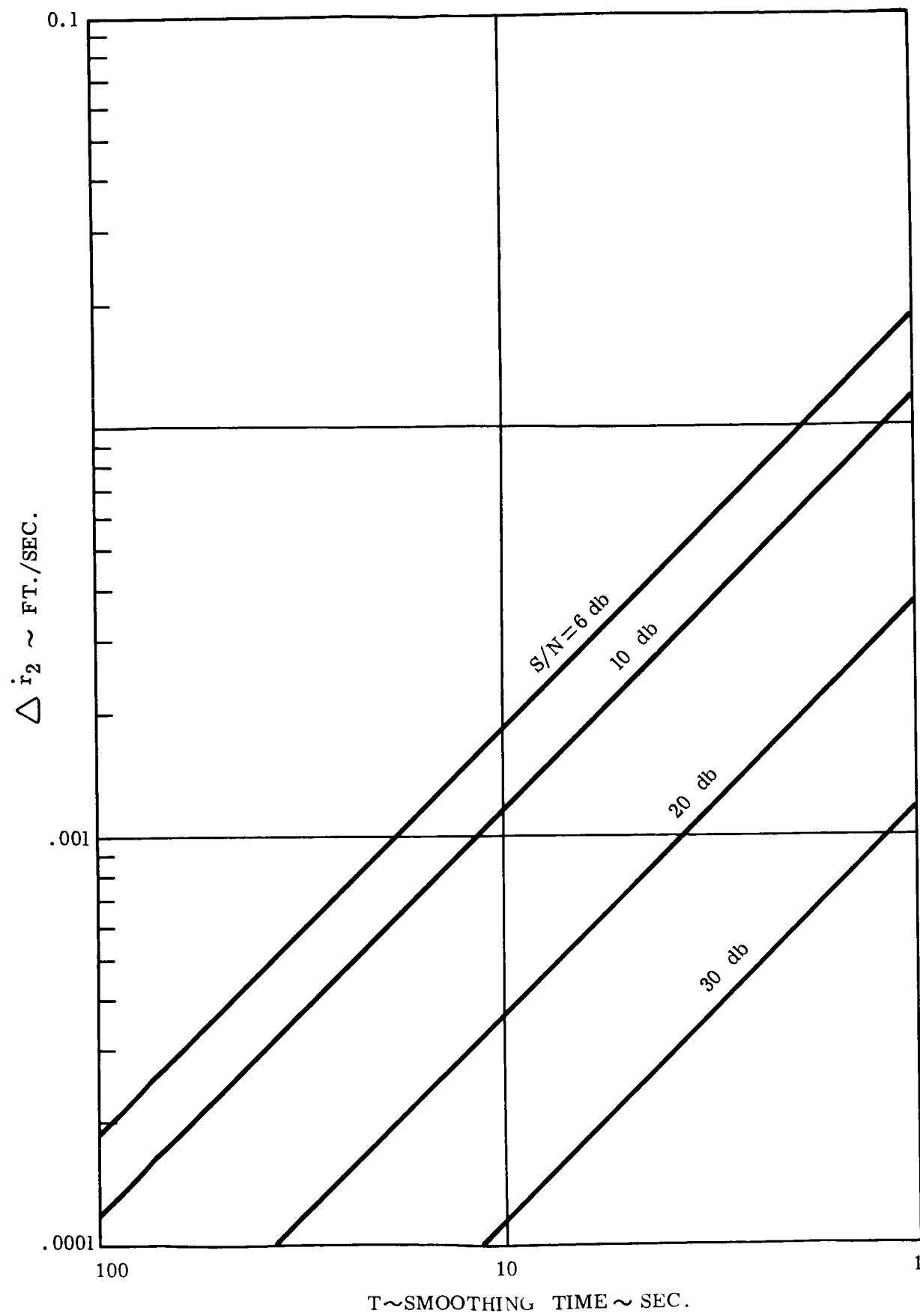


Figure 1.6.4-4. RMS Range Rate Error ($\Delta \dot{r}_2$) Due to Receiver Thermal Noise

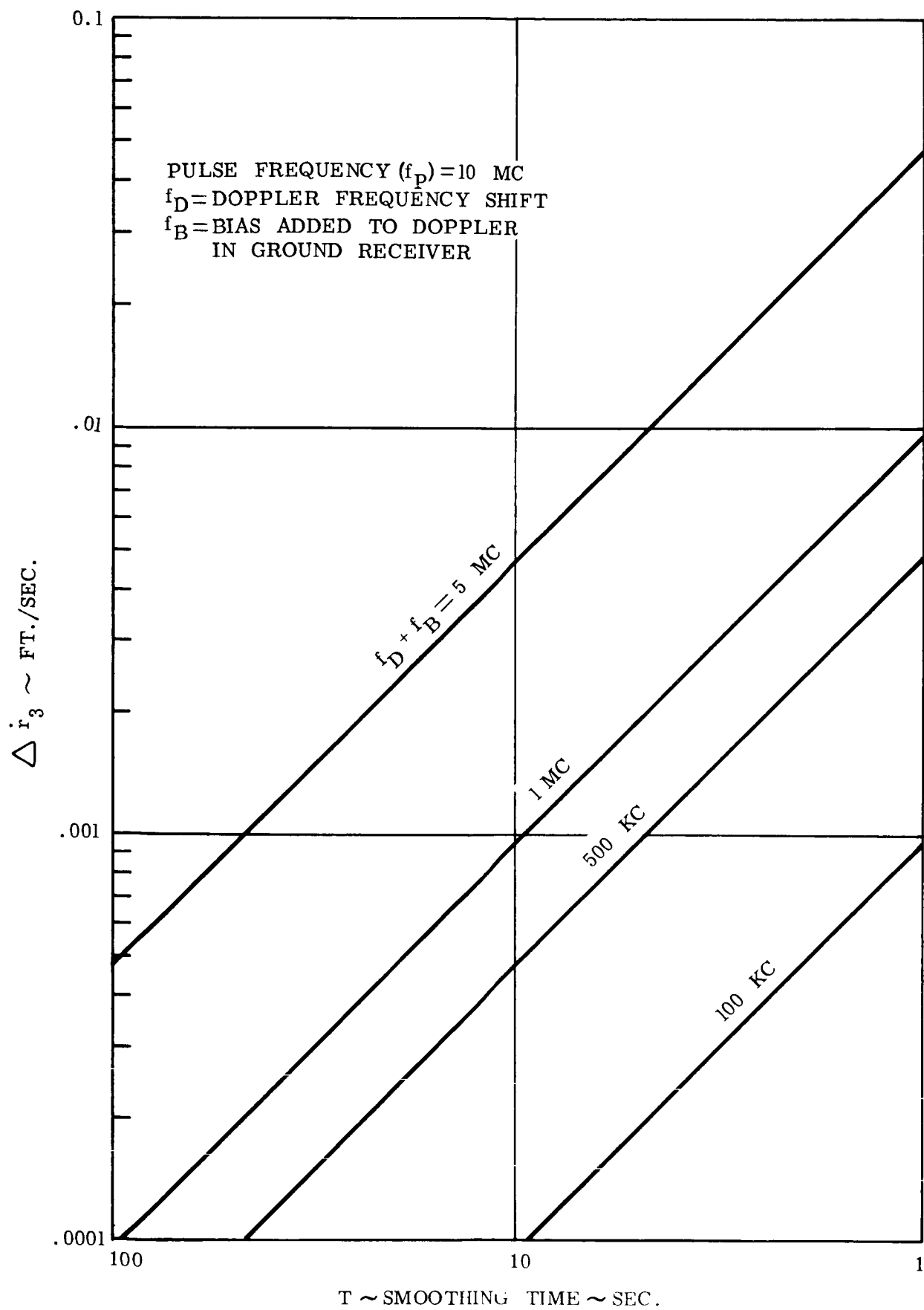


Figure 1.6.4-5. RMS Range Rate Error ($\Delta \dot{r}_3$) Due to Quantization Interval in Cycle Counting

D. Conclusions

From the foregoing results it is obvious that the limiting factor in the accuracy of the range rate measurement is the stability of the master oscillator in the DSIF transmitter. Based on the quoted stability², the oscillator has a coherence time of approximately 0.1 seconds at the transmitted frequency of 2113 mc. With this coherence time, a cycle counting interval of 270 seconds is required to limit the instrumentation error in range rate measurement to ± 0.01 ft/sec rms. If the oscillator coherence time can be improved, the required smoothing time will decrease linearly with the increase in coherence time.

1.6.5 Command Signal Structure

The recommended command signal structure and utilization is similar to that described by Springett* and is outlined below:

1. Bit Structure (two symbols per bit)
 - a. data and parity bits: 01 transmitted for "1"
10 transmitted for "0"
 - b. word-start bits: 111000
 - c. zeros (10) transmitted between words
2. Word Structure
 - a. total number of bits per word: 65
 - b. number of command data bits: 61
 - c. number of word-start bits: 3
 - d. number of parity bits: 1
3. Verification Procedure
 - a. word-start sequence must occur to activate decoder
 - b. the symbols 01 and 10 are decoded in part to reconstruct "1" and "0"
 - c. occurrence of symbols 00 or 11 after word-start causes entire word to be rejected
 - d. failure of final parity check causes word to be rejected
 - e. parity bit is retained in stored command words and rechecked before word is accepted from storage.

Figure 1.6.5-1 shows a typical signal structure. In order that a command be accepted even though it is corrupted by noise and therefore incorrect, an even number of data and parity bits must be incorrect (an odd number of errors will be detected by the parity bit). In addition, each of the bits must be corrupted so that a 10 becomes a 01 or vice versa. The probability of such an occurrence is then approximately

$$P_{ai} \approx (122 P_e^S P_e^S) (120 P_e^S P_e^S) \quad (1)$$

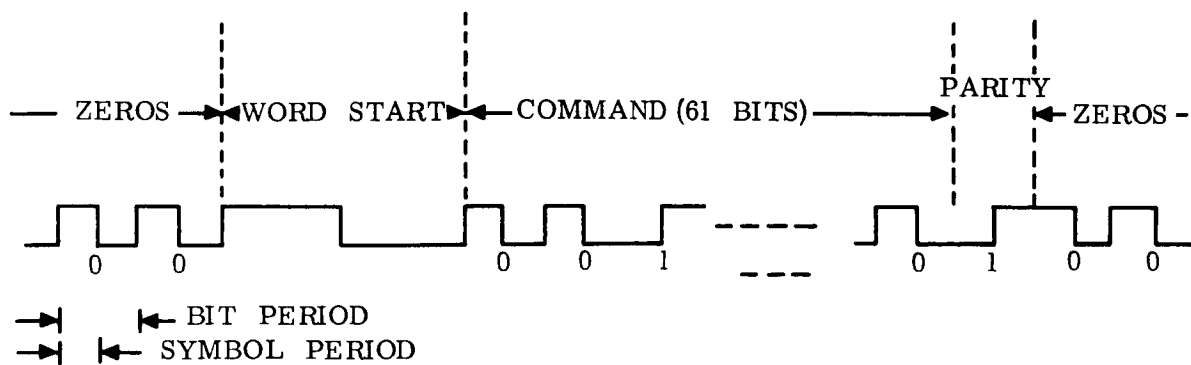


Figure 1.6.5-1. Command Signal Structure

where P_{ai} is the probability of accepting an incorrect command

P_e^S is the probability of symbol error

Then, at the maximum design value of 10^{-5} for P_e^S , this becomes

$$\begin{aligned} P_{ai} &\approx 1.5 \times 10^4 (10^{-5})^4 \\ &= 1.5 \times 10^{-16} \end{aligned} \quad (2)$$

The probability of a command being rejected is

$$P_{ri} \approx 130 P_e^S = 1.3 \times 10^{-3} \quad (3)$$

That is, at the design value of $P_e^S = 10^{-5}$, approximately one command per thousand transmitted will be rejected.

* Springett, J.C.; "Command Techniques for the Remote Control of Interplanetary Spacecraft" JPL Technical Memorandum No. 33-88, May 21, 1962

1.7 COMPONENT SELECTION

1.7.1 S-BAND POWER AMPLIFIER

The electrostatically focused klystron (ESFK) is recommended as the power amplifier tube for communication from the spacecraft to the Earth. No fully qualified device that exactly meets the requirements was identified during the study, but a number of candidate devices were compared, and several were found to be potentially useful. Both the ESFK and the traveling wave tube (TWT) can be developed to meet the mission requirements within the time scale and would provide approximately equal efficiency. The ESFK is favored because it does not have an external magnetic field and because it can be operated over a power range as great as 10 db by changing the high voltage. Over this range, the change in efficiency is only 5 to 10% with higher efficiency at higher power. The tube can thus be designed for mission flexibility, as the amplifier used for the first mission can be used for later missions requiring higher power. The ESFK has a simpler and less critical structural design than the TWT, and thus may have a higher reliability.

Voyager requirements can be met by adapting existing designs of the ESFK. It is interesting to note that useful life test information on linear beam devices such as the ESFK and the TWT can be derived before the final design is completed by life testing the cathode designs that will be used. This cannot be done with crossed-field devices because cathode life is limited by back bombardment of the cathode and thus cathode life test data derived external to the tube is not valid.

The four basic tube types considered for the Voyager application were examined mainly with respect to life, power output and efficiency. These three requirements eliminate crossed-field devices and planar triodes. The remaining devices (Klystron and TWT) then were re-examined and the klystron selected. In the course of the study meetings with several vendors in the power tube field were conducted and data assembled on the various types. Power tube engineers from the GE Research Laboratory (Schenectady, N. Y.) assisted in this study and evaluation of the various amplifier designs. By comparing the vendor's data with the requirements given below the selection of the electrostatically focused klystron was made.

A. Summary of Requirements

The requirements for the S-band amplifier may be summarized as follows:

Frequency	2295 mc
RF Output Power	50 watts
Efficiency	≈ 35%
Driver Power	100 milliwatts or less (27 db gain)
Bandwidth	100 kc
Supply Voltage	Not Restricted
External Magnetic Field	2 gamma at 3 ft
Operating Life	≈ 12,000 hours

Cooling	Conduction
Modulation	Phase-Shift Keying
Shock	150g for 5 milliseconds
Vibration	6g from 20 to 2000 cps
Acceleration	5.6g axial 0.9g transverse
Temperature	-18°C to + 100°C operating + 145°C sterilization

B. Comparison of Candidate Devices

Several candidate devices were compared with respect to important parameters that determine their usefulness for Voyager. In addition, consideration was given to unique characteristics of particular devices that have either favorable or unfavorable influence on their choice.

(1) Amplitron

The amplitron is a crossed-field amplifier manufactured by Raytheon Corp., Waltham, Mass. Its most valuable characteristic for space applications is its unusually high efficiency. In addition, it has a unique redundancy feature. Amplitron tubes may be connected in series to add their powers, or if one of the tubes in the series is not activated or has failed electrically, it has an insertion loss of only 0.5 to 0.6 db, so that the other tube or tubes in the series connection can operate normally without disconnecting the unused tube.

The amplitron requires a relatively complex circuit to control its operating current and prevent oscillation. Crossed-field devices, a family that includes the amplitron and magnetrons, tend to have short life due to back bombardment of the cathode. Raytheon engineers have suggested techniques that should make adequate life possible, but the techniques have not yet been fully tested. Advantages and disadvantages tabulated below are based on performance predicted for tubes designed for Voyager.

Advantages

Small (3-inch diameter x 3 1/2 in.)

Light Weight (2 lbs for 50 watts)

High Efficiency (50%)

Unique Redundancy Feature

Disadvantages

External magnetic field (requires double shield to meet requirement)

Reliability and life not established (comes from short-life family)

May be unstable

Moderate power gain (less than 20 db: 27 db required)

Requires isolation

Requires further development and qualification tests.

(2) Electrostatically Focused Klystron (ESFK)

The electrostatically focused klystron is a linear beam device manufactured by Litton Industries, San Carlos, California. Linear beam devices have been shown to have long life. The simple structural design of the ESFK should make it one of the most reliable devices in this family. Electrostatic focusing eliminates the need for heavy magnets and the external magnetic field. The tube is designed to connect the cathode to the beam focusing electrodes, so that the tube requires only two voltages for its operation, the filament and beam voltage. As an additional feature, power output can be reduced as much as 10 db with only a small reduction in efficiency.

Only experimental samples of the device have been built. None of these exactly meets the requirements of Voyager. A 40-watt, S-band tube was built with 25% efficiency. It has a 6-mc bandwidth. Litton engineers stated that efficiency can be increased if bandwidth can be reduced.

Advantages tabulated below are based on performance predicted for a tube designed for Voyager.

Advantages

Small (3-inch diameter x 4 in.)	
Light Weight	1.5 lbs for 50 watts
High Gain	30 db
High Efficiency	40%
High Reliability	12,000 hours life
No External Magnetic Field	
Low Phase Jitter	3°/volt

Disadvantages

Requires further development and qualification tests

(3) Traveling Wave Tube (TWT)

The TWT is a linear electron beam device. Amplification is accomplished by the interaction of the electron beam and a slow-wave RF signal on the helical structure. The electron beam must be carefully focused so that it does not intercept the helical structure. This focusing is accomplished by placing permanent magnets along the length of the tube, thus creating an external magnetic field. The electrical length of the tube is considerable (approximately 30 wavelengths) and as a result the mechanical and electrical tolerances required are an order of magnitude more severe than the klystron. The beam voltage must be regulated precisely and lower output powers are not possible except by changing the drive level. The TWT is a glass-metal configuration with the attendant difficulty and reduced ruggedness.

TWT's in the 20-watt power range have been built, and it is believed that TWT's are applicable to the 100-watt range. However, the efficiency will be approximately 33% and two high-voltage power supplies are required which will lower the overall DC-to-RF efficiency factor.

The advantages and disadvantages of a TWT for Voyager use are listed below:

Advantages

Small	2 in. dia. x 20 in.
Light Weight	2.5 lbs
High Gain	40 db
High Reliability	MTBF = 40,000 hours
Moderate Efficiency	33%

Disadvantages

High External Magnetic Field

Two High Voltages Required { Collector Voltage 1500 volts
Beam Voltage 3000 volts

Complexity - Alignment of Magnetic Focusing with Slow-Wave Helical Structure

Phase Jitter - 4 times greater than klystron.

(4) Planar Triode

The planar triode power amplifier is essentially a class-C vacuum-tube amplifier. Such a tube is manufactured by the GE Power Tube Department. Amplification is accomplished by applying the RF drive signal to the grid of the unit. The output is then available from a plate-to-cathode coaxial cavity. Some bias circuits are also required.

The triode has a low life expectancy because of cathode back-bombardment, and planar triodes operating at the desired power levels in S-band have not yet been built.

A summary of advantages and disadvantages is given below:

Advantages

Small	3 in. x 2 in. diameter
Light Weight	4 lbs (including cavity)
No External Magnetic Field	

Disadvantages

Low Reliability	
Low Gain	13 db
Poor Efficiency	25% or less

1.7.2 ANTENNAS

A. Orbiter Antennas

The Orbiter has four antenna configurations which serve the Communications Subsystem. DSIF communications with earth are maintained by a high-gain S-band antenna during stabilized flight phases. An "isotropic antenna" pair is used during early mission stages before deployment of the high-gain antenna, during maneuvers, and as a back-up in the event of loss of pointing of the high-gain antenna. A medium-gain VHF yagi antenna and a low-gain VHF turnstile are used for communication with the Lander.

(1) High-Gain Antenna

The high-gain antenna recommended is a ten-foot diameter horn-fed parabolic dish. This choice of antenna satisfies system requirements in an optimum fashion. In addition, the advanced state of parabolic antenna design techniques permits minimizing development time and cost. The performance of the design will be optimized at 2295 mc where the system margin is smallest. The gain at 2115 mc will be within 1 db of the peak value.

(a) Parabolic Antenna Design

The paraboloid is of honeycomb construction; the tradeoff study of various alternative materials is given in the structure section, Volume IV, Section 2.5. An f/D ratio of 0.35 has been selected because this represents a fairly good compromise among the various desires for dish flatness, short feed supports, low primary pattern path taper, minimum aperture blockage by the feed, and ease of feed design. A circularly polarized horn, tripod-mounted from the parabola, has been selected for the feed. However, other feed designs — a turnstile over a ground plane, a short helix with a conical ground plane, or a printed spiral — offer possible weight saving advantages and the possibility of vertex mounting. The final feed design should not be made until experimental investigation of the feed radiation pattern has been completed.

(b) Performance

1) Gain

The gain of a parabolic antenna is given by the expression

$$G = E \frac{4 \pi A}{\lambda^2} \quad (1)$$

where A is the area of the aperture, λ is the wavelength, and E is the aperture efficiency, an empirically derived factor which is a function of the illumination of the dish by the feed, the blocking effect of the feed, and mechanical construction tolerances. A conservative value of E is 0.6; this can usually be achieved without undue effort for a pencil beam when sidelobe level requirements are not stringent. The predicted gain for the ten-foot diameter dish is then 3180, i. e., 35 db.

2) Beamwidth

The 3-db beamwidth is approximately related to the gain of a high-gain pencil beam antenna by

$$\theta_{3db} = \frac{A}{G} \quad (2)$$

where A is a factor which is a function of aperture distribution, blockage, surface losses and tolerances (and, therefore sidelobes). Taking $A = 3 \times 10^4$, the 3-db total beamwidth is then 3.1° . Alternatively, the beamwidth of a dish is related to the dish size, in wavelengths, by the formula

$$\theta_{3db} = f \frac{\lambda}{D} \quad (3)$$

where the factor f is again a function primarily of aperture distribution but is also somewhat influenced by tolerances and blocking. For a 10 to 12 db total illumination taper, with an approximately Gaussian distribution, $f = 68$. This gives a half-power beamwidth of 2.93° . This figure should probably be considered more accurate.

On the same basis, the 20-db beamwidth is

$$\theta_{20db} = 147 \frac{\lambda}{D} = 6.32^\circ \quad (4)$$

at 2295 mc.

3) Sidelobes

The sidelobe level in db below peak gain is primarily a function of the aperture distribution, i. e., the taper of the dish illumination. Since in this application gain is more important than low sidelobe level, the design goal will be maximum gain. It is expected that the sidelobe level will be approximately 20 db down. Suppression greater than 25 db would be expected as the result of aperture distribution alone. The 5 db degradation has been added to account for the effects of feed and feed support blockage.

4) Circularity

No difficulty should be experienced in obtaining an ellipticity less than 0.5 db with any of the feed designs considered. This will deteriorate to perhaps one db at the half-power points.

5) Thermal Distortion

Calculation of thermal distortion effects on the parabolic dish (as given in Section 2.5.4G of Volume IV) shows a worst-case dish edge movement of the order of 0.114 in. or 0.022λ for Mars. This will cause insignificant pointing errors and gain changes at S-band.

(c) Alternative Designs

Several alternative designs have been considered for use as the high-gain antenna. These are described below, and the relative advantages and disadvantages are discussed.

1) Array of End-Fire Elements

An array of circularly polarized end-fire antennas such as helices or crossed-yagis can be used to achieve the desired 35 db gain. An approximate calculation indicates that 49 helices each 3λ or 1.3 feet long, at optimum spacing of 2.2λ or 0.95 feet would theoretically provide 35 db gain. The square configuration of Figure 1.7.2-1 is shown for illustrative purposes; the optimum array would probably occupy a rounded area of a smaller maximum dimension. It should be noted that higher gain longer elements would require even less area. The helices would be imbedded in lightweight foam for support. If a more compact array were desirable for stowage, the helices could be compressed into a flatter structure; restraining dielectric intra-turn cords would damp out vibration and hold the desired configuration after erection in orbit.

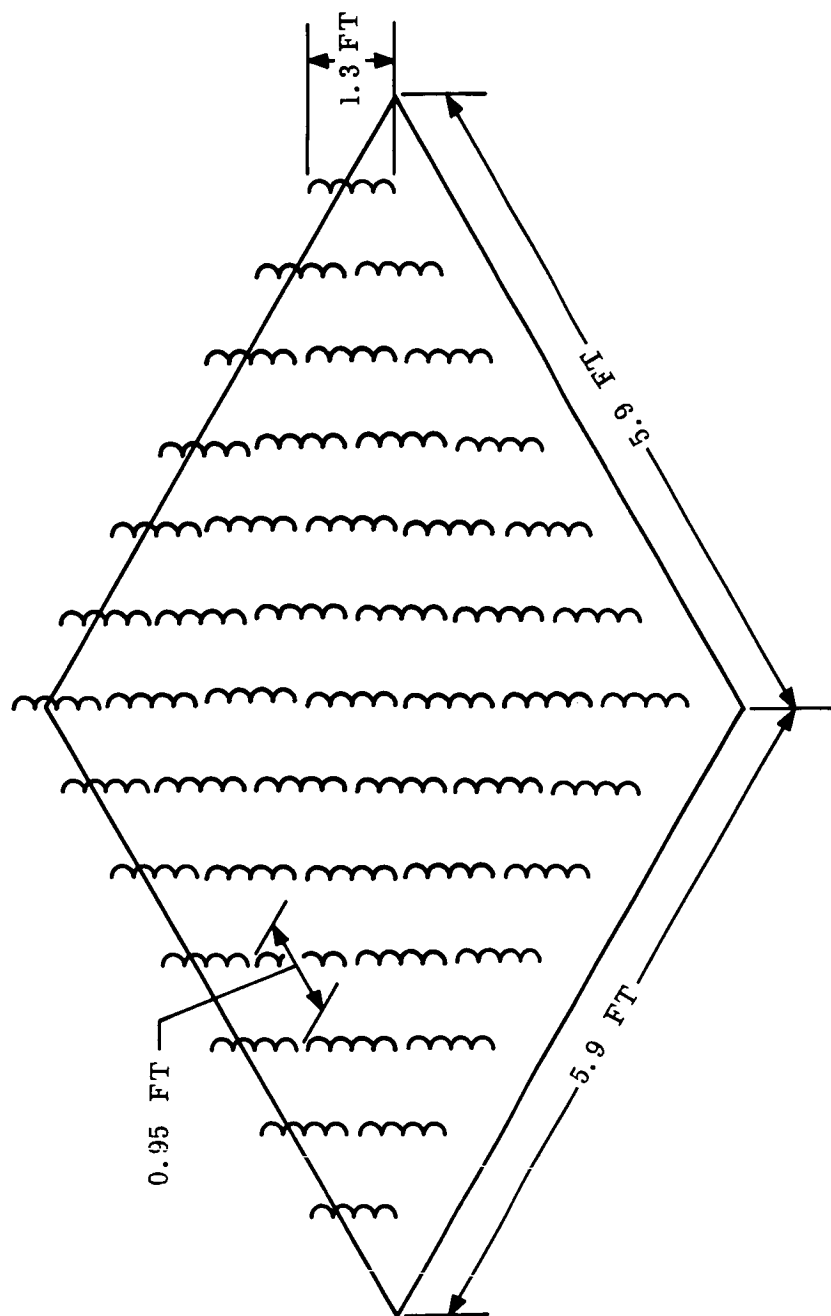


Figure 1.7.2-1. Alternative Design for High-Gain Antenna (Array of 49 Helices)

The feed harness arrangement would utilize strip-line techniques and be printed on the back of a printed circuit board, thus avoiding the weight of coaxial cables and connectors. The front foil surface of the board would serve as the ground-plane and mounting structure for the end-fire elements and as the ground-plane for the strip-line feed.

The implementation of this design would require considerable development effort. A detailed study would be needed to determine the optimum end-fire element length versus number of elements. The strip-line feed design will determine the bandwidth achievable and the optimum design must be determined experimentally because of its dependence on mutual impedance effects.

2) Planar Printed Circuit Array

Linearly polarized planar arrays of collinear radiating elements backed by a reflector have been built using printed circuit techniques and aperture efficiencies approaching 100% achieved⁽¹⁾. Thus for 35-db gain and linear polarization, an array physically approximately 8 feet in diameter by 1.3 inch thick would be equivalent to a 10-foot diameter parabola. The construction would employ two printed circuit boards supported and separated by a layer of foam. Radiating elements and feed lines would be etched on the upper board; the back of the bottom board could be used for the necessary strip-line baluns.

Such a tentative design is not immediately applicable to Voyager, since circular polarization is highly desirable. Although planar printed circularly-polarized radiating elements exist — spiral antennas, for example — they cannot be fed collinearly, and each element requires its own feed line. Since approximately 1000 elements are necessary, this complicates the design and makes the achievement of the bandwidth required for DSIF use (8%) unlikely. If a linearly polarized unit is used, an 11-foot diameter would be required to achieve the required 38 db linearly polarized gain.

3) Unfurlable Antenna

Unfurlable or space-erectable antennas have been considered. However, a rigid parabola is consistent with the system packaging requirements. It is evident that any erectable space antenna will be less reliable than one which is rigid, and an erectable antenna will probably weigh as much as a rigid antenna when both are designed to meet the same environments, if the weight of erecting mechanisms, boost-phase, tie-down straps, etc., are considered as part of the weight of the erectable antenna. Thus the only significant advantage that the erectable antenna has is its packaging. If our present concept of the Voyager spacecraft did not have room to package a 10-foot diameter dish conveniently, then serious consideration would have to be given to a space-erectable antenna. However, since the 10-foot dish fits conveniently into the overall vehicle configuration, a rigid design has been recommended.

On later versions of the Voyager spacecraft, there will be no penalties incurred by using an unfurlable antenna with up to a 30-foot diameter packaged in the same general volume as the present 10-foot rigid dish.

4) Parabolic Cylinder and Other Antennas

For certain vehicle configurations it is apparent that antennas other than those described may be optimum. For example, with a cylindrical vehicle, where the ends are not available for antenna purposes, it would be a good packaging scheme to have a parabolic

(1) McDonough, J. A., Malech, R. G., and Kowalski, J., "Final Report on Study of Printed Antenna," AD-76753, Airborne Instruments Laboratory, August 1955.

cylinder fold in against or inside the vehicle. Such an antenna would be fed by a line source — perhaps a waveguide with crossed slots. However, it is not necessary to resort to any such design with the present vehicle concept.

Needless-to-say, there are probably as many possible variations and modifications to the various basic designs presented as there are antenna designers. Cassegrain feed systems for dishes, arrays of slotted lightweight waveguide, and cigar end-fire elements are some of the ideas that come to mind. It is not claimed that these ideas or others are inferior to the antennas we have considered. However, it is felt that the ones investigated are representative. Moreover, it is felt that the rigid 10- foot dish as described represents an optimum in regard to the following areas of concern:

- Reliability
- Simplicity
- Compatibility with other systems
- Advanced design knowledge

The rigid dish can be considered adequate even if not definitely superior to all other designs in the following areas:

- Gain/weight ratio
- Gain-beamwidth product
- Circularity
- Resistance to environmental deterioration

(2) "Isotropic" DSIF Antenna

The design goal for the radiation pattern of this antenna is, as the name implies, uniform radiation in all directions. An isotropic circularly polarized source is, of course, even theoretically impossible, and the situation is further complicated by shadowing due to the vehicle on which it is mounted. Since the system design philosophy dictates the utmost reliability for this antenna, the design choice which has been made does not utilize any active elements such as switches, phase-shifters, or deploying booms.

(a) Selected Design

A pair of small turnstile antennas is recommended, mounted as shown in Figure 1.7.2-2 so that only one antenna can be "seen" over most of the solid angle. The two units are fed by a power divider. Construction of each unit is shown in Figure 1.7.2-3: its radiation pattern can be made to be either of the two patterns shown in Figure 1.7.2-4, or a compromise, by adjustment of turnstile height over the ground plane. The total radiation pattern of the antenna system will be of the form of Figure 1.7.2-5 which also indicates the polarization of the radiation. Experimental pattern measurements using an accurate vehicle mockup will be necessary for the final design because of reflection and diffraction effects which are not amenable to analysis.

(b) Alternate Methods

1) Dual Receiver-Transmitter

By using two receivers and transmitters, one of each being connected to one of the turnstile antennas described above, the partial interference nulls which exist in the meridial

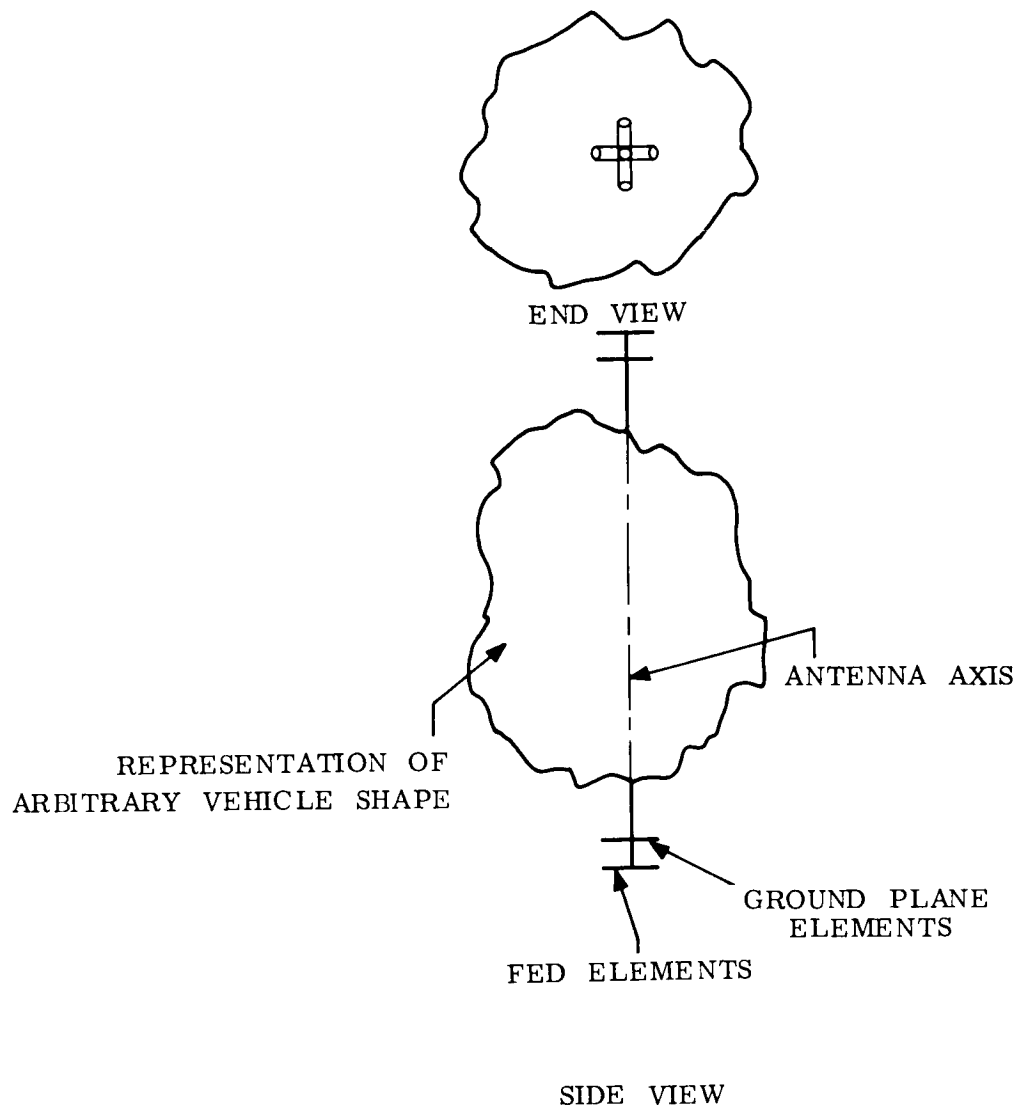


Figure 1.7.2-2. S-Band Orbiter Low-Gain Antenna Array

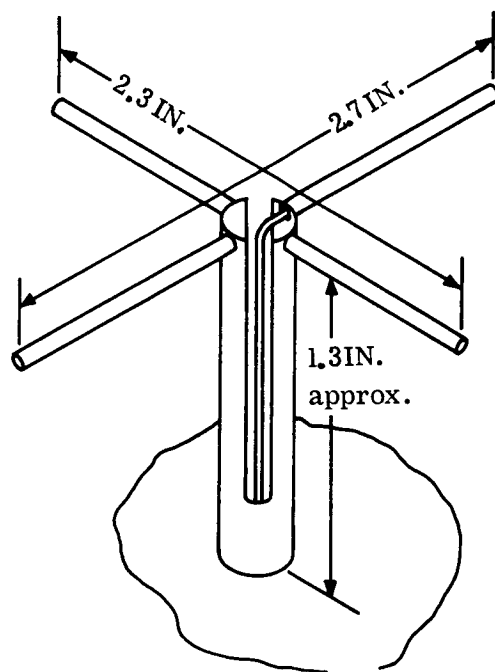


Figure 1.7.2-3. Turnstile Antenna (S-Band Split Balun Feed)

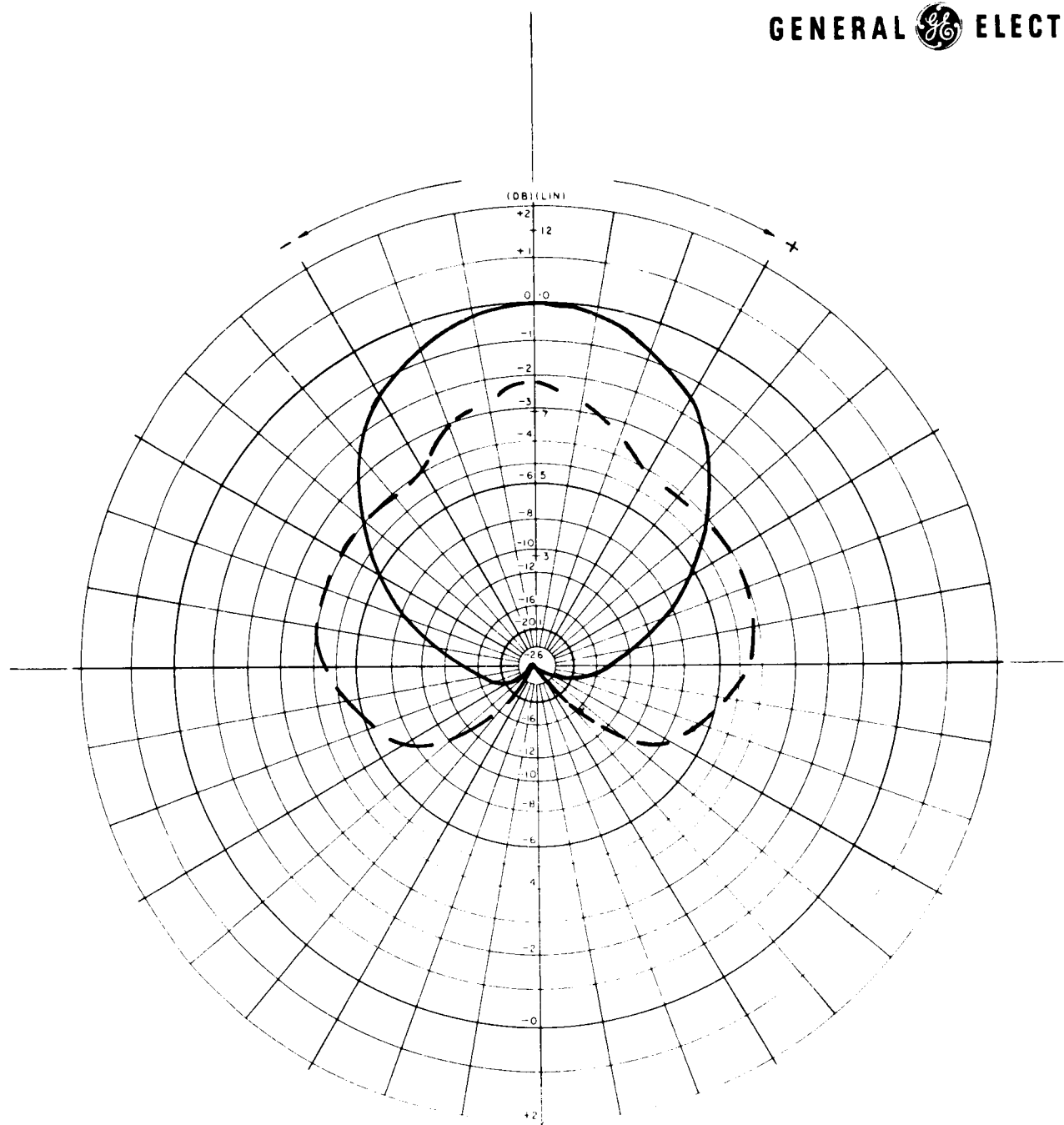
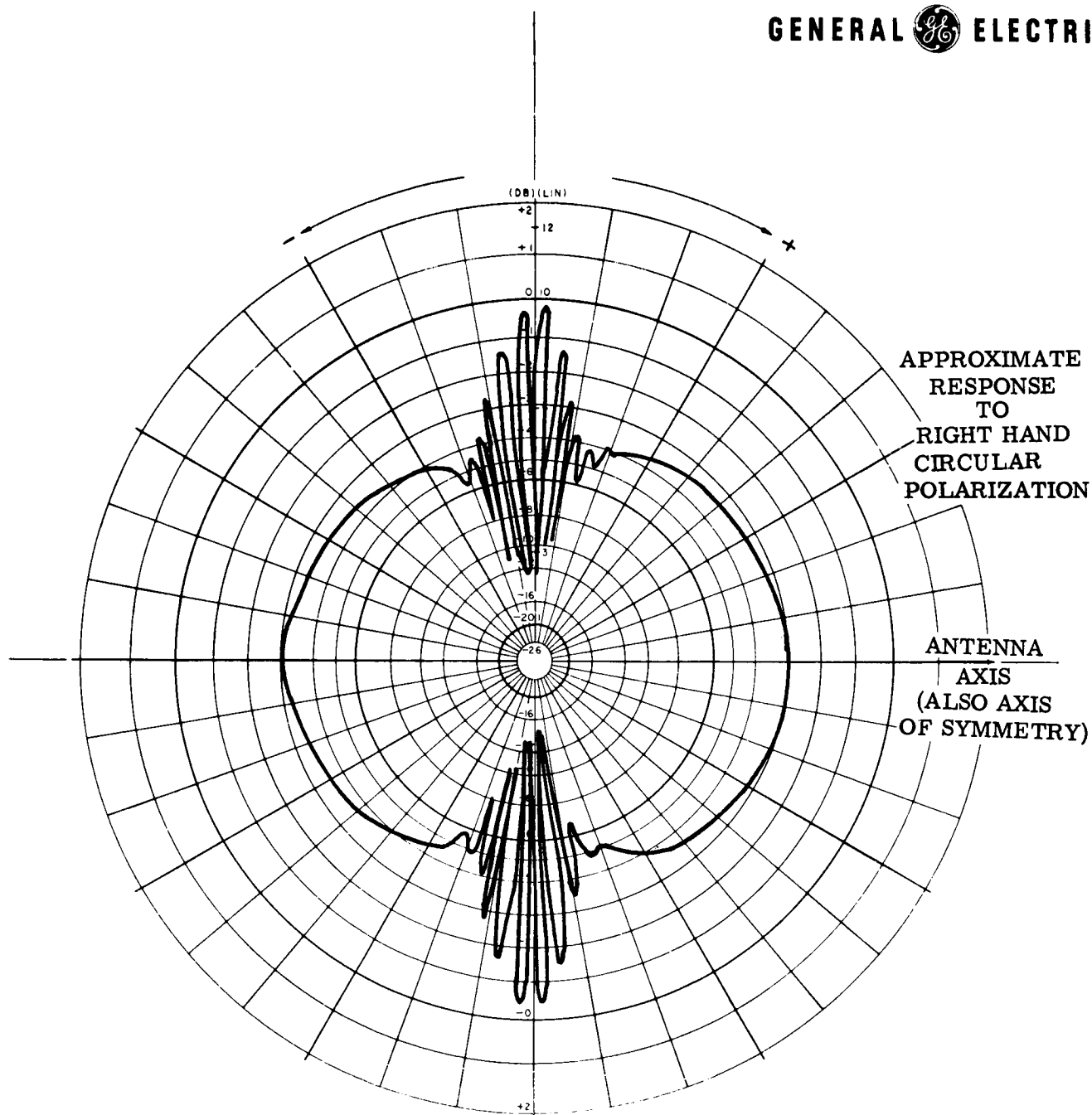


Figure 1.7.2-4. Turnstile Antenna Over a Ground Plane
(Two Different Turnstile Heights)



1-197

plane of the system described above can be eliminated. The receiver outputs can be combined after first detection, i. e., after RF signal phase has been eliminated, and both receivers can be at the same frequency. To eliminate the interference nulls on the transmit patterns, separate transmission frequencies are required. This system suffers the obvious disadvantages of requiring additional equipment.

2) Adaptive Phase Systems; Switched Systems

Varying degrees of additional sophistication can be employed to increase effective gain. Feedback systems, which detect and adjust the relative phase of the signals received from the two antennas so that they add, or switching systems, which switch to the antenna receiving the stronger signal, will eliminate the partial nulls of the chosen design and increase the overall gain by 3 db. The necessary added complexity and consequent unreliability of such systems is undesirable and has eliminated such systems from further consideration.

(3) Relay Link Crossed-Yagi

A 100-mc antenna is required for communications with the Lander. This unit must operate over an 11% bandwidth. The highly elliptical orbit places contradictory requirements on this antenna: at periapsis a wide-beamwidth low-gain antenna is desirable; at apoapsis high gain is needed, and the consequent narrow beamwidth will still subtend the entire planet.

Considerations of communications link margin and antenna size versus gain have yielded a gain of ten db as a compromise. The 3-db beamwidth is then approximately 55° . A turnstile-fed crossed-Yagi design has been selected because of the simple structure required, the low weight as compared to alternate designs, and the adaptability to folding necessary for stowage. The antenna is approximately 13 feet long as shown in Figure 1.7.2-6. Although Yagi antennas are usually designed for narrow-band applications, broad-band designs exist which substantiate the desired performance.

Alternate designs which could be used are a helix or a disc-on-rod antenna. The helix requires additional support structure to maintain proper shape and is not susceptible to folding, and the disc-on-rod design is inherently heavier than a crossed Yagi.

(4) Relay Link Turnstile

Prior to deployment of the PHP, it will be necessary to have an antenna on the main body of the Orbiter to maintain communications with the descending Landers. This antenna will be a turnstile with elements 4.2 feet in length, erected about 2.5 feet above the sides of the vehicle. The pattern of this antenna, roughly between the two patterns shown in Figure 1.7.2-4, will provide sufficient coverage to maintain the VHF link during the descent phase.

B. Lander Antennas

The Lander requires several antennas: a low-gain antenna for direct communication with Earth at DSIF frequencies; high-gain pointed DSIF antennas with two different designs for two missions; a low-gain 100-mc antenna for communication with the Orbiter, and a 100-mc, low-gain antenna for use during descent.

(1) High-Gain DSIF Antennas

(a) Mars 1969 Lander

The Mars 1969 mission requires a right-hand circularly polarized antenna with 21 db gain. The 3-db beamwidth is then approximately 14.5° . A helix, 28-inches long by

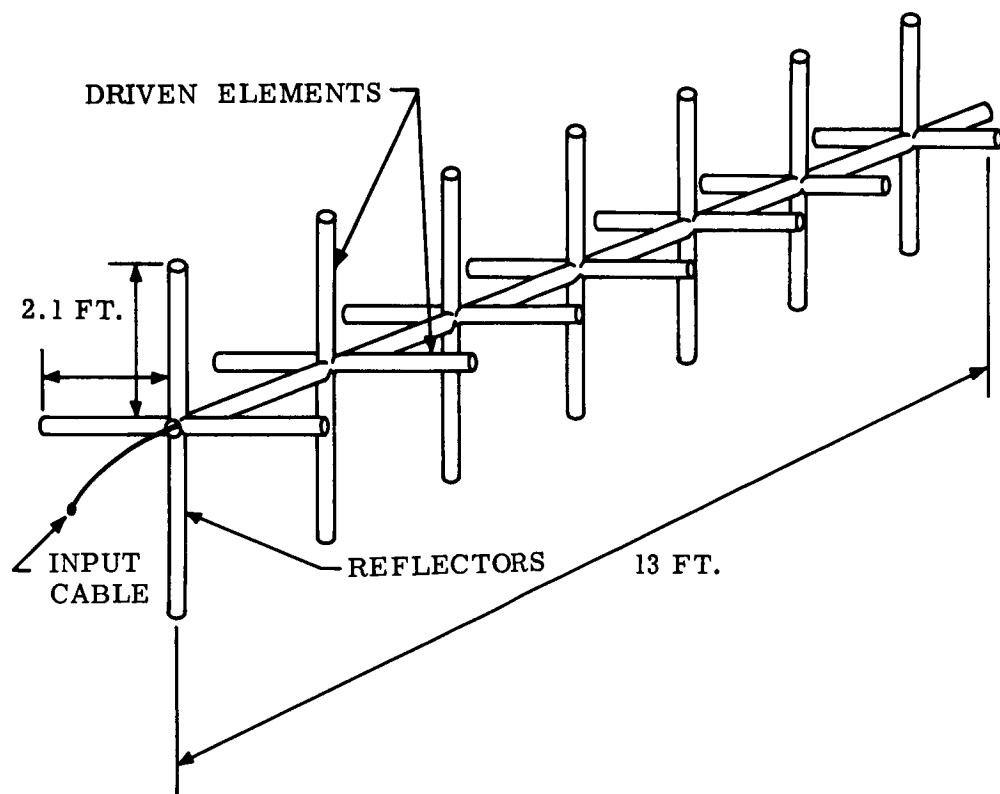


Figure 1.7.2-6. Orbiter VHF Crossed Yagi

3.3 inches diameter, has been selected as the optimum overall design which can be stowed in the Lander configuration. The helix can be supported from a central rod, and simplify stowage problems; it is feasible to make the unit either slightly flexible or compressible.

Alternate designs include a crossed-yagi or other end-fire arrays which offer no advantages over a helix for required gain or an erectable two-foot diameter parabola. Erectable parabolas are not quite state-of-the-art, and the required complicated erection mechanism is susceptible to damage during the rough landing environments.

(b) Mars 1971, 1973, and 1975 Landers

The high-gain antenna for the 1971, 1973, and 1975 Mars Landers will consist of an array of 12 helices each nine inches long potted in lightweight foam material (see Figures 1.7.2-7 and 1.7.2-8). Each helix will be 1.25λ (wavelengths) in circumference at midband frequency (2.2 kmc), and its directive gain will be:

$$(1) G_D = 15 (1.25)^2 \times \frac{9}{\lambda} = \frac{211}{5.37} = 39.3 \quad (5)$$

The directive gain of the optimally space array will be

$$G_T = 39.3 \times 12 = 461 \text{ or } 26.75 \text{ db.} \quad (6)$$

The spacing is given by⁽³⁾

$$S_P = \frac{\lambda}{\sin \phi/2} \quad (7)$$

where ϕ is the element null beamwidth.

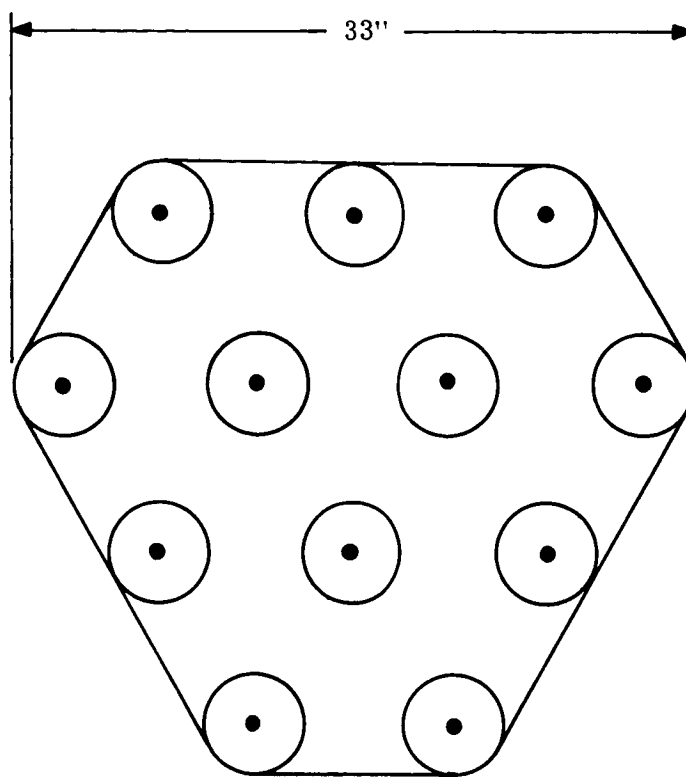
$$(2) \phi = \frac{115}{1.25 \sqrt{9/5.37}} = 71^\circ \quad (8)$$

$$(3) S_P = \frac{\lambda}{\sin 35.5^\circ} = 1.725 \lambda = 9.25 \text{ in.} \quad (9)$$

The design of an individual element is shown in Figure 1.7.2-8. The base upon which the helices are mounted will be of 1/8-inch Teflon fiberglass covered with a copper foil on the helix side with strips of copper on the other side, thus forming a microstrip feed and power division network (see Figure 1.7.2-9). Each helix will have a characteristic impedance of 150 ohms and will feed through the Teflon fiberglass dielectric material to 150-ohm microstrip. Equal lengths of 150-ohm microstrip lead from each of three helices will meet at a junction with a 50-ohm microstrip lead. The four 50-ohm microstrip leads thus formed will feed into two microstrip 3-db hybrid junctions, again with equal length lines. The third arms of the two hybrids will again feed into a third hybrid through equal-length lines and the fourth arm of all three hybrids will be terminated in 50 ohms. The third arm of the third hybrid will be the terminals of the array. To compensate for

(1), (2) Kraus, J. D., Antennas, McGraw-Hill Book Co., New York, 1950.

(3) Yen, K., "Coupled Surface Waves and Broadside Arrays of End-Fire Antennas," Trans. PGAP-IRE, May 1961.



ARRANGEMENT OF HELICES IN ARRAY
(MARS 1971, 1973, and 1975 LANDERS)

Figure 1.7.2-7. Arrangement of Helices in Array
(Mars 1971, 1973, and 1975 Landers)

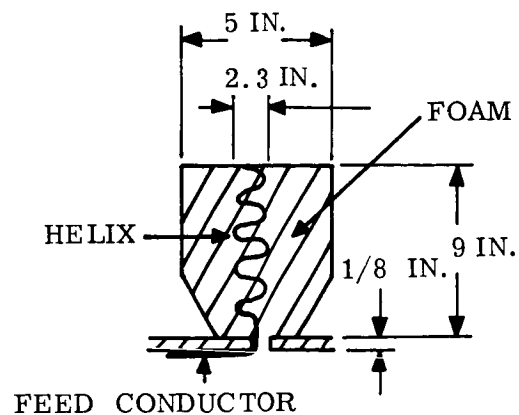


Figure 1.7.2-8. Individual Helix Element

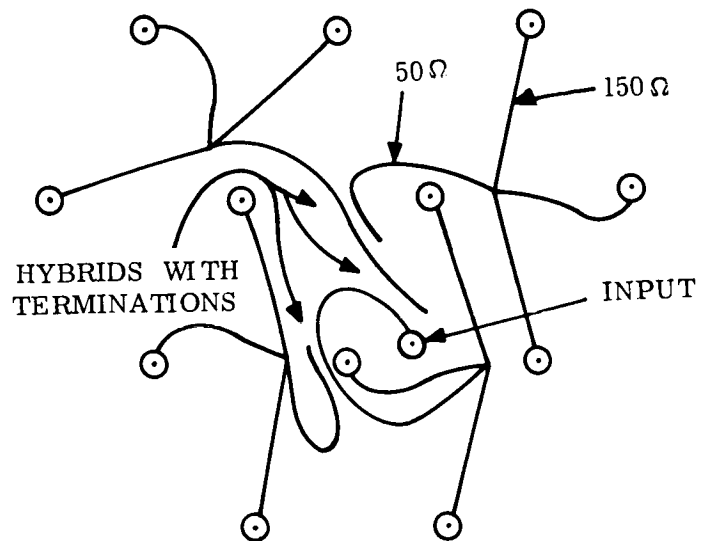


Figure 1.7.2-9. Microstrip Feed Network

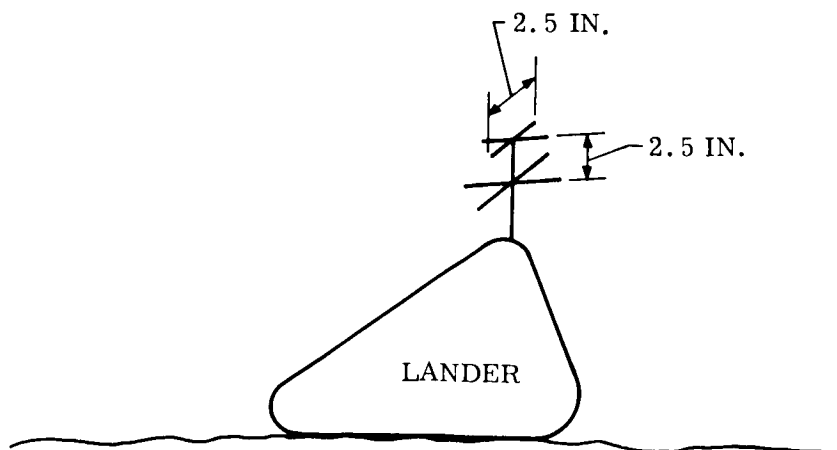


Figure 1.7.2-10. Mars Lander Low-Gain S-Band Antenna

the 90° phase shifts introduced by the hybrids, three of the helices will be rotated 180° and six will be rotated 90° about their axes with respect to the remaining three.

(2) Low-Gain DSIF Antenna

This antenna will provide low data rate communications with the Earth in the event of failure of the other higher data rate systems. It will be erected on a boom along the local vertical after the Lander has come to rest, as in Figure 1.7.2-10. The upper elements will be fed as indicated in Figure 1.7.2-3 and an additional parasitic crossed-reflector will be used to achieve the patterns of Figure 1.7.2-11 — hemispherical coverage. Gain will be approximately three db along the vertical and zero db in the plane tangent to the local terrain.

(3) VHF Relay Antenna

This unit is electrically identical to the low-gain DSIF antenna and will provide the same electrical performance. Physically no parasitic reflectors will be used: the active turnstile elements will use the body of the Lander as a reflector ground plane (Figure 1.7.2-12). This unit could be mounted on the same erected boom as the DSIF low-gain antenna, below the DSIF unit, utilizing a triaxial cable to feed both antennas independently.

(4) Pre-Entry and Post-Entry Antennas

Communications between the Orbiter and Lander from after their separation to the landing will be maintained by a 100-mc link. A "transmission line" antenna is envisaged as the best solution to the resulting antenna problem. This antenna, shown in Figure 1.7.2-13, would be a quarter-wave stub bent and folded against the periphery of the aft end of the vehicle. Installation of the antenna on the Lander is shown in Figure 1.7.2-14. Such an antenna has been required because of the serious interference presented to other designs by the aft-cover brake and the retro-thrust rocket and supports.

The recommended antenna will be narrow-band because of its close proximity to its ground plane. However, since it will only transmit, this is not a serious problem. The antenna will be highly sensitive to changes in nearby pieces of metal as well as to changes in environment — particularly temperature. Thus, it is recommended that it be designed to be self-tunable. This can be accomplished by using a reflected-wave sensor to drive a Varactor pair to introduce the proper amount of capacitance to cancel the detuning of the antenna. Such a device — a breadboard model of which has been produced by GE — would weigh 0.5 pound, fit in a package of 1/2 inch x 1 inch x 8 inches and draw negligible current.

An alternate — considered less desirable for weight reasons alone — would be to use two antennas, one on either side at the aft of the entry vehicle. One antenna would be tuned for the case before the rocket supports and the separation ring are jettisoned, while the other would be tuned to work afterward. If necessary, a third antenna could be tuned for use after the aft-cover is deployed. Switching between these could be accomplished by energizing separate power-amplifier stages, so that no RF switching would be necessary.

1.7.3 RECORDERS

A. Survey of Recording Devices

To determine the type of data storage device most suited for use on the Voyager Program, a brief survey of the data storage field was conducted. This included the following types of devices:

1. Magnetic drums
2. Magnetic cores

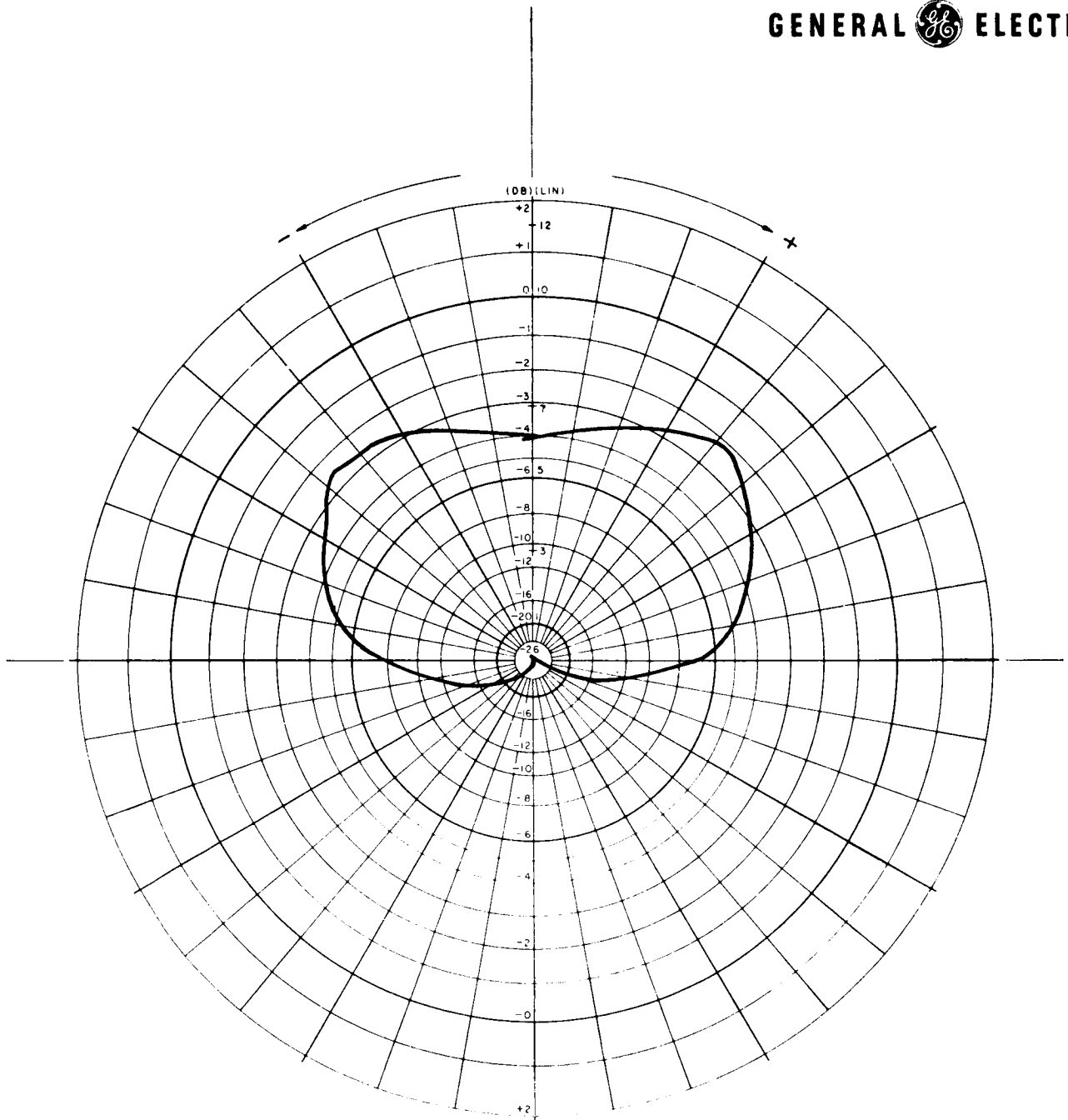


Figure 1.7.2-11. S-Band Turnstile Pattern

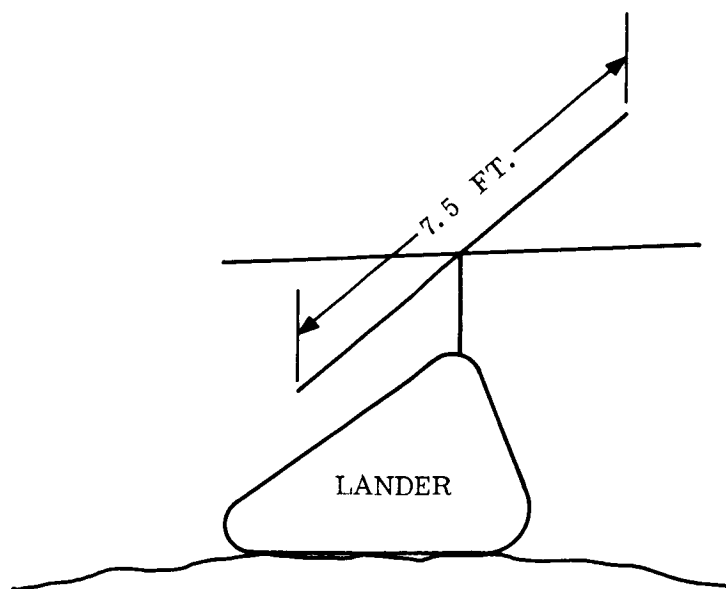


Figure 1.7.2-12. Lander Turnstile Antenna

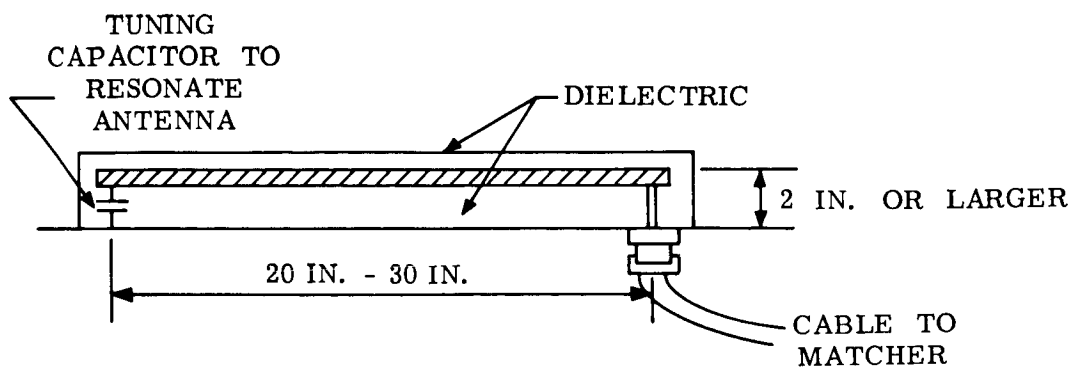


Figure 1.7.2-13. Lander "Transmission Line" Antenna

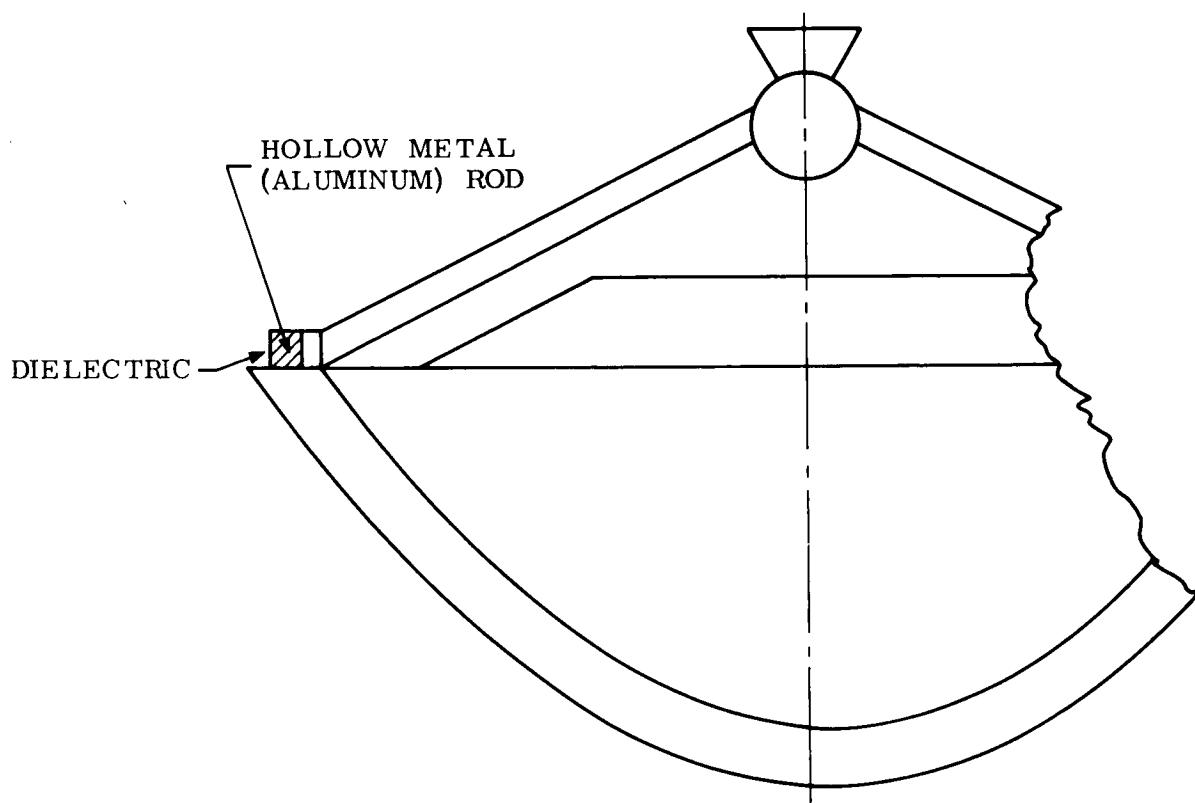


Figure 1.7.2-14. Installation on Lander

3. Magnetic plated-wire
4. Thermoplastic recording
5. Magnetic tape recording

In addition to the environmental requirements, the criteria for selection included weight, volume, power consumption, cost and availability.

Magnetic drums and cores were discarded on the basis of volume, since storing 10^9 bits in these devices is unfeasible. The magnetic plated-wire memory, a Univac development, also proved to be impracticable for the bulk storage, due to the required volume. However, because of its flexibility in reading and writing rates, low power consumption, and mechanical simplicity, this device should be considered for use in low capacity (10^5 bits) applications. After the elimination of these three techniques, a detailed evaluation of thermoplastic recording and magnetic tape recording was conducted. This resulted in the selection of the thermoplastic recording technique as the superior method for this application. A discussion of the two techniques as applied to the Voyager requirements is given in the following sections.

B. Magnetic Tape Recording

The most promising recording system evaluated was a modified version of the RCA SL-100, designed for use on the Gemini Program. This was selected as the basic unit because of its potentially high data storage capacity. The characteristics of the modified recorder are as follows:

Data Format	Four bits parallel, NRZ
Five Operating Modes:	
Mode 1	Erase and record at 256,000 bits per second (64,000 per track)
Mode 2	Playback at 16,000 bits per second (4,000 per track)
Mode 3	Playback at 8,000 bits per second (2,000 per track)
Mode 4	Playback at 4,000 bits per second (1,000 per track)
Mode 5	Playback at 2,000 bits per second (500 per track)
Readout Format	NRZ serial
Error rate	1 bit error in 10^4 bits, maximum
Volume	Approximately 1,000 in. ³
Weight	Approximately 18 pounds
Power	20 watts @ 28 vdc

Two of the above recorders would be utilized to store Orbiter data. Each recorder would have 2500 feet of 1/4-inch tape, 4 tracks, and would record on both sides of the tape. The packing density would be 2000 bits per track inch. On this basis the storage capacity per recorder would be as follows:

$$\frac{2000 \text{ bits}}{\text{track-inch}} \times 8 \text{ tracks} \times \frac{12 \text{ inch}}{\text{foot}} \times 2500 \text{ feet} = 4.8 \times 10^8 \text{ bits} \quad (10)$$

While the required playback rates are not precisely defined, those listed above are considered typical.

The data storage capacity of the recorder has been doubled by recording on both sides of the tape. This is accomplished as follows. The depth of flux penetration into the tape is approximately equal to the width of the gap in the recording head. Normally, this gap is wide compared to the reproduce head. In this application, the gap is made narrow, on the order of 100 micro-inches. The flux, therefore, does not penetrate to the oxide on the opposite side of the tape.

On playback, as the distance between the oxide layer and the head is increased, the signal is attenuated according to:

$$\text{attenuation} = 54.6 (d/\lambda) \text{ db} \quad (11)$$

Consequently, if the distance between the reproduce head and the outer oxide layer is greater than λ , the recorded wavelength, the crosstalk during reproduce will be negligible. This technique requires two complete sets of heads, one for each side of the tape.

Two recorders would give the required 10^9 bits. An additional, less complex recorder would still be required to handle Lander data in the Orbiter - a total of about 6×10^7 bits. This data is to be read in at a relatively low rate - approximately 8000 bits per second. In addition it has a six-bit-per-word format. While the basic recorder could be built to handle this input it would make it unduly complex.

While the above recorders can meet most of the requirements, they have the following disadvantages:

1. The high ratio of record to minimum playback speed, 150:1, would be difficult to implement.
2. The 10^9 bit storage requirement can only be met within a reasonable volume by adding complexities to the recording, such as recording on both sides of the tape.
3. The above technique does not offer complete redundancy in case of a failure. This would require the addition of a third recorder with the corresponding penalties in weight and power.
4. The recorders do not have the desired flexibility of read-in, read-out rates.
5. Maximum storage volume cannot be realized because of tape wasted during the frequent stopping and starting periods between TV frames.
6. Efficient bit-sync techniques are more difficult to implement because of non-synchronous readout.

The above disadvantages do not disqualify recorders from consideration. They have the major advantage of being within the present state-of-the-art. But, because of the constraints which they place upon the Communications Subsystem, they will be considered only as a backup to thermoplastic recorders.

C. Thermoplastic Recording

General Electric's experience in Thermoplastic film recording, a new and powerful technique for the recording, storage and display of information, was invented by Dr. W. E. Glenn of the General Electric Research Laboratory, where he has demonstrated both black and white and full-color high-quality video recording.

In 1957, the General Engineering Laboratory of the General Electric Company began development work on the storage system, and studies were made of various applications of thermoplastic film storage of analog and digital information. The feasibility of high-density recording and readout of information was demonstrated using facilities built as part of the General Engineering Laboratory's advanced work program.

In addition to several Company funded efforts, there has been a feasibility study made as part of the Air Force Contract AF 04(647)269. This work was done by the General Engineering Laboratory as part of the advanced instrumentation study of the General Electric Missile and Space Division for application to nose cone instrumentation recording. Following this study, there have been a number of contracts for the construction of specific-purpose thermoplastic equipment at the General Engineering Laboratory. These include a recently delivered High Density Large Capacity Thermoplastic Film Digital Data Storage System (Signal Corps Contract DA 36 039 SC 85118) as well as several classified analog signal recording contracts.

Thermoplastic recording is accomplished by writing data to be stored as a pattern of electrons on a film of thermoplastic material. The film is then heated until it will flow, and the electrons will deform the film into a pattern of grooves. Upon cooling, the ridges are frozen in the surface of the film.

Figure 1.7.3-1 shows a cross-section of a typical thermoplastic storage material. The substrate may be a plate of glass or a tape made of relatively high melting point plastic such as Lexan or Mylar. A transparent conductive coating is deposited on the surface of the substrate. The purpose of the conductive coating is to provide both a resistive coating for heating and melting the thermoplastic film and an equipotential surface to attract surface electrons producing surface deformations. The thermoplastic film is applied on top of the conductive coating and is usually less than one mil thick.

In order to write information on the thermoplastic, an electron beam of appropriate diameter is focused on the surface. The electron beam deposits a charge on the surface of the thermoplastic. By deflecting the beam, a pattern of charge is produced which corresponds to the information to be stored. Writing is usually accomplished by laying down line charges which are modulated in accordance with the data.

Figure 1.7.3-2 shows the forces produced by a charge pattern due to the attraction of the charge to the equipotential surface provided by the conductive coating. If electrical current is caused to flow in the conductive coating, the heat produced in the coating will quickly melt the thermoplastic film. When the thermoplastic becomes fluid, the force of the charges deforms the surface against the opposing force of surface tension in a pattern corresponding to the information pattern written by the electron beam. This is shown in Figure 1.7.3-3. The process of melting and deforming is referred to as development of the image.

The charges will remain on the cool thermoplastic for a matter of hours, and much information may be written before development need be performed. Once the charges have leaked away, it is only necessary to re-melt the thermoplastic, and surface tension will cause the surface to become smooth again. The information has been erased, and the material is again ready for writing.

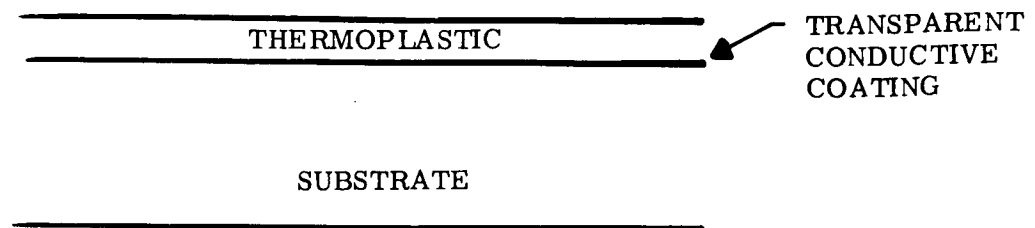


Figure 1.7.3-1. Cross Section of Thermoplastic Film

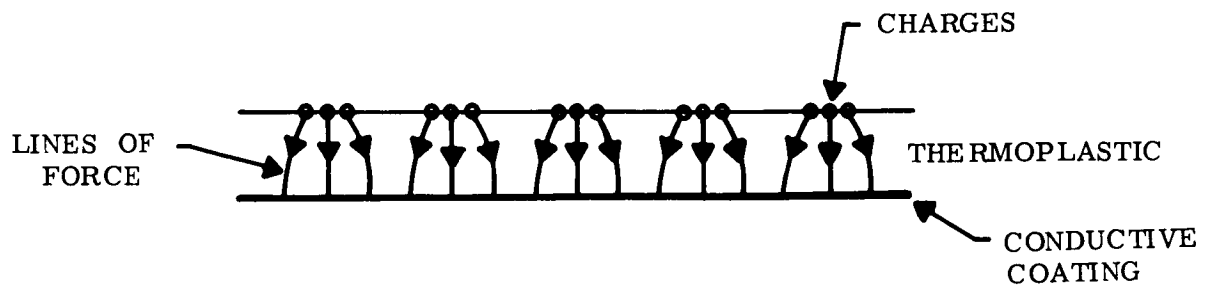


Figure 1.7.3-2. Force on Surface Charges

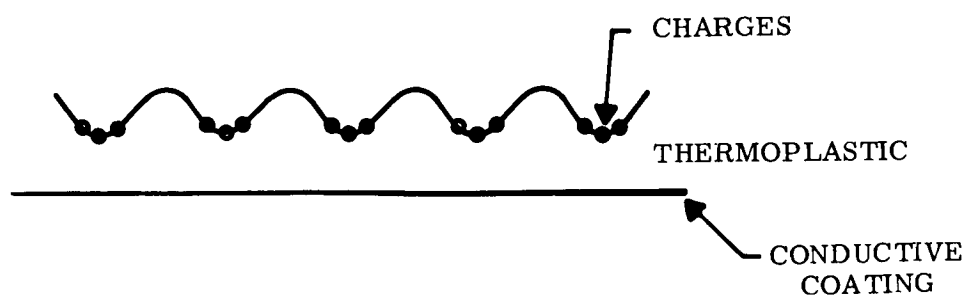


Figure 1.7.3-3. Deformation After Developing

The time required to melt the thermoplastic film can be very short, 10 milliseconds being typical, and the substrate remains relatively cool. When the heating current is removed, the substrate acts as a heat sink, and the thermoplastic film quickly cools and solidifies. Charges leak off much more rapidly when the thermoplastic film is hot, but it has been found that the development can be completed before the charges have noticeably diminished. The ratio of charge decay time constant to image formation time constant is about 50:1.

The effect of increased charge leakage with melting is used to advantage in situations where the material is to be reused shortly after a previous writing. The rate at which heat is added to the thermoplastic is not critical, and developing can be conducted over very wide time ranges, varying from milliseconds to minutes. On all thermoplastic recorders built to date, playback of stored material has been done by optical reading. In this technique a finely focused beam of light illuminates the grooves on the thermoplastic film. A very versatile light source for reading is the cathode-ray tube flying-spot scanner. The light can be deflected at very high rates in two coordinates, making possible the use of flat plates that use no mechanical motion for readout of the stored data. It also makes possible readings at rates that are in the video range. This technique does not lend itself to spacecraft applications, however, because of size and mechanical complexity. An alternate technique, electron beam readout, does not have these disadvantages. This technique is under development by the General Electric Company at this time. Assuming successful development, it is recommended for the Voyager thermoplastic recorder. It involves the detection of the secondary emission from the slopes on each side of the recording groove. Since the method does not involve the detection of charges in the thermoplastic laid down by the recording process, the recording is permanent and unaffected by the reading process or other charge-disturbing processes.

It has another advantage — an inherent groove-following servo error signal. This has been found to be very helpful in reading high-density information. The method of readout is shown in Figure 1.7.3-4.

The modulation of both the magnitude and direction of emitted electrons by the thermoplastic slope is shown in the figure. The primary reading beam is shown striking the thermoplastic surface at three significant points — zero slope, and positive and negative values of maximum slope. The total number of secondary electrons emitted is greater where the surface has a slope than at zero slope, and the majority are emitted with directions around the normal to the surface. The readout method utilizes this modulation of direction by the surface slope by placing two electron-multiplier collectors in appropriate positions to collect the secondary electrons emitted at an angle to direction of incidence. Good detection of slope by such collection becomes possible with groove slopes of about 45° . Figure 1.7.3-5 shows such an arrangement of multiplier-collectors.

If the outputs of such a pair are electronically subtracted, an error signal is produced as the electron spot moves across a groove. Such a signal may be used to lock an electron spot to the center of the groove by feeding it back into the CRT sweep circuits to redirect the beam to the center of the groove. If lateral modulation of groove position is used to record information, the servo may be used to follow the center of the groove precisely at low frequencies. At high frequencies this is not possible, and the servo is designed to follow the average position of the groove while the lateral motion of the groove beneath the readout electron beam modulates the secondary electrons direction back and forth between the collectors. This will produce a push-pull signal in the two multipliers. Signal-to-noise ratios exceeding those obtainable with flying-spot scanners may be obtained, since it is not necessary to contend with the inefficiencies of the cathode-ray tube phosphor and optical system. Maximum frequency response is greater, since the time-constant of phosphors is no longer a limitation — having been replaced by the frequency limitations of the collector-multiplier combination, which is at a much higher frequency.

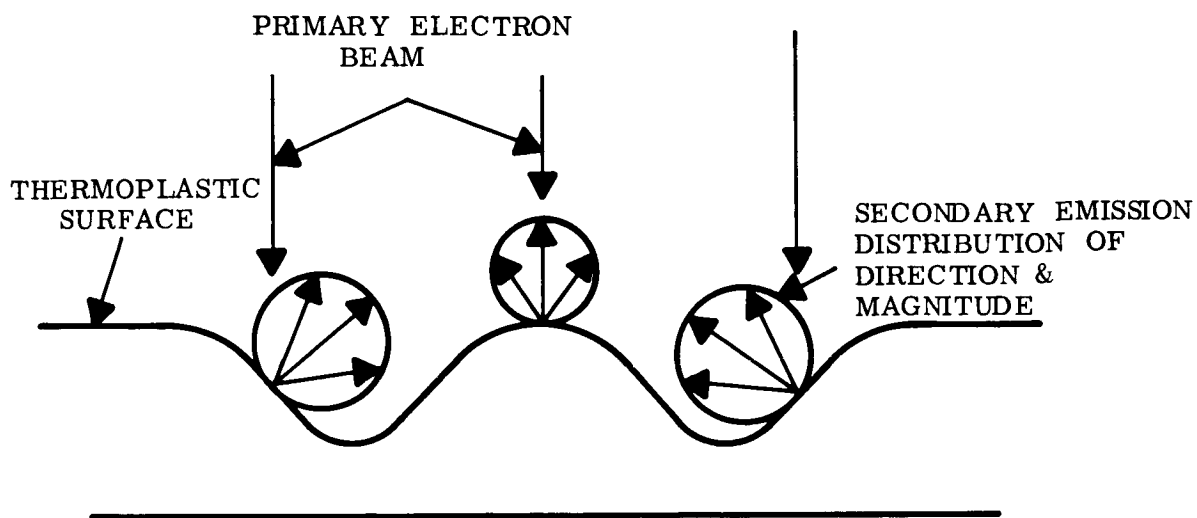


Figure 1.7.3-4. Principle of Electron Beam Readout

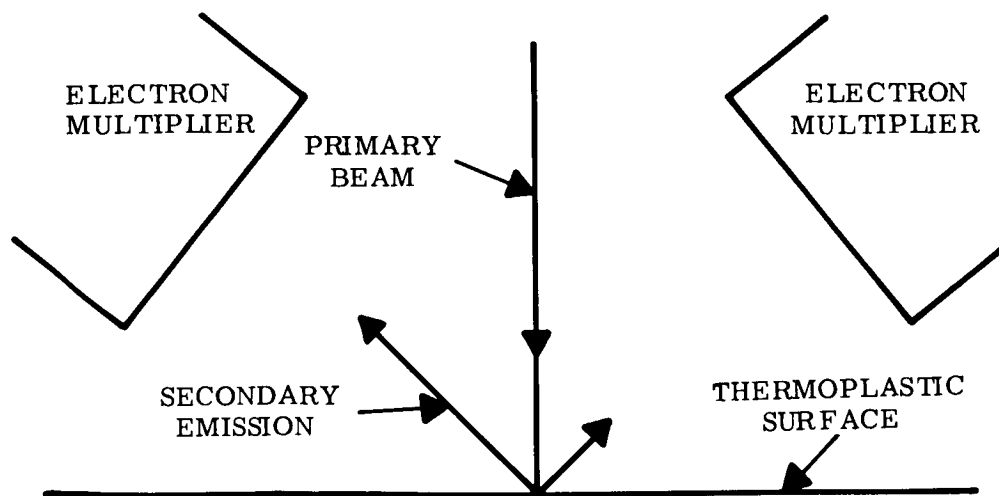


Figure 1.7.3-5. Arrangement of Multiplier Collectors for Electron Beam Readout

In addition to the specific technical advantages mentioned, the thermoplastic process has other plus values. Since both recording and playback scanning can be accomplished with an electron beam, the mechanical complexity can be greatly reduced. The use of electron beam scanning allows very fast access to the recorded data. The record is in the form of mechanical deformation, and, since non-contacting methods are used for reading, should provide a reliable, long-life storage medium. The thermoplastic recording process also allows completely synchronous recording and playback, thus eliminating loss of capacity due to starting and stopping and allowing constant output bit rate without an auxiliary buffer.

The salient technical features which make thermoplastic recording one of the most significant developments in the field of information storage may be summarized as follows:

(1) High Storage Density

Densities of 40 million bits of information per square inch have been demonstrated; no known medium exceeds this density.

(2) High Information Rate

Direct recording of signals at rates of tens of megacycles has been demonstrated.

(3) Selective Erasure

Thermoplastic film can be selectively erased and reused at least several thousand times; the limit is believed to be about 100,000.

(4) Analog or Digital Recording

The information stored can be modulated continuously or can be recorded as "on-off" data. Thus, the medium is suitable for recording of either analog signals or digital data.

(5) Fast, All-Electronic Process

The input to the process is an electrical signal. Heat is used to develop the information for permanent storage and use (until erasure is desired). Heat development times can be as low as a few milliseconds. Thus, the process is all-electronic and the recorded information is ready for use or permanent storage in only a few milliseconds.

(6) Relative Insensitivity to Nuclear Radiation

The materials and processes used are relatively unaffected by moderate amounts of nuclear radiation. The radiation dosage by the electron beam is usually many times that of ambient radiation levels.

(7) Readout Independent of Speed

Because of the manner of storing the information, the output signal is essentially independent of the relative speed between the storage medium and the output sensor. This is of great utility in the area of signal processing and analysis where it is often desirable to perform recording and playback at widely differing speeds. The peak-to-peak, signal-to-rms noise ratio in this instance is about 20 db, but more recent work indicates that much better ratios may be achieved. At lower playback rates, such as contemplated for this application, the signal-to-noise ratio should be much better.

It was concluded in the final evaluation that thermoplastic recording was far superior to magnetic tape recording for this application. All requirements could be met with a TPR weighing 20 pounds plus five pounds for the plate-changing mechanism. A second TPR would be added for reliability and to simplify the recording sequence.

1.7.4 S-BAND TRANSPONDERS

A. General

The S-Band transponder receives a PCM/PSK signal from Earth, phase locks to the carrier, demodulates command signals and provides modulated, coherent carrier to a power amplifier for subsequent transmission to Earth. The transponder consists of two subassemblies: a phase-lock receiver, and a transmitter. Suitable equipments are available from several sources. The table below summarizes the characteristics of transponders developed or actively being developed.

TABLE 1.7.4-1. CHARACTERISTICS OF AVAILABLE TRANSPONDERS

	Hazeltine	STL	Motorola
Size	480 cu in.	184 cu in.	204 cu in.
Weight	18 lbs	5.4 lbs	12.5 lbs
Power	35 watts	2 watts	9.6 watts
Noise Figure	13 db	10 db	10 db
Sensitivity (threshold lock)	-	-154 dbm	-154 dbm
Loop Bandwidth	-	10 cps	10 cps
S-Band Power Output	1 watt	0.05 watts	0.03 watts
MTBF (hrs)	-	38,900 hrs	15,200 - 20,100 hrs

The STL reliability numbers were received as 0.903 probability of success for six months for the receiver portion and 0.989 probability of success for six months for the transmitter portion. These numbers were converted to an MTBF of 38,900 hours in order to compare with Motorola's numbers. Both the Motorola and STL units are constructed from high reliability parts. Motorola's figure of 20,100 hours is based on substitution of new, more reliable parts into the existing transponder.

The Hazeltine and Motorola receivers are double-conversion units, while the STL receiver is triple conversion. Motorola and STL have units with similar functional requirements which have successful flight histories in the 960 mc and 400 mc frequency bands, respectively. Based on superior performance, reliability, size, and weight, the STL unit is the recommended S-Band Transponder at this time.

B. Receiver

Figure 1.7.4-1 is a block diagram of the STL receiver. Triple conversion keeps the gain of each IF amplifier down to a level such that oscillation and self-locking are not problems. Frequencies are chosen to minimize spurious signals and for ease of filtering after mixing. The output frequency $12 f_1$ is truly coherent with the incoming signal, since the reference local oscillator frequency stability is completely eliminated by mixing twice. Command signals which are phase modulated on the carrier are demodulated by the loop phase detector. The "Signal-Present Phase Detector" is fed from the reference oscillator phase shifted by 90° so that its product with the incoming carrier results in a dc voltage indicating phase lock.

Command modulation is of the form NRZ pseudo random noise multiplied by a square-wave clock at a frequency $2f_s$ equal to the PN bit rate. The resulting power density spectrum has broad nulls at 0 and $4f_s$. The RF spectrum, then, has an uncluttered carrier

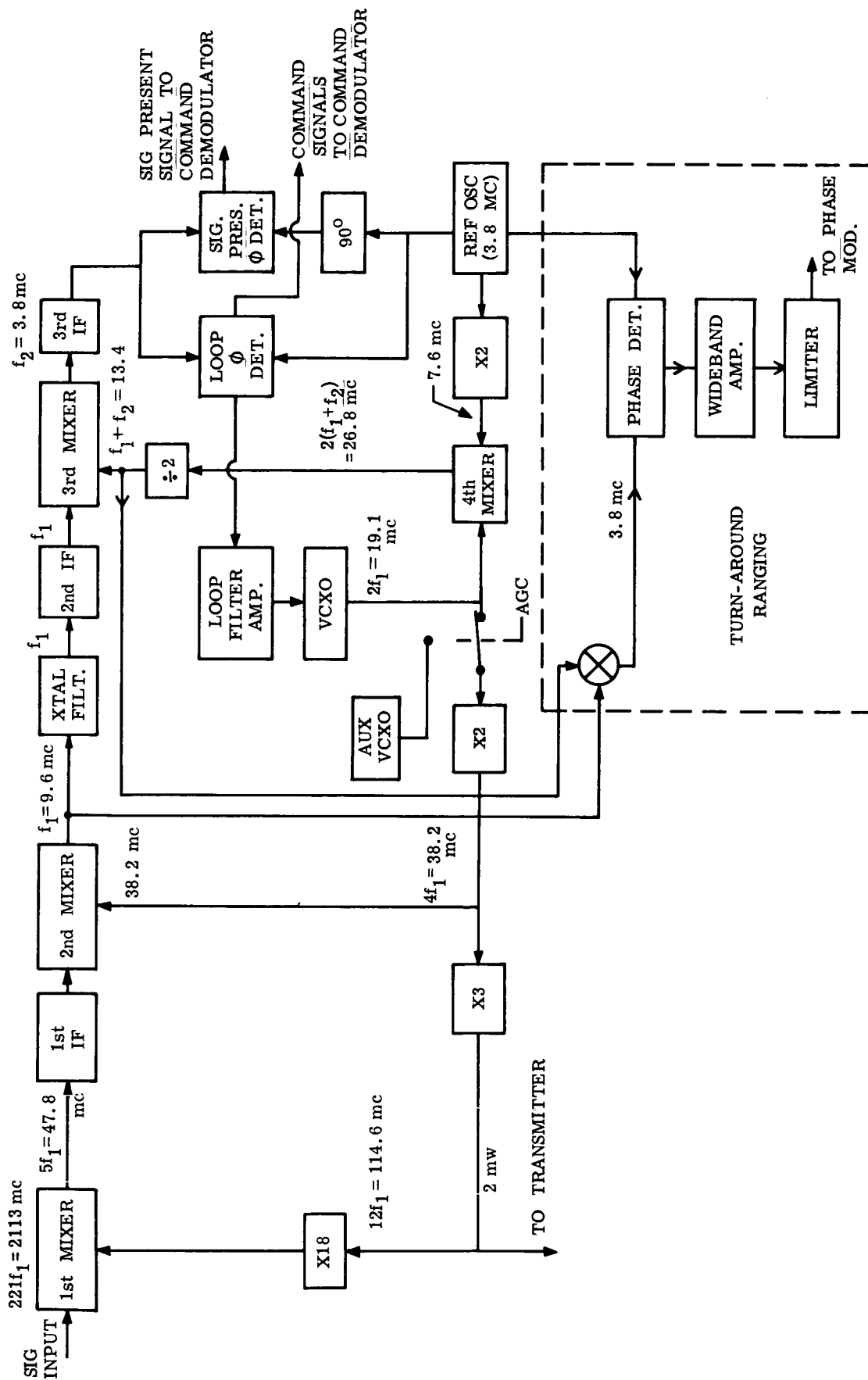


Figure 1.7.4-1. Modified STL Receiver

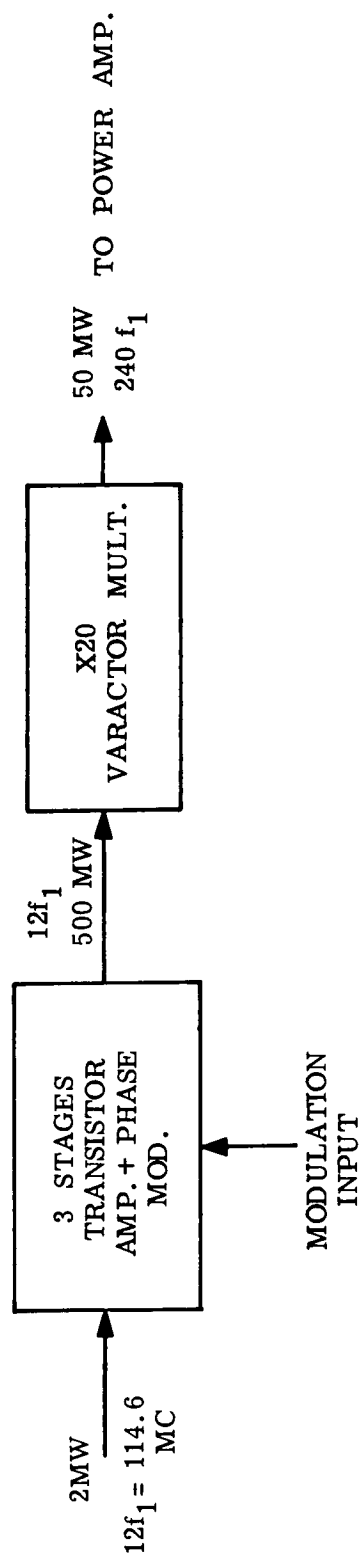


Figure 1. 7. 4-2. Transponder-Transmitter Portion

(i.e., no modulation frequencies lie near it). The final IF amplifier must be wide enough to accommodate this signal (approximately $8f_s$), plus twice the instability of the reference oscillator and IF crystal filter. The IF and phase-lock-loop filters are the only component differences in the receivers recommended for all missions. The two phase-lock-loop bandwidths recommended are 10 cps and 20 cps resulting in carrier acquisition sweep rates of 36 cps² and 9 cps² respectively (sweep rate $\approx 0.09 (2 B_{LO})^2$ for 90 per cent probability of lock in single sweep at SNR = 6 db, where $2 B_{LO}$ is the double-sided loop noise bandwidth)⁽¹⁾.

While the noise figure of 10 db is state of the art for diode mixers, it will be possible in the near future to utilize a tunnel diode or transistor preamplifier to achieve noise figures of the order of 3 to 4 db. A tunnel diode preamplifier is presently available with a noise figure of 4 db and a gain of 17 db (from Micro State Electronics). The pre-amp weighing 2 lbs is about 140 cu inches in size and requires a heater for operation in cold temperatures. The diode is Gallium Antimonide and can withstand non-operating temperatures of 125°C. With a Germanium diode the non-operating temperatures can go up to 135°C but the noise figure is degraded by approximately 0.7 db. Saturation of the diode occurs at signal strengths of about -40 dbm, while burn-out occurs at about -20 dbm.

C. Transmitter

Figure 1.7.4-2 is a block diagram of the transmitter.

The transmitter consists of a transistor amplifier modulator and a times 20 Varactor frequency multiplier. The transmitter drive at 114.6 mc ($12 f_1$) is obtained from the receiver assembly at a two-milliwatt level and is amplified, modulated, and multiplied to yield 50 milliwatts output at 2295 mc ($240 f_1$).

The amplifier uses three cascaded stages of amplification to provide 500 milliwatts to the times 20 Varactor frequency multiplier. This portion of the transmitter operates reliably with an overall efficiency exceeding 50 per cent.

The times 20 Varactor frequency multiplier is a single-stage design rather than a cascaded low-order multiplier configuration. Idler circuits are included at selected multiples of the input frequency to achieve high conversion efficiency. The use of a single-stage high-order multiplier offers several unique advantages over a cascaded low-order chain, including: 1) a much smaller and lighter package, 2) insensitivity to long-term drifts in circuit elements, 3) ease of alignment and, 4) insensitivity to load VSWR at and outside the frequency band of interest.

D. Turn-Around Ranging Unit

The dotted section of Figure 1.7.4-1 illustrates a method of obtaining "turn-around" ranging. The second IF signal is tapped before the narrow crystal filter and is mixed down to the third IF frequency where it is compared in a phase detector with the reference oscillator which is locked to the carrier. The demodulated output is amplified, limited, and then used to phase modulate the transmitted carrier.

1.7.5 DIPLEXERS AND RF SWITCHES

A. S-Band Diplexer Requirements

The S-Band receiver, transmitter, power amplifier, and diplexer will be connected as shown in Figure 1.7.5-1.

⁽¹⁾J. P. Frazier, J. Page, "Phase-Lock-Loop Acquisition Study," GE Tech. Info. Series No. R61DS25, 1 September 1961.

The diplexer performs a number of important filtering tasks, each of which must be considered in determining its requirements. Basically it consists of two bandpass filters, one tuned to the transmit center frequency (T-A) and one tuned to the receiver center frequency (A-R).

The transmit section must: 1) have low loss at transmit frequency; 2) reject transmitter noise at the receive frequency in order that receiver noise figure is not degraded; 3) appear as an open circuit to the antenna at the receive frequency.

The receive section must: 1) have low loss at receive frequency; 2) reject transmitter frequency; 3) appear as an open circuit to the transmitter; 4) reject receiver image frequencies. Losses, of course will be minimized by high-Q elements which may be made to appear as open circuits at a particular off-band frequency by proper phase shifting. A value of 80 db image rejection is reasonable. Therefore, the major requirements to be met are the receive and transmit frequency rejections in the respective arms.

It appears that a diplexer having 80 db rejection in the receiver section and 20 db rejection in the transmitter section will be adequate.

B. Diplexer Availability

The diplexer requirements described in the preceding paragraph can be met with state-of-the-art components.

An S-Band cavity filter exists with the following characteristics:

Weight:	1 lb
Volume:	40 cu in.
Insertion loss at 2115, 2295 mc:	1.0 db max
Isolation between receive and transmit terminals at 2295 mc:	80 db min

For the relay link a 100 mc-lumped-constant filter may be used, having the following characteristics:

Weight:	1 lb
Volume:	8 cu in.
Insertion loss at 95 mc:	1.0 db max
Insertion loss at 105 mc:	2.0 db max
Isolation between receive and transmit terminals at 95 mc:	80 db min

C. RF Switching

RF switching is state-of-the-art at S-Band using either diode switches, coaxial mechanical switches, or circulator switches. At 100 mc either coaxial switches or diode switches may be used.

1. 7. 6 HIGH VOLTAGE POWER SUPPLY

The High Voltage Power Supply is a dc-to-dc converter which provides the cathode voltage and the filament voltage to the klystron. The filament voltage (5vdc) floats at -2,500 v. A schematic of the connections is shown in Figure 1. 7. 6-1.

The design of this power supply is based on a constant-frequency variable pulse-width voltage waveform applied to a transformer. The output of the transformer is then rectified, filtered and series-regulated.

The pulse width is controlled by comparing the output voltage to a Zener reference voltage and driving the difference voltage to zero.

The characteristics of the Orbiter Unit are given below:

Size:	4 x 4 x 6 inches
Weight:	5 lbs
Efficiency:	75 per cent
Inputs:	28 volts dc \pm 10 per cent 2,500 cps Square Wave, Relay Drive Lines
Outputs:	2,500 volts @ 20 milliamperes for cathode 7.5 volts peak-to-peak ripple 1 per cent regulation 5 volts @ 1 ampere on 3 lines for filaments

The output of the unit can be provided on any one of three lines. Line selection is accomplished by energizing one of the three relay coil lines. By selecting one line, the other two are opened. No provision is made to switch under load conditions. A block diagram is shown in Figure 1.7.6-2.

The characteristics of the Lander Unit are given below:

Size:	4 x 4 x 6 inches
Weight:	5 lbs
Efficiency:	75 per cent
Inputs:	28 vdc \pm 10 per cent 2,500 cps Square Wave
Outputs:	2,500 volts @ 24 milliamperes for cathode 7.5 volts peak-to-peak ripple 1 per cent regulation 5 volts @ 1 ampere for filament

The Lander unit is supplied with 28 vdc through the Power Conversion and Control Unit, which can switch the unit on and off by controlling this voltage. A block diagram is shown in Figure 1.7.6-3.

1.7.7 VHF TRANSMITTERS FOR RELAY LINKS

The phase-modulation VHF transmitter block diagram shown in Figure 1.7.7-1 is an all solid-state unit to be used for the Orbiter-to-Lander command links and the Lander-to-Orbiter telemetry links. This transmitter is identical for all links except for the plug-in oscillator module which is to be selected according to its use. It is similar in circuitry and components to the low-frequency portion of a 250-mc stable transmitter (GE-RSD Dwg. 111C5822) recently developed by GE-RSD for miss-distance measurement.

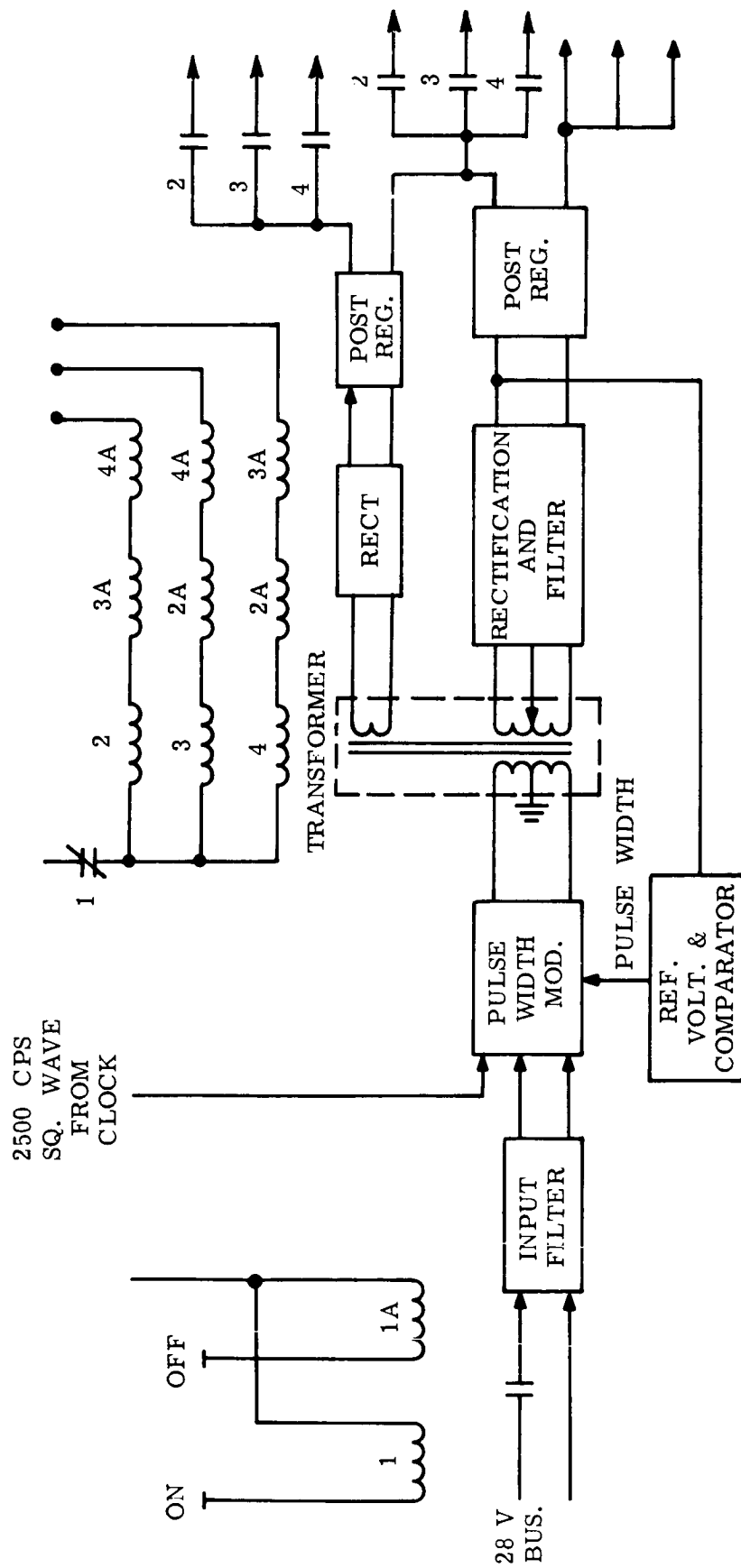


Figure 1. 7. 6-2. Orbiter High Voltage Power Supply

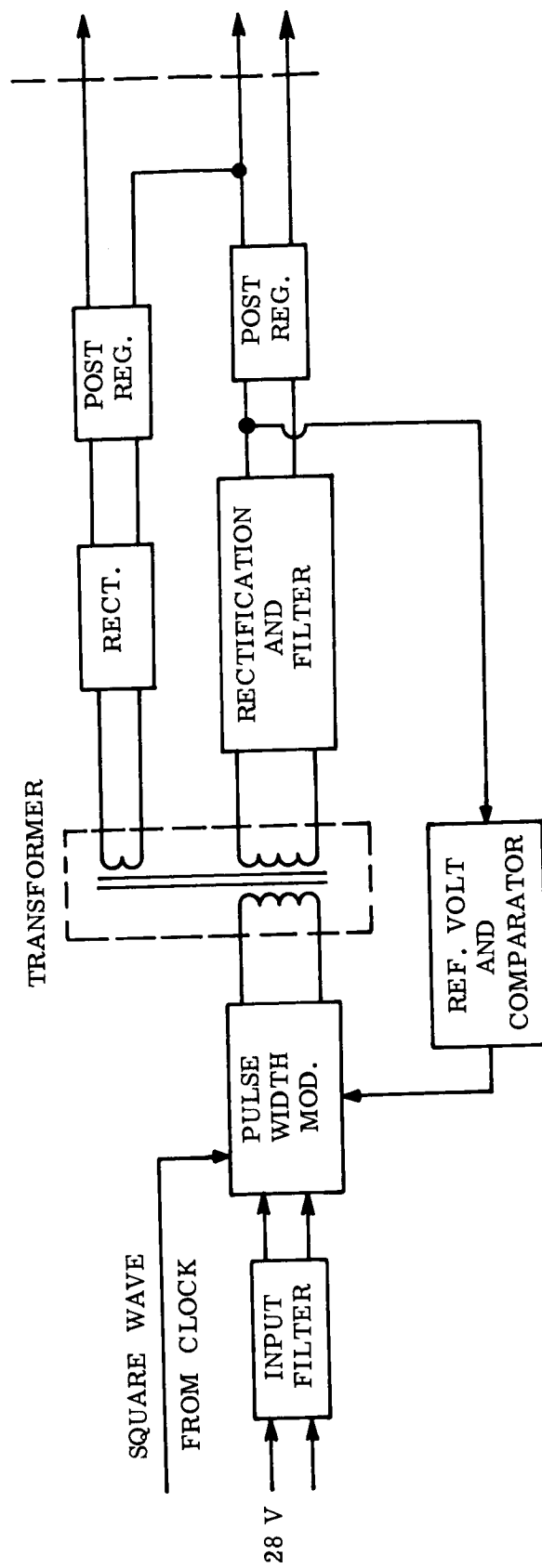


Figure 1.7.6-3. Lander High Voltage Power Supply

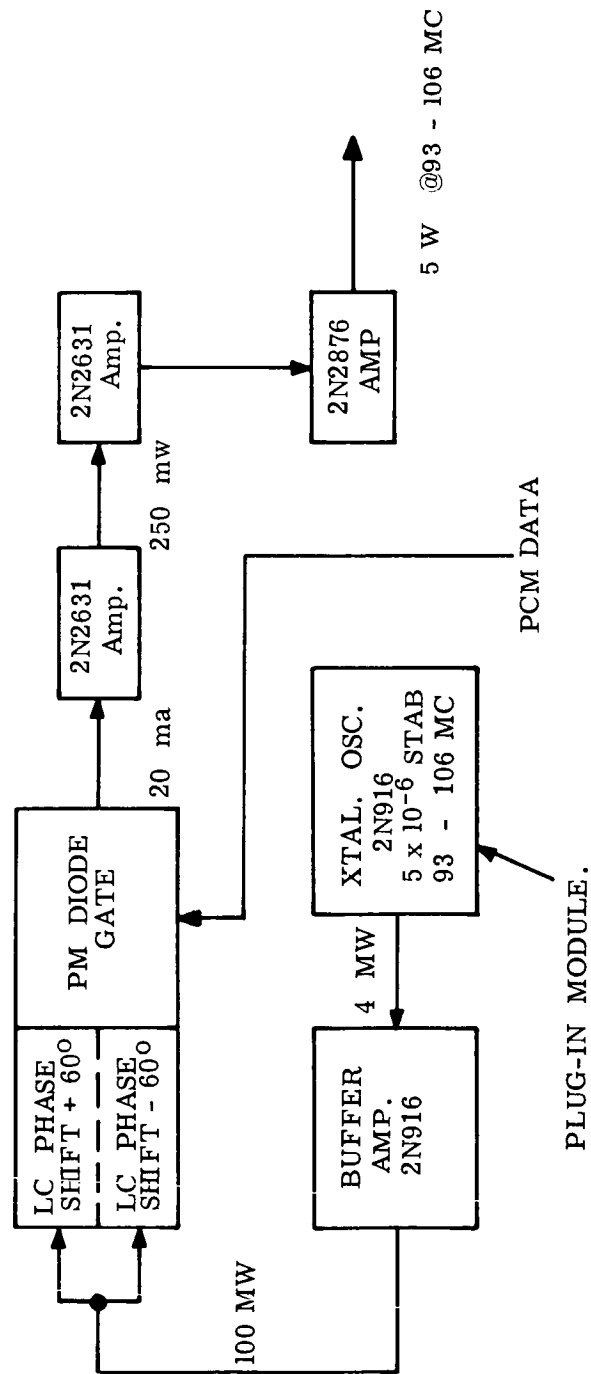


Figure 1.7.7-1. VHF Phase Modulated Transmitter

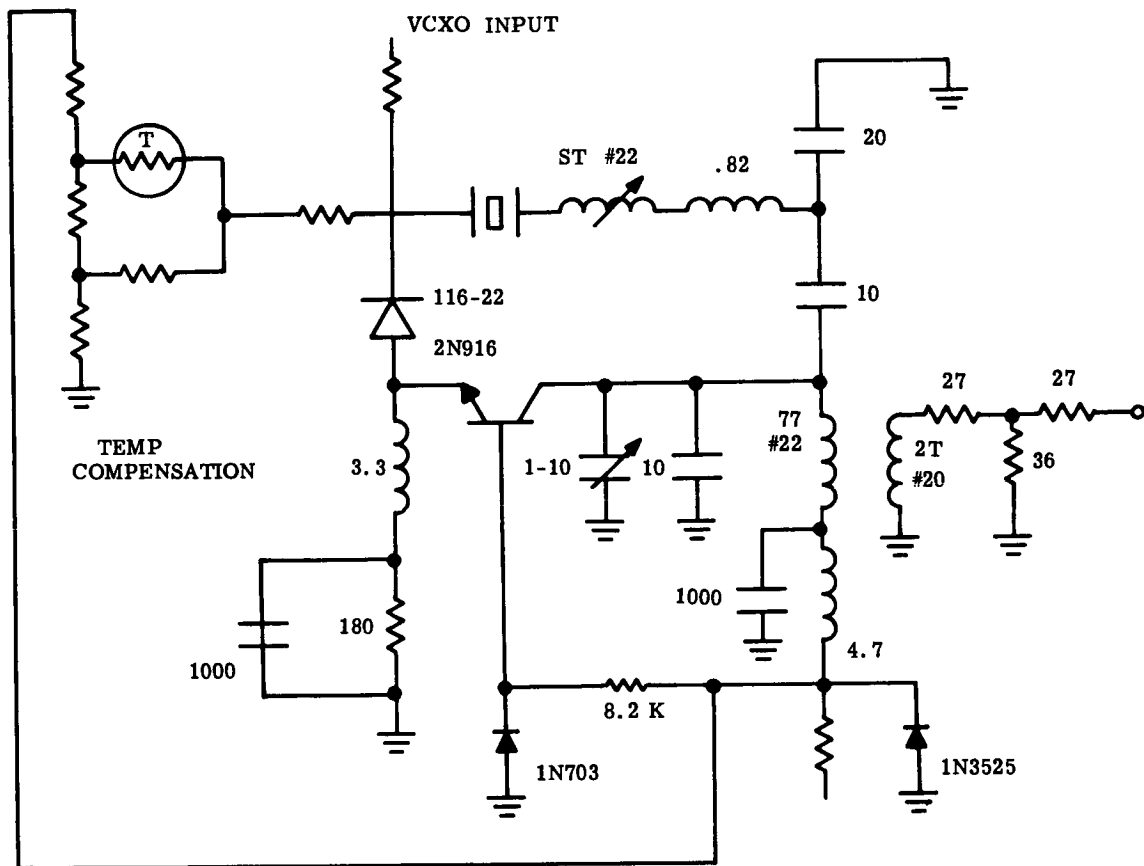


Figure 1. 7. 7-2. Oscillator Schematic

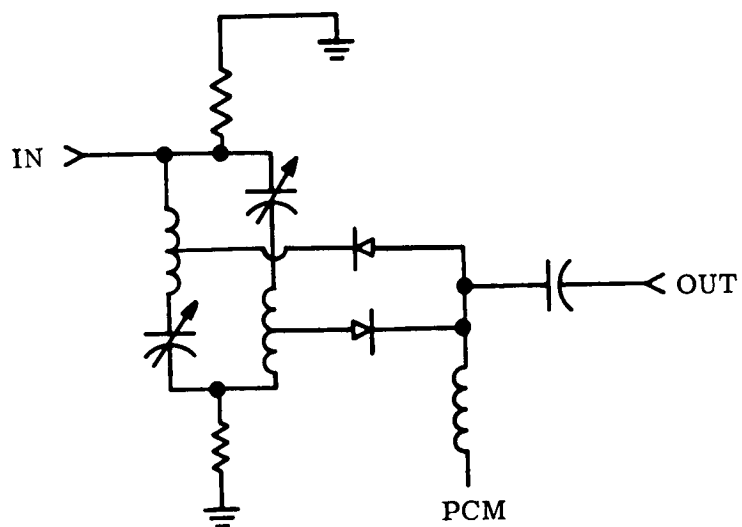


Figure 1. 7. 7-3. Phase Modulator

A. Oscillator

A desired transmission link long-term frequency stability of one part in 10^5 (transmitter plus receiver) requires a frequency stability of ± 5 parts in 10^6 at each end of the link, assuming equal division of instability. A quartz crystal oscillator will provide this moderate frequency stability with minimum weight, volume and power requirements. An oven could be used to stabilize the quartz crystal oscillator temperature, but this would significantly reduce the overall transmitter efficiency and increase the volume. Also, the high temperature required (above maximum environment) would tend to accelerate crystal aging and an oven failure could cause complete communications link failure because of the large temperature coefficient (TC) of a quartz crystal cut for oven operation at, say, 70°C .

The oscillator employed here makes use of a thermistor-derived compensating voltage to correct for the TC of the quartz crystal, thus eliminating the liabilities associated with the oven. A schematic of the oscillator is shown in Figure 1.7.7-2. It is a common-base Colpitts oscillator employing a fifth overtone HC-26/U crystal, cut for an 80°C temperature turnover point. The TC of the thermistor bridge voltage is adjusted with the fixed resistors to decrease the varactor capacitance and compensate exactly for the negative crystal TC at three points between -10°C and $+80^\circ\text{C}$. This oscillator, operating at 65 mc was installed in a prototype unit Miss-Distance Indicator (MDI). The unit was subjected to the following environments and maintained frequency within $\pm 2.5 \times 10^{-6}$ long term, and $\pm 10^{-8}$ in a 2-second period:

Temperature	-10°C to $+70^\circ\text{C}$ (with voltage profile)
Vibration	+10 g @ 5-2000 cps
Shock	115 g for 11 ms
Acceleration	175 g for 1 minute

As shown in the block diagram of Figure 1.7.7-1, the oscillator is isolated from the phase modulator by a buffer amplifier to prevent the introduction of incidental FM by the PCM/PS data.

B. Phase Modulator

Several possible circuits could be used to accomplish the required phase-shift modulation, but most leave much to be desired in terms of time and environmental stability, or incidental amplitude modulation. A significant change in the phase-modulation index could reduce either the RF carrier or the sideband power below a desirable level. Amplitude modulation will reduce the useful energy in both the carrier and subcarrier spectrum, can cause undesired phase-modulation of the locked oscillator at the receiver, and may in other manners interfere with proper receiver operation.

Phase-shift modulators which employ a voltage-variable reactance such as a varactor diode, require tight regulation of data and bias voltages to prevent changes in modulation index, and if operating in a circuit without considerable post-modulation frequency multiplication or limiting, they may also introduce considerable amplitude modulation. Those phase-shift modulators which employ active elements (transistors/diodes) such as two-channel gated amplification are time-sensitive (due to active component parameter change) in terms of both modulation index and incidental AM. The phase-shifter used here, shown schematically in Figure 1.7.7-3, employs identical passive components for phase shift, and the two switching diodes used result in insignificant PM index changes or incidental AM with changes in characteristics or voltage short of catastrophic failure.

C. VHF Medium-Power Amplifiers

The power amplification stages are all un-neutralized common emitter circuits. The first is operated class A and the latter two stages class C. Operating characteristics of the two transistors used in a class C un-neutralized common emitter circuit at 100 mc with a +28 volt collector supply and 80°C case temperature are shown in Table 1.7.7-1.

TABLE 1.7.7-1. OPERATING CHARACTERISTICS OF POWER TRANSISTORS

	Dissipation Limit	Power Out	Gain	Eff.
2N2631	6 watts	3.5 watts	8.5 db	40%
2N2876	12 watts	7.0 watts	5 db	40%

The power outputs shown in the block diagram are minimum, having been calculated for the worst-case condition of high temperature and low voltage. Nominal power output (+28 V @ room temperature) with the identical components and circuitry as used in the GE-RSD Solid-State Telemetry Transmitter (GE-RSD 111C3147) and MDI Transmitter (GE-RSD 111C5822) at 125 mc, is about 1.5 db above minimum.

D. VHF High-Power Amplifier

The state-of-the-art in high-power VHF transistors is progressing rapidly. The U. S. Army Signal Corps is presently sponsoring a program for a transistor capable of 50 watts output at 150 mc (25°C case temperature), which should be available in about one year. Presently the transistor which appears to offer the greatest power output at 100 mc is the PSI PDT 685. This transistor is capable of providing 25 watts output at 100 mc with 10 db gain at 50 volts and 25 per cent efficiency. Two of these PDT 685's will be used in parallel to provide an output of 35 watts nominal and 25 watts minimum at high temperature (70°C). The physical parameters of this high-power amplifier stage are:

Weight: 0.35 lbs
Volume: 6 cu in. @ 1 x 2 x 3
Power: 100 w. @ +50 volts dc \pm 5 per cent

1.7.8 VHF RECEIVERS FOR RELAY LINKS

A block diagram of the VHF Pre-amplifier and the Command/Telemetry Receiver is shown in Figure 1.7.8-1. The performance characteristics for each link are shown in Table 1.7.8-1.

As indicated in the block diagram, the receiver circuits are standard for each application except for plug-in modules for the VCXO and crystal filter, second RF-amplifier band-pass alignment, and resistor selection for sweep-rate and loop bandwidth.

A. Preselector and Receiver Front End

The preselector is a three stage LC filter with a 3 db bandwidth of 4 mc and a 40 db bandwidth of 20 mc. The block diagram of Figure 1.7.8-1 assumes the use of a diplexer with a rejection of the transmitted signal in the receiver port of 75 db. Using a selected low-noise transistor (TA 2333) to provide 15 db of gain at RF before the preselector, an overall receiver noise figure of 4 db can be obtained, resulting in a receiver sensitivity of approximately -170 dbm.

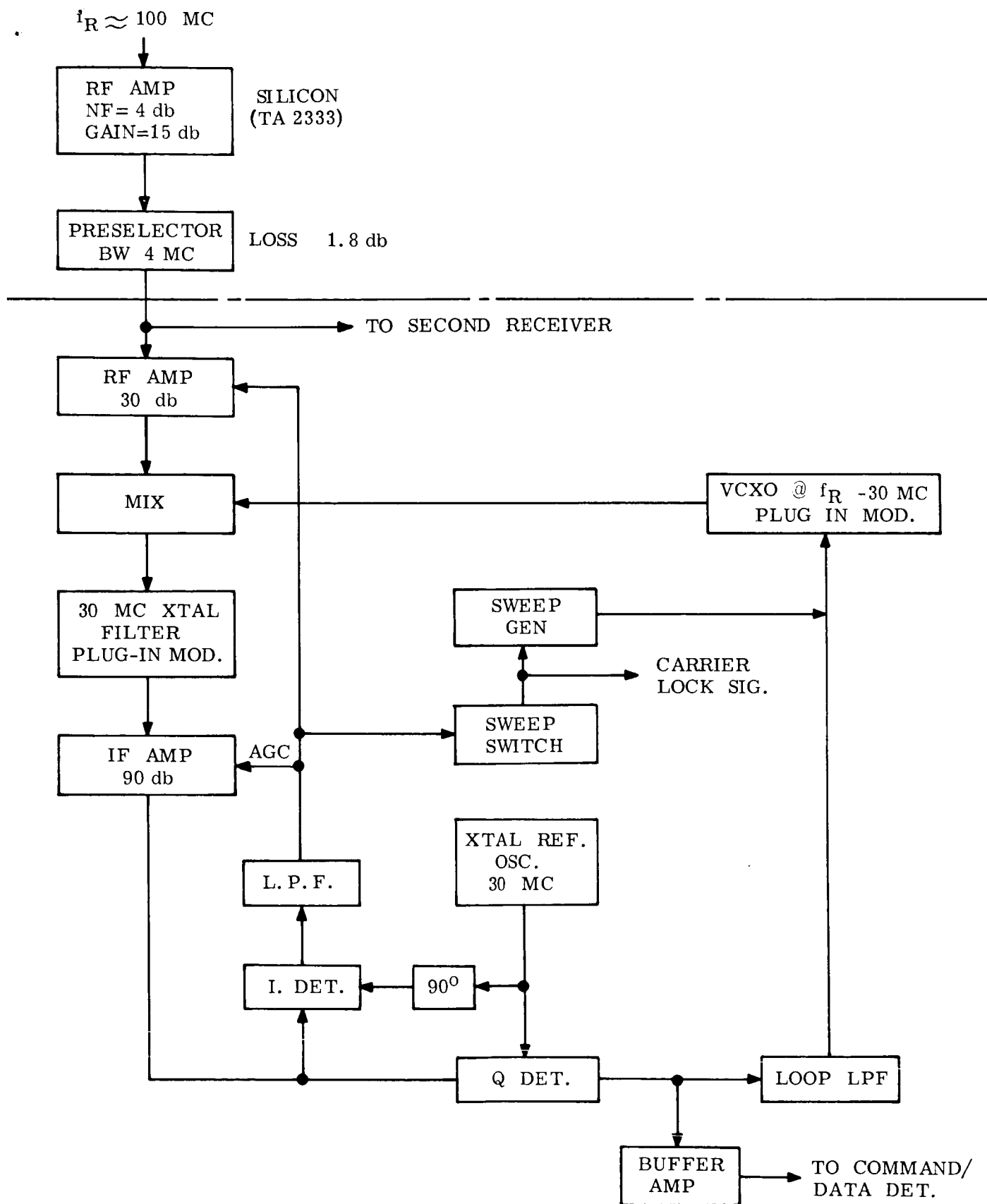


Figure 1.7.8-1. VHF Pre-Amplifier and Command/Telemetry Receiver

TABLE 1.7.8-1. PERFORMANCE CHARACTERISTICS OF VHF RECEIVERS

Characteristic Link	Nominal Carrier Frequency	VCXO Frequency	Maximum Bit Rate (Bits/Sec)	PN Sequence Length (Bits/Bit)	IF Bandwidth (KC)	2BLO-Loop Bandwidth (cps)	Sweep Range and Sweep Rate	Maximum Acquisition Time
(5)* Lander-Orbiter (Prime)	95 mc	65 mc	16000	3	192	85	± 2000 cps @ 800 cps/sec	5 sec
(6)* Lander-Orbiter (Descent)	95 mc	65 mc	500	3	6	85	± 2000 cps @ 800 cps/sec	5 sec
(11)* Orbiter-Lander (Command)	105 mc	75 mc	20	31	2.5	85	± 2000 cps @ 800 cps/sec	5 sec

*For numerical link designations, refer to Section 1.1.

B. Receiver Characteristics

The average time required to attain carrier lock depends on the sweep bandwidth (bandwidth to be searched) and the phase-lock-loop (PLL) bandwidth. A good approximation for this relationship for a 90 per cent probability of locking during one sweep with a 6 db SNR in the PLL bandwidth is⁽¹⁾:

$$\frac{B_s}{T_L} \approx 0.11 (2 B_{LO})^2$$

where B_s = sweep bandwidth (cps)

$2 B_{LO}$ = phase lock loop bandwidth (cps)

T_L = time required to sweep through B_s (sec)

The sweep bandwidth for the relay links should be equal to the frequency uncertainty due to long term oscillator instability and doppler shift, each of which is approximately ± 1000 cps. Therefore, $B_s \approx 4000$ cps. Also, a sweep time of 5 seconds will be assumed. The resulting sweep rate of $4000/5 = 800$ cps/sec leads to the required value of the PLL bandwidth

$$2 B_{LO} = \sqrt{9 \frac{B_s}{T_L}} = \sqrt{9 (800)} \approx 85 \text{ cps}$$

The IF bandwidths must be broad enough to include all the subcarrier spectrum out to the first nulls resulting from the modulation. These nulls are at $f_0 \pm 4f_s$ where f_0 is the IF center frequency and $2f_s$ is the product of the bit rate "R" and the length of the PN sequence (see Section 1.7.8). The total IF bandwidth for each receiver is therefore $B_{IF} = 4 R L_{PN}$. The resulting values are given in Table 1.7.8-1.

1.7.9 COMMAND/DATA DETECTORS

The function of the Command/Data Detector is to lock to the received synchronizing signals, demodulate the command or telemetry subcarrier to recover the data bits, and supply the decoder with all the necessary synchronizing and timing signals. The output of the detector consists of data bits, bit sync signals, and a lock indicator signal. The bit sync signal is also used for the integrate-and-dump and decision circuits within the detector itself. The technique and implementation described here are as given by Springett⁽¹⁾.

The baseband signal into the detector consists of data \oplus PN $\oplus 2f_s$, where PN $\oplus 2f_s$, consisting of a pseudo noise (PN) sequence half added with its clock ($2f_s$), is bi-phase modulated by the data. Each of these waveforms and the resulting composite waveform are shown for a seven bit PN sequence in Figure 1.7.9-1. This signal is demodulated by two multipliers as shown in Figure 1.7.9-2. The switching reference signals into the multipliers are PN $\times f_s$ and PN resulting in outputs of data $\times f_s \angle 90^\circ$ and data $\times f_s$, respectively. Each output is then filtered by bandpass filters of noise bandwidth equal approximately to $2 R$ cps, where R is the data rate in bps. The two signals are then product-detected in a common multiplier to produce f_s , which is passed through a bandpass limiter. The bandpass limiter acts to reduce or eliminate residual AM on f_s at the data rate caused by narrow-band filtering before the product detector in filters 2 and 3. Reduction of AM on f_s allows the maximum loop bandwidth in the following circuits to be limited only by signal-to-noise ratio and not by errors caused by AM on f_s .

⁽¹⁾ Frazier, J. P. and Page, J., "Phase-Lock-Loop Frequency Acquisition Study," GE-TIS No. R61SD25.

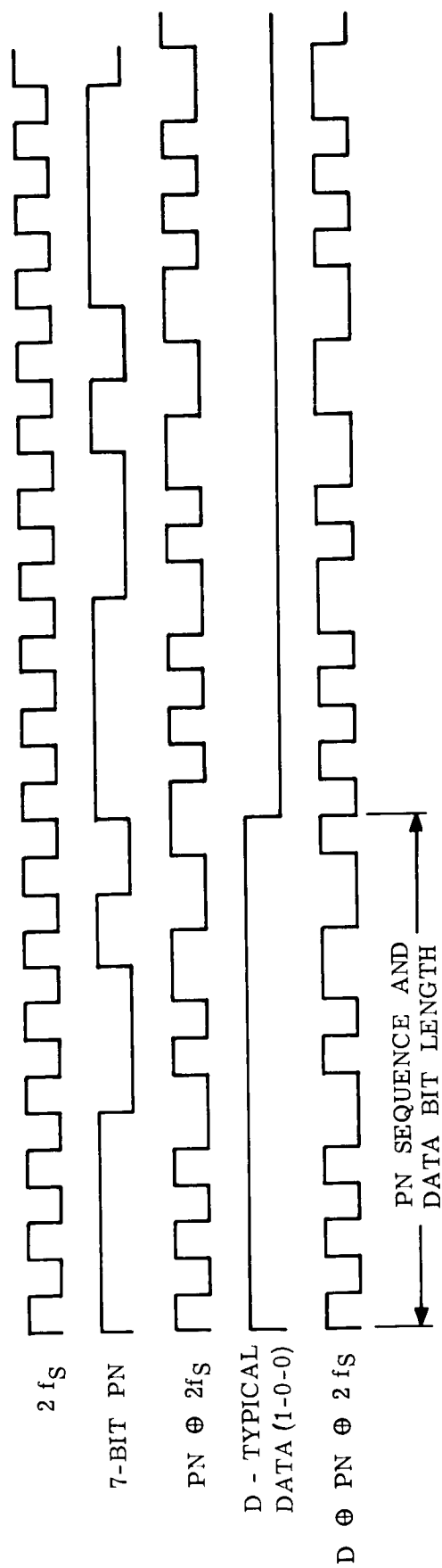


Figure 1.7.9-1. Construction of Modulating Waveform Utilizing 7-Bit PN Sequence

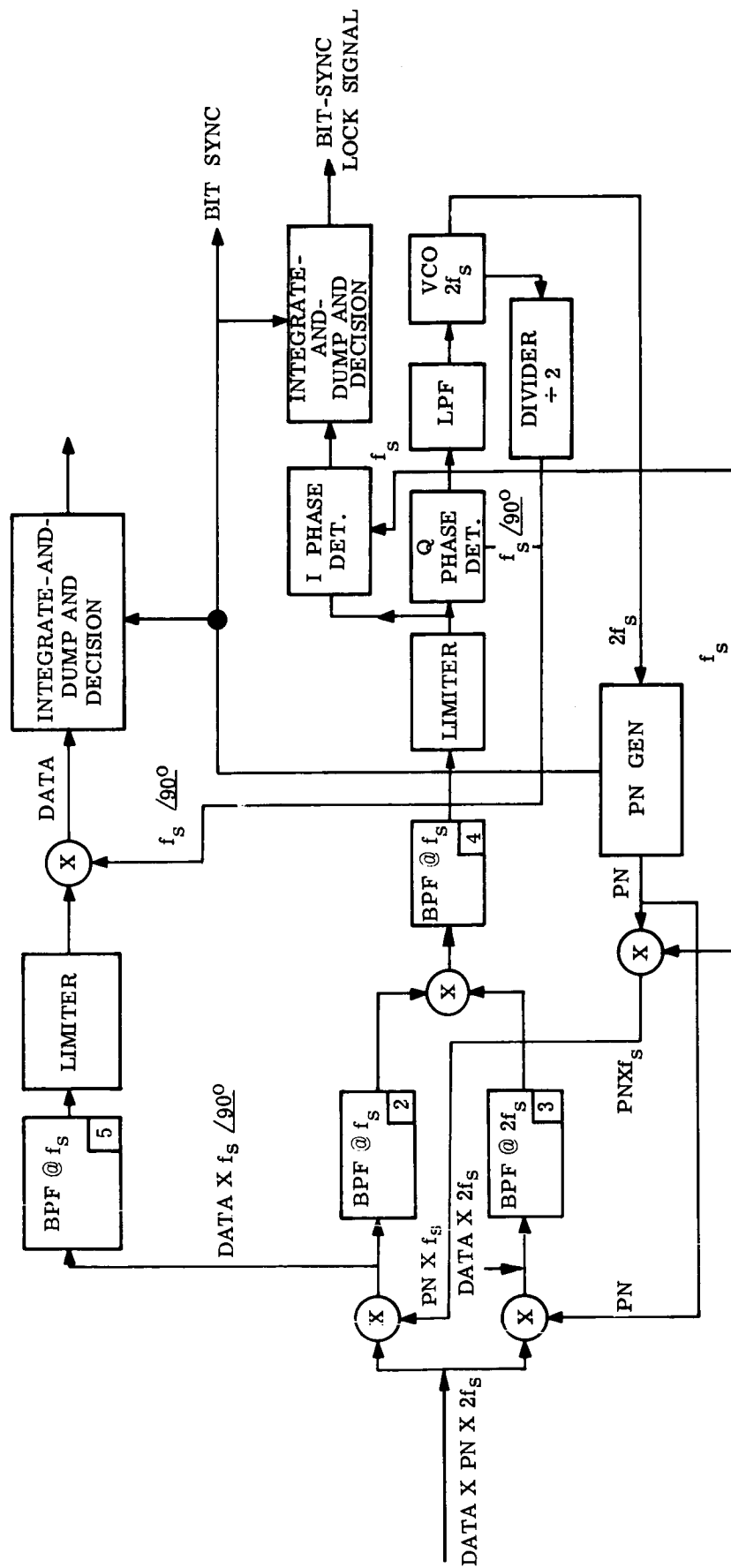


Figure 1.7.9-2. Command/Data Detector Functional Block Diagram

The VCO operating at $2f_s$ is used to drive the PN generator at half that frequency, or $f_s / 90^\circ$, to recover the data from data $\times f_s / 90^\circ$. Bit sync is obtained from the PN generator by a word detector which detects the proper states of the stages in the shift-register or PN generator. Each time the sequence is repeated, the word detector emits a pulse which serves as bit sync. The VCO shown running at $2f_s$ will actually be derived from some higher frequency where stable crystal oscillators are available.

Table 1.7.9-1 lists the characteristics of the Detectors required for the various links of the Mars 1969 and 1971 missions along with estimated size, weight, and power of each. One detector will be used for reception from each Lander for links 5 and 6 with switching capability, by command, to the various bit rates. Since the various bit rates for links 5 and 6 change by multiples of two, a common clock will be used with appropriate switches in the countdown chain.

(1) Springett, J.C., "Command Techniques for the Remote Control of Interplanetary Spacecraft," JPL Technical Memorandum No. 33-88, May 21, 1962.

TABLE 1.7.9-1. CHARACTERISTICS OF COMMAND/DATA DETECTORS (MARS 1969 AND 1971)

Characteristic Link	Bit Rate (Bits/Sec)	PN Bits Per Data Bit	f_s (cps)	Size (cu. in.)	Weight (Lbs.)	Power (Watts)
(5) and (6) Lander-Orbiter Telemetry (Two Required)	16000 8000 4000 2000 500	3 3 3 3 3	24000 12000 6000 3000 750	90	3.5	1.75
(11) Orbiter-Lander Command	*20	†	†	80	3	1.75
(7) Earth-Orbiter Command	*20	†	†	80	3	1.75
(8) Earth-Orbiter Command	*1	†	†	80	3	1.75
(9) and (10) Earth-Lander Command	*1	†	†	80	3	1.75

*Symbol rate (two symbols per command bit)

† As required for link security

1.3 TYPICAL OPERATING SEQUENCES - MARS 1969

1.8.1 ORBITER TV SEQUENCES

For the first two orbits, a nominal mapping sequence will be programmed based on a 1,000 x 19,000 nm orbit. The sequence will commence when the light level is sufficient for the first set of pictures (nadir vidicon and I.O. cluster). Thus, the Command and Computer Subsystem must be able to update the sequence based on the time of the first set of pictures. A time label will be assigned to the first commands (camera electronics on, exposure control electronics on and filaments on), so that the units will be in a ready state when the terminator is crossed on an extreme orbit. However, the sequence will be planned for the nominal orbit.

After four sets of nadir vidicon pictures are taken, the fifth sequence of vidicon pictures will include the forward-looking stereo camera (#2). The next vidicon sequence will include both stereo cameras and the nadir camera. The nadir camera will not be used after the tenth vidicon sequence. Midway in time between the vidicon sequences will be the image orthicon sequences. Typical operations are shown in Table 1.3.1-1.

TABLE 1.8.1-1. TYPES OF FRAMES

Sequence Number	Vidicon				Image Orthicon		
	Stereo #1	Stereo #2	Nadir	Red	Yellow Green	Blue	High Res.
1, 3, 5, 7			X				
Even Numbered Sequences 2 to 104				X	X	X	X
9		X	X				
11, 13, 15, 17 and 19	X	X	X				
Odd Numbered Sequences 21 to 85	X	X					
87, 89, 91, 93 and 95	X	X	X				
97	X		X				
99, 101, 103, 105			X				

On the second orbit the same procedure will be followed. It is realized that the actual pictures taken for these initial sequences will not be optimum, but they will be of use since the time will be indicated on each frame, the accuracy of the PHP will be known, and the orbit will be determined from tracking data. At this time (during the first and second orbits) the orbit information can be transmitted to the vehicle for use by the computer, or the actual camera sequence can be computed on earth and transmitted to the vehicle. Changes in the sequences dictated by results of the first two orbits can be included at this time.

Both TPR units will be used simultaneously for sequences 37 to 70, since the short period between image orthicon pictures at periapsis would require the A/D encoder to operate in excess of 300 kbps if only one TPR were used at that time. In the event of a TPR failure, some image orthicon pictures will be eliminated near periapsis.

The number of frames of each type for a nominal orbit is shown in Table 1.3.1-2.

TABLE 1.8.1-2. SUMMARY OF NUMBER OF TV FRAMES PER ORBIT

Sequence/Orbit 105	Vidicon			Image Orthicon			
	Stereo # 1	Stereo # 2	Nadir	Red	Yellow- Green	Blue	High Res.
	44	44	20	52	52	52	52
	108			208			
Total Frames Per Orbit	316						

1.8.2 TELEVISION OPERATION

The inputs and outputs of each Television Camera Unit are listed in Tables 1.8.2-1 and 1.8.2-2.

TABLE 1.3.2-1. INDIVIDUAL CAMERA INPUTS

<u>General</u>
1. Electronics On-Off
2. Filament Voltage On-Off
3. Clock and Time Code Inputs
4. Destination Commands (TPR # 1 or TPR # 2)
<u>For Each Picture</u>
1. Take picture commands.
2. Read-out command. (Can come from another camera.)
3. Read-out inhibit. (From TPR Unit.)
<u>Self-Generated Functions</u>
1. Camera Identification
2. Line and Frame Sync
3. Light Level
4. Pertinent Voltages
5. Line Count
6. Target Voltage (if applicable)

TABLE 1.8.2-2. CAMERA OUTPUTS

1. Serial PCM (NRZ) data with sync, camera number, etc. (see below)	
2. End-of-frame signal	
3. Erasure-complete signal (inhibits "Take Picture" command)	
4. Data-Present Signal	
<u>Output Format</u>	<u>Number of Bits</u>
1. Frame Sync Word	50
2. Camera Number	3
3. Time	20
4. Light Level	7
5. Target Voltage	6
6. Line Sync	30
7. Line Number	10
8. Line Data (1st)	2043 or 4096 (I. O.)
9. Line Number	10
10. Line Sync	80
11. Line Number	10
12. Line Data (2nd)	2043 or 4096 (I. O.)
13. Line Number	10
' '	
' ' (etc.)	
' '	
2049. or 4097. Line Number	10
2050. or 4098. Camera Number	3
2051. or 4099. End-of-Frame Sync Word	50

In the normal mode, all the camera electronics and filaments will be energized before the sequence starts. A command to take the first nadir vidicon picture will be sent from the Command and Computer Subsystem to the vidicon camera. Approximately one second later, the readout command will be given to the camera unit, which will then generate its unique "frame synchronization word", camera number and time label, as drawn in Figure 1.8.2-1. This time label will be stored in a 15-stage register which is inhibited from changing state by the "Take Picture" command. Next, the quantized light-level measurement will be inserted, then the target voltage, line sync (a unique 30-bit word), and line number, followed by the 512 or 1024 four-bit words of quantized element illumination. This serial PCM wavetrain will be present on either of two output lines, one going to each TPR unit. A "Data Present" line will indicate to the TPR unit that data is

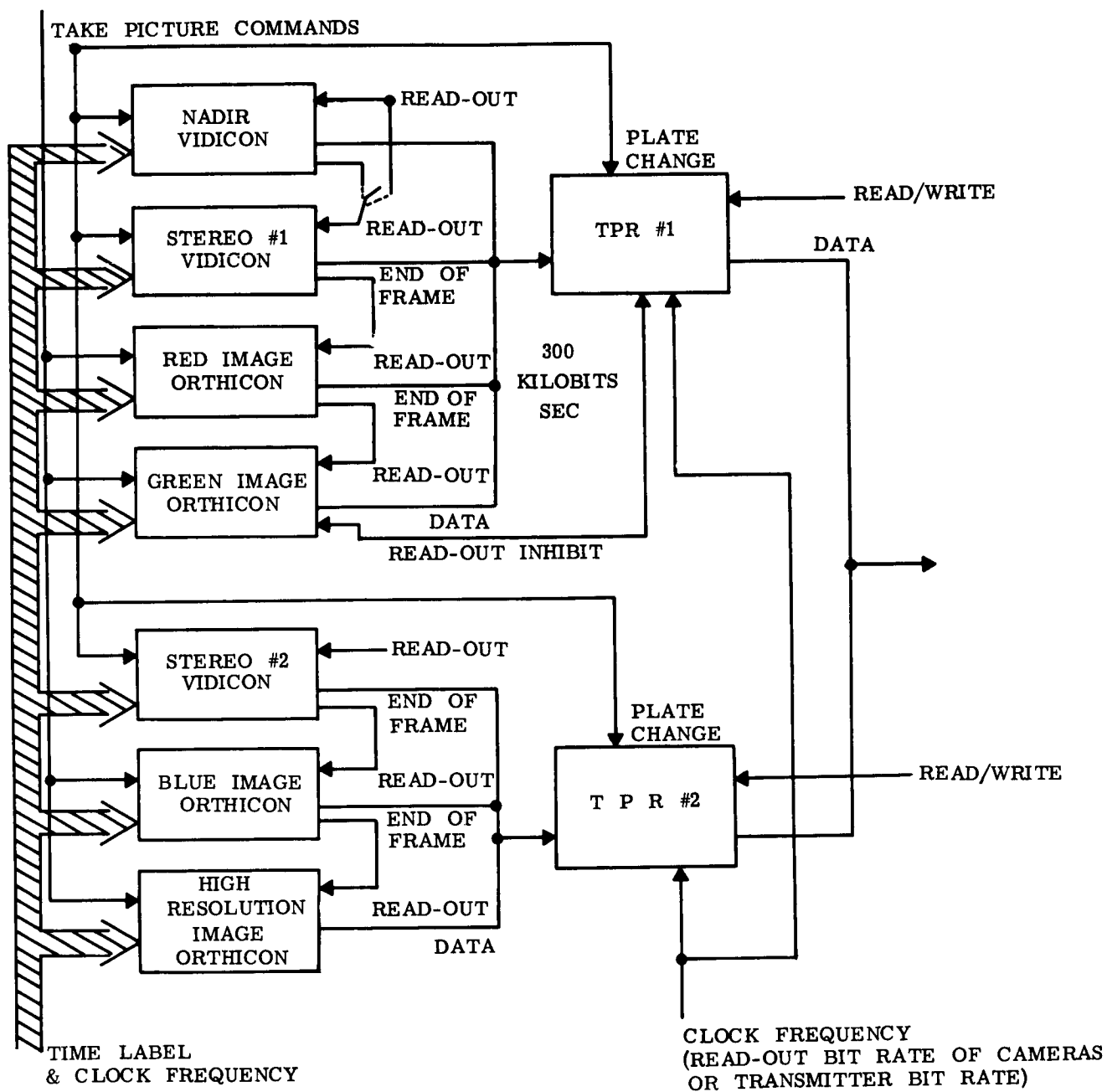


Figure 1.8.2-1. Television and TPR Interconnection

forthcoming. The camera unit will automatically cycle through the readout format as shown in the diagram. When the "End Frame Sync Word" is completed an "End of Frame Signal" will be present at the camera output. In the case of the first frame, this will not be used. However, in succeeding frames this signal can be connected to the "Readout Command" input line of the next camera in the sequence. When one frame has been read out of a camera, the frame from the next camera can follow immediately. The clock in the Programmer and Computer Subsystem will be used as the source for the sync signals. The frames will be read out of the camera unit and into the TPR unit at a 300 kbps rate. The TPR unit will generate its own vertical and horizontal sweep signals from this clock. The first nadir vidicon frame and the red and green image orthicon frames will be stored on Plate No. 1 of TPR # 1. The No. Plate of TPR #2 will contain the digital data from the blue and high-resolution image orthicon pictures.

The plates will be changed each time the command to take vidicon pictures is given. The plates can also be changed by direct command, but this mode of operation is not necessary during the normal photographic mapping operation, since the sequence is such that two image orthicon frames and one vidicon frame can be put on a single plate in each TPR unit. The exception to this operation is at the beginning and end of each mapping sequence when three vidicon frames and four image orthicon frames are taken in a sequence pair. In this case, one TPR unit will be used to record two I. O. frames and two vidicon frames. Thus, one of the I. O. frames will be on two plates. In this mode each plate on TPR # 1 will be filled with data. When the end of the plate is reached, a "Read-Out Inhibit" signal will be sent to the camera unit which is presently reading out data to the TPR unit. The "Read-out Inhibit" signal will also cause the TPR unit to change plates. Once the plates are changed, the "Read-out Inhibit" signal will cease, and the camera unit will begin to read out data again.

As shown in Figure 1.8.2-1, the nadir and No 1 stereo vidicon and the red and green image orthicons normally feed TPR # 1. No. 2 stereo vidicon, the blue and the high-resolution image orthicon feed TPR #2. This, of course, is not the only possible mode of operation. Since the camera units can be connected to either of the TPR units, any combination is possible.

When the TPR units are being used to playback TV data, the C & C Unit Clock is used to control the read-out rate. When the end of a plate is reached, a signal is sent to the other TPR unit, which will begin to read-out the plate which is in position. Thus the read-out of all data is accomplished in this manner by switching back and forth between the two TPR units. Note, that the method of readout will not interfere with the logical transmission of data. The first TPR plate on unit #1 will contain the nadir vidicon and, red and green I. O. pictures. The second plate read out (from TPR # 2) will contain the blue and high resolution I. O. picture taken at the same instant as the red and green scenes. This sequence will continue throughout the readout.

1.8.3 ORBITER-LANDER RELAY LINK OPERATION — MARS 1969

Before transmission from a Lander to the Orbiter can be initiated, several conditions must be satisfied simultaneously. They are:

1. Power must be available in the Lander
2. Line of sight condition must exist between Lander and Orbiter
3. Slant range must be within acceptable limits

The simultaneous occurrence of these conditions during the first few orbits can be predicted prior to launch with enough accuracy to pre-program the transmission periods. Later, however, pre-programming is not adequate because of the possible variations of orbital period. Therefore, the transmission periods must be commanded from Earth

after the orbit and landing site have been accurately determined. When the commands are to be transmitted to the Lander, they are read into a buffer storage and a relay link acquisition process is initiated.

First an unmodulated carrier is transmitted to the Lander. The Lander receiver, which is continually searching for the carrier, locks to the carrier. A carrier lock signal from the receiver then initiates the transmission of an unmodulated carrier to the Orbiter. When carrier lock is achieved in the Orbiter, a lock signal is provided to the Command and Computer Subsystem which initiates modulation of the transmitted carrier. The modulating waveform is the repetition of selected commands and the associated bit sync waveform. The commands designate which Lander is being addressed (both can operate simultaneously if desired) and the bit rate at which the Lander is to transmit, since it is capable of sending at any one of several bit rates. (The desired operating bit rate will have been estimated on the Earth and the command designating it will have been transmitted from the Earth to the Orbiter prior to the initiation of the acquisition process)

The Lander will now receive the modulated carrier and the data detector will lock to the bit sync waveform. The sync lock signal initiates operation of the Lander command subsystem, which detects the bit rate command and initiates modulation of the transmitted carrier at the designated bit rate (the modulating waveform comprises an arbitrary bit sequence and associated bit sync information). When bit sync lock is attained in the Orbiter, both links are ready for operation. The sync lock signal from the Orbiter data detector initiates the transmission of the stored commands from the Orbiter to the Lander. These commands then control the subsequent operation of the Lander including that of data transmission to the Orbiter.

SECTION 2. TELEVISION SUBSYSTEM

2.1 SUMMARY

In general, the mission for the Voyager television is to obtain biological and geological information about Mars and information about cloud movements and possibly geological features of Venus. The television mission for the various vehicles and mission opportunities is given in Tables 2.1-1 and 2.1-2 while Table 2.1-3 lists the systems constraints imposed on the television subsystem in the form of orbital geometry and transmission bandwidths. The characteristics that are required of the television camera to perform these missions are listed in Table 2.1-4.

2.1.1 ORBITER TELEVISION

The daylight portions of the Martian surface and the Venus cloud cover are to be mapped by television cameras having various resolutions installed in an Orbiter. The Mars Orbiter television cameras are designed to provide optical resolutions of 1 km, 140 m (in color), and 20 m at the periapsis. The low resolution cameras provide a stereo pair having a height resolution of 345m. The Venus cloud cover will be mapped with an optical resolution of 2 km at periapsis.

2.1.2 LANDER TELEVISION

The Mars Landers are equipped with one television camera with steerable optics such that clouds, the horizon, and the terrain in the immediate vicinity of the landing site can be scanned through 360 degrees during daylight hours. A television camera attached to a microscope is also provided for examination of soil samples and for planned biological experiments. The panoramic camera will resolve three minutes of arc (in color); the microscope will resolve 1μ , 5μ , and 50μ (in color). The Venus Lander television will provide infrared surface information during descent and limited panoramic surface coverage in the visible spectrum, using flash illumination. A microscope has been incorporated only in the longer-life Venus 1972 Lander.

2.1.3 RESOLUTION PARAMETERS

For optimum bandwidth utilization, four bits per sample has been chosen in the Orbiter digital television cameras while the tube raster contains the maximum number of resolvable lines (512 for a one-inch vidicon and 1,024 for a two-inch image orthicon). The four-bit quantization was selected after studies including study of photo-interpretation techniques and in consideration of the low resolution obtainable. The number of raster lines was made large to maximize the field of view. In the Lander television, full tonal rendition (6 bits per sample) seems necessary, while 256 lines per raster provides a reasonable field of view (about $4\frac{1}{2}$ degrees).

2.1.4 CAMERAS

Since the vidicon is an inherently simple and rugged camera tube which has been used previously in space applications and can be built to withstand heat sterilization, it is used where practicable in the recommended subsystem. Although the image orthicon does not offer these features, it is recommended for the medium - and high-resolution Orbiter cameras, since its high sensitivity allows the use of much smaller lenses. The minimum signal-to-noise current ratio in the camera video signal has been set at 35. The slow-scan vidicon was analyzed and an appropriate derating factor was found to account for the long frame times necessary at Voyager bandwidths. The tube was considered noiseless. All noise was considered as originating in the pre-amplifier. The sensitivity at three-second frame rates was calculated to be approximately 0.33 foot-candle-seconds.

TABLE 2.1-1. MARS TELEVISION MISSION

Function	Mars '69 & '71 Orbiters*				Mars '69, '71, '73 & '75 Landers	
	Map	Map	Map	Map	Panorama	Microscope
Number of Cameras	2	1	3	1	1	1
Optical Resolution	1 Km	1 Km	140 m	20 m	3 Min. of Arc	1 μ , 5 μ , 50 μ
Stereo	345 m	no	no	no	no	no
Color	no	no	yes	no	3 filters	3 filters
Camera Designation (Section 2.4)	(a)	(a)	(b)	(c)	(d)	(e)

*(The Mars '73 Orbiter and '75 flyby do not carry TV)

TABLE 2.1-2. VENUS TELEVISION MISSION

Function	Venus '70 & '72 Orbiters		Venus '70 Lander		Venus '72 Lander	
	Map Clouds	Descent	Panorama	Descent	Panorama	Microscope
Number of Cameras	1	1	1	1	1	1
Optical Resolution	2 Km	1 Min. of Arc Max.	3 Min. of Arc	1 Min. of Arc Max.	2 Min. of Arc	1 μ , 5 μ , 50 μ
Stereo	no	no	no	no	no	no
Color	no	no	3 Filters	no	3 Filters	3 Filters
Camera Designation (Section 2.4)	(f)	(g)	(h)	(g)	(h)	(e)

TABLE 2.1-3. VOYAGER SYSTEMS CONSTRAINTS

	<u>Mars '69</u>	<u>Mars '71</u>	<u>Venus '70</u>	<u>Venus '72</u>
Orbit (n. m.)	1000 x 19, 000	1000 x 19, 000	1000 x 4300	1000 x 7300
Inclination	55°S	45°N	68°	90°
Number of Recorders	2	2	2	1
Recorder Input	300 kbps	300 kbps	100 kbps	100 kbps
Transmission Bandwidth	2-16 kbps	2-16 kbps	8-64 kbps	2-16 kbps

TABLE 2.1-4. TELEVISION CAMERA CHARACTERISTICS

<u>Module</u>	<u>Camera</u>	<u>No. of Lines</u>	<u>No. of Bits/Sample</u>	<u>No. of Bits/Frame</u>
Orbiters	Low Resolution (Vidicon)	512	4	1, 048, 576 + Sync. and Ident. $\approx 1.1 \times 10^6$
	Medium Resolution (Image Orthicon)	1024	4	4, 194, 304 + Sync. and Ident. $\approx 4.3 \times 10^6$
	High Resolution (Image Orthicon)	1024	6	6, 514, 584 + Sync. and Ident. $\approx 6.6 \times 10^6$
	Descent (Vidicon)	512	6	1, 572, 864 + Sync. and Ident. $\approx 1.7 \times 10^6$
	Panorama & Microscope (Vidicon)	256	6	393, 216 + Sync. and Ident. $\approx 4.2 \times 10^5$

The sensitivity of an image orthicon at a signal-to-noise current ratio of 35 was found to be approximately 3.3×10^{-4} foot-candle-second. The noise originating at the photocathode, the target, the first dynode, and in the beam was considered the major noise contribution in the system.

The dependence of the signal-to-noise ratio on the scan velocity indicates that the dwell time of the beam on each picture element should be minimized while the frame time remains long. A digital scan, therefore, is recommended. In this type of scan, the beam remains only a short time on the element to be sensed and then returns to a dormant part of the target.

Special automatic control circuits are needed to operate the cameras without adjustments over a long period of time. Automatic vidicon cameras have already been developed. Self-adjusting image orthicon cameras are now being designed by the Hazeltine Corporation and the General Electric Advanced Electronics Center. Highlight determination, using the camera tube as a sensor, and protection of the tube face from direct sunlight will also be accomplished. A computing circuit designed for Project Mariner is selected for high-light determination. A separate sun sensor will be incorporated for sunlight protection.

2.1.5 OPTICS

Optical systems have been calculated for the various vehicles and missions. A simple telescopic lens was found sufficient for the low resolution Orbiter stereo cameras. Maksutov folded optics are selected for the medium and high resolution Orbiter cameras. A double Gaussian type lens is selected for the Lander panoramic television. The microscope and the infrared descent optics are also state-of-the-art design.

2.1.6 STEREO

The height resolution of the stereo cameras was calculated using empirical factors obtained from the experimental data of photo-interpretation experience. The 1 km resolution cameras will resolve 345 meters at a canting angle of 20 degrees to the local vertical. This height resolution is to be interpreted as the ability of the television system to deliver stereoscopic pictures on which spot height differences of 345 meters can be recognized with 95 percent confidence while lesser heights cannot be determined. It is expected that a general physiographic map of the planet can be assembled from the information obtained.

2.1.7 ARTIFICIAL ILLUMINATION FOR VENUS

Artificial illumination is considered necessary to obtain television pictures from the Venus Lander in the visible spectrum. Electronic flash equipment and chemical flares were investigated for this mission. Both appear feasible. The electronic flash equipment is recommended, however, on the basis of repeatability, reliability, and the uncertain atmospheric information available for the development of usable chemical flares.

2.2 ESTABLISHMENT OF SUBSYSTEM REQUIREMENTS

Several trade-offs among TV subsystems component parts are possible while the subsystem as a whole still performs the mission. Examination of the subsystem requirements in terms of maximum possible information content, terrain coverage and data reduction problems, however, leads to a better definition of the components and their operation.

2.2.1 INFORMATION CONTENT

The information content in a television picture is limited by the picture quality in terms of the signal-to-noise ratio, the resolution obtained, and the number of gray shades that can be reproduced.

It is standard broadcast practice (and applicable in this case) to define an acceptable television picture by a signal-to-noise ratio (ratio of peak-to-peak signal current to rms noise current) of 35. Experiments performed by JPL (Reference 1 of Section 2.6) on space television subsystems have also shown that a signal-to-noise ratio (S/N) of 35 is satisfactory. This corresponds to 30.9 db.

The resolution requirements are stated as part of the mission and were given in Section 2.1. They define an area on the planet surface over which light is integrated by the sensor. The resolution of a camera, therefore, defines not only the minimum distance between two points which can be resolved but also an area in which changes in brightness affect only the average and are not sensed per se.

The number of gray shades that can be reproduced in a digital television system is directly related to the number of quantization levels into which the black-to-white signal is divided. Experiments (Reference 2 of Section 2.6) have shown that 64 quantization levels (six bits/sample) give a complete rendition of the ten gray levels conventionally used in broadcast television charts. Experiments by EMR with color scenes supplied by GE (Reference 3 of Section 2.6) confirm no loss of tonal information for six bit/sample encoding.

For low-resolution mapping, however, no significant information is contained in an apparent small change in scene brightness; in fact, a contouring effect is noted when the number of quantization levels is decreased which enhances the information that is present. EMR experimental results (Reference 3 of Section 2.6) with degraded resolutions confirm this conclusion and consultation with professional photo-interpreters (Reference 4 of Section 2.6) led to the selection of only four bits/sample for the low resolution Orbiter cameras. In the 20-meter resolution Orbiter camera and the Lander camera, full rendition of tonal values is necessary, however, and six bits/sample have been selected there.

2.2.2 TERRAIN COVERAGE

Complete coverage of the sunlit portion of the planet is required of the low-resolution Orbiter cameras, and the Lander "panoramic" camera must scan through an angle of 360 degrees. The total number of pictures per orbit (or per 360 degree Lander scan) is, therefore, dependent on the field-of-view of the cameras. The field-of-view should be large, if bandwidth is to be conserved, since at least ten percent overlap of adjacent pictures is required.

The field-of-view of the Orbiter cameras is fixed by the resolution requirement, the canting angle, and the number of lines in the television tube raster.

The resolution requirement is given, and the canting angle is established for the minimum discernable height increment (see Section 2.3). The maximum number of lines resolvable on slow-scan electrostatic vidicon camera tubes is 400-500 lines (Reference 5 of Section 2.6) and that on the electrostatic image orthicon (being developed by the GE Power Tube Department) is 600-800 lines per raster height (Reference 6 of Section 2.6). The number of raster lines for the Orbiter cameras was, therefore, established as 512 lines for those using one-inch vidicon tubes and 1024 lines for those using two-inch image orthicon tubes (the nearest binary number to the limiting resolution divided by the Kell factor, as indicated in Section 2.3).

In the Orbiter television, the requirement of complete coverage also establishes the minimum time between exposures, and the camera tubes must be read out in this time period. This minimum time between pictures of one minute which occurs at periapsis is equal to the maximum frame time. The storage requirement that is so established is discussed in Section 1.3.

In the Lander panoramic camera, the total number of pictures per scan will again be minimized. In this unit, however, the parts of the pictures that carry no significant information, the foreground and the sky in a horizon view, are increased with the field-of-view. A compromise design was, therefore, needed and a field-of-view of approximately six degrees has been selected. This field-of-view could be covered by 256 television lines at the required resolution.

2.2.3 DATA REDUCTION

The data reduction problems of display and interpretation are reflected into the subsystem design. Sufficient time must be allowed between lines and frames for insertion of synchronization and identification. Appropriate circuitry must be provided for these purposes.

It is assumed that existing display equipment using pseudo-noise sequence synchronization will be used.

A pseudo-noise sequence will consist of $(2^n - 1)$ bits. Thirty-one bits for synchronization was selected as reasonably far removed from the six-bit video code. The sync will be inserted at the beginning and the end of each line and frame.

It is required that complete maps be assembled from both the Orbiter and the Lander pictures. Good identification of each frame and line is, therefore, necessary. Line and frame requirements are as follows.

Each line will be identified with 89 bits:

- a. Line number = 10 bits
- b. Frame number = 14 bits
- c. Camera number = 3 bits
- d. Sync = 62 bits

Each frame will be labelled with 130 bits:

- a. Frame number = 14 bits
- b. Camera number = 3 bits
- c. Orbiter or Lander code = 2 bits
- d. Orbit number = 14 bits
- e. Mission time at exposure = 20 bits
- f. Filter number = 2 bits
- g. Azimuth angle = 10 bits
- h. Elevation angle = 3 bits
- i. Sync = 62 bits

A total of 45,698 bits is then needed in each 512-line frame for identification and synchronization. A 256-line frame will increase by 22,914 bits and a 1024-line frame by 91,266.

2.3 ANALYSIS

The three major components of the television subsystem are: Optics, Sensors, Camera Electronics.

These components are analyzed in the following sections taking into consideration the restrictions listed in Table 2.1-4. Those areas which are particular to the Voyager mission are treated in detail. Standard television design is used in all other portions of the discussion.

2.3.1 OPTICS

The optical parameters that define the lens are based on the requirements of the individual systems that are given in Table 2.1-1. These parameters and method of solution are listed below.

A. Focal Length

The focal length is given by the geometrical relationship:

$$F = (\text{Resolution Element at Camera Tube}) \left(\frac{\text{Altitude}}{\text{Resolution Element on Ground}} \right) \quad (1)$$

B. Minimum Diffraction Aperture Diameter

The physical optics formula

$$D = \frac{1.22}{\text{Angular Resolution Required}} \quad (2)$$

gives the aperture at which the central disk of the diffraction pattern of a point source coincides with the first minimum of another source when the two subtend the required angle. The two sources are then just resolved.

C. Exposure Time

In the case of the Orbiter optics, there are three separate contributions to the relative motion between the camera and the subject area on the planet. These are the angular velocity of the camera about the c.g. of the vehicle, the orbital trajectory of the vehicle about the planet, and the rotation of the planet about its axis. The latter contribution is small in this application. The formula relating the other contributions is:

$$t_E = \frac{\frac{1}{4} R_G}{W_S h + \frac{r}{r+h} V_h} \quad (3)$$

where

t_E = exposure time

R_G = linear dimension of resolution element on ground

W_S = angular velocity of vehicle about its c.g.

r = radius of planet

h = altitude of vehicle

V_h = horizontal velocity of vehicle in orbit.

Exposure time during Lander descent is influenced by the angular motion of the Lander about its c.g., the rotation of the planet about its axis, and the horizontal drift of the Lander during descent. The rotation of the planet is a minor contribution. Horizontal drift of the Lander is also minor during the picture-taking period. The other contribution, the swing of the Lander caused by the parachute, is indeterminant. Television pictures during this mode are, therefore, on a best-efforts basis. Exposure time at the surface is influenced only by motion within the subject area. Such motion will be primarily due to winds. A maximum exposure time of 1/4 second was chosen for this purpose.

D. Relative Aperture

A minimum acceptable exposure is first selected for the sensor. In the case of the vidicon, this is 0.33 ft-cdl-sec; for the image orthicon 0.33×10^{-3} ft-cdl-sec; for photographic film, the exposure corresponding to the center of the straight line portion of the H and D curve for the film. This usually corresponds to a photographic density of 1.0 to 2.0. Calling this quantity E_{\min} , the formula for the relative aperture is

$$F/\text{no} = \sqrt{\frac{t_E \pi B \tau}{4E_{\min}}}$$

where τ = transmission of the optics

B = scene brightness

(4)

E. Field of View

The field-of-view is given by the geometrical formula:

$$\tan 1/2 (\text{FOV}) = \frac{1/2 \text{ Frame Size}}{\text{Focal Length}} \quad (5)$$

F. Calculations for Required Optics

An example calculation follows for an Orbiter vidicon camera that always points to the nadir and is required to resolve 1000 meters on the ground at an altitude of 1000 nautical miles. The vidicon raster is 11 x 11 mm. The number of television lines is 512, of which $0.7 (512) = 350$ television lines may be used in resolution calculations. There are then 175 optical resolution lines (since two television lines constitute one optical line pair).

$$f = 11/175 \frac{1852 \times 10^3}{1000} = 116.4 \text{ mm} = 4.58 \text{ inches} \quad (6)$$

$$D = \frac{1.22 (22 \times 10^{-6})}{1000} = 0.0497 \text{ inches} \quad (7)$$

$$\frac{1852 \times 10^3}{1852 \times 10^3}$$

$$t_{E/0^\circ} = \frac{1/4 (1000) (3.28)}{(.00005) (1000) (6080) + \frac{1800}{2800} (12500)} = 0.0983 \text{ sec. at periapsis} \quad (8)$$

$$t_{E/90^\circ} = \frac{787.5 (3.28)}{(.00005) (3150) (6080) + \frac{1800}{4950} (7100)} = 0.7297 \text{ sec. at } 90^\circ \text{ from periapsis} \quad (9)$$

TABLE 2.3.1-1. OPTICAL CHARACTERISTICS

Function	Focal Length	Diffraction Aperture Diameter	Minimum Exposure Time	Maximum Speed F/No.	FOV	Actual Aperture Diameter
(a)	4.58 in.	0.0497 in.	0.0983 sec	1:3.45	5°24'	1.33 in.
(b)	40.16 in.	0.355 in.	0.0138 sec	1:20.4	1°30'	1.97 in.
(c)	281.2 in.	2.485 in.	0.002 sec	1:23	0°12'	12.23 in.
(d)	5.68 in.	0.031 in.	0.25 sec (max)	1:1	4°22'	5.68 in.
1	3mm (min.)	Not Appl.	Not Appl.	0.25 Num. Apt. (min)	0.175mm	Not Applicable
(e) 5	14mm (min.)	Not Appl.	Not Appl.	0.05 Num. Apt. (min)	0.875mm	Not Applicable
50	50mm (min.)	Not Appl.	Not Appl.	0.005 Num. Apt. (min)	8.750mm	Not Applicable
(f)	2.29 in.	0.0249 in.	0.1966 sec	1:25	10°48'	0.1 in.
(g)	16.65 in.	0.75 in.	0.01 sec	1:5	1°27'.5	3.33 in.
(h)	5.68 in.	0.031 in.	0.25 sec (max)	1:1	4°22'	5.68 in.

(Corresponding lens weights and sizes are given in Table 2.4-1.)

Brightness of Mars (see appendix):

$$820 \cos 31^\circ = 703 \text{ ft-lamberts at periapsis} \quad (10)$$

$$28.7 \text{ ft-lamberts at } 90^\circ \text{ from periapsis} \quad (11)$$

Exposure for vidicon is 0.33 ft-cdl-sec.

$$f/\text{No.} = \frac{(.0983)(703)(.75)}{4(.33)} = 6.27 \text{ at periapsis} \quad (12)$$

$$f/\text{No.} = \frac{(.7297)(28.7)(.75)}{4(.33)} = 3.45 \text{ at } 90^\circ \text{ from periapsis} \quad (13)$$

$$\tan 1/2 \text{ FOV} = \frac{5.5}{116.4} = 0.04725 \quad (14)$$

$$\text{FOV} = 5^\circ 24' \quad (15)$$

Table 2.3.1-1 lists the optical characteristics for the various functions described in Table 2.1-1.

Following Table 2.3.1-1 are Figures 2.3.1-1 to 2.3.1-4 that illustrate the variation of the parameters, focal length, relative aperture, exposure time and field of view with resolution required at 1000 nautical miles altitude. It will be noted that in all cases the parameter increases rapidly with higher resolution requirement.

G. Extension Of Analysis To One-Meter Ground Resolution

The physical dimensions of the lens needed to produce a resolution of one meter on the ground become inordinately large at the 1000 nautical mile altitude discussed previously. The focal length, for instance, becomes 469 feet. The analysis of this section is, therefore, limited to orbits in which the periapsis altitudes are 100, 300 and 700 nautical miles; the orbits having the dimensions, 100 x 19000, 300 x 19000, and 700 x 19000 nautical miles, respectively.

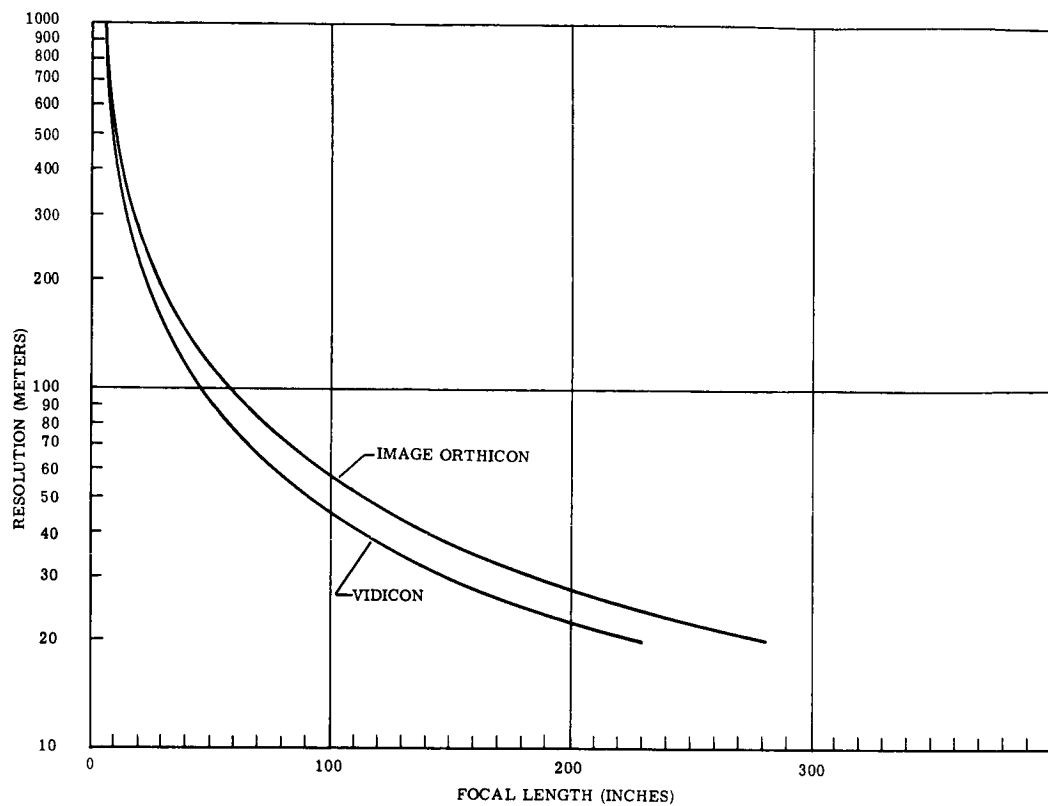


Figure 2.3.1-1. Focal Lengths of Lenses Vs. Resolution, Vidicon and Image Orthicon

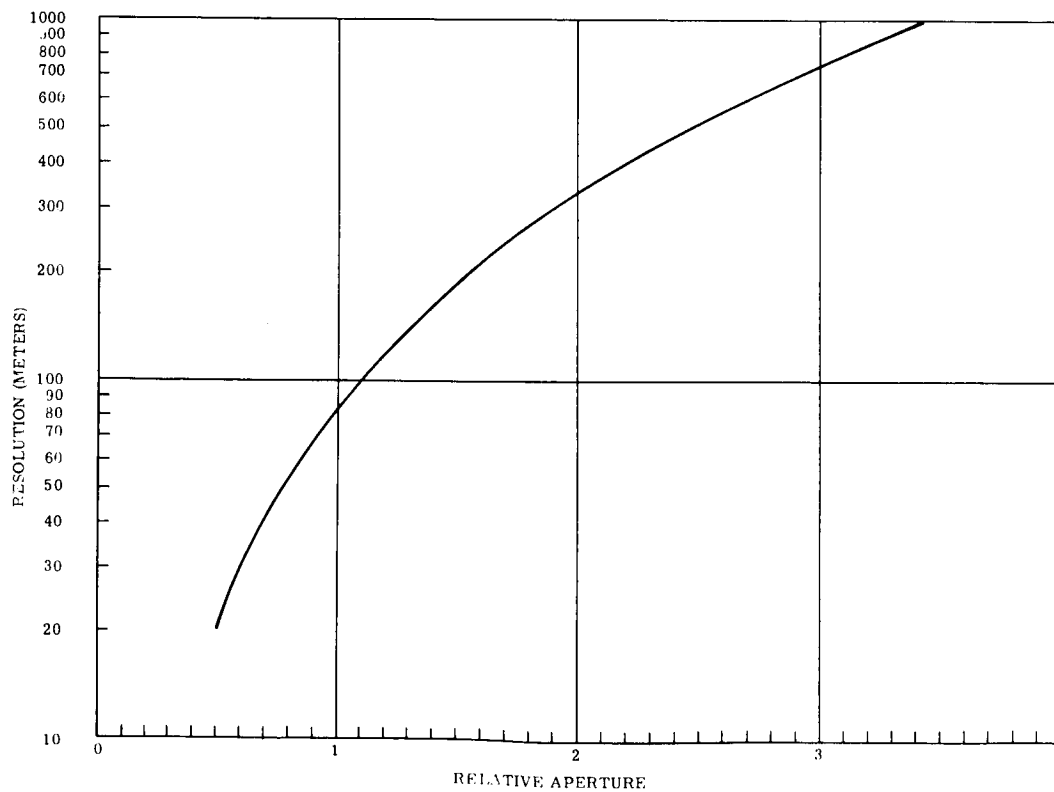


Figure 2.3.1-2. Relative Aperture Vs. Resolution

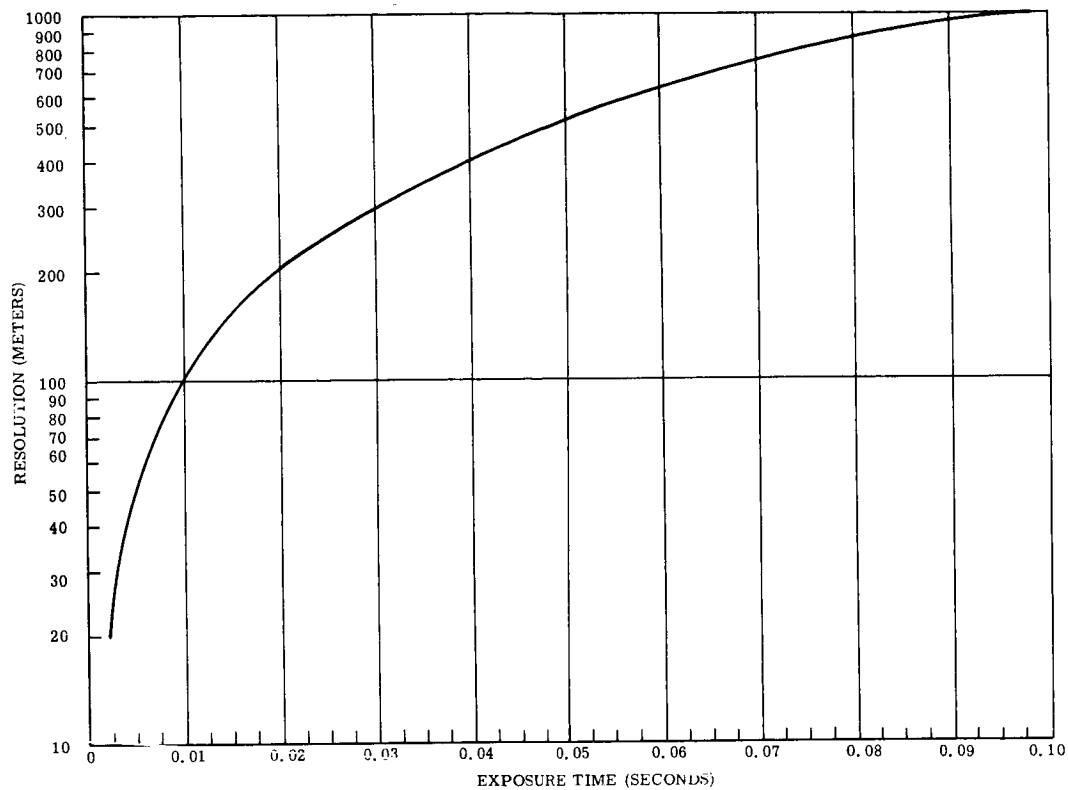


Figure 2.3.1-3. Maximum Exposure Time Vs. Resolution

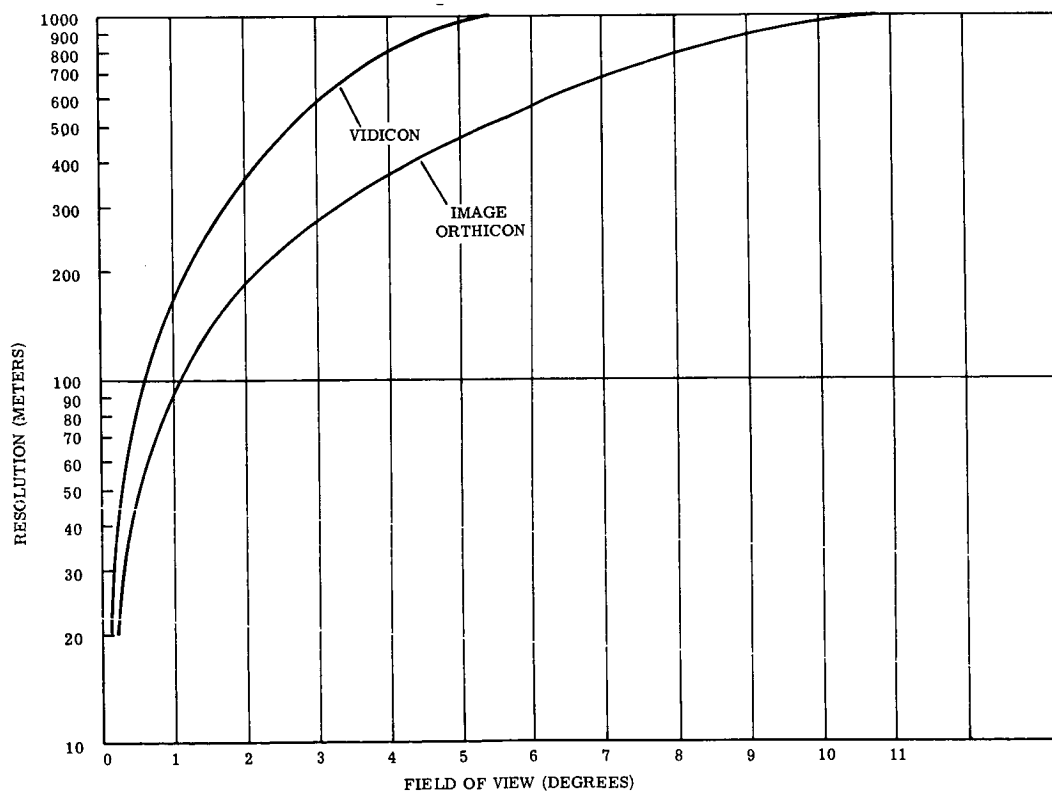


Figure 2.3.1-4. Field of View Vs. Resolution

The analysis involves the same quantities of focal length, exposure time, f/no., field-of-view, etc. as in the previous sections. An image orthicon camera having a minimum highlight response of 0.00033 ft-cdl-sec is assumed. Table 2.3.1-2 lists the results. Because of the large dimensions of the lenses, no attempt is made to estimate their weights. The gross difference, between required diffraction-limited aperture diameter and exposure aperture diameter, emphasizes the fact that, if high resolution is to be attained, image motion compensation (thus permitting longer exposure time) will be required.

The application of photographic techniques to this application is given in Appendix B.

TABLE 2.3.1-2. TELEVISION LENS CHARACTERISTICS FOR ONE-METER GROUND RESOLUTION

Altitude (Nautical Miles)	Focal Length (Feet)	Max. Exposure Time (Milliseconds)	Relative Aperture (Maximum)	Diameter (Feet)	Diffraction Aperture Diameter (Feet)	Field-of- View (Degrees)
100	46.9	Periapsis: 0.0557 90° from Periapsis: 2.828	4.72	9.94	0.414	0.108
300	140.6	Periapsis: 0.0647 90° from Periapsis: 1.226	4.47	31.45	1.243	0.036
700	328.1	Periapsis: 0.0835 90° from Periapsis: 0.814	3.63	90.39	2.899	0.0154

2.3.2 SENSORS

Of the various types of camera tubes, only the vidicon and the image orthicon are suitable when considering sensitivity, weight, and absence of magnetic fields due to deflection and focus coils.

A. Vidicons

Vidicons, due to their simplicity, are small, light, rugged, and reliable. They have operational histories in space missions. On consideration to the accumulated experience and reliability data alone, they are the most preferred tube to use in the voyager television subsystem.

Another important advantage of vidicons is that, by their nature, they are not limited to storage below the sterilization temperature of 145°C. Considerable development is necessary, however, to qualify them for sterilization at that temperature. From a quotation received from the General Electrodynamics Corporation for the development of such a camera tube, however, it appears to be a solvable problem.

The photosensitive surface on a vidicon is a photoconductive semiconductor with an equivalent circuit as shown in Figure 2.3.2-1 (Reference 1 of Section 2.3).

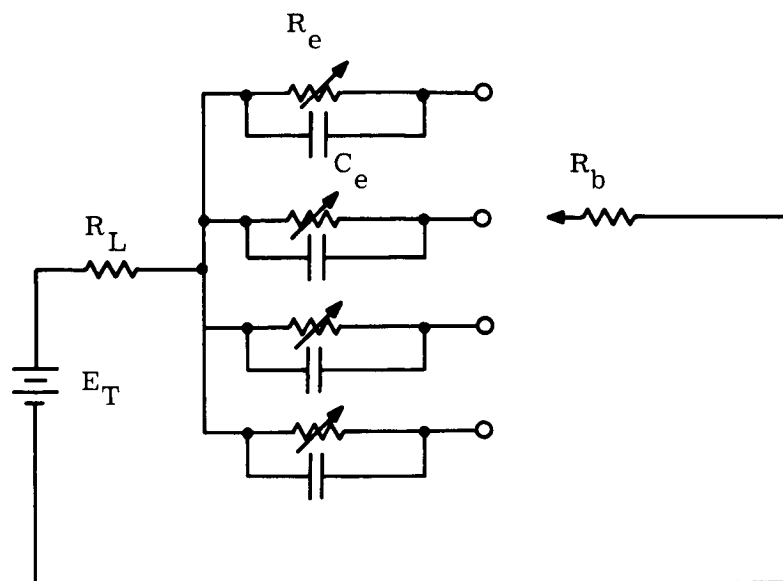


Figure 2.3.2-1. Equivalent Circuit

The symbols used in Figure 2.3.2-1 are defined as follows:

C_e = target element capacitance

R_e = target element resistance

R_b = Beam resistance

R_L = load resistance

E_T = applied target potential

The value R_e changes with the incident light level and C_e is discharged through R_b . The charge is then replenished by the scanning beam.

The vidicon signal is practically noiseless, the noise present in the video being mostly due to the preamplifier. The output signal-to-noise ratio (S/N) is defined as:

$$S/N = \frac{\text{Signal Current}}{\text{RMS Amplifier Noise Current}} \quad (21)$$

The signal current, $\frac{dq}{dt}$, at a certain incident light level is directly proportional to the scanning rate, while the preamplifier noise current is approximately proportional to the square root of the video bandwidth. Slow-scan operation, therefore, decreases the sensitivity of the tube.

The signal current in a vidicon varies as approximately the 0.7 power of the scene illumination, such that the sensitivity varies as

$$\log E_2 = \frac{0.7 \log E_1 + \log i_1/i_2}{0.7} \quad (22)$$

where

E_n = the minimum faceplate illumination at frame rate, T_n

i_n = signal current at frame rate T_n

For $E_1 = 0.6$ foot-candles at broadcast rates, $E_2 = 10$ foot-candles at a frame rate of 3.3 seconds and constant S/N.

This value of minimum faceplate illumination is used in the optical calculations. Other vidicon parameters are listed in Table 2.3.2-1.

B. Image Orthicons

Image orthicon camera tubes are two-to-three orders of magnitude more sensitive than vidicons. However, they have not been used for space applications so far, mostly due to their complexity, large size, and the excessive weight of magnetic deflection and focus coils. Electrostatic image orthicons are being developed, however, and a contract for the development of an image orthicon camera for space use has been awarded by NASA. It is felt, therefore, that it will be reasonable to assume successful space operation of image orthicons prior to the time of a Voyager design program.

Image orthicons employ a photoemissive surface which is sensitive to heat, however, and will be permanently damaged if stored at temperatures above 75°C. Therefore, this type of tube cannot be used in modules where sterilization is a requirement.

For the medium and high resolution Orbiter cameras, the higher sensitivity results in considerable reduction in optics weight and size, so the image orthicon tubes are recommended for these applications.

The sources of noise in an image orthicon are the photocurrent, the target, secondary emission, the beam, and the dynode of the electron multiplier. The effects of the photoemissive properties of the photocathode, the secondary emission ratio of the target and the dynode, and the beam shot noise can be lumped into one constant, F . $F = 2.5$ for a modulation ratio of 0.3 in a typical I.O., and the signal-to-noise ratio becomes (Reference 12 of Section 2.6):

$$S/N = \frac{E_o A_r S}{2e B F} \quad (23)$$

where

E_o = faceplate illumination

A_r = sensitive area of the tube in cm^2

S = sensitivity in amperes/lumen

e = electronic charge = 1.6×10^{-19} coulombs

B = bandwidth in cps

TABLE 2.3.2-1. VIDICON PARAMETERS

Sensitivity: 0.02 ft-cdl-sec
 Raster Area: 11mm x 11mm
 Heater Power: 0.6 watts
 Size: 1.125" dia x 6.5" long
 Max. Readout Time: 5-20 sec
 Max. Storage Time: Several minutes

The minimum faceplate illumination for an I.O. is then

$$E_o = \frac{S^2}{N} \frac{2te\pi BF}{A_r S} \quad (24)$$

$$A_r = 7.29 \text{ cm}^2 \text{ and}$$

$$S = 150 \text{ A/lumen}$$

$$B = \frac{(\text{Number of Lines})^2}{2 (\text{Broadcast Frame Time})} \quad (25)$$

$$e = 1.6 \times 10^{-19} \text{ coulombs}$$

$$S/N = 35$$

$$E_o = 1.41 \times 10^{-5} \text{ lumens/cm}^2$$

$$= 1.31 \times 10^{-2} \text{ foot-candles}$$

A value of 3.3×10^{-4} foot-candle-seconds has been used for optical calculations. Other image orthicon parameters are listed in Table 2.3.2-2.

TABLE 2.3.2-2. IMAGE ORTHICON PARAMETERS

Sensitivity: 3.3×10^{-4} ft-cdl-sec
 Raster Area: 11 mm x 11 mm
 Heater Power: 0.6 watts
 Size: 1.125" dia x 6.5" long
 Max. Readout Time: 1 min
 Max. Storage Time: several hours

Preamplifier noise considerations are the same as those for the vidicon. The tube noise is independent of scan velocity while the preamplifier noise is not. However, the tube noise is the limiting factor and low-noise circuits are available (Reference 13 of Section 2.6) which do not significantly affect the S/N.

2.3.3 CAMERA ELECTRONICS

The camera electronics will consist of standard television circuitry plus circuitry which is necessary for the space application.

In order to increase the sensitivity of the sensors, scan conversion circuitry will be used which keeps the scan rate high while the frame rate is still in the order of 5 seconds.

Space cameras must also be fully self-adjusting over long periods of time and automatic control circuitry will be provided for this.

The video signal-to-noise ratio depends on the scan rate, which should be kept as high as possible, while the frame rate remains low to decrease the bandwidth needed.

A buffer storage will be needed in which one line is recorded at a high scan rate while it is read out at a low frame rate. This must be supplied for analog readout and storage of one line; or, for a digital scan, the tube face can be used to store while each element is read out. The digital scan involves lighter equipment and is available from Electromechanical Research Inc. (Reference 3 of Section 2.6).

Control circuitry must be present to interpret the highlights on the tube face and to adjust tube parameters and iris settings. JPL (Reference 14 of Section 2.6) has developed a highlight computing circuit that can be used for both the vidicon and the image orthicon beam current and target voltage control. A sun sensor must also be incorporated that closes an iris to protect the tube from direct sunlight. Both Hazeltine Corp. and the G. E. Advanced Electronics Center are developing automatic focusing circuits for the image orthicon (Reference 13 of Section 2.6).

2.3.4 STEREO CALCULATIONS

A. Minimum Detectable Height (1 KM System)

Previous research (Reference 7 of Section 2.6) on the minimum heights detectable by typical observers on stereoscopic imagery indicates that the following equation provides an accurate estimate of observer performance:

$$h_{(\min)} = \frac{(H/f) \times C}{(B/H) \times R \times 2} \quad (26)$$

where:

- $h_{(\min)}$ = smallest increment of height detectable stereoscopically
- H = altitude of exposures above datum
- f = focal length of camera
- C = factor to correct for change in optical path length due to tilting of camera axis and planet curvature
- B = air base distance between exposure stations
- R = resolution of imaging system, in optical line pairs per unit distance
- 2 = empirical factor derived from performances of 10 observers

The factors in this equation as written are adapted to earth imaging situations and require minor modifications.

The numerator of the equation is simply the calculated scale factor (reciprocal of the representative fraction) of the image on the focal plane of the camera. Since camera altitude is large in comparison to the radius of the planet, the scale factor is more simply derived from the slant range (from camera to object) divided by the camera focal length, both expressed in identical units of measure. Figure 2.3.4-1 shows the geometric relationships. An orbital altitude of 1,000 nautical miles is assumed and camera tilt angles (converging) of 19.79° from the vertical are assumed. The calculated slant range is 1104.9 nautical miles ($1104.9 \times 6080.2 = 6,718,013$ feet). The camera focal length is 5.9 inches (0.49167'). The scale factor of the image is therefore $6,718,013 / 0.49167 = 13,663,662$.

The B/H factor in the denominator is the ratio between the distance separating the exposure stations and the height of the base line above the point imaged. This geometry is illustrated in Figure 2.3.4-2. It can be seen that the B/H is equal to twice the tangent of the angle $31^\circ 52.8'$ ($= 1.24392$).

The factor R is the effective resolution of the imaging system expressed in line pairs per unit length which in the current case has been given as 15.9 line pairs per millimeter. Therefore, solving for the minimum detectable height we obtain a value of:

$$h_{(\min)} = \frac{13,663,682}{1.24392 \times 15.9/\text{mm} \times 2} = \frac{13,663,662}{39.5567} = 345.4 \text{ meters} \quad (27)$$

Equation (26) is derived from photogrammetric parallax formulae and the work of Aschenbrenner (Reference 8 of Section 2.6) wherein he states that the minimum differential parallax (image shift between two photos of a stereo pair) which an observer can perceive and translate into a third dimensional effect is equal to

$$p_{(\min)} = \frac{1}{R F} \quad (28)$$

where:

R = resolution in line pairs per unit distance

F = personal factor derived empirically found by Aschenbrenner to range from 2 to 4 for various individuals

Research at Aero Service Corporation (Reference 7 of Section 2.6) on performances of ten observers on aerial photography simulating extremely high altitude imaging systems and electronic readouts of this photography indicates that a value of 2 for the F factor fits the empirical data best. Thus, this value is used in equation (26). This value was found to be equally valid for performance on the original silver halide photography and for the electronically scanned images.

In comparison with the reports by Hackman (Reference 9 of Section 2.6) on his work on lunar photography, this estimate of perceptible height would appear to be quite conservative. Hackman reports: "With photographs having 12 degrees or more of libration, relief of 1,000 feet or more can be discerned in normal stereoscopic models." He also reports that: "The smallest object that can be seen on the best lunar photograph is about half-a-mile across..."

Using these data to calculate an effective (F) empirical factor, we find a value of 6.28. Thus, it is apparent that our value of 2 is conservative in comparison with Hackman's experience.

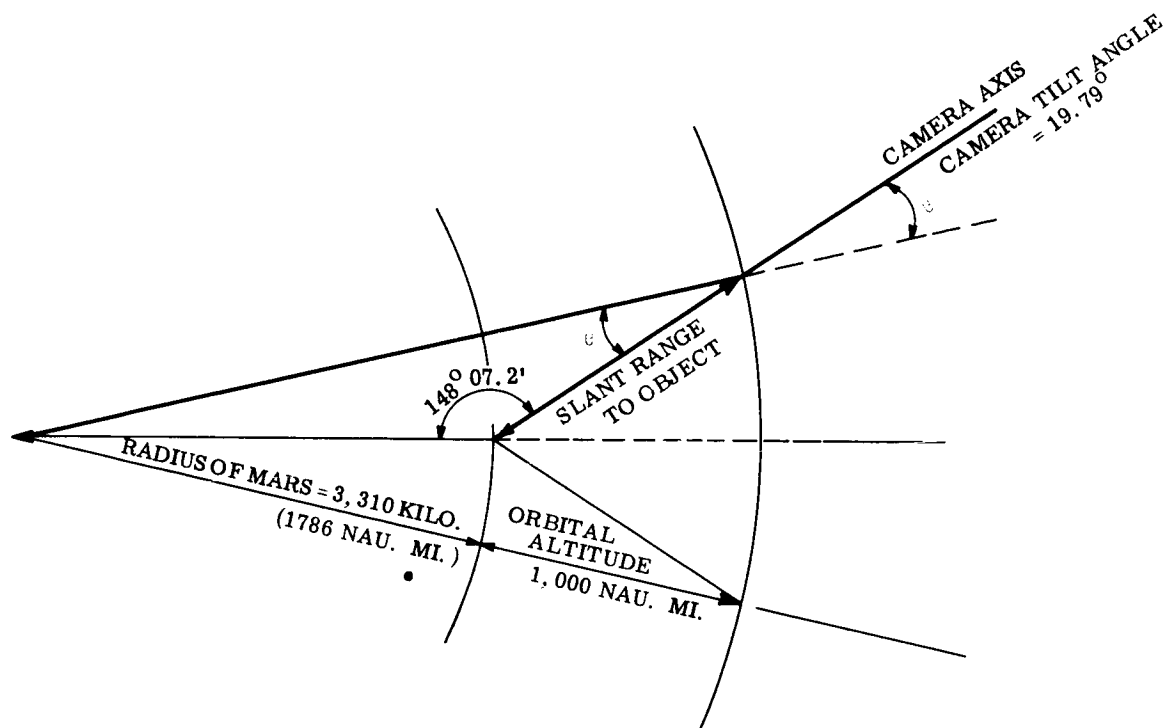


Figure 2.3.4-1. Geometric Relationships, Camera to Objective

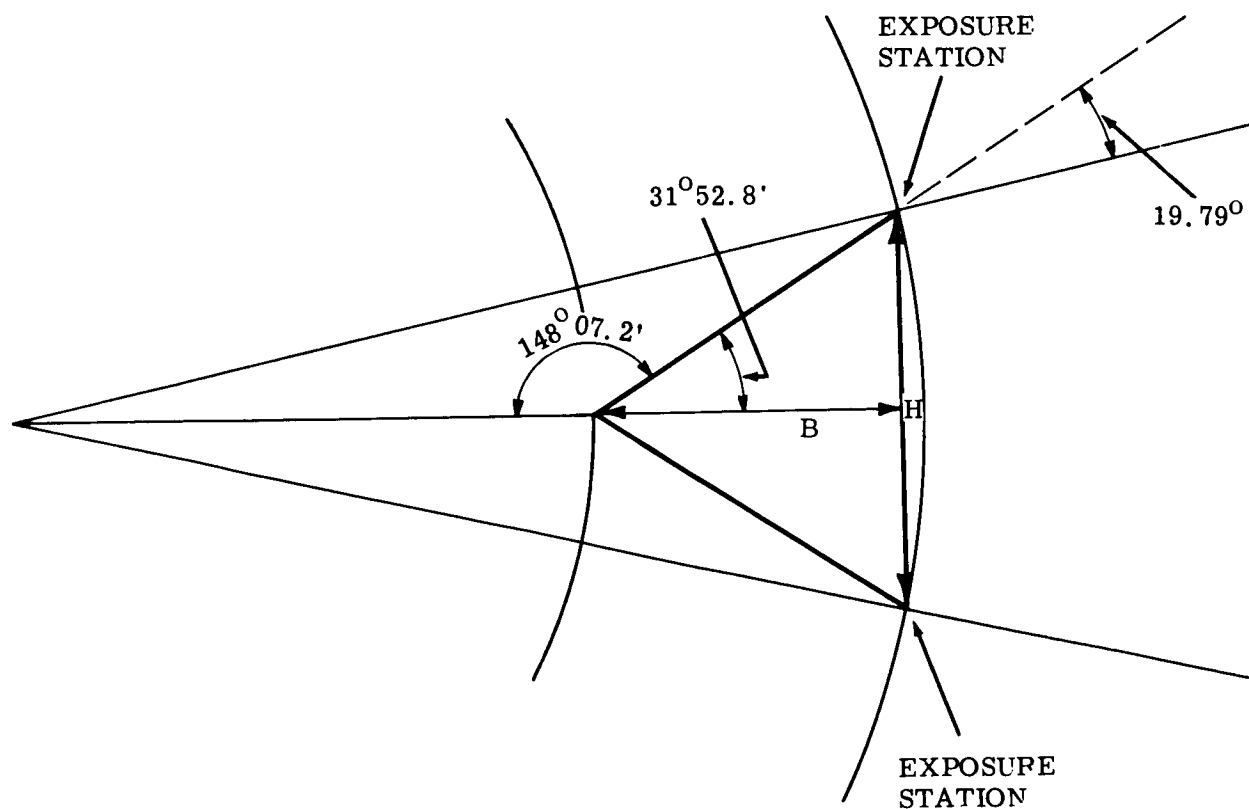


Figure 2.3.4-2. B/H Factor Geometry

The calculated minimum detectable height is 345 meters. This means that an observer can see all objects more than 345 meters above or below the surroundings in third dimension and can, with an accuracy of 95 percent, judge whether the object lies above or below the elevation of the surroundings. For example, he can differentiate between a ridge and a linear depression if the height or depth exceeds 345 meters. Objects of less elevation difference from their surroundings than 345 meters cannot be appreciated stereoscopically and cannot reliably be seen to be above or below the surroundings. With low angles of illumination however, it will be possible to deduce general landform shapes for some of the lesser elevation changes.

For elevation differences well above 345 meters, the observer will be able to make general height comparisons within the stereoscopic model; e.g., this ridge is higher than that one, etc.

B. Expected Height Measurement Accuracy

It is more difficult to predict the accuracy with which observers can be expected to make spot height measurements due to the absence of a general mathematical model for observer performance predictions and due to the many effects which the electronic scan system can impose on the measurement operation. However, previous research (Reference 10 of Section 2.6) indicates that the standard error of height measurements on electronically scanned images with 40° angle of convergence is approximately equal to the minimum detectable height increment for the same imagery. Therefore, it is not unreasonable to assume a standard deviation of ± 345 meters for height measurements on the proposed 500 meter system. This means that spot height measurements will, on the average of 2 times out of 3, be within 345 meters of the true spot height of the point being measured. It should be noted that this accuracy applies only to measurements of discrete points with respect to the height of nearby surroundings and does not refer to height above a reference datum. To accomplish the latter, which would result in true elevation determinations, would require a complete network of control points across the planet for which accurate elevations were known or determined. Anticipated distortions in the electronic imagery will prohibit establishment of such a comprehensive control net from the proposed system.

2.3.5 FLASH ILLUMINATION ON SURFACE OF VENUS

Two practical methods exist for illuminating the surface of Venus for television pictures in the visual region: electronic flash and chemical flares. The exposure time must be relatively short (fraction of a second) because of the possibility of high winds and dust in motion across the scene.

To compare the efficiency of the two methods, the exposure time will be assumed to be 1/60 second and the region to be illuminated 100 feet from the light source. The lens is f/2 and covers a six degree field-of-view.

A formula for determining the size of the electronic flash unit that is needed for given conditions is obtained from the General Electric Flashtube Data Manual (Reference 11 of Section 2.6):

$$J = \frac{GN^2}{0.005 \times (L/w) \times M \times S} \quad (29)$$

where:

J = watt-sec

GN = guide number = (100) (2) = 200, from above conditions

L/W = lumen-sec. per watt-sec = 35, for average conditions

M = reflector factor = 100, for 6° field-of-view

S = exposure index of film = 15, for vidicon tube, 1/60 sec. and 10 ft cdl. on face

$$J = \frac{(200)^2}{.005 \times 35 \times 100 \times 15} = 152 \text{ watt-sec.} \quad (30)$$

An electronic flash unit of this size will have approximately 75,000 center beam candle power seconds for a six degree field. The unit will weigh about six pounds and will require about 2.5 watts input power at a rate of one flash per minute.

Chemical flares are somewhat unique for this purpose in that they can be launched to a remote location before ignition takes place. For instance, a flare might be launched to a great height above the area to be ignited such that illumination is fairly uniform over that area and the problem of over and under exposure eliminated. Increased penetration into the area surrounding the Lander can be effected by launching the flare to a great distance. These features distinguish chemical flares from electronic flash which remains in a fixed position and illumination decreases with increased distance from the unit.

Flares are available which have the capability of producing 5,000,000 candle seconds in a four-pound package which is nearly two orders of magnitude greater than that of the electronic flash. The size of the unit is about 8 in. long by 3 in. diameter.

The main drawbacks to using chemical flares are:

1. Development would have to be done on a flare mixture for the Venus atmosphere.
2. Reliability is about 95 - 98 percent. In this case, reliability refers to a failure in ignition due to adverse atmosphere or other causes. Premature ignition is a very rare occurrence because of built-in safety features although such an occurrence would destroy the vehicle. The unit itself can be made safe for temperatures under 500°F (260°C), so that sterilization temperatures could be tolerated.
3. Photoflash units such as these have never been qualified for space missions.
4. Because of the high atmospheric pressure at the surface of Venus, the combustion smoke may attenuate the radiated light considerably. On the other hand, the very short flash interval may minimize this effect.
5. The chemical flare can be used only once whereas electronic flash is repeatable.

For these reasons, electronic flash is recommended and is included in the hardware list.

2.4 RESULTS

From the optical characteristics of the various lenses shown in Table 2.3.1-1, a selection of actual lens hardware was made. Examination of the FOV column indicates that the lenses are of the narrow field type, no FOV being greater than $5\frac{1}{2}^\circ$. This means that the lenses need not be very complex. The focal lengths range from 4.5 to 281 inches. It is apparent that folded lenses will be needed in the longer focal lengths. Very fast lenses will be required in the Landers because of the need for color filters, for penetration into the darkness in the Venus mission, and the possibility of motion within the scene. The microscope lenses are not unusual because the experiment with

which they are involved is internal and completely controlled so that standard lenses may be used. The IR lens for the Venus descent has a very narrow field so that the speed of the lens is the most important criterion. A large assortment of stock IR lenses is available for this purpose. Generally, they consist of a single element of an IR transmitting material such as the IRTAN series, silicon or germanium. All reflective optics become too complex and unwieldy in this application.

The lens for function (a) (See Table 2.1-1) is not an unusual lens and may be obtained as a stock item. The lens is approximately six inches long from the front of the lens to the vidicon tube face. It will have a diameter of two inches.

Variable iris and shutter rings on the lens will be controlled by a light meter. Its weight will be one pound.

For the lenses of functions (b) and (c), a Maksutov type will be used. The characteristics of a basic Maksutov lens are listed below:

$f = 140$ inches

$F/\text{No.} = F/23$

Physical length = 20 inches

Diameter = 6.5 inches

Weight (with beryllium mirror 1/4" thick) = 2.321 lbs.

Using these dimensions, the lens of function (b) has the following characteristics:

$f = 40.16$ inches

$F/\text{No.} = F/20.4$

Physical length = 6.38 inches

Diameter = 2.2 inches

Weight = 1 lb.

The lens of function (c) becomes:

$f = 281.2$ inches

$F/\text{No.} = F/23$

Physical length = 40.1 inches

Diameter = 13 inches

Weight = 18.8 lbs

The lenses of functions (d) and (h), the panoramic scan lenses for the Mars and Venus Landers, have short focal lengths, are extremely fast, and have narrow fields. They will most likely be of the double Gauss type consisting of 6 elements. The lens will include a variable iris and shutter which will be controlled by a servo from within the Lander. The distance from the front of the lens to the camera tube face will be eight inches and the diameter of the lens, seven inches. Its weight will be three pounds.

Considerable weight and size can be eliminated on this lens if picture-making is limited to the periods around noon on the Martian day and if only distances up to about 50 feet on Venus are recorded. The above lens was based on color recording the terminator on Mars and for distances up to 100 feet on Venus.

The microscope objectives listed for function (e) are readily available. The focal lengths were based on a tube length, object to vidicon tube face distance, of 200 mm. The three objectives would be located in a turret which is programmed to rotate and obtain three magnifications of the specimen. The entire microscope tube, objective turret, and vertical illuminator source are estimated to weigh 2 pounds and occupy a space of 8 in. x 5 in. x 2 in. A color filter disk will also be included in the tube and will be programmed to produce a series of images throughout the visible spectrum.

The lens for cloud mapping in the Venus mission is also readily available and is quite small. Its weight is estimated at 0.5 lbs. Its dimensions are three inches from the front of lens to the tube face with a 0.5 inch diameter.

The infrared lens for function (g) was mentioned previously. It will weigh about one pound and will be located 17 inches from the tube face. Its diameter is listed as 3.33 inches. Because of the uncertainties of the IR content of the Venus atmosphere and surface, the F/no. is based on practical size limitations.

The hardware data on the lenses is listed for convenience in Table 2.4-1.

In addition to the lenses, equipment is needed to control shutters, irises, color filter wheels, panoramic scanning, elevation, erection of optics on Landers, etc. These accessories together with a summary of the television subsystem characteristics are listed in Table 2.4-2. A block diagram of the television cameras is given in Figure 2.4-1.

TABLE 2.4-1. LENS WEIGHTS & SIZES

<u>Function</u>	<u>Wt (Each - lb)</u>	<u>Physical Size (in.)</u>
(a)	1.0	6 x 2 dia.
(b)	1.0	6.38 x 2.2 dia.
(c)	18.8	40.1 x 13 dia.
(d)	3.0	8 x 7 dia.
(e) microscope	2.0	8 x 5 x 2 dia.
(f)	0.5	3 x 0.5 dia.
(g)	1.0	17 x 3.33 dia.
(h)	3.0	8 x 7 dia.

2.5 CRITICAL PROBLEM AREAS

Three critical problem areas presently exist in the television subsystem: vidicon sterilization, image orthicon tube development, and image orthicon camera development.

TABLE 2.4-2. TELEVISION SUBSYSTEM CHARACTERISTICS

Subsystem Components	Camera Head, Vidicon	Camera Head, Vidicon	Camera Head, I.O.	Camera Electronics, I.O.	Exposure Control (Iris and Shutter)	Light Meter	Control Electronics	Color Wheel	Color Wheel Actuator	Boom Erect. (Panoramic)	Boom	Azimuth Mechanism	Elevation Mechanism	Focus Control	Electronic Flash	Ablation Mat'l Remover	Mirror	Lens Weight (lbs)	Total Weight (lbs)	Total Power (watts)
Component Characteristics																				
Power (Watts)	2	16	3	20				0	1	1	0	1	1	0.5	2.5	1	0			
Size (Inches)	8 x 2 1/2 D	9 x 6 x 4	17.5 x 3 D	9.2 x 8 x 5	2.6 x 2.6 x 1	3 x 0.5 D	5 x 3 x 3	0.5 x 5 D	2 x 2 x 2	4 x 1 D	16 x 1 D	2 x 2 x 3	2 x 2 x 3	2 x 2 x 3	12 x 4 x 4	4 x 1 D	5 x 8 x 0.25			
Weight (lbs)	2.5	5.0	4.0	13.5	2.0 (each)	2.0 (each)		0.5	0.5	0.3	2.0	2.0	2.0	2.0	0.0	0.3	2.0			
FUNCTION																				
MARS '69 and '71																				
Orbiter, Vidicon, Nadir, 1000 meter	X	X			X	X	X											1	10	20
Orbiter, Vidicon, Stereo, 345 meter height	X	X			X	X	X											1	20	40
Orbiter, I.O., Nadir, 440 meter height			X	X	X	X	X											1	57	75
Orbiter, I.O., Nadir, 20 meter			X	X	X	X	X											18.8	37.8	25
*Lander, Vidicon, 3 minute, color	X	X			X	X	X	X	X	X	X	X	X	X			X	3	23.3	24.5
*Lander, Microscope, color (*Also '73 and '75)	X	X						X	X						X			2	16	21.5
VENUS '70																			164.1	207.0
Orbiter, Vidicon, Nadir, 2 km clouds	X	X			X	X	X											1	10	20
Descent, Vidicon, I.R., surface	X	X			X	X	X									X	X	1	12.3	21
Lander, Vidicon, 3 minute, color, panorama	X	X			X	X	X	X	X	X	X	X	X	X	X		X	3	29.3	27
VENUS '72																			51.6	68
Orbiter, Vidicon, Nadir, 2 km, clouds	X	X			X	X	X											1	10	20
Descent, Vidicon, I.R., surface	X	X			X	X	X									X	X	1	12.3	21
Lander, Vidicon, 3 min., color, panorama	X	X			X	X	X	X	X	X	X	X	X	X	X		X	3	29.3	27
Lander, Vidicon, Microscope, color	X	X						X	X						X			2	16	21.5
Totals/vehicle																			67.6	89.5

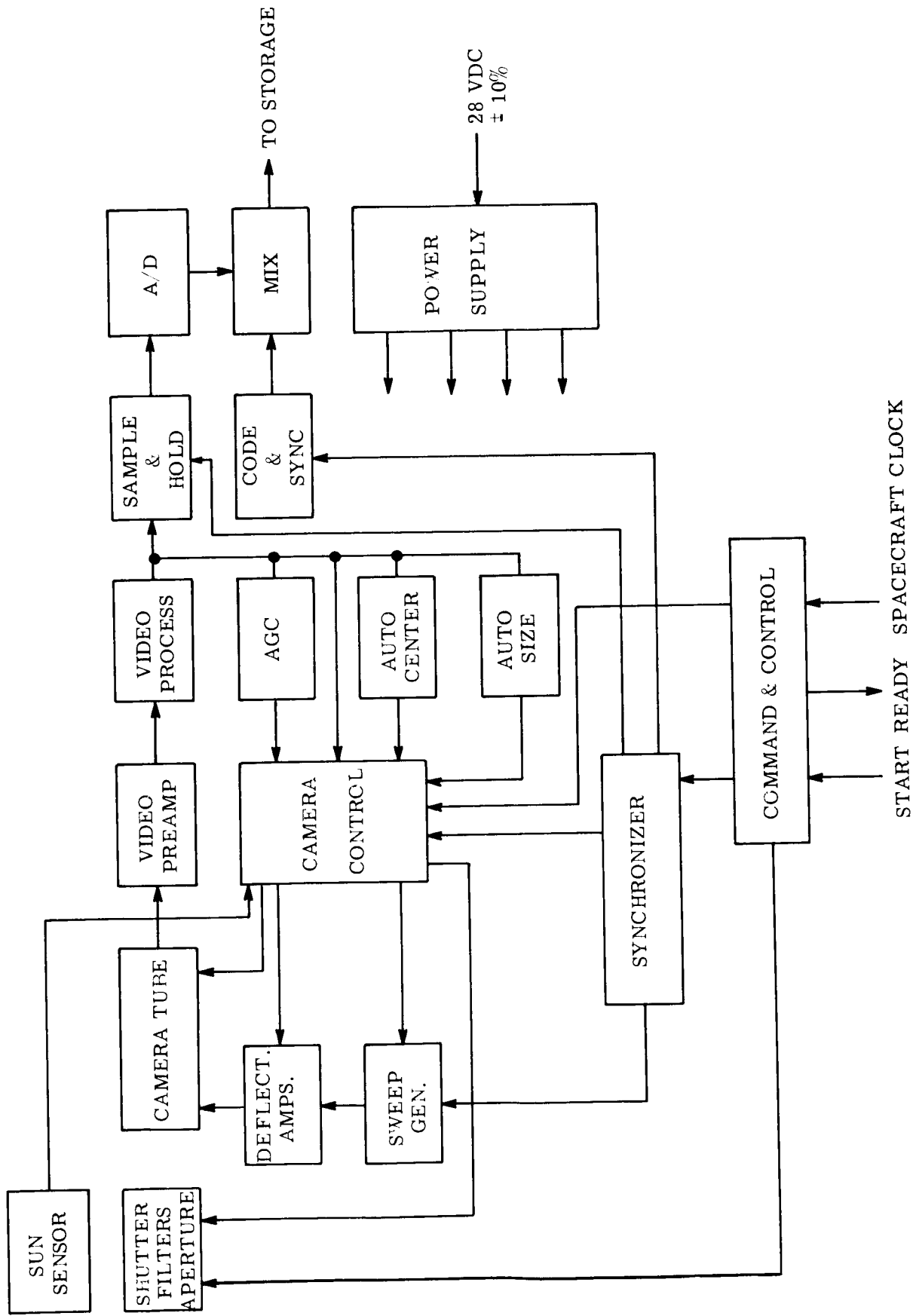


Figure 2.4-1. Television Subsystem Block Diagram

2.5.1 VIDICON STERILIZATION

Although semiconductors are basically able to withstand high storage temperatures, several problems are apt to occur during sterilization. General Electrodynamics Corp. (GEC) lists them as follows (Reference 16 of Section 2.6):

1. Modifications in the semiconductors
2. Interdiffusion of successive layers
3. Shifting of spectral response
4. Changes in secondary emission characteristics
5. Structural Changes
6. Changes in dark conductivity affecting sensitivity and storage characteristics

Beyond these GEC lists vacuum tube problems which could arise due to sterilization:

1. Outgassing of components
2. Deterioration of the thermionic cathode
3. Leakage in the faceplate seal.

The faceplate seal leakage was pointed out by RCA (Reference 17 of Section 2.6) as the most serious sterilization problem.

However, information received from General Electrodynamics Corp. indicates that a sterilizable, ruggedized vidicon having high sensitivity is indeed feasible (Reference 16 of Section 2.6).

2.5.2 IMAGE ORTHICON TUBE DEVELOPMENT

The electrostatic image orthicon is at this time being developed at the G.E. Power Tube Department, Syracuse, N.Y. Electrical tests have not shown completely satisfactory performance, especially concerning resolution. No environmental tests as severe as those required for Voyager have been performed on the tube (References 6, 13 of Section 2.6). G.E. Power Tube Department, however, expects to have a ruggedized, high resolution tube developed within the next year.

2.5.3 IMAGE ORTHICON CAMERA DEVELOPMENT

Employment of image orthicons for the Voyager mission also depends on successful development of automatic control circuitry for long-periods of unattended camera operation. A NASA contract has been awarded to Hazeltine Corp. (Reference 18 of Section 2.6) for development of a space-qualified image orthicon camera which is scheduled for completion by 30 January 1964. The G.E. Advanced Electronics Center, Ithaca, N.Y. is also doing independent development work on a ruggedized, automatic image orthicon camera. It is, therefore, reasonable to assume availability of this equipment at the time of a Voyager design contract if the current developments are successful.

2.6 REFERENCES

1. Space Programs Summary No. 37-19, Volume VI, Space Exploration Programs and Space Sciences, Jet Propulsion Laboratory, Pasadena, California, Feb. 28, 1963.

2. W.M. Goodall, Television by PCM, BSTJ, January 1951.
3. Electromechanical Research Corporation, "Digital Television Subsystem for Project Voyager, Project Voyager Study Report, Volume VIII, Part 1."
4. Consultations with Aero Service Corporation, Philadelphia, Pa.
5. Consultation with General Electrodynamics Corporation, Garland, Texas.
6. Consultation with General Electric Company, Power Tube Department, Syracuse, N.Y.
7. Aero Service Corporation, "Study of Stereoscopic Imagery" RADC TR - 59 - 78, June 1959 (Secret).
8. Aschenbrenner, Olaus M. "High Altitude Stereo Techniques" Photogram-metric Engineering Vol. 16, No. 5, p. 712, 1950.
9. Hackman, Robert J. "Photointerpretation of the Lunar Surface" Photogram-metric Engineering Vol. 27, No. 3, June 1961.
10. Aero Service Corporation, "Photogrammetric Analysis of Small Scale Images" RADC TR - 60 - 100, 1960 (Secret).
11. General Electric Flashtube Data Manual, General Electric, Photo Lamp Department, Cleveland, Ohio.
12. Vine, "Analysis of Noise in the Image Orthicon," JSMPTE, No. 6, 1961.
13. Consultation with General Electric Advanced Electronics Center, Utica, N. Y.
14. Space Programs Summary No. 37-20, Vol. VI, Space Exploration Programs and Space Sciences, Jet Propulsion Laboratory, Pasadena, California, 1963.
15. Hazletine Corporation, "Analog Television Subsystem for Project Voyager, Project Voyager Study Report, Vol. VIII, Part 2."
16. Proposal for the Development of a High "G" Sterilizable Slow Scan Vidicon with Electro-Static Focus and Deflection, General Electrodynamics Corporation, Garland, Texas.
17. Consultation with RCA, Tube Division, Lancaster, Pa.
18. Consultation with Hazeltine Corporation, Little Neck, N. Y.

APPENDICES TO SECTION 2

Appendix

- A. Photographic Methods for Low Resolution
- B. Photographic Methods for One-Meter Resolution
- C. Solar Radiation Intensity for Mars

APPENDIX A. PHOTOGRAPHIC METHODS FOR LOW RESOLUTIONS

Photography, as a replacement for direct television image recording, offers many advantages.

1. Resolution is higher. Films are available which will adequately resolve 200 optical lines/mm whereas television is limited to uses of more than 20 optical lines/mm.
2. Frame format and size are quite flexible. The limitation on size is mainly that of the vehicle packaging limitations.
3. Film is a permanent storage device. No further storage means are necessary. It is also a very compact storage device compared with magnetic tape because of the resolution ability mentioned above.

However, the disadvantages associated with photography are sufficient to relegate the method to a back-up status. Among the disadvantages are:

1. Adequate shielding of film from space radiation may require inordinately heavy materials. The main radiation offenders are solar flares and the radioisotope power generator within the vehicle itself.
2. Photographic film cannot be heat sterilized. Therefore, film must be eliminated from Landers and low altitude Orbiters.
3. The film processing equipment might become a difficult task because of the lack of gravity and low pressures in the space environment.
4. Developing chemicals may not withstand a long dormant period.

Despite the disadvantages of photography, the characteristics of such systems have been determined for comparison with the equivalent television systems. Table A compares the two methods.

In every function but the last one (20 meter resolution), the photographic system has obvious advantages over the equivalent television system. The latter system is rejected because of lack of a film with 100 lines/mm resolution which is fast enough.

A similar study was made to investigate the possibility of using the photographic method for lower altitude orbits in which it would be desirable to resolve one meter on the ground. In every case, the maximum exposure time required to prevent smear was much too short for photographic purposes.

If the photographic approach were used for orbital pictures in either the Mars or Venus mission, the film processing would be done in somewhat the following manner. The film would be fed and stored from two end take-up reels between which the various processing stations would be located. The take-up reels would be mechanized such that any particular film frame could be programmed to appear at a selected station. The stations consist of the lens locations, the film developing and processing unit, and the readout device.

Rapid film development has progressed to the point where acceptable pictures can be made in 5 seconds. The processing units are quite small, having dimensions slightly larger than the film frame being processed and a thickness of 1 to 2 inches. Descriptions of such processing units many times include provisions for modification to space applications. 1, 2, 3, 4, 5

The readout station would consist of either a flying spot scanner and photomultiplier or a television camera and flash illumination. In these circumstances, because of the lower resolution of the television equipment, it is probable that only a portion of the film frame would be read out on one television frame. It is also conceivable that the photographic mapping would be completed long before the information could be telemetered, thus lifting a restriction on readout times on the eraseable television picture.

TABLE A. COMPARISON-TELEVISION VS PHOTOGRAPHY

	Television	Wt (Lbs)	Size (Inches)	Photographic	Wt (Lbs)	Size (Inches)
<u>1000-Meter Resolution</u>						
Focal Length	4.58 inches	1	6 x 2D.	0.73 inches	0.25	1 x 1D.
F/no.	3.45			1		
FOV	5° 24'			70°		
<u>140-Meter Resolution</u>						
Focal Length	40.16 inches	1	6.38 x 2.2D.	5.2 inches	3	6 x 5.5D.
F/no.	20.4			1		
FOV	1° 30'			50°		
<u>20-Meter Resolution</u>						
Focal Length	281.2 inches	18.8	40.1 x 13D.	36.4 inches*	High	37 x 23D.
F/no.	23			1.6 (22.8 inch dia. required but not practical)		
FOV	0° 12'					

*Film speed of ASA 1250 not fast enough unless indicated diameter is used.

1. E.R. Townley, Some Design Considerations of Rapid Access Photographic Systems, Photographic Science and Engineering, Vol. 6, No. 1, 1962.
2. Robert P. Mason, An Advanced Technique for Short Delay Processing of Photographic Emulsions, Photographic Science and Engineering, Vol. 5, No. 2, 1961.
3. Seymour L. Hersh and Frank Smith, Rapid Processing: Present State of the Photographic Science and Engineering, Vol. 5, No. 1, 1961.
4. John R. Mertz, Ansco Recording Films and Rapid Processing Techniques, Photographic Science and Engineering, Vol. 5, No. 2, 1961.
5. Karl-Heinz Lohse and Marvin B. Skolnik, The Capillary Chamber Process for Ultrarapid Negative Processing, Photographic Science and Engineering, Vol. 5, No. 2, 1961.

APPENDIX B. PHOTOGRAPHIC METHODS FOR ONE-METER RESOLUTION

The analysis of this section is similar to that for the television lenses in a previous section. The differences exist mainly in the resolution and minimum exposure characteristics of photographic film. It is assumed in this analysis that the film is capable of 100 optical lines/mm resolution and that the exposure should be 0.00099 foot-candle-seconds for the fastest film available that is capable of 100 optical lines/mm resolution.

Table B lists the results. It will be noted that the diameters and focal lengths are considerably smaller than those of the equivalent lenses for television recording. Nevertheless, practical lenses of these sizes would be quite bulky for the Voyager mission except for low orbital altitudes. For instance, an estimate of the weight of the smallest lens for 100 nautical miles altitude is 25 pounds. The lenses for much higher altitudes would be completely impractical for the mission. The best solution to the problem, if high resolution is required, is, again, image motion compensation.

TABLE B. PHOTOGRAPHIC LENS CHARACTERISTICS FOR ONE-METER GROUND RESOLUTION

Altitude (Nautical Miles)	Focal Length (Feet)	Max. Exposure Time (Milliseconds)	Maximum Relative Aperture	Diameter (Feet)	Aperture Diameter Diffraction (Feet)	Field of View (Unlimited Below for 5" x 5" Format)
100	6.08	Periapsis: 0.0557 90° from periapsis: 2.828	2.72	2.24	0.414	3.93°
300	18.24	Periapsis: 0.0647 90° from periapsis: 1.226	2.58	7.07	0.1243	1.31°
700	42.56	Periapsis: 0.0835 90° from periapsis: 0.81	2.09	20.36	2.899	0.56°

APPENDIX C. SOLAR RADIATION INTENSITY FOR MARS

The basic assumptions of this study are:

1. The Martian atmosphere can be approximated by a model atmosphere and computations based upon the model will be applicable to Mars.
2. The Orbiter will be sufficiently close to the planet that solar radiation computations based upon the model atmosphere will yield light levels as seen by the Orbiter as though the Orbiter were seeing the true Martian atmosphere.

The Mars model II atmosphere is used as the basis for the computations. The computations assume this model to be characterized as being:

1. plane parallel --- no variation in the horizontal
2. non-absorbing
3. a "Rayleigh atmosphere"
4. of finite optical thickness
5. bounded at the top by a perfect vacuum
6. bounded at the bottom by a uniform surface of infinite extent.

The flux of radiation through a unit area perpendicular to the vertical will be computed at the bottom and at the top of the atmosphere.

Radiation Reaching the Bottom of the Atmosphere. The total energy perpendicular to the surface will be computed. This total will include direct radiation plus all Rayleigh scattering of all orders except as noted.

Let G_λ = energy per unit area at wavelength λ arriving at the bottom of the atmosphere¹

$$G_\lambda = (1/2) \pi F_{O\lambda} \mu_O \frac{V_\ell(\mu_O) + V_r(\mu_O)}{1 - A \bar{s}} \text{ watts cm}^{-2} \mu^{-1}.$$

where:

$\pi F_{O\lambda}$ = the net flux of monochromatic radiation of wavelength λ incident at the top of the atmosphere.

μ_O = $\cos \theta_O$ where θ_O = sun zenith angle

A = surface albedo

\bar{s} = a function of optical depth,

V_ℓ = a function of optical depth, τ , and μ_O

V_r = a function of optical depth, τ , and μ_O

\bar{s} , V_ℓ , V_r , are functions introduced by Chandrasekhar in formulating the theory of Rayleigh scattering of planetary atmospheres.

In order to save carrying along the constant, $\pi F_{0\lambda}$, we shall compute the relative flux, $(G_{1\lambda})$
 $(\pi F_{0\lambda})^{-1} = G_{1\lambda}$. At the end of the computations, the constant $\pi F_{0\lambda}$ will be made use of.

Radiation Emerging from the Top of the Atmosphere: The total energy emerging perpendicular to the surface will be computed. This includes reflected radiation and Rayleigh scattering to the highest significant order.

Let D_{λ} = energy per unit area at wavelength λ emerging from the top of the atmosphere².

$$D_{\lambda} = \pi F_{0\lambda} \mu_0 \left\{ 1 - \left[\frac{V_e(u_0) + V_n(u_0)}{2} \right] \left[\frac{1 - A}{1 - A\bar{5}} \right] \right\} \text{watts cm}^{-2} \mu^{-1}.$$

where the symbols are the same as for G_{λ} .

By direct substitution we can write:

$$D_{\lambda} = \pi F_{0\lambda} \mu_0 - (1 - A) G_{\lambda}$$

Again, we shall compute the relative flux, $(D_{\lambda}) (\pi F_{0\lambda})^{-1} = D'_{\lambda}$

$$D'_{\lambda} = \mu_0 - (1 - A) G'_{\lambda}.$$

A compilation of value of G'_{λ} and D'_{λ} for various values of the albedo and sun zenith angles is given in reference 3.

In order to obtain the absolute fluxes, we multiply the values of D'_{λ} and G'_{λ} by πF_0 , the incident solar flux at the position of Mars. Figure C1 shows the solar flux as a function of wavelength at the average distance of Mars from the sun. This distance is taken to be 2.281×10^8 Km (141.69×10^6 mi.) or 1.524 astronomical units.

Typical curves of D_{λ} versus λ are given in Figures C2 and C3, where the curve of Figure C2 is that for 0° sun zenith angle, and Figure C3, an approximate 90° sun zenith angle. A good approximation to the relative illuminations between the two conditions was obtained by finding the ratios of areas under the curves. The ratio used for determining the maximum F/Nos. for the lenses in this report was 3.5 percent.

By convolving a D_{λ} versus λ curve with the standard visibility function and multiplying the result by the reciprocal of the mechanical equivalent of light, 680 lumens/watt, a value for the illumination of Mars in photometric units may be obtained. The value used in this report, for the representative albedo of $A = 0.15$, and for 0° sun zenith angle, is 820 lumens/ft.². Up to zenith angles of 60° the illumination may be approximated closely by multiplying 820 lumens/ft.² by the cosine of the sun zenith angle. Beyond 60° zenith angle the illumination may be approximated by comparison of areas under the D_{λ} versus λ curves as had been described previously. Thus, for 820 lumens/ft.² at 0° sun zenith angle, the illumination at 90° sun zenith angle is $820 (.035) = 28.7$ lumens/ft.².

1. D. Deirmendjian and Z. Sekera, "Global Radiation Resulting from Multiple Scattering in a Rayleigh Atmosphere". Tellus, 6, 4, pp 382-398, Nov., 1954.
2. K. L. Coulson, "The Flux of Radiation from the Top of a Rayleigh Atmosphere". University of California at Los Angeles, Department of Meteorology Scientific Report No. 1, (AFCRC TN 59 402 & ASTIA AD216 317)
3. G. M. B. Bouricius, "Solar Radiation Intensity for Mars" GE-PIR No. 2640-401, 18 June 1963.

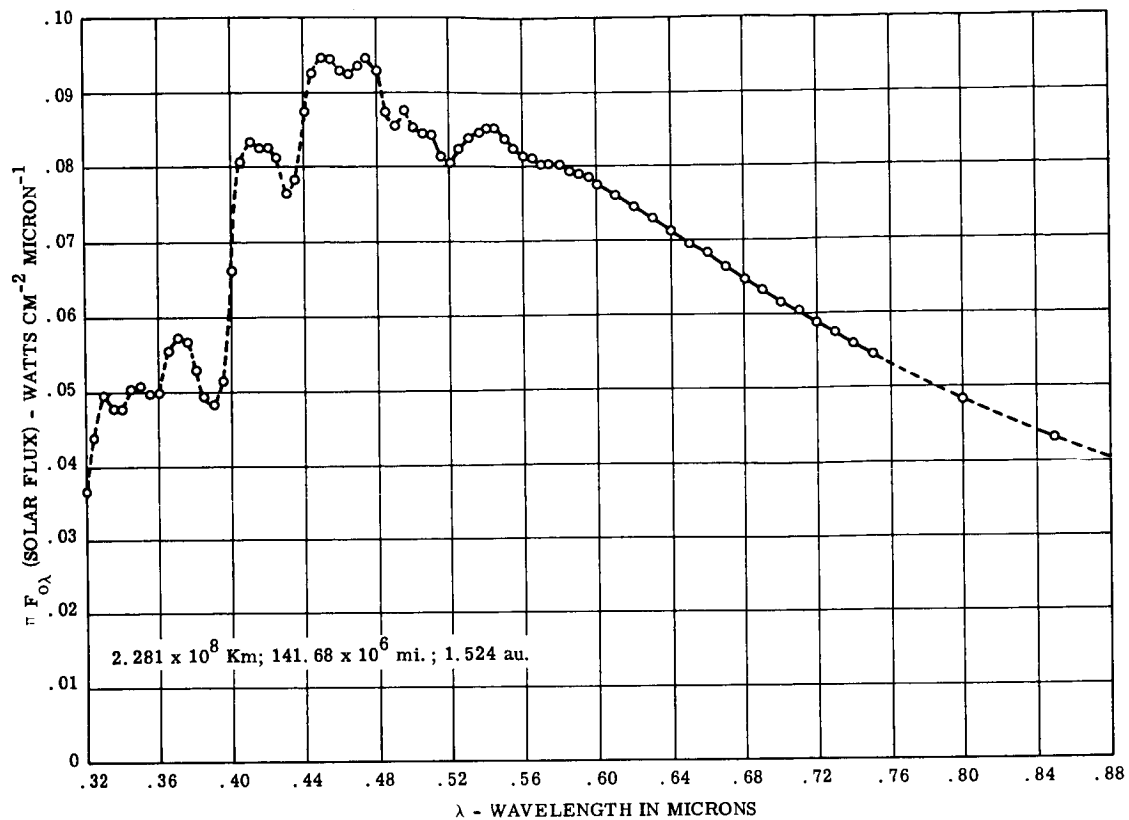


Figure C-1. Solar Flux at the Average Distance of Mars Orbit

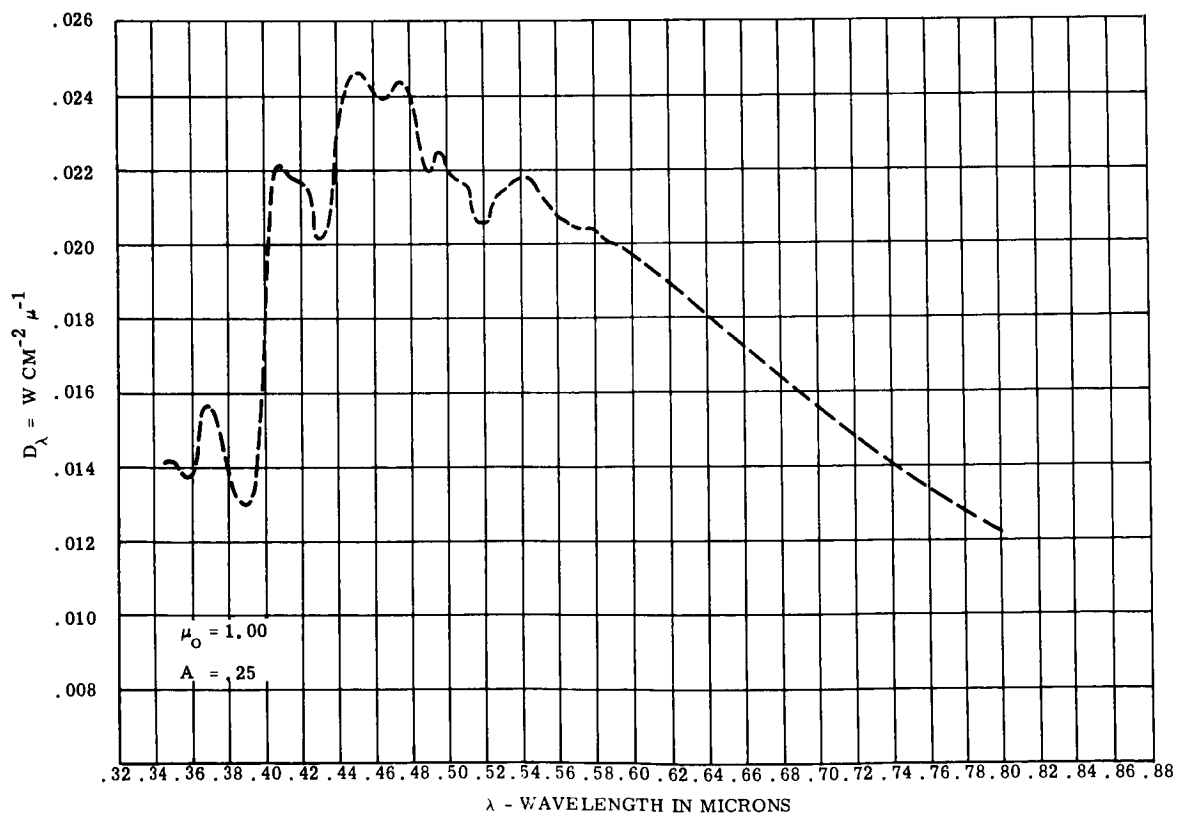


Figure C-2. D_{λ} For a Sun Zenith Angle of 0°

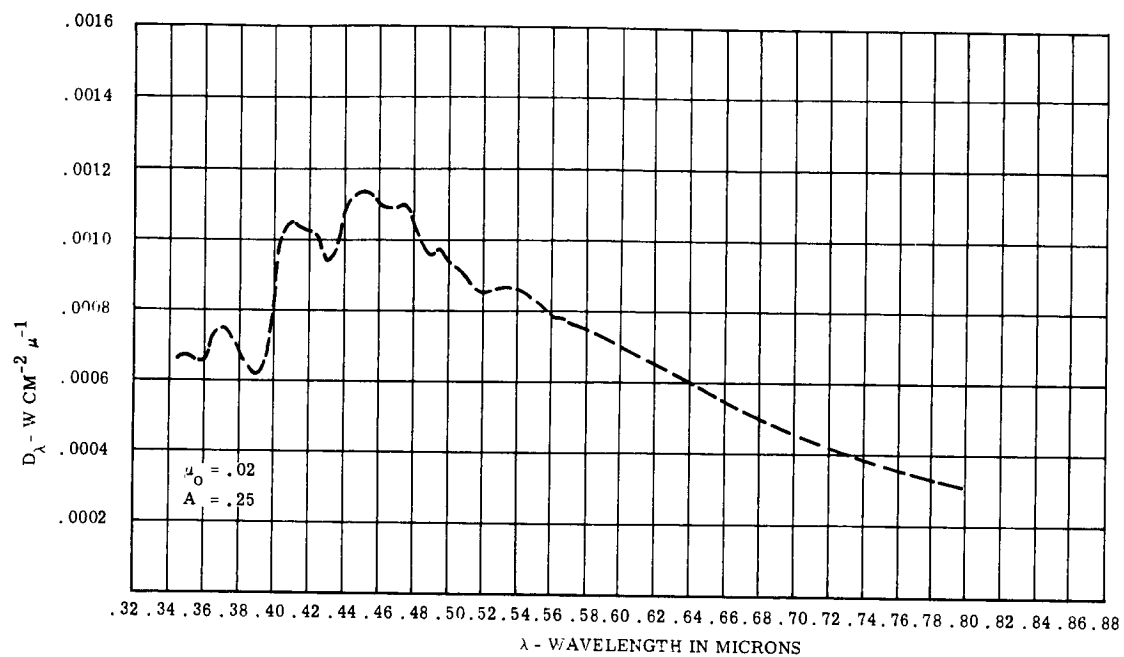


Figure C-3. D_λ For a Sun Zenith Angle of $88^\circ 48'$

SECTION 3. RADAR

3.1 SUMMARY

The presence of extensive cloud cover about the planet Venus makes it expedient to obtain information about the planet by the use of frequencies outside the optical portion of the spectrum. In particular the microwave and UHF frequencies are attractive.

The following missions can be performed using information gathered by radar sensors on an Orbiter about Venus:

- (1) A topographic map* of the terrain can be generated for all or part of the planet's surface.
- (2) Surface characteristics can be determined for particular areas on the planet.
- (3) The surface temperature can be determined by radiometry for particular areas.
- (4) The height of the ionosphere and the electron density can be measured.
- (5) The altitude of the Orbiter above the surface of the planet can be measured to aid in establishing the actual ephemeris of the Orbiter.

The Mars and Venus Landers will use radar altimeters to give height above terrain to be used for the correlation of scientific measurements made during descent. The Venus Lander will also carry doppler radar to measure the effect of winds. These equipments are the same as those used for Surveyor with minor modifications.

3.1.1 TERRAIN MAPPING

The terrain mapping methods considered would generate narrow strip maps which could be combined into a continuous terrain map of the planet. The planetary map will provide a basic reference against which all subsequent atmospheric and surface measurements may be evaluated. It will show areas of differing radar reflectivity and it will show radar shadows. The total effect is similar to that obtained by a black-and-white aerial photograph with the sun casting distinct shadows. The terrain mapping radar is considered to be the primary sensor for the Venus 1970 Orbiter.

Two synthetic aperture radars were compared for this application. A synthetic aperture radar obtains, by means of special signal processing, a finer resolution than that obtained by virtue of the antenna beamwidth in a conventional radar. The Synthetic Aperture High Altitude Radar (SAHARA) designed by the Light Military Electronics Department of General Electric Co. is compared in this study with a coherent pulse doppler radar designed by the Conduccion Corporation. The pulse doppler radar extracts the radar map information from a series of short pulses, whereas, SAHARA obtains this data from a single long pulse.

The pulse doppler radar obtains finer resolution and requires less communications bandwidth than SAHARA radar, because processing in the Orbiter is feasible. However, due to the pulsed nature of the pulse doppler system, there are potential range and azimuth ambiguities which require a 14-foot diameter antenna operating at a wavelength of 3.2 cm in

* A map in this report does not mean a survey or chart but a representation of the surface from which approximate sizes, separation, locations, and altitudes of features can be obtained.

order to obtain directivity to suppress them adequately. The SAHARA radar can use a 10-foot diameter antenna operating at a wavelength of 13 cm. The 14-foot antenna at the 3.2 cm wavelength requires a significant increase in antenna weight because of its increased size and smaller tolerance due to the shorter wavelength.

It is recommended that the SAHARA radar system be used for the Venus 1970 Orbiter. The recommendation is based primarily on the fact that the antenna required for SAHARA is 60 to 70 pounds lighter than that required for a coherent pulse doppler radar.

The SAHARA radar has the following characteristics:

Frequency:	2295 mc (S-band)
Antenna diameter:	10 ft.
D. C. power requirement:	440 watts
Weight:	109 pounds
Volume:	2.0 ft. ³ , (excluding antenna)
Polarization:	circular
Peak transmitter power:	302 watts
Final map resolution:	1.0 nm x 1.0 nm
Required data transmission rate:	63,000 bits/sec

The video signals at the output of the radar must be transmitted to the earth for the processing required to obtain a map.

One nautical mile azimuth and range resolutions are obtainable from 1000 nm altitude. The range resolution can be made constant with altitude but the azimuth resolution degrades with altitude, (e.g., it is 1.6 nm for a 2500 nm altitude). Map quality is a function of signal-to-noise ratio which, in turn, is a function of altitude. A good quality map can be obtained with average terrain reflectivity up to an altitude of 1200 nm and a fair quality map up to an altitude of 1600 nm. A calculation was made of the radar system weight if the transmitter power is increased to give constant map quality over the altitudes of interest. These weights are large and cannot be accommodated in the Venus 1970 Orbiter. With an elliptical orbit, mapping will be limited to the lower altitude regions.

3.1.2 RADAR SURFACE SOUNDER

The surface roughness of the planet may be determined by using multi-frequency sounding radar in the microwave frequency range. The variations in polarization and amplitude of the radar return are evaluated as a function of the aspect angle to determine the dimensions of the surface roughness. Since the system requires a scan of ± 50 degrees about the nadir, the terrain mapping antenna is used.

3.1.3 RADIOMETER

Radiometer experiments will be conducted from the Orbiter. These will extend the information obtained from Mariner II and, especially, make measurements with finer spatial resolution. Data will be obtained which will give surface temperature, roughness, and perhaps composition. The radiometer will use the radar antenna, part of the radar surface sounder equipment, and five pounds of additional equipment.

3.1.4 IONOSPHERIC SOUNDING

Ionospheric sounding measurements of the height, thickness, and electron density of the ionosphere of Venus may be obtained from the Orbiter. The ionospheric sounding equipment would direct RF pulses towards the ionosphere at various frequencies. The amplitude, polarization, and time delay of the return would provide the basic data from which ionospheric measurements can be deduced. Discrete frequencies between 5 and 15 megacycles are transmitted using a long extensible rod or whip antenna.

3.1.5 ORBITER RADAR ALTIMETER

The mapping radar for the Venus 1970 Orbiter may also be used in a radar altimeter mode. The nominal orbit for the Venus 1970 mission is an ellipse with a minimum altitude of 1,000 nm and maximum altitude of 4,300 nm. The eccentricity of the orbit actually attained may be obtained from measurements of height-above-terrain using a radar altimeter. If such information is obtained for a few orbits then the effects of uneven terrain may be smoothed out. An accuracy of ± 0.66 nm is estimated for the altitude measurements.

3.1.6 LANDER RADARS

A radar altimeter will provide a data base for atmospheric measurements made during the sub-sonic portion of the descent of the Mars-Venus Landers. Present Lander design studies indicate that the vehicles will not be subsonic until below an altitude of 200,000 feet. Altitude requirements for the atmospheric experiments for Mars and Venus entry vehicles are:

- (1) Accuracy of ± 2 percent of altitude, or ± 100 feet, whichever is larger.
- (2) Measurements to be made every 1,000 feet after subsonic velocity is attained.

The altitude measurements for the Mars Landers can be made with a pulsed radar altimeter. The altimeter will be mounted behind a radome constructed of ESM* which has been found to have acceptable electrical characteristics. The altimeter is a modification of the Surveyor Altitude Marking Radar. The modifications consist of a new antenna and circuitry to allow altitude to be measured continuously.

For the Venus Landers there is an additional requirement to measure the horizontal displacement of the capsule during descent. Measurements of horizontal displacement rate may be used to deduce horizontal wind velocities. The Surveyor Radar Altimeter and Doppler Velocity Sensor which integrates the velocity and altitude functions is recommended for use in this application. It measures altitude to an accuracy of ± 2 percent and horizontal velocity to an accuracy of ± 1 percent, which is adequate for the Voyager mission. The antennas, which would be deployed when subsonic velocity is attained, would be re-designed for mounting in the Venus Lander. A solid-state transmitter will be used, which will result in a lower input power requirement and will be able to withstand the entry deceleration.

3.2 INTRODUCTION

There are a number of general or common objectives which should be followed in the selection of radar sensors for Voyager. To save weight, the sensors should be integrated as much as possible. The Orbiter radar altimeter function should be integrated with the terrain mapping radar and the radiometer function should primarily employ terrain mapping and radar surface sounding equipment.

*Elastomeric Shield Material

Another objective is to have data from one sensor complement data from other sensors. It must be kept in mind that these planets are being observed without the familiar frame of reference available on earth. A terrain map of Venus to the detail contemplated would not be so easily interpreted as a terrain map of the Earth. The radar surface sounder and radiometer would supply data which are useful and perhaps necessary to interpret the terrain map. The terrain map, in turn, would supply a spatial reference for the other experiments.

The use of existing equipment wherever possible is a desirable objective. The use of space-qualified hardware in this application will save cost and development problems. If qualified equipment does not exist, the minimum requirement is that proven techniques be used and that no advances beyond the state-of-the-art be required.

There are two promising approaches to fine-resolution radar mapping. One is the coherent pulse doppler technique, which has been developed by the Conduction Corporation and flown in aircraft but has not yet been developed for satellite operation. The other technique is Synthetic Aperture High Altitude Radar (SAHARA) that is designed by the GE Light Military Electronics Department but is not yet developed. Its specific method of implementation gives it qualities which may be more appropriate for mapping Venus in 1970.

Radar sensors may also be used in the Orbiter to perform additional scientific experiments which cannot be performed so well from Earth, such as surface and ionospheric soundings and radiometer measurements.

The primary objective of the radar in the Landers is to measure altitude above the terrain to correlate scientific measurements made during descent. An experiment is also performed using radar to measure the effect of winds on the Venus Landers.

3.3 ANALYSIS

3.3.1 TERRAIN MAPPING RADARS

Conventional radar resolution is determined by the antenna beamwidth, which is a function of antenna size and wavelength. A typical antenna beamwidth is two degrees, which for 1300 miles slant range (1000 miles altitude) permits a resolution of 43 miles. A synthetic aperture radar can give resolutions of one mile, or finer, using antenna sizes similar to that in the example above. This is accomplished by special processing of the signals received by a coherent radar system.

Figures 3.3.1-1 and 3.3.1-2 are samples of radar images obtained with a coherent pulse doppler radar, which illustrate the value of this type of sensor as a large area surface mapping tool. The recordings shown represent the state-of-the-art of five years ago. The performance presently available in fine resolution radar systems is much improved compared to these examples although details are not available because of security classification. The images shown are good examples of how well this type of radar sensing emphasizes surface features and roughness, a primary mission of the Voyager spacecraft. A wealth of geologically significant information can be extracted from side-looking radar recordings. Slopes and protuberances on the surface will produce effects in terms of both shadows and specular reflections that will allow detailed interpretation of terrain features and patterns. Also, this sensor is an excellent tool for observing large area stratigraphic structural and geomorphic configurations to infer existing surface conditions.

Another very important feature of side-looking radar as a planet reconnaissance sensor is that this sensor is capable of providing imagery and contour data for use in establishing a planet grid reference and for use in the production of topographic maps. Radar-grammetric techniques and equipment have been developed for obtaining planimetric data and parallax measurements for surface elevation data.



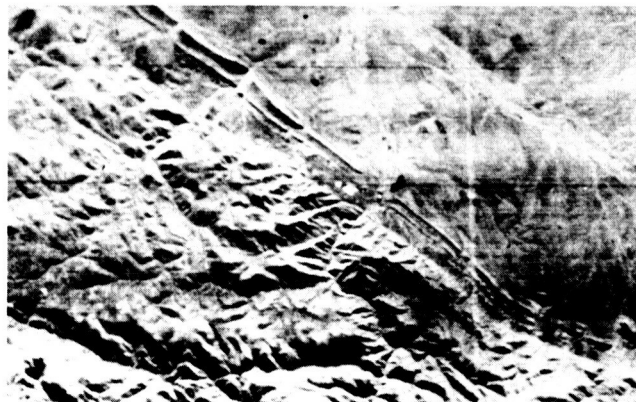
SCALE: 1:300,000

NOTE: This unclassified image made several years ago, illustrates the performance of synthetic aperture radar as a mapping tool. The state-of-the-art in range and resolution today is an order of magnitude improved over that shown here.

Figure 3.3.1-1. Sample Side-looking Radar Strip Map with Coordinate Grid and Point Elevation Data



AERIAL PHOTO



B. SIDE LOOKING RADAR

NOTE: This example illustrates how side looking radar emphasizes texture and contour of the surface.

Figure 3.3.1-2. Comparison of Aerial Photograph and Side-looking Radar Image of the Same Area

There are two different approaches to synthetic aperture radar. The SAHARA approach involves the transmission of a long coded pulse and processes signals within the pulse. The other approach transmits short pulses, receives and stores these pulses, and simultaneously processes them to extract the information. This latter system is sometimes referred to as the University of Michigan Radar and has been developed and used in various low-altitude applications. The radar is also described as the coherent pulse doppler type. The detailed reports of the Light Military Electronics Department of GE and the Conduction Corp. on these two radars are included in Volume VIII, Sections 5 and 6, of this report.

A. SAHARA Radar

(1) Basic Concept

As the antenna pattern moves over the terrain due to the velocity of the vehicle, the frequency of the signal from a particular reflector varies due to the doppler effect. If the radar receiver contained a filter that passed only a narrow interval of doppler frequencies, only signals from reflectors having their doppler in this interval would be passed. Signals from other reflectors in the beam pattern would not be passed and the radar system would then have a finer resolution than that allowed by the antenna size and wavelength. This is the principle of synthetic aperture radars although they do not necessarily use filters.

The doppler frequencies involved here are relatively low and the radar must receive signals for a rather long time in order to pass the low-frequency doppler. The synthetic aperture radars that have been developed and that have attained operational status transmit short pulses and extract a sample of the doppler wave from each received pulse. This method has been effective but, due to cross-products of the doppler and pulse-repetition frequencies, the pulse-doppler approach has certain limitations that would require a very large antenna to overcome for the Venus application.

The SAHARA system takes advantage of the high velocity and high altitudes of space vehicles. A very long pulse is transmitted. This pulse is long enough to contain full cycles of the doppler frequencies. Interaction with the pulse-repetition frequency is avoided and, with sufficient processing equipment, a "map" can be obtained from a single pulse. Pulse-to-pulse integration is used, though, to improve the signal-to-noise ratio.

The time duration of the long pulse transmission of SAHARA radar is chosen so that transmission ends just prior to the arrival of the leading edge of the returned pulse. Thus, the duration of the pulse is given as:

$$T = \frac{2R_{s_{\min}}}{c} \quad (1)$$

where $R_{s_{\min}}$ is the slant range to the nearest target of interest. When the orbit is elliptical, the pulse length is determined by the slant range at the lowest altitude. If computed and designed for the higher altitude, the transmitter would still be on and interfere with the received signals when near periapsis. Consideration was given to changing the pulse length with altitude but this was not favored due to the resulting complication of the transmitter.

If SAHARA were operated at a single altitude, transmission and reception could alternate at equal time intervals and the pulse repetition frequency would be $1/2T$; but this is not so when the design uses a constant PRF and when the altitude varies. The time between the start of transmission and the reception of the first return signal is longer at the maximum altitude and is $1/\tau$. Since the pulse length is constant with altitude, the signal is received for a duration T . The pulse-repetition frequency is then given by

$$\text{PRF} = \frac{1}{T + \tau} \quad (2)$$

This assumes a single, point target at range R_s . In reality, signals are received from a finite strip width on the ground and the PRF would be slightly lower. Table 3.3.1-1 gives, as a function of altitude, the antenna depression angle, minimum slant range R_s , and the time between the start of transmission and the first reception. Times can be selected from this table to compute the PRF. If the minimum and maximum altitudes are 1000 and 4500 miles, respectively, the PRF is 13 pulses per second.

TABLE 3.3.1-1. MAPPING CONDITIONS

Altitude (Miles)	Depression Angle (Degrees)	Slant Range (Miles)	2-Way Propagation Time (msec.)
1000	77	1360	16.7
2500	68	3050	37.5
4500	62	5150	63.0

In order to determine the quantities in the table, it is assumed that the angle, ϕ , between the direction of propagation and the planet's surface is 45 degrees. If this angle is decreased, the slant range increases and the required transmitter power increases. Increasing this angle decreases the required power but the ground range resolution for a given slant range resolution becomes coarser fairly rapidly, since it is proportional to $1/\cos \phi$. A grazing angle of 45 degrees is not mandatory but represents a good nominal value.

When this long pulse transmission is coupled with the high velocity inherent to the vehicle, a prime advantage results, that of increased azimuthal resolution at $R_{s \min}$. The Voyager Radiogrammetry. Appendix (Volume VIII, Section 6) shows that the resolution achievable from a single pulse is:

$$\Delta S = \frac{\lambda c}{4v} \quad (3)$$

where

λ = transmitted wavelength

v = velocity of vehicle

c = velocity of light

This expression for the azimuth resolution is derived by using the reciprocal of T , the pulse duration, as the minimum resolvable frequency interval and by assuming a linear relation between doppler frequency and azimuth angle. This relation is linear in the vicinity of zero doppler.

The azimuth resolution is now independent of antenna size and is proportional to the transmitter wavelength. A transmitter frequency in S-band has been chosen mainly in consideration of antenna tolerance limitations.

The vehicle velocity to be used in the above equation is not the orbit velocity but the velocity relative to the ground. At 1000 miles altitude, this velocity is about 16,400 feet per second.

With a transmitter frequency of 2295 mc, for example, the azimuth resolution is one mile from this altitude. Table 3.3.1-2 gives azimuth resolution at other altitudes.

TABLE 3.3.1-2. AZIMUTH RESOLUTION

Altitude (Miles)	Ground Velocity (Feet Per Sec.)	Azimuth Resolution (Miles)
1000	16,400	1
1200	15,300	1.1
1600	13,400	1.2
2200	11,250	1.5
2500	10,300	1.6

A further significant result is the removal, on a single pulse basis, of essentially all azimuth ambiguities. It might appear, initially, that the improved azimuthal resolution has been achieved at the expense of a degradation in range resolution. In actuality, range resolution is maintained by dividing the long transmitted pulse of the SAHARA system into η subpulses, where the subpulse duration is τ , according to the relation:

$$\tau = \frac{2\Delta R_s}{c} \quad (4)$$

where

ΔR_s is the range resolution measured in slant range units.

Thus

$$T = \eta \tau \quad (5)$$

and:

$$\frac{T}{\tau} = \frac{R_s}{\Delta R_s} = \eta \quad (6)$$

where η is defined as the pulse compression ratio.

The desired ground range resolution is one mile, a value that was chosen to be compatible with the approximately one mile azimuth resolution. To give this ground range resolution, the slant range resolution, ΔR_s , should be 0.707 mile according to equation (7). The slant range in the previous formula for pulse compression ratio is about 1300 miles corresponding to a 1000 mile altitude above the surface of Venus. This value is used although the radar may operate at higher altitudes because a constant pulse length system has been chosen and the pulse length must be designed for the lower altitude.

This gives a pulse compression ratio, then, of about 1800. From the geometry of the system, the range resolution on the ground is given as:

$$\Delta R_g = \frac{\Delta R_s}{\cos \theta} \quad (7)$$

where θ is the acute angle described by the ground plane and the line of sight from the antenna to target. It follows that the ground range resolution deteriorates as the look angle becomes large; or, conversely, that ground range resolution, ΔR_g , approaches ΔR_s at grazing incidence.

In order to preserve the identity of the subpulses within the long pulse transmission, each subpulse is phase coded. The coding is such that the phase of each subpulse is either 0 or 180 degrees with respect to a transmitter RF reference signal. The range information contained in each pulse can now be recovered by a suitable data processing technique. Note that the video bandwidth must be $1/\tau$.

For a uniform beam pattern, the long coded pulse transmission may be regarded as a means of dividing the illuminated ground patch into a matrix of resolution cells. Each of these resolution cells within the beam is uniquely characterized by a range increment, ΔR_g , and an azimuthal increment, ΔS , related to doppler shift. Thus, there is sufficient information in one long pulse return to obtain a map of the ground patch illuminated by the antenna beam. Additional enhancement of this map is achieved by superimposing the returns from several successive long pulse transmissions.

The information contained in the long pulse transmission must be recovered to reconstruct the ground map. This is accomplished in the SAHARA system through the use of a correlation technique. The returned signal is multiplied by the stored transmitted reference signal and the product is integrated in time. This process yields the zero doppler line of the ground. The method of obtaining the information pertinent to the off-zero lines is conceptually equivalent to shifting the reference signal in frequency by an amount equal to the doppler line of interest and then repeating the previous process.

In the SAHARA system, the correlation is performed by using a shift register with resistors connected to each stage. The shift register contains all the received signals in their time sequence. While illuminated by the long pulse, a particular resolution element will move relative to the vehicle and a doppler frequency will result which will change with time. One function of the resistors is to weigh the shift register outputs according to the doppler variation in order to allow correlation. Integration is accomplished by combining the outputs of a bank of resistors.

The proper values of these resistors are a function of the variation in doppler frequency with time. This relationship changes with altitude. Because of the anticipated elliptical orbit, a decision has been made to do the processing on the Earth to avoid complicating the processor.

In order to reduce propulsion requirements, a 1000 x 4300 nm orbit has been selected. Earlier in the program less elliptical orbits were considered. The radar was designed and the performance obtained was limited by the weight and power possible within the Orbiter. The characteristics of this system are given in Section 3.3.1.A(5). A particular value of average power, 90 watts in this case, requires a minimum value of terrain reflectivity. With fixed power, the reflectivity must increase as the altitude increases. Figure 3.3.1-3 shows the required reflection coefficient as a function of altitude. The curve is for a signal-to-noise ratio (S/N) equal to unity after post-detection integration. A higher S/N is required to give a good display of terrain having a particular value of reflection coefficient. A typical design value for this S/N is 10 db. To illustrate the application of this curve, the situation at 4500 miles altitude is examined. Figure 3.3.1-3 shows that a reflection coefficient, γ , of -4 db is required for S/N = 1. Then for S/N = 10, γ must be +4 db. But values of this order are only encountered, on Earth, for normal incidence with smooth water. A more typical value of γ , -12 db, is also in agreement with radar observations of Venus. To obtain the altitude at which a good display of this average terrain can be obtained, the 10 db S/N must be considered. Figure 3.3.1-3 is then entered at -12, -10, or -22 db and an altitude of 1250 miles is obtained. These figures mean that if the system is designed for $\gamma = -22$ db and the orbital altitude is 1250 miles, then an average γ of -12 db will produce a signal-to-noise ratio of 10 db after processing.

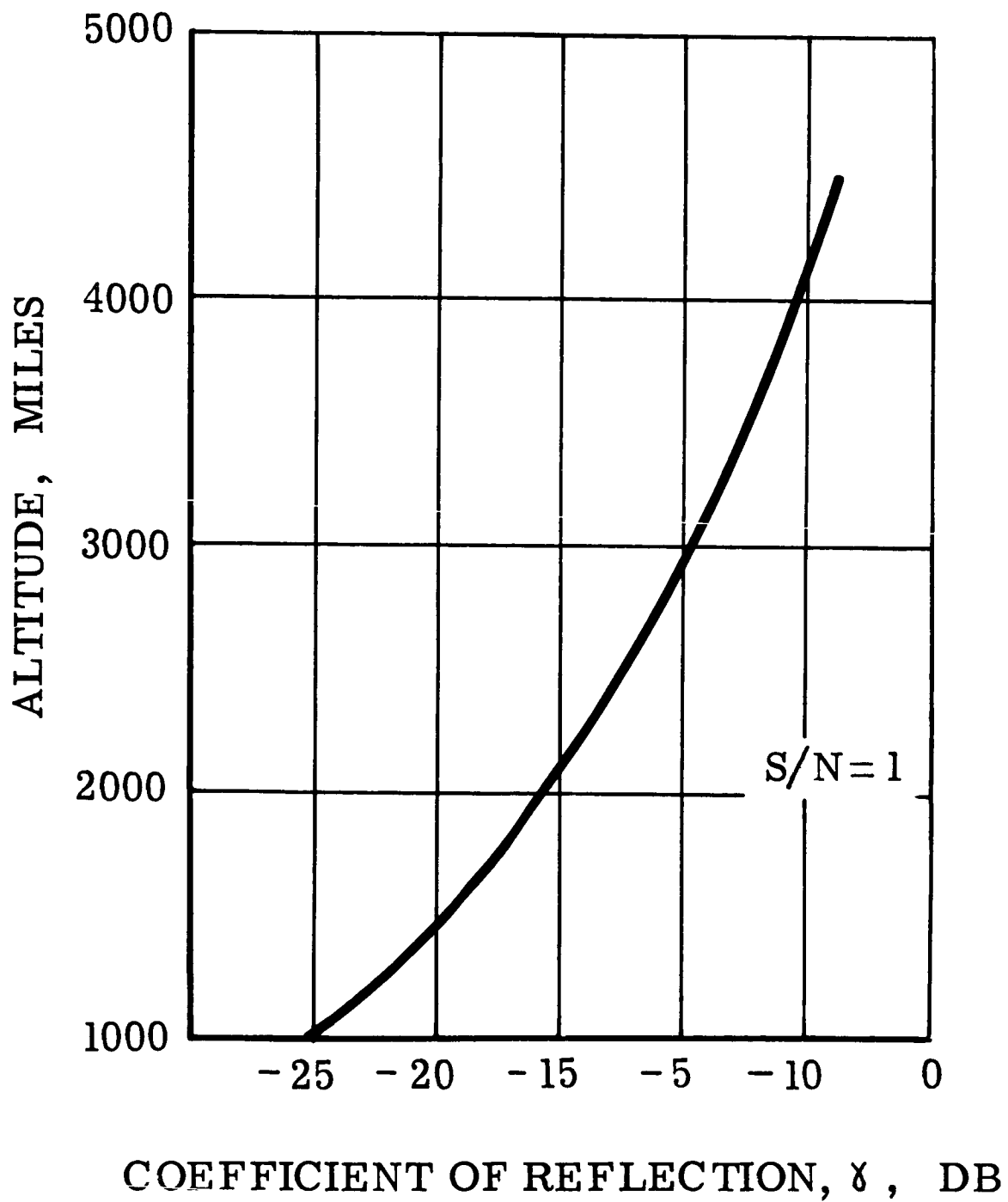


Figure 3.3.1-3. Required Reflection Coefficient vs. Altitude

To have the same performance at higher altitudes as obtained from 1250 miles, the transmitter average power must be increased by an amount approximately equal to the deficit in γ . The variation in velocity and ground illumination will affect the required transmitter power but the approximation is valid for the purpose here. The weight of about half of the radar system (50 lbs. out of 109 lbs.) is a function of average transmitter power and is assumed to have a linear relation to power. Table 3.3.1-3 gives the weight and power required for equal performance at 1250 miles and at higher altitudes for the same antenna size. A large weight penalty is incurred at higher altitudes. Therefore, it is not practical to change the radar power to accommodate the highly elliptical orbit.

Mapping will be done when the Orbiter is sufficiently close to the planet to give the required performance. This altitude is 1250 miles for a good map and 2000 miles for a fair map ($S/N = 4$ db). Because of the small displacement of the orbital tracks from one orbit to the next, the same terrain can be mapped a number of times. This will allow prominent terrain features to be distinguished from noise peaks and mapping may be done from higher altitudes.

TABLE 3.3.1-3. WEIGHT AND POWER FOR EQUAL PERFORMANCE
AT ALL ALTITUDES

Altitude (Miles)	Rel. Transmitter Power (db)	Power (Factor)	Trans. Avg. Pwr. (Watts)	System Weight (Lbs.)
1250	0	1	90	107
2500	9	8	720	457
3500	14.5	28	2500	1457
4500	18	62	5600	3147

(2) Variable Parameters

Many system parameters may be varied within the general configuration imposed by a 1,000 nm x 4,300 nm orbit and the mission goal of mapping the entire surface of the planet. Among the parameters which may be varied in the course of the design are: frequency, polarization, swath width and length, proportion of time spent mapping, recording capability, radar system cost, antenna area, map resolution (in range and in azimuth), signal-to-noise ratio of the final map, proportion of data reduction to be performed on the vehicle, data transmission capability, and required DC power input. Some of these parameters may be optimized by quantitative trade-offs. Other parameters are selected by qualitative trade-offs. For instance, trade-offs between antenna diameter and radar transmitter power were performed and are described below. It is observed that the radar system weight goes through a minimum at a particular value of antenna diameter. On the other hand, the selection of radar frequency is qualitative in nature.

The frequency recommended for the radar is S-band. It is recommended because it is one of several frequency ranges in which considerable design experience is available and because its wavelength is large enough that the antenna will retain its required dimensional stability (parabolic to within one-tenth of a wavelength) in the presence of the thermal stresses caused by partial solar illumination. An analysis of the dimensional stability of a parabolic dish was performed for vehicles orbiting Mars and is described in Section 2.3 of Volume IV, entitled "Structural Analysis." The analysis also shows that an X-band antenna is marginal. Since the solar environment is more severe for a Venus orbit, it is anticipated that the antenna deformation problem will be more pronounced for that case. It is recommended that this be investigated in detail in future design studies. Therefore, the dimensional stability problem precludes the use of the X-band frequency and possibly of C-band for a Venus Orbiter's radar. Another influence on the choice of S-band for the radar is the use of S-band in the data transmission system. There is the possibility that common or similar hardware can be developed for both the radar and for the communications, thereby, saving both time and money during the development program.

(a) Trade-offs Made to Optimize the Mission Performance

Trade-offs of antenna area vs. transmitter power were made and are described below, as well as a trade-off between vehicle-borne data reduction and required communications bandwidth. In both cases the selection of S-band as the radar frequency was assumed. In addition, the radar is not designed to produce uniform map quality at all altitudes in the orbit. The design philosophy is to obtain a "desired" map quality at the minimum orbital altitude and to accept a "less desirable" map quality at the higher altitudes in the orbit. The resultant map of the planet's surface is significantly better in one hemisphere, approaching the "desired" map quality.

(b) Trade-offs of Antenna Area vs. Transmitter Power

Using the S-Band frequency selected as described above, the antenna area and required transmitter power needed to illuminate the surface with a given power per unit area may be calculated. The power per unit area is determined from the radar range equation (as modified for SAHARA) and the signal-to-noise ratio to be obtained for a given resolution with a given surface reflectivity. Two resolutions were considered: a 1 nm x 1 nm resolution and a 2 nm x 2 nm resolution. The range resolution depends only on the number of sub-pulses in a transmitted pulse and the angle of incidence between the pulse and the surface (45°). However, the azimuth resolution for the SAHARA system is given by:

$$\text{azimuth resolution} = \frac{\lambda c}{4 v} \quad (8)$$

where

λ = Radar wavelength

c = velocity of light

v = ground velocity

For S-band ($\lambda = 0.12$ m) and the ground velocity at 1,000 nm altitude ($\approx 5,000$ m/sec), the azimuth resolution is approximately 1.0 nm. Therefore, a surface resolution of 1 nm x 1 nm is the finest resolution to be obtained from an S-band SAHARA system, assuming range resolution is set equal to azimuth resolution. A surface resolution of 2 nm x 2 nm is also considered for comparison.

If a 1 x 1 nm resolution system is examined, it is found that $S/N = 1.0$ for a surface reflectivity of -25 db when the power per unit area incident on the surface is approximately $0.43 \text{ watts}/(\text{nm})^2$. For 2 nm x 2 nm resolution, $0.125 \text{ watts}/(\text{nm})^2$ is required. This illumination may be obtained by using a high transmitter power with a small antenna and illuminating a large area, or by using a lower transmitter power with a larger antenna and illuminating a smaller surface area. It is noted that in the cases considered, the total area illuminated over the entire mission is constant since the entire planet is mapped. The area illuminated with a given pulse then determines the proportion of time to be used in gathering mapping information and the proportion of time during which no mapping is carried out. The trade-off is made by evaluating the weight of the SAHARA system for antenna diameters between 6 feet and 15 feet and examining the results for a minimum weight. The minimum weight criteria is then used to select the optimum antenna diameter.

The antenna weights are based on a paraboloid of revolution constructed of aluminum honeycomb, the required feed structure, launch support structure, and antenna boom and motor. Volume IV contains a detailed analysis of the antenna designs.

The weight vs. diameter is given in the table below:

TABLE 3.3.1-4. ANTENNA WEIGHT VS DIAMETER

<u>Antenna Diameter (Ft.)</u>	<u>Antenna Weight (Lbs.)</u>
6	13.8
8	20.4
10	32.0
12	61.3
14	102.5
15	130.0

As the antenna diameter decreases, the required S-band power output must increase. This requires an increase in the weight of the modulator, transmitter, and radar power supply (to convert DC power to S-band power). Also the weight of the DC power source must be increased since there must be greater weight allotted to solar cells and support structure, batteries, wiring, etc. In calculating the weight penalty for a given S-band power, a 25 percent conversion efficiency from DC to S-band is assumed. Also, it is assumed that the radar will be mapping during only one-sixth of orbit time since this will provide a map of the entire surface with allowance for overlap. The DC power supply weights are shown in Tables 3.3.1-5 and 3.3.1-6. The weights are based on 200 pounds per kilowatt, as shown in the power supply analysis (Section 6 of Volume III). The radar receiver and the limited data processing required represent fixed weights. The weight allotted for these fixed items is 30 pounds.

The following tables and graph show the total radar system weight for a given antenna diameter. They include the weights of the major subsystems. An Orbiter altitude of 1,000 nm is assumed for each table. The resolutions are 1 nm x 1 nm and 2 nm x 2 nm. A summary of data is given by Figure 3.3.1-4.

For both resolutions considered, the total system weight goes through a minimum. For 1 nm x 1 nm resolution, the system weight is a minimum for a 10-foot diameter. For a 2 nm x 2 nm resolution, the minimum extends from an 8-foot diameter to a 10-foot diameter.

The 1 nm x 1 nm resolution system represents the finest resolution obtainable with an S-band SAHARA system. It is 35 pounds heavier (33 percent heavier) than the 2 nm x 2 nm resolution system. It is recommended that the 1 nm x 1 nm resolution system be used since the weight penalty is not unduly severe for the four-fold increase in map information obtained.

The antenna diameter vs. transmitter trade-offs clearly show that 1 nm x 1 nm resolution may be obtained with an optimized radar system based on a 10-foot diameter antenna and a 109 pound total radar system weight.

(3) Antenna Pointing Accuracy Requirements

A side-looking antenna pointed at a depression angle of 45 degrees, nominal, is used in the mapping mode. The question naturally arises as to the required antenna pointing accuracy. To answer this question, antenna pointing accuracy in the vertical plane will be discussed first, and it will be followed by a discussion of accuracy requirements in the horizontal plane.

(a) Five Vertical Pointing Accuracy Effects

Five effects are considered in discussing vertical pointing accuracy in the following paragraphs.

TABLE 3.3.1-5. POWER REQUIREMENTS FOR THE SAHARA RADAR,
FUNCTION OF ANTENNA DIAMETER, 1 NM X 1 NM RESOLUTION

Antenna Diameter (Ft.)	Peak S-Band Power (Watts)	Average S-Band Power (Watts)	Required DC Power (Watts)	DC Power Supply Weight (Lbs.)
6	400	66.7	267	53
8	170	28.4	114	23
10	87	14.5	58	12
11	65	10.8	43	9
12	50	8.3	33	7
13	40	6.7	28	6
14	25	4.2	17	3
15	15	2.5	10	2

RESOLUTION FROM AN ALTITUDE OF 1,000 NM

TABLE 3.3.1-6. POWER REQUIREMENTS FOR THE SAHARA RADAR,
FUNCTION OF ANTENNA DIAMETER, 2 NM X 2 NM RESOLUTION

Antenna Diameter (Ft.)	Peak S-Band Power (Watts)	Average S-Band Power (Watts)	Required DC Power (Watts)	DC Power Supply Weight (Lbs.)
6	100	17.0	68	13
8	45	7.5	30	6
10	25	4.0	16	3
12	15	2.5	10	2
14	10	1.6	6.5	1

RESOLUTION FROM AN ALTITUDE OF 1,000 NM

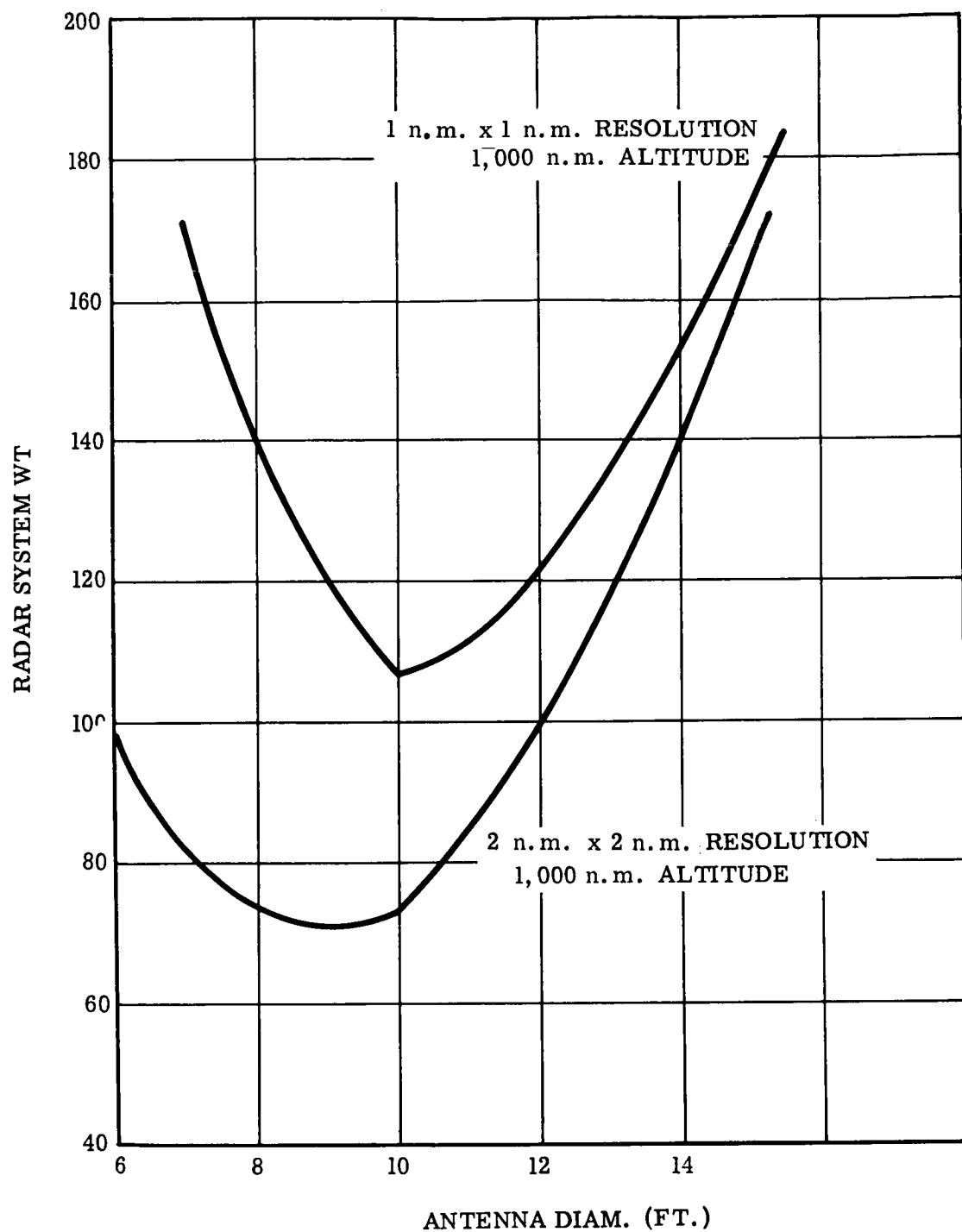


Figure 3.3.1-4. Graph of Radar System Weight vs. Antenna Diameter for 1 n. m. x 1 n. m. Resolution and 2 n. m. x 2 n. m. Resolution at an Altitude of 1,000 n. m.

TABLE 3.3.1-7. TOTAL RADAR SYSTEM AND SUBSYSTEM WEIGHTS, FUNCTION OF ANTENNA DIAMETER,
1 NM X 1 NM RESOLUTION

Antenna Diameter (Ft.)	Total Radar System Weight (Lbs.)	Antenna Weight (Lbs.)	Transmitter Modulator & Power Supply (Lbs.)	DC Power Supply (Lbs.)	Fixed Weights (Receiver, etc.) (Lbs.)
6	257	14	160	53	30
8	141	20	68	23	30
10	107	30	35	12	30
11	110	45	26	9	30
12	120	63	20	7	30
15	172	130	10	2	30
RESOLUTION FROM AN ALTITUDE OF 1,000 NM					

TABLE 3.3.1-8. TOTAL RADAR SYSTEM AND SUBSYSTEM WEIGHTS, FUNCTION OF ANTENNA DIAMETER,
2 NM X 2 NM RESOLUTION

Antenna Diameter (Ft.)	Total Radar System Weight (Lbs.)	Antenna Weight (Lbs.)	Transmitter Modulator & Power Supply (Lbs.)	DC Power Supply (Lbs.)	Fixed Weights (Receiver, etc.) (Lbs.)
6	97	14	40	13	30
8	73	20	17	6	30
10	72	30	9	3	30
12	100	63	5	2	30
15	166	130	5	1	30
RESOLUTION FROM AN ALTITUDE OF 1000 NM					

1) Change in Radar Range

The radar range is larger at smaller depression angles; hence, the signal-to-noise ratio would be decreased, thereby reducing the range capability at these angles. A special case occurs at minimum altitude and large depression angles. In the condition of this case, radar returns would be received before the transmission stops. Since the receiver is blanked during transmission, the range resolution of targets at the near edge of the beam would be degraded accordingly. Shortening the length of the transmitted pulse would eliminate this effect. The above two effects can be considered negligible if the vertical pointing error is held to ± 5 degrees.

2) Change in Range Resolution

Range resolution is given as:

$$\Delta R = c/2 \tau \sec \theta \quad (9)$$

where

ΔR = range resolution

c = velocity of light

τ = subpulse length

θ = graze angles

As can be seen by the equation, a ± 5 degree error would not seriously affect the range resolution for a nominal graze angle of 45 degrees.

3) Change of the Target Coefficient of Reflection (γ)

This effect will be discussed later. Again ± 5 degrees is sufficient.

4) Different Doppler Histories of Targets at Different Ranges

Ground processing will permit compensation of this effect.

5) Accuracy of Map

It should be obvious that positional accuracy of the ground map depends on the accuracy in antenna pointing. However, if the Orbiter's orbit is known, a range accuracy of one mile can be obtained by radar range timing in the ground processor. Another factor to consider is that if a large area is to be mapped by over-lapping several strip maps, the overlap must be sufficient to allow for vertical antenna pointing error.

(b) Discussion

Antenna pointing accuracy in the horizontal plane is associated with doppler processing and the doppler clutter lock. Recalling that a side-looking antenna requires that the zero isodoppler line be illuminated for proper operation and that a doppler clutter lock is employed, the factors which change the position of the zero isodoppler lines should be reviewed. The following three factors will displace the zero isodoppler line from abeam the Orbiter's ground-track velocity:

- 1) Planet's rotation
- 2) Vertical velocity component of Orbiter
- 3) Horizontal antenna pointing error

Since Venus rotates approximately one revolution every 225 Earth days, the shift of the zero isodoppler line based on this factor is negligible. The elliptical orbit of the Orbiter is such as to give a vertical velocity component on the order of 0.5 mile/second at the extreme.

Since the doppler clutter lock must correct each of these factors, it is desirable to keep the horizontal pointing error to within ± 1.5 degrees. Further, a second clutter lock, ground-based, can be employed to allow a greater pointing error in the event of a partial failure.

Since the clutter lock signal is telemetered to Earth, the horizontal pointing error can be computed and the horizontal positioning accuracy can be improved to one mile. The other effects on horizontal pointing accuracy (radar range for example) are negligible if the ± 1.5 -degree limit is maintained.

The required horizontal and vertical attitude accuracy requirements are within the capability of the vehicle's attitude control system.

(4) System Operation

The block diagram of the radar equipment carried in the orbiting vehicle is shown in Figure 3.3.1-5. Processing of this data will be done on the ground. This equipment block diagram is given in Figure 3.3.1-6.

Three highly stable oscillators are required in this system: the microwave source or STALO, the IF oscillator or COHO, and the clock-pulse generator. The clock-pulse generator is necessary to control the spacing of all the subpulses in the long transmitted pulse as well as to control the data propagation rate in the shift registers.

At the beginning of the transmit period, the PRF generator connects the clock-pulse generator to the shift register encoder and keys the modulator for the power amplifiers. The shift register coder produces a train of video pulses whose polarity reverses in a random manner. This train of video pulses modulates the COHO signal to produce a train of IF pulses whose phase alternates between zero and 180 degrees. This modulation is performed with a suppressed carrier, balanced modulator. The output drives a single sideband modulator which, in turn, modulates the microwave signal with a 180-degree random phase reversal modulation. This microwave signal is subsequently amplified and passed through the duplexer to the antenna. After the long pulse has been transmitted, the power amplifiers are turned off and the equipment is ready for reception of the target signals. When the radar returns are received, they are immediately mixed with the STALO to produce an IF signal centered at the COHO frequency. The signals are then amplified in a conventional 30 megacycle IF strip having the necessary bandwidth.

The signal from the intermediate frequency amplifiers is coherently detected in two channels to give in-phase and quadrature components. The coherent or phase-sensitive detectors are essentially balanced modulators in which extra care has been taken to balance capacitances at the expected IF frequencies.

The COHO (COherent High Frequency Oscillator) is shifted by 90 degrees for the quadrature channel. This is preferable to shifting the IF information, since such a shift would be a function of frequency and, therefore, different for the various doppler frequencies.

It will be recalled that a side-looking radar requires that the zero doppler line be illuminated for proper operation. There are conditions during which the zero doppler line will not be illuminated due to antenna pointing error and rotation of the planet. Doppler clutter lock can be employed to overcome these restrictions. This technique is used to determine the average doppler frequency present in the radar returns. This average doppler frequency, now called the off-setting frequency, modulates a single-sideband generator which offsets the radar return. Thus, the radar returns at the output of the single-sideband generator have an average doppler frequency of zero. If neither the antenna pointing error nor the planet rotation are considered serious, the doppler clutter lock circuitry can be eliminated.

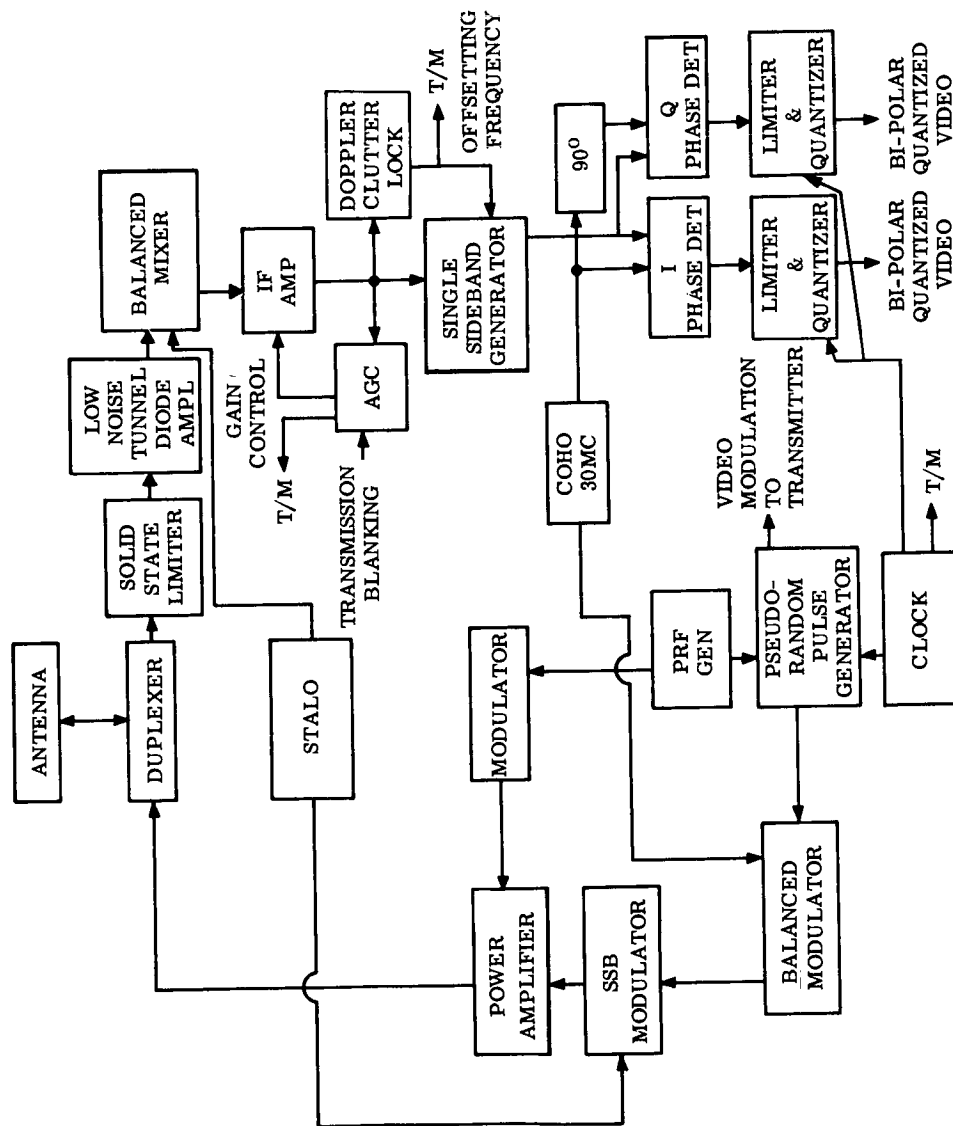
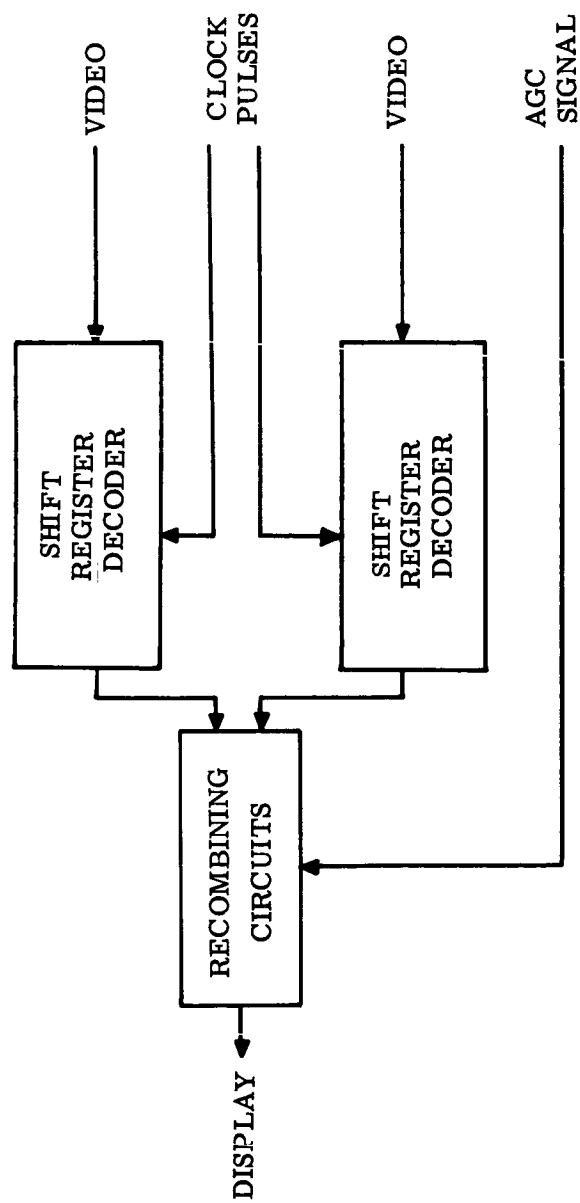


Figure 3.3.1-5. Equipment in Vehicle



FROM TELEMETRY

Figure 3.3.1-6. Processing on Ground

However, the doppler clutter lock would provide information via telemetry regarding antenna pointing errors that occur as a result of a malfunction.

As shown in the schematic diagram, the synchronous detectors are followed by limiters. Thus, the subsequent circuits are insensitive to changes in signal amplitude and can react to changes in polarity alone. The useful information in the waveform, after limiting, is contained in the zero crossings only. As shown in Volume VIII, Section 6, Voyager Radargrammetry, the process of recovering the relative amplitude information from the various targets is a linear process. To prevent false signals from being propagated down the shift register chain, the limited waveform is passed through a time quantizer or boxcar circuit which is triggered by the same clock-pulse that triggers the shift register chain. This prevents changes of state during a subpulse interval.

Recovery of the short pulse information from the long coded pulse is performed in a shift register data processor on the ground. The analysis and theory of operation of this type of processor is considered in detail in Volume VIII, Section 6. A general block diagram of the processing system is shown in Figure 3.3.1-7.

The output of each element of the shift register chain will be fed into a number of resistively loaded parallel paths, each path being a different doppler channel.

In many shift register chain configurations, both positive and negative outputs will be available. If both are available, only one summing bus is required for each amplitude weighting function. The analysis of the required sinusoidal space weighting functions is presented in Volume VIII, Section 6. Figure 3.3.1-7 shows a shift register chain with a desired sine wave weighting function.

Each resistor must have a different value to give the proper shape to the amplitude function. It is noted that a negative value is achieved by connecting a normally negative output to the positive bus and vice-versa. The resistors at the peak of the sine wave, cells 6 and 7 for instance, will have the unit or minimum value. If the filter is centered at doppler frequency, f_d , then there will be $\eta/f_d T$ shift register elements per cycle of amplitude variation. The amplitude function can, therefore, be expressed as:

$$A = \sin \left(2 \pi \frac{f_d T}{\eta} n \right) \quad (10)$$

where n is the number of the element in the shift register.

Assuming the summing is accomplished in a feedback adder, the impedance of the summing point will be a virtual ground. The value of the n^{th} register's adding resistor is then given by:

$$R_n = \frac{R_1}{A} \quad (11)$$

where R_1 = Base or unit resistance.

This process requires a large number of tap resistors. An example will illustrate the magnitude of this problem. Consider a system with η of 3000 and consisting of 31 parallel channels (15 positive, 15 negative, and 1 zero doppler channel). The 30 non-zero doppler channels require 15 sets of 4 weighting functions, 2 each on the in-phase and the quadrature channels. The zero doppler channel requires two uniform weighting functions. Each of these weighting functions requires η tap resistors. Summing all these, the total number is $(15 \times 4 + 2) (3000)$ or 186,000 resistors. This factor is the primary reason for having the processor on the ground.

The summed outputs from the weighted channels are added or subtracted to obtain the in-phase and quadrature components of the negative and positive doppler frequencies.

This is followed by an RMS combining process. Usually, a simple addition of the full-wave rectified values of the two quadrature signal components is an adequate approximation to the RMS process.

The relative strengths of the signals have been preserved throughout this process. However, the pulse-to-pulse variations have been lost. To recover the relative strengths of targets many beamwidths apart, it is necessary to weight the shift register outputs on a pulse-to-pulse basis. This must be done with a signal proportional to the strength of the average target in the physical beam. It can be accomplished, quite simply, by weighting the data processor output with the AGC signal. If desired, additional accuracy and sophistication can be achieved by using the integrated output of the synchronous detectors before limiting as the weighting signal.

The outputs from the parallel doppler channels are scanned or commutated at a rate commensurate with the sub-pulse length. This results in a display as shown in Figure 3.3.1-8. The raster offset in the range direction is controlled by an analog signal proportional to the ground range.

Each separate SAHARA pulse will generate a complete, but small, map. The size of this map is roughly the size of the patch on the ground illuminated for each position of the physical beam. The width of the ground map in range for a given compression ratio, R , is directly related to the quality of map desired. A discussion of the transverse scanning method for achieving a wider map in a direction normal to the vehicle, is presented in the Voyager Radargrammetry Appendix (Volume VIII, Section 6).

The process of overlaying single pulse maps to achieve post-detection integration, in a direction parallel to the vehicle's motion, presents two problems. First, there is the problem of accuracy of overlay, assuming perfect single maps. One simple method of accomplishing this overlay is to focus the display tube on a carefully synchronized moving photographic film. Assuming the film speed to be integrally related to the vehicle motion and the display's azimuth scale, then, a given target will progress across the tube on successive pulses in such a manner that it will track the same point on the moving output film. Second, since pulse length is determined by the inside or minimum range, points at longer ranges have poorer resolution. The doppler filter outputs will represent increasing physical separation at ranges greater than the minimum. This will require the azimuth scan raster to change as a function of ground range, R_g , to prevent map distortion.

(5) Radar Map Data Acquisition and Data Rates

The radar mapper will be operated at times when the following two conditions prevail: (1) the vehicle orbital altitude is less than 2,500 nm, (2) the area has not been previously mapped (within a fixed percentage of overlap).

Since the radar beam must strike the surface of the planet at 45 degrees to the horizontal, the antenna angle from the local vertical through the Orbiter will vary from 22.8 degrees at 2,500 nm altitude to 32 degrees at 1,000 nm altitude. If both poles of the planet are to be mapped, the plane of the orbit must be inclined to the pole by an angle which will depend on altitude when passing over the pole. Also, the antenna must be capable of looking to the right and to the left of the orbital plane.

A schedule for obtaining radar data will have the radar antenna looking: to the right on the first orbit, straight down on the third orbit (for altimeter mode operation), and to the left on the fifth orbit. By the seventh orbit, the cycle will return to the pointing angle of the first orbit. In this way, every sixth orbit will provide a map adjacent to the one taken before.

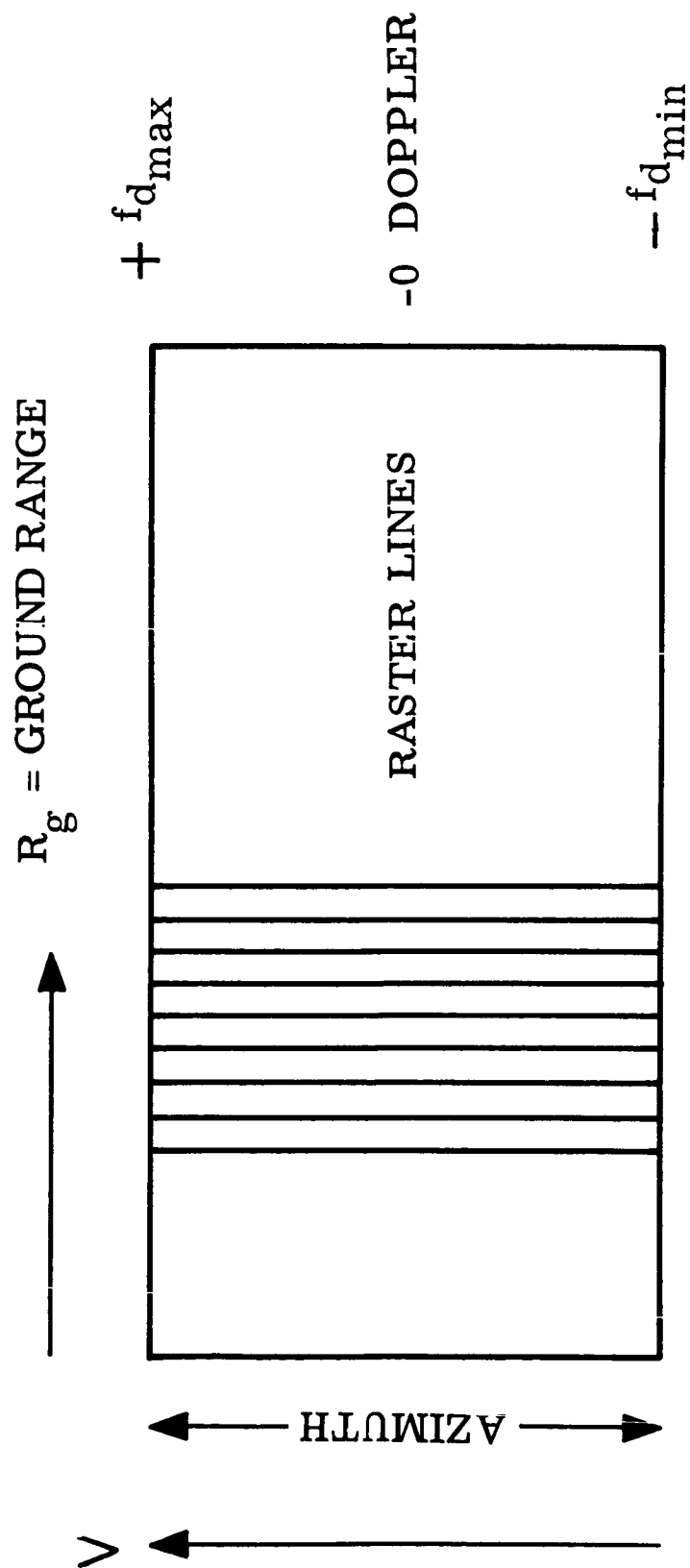


Figure 3.3.1-8. Display Raster-Single Pulse Map

For the radar to have constant pulse characteristics over the slant range of from 1,270 nm to 2,920 nm, the pulse length will be 15.6 milliseconds with a pulse repetition period of 52.3 milliseconds. For one nm range resolution, the transmitted pulse will be made up of 1,755 subpulses of 8.9 microseconds each. Since the period of reception will be 16.4 milliseconds (this includes the time taken to cover the 90 nm of the map), then, each radar channel will generate a total of 1,845 bits per pulse period. The number to be stored for each period consists of 3,690 radar bits, 63 sync bits, and 12 bits to indicate the slant range of the map, a total of 3,764 bits. For an orbit of 205 minutes, 95.8 minutes may be used to take radar data and the remainder of the period used to transmit to earth at 63,000 bits per second. During the record period, a total of 41.4×10^7 bits will be stored in a thermoplastic recorder.

Transmission of digital data from the radar limiters to the storage buffer units will be under the control (on - off) of the Slant and Ground Range Register. This will eliminate the storage of noise bits. The slant range data, a function of the Orbiter height, and a frame sync word will be included with each set of data stored.

(6) Recommended Terrain Mapping Radar Subsystem

The recommended terrain mapping radar subsystem for the Venus 1970 Orbiter is a SAHARA radar operating at S-band frequency with a 90-watt average power output during mapping and a 10-ft. diameter parabolic antenna. The data processing on the Orbiter includes phase detector, limiters, and the required data storage and playback equipment. The recommended radar system is compatible with the attitude sensing and control system and the Orbiter-to-earth communications system designed for the Mars 1969 Orbiter. The radar pulse length and pulse-repetition frequency are chosen to allow operation between the altitudes of 1000 and 2500 nm. The radar maps will not have constant quality over this altitude range.

System losses of about 10 db were included in establishing the transmitter power.

The total radar system weight is approximately 109 pounds as shown in Table 3.3.1-9.

TABLE 3.3.1-9. TOTAL RADAR SYSTEM WEIGHT OF
RECOMMENDED SYSTEM

Antenna	32 pounds
Low Voltage Power Supply	7 pounds
High Voltage Power Supply	8 pounds
Transmitter	27 pounds
Receiver	10 pounds
Packaging Structural Support	13 pounds
D. C. Power Supply	12 pounds
Solar Cell Array	7.88 pounds
Batteries	2.79 pounds
Regulation, control and distribution	1.33 pounds
	<u>12.00</u>

Total

109 pounds

Other radar system parameters are contained in the following list, Table 3.3.1-10.

TABLE 3.3.1-10. RADAR SYSTEM PARAMETERS OF RECOMMENDED SYSTEM

Peak Power Transmitted	302 watts
Average Power Transmitted	90 watts
Duty Cycle	0,298
PRF	19,1 PPS
Transmitted Pulse Length	15,6 milliseconds
Subpulse Length	8,9 μ s
Range Compression Ratio	1755
Azimuthal Beam Sharpening Factor	67
System Noise Temperature	800°K
System Noise Figure	5,7 db
Receiver Noise Figure	3,5 db
Transmitted Frequency	2295mc
Stability Requirements of Transmitter:	
Long Term Stability	1 part in 10^4
Short Term Stability	1 part in 10^9
Prime Power Input: Standby--	
Expected Value	27 watts
Maximum Value	35 watts
Radiate --	
Expected Value	440 watts
Maximum Value	570 watts
Average Output Data Rate	63 kbps
Size (excluding antenna)	
Expected Value	2,0 ft. ³
Maximum Value	3,2 ft. ³
Weight	
Expected Value	107 pounds
Maximum Value	141 pounds
Antenna	
Beamwidth	3°
Sidelobes:	
Vertical Below Main Beam	-20 db
Others	-15 db
Beam Shaping	None Required
Pointing Accuracy	$\pm 1,5^\circ$ max.
Cooling Requirements	No Special Cooling Required - Will conduct heat to Vehicle
Number of Post-Detection Integration Channels	67
Switching Required from Mapping Mode to Altimeter Mode	None-Identical Operation.

Recommended system input-output parameters are given in Table 3.3.1-11.

TABLE 3.3.1-11. INPUT-OUTPUT
PARAMETERS OF RECOMMENDED
SYSTEM

RADAR INPUT

Standby Command	Applied 1 to 2 minutes before Radiate Command
Radiate Command Prime Power	

RADAR OUTPUT

In-Phase Video Radar Signal	8.9 μ sec Random Pulses at a 112.4 kc Rate for 16.8 ms, Repeated at a Rate of 19.1 cps
Quadrature Video Radar Signal	Same as above, occurring at the same time
PRF Sync Pulse	T/M One Pulse every 52.3 ms
Clock Signal	112.4 kc Sync (for Storage Only)
Receiver AGC Signal	T/M to Ground for Determining γ
Doppler Clutterlock Signal	T/M to Ground to Determine if Antenna is Pointing Properly
Several In-Flight Monitor Signals	T/M to Ground, used to evaluate Radar Subsystems Operation

Operating mode parameters for the recommended system are given in Table 3.3.1-12.

TABLE 3.3.1-12. OPERATING MODE
PARAMETERS OF RECOMMENDED
SYSTEM

OPERATING MODE

Mapping

Information Gathered

Reflectivity of Planet

Ground Map (Giving MTI)

Three-Dimensional Map

Swath width of Strip Map (at 1000 nm altitude)	Any value up to 95 nm
--	--------------------------

TABLE 3.3.1-12. OPERATING MODE PARAMETERS
OF RECOMMENDED SYSTEM (Cont'd)

Length of Strip Map for 10 min. Mapping
Time (at 1000 nm altitude) 1620 nm

Range Resolution (at 45° Graze Angle) 1 nm

Target Coefficient of Reflection, (γ), To
Give a Signal-To-Noise Ratio of 1 and
Azimuthal Resolution Vary with Altitude.
Several Values are Given in the Following.

Altitude (N. Miles)	Slant Range* (N. Miles)	Ground Velocity (Ft./Sec.)	γ ** (db)	Azimuthal Resolution (N. Miles)	Range Resolu- tion (N. Miles)
1000	1280	16,400	-25.0	1.0	1.0
1200	1520	15,300	-22.4	1.1	1.0
1600	1970	13,400	-18.7	1.2	1.0
2200	2650	11,250	-15.5	1.5	1.0
2500	3000	10,300	-12.8	1.6	1.0

* Assuming a grazing angle of 45°

** γ for S/N = 1 after post-detection integration

B. Coherent Pulse Doppler Radar

(1) Basic Concepts

In the synthetic aperture radar, only a single radiating element is used. This element is moved so that it occupies, in turn, each of the positions of a long linear array. At each of these positions, a signal is transmitted and the radar echoes are received. The received signals are put into storage. Subsequent operation on this data is used to combine these signals in a manner appropriate to synthesize a long aperture antenna. To do this, the storage and data processing operations must preserve the essential vector character of the signals. Therefore, a coherent radar system preserving both phase and amplitude is required.

It is evident that, if the signals are in storage, there is considerable freedom available as to the exact way in which the signals are combined to produce the synthetic antenna. Two principal methods of signal combination are currently in use. These lead to two principal types of synthetic aperture radar: the focussed and the unfocussed.

(a) The Unfocussed Synthetic Antenna

The simpler of the synthetic antenna techniques is that which generates an unfocussed synthetic aperture. In this case, the coherent signals, received at the synthetic array points, are integrated with no attempt made to shift the phases of the signals before integration. This lack of phase adjustment imposes a limit on the maximum length of synthetic antenna which can be generated. This maximum length depends upon the target range and occurs when the round-trip distance, from a target to the center of the synthetic array, differs by $\lambda/4$ from the round-trip distance between that target and the extremities of the synthetic antenna array.

The pertinent geometry is shown in Figure 3.3.1-9. In this figure, R_0 , represents the range from a radar target to the center of the array and, L_{eff} , represents the maximum synthetic antenna length for which the distance from the target to the extremities of the synthetic antenna does not exceed $R_0 \pm \lambda/8$.

It is evident from this geometry that

$$(R_0 + \frac{\lambda}{8})^2 = \frac{(L_{eff})^2}{4} + R_0^2 \quad (12)$$

If this expression is solved for L_{eff} , subject to the assumption that $\lambda/16$ is small compared to R_0 , the result is

$$L_{eff} = \sqrt{R_0 \lambda} \quad (13)$$

Because of coherence, the relative phase of signals received from a target depends on the round-trip distance to it. Consequently, the beamwidth of the synthetic antenna is one-half that of a conventional array of the same length, i. e.,

$$B = \frac{\lambda}{2 L_{eff}} \quad \text{radians} \quad (14)$$

The resolution is now taken to be the product of beamwidth and range, R , that gives as a result

$$\text{Resolution} = 1/2 \sqrt{R \lambda} \quad (15)$$

which is the resolution equation for the unfocussed synthetic aperture.

As shown in (15) above, the linear azimuth resolution is independent of the antenna aperture size. For the unfocussed case, fineness of resolution is increased by the use of shorter wavelengths but, in comparison with the conventional case, the improvement in fineness of resolution varies as the square root of λ rather than directly as λ .

Most significant is the fact that resolution is degraded in proportion to the square root of range, rather than directly with range, as in the conventional radar.

(b) The Focussed Synthetic Aperture

In the unfocussed radar, the received signals were combined by in-phase addition of all signals received over the synthetic aperture length, giving rise to the equivalent of a linear antenna array. In the focussed radar phase, corrections are applied to the several signals before they are combined. These corrections are range dependent. They give rise to the equivalent of a curved array, the curvature of which correctly focusses the array for every target range. Under these conditions the phase discrepancies that limit the length of the unfocussed aperture no longer apply and a longer synthetic aperture can now be realized.

The new limitation on aperture length is found by considering that the target must be illuminated by radar energy at all times while it is within the pattern of the synthetic array. Thus, the limitation on synthetic antenna length is due to the finite beamwidth of the physical antenna and, hence, depends upon the length, D , of the physical antenna.

The synthetic aperture length is given by

$$L_{eff} = \frac{\alpha \lambda R}{D} \quad (16)$$

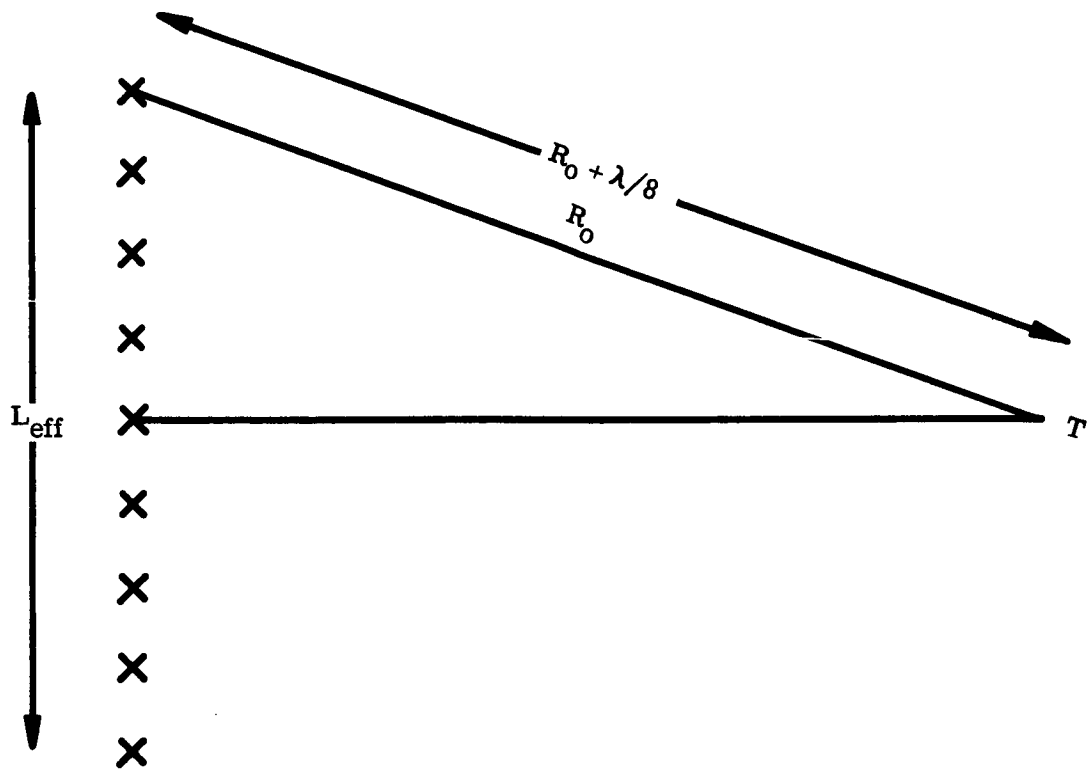


Figure 3.3.1-9. Geometry for Unfocused Synthetic Antenna

and the resolution is

$$\text{Resolution}_{\text{foc}} = \frac{D}{2\lambda} \quad (17)$$

The coefficient α has been introduced because, in some situations, a resolution coarser than $D/2$ may be sufficient. In this case, a fraction of the maximum synthetic antenna length will actually be employed.

For those situations for which the synthetic antenna length given by (17) is less than or equal to the unfocussed length, only a limited improvement in resolution can be obtained by focussing. However, if sufficient resolution cannot be obtained with the unfocussed technique, then focussing should be used. The use of focussing, in effect, removes the restriction on synthetic antenna length which would otherwise apply.

(c) Summary

The azimuth resolutions for these radars and a conventional radar are as follows:

$$\text{Resolution}_{\text{conv}} = \frac{R\lambda}{D} \quad (18)$$

$$\text{Resolution}_{\text{unfoc}} = 1/2 \sqrt{R\lambda} \quad (15)$$

$$\text{Resolution}_{\text{foc}} = \frac{D}{2\alpha} \quad (17)$$

The above equations indicate that the resolution capabilities of the three types of radar are substantially different. It has been shown that the fineness of resolution, other parameters being fixed, varies directly as λ for the conventional case, as the square root of λ for the unfocussed case, and is independent of λ for the focussed case.

The dependence of fineness of resolution on physical antenna size has been shown: to improve for larger apertures in the conventional case, to be independent of aperture in the unfocussed case, and to improve with smaller apertures in the focussed case.

The dependence of fineness of resolution on range has been shown: to deteriorate directly with range in the conventional case, to deteriorate as the square root of range in the unfocussed case, and to be independent of range for the focussed case.

(2) Variable Parameters

The selection of frequency and physical antenna size tend to be limited by practical considerations. Consequently, it is instructive to fix these parameters with reasonable values and to plot theoretical resolution versus range for the three types. The results are plotted in Figure 3.3.1-10. This plot is for an antenna aperture of 10 ft. and a wavelength of 0.1 ft., which are considered reasonable values for a spacecraft radar. For ranges in excess of 1,000 nautical miles, the best resolution that can be obtained by the conventional technique with the above parameters is on the order of 10 nautical miles. Generally speaking, resolution of this order is inadequate for most terrain mapping applications. Thus, the conventional technique is not very suitable. The resolution of a radar using unfocussed processing at 0.1 ft. wavelength will have an optimum resolution of approximately 390 ft., which is considerably better than can be obtained with a brute force approach. For the 10 ft. antenna length, the theoretical limit on resolution of a focussed synthetic antenna is 5 feet.

For the unfocussed case, the figure also gives the results for a wavelength of 13 cm. Because of the square root relationship, the resolution degrades by only a factor of 2.

It is shown below that the transmitter power capability and realizable antenna size which can be provided in the Voyager spacecraft limit the realizable resolution to a value of about 1,000 feet. Examination of Figure 3.3.1-10 then indicates that the unfocussed technique is most suitable when a resolution of about 1000 feet is acceptable at Orbiter altitudes in the assumed range from 1,000 to 4,300 miles.

Many parameters are involved in the specification of the satellite-borne radar. Each of the following sections contains a discussion of an important item required to specify the recommended radar system.

(a) Antenna

Several conflicting considerations enter into the choice of antenna geometry. These include:

- (1) The area of the antenna must exceed a minimum value in order to avoid ambiguities in the interpretation of signal returns. This minimum value depends upon: the radar resolution, the Orbiter speed with respect to terrain, and the pointing angle of the antenna.
- (2) Depending on the weight penalty per unit area of antenna, a larger-than-minimum antenna may be desired for the increased gain that will reduce the radar transmitter power requirement. However, a more directive antenna may undesirably reduce the terrain mapping rate because of the reduced area of terrain illuminated.

The minimum antenna area requirement is dictated by ambiguity considerations. Basic ambiguity considerations come from two sources. First, the maximum doppler shift of target returns observed in the antenna beam must be sampled by the PRF at least twice per cycle of this maximum shifted frequency. Second, on the other hand, the ground range interval to be covered by the radar must be sufficiently narrow that no more than one transmitted pulse impinges in the region at any instant. This limited ground range coverage is obtained by making the vertical antenna beamwidth narrow or by making the height of the antenna large. The required PRF is kept below a certain level by making the length of the antenna great, so that the beamwidth of the antenna in the horizontal direction is sufficiently small that the maximum doppler frequency return illuminated by the antenna is held below a given level. By combining the above considerations, the minimum antenna area for a given radar vehicle can be determined by the following equation

$$A_{\min} = \frac{9 V_{gs} R \lambda}{c \tan \alpha} \quad (19)$$

where V_{gs} is the speed of the Orbiter with respect to the terrain, R is the radar range, λ is the radar wavelength, c the speed of light, and α the angle of grazing incidence (assumed here at 45°). Smaller antenna areas can be used; however, it will always be at a sacrifice because the ambiguous signal returns will become larger with respect to the desired radar signals.

In the above expression, the speed and velocity are dependent upon Orbiter altitude. Thus, the required minimum area is a function of altitude. Figure 3.3.1-11 shows a plot of minimum area versus altitude for a wavelength of 3.2 cm.

A 14 ft. diameter antenna is a possibility on the spacecraft. Assuming that the effective area is 80 percent of the physical area, this antenna would have an effective area of 123 square feet which is somewhat less than the desired minimum area of

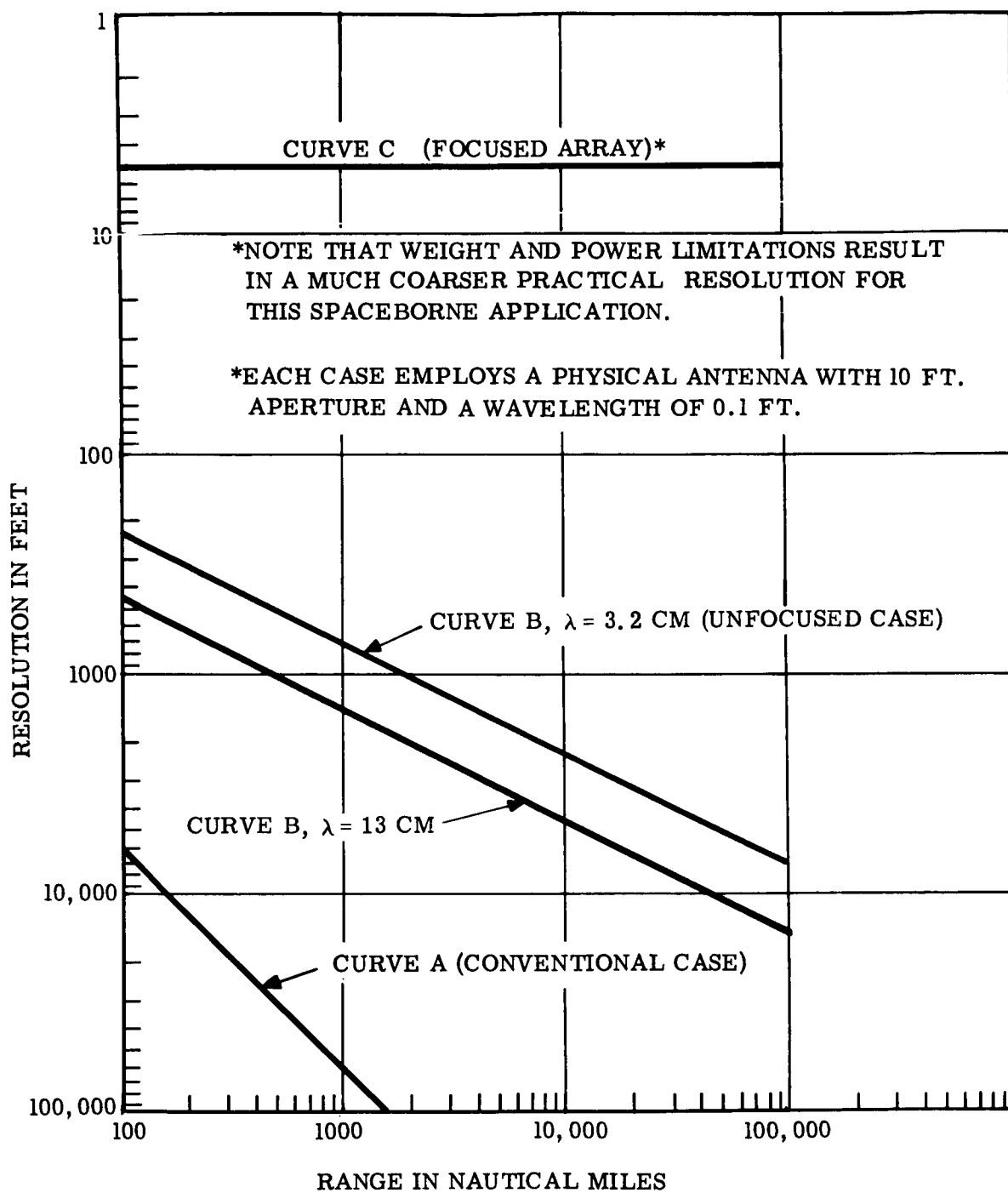


Figure 3.3.1-10. Azimuth Resolution as a Function of Range for Three Types of Radars

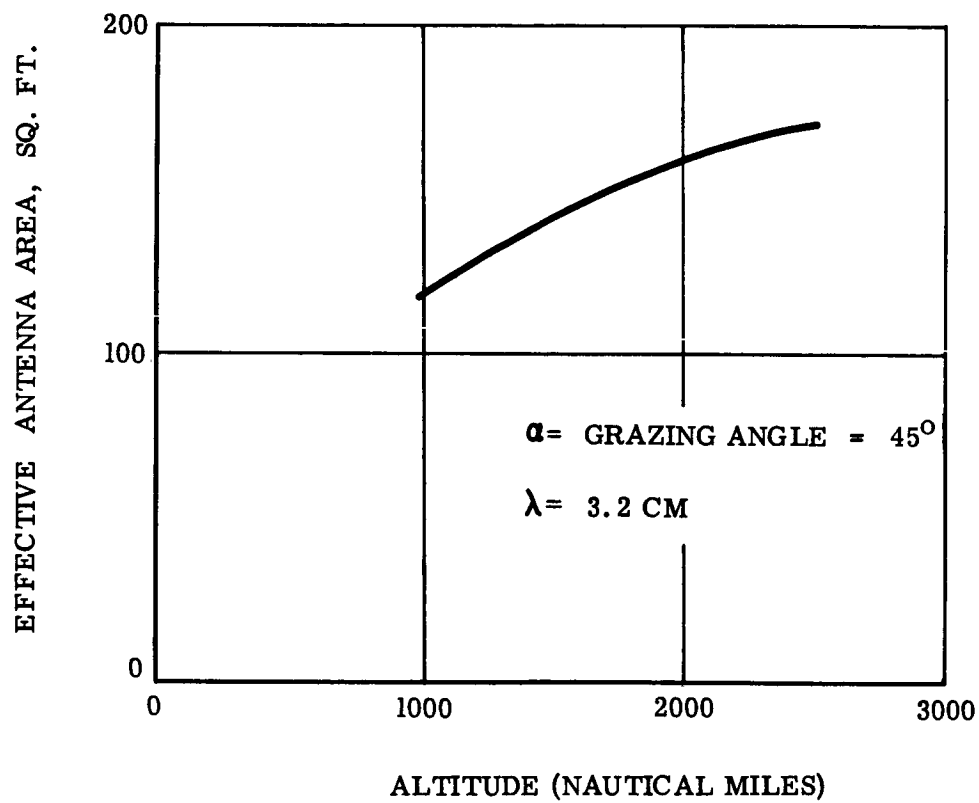


Figure 3.3.1-11. Minimum Antenna Area for Ambiguity Avoidance vs. Altitude

170 square feet shown in Figure 3.3.1-11 for a wavelength of 3.2 cm and at 2500 miles altitude. The effect is to increase the level of ambiguous signals that will be found in the radar returns. However, the ambiguous return should still be from 15 to 20 db below the desired signal and no serious degradation in the quality of the map data should result. Therefore, the 123 sq. ft. of effective possible antenna area on the vehicle, while not as large as desired, will perform adequately over the given altitude range of the satellite. While the case of operating with a 13 cm wavelength (S-band) looked attractive from the resolution viewpoint, the physical area of the antenna required is about 600 sq. ft. Therefore, wavelengths other than 3.2 cm will not be considered further.

(b) Transmitter Power

The required average power for a synthetic aperture radar is given by the following equation which is developed in Volume VIII, Section 5, a report by Conductron Corp.

$$P_a = \frac{8\pi \frac{S}{n} R^3 V k T \lambda}{\delta \gamma \sin \alpha A^2} \quad (20)$$

where

$\frac{S}{n}$ = required signal-to-noise ratio = 10

k = Boltzman's Constant = 1.38×10^{-23}

T = Effective receiver temperature = 1,000°K

γ = Backscattering coefficient per unit projected cross section area

δ = Resolution

and the remaining quantities have been previously defined.

In this equation, range and velocity are both dependent on Orbiter altitude. The antenna area can be fixed at the value previously specified. The equation can then be used to plot required transmitter power as a function of resolution with Orbiter altitude as a parameter. This plot is shown in Figure 3.3.1-12, where a constant backscatter coefficient has been assumed. Examination of this curve, together with a consideration of the weight available for the transmitter, suggests that a reasonable operating point may employ a resolution of about 1000 feet and a transmitter average radiated power of about 20 watts.

Once the above parameters have been selected, the threshold detection capability of the radar (in watts) has been fixed. The value of terrain backscatter coefficient then required to exceed the detection threshold will vary with the altitude of the Orbiter. This dependence is shown in Figure 3.3.1-13.

The peak power of the radar transmitter is determined by considering the PRF and pulse length. The radar PRF is dictated by the maximum doppler shift of a target located in the antenna beam. This PRF must be at least twice the maximum frequency shift and is given by the following equation:

$$\begin{aligned} \text{PRF} &= \frac{2V}{D} = 2700 \text{ PPS @ } h = 1000 \text{ nm} \\ \text{or} & \\ &= 1000 \text{ PPS @ } h = 5000 \text{ nm} \end{aligned} \quad (21)$$

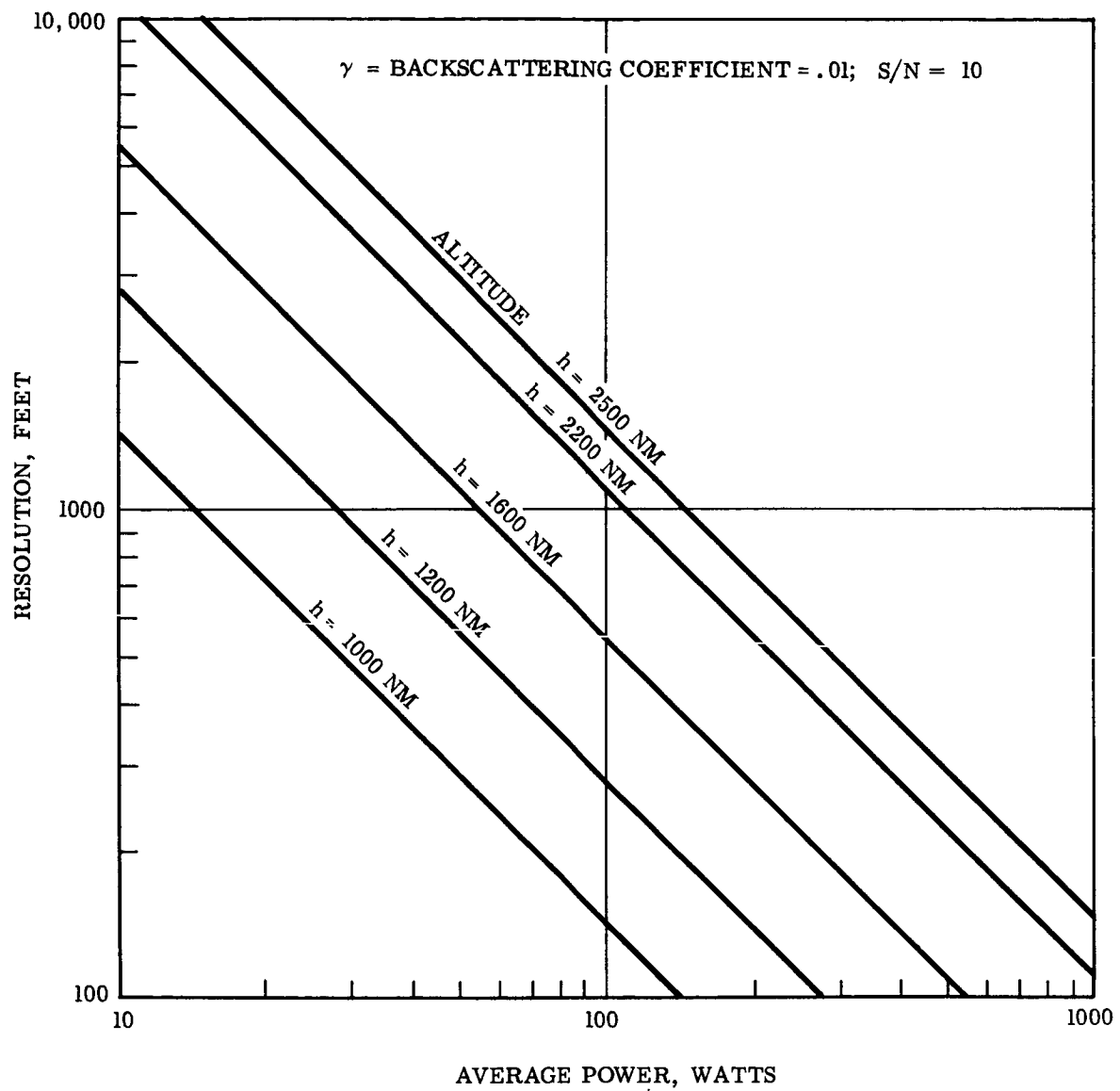


Figure 3.3.1-12. Resolution vs. Average Radiated Power

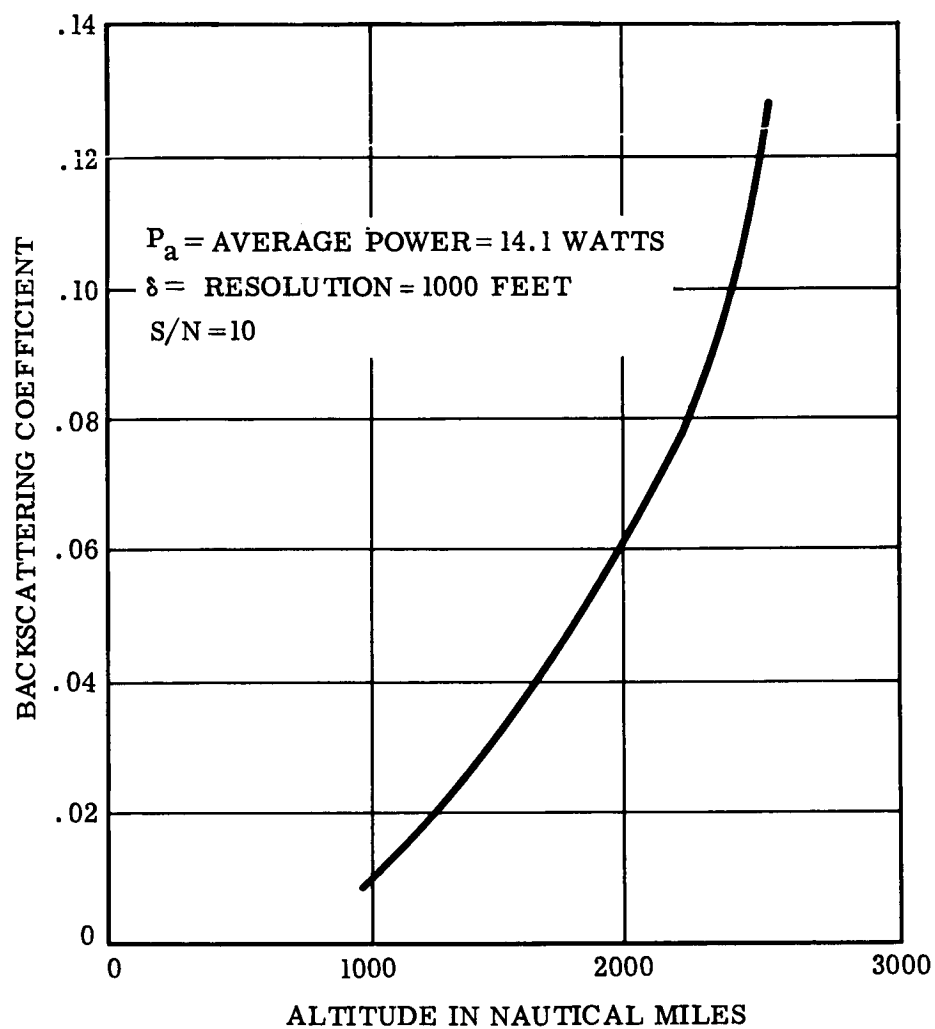


Figure 3.3.1-13. Backscattering Coefficient vs. Altitude

Furthermore, if it is assumed that the 1,000 ft. range resolution is obtained by a straight pulsed radar technique, then the pulse width required to obtain 1,000 ft. resolution is 2 microseconds. With the PRF available and the pulse width known, it is possible to compute the required peak power for the radar from the average power in these other two parameters. The following equation shows this relationship.

$$P_P = \frac{P_a}{\tau \text{ PRF}} = 3.7 \text{ kw for } P_a = 20\text{w} \quad (22)$$

If a design value of 1,000 ft. resolution at 1,000 nm altitude is chosen, then the resolution will be degraded at higher altitudes as shown in Figure 3.3.1-14. This is indicated by the average power formula in Volume VIII, Section 5.

(3) Mapping Coverage Capability

Many of the parameters influencing coverage capability have been limited to a narrow range of choice due to constraints imposed by the spacecraft and the nature of the radar technique. The Orbiter will operate in a nearly polar orbit for a period of about two months. Since the rotation period on Venus is about eight months, the Orbiter, during its operating life, will pass over about one-half of the planet's surface.

The orbiter period is about two hours. During each orbiter revolution, a point on the Venusian equator moves about six miles due to planetary rotation. For the nominal values of orbit altitude and antenna aperture, the radar strip width will be about 1 1/2 times as large. Thus, the strip maps will have about a 50 percent overlap in the equatorial region. The overlap will be progressively more at higher latitudes. The radar could be programmed to look sometimes to the right and sometimes to the left of the orbit. By means of such programming, the total area mapped could be made larger than one-half the total area of the planet. At latitudes above 45°N and 45°S, the range of the radar is sufficiently large that substantially all of the area above these latitudes could be mapped. At lower latitudes the technique would be employed less fruitfully.

Thus, with suitable programming, approximately 3/4 of the planet's total area may be mapped in a two month period.

(4) Data Processing and Communication

Two approaches may be considered for processing and communicating the radar data: (a) transmission of the radar video followed by processing at an Earth station, and (b) performing signal processing in the Orbiter and communicating only the resulting information.

The transmission of radar video approach is considered first. Using the Mars 1969 communications subsystem at Venus ranges, the capacity of the communications link for the output data (for moderate dynamic range, moderate noise transmission as needed here) is about 64 bps. Thus, if the radar signal bandwidth is kept below this value, then simple real-time telemetry of the radar data is feasible. The corresponding range resolution is about 0.5 nautical mile. However, previous discussion of this section indicates that the radar should be capable of finer resolution. Therefore, direct telemetry appears undesirable.

In the second approach, if processed data is to be transmitted, the communication requirement is greatly reduced. At the resolution and for the strip width required, including a factor of two excess width for overlap, the output data rate is only 150 samples per second; thus, gross redundancy would exist in the link if the full video output were relayed. Pre-processing of the data is, therefore, clearly indicated.

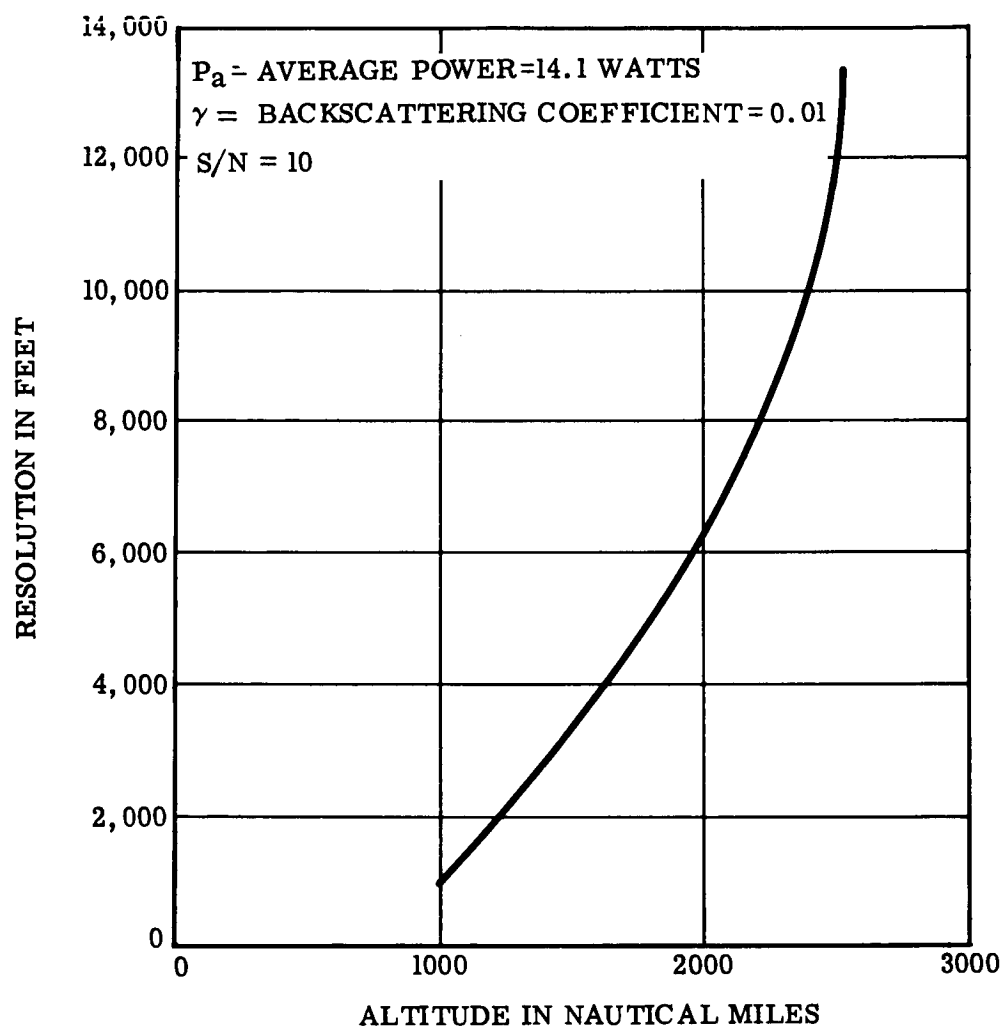


Figure 3.3.1-14. Resolution vs. Altitude

Unfocussed signal processing, which is simple to perform, can produce a resolution of about 0.2 nautical miles at the stated range and wavelength. At this resolution and for the same overlap, some 60 independent range elements would need to be processed, and the output data rate would be approximately 1,000 samples per second. Allowing approximately 30 gray-scale levels in the output data, the bit rate would be 5,000 bits per second, a reasonable value.

Data processing for the unfocussed coherent synthetic aperture radar consists only of the coherent integration of the received signals within the doppler spectrum defined by the effective length of the synthetic aperture. The necessary processing can be performed by range gated integrating filters. Approximately 60 filters are required to accommodate the number of range quantization levels. The output from the filters would be digitized and stored for subsequent transmission over the digital data link.

(5) Coherent Pulse Doppler Radar System for Venus 1970 Orbiter

(a) Transmitter

The transmitter for this radar will employ an X-band pulsed, four cavity klystron output power amplifier, driven from a stable frequency crystal oscillator through a varactor frequency multiplier. At the relatively narrow bandwidth required for this transmitter, a gain of 55 to 60 db can be obtained in the single klystron, so that it will be unnecessary to use more than one tube at the transmission frequency. The klystron is an efficient, rugged tube with adequate operating life.

(b) Receiver

A tunnel diode amplifier receiver will be used. It consists of five cascaded tunnel diode radio frequency stages, giving approximately 20 db gain each stage, followed by a coherent phase detector, then by a solid state video amplifier.

(c) Signal Processor

A processor comprising 60 separate range-gated integrating filters will be used. Each filter is a module approximately 2 cubic inches in volume and weighing 0.3 lbs., resulting in a net weight of 18 lbs. for the processor. The accompanying signal and synchronizing distribution circuitry will weigh an additional 7 lbs.

(d) Weight, Volume and Power Summary

Weight, volume, and power for the Coherent Pulse Doppler Radar System for the Venus 1970 Orbiter is given in Table 3.3.1-13.

TABLE 3.3.1-13. SUMMARY OF WEIGHT, VOLUME AND POWER REQUIREMENTS FOR COHERENT PULSE DOPPLER SYSTEM

	Weight (Lbs.)) Volume (Ft. ³)	Power Consumption (Watts)
Transmitter	60	1	240
Antenna	approx. 100	--	--
Receiver	15	0.3	15
Processor	25	0.2	90
Total	200 (approx.)	1.5	345

It is noted that the radar can be turned off during the orbit portion that is near the poles of most orbits. Very redundant coverage is produced of this area otherwise. The effective power usage duty cycle over the mission can be reduced to about one-half by such a method.

3.3.2 RADAR TO DETERMINE SURFACE CHARACTERISTICS

Earth-based radar measurements of the Moon have made significant contributions to our knowledge of the Moon's surface characteristics. Similar measurements of Venus have produced some information, although less than the lunar measurements, largely because of the greater distance between Venus and Earth. It has been found, for example, that the Moon is smooth at the longer radar wavelengths and begins to show evidence of roughness only at centimeter wavelengths. On the other hand, Venus presently appears rough at all radar wavelengths used. Radar investigations of planets like Venus and Mars from an orbiting vehicle would yield much more detailed information than radar investigations performed from the Earth.

Radar sounding experiments, designed to measure the topographical features of the planet, are outlined below. These experiments comprise a series of measurements of return as a function of angle of incidence over a wide range of wavelengths. (This section is adapted from the report submitted by the Conductron Corporation which is presented as part of this report.)

A. . Theoretical Background

A measurement of the scattering matrix of the Martian or Venusian surface at various frequencies will provide information about the scales of roughness present, since depolarization effects (see Table 3.3.2-1) can be expected to occur when the wavelength is comparable to the radius of curvature of a typical perturbation in the surface*. Depolarization will not occur when the perturbations are much smaller than a wavelength. However, backscattering will occur at angles other than specular even for fairly small scales of roughness. Hence, lack of scattering at non-specular incidence would indicate relative smoothness of the surface at the wavelength of the measurements. A tabulation of return characteristics for various aspect angles can be found in Table 3.3.2-2.

In order to take advantage of these effects, a sequence of measurements is proposed such that, during a portion of the orbit, a single fixed "patch" of surface will be sounded by the radar at various frequencies and angles of incidence. One of the angles of incidence is normal incidence so that the back-scattered return includes the specular (see Figure 3.3.2-1). If the "patch" being sounded is smooth, the non-specular return will be very small compared to the specular. In this case, the numerical value of the return at two different frequencies at normal incidence will allow the computation of the average surface impedance and loss tangent. Estimates thus obtained can be compared with those obtained for the permittivity and conductivity from radiometer measurements.

TABLE 3.3.2-1. POLARIZATION EFFECTS

No Cross Polarized Term	Smooth at Wavelength
(Down 10-15 db from direct)	
Cross Polarized Terms	Perturbation of Order of Wavelength
(Approximately 3-6 db down)	

*Cf. T. B. A. Senior and K. M. Siegal, "A Theory of Radar Scattering by the Moon", J. Res. Nat. Bur. St.-D. Rad. Prop., 64D, 217-229 (1960).

TABLE 3.3.2-2. RETURN VS. ASPECT ANGLE

<u>Pattern as Function of Aspect Angle</u>	<u>At Grazing Incidence</u>	<u>Conclusion</u>
Sharp specular return order of $kd \sin \theta \geq \pi$ where d = illuminated length or width, θ = angle of incidence	No return	Smooth surface
Wider peak width as function of aspect	Moderate return (Use standard theory such as that of Hayre and Moore, J. Res. Nat. Bur. St.-D, Rad. Prop., <u>651</u>), 427-432 (1960)	Small roughness but no topographical features
Smooth return as function of aspect	Relatively large return	If λ^0 dependence: smooth rolling hills and craters If λ^{-1} dependence: volcanic peaks and rock spires If λ^{-2} dependence: elevated plateaus

It is important to note that only relative magnitudes are important. Therefore, accurate absolute calibration of the system is not vital. Only the variation of return with aspect and frequency will be needed. For surface roughness, a transition in the type of cross section vs. aspect curves at various frequencies would be observed that would give an estimate of the magnitude of the roughness.

B. Recommended System

A multi-frequency radar that illuminates a "patch" of the Venus surface continually as it passes over that "patch" will provide a measurement of surface roughness. By operating at various frequencies, information relative to the size of this roughness may be obtained. Through the use of a single broadband antenna, programmed to illuminate a given area of surface, and through shared radar equipment functions, it is possible to utilize four or more different frequencies in this method of radar sounding.

Frequencies of 2 kmc, 1 kmc, 500 mc and 250 mc are recommended utilizing the single large spacecraft parabolic antenna. A spacecraft altitude of 1000 miles, with the radar operational through an angle of $\pm 50^\circ$ of the Venus nadir, has been used for estimating equipment parameters. Through diligent design of feeds the radar antenna can be made sufficiently broadband to cover the range of 0.25 to 2 kmc. The ability to transmit and receive with both vertical and horizontal polarization, can be achieved through an arrangement of crossed-dipole antenna feeds with either dipole utilized for each transmission through diode switching.

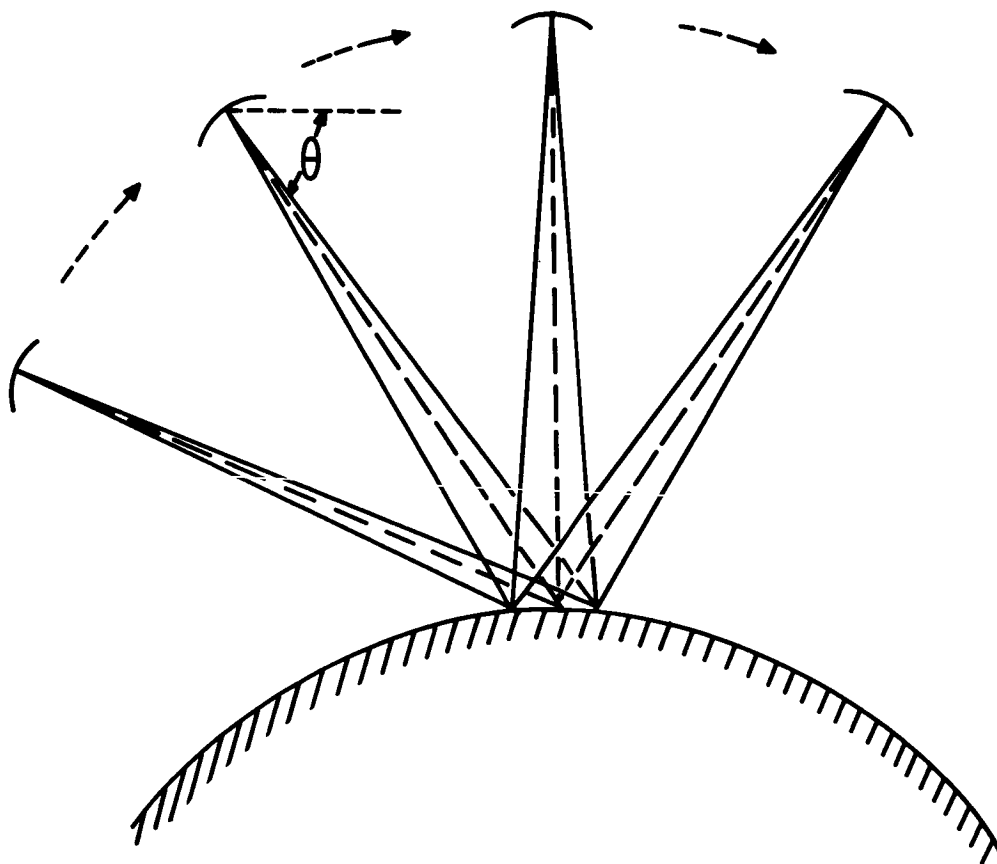


Figure 3.3.2-1. Radar Sounding of the Planetary Surface at Different Aspects

The radar equation is given by

$$P_T = \frac{4 \pi \lambda^2 R^4 \left(\frac{S}{N}\right) k T B}{A^2 \sigma} \quad (23)$$

where:

$R = 1500$ nautical miles range

$\frac{S}{N} = 16$ db = 40 signal-to-noise ratio

$k = 1.4 \times 10^{-23}$, Boltzman's constant

$T = 900^\circ\text{K}$ receiver noise temperature

$B = 10$ kc bandwidth

$A = 100 \text{ ft}^2$ effective antenna area (14 ft diameter)

$\sigma = 100$ square miles Venus radar cross-section.

Substituting the above in Equation (23) gives a required peak transmitted power of 11 watts for 1 kmc. At other frequencies power required is proportional to the square of the wavelength. Using coherent integration of groups of 30 pulse provides an improvement that can reduce the peak power required to 2 watts. With this magnitude of RF power required, transmission and reception at the four different frequencies could easily be accomplished through use of four separate transmitters and receivers. Should a 10 foot diameter antenna be employed in place of the 14 foot diameter antenna used in the preceding calculation, the effective antenna area, A , in the radar equation would be reduced by a ratio of the antenna diameters squared:

$$\left(\frac{D_{10}}{D_{14}}\right)^2 = \frac{100}{196} \approx \frac{1}{2} \quad (24)$$

which is squared again since the effective antenna A is used both in transmission and reception. Therefore, a 10 foot diameter antenna will require 16 watts peak transmitter power.

A single stable frequency reference and the use of solid-state harmonic generator methods could provide the four separate transmitter signals utilizing all solid-state devices. Switching of the separate transmitter signals would be accomplished through activating RF diode switches sequentially programmed after receipt of a radar-activate command. For the 2-watts peak power requirement (14 foot diameter antenna), the entire radar transmitter could utilize solid-state devices. Where 16 watts peak power is required (10 foot diameter antenna), vacuum tubes will be utilized for the final power amplifier at the two highest frequency transmitters: 2 kmc and 1 kmc. The radar receivers would be completely designed with solid-state devices with passive pre-selection filters and with RF pre-amplification separating the received signals for each receiver. A tunnel diode RF pre-amplifier design can provide a receiver noise figure of 6 db with little development effort. Conventional solid-state components and techniques will be employed for the receiver circuitry.

Since information provided by the radar is found in the relative energy, polarization, and time delay for transmitter pulse as the spacecraft passes over the illuminated surface, no requirements for calibration are anticipated.

A tabulation of estimated radar physical and electrical characteristics, utilizing both a 10-foot and a 14-foot diameter antenna, is shown in Table 3.3.2-3.

Data handling requirements for the radar sounder are shown in Figure 3.3.2-2. A gate waveform is generated in the period between transmitted and received pulses in which a group of clock pulses are counted. This count is inserted into the experiment data storage for relay to earth by the spacecraft telemetry subsystem. The relative intensity of received signals is, first, integrated in an analog integrator, then converted into a digital number, and then inserted into the data storage. Relative vertical-to-horizontal polarization of the received signal is obtained by alternately switching the antenna polarization during reception between transmissions. Two separate outputs are provided, one for each polarization sense, that are also converted in a similar analog-to-digital converter and inserted into storage.

(1) Expected Data Rate

The number of bits of information for each aspect angle and polarization test is:

$$n m p q = 640 \text{ bits,} \quad (25)$$

where

n = number of aspect angles sampled = 20 ($\pm 50^\circ$ at 5° increments)

m = number of frequencies = 4

p = number of polarizations = 2

q = number of bits of dynamic range = 4 (16 grey levels)

The total number of bits depends upon how many ground areas are to be tested. Clearly, the experiment can be performed hundreds or even thousands of times without overloading the transmission channel.

TABLE 3.3.2-3 - ESTIMATED (HIGH FREQUENCY) RADAR CHARACTERISTICS
Radar Sounder - 10-Ft Antenna

Equipment	Weight (lbs.)	Volume (in. ³)	Power (watts)
Antenna	-	-	-
Diplexer and Diode Switching	1.5	30	-
Transmitters	3.8	160	3.5
Receivers	3.5	144	1.0
Power Supply	2.4	36	0.8
Total	11.2 lbs.	370 in. ³	5.3 watts

Radar Sounder - 14-Ft Antenna

Equipment	Weight (lbs.)	Volume (in. ³)	Power (watts)
Antenna	-	-	-
Diplexer and Diode Switching	1.5	30	-
Transmitters	3.0	120	1.5
Receivers	3.5	144	1.0
Power Supply	1.5	24	0.5
Total	9.5 lbs.	318 in. ³	3.0 watts

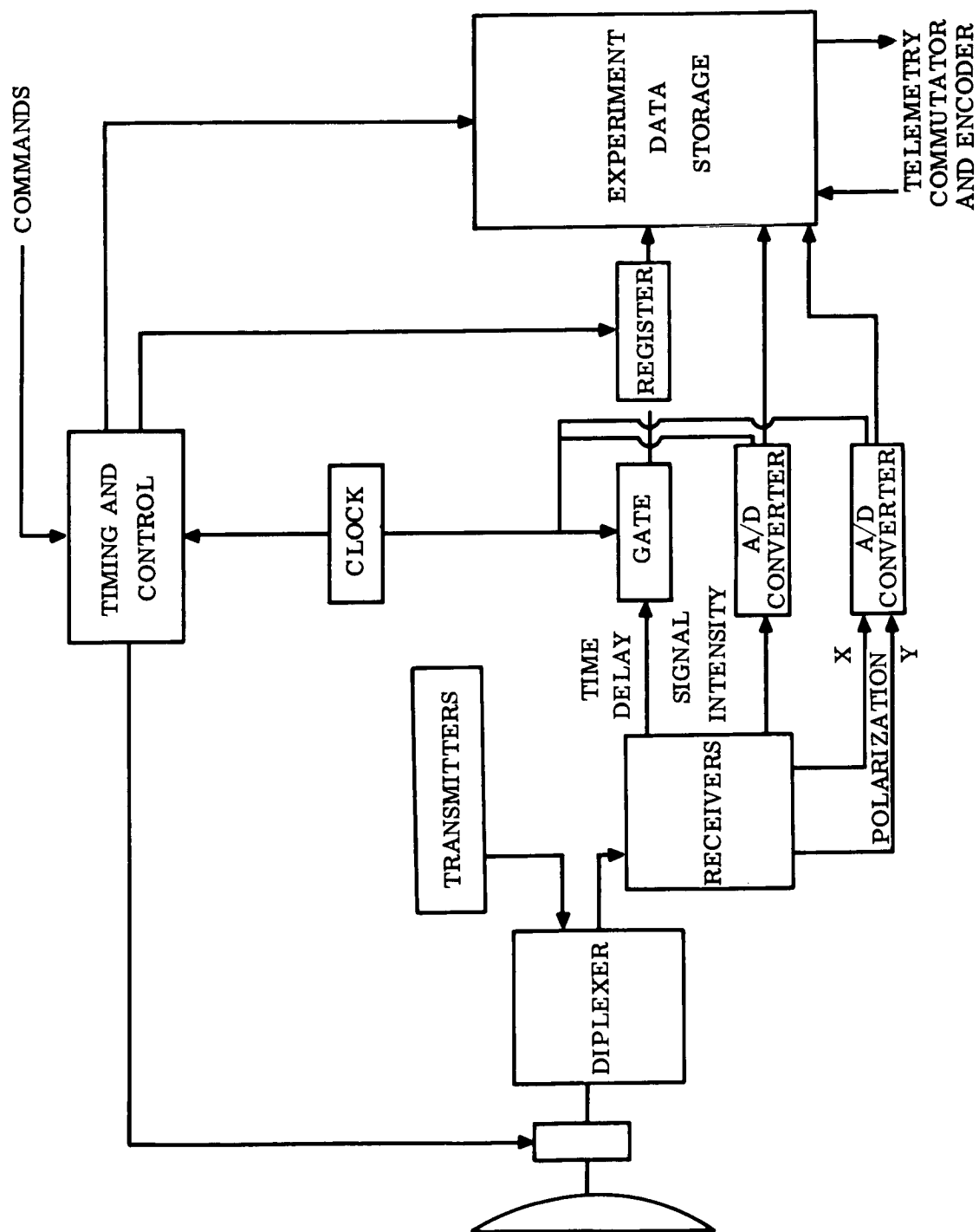


Figure 3.3.2-2. Surface Sounder Data Handling

3.3.3 IONOSPHERIC SOUNDING

The density of the ionosphere of Venus has not been clearly established. Sounding experiments, similar in principle to those for determining the surface roughness characteristics, can also provide information on the ionosphere if one is in fact present. For, at the longer wavelengths, the absorption and reflection by the ionosphere will be visible in the records made. However, a separate radar for this purpose will actually be required, since the frequencies required for detailed ionospheric soundings are necessarily low and should cover an almost continuous band. The high reflectivity of an ionosphere at low frequencies (except near a critical frequency) results in a much lower power requirement for this radar than for that used to measure the planetary surface characteristics.

A. Theoretical Background

In the case of the earth's ionosphere and at the long wavelengths (e.g., for the band between 5 to 15 mc), standard ionospheric sounding measurements have been made for decades by measurement of the time delay for pulses transmitted from the earth at normal incidence over a continuous sweep of frequencies and through a band which covers the maximum plasma frequency of the ionosphere. The result of such a series of measurements is an ionogram, Figure 3.3.3-1, which is a curve of time delay versus frequency. At each frequency below the critical frequency, the pulse will be totally reflected by the ionosphere. When the critical frequency is approached, the return will fall off sharply due to an increase in absorption.

If a constant planetary magnetic field is present, the ionosphere becomes anisotropic. The phenomenon of double refraction and reflection can, then, take place at frequencies above some minimum value which depends on the relative strength and orientation of the constant magnetic field. This effect takes the form of two pulses returned at different time delays for each transmitted pulse. The ionogram curve of time delay versus frequency, then, splits into two branches. The returns corresponding to the two branches will be circularly polarized with opposite orientations if the constant magnetic field is oriented in the direction of propagation. If the imposed magnetic field is transverse to the propagation direction, the returns will be plane polarized.

From data obtained from this kind of measurement, a detailed knowledge of the electron distribution as a function of distance can be deduced. In particular, the critical or plasma frequency can be estimated. The splitting effect can be used to estimate the strength and orientation of the planetary magnetic field. In fact, if the experiment is carried out over a map area, magnetic lines of force can be constructed from the data.

For example, if

$$\omega = 2\pi f \quad (26)$$

is less than the collision frequency ω_c of the free electrons with heavy particles, then the magnetic field H is given in terms of the critical frequencies f_o and f_x for the ordinary and extraordinary waves by:

$$H = \frac{2\pi mc}{e} \frac{f_x^2 - f_o^2}{f_x}, \quad (27)$$

where m = electron mass, e = electron charge, and c = free space speed of light.

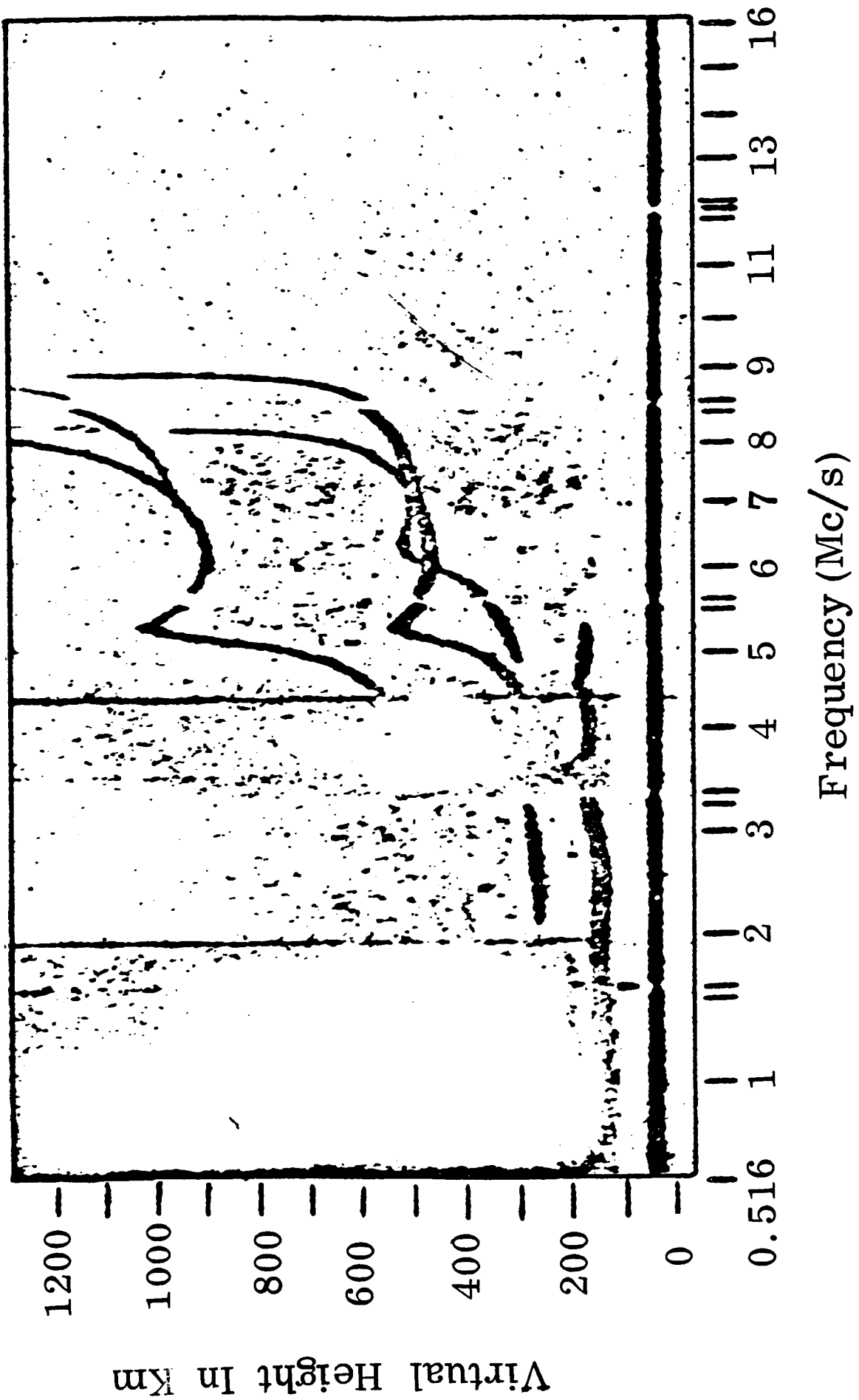


Figure 3.3.3-1. Ionogram

On the other hand, if $\omega > \omega_c$, H is given by

$$H = \frac{2\pi mc}{e} (f_x - f_o) . \quad (28)$$

Whether ω is greater than ω_c or less than ω_c can be determined by observing the nature of the polarization ellipses for the two returned pulses. If they are nearly circularly polarized in opposite directions, then $\omega > \omega_c$. If they are nearly linearly polarized, then $\omega < \omega_c$.*

B. Recommended Systems

Since the reflective properties of the earth's ionosphere lie in the frequency range of 5 to 15 mc, it is assumed that this frequency range is also of most interest in determining the existence and characteristics of an ionosphere about Venus. The method of implementation for the other sounding experiment would not be applicable here due to the difference in frequencies. Implementation of radar sounding of a possible Venus ionosphere in the 5-15 mc range is made easier because of the larger radar reflecting cross-section which the ionosphere will present. This cross section can be approximated by**

$$\sigma = \pi r^2 \quad (29)$$

where r is the distance from the reflecting surface that in this case is the ionosphere. This formula applies because the vehicle is assumed to be orbiting in the near zone of the ionospheric surface. With the spacecraft at an altitude of 1000 nautical miles, a σ of 36×10^6 square miles is indicated. This is many orders of magnitude greater than the cross-section calculated for the other sounding experiment to determine surface roughness which indicates that little transmitted power is required to sound the possible Venus ionosphere.

Implementation of this experiment would consist of a low-power pulsed radar where the transmitter and receiver frequencies are swept in discrete steps in the frequency range of 5-15 mc. A single frequency synthesizer, employing two stable crystal oscillators and a combination of frequency multiplex and mixers, would provide 0.1 mc steps in the range 5-15 mc, so that 100 discrete frequencies may be used. This same synthesizer would provide the receiver mixer local oscillator injection frequency offset by the receiver IF amplifier frequency. Similar to the surface roughness sounding radar, the switching of frequencies will be sequentially programmed and controlled by command signals from the spacecraft command link.

A long extensible rod, or whip, antenna may be employed. This could be of the spring-loaded type that will be extended by an explosive squib upon a command to the spacecraft. This antenna form has been used successfully in previous satellites.

With an RF peak power output of 1 watt, a more than adequate received signal-to-noise ratio may be assured. Both transmitter and receiver may be completely designed with solid state devices using components and techniques presently well within the state-of-the-art. A tabulation of electrical and physical characteristics is shown in Table 3.3.3-1.

* Cf. S. K. Mitra, The Upper Atmosphere, Chapter 6, Hafner Publishing Co., New York, January 1952.

**Cf. T. B. A. Senior and K. M. Siegel, "A Theory of Radar Scattering by the Moon", J. Res. Nat. Bur. St., 64D (1960).

TABLE 3.3.3-1. ESTIMATED IONOSPHERIC SOUNDER CHARACTERISTICS

<u>Equipment</u>	<u>Weight (lbs)</u>	<u>Volume (in. ³)</u>	<u>Power (watts)</u>
Antenna	2.5	-	-
Diplexer and Diode Switching	1.5	30	-
Transmitter	2.0	100	4.0
Receiver	1.2	24	0.75
Frequency Synthesizer	1.5	30	0.5
Power Supply	3.0	40	1.0
Total	11.7 lbs.	224 in. ³	6.25 watts

Data processing and storage for this equipment would be similar to that described for the surface radar sounding experiment.

(1) Expected Data Rate

The number of bits of information for each ionospheric sounding is

$$r s t = 2000 \quad (30)$$

where:

r = number of frequency samples = 100

s = number of types of waves = 2

t = number of bits for time delay accuracy = 10 bits (1 mile accuracy in 1000 miles).

The total number of bits depends upon how many soundings are to be made.

(2) Equipment Required

The equipment required is listed in Table 3.3.3-1 with applicable weights, volumes and powers.

3.3.4 RADIOMETER MEASUREMENTS

This section is adapted from a Conductron Corporation report.

As proved by the Mariner II experiment, microwave radiometer measurements of Venus are feasible from a satellite and can provide valuable scientific information. The primary objective of this first successful deep space probe microwave radiometer experiment was thermal mapping of the planet's surface. Because of a deep, dense atmosphere and extensive cloud cover over the planet, conventional infrared wavelengths could not be utilized for this purpose. Earth based receivers have been able to obtain only an average temperature for the entire visible disk, and even improved interferometric techniques appear unlikely to provide any detailed mapping of the planet from the earth in the next ten years or so.

Additional radiometer measurements, similar to those performed by Mariner II, are proposed for the Voyager spacecraft with several wavelengths being selected. Information will be provided by these experiments on: surface temperature, roughness, and composition; the density and composition of the atmosphere; and the ionosphere. Equipment analogous to Mariner II equipment is proposed. The equipment will share many elements with the other radar equipment proposed.

A. Selection of Wavelengths

The wavelength range most widely used in microwave radiometer measurements is the spectrum between 0.5 cm (6×10^{10} cps) and 100 cm (3×10^8 cps). At these wavelengths the radiation detected is believed to be predominantly radiation from the surface of the planet. At shorter wavelengths, the radiation detected arises primarily from the atmosphere. At longer wavelengths, the radiation arises from the ionosphere (or arises from the galaxy and is reflected by the ionosphere).

The wavelength range that is first defined is the region of greatest interest, primarily because the data there should be affected by a relatively small number of factors whose effects can be separated, so that definitive information can be deduced regarding the gross physical conditions on the planet. Until these gross conditions have been determined with some certainty for the planet, the additional information, that would be made available by extending the frequency range further, is probably of secondary importance.

Measurements from earth at wavelengths of 2 to 20 cm have given an average effective temperature of about 600°K . Measurements at wavelengths of 0.4 to 1.0 cm and at 40 cm have given an average effective temperature of about 300 to 400°K . The Mariner II data, at 1.9 and 1.2 cm wavelengths, indicated that the temperature of the planet is about 800°K over both dark and lit areas. It has been generally assumed that the wavelengths giving the higher temperature values indicate the surface temperature and that the drop-off at either end is due to the intrusion of additional effects.

The earth based measurements at 3 cm and 10 cm have shown a certain amount of sensitivity to planet rotation phase. The size of this effect and its angular displacement are not the same at 3 cm as at 10 cm. The effect is ascribed to a difference in penetration of the atmosphere or emissivity of the surface at these two frequencies. The layer which gives rise to the 10 cm radiation presumably has somewhat less thermal fluctuation than the layer where the 3 cm emissions originate. The theoretical relationship which should apply between the phase effect and the properties of the surface material is set forth in the Conductron Report. In order to obtain adequate data on this rotation phase effect, measurements for at least two, and preferably more, test wavelengths within the range from 2 cm to 20 cm should be made from the satellite over a period of several months.

Assuming that the surface temperature data can be refined by measurements in the wavelength range described above, it is then practical to investigate the effects of atmospheric absorption through the use of wavelengths outside the initial range. As was mentioned earth based measurements give a much lower average temperature at 1 cm and below than at 2 cm and above. This is generally attributed to molecular absorption in the lower atmosphere. A detailed study of this absorption, over the planetary surface and over a range of angles of incidence, could provide useful information about the uniformity and height distribution of this absorbing layer. The water vapor absorption line at 1.35 cm is of particular interest. A recent earth-based measurement appears to indicate virtually no absorption at this wavelength in the Cytherean atmosphere. The data from the Mariner II experiment at this wavelength apparently was not conclusive. A further comparison of this line with nearby wavelengths, especially shorter wavelengths, would be of value.

A single earth based measurement at 40 cm has indicated an emission temperature at this wavelength of 400°K . One explanation has been advanced that a decrease in the ratio of roughness to wavelength takes place, thereby causing the planet to look smoother at 40 cm than at 20 cm or less. A "rough" planetary surface would appear uniformly bright over the entire disk, while a "smooth" surface would have a decreasing emissivity toward the limb where the angle of emission is large, thereby giving a smaller total emission from the planet (see Conductron Report later in this study). This explanation appears to be in conflict with radar data which indicate that the planetary surface is relatively smooth even at 12.5 cm. However, it is not certain that a roughness capable of producing the observed emission effects is necessarily incompatible with a "smooth" radar reflecting surface for the wavelengths thus far observed.

Another possible explanation for the 40 cm drop-off is ionospheric absorption of the surface emissions. Although radar data has shown no such absorption even for 68 cm radiation, the path lengths toward the limb of the disk are considerably longer than those for radar which is essentially specular at present. Absorption toward the edges could account for the decrease in effective temperature. In either case, the use of one or more wavelengths larger than 40 cm should enable us to determine the causes of this effect. If the ionosphere is causing the drop-off, it should become much more severe at longer wavelengths. This effect will be more observable at the more nearly vertical angles of incidence.

Additional indications of surface roughness can be obtained by measurements over a range of aspect angles. The emissivity of a smooth, solid surface as a function of angle and polarization is described in the Conductron Corporation Report. If measurements of the same surface area from several different angles show very little aspect variation, then the surface almost certainly is "rough" at this wavelength scale. If the data do, however, show clear aspect sensitivity, the surface almost certainly must be relatively "smooth", and a plot of emissivity versus angle will enable estimates to be made of the dielectric constant and the conductivity of the surface.

In summary, primary interest should be to obtain measurements in the 2 cm to 30 cm wavelength range, a range at which atmospheric effects are believed secondary, to provide further data on surface temperature, roughness, and perhaps composition. Measurements to provide information on ionospheric and surface roughness effects in the range of 30 cm to 80 cm would be next in importance. Finally, measurements at millimeter wavelengths could extend our knowledge of the atmosphere.

Accomplishment of the first two objectives is recommended. The equipment needed is available almost in total from the radar measurements planned for other purposes. The specific wavelengths proposed are wavelengths utilized by the radars, namely: 3 cm, 15 cm, 30 cm, and 60 cm. The third objective, measurement at millimeter wavelengths, may be accomplished if weight tolerances will allow additional lightweight antenna equipment.

B. Thermal Sensitivity and Angular Resolution

The thermal sensitivity required for the above purposes is about 5°K to 15°K . The finer resolution is required only for inversion of the radiation integral vs. aspect. This level of performance is available at the frequencies planned at which the sum of the receiver noise temperature plus input radiation temperature will in general not exceed 5000°K . This is achieved by use of a receiver bandwidth-time product of about 10^6 . This value is attainable with the receivers planned with integrating times of about 10 seconds, a reasonable value.

The angular resolution required is low. The radar equipment will provide an angular resolution of about 0.1 radian at the mid wavelength, and a proportionately coarser and finer resolution at the other wavelengths.

C. Data Output

The temperature measurements made by the recommended equipment will produce one datum of about 6-bit (64-level) gray scale per 10 seconds, or about 0.6 bit per second.

D. Equipment

The same basic large reflector antenna as that used for the radars and communications can be used for the several radiometers. Sufficient time will be available for radiometer use during each orbit to obtain a large quantity of data since a full map is not essential. Data will be taken only when the viewing direction points well away from the sun. Four wavelengths are planned, as discussed above. A multiple nested feed will be used. At the longer wavelengths, the feed will be made to under-illuminate the reflector to provide low backlobes. A Cassegrain feed could be used but should not be necessary.

For each frequency used in this experiment, the receiver associated with the companion radar will be used, and a demodulator and integrator will be supplied.

Reference temperature radiation signals will be obtained, as in Mariner II, from both a separate small antenna pointing toward a cold region of space and an absorptive termination at satellite structure temperature. Chopping modulation will be performed, using diode switches, to provide calibration.

The equipment required is primarily that provided by the radar sounder system described above. The additional switching and integrator circuitry needed will weigh approximately 5 lbs.

3.3.5 RADAR ALTIMETERS AND DOPPLER RADAR

A. Recommended System for the Venus 1970 Orbiter

Height-above-terrain may be measured for the Orbiter by using the SAHARA system. The antenna from the mapping radar can be pointed towards the local vertical. The pulse compression used to obtain range resolution for the mapping mode would be used to obtain height-above-terrain for the altimeter mode. Antenna duplexing would not be required. The accuracy of the height-above-terrain measurements would be approximately 0.66 nm.

B. Recommended System for the Mars Entry Vehicle

(1) Radar Equipment

For the Mars mission, height-above-terrain is required to provide a data base for atmospheric measurements during the parachute descent. This requirement may be satisfied by a pulsed radar altimeter which can be a modification of the Altitude Marking Radar made by Hughes Aircraft Company for the Surveyor.

The Altitude Marking Radar in its Surveyor configuration is range-gated to provide a signal to the Surveyor retro-rocket when a specified height-above-terrain is measured. By redesigning the Video Processor, the Altitude Marking Radar can give continuous altitude readings in the range from 200,000 feet to 1,000 feet, as required for the Mars entry vehicles.

The characteristics of the radar are given in Tables 3.3.5-1 and 3.3.5-2.

TABLE 3.3.5-1. MARS ALTIMETER PARAMETERS AND PERFORMANCE

<u>Parameter</u>	<u>Value</u>
Altitude Range	1,000 to 200,000 feet
Accuracy	Maximum error will not exceed ± 100 ft. or 2 percent, whichever is larger
Velocity	200 ft/sec. maximum
Radar reflection coefficient	Similar to extremes experienced with earth terrain
Data rate	One reading per second minimum
Antenna beamwidth	20°
Power consumption	10 to 15 watts average
Transmitting frequency	X-Band

TABLE 3.3.5-2. MARS ALTIMETER PHYSICAL CHARACTERISTICS

<u>Unit</u>	<u>Outline Dimensions (Inches)</u>	<u>Approximate Weight (Ounces)</u>
Antenna	5 in. dia. paraboloid 60 cubic inches displaced volume	3
R. F. Assembly	$5 \times 3 \frac{1}{4} \times 1 \frac{3}{4}$	16
Mixer	$2 \frac{1}{8} \times 1 \frac{5}{8} \times 1 \frac{15}{16}$	$3 \frac{1}{2}$
Modulator	$4 \times 2 \frac{11}{16} \times 2$	16
I. F. Amplifier	$6 \frac{1}{2} \times 1 \frac{1}{8} \times 1 \frac{1}{2}$	8
Local Oscillator	$6 \times 1 \frac{1}{2} \times 1 \frac{1}{2}$	8
Video Processor	$6 \times 5 \times 2 \frac{1}{4}$	17
Electric Conversion Unit	$4 \frac{1}{4} \times 3 \frac{1}{4} \times 2 \frac{1}{8}$	12
Harness, Brackets, etc.		4
Total		<u>$5 \frac{1}{2}$ POUNDS</u>

(2) Mars Lander Radome Characteristics

The radar altimeter is mounted in the nose of the Mars Lander and transmits through a radome. The radome is made of non-charring ESM having a nominal thickness of one inch. This is backed with fiberglass honeycomb about two inches thick in the vicinity of the antenna. The holes in the honeycomb are parallel to the direction of radar propagation.

The ESM has a dielectric constant of 2.32. Tests have been made of the transmission characteristics of a 1/2-inch flat sheet of ESM at a frequency of 2400 megacycles. In these tests, the percentage power transmission was 99 before heating and 97 after being subjected to 6 btu/ft²/sec for 840 seconds. The material was also heated at a rate of 89 btu/ft²/sec. Although electrical measurements were not made after this heat was applied, char did not form and it is known from the nature of the material that char will not form at higher heat rates*.

The power transmission is a function of the dielectric constant, loss tangent, and the thickness of the material. The thickness of the material tested was $0.152 \lambda_s$ where λ_s is the wavelength in the material. Figure 10.5 of the text, Radar Scanners and Radomes**, relates these quantities and by referring to the curves it can be seen that the loss tangent of the material is extremely small.

For thicknesses of less than a few inches, losses within the material can be neglected due to the low loss tangent. Therefore, only losses due to reflections need be considered. Minimum transmission occurs at odd multiples of quarter-wavelength thicknesses and maximum transmission occurs at multiples of a half wavelength. The radar altimeter operates at 9.6 kmc. The wavelength in the material is 0.83 inch. The nominal design thickness of the ESM of one inch is very close to an odd multiple of a quarter wavelength and, thus, minimum transmission occurs. Extrapolating the ESM test results, it is estimated that the minimum transmission, $0.25 \lambda_s$, would be 98 percent before heating and 95 percent after heating. This indicates that material thickness is not critical and, although there are preferred thicknesses (for example, 0.83 or 1.24 inch), it is feasible to allow a variation from these if required for mechanical or thermal reasons.

The effect of the honeycomb, as arranged, should be small because of its alignment and low density. The honeycomb is without a skin on either side, as a conventional honeycomb sandwich panel would have, and butts against the ESM. Data is presented in Radar Scanners and Radomes, page 334, for a sandwich radome consisting of a honeycomb cone with a skin on either side. This skin is known to be the major cause of power transmission decrease through a honeycomb panel. As the thickness of the skin decreases, the transmission increases. For a skin thickness of 0.020 inch and panel thickness of 0.489 inch the power transmission is 97 percent. Similarly, high transmission is expected in this application of honeycomb.

The radar power is transmitted through the radome in two directions: from the antenna to the ground and back to the antenna. Using power transmission percentages of 95 for the ESM radome and 97 for the honeycomb, the 2-way loss can be calculated,

$$\begin{aligned} \text{Loss (db)} &= 2 \times 10 \log \left[\frac{1}{(0.95)(0.97)} \right] \\ &= 0.72 \text{ db} \end{aligned} \quad (31)$$

A loss of 1.5 db has been allowed in the radar altimeter design which, as can be seen, is conservative.

C. Recommended System for the Venus Entry Vehicle

The requirement for height-above-terrain for the Venus Entry Vehicle and for horizontal velocity can be satisfied by modifying the doppler radar being built for Surveyor.

*For a discussion of the material and its tests, see Section 1.3.9A(4) of Volume IV

**Radar Scanners and Radomes, Vol. 26, Radiation Laboratory Series, 1948, McGraw-Hill

A solid-state transmitter is substituted for the klystron transmitter. This decreases the input power requirement and allows the equipment to withstand the 125 g's (design value) during initial entry. The Surveyor paraboloidal antennas are replaced by flat arrays which are able to take aerodynamic loads better.

The Radar Altimeter and Doppler Velocity Sensor, being built for Surveyor, has a one-sigma error of ± 2 percent on altitude measurements and a one-sigma error of ± 1 percent on horizontal velocity. The doppler radar operates at 12.9 Gc for the altimeter and 13.3 Gc for the horizontal velocity measurements. Two antenna arrays, 15 in. x 19 in., are deployed from the Venus entry vehicle after the vehicle has entered the atmosphere and slowed to subsonic velocity. Each antenna provides two beams which gives a total of four beams for the system. One is vertical (for altitude measurement) and the other three form a tripod (for horizontal velocity measurement).

The total radar system weight for the Venus entry vehicles is estimated to be 25 pounds. The input power is 200 watts average when operating and zero for standby. It is possible to design the equipment to time-share the altimeter and velocity functions. The input power would then be 100 watts and the weight would remain the same.

3.4 RESULTS AND CONCLUSIONS

3.4.1 TERRAIN MAPPING

A. Choice Between SAHARA and the Coherent Pulse Doppler Radars.

The main points considered in choosing between the two mapping radars are:

- (1) The SAHARA system transmitter power calculation included higher losses than did the coherent pulse doppler radar calculation. When an adjustment is made for system losses, the values of terrain reflectivity coefficient, signal-to-noise ratio and transmitter power are comparable for both systems.
- (2) The resolution obtainable with the coherent pulse doppler radar is about 1/6 of that obtainable with the SAHARA system but the SAHARA resolution of one mile is acceptable. The resolution of both systems degrades with increasing altitude.
- (3) The coherent pulse doppler radar system can perform on-board data processing, which decreases the communication bandwidth requirement.
- (4) The coherent pulse doppler radar requires twice the antenna area that SAHARA requires. This adds a minimum of 30 pounds additional weight. The coherent pulse doppler wave length (a requirement) is 3.2 cm. To hold the required antenna tolerance for this wave length with the thermal stresses anticipated requires a weight addition of 30 to 60 pounds. These factors result in an additional weight of 60 to 90 pounds in the antenna system.
- (5) The vehicle attitude rate (50 microradians per sec.) causes, during the radar integration time, an angle error which is very much smaller than the beamwidth of either radar and, therefore, does not degrade the data. Both systems use a clutter-lock circuit in the receiver to adjust for a vehicle attitude angle error in the azimuth plane. Although the antenna pointing accuracy requirement of the coherent pulse doppler radar is more stringent, the use of clutter lock will meet its requirement.
- (6) The coherent pulse doppler radar has been developed and operated in aircraft. Satellite operation adds additional requirements, but aircraft operation has uncovered some problems which have been solved. Although the SAHARA design has been examined in detail, and it uses electronic building blocks which, at least functionally, have been used before, there are liable to be unforeseen problems which invariably arise during development.

Based upon the analysis to date the SAHARA system was chosen because of its antenna weight advantage. However, the coherent pulse doppler radar has certain advantages listed above which warrant a more detailed examination of the antenna problem to determine if its strong weight disadvantage could be removed.

B. Recommended Terrain Mapping System

The SAHARA system for the Venus 1970 Orbiter uses a 10-foot parabolic dish. The total weight of the terrain mapping radar system equipment carried in the Orbiter is approximately 109 pounds. This weight is broken down as given earlier in Table 3.3.1-9 as follows:

Antenna		32 pounds
Low Voltage Power Supply		7
High Voltage Power Supply		8
Transmitter		27 pounds
Receiver		10
Packaging Structural Support		13
DC Power Supply		12
Solar Cell Array	7.88	
Batteries	2.79	
Regulation, Control, and Distribution	1.33	
Total	12.00 pounds	109 pounds

The volume occupied by the equipment, less antenna and primary power, is estimated as 2 cubic feet.

The outputs of this equipment comprise video signals which are transmitted to the earth for processing. The result of the processing is a map of the surface with a 1 mile x 1 mile resolution of terrain features having an average value of reflectivity of -15 db. This result is obtained when the Orbiter is at 1000 miles altitude. The azimuth resolution will degrade with increasing altitude. At 2500 miles, the azimuth resolution is 1.6 miles. The map quality also degrades with altitude because of a decreasing signal-to-noise ratio. At 2500 miles altitude a reflection coefficient of about -3 db is required for a good quality map. This value of reflectivity is only encountered on the earth for near-normal incidence with a relatively smooth water surface. The maximum altitude, for a fair quality map with average terrain reflectivity, is about 1600 miles.

3.4.2 RADAR SURFACE SOUNDER

Frequencies of 2 kmc, 1 kmc, 500 mc and 250 mc are proposed utilizing the single, large spacecraft parabolic antenna. A spacecraft altitude of 1000 miles has been used for estimating equipment parameters, with the radar operational through an angle of $\pm 50^\circ$ of the Venus nadir. The high-gain spacecraft antenna is assumed to be optimized at 2 kmc for Earth-Venus communications and, through diligent design of antenna feeds, it is assumed that it can be made sufficiently broad-band over the range of 0.25 to 2 kmc. The

ability to transmit and receive with both vertical and horizontal polarization can be achieved through an arrangement of crossed-dipole antenna feeds with either dipole utilized for each transmission through diode switching. Table 3.4.2-1 summarizes the radar surface sounder characteristics.

TABLE 3.4.2-1. RADAR SOUNDER - 10-FT. ANTENNA

<u>Equipment</u>	<u>Weight (Lbs.)</u>	<u>Volume (In. ³)</u>	<u>Power (Watts)</u>
Antenna	(uses Terrain Mapping Radar Antenna)		
Diplexer and Diode Switching	1.5	30	-
Transmitters	3.8	160	3.5
Receivers	3.5	144	1.0
Power Supply	2.4	36	0.8
Total	11.2 Lbs.	370 in. ³	5.3 Watts

3.4.3 IONOSPHERIC SOUNDER

The recommended ionospheric sounder would consist of a low-power pulse radar with capacity to emit 100 discrete frequencies in the range from 5 mc to 15 mc. The transmitter and receiver would both be entirely solid-state in design and a spring-loaded, long extensible-rod antenna would probably be used.

The total ionospheric sounder weight would be 11.7 pounds. It would occupy 225 cubic inches and require 6.25 watts of input power. The rod antenna would be directed broad-side to the planet.

3.4.4 RADIOMETER

Radiometric measurements can be made utilizing the terrain mapping radar antenna and radar surface sounder equipment. In addition to this equipment, 5 pounds of additional equipment is required. Because of the better spatial resolution, the measurements will obtain data to extend the Mariner II experiments. A recommendation is made that this function be performed.

3.4.5 VENUS 1970 ORBITER RADAR ALTIMETER

It is recommended that the radar altimeter function for the Orbiter be performed by the equipment used for terrain mapping during intervals when terrain mapping is not being performed. It is, therefore, necessary to be able to orient the antenna of the terrain mapping radar directly to the local vertical. The additional equipment required to derive height-above-terrain information from the re-oriented terrain radar antenna is incidental. The accuracy of the measurement is estimated as 0.66 mile.

3.4.6 RADAR EQUIPMENT FOR MARS-VENUS ENTRY VEHICLES

The entry vehicles for Mars and Venus require a measurement of height-above-terrain to ± 100 feet, at least every 1,000 feet. The Venus entry vehicle also requires a doppler radar so that horizontal velocity may be measured. Equipment developed for Surveyor can meet these requirements with modifications. The one sigma velocity error of \pm one percent of the Surveyor Doppler Velocity Sensor meets the Voyager requirements.

The Radar Altimeter and Doppler Velocity Sensor antennas used on the Venus entry vehicle are deployed at sub-sonic speeds and, therefore, entry heating is not a problem. The Mars altimeter is behind a radome constructed of non-charring ESM material (see Section 1.3.9A(4)). This material is very suitable for a radome when taking into consideration its non-charring characteristic, and its values of dielectric constant and loss tangent.

3.5 CRITICAL PROBLEM AREAS

There are no critical radar problem areas in the strict sense that there is no component or subsystem which requires an advance in the state-of-the-art to develop. However, there are many systems problems to be solved.

The entry vehicle altimeters and doppler radar are modifications of Surveyor equipment. The radiometer is mainly composed of terrain mapping radar and radar surface sounder equipment and, therefore, is not considered a unique piece of equipment. This also applies to the Orbiter radar altimeter which is a function of the terrain mapping radar.

The basic radar subsystems to be developed are, then, the:

- a) Terrain mapping radar
- b) Radar surface sounder
- c) Ionospheric sounder

The terrain mapping radar development will require the most effort because of its complexity and significant interfaces with other subsystems. It is recommended that development of this radar start as soon as possible. The use of simulators and flight tests with scaled parameters in an aircraft can be used as interim steps in the evaluation of this radar. But its performance is an intimate function of velocity and altitude and it should ultimately be tested in a satellite.

Radar surface sounders have been operated before from low altitudes and their nature is such that performance can be accurately extrapolated to higher altitudes and velocities.

Ionospheric sounders have been developed for space application. The development of this equipment will consider the greater ranges involved and the interface between the antenna and the vehicle. The required characteristics for the increased range are easily obtained.